Distribution, interacting partners, and function of polysialic acid in the brainstem and spinal cord of adult rodents

Shila Shahbazian (PharmD, MBiotech)

Faculty of Medicine and Health Sciences

Macquarie University

A thesis submitted to Macquarie University in fulfilment of the requirements for the degree of Doctor of Philosophy

Principle Supervisor**: Associate Professor Ann K Goodchild**

Associate Supervisor: **Professor Nicolle H Packer**

2017

Contents

Abstract

Glycans, a major class of biomolecules, are expressed on every cells surface and play an important role in maintaining health with their perturbation causing disease. Polysialic acid (polySia) is a large cell surface glycan widely expressed in the developing brain with an essential role in brain development. Mice deficient in polysialyltransferases ST8SiaII and ST8SiaIV, enzymes required for polySia synthesis, show severe developmental deficits in their nervous system with mostly dying within a month. In adult brain, however, polySia exhibits a discrete expression pattern which in the higher brain regions is often associated with plasticity. The expression and function of polySia in the brainstem and spinal cord is poorly understood.

We investigated the distribution and cellular localization of polySia in the adult rat brainstem, spinal cord, and trigeminal ganglion resulting in the identification of novel polySia positive regions including the spinal trigeminal nucleus caudalis (Sp5C) and the intermediolateral cell column (IML). PolySia was associated with neurons and fine astrocytic processes, confirmed by ultrastructural analyses. Within the superficial laminae of the dorsal horn, some association of polySia with inhibitory neurons was found. The sugar also coated some neurons, satellite glial cells, and fibres in the trigeminal ganglia, which provides input to Sp5C. Comparing the expression pattern of polySia in rats and mice showed mostly common patterns of labelling although areas such as the spinal cord dorsal horn differed between species. Moreover, comparison of the pattern of polySia immunolabelling using the two most common antibodies, mAb 735 and mAb 5324, demonstrated similar patterns of expression.

Next, in order to understand the function of polySia in the spinal cord and the biological processes it regulates, binding partners of polySia in the dorsal horn were investigated using co-immunoprecipitation (IP) followed by label-free liquid chromatography tandem mass spectrometry. Thirteen potential protein partners were identified, with more than half associated with signalling. Five proteins (receptor expression-enhancing protein 5, guanine nucleotide-binding protein G(o) subunit alpha, sodium/potassium-transporting ATPase subunits alpha-2 and alpha-3, and clathrin heavy chain) were further validated using co-IP/reverse co-IP followed by western blotting and confocal microscopy. The interaction with validated candidates was also demonstrated in the Sp5C and IML of adult rats as well as in the dorsal horn of adult mice, indicating that the interactions were neither region nor species specific.

Recently our laboratory found that polySia is required for the normal transmission of information through the nucleus of solitary tract (NTS). Information from the NTS is conveyed to the rostral ventrolateral medulla (RVLM), which generates vasomotor tone and integrates a range of cardiorespiratory reflexes. We used a viral vector that drives the expression of polysialyltransferase ST8SiaIV in the RVLM where polySia expression is normally low. We determined the consequences of increasing polySia expression in basal cardiorespiratory and reflex function. Induced expression of polySia was demonstrated but did not change baseline cardiorespiratory function or alter four reflexes tested (Bezold-Jarisch reflex, responses to hypercapnia, hypoxia, and acute intermittent hypoxia). The lower plateau of sympathetic baroreceptor reflex curve was elevated, possibly due to increased non-barosensitive sympathetic activity; however, total activity was unchanged. Due to substantial variability it remains unclear whether polySia did not alter neurotransmission in the RVLM or its expression, particularly in cardiorespiratory neurons was not enough to alter its function.

These data greatly expand the lists of polySia positive regions and potential binding partners in the brainstem and spinal cord that will help in delineating the function and mechanisms of action, particularly with respect to signalling, of polySia in these regions.

Declaration of originality

I acknowledge that the work conducted in this thesis entitled “Distribution, interacting partners, and function of polysialic acid in the brainstem and spinal cord of adult rodents” has not been submitted for a degree nor has it been submitted as part of the requirements for a degree to any other university or institution other than Macquarie University. I declare that the contents of this thesis represent the original experimentation and written work of the candidate expect where due reference is stated. Any contribution made to the research by others is explicitly acknowledged (see Declaration of contribution).

All work in this thesis was conducted in the Faculty of Medicine and Health Sciences. All research in this thesis was conducted with the consent of Macquarie University Ethics Committees (Animal Research Authority: 2014/041, 2015/040, and 2015/041).

Shila Shahbazian

Declaration of contribution

Chapter 2: The candidate was the major contributor to this work. Experiments were designed by the candidate and A/Prof. Ann K Goodchild. The candidate performed all experiments except for the electron microscopy, performed by Miss Britt Berning.

Chapter 3: The candidate was the major contributor to this work. Experiments were designed by the candidate and A/Prof. Ann K Goodchild. Prof. Nicolle H Packer and Dr. Albert Lee provided essential intellectual contribution for the development of this chapter. All experiments as well as data collection and analysis were performed by the candidate.

Chapter 4: The candidate was the major contributor to this work. Experiments were designed by the candidate and A/Prof. Ann K Goodchild. Vector injections were performed by Dr. Anita Turner. Electrophysiological experiments were performed in collaboration with Dr. Anita Turner. The candidate performed all histological processing, imaging, and analyses. Electrophysiological analyses were performed in collaboration with Dr. Anita Turner and A/Prof. Ann K Goodchild. The plasmid (pRRL_Syn_PST-GFP_Syn-mCherry) was kindly made and provided by Dr. Xuenong Bo (UCL, UK).

Dr. Martina Mühlenhoff and Prof. Rita Gerardy-Schahn (Hannover Medical School, Germany) provided endo-N-acetylneuraminidase (endoN and endoNF) and monoclonal antibody 735 directed against polySia (mAb 735) used throughout this thesis.

Publications arising during candidature

BOKINIEC, P., **SHAHBAZIAN, S.**, MCDOUGALL, S. J., BERNING, B. A., CHENG, D., LLEWELLYN-SMITH, I. J., BURKE, P. G., MCMULLAN, S., MÜHLENHOFF, M., HILDEBRANDT, H., BRAET, F., CONNOR, M., PACKER, N. H. & GOODCHILD, A. K. 2017. Polysialic acid regulates sympathetic outflow by facilitating information transfer within the nucleus of the solitary tract. *Journal of Neuroscience*, 0200-17.

In preparation

SHAHBAZIAN, S., BOKINIEC, P., MÜHLENHOFF, M., PACKER, N. H. & GOODCHILD, A. K. Polysialic acid distribution within the spinal cord, brainstem, and trigeminal ganglion

SHAHBAZIAN, S., LEE, A., BOKINIEC, P., MÜHLENHOFF, M., PACKER, N. H. & GOODCHILD, A. K. Identification of polysialic acid interacting partners in the dorsal horn of rat and mouse and the trigeminal nucleus of rat

SHAHBAZIAN, S., BOKINIEC, P., MÜHLENHOFF, M., PACKER, N. H. & GOODCHILD, A. K. Viral vector induced expression of polysialic acid in the RVLM: expression pattern and cardiorespiratory effects

Communications

SHAHBAZIAN, S., LEE, A., EVEREST-DASS, A., BOKINIEC, P., PACKER, N. & GOODCHILD, A. 2016. Location and Partners of Polysialic Acid in the Dorsal Horn and Trigeminal Nucleus of Adult Rat. *The FASEB Journal*, 30, 1096.1-1096.1.

BOKINIEC, P., **SHAHBAZIAN, S.**, MCMULLAN, S., PACKER, N. H. & GOODCHILD, A. K. 2015. Polysialic acid controls neuronal activity in the nucleus of the solitary tract (NTS), influencing the tonic and reflex control of blood pressure. Central Cardiovascular and Respiratory Control: Future Directions. Poster Presentation.

BOKINIEC, P., **SHAHBAZIAN, S.**, MCMULLAN, S., PACKER, N. H. & GOODCHILD, A. K. 2015. Polysialic acid controls neuronal activity in the nucleus of the solitary tract influencing the tonic and reflex control of blood pressure. International Society for Autonomic Neuroscience (ISAN) in conjunction with the American Autonomic Society (AAS), Federation of European

Autonomic Societies (EFAS), and Japanese Society for Neurovegetative Research (JNSR). Oral Presentation.

BOKINIEC, P., **SHAHBAZIAN, S.**, MCMULLAN, S., PACKER, N. H. & GOODCHILD, A. K. 2015. Polysialic acid controls neuronal activity in the nucleus of the solitary tract (NTS), influencing the tonic and reflex control of blood pressure. The 25th ISN-APSN Join Biennial Meeting in conjunction with the Australian Society for Neuroscience (ANS). Poster Presentation.

BOKINIEC, P., EVEREST-DASS, A., **SHAHBAZIAN, S.**, GOODCHILD, A. K. & PACKER, N. H. K. 2014. Polysialic acid controls neuronal activity in the nucleus of the solitary tract (NTS), influencing the tonic and reflex control of blood pressure. The 25th ISN-APSN Join Biennial Meeting in conjunction with the Australian Society for Neuroscience (ANS). Poster Presentation.

SHAHBAZIAN, S., BOKINIEC, P., EVEREST-DASS, A., PACKER, N., GOODCHILD, A. 2014. Location and partners of PSA-NCAM in the brainstem and spinal cord of adult rat. The 2nd Proteomics & Beyond symposium. Poster Presentation

SHAHBAZIAN, S., BOKINIEC, P., EVEREST-DASS, A., PACKER, N., GOODCHILD, A. 2014. Location and partners of PSA-NCAM in the brainstem and spinal cord of adult rat. Sialoglyco 2014. Poster Presentation

Awards arising during candidature

Macquarie University Postgraduate Research Fund 2015.

Student Poster Certificate of Merit. Sialoglyco 2014.

Acknowledgments

I would like to acknowledge and thank my supervisor, A/Prof. Ann K Goodchild, for her tremendous guidance, knowledge, and insightful mentorship. She guided me through the whole journey with her inspiration and support.

In addition, I would like to take the opportunity to appreciate my associate supervisor, Prof. Nicolle H Packer, for her continuous help, guidance, and expertise.

I am grateful to Dr. Albert Lee and Dr. Simon McMullan for their great support and feedback, which contributed towards improving this thesis.

I would like to thank Dr. Anita Turner, Ms. Katherine Robinson, Dr. Ardeshir Amirkhani, and Dr. Sheng Le for their help.

My thanks also go to my friends: Parisa, Mahdieh, Mojdeh, and Daniel for helping me print this thesis.

I would like to dedicate my dissertation to my loving family. None of this would have been possible without you; my parents, whose words of encouragement and unconditional love kept me focused and motivated; my sister and brother, who never left my side and never ceased to love me.

List of figures

List of tables

Abbreviations

ACN	Acetonitrile
AIH	Acute intermittent hypoxia
AMPA	α-amino-3-hydroxy-5-methyl-4-isoxazole propionate
AP	Arterial blood pressure
ATP1A2	Sodium/potassium-transporting ATPase subunit alpha-2
ATP1A3	Sodium/potassium-transporting ATPase subunit alpha-3
BDNF	Brain-derived neurotrophic factor
CCL21	Chemokine (C-C motif) ligand 21
CCR7	C–C chemokine receptor type 7
CGRP	Calcitonin gene-related peptide
ChAT	Anti-Choline Acetyltransferase
CLTC	Clathrin heavy chain
CMP	Cytidine 5’-monophosphate
CNS	Central nervous system
CVLM	Caudal ventrolateral medulla
DA	Dopamine
DC	Dendritic cell
DH	Dorsal horn
DiSia	Disialic acid
DP	Degree of polymerization
DVC	Dorsal vagal complex
EAAT2	Excitatory amino acid transporter 2
endoN	Endo-N-acetylneuraminidase
ESL-1	E-selectin ligand-1
FGF2	Fibroblast growth factor-2
GAD	Glutamic acid decarboxylase
GFAP	Glial fibrillary acidic protein
GNOA1	Guanine nucleotide-binding protein G(o) subunit alpha
GPCR	G protein-coupled receptor
GPI	Glycosylphosphatidylinositol
GS	Glutamine Synthetase
HR	Heart rate
HSPG	Heparan sulphate proteoglycan
Ig	Immunoglobulin
IML	Intermediolateral cell column
IP	Immunoprecipitation
ir	Immunoreactivity
kDa	kilodalton
KDN	2-keto-3-deoxy-nonulosonic acid

LPS	Lipopolysaccharide
LTD	Long-term depression
LTP	Long-term potentiation
LV/GFP	Lentiviral vector encoding GFP
LV/PST	Lentiviral vector containing PST cDNAs
mAb 5324	Monoclonal antibody 5324 directed against oligo/polySia
mAb 735	Monoclonal antibody 735 directed against polySia
MAP	Mean arterial pressure
MARCKS	Myristoylated alanine-rich C kinase substrate
MBP	Myelin basic protein
NCAM	Neural cell adhesion molecule
NEU	Neuraminidase
Neu5Ac	N-acetylneuraminic acid
Neu5Gc	N-glycolylneuraminic acid
NeuN	Neuronal nuclear antigen
NMDA	NR2B subunit-containing N-methyl-D-aspartate
NRP-2	Neuropilin-2
NTS	Nucleus of the solitary tract
OligoSia	Oligosialic acid
PBG	Phenylbiguanide
PE	Phenylephrine
PNA	Phrenic nerve activity
PNamp	Phrenic nerve amplitude
PNf	Phrenic nerve frequency
PolySia	Polysialic acid
PolyST	Polysialyltransferase
PST	Polysialyltransferase ST8SiaIV
REEP5	Receptor expression-enhancing protein 5
RVLM	Rostral ventrolateral medulla
SGC	Satellite glial cell
Sia	Sialic acid
SNA	Sympathetic nerve activity
SNP	Sodium nitroprusside
Sp5C	Spinal trigeminal nucleus caudalis
SPN	Sympathetic preganglionic neuron
SSTR2A	Somatostatin Receptor 2A
Syn	Synapsin
SynCAM 1	Synaptic cell adhesion molecule 1
TBST	Tris-buffered saline containing Tween-20
TG	Trigeminal ganglion
TPBS	Tris-phosphate buffered saline

TUBB5	Tubulin beta-5 chain

Chapter 1 : Introduction

1.1. Glycans

Every living cell has a dense and complex coat of an array of sugars (carbohydrate; glycan). Cell surface sugars appear to be as crucial for life as having DNA, RNAs, the vast collection of proteins, and lipid-based membranes that regulate cellular activity (Varki, 2011). In the 1960s and 1970s, during the initial phase of the molecular biology revolution, the understanding and investigation of glycans was far behind comparable studies of three other building blocks of life (DNA, RNAs, and proteins). This slow progress was due largely to the structural complexity of glycans and the resultant difficulty in identifying their sequences, due largely to the fact that sugar biosynthesis is not template-driven (see below). In the 1980s, development of new technologies specialized for the structural and functional examination of glycans led to a much greater understanding of the cellular and molecular biology of glycans. The term glycobiology was coined in the late 80s to recognize the joining together of the traditional disciplines of carbohydrate chemistry and biochemistry with a modern understanding of the cell and molecular biology of glycans (Varki and Sharon, 2009).

Glycans are made from any form of mono-, oligo-, or poly-saccharide, either free or covalently bound to another molecule. Monosaccharides are linked together in either linear or branched forms using glycosidic linkages to form glycans (Varki and Sharon, 2009). Glycosylation refers to the enzymatic process that produces glycosidic linkages of saccharides to other saccharides, proteins or lipids (Pinho and Reis, 2015). In eukaryotes, glycans are mainly present as glycoconjugates, molecules composed of glycans covalently attached to a non-carbohydrate moiety (Figure 1.1) (Varki and Sharon 2009, Hart and Copeland 2010, Taylor and Drickamer 2011). Glycoconjugates are usually found as membrane-bound (for instance, in the glycocalyx) or secreted molecules and can become integral parts of the extracellular matrix (Fuster and Esko, 2005). The main classes of glycoconjugates are proteoglycans, glycolipids, and glycoproteins (Schnaar et al., 2014).

Proteoglycans are macromolecules consisting of a protein core with one or more covalently attached glycosaminoglycan chain(s) (Kjellén and Lindahl, 1991). The glycosaminoglycans (Figure 1.1) are linear glycans present as free polysaccharides (such as hyaluronic acid) or as part of proteoglycans (such as heparan sulphate and chondroitin sulphate) (Fuster and Esko, 2005).

Glycolipids come in several forms. Glycosphingolipids (Figure 1.1) are one form consisting of a glycan attached to ceramide that is composed of sphingosine and a fatty acid. Glycosphingolipids are present in the cell membranes of organisms ranging from bacteria to humans (Schnaar et al.,

2009). Conventionally, all sialylated glycosphingolipids are known as gangliosides that are found at the highest concentration in the grey matter of the brain (Rapport, 1981, Schnaar et al., 2009). Glycosylphosphatidylinositols (GPIs) are glycolipids covalently bound to the carboxyl terminus of proteins and act as membrane anchors (Schnaar et al., 2009).

Glycoproteins, one of which is the focus in this thesis, are a class of glycoconjugates in which one or more glycans are covalently attached to polypeptide side-chains of a protein carrier (Varki and Sharon, 2009). Glycoproteins have a broad phylogenetic distribution ranging from eubacteria and archaea to eukaryotes (Kornfeld and Kornfeld, 1980, Spiro, 2002). Eukaryotic protein glycosylation usually occurs via N or O linkages (Guzman-Aranguez and Argüeso, 2010). An N-glycan is formed when a sugar chain covalently binds to an asparagine residue of a polypeptide chain followed by any amino acid (except proline) ending with serine or threonine (Figure 1.1) (Varki and Sharon, 2009, Aebi et al., 2010). An O-glycan is mainly linked to the polypeptide via N-acetylgalactosamine to a hydroxyl group of a serine or threonine amino acid residue (Figure 1.1) (Varki and Sharon, 2009, Strous and Dekker, 1992) and predominates on secreted and membrane bound mucins (Pinho and Reis, 2015). Currently, 13 different monosaccharides and 8 amino acids have been found to be involved in glycoprotein linkages resulting in at least 41 linkages (Spiro, 2002). Glycans bound to proteins can have extremely complex structures which together with

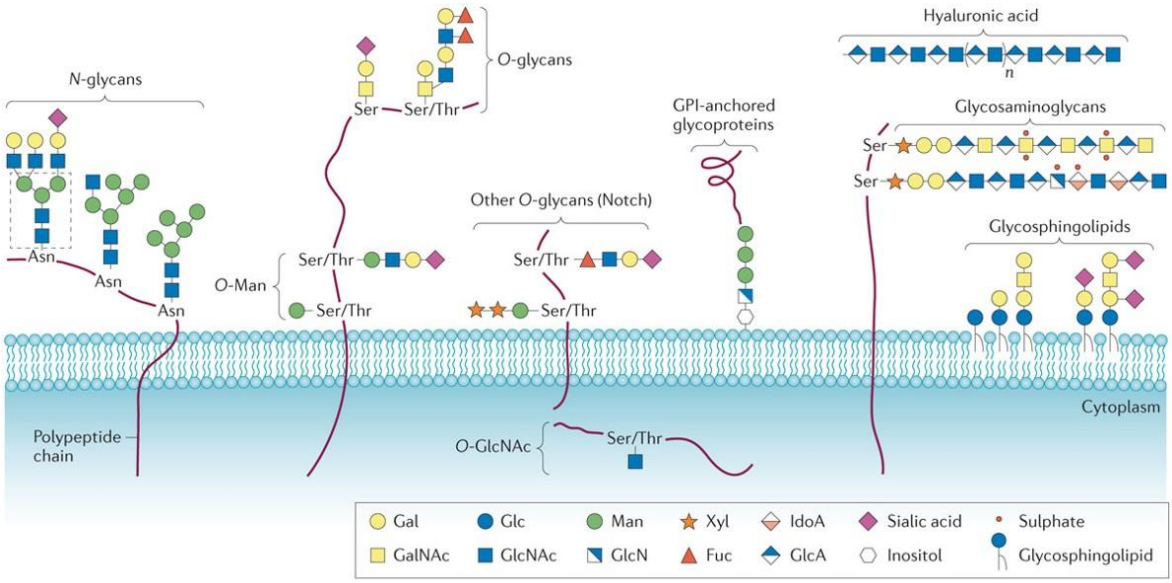

Figure 1.1. Schematic representation of major classes of glycoconjugates in vertebrate cells. Asn, asparagine; Fuc, fucose; Gal, galactose; GalNAc, N-acetylgalactosamine; Glc, glucose; GlcA, glucuronic acid; GlcN, glucosamine; GlcNAc, N-acetylglucosamine; GPI, Glycosylphosphatidylinositols; IdoA, l-iduronic acid; Man, mannose; Ser, serine; Thr, threonine; Xyl, xylose. From (Pinho and Reis, 2015)

various glycosidic linkages means that there is much more structural diversity than that found for linear nucleic acid or polypeptide structures (Moremen et al., 2012).

Until the second half of 20th century, glycans were mainly regarded as an energy source or as structural components and were assumed not to have other biological activities (Varki and Sharon, 2009). However, it is now recognized that glycans are involved in a diverse range of functions such as protein quality control (Moremen and Molinari, 2006), adhesion, motility (Brown et al., 2007, Todeschini and Hakomori, 2008, Paszek et al., 2014), cell signalling (Yen et al., 2015, Fernandez-Valdivia et al., 2011, Coskun et al., 2011), endocytosis (Weigel and Yik, 2002, Christianson and Belting, 2014), and the response to immunity (Marth and Grewal, 2008, Garner et al., 2015, Park et al., 2016a).

Protein glycosylation is the most common and most complex posttranslational modification with more than 50% of human proteins estimated to be glycosylated, most of which contain N-glycan structures (Apweiler et al., 1999, Wong, 2005). Glycosylation changes physiochemical and biological properties of the underlying protein. Glycans can alter solubility, electrical charge, mass, size, and viscosity of their carrier proteins in solution. Glycans can control folding and stabilize conformation (three dimensional folding) of their bearing proteins and they can also confer proteins' thermal stability and protect them against proteolysis. Biological actions of glycans on their carrier proteins include, but are not limited to, mediating intracellular traffic and localization of glycoproteins, changing the lifetime of glycoproteins, modifying immunological properties, regulating the activity of enzymes and hormones, acting as cell surface receptors for molecules such as lectins, antibodies and toxins, and participating in cell-cell interactions (Lis and Sharon, 1993, Varki, 1993, Varki, 2017). Changes in glycosylation states in the central nervous system (CNS) is commonly associated with disease states (for review see (Abou-Abbass et al., 2016)). For example, the glycosylation status of acetylcholinesterase is shown to be altered in brain and cerebrospinal fluid of patients with Creutzfeldt–Jakob disease (Silveyra et al., 2006) and Alzheimer's disease (Sáez-Valero et al., 1999, Sáez-Valero et al., 2000). The glycome of amyotrophic lateral sclerosis patients' sera was found to have high levels of sialylated glycans versus low levels of core fucosylated glycans compared to that of healthy volunteers (Edri-Brami et al., 2012). In addition, manipulating the level of some glycans have been implicated in alleviating some brain diseases (for review see (Abou-Abbass et al., 2016)). For instance, increasing O-linked β-N-acetylglucosamine (O-GlcNAc) has been reported to slow neurodegeneration and stabilize tau,

an important protein in Alzheimer's disease, protecting against aggregation (Borghgraef et al., 2013, Yuzwa et al., 2012).

The functional specificity of glycans is often dominated by sugars at the outermost ends of glycan chains. In mammals, a large number of glycans on cell surface glycoproteins or glycolipids are terminated with sialic acids (Schnaar et al., 2014).

1.2. Sialic acid

Sialic acid (Sia) is a derivative of nine carbon neuraminic acid with a carboxylic acid, a glycerol side chain, and an N-acyl group (Figure 1.2A) and is usually found terminating N-glycans, O-glycans, glycosphingolipids and occasionally capping side chains of GPI anchors (Figure 1.2B) (Varki and Schauer, 2009). Sias are added enzymatically to the terminal non-reducing positions of glycan chains via the C-2 carbon of the Sia, mainly in one of five linkages: α2,3- or α2,6-linked to galactose, α2,6-linked to N-acetylgalactosamine or N-acetylglucosamine, or α2,8-linked to another sialic acid (Harduin-Lepers et al., 2005).

Sias typically exist in N-acetylneuraminic acid (Neu5Ac), N-glycolylneuraminic acid (Neu5Gc), or 2-keto-3-deoxy-nonulosonic acid (KDN) forms (Figure 1.2.A) (Schnaar et al., 2014, Varki and Schauer, 2009). Most vertebrate tissues (except for those of healthy humans which do not express Neu5Gc) express large amounts of Neu5Gc as well as Neu5Ac. However, in the brains of non-human animals the level of Neu5Gc is always very low or absent, regardless of its level in other organs of the body (Chou et al., 2002, Varki, 2007). Sias show a great diversity with more than 50 structurally distinct types of Sia so far described (Angata and Varki, 2002). This diversity is not only due to the different Sia backbone components, but also derives from the different α-glycosidic linkages between carbon 2 of Sias, their underlying sugars as well as from Sia modifications such as O-lactylation, O-acetylation, and O-sulphation (Varki and Schauer, 2009). Sias are found predominantly in animals of the deuterostome lineage (vertebrates and some higher invertebrates), from echinoderms (sea urchins and starfish) to the great apes (Schauer, 2000, Varki and Schauer, 2009). In other lineages including bacteria, archaea, fungi, protozoa, and protostomes, Sia expression is seen in only a small minority of species (Vimr et al., 2004, Varki and Schauer, 2009). Compared to other sugars, Sias are distinct as they can bind covalently together to form disialic

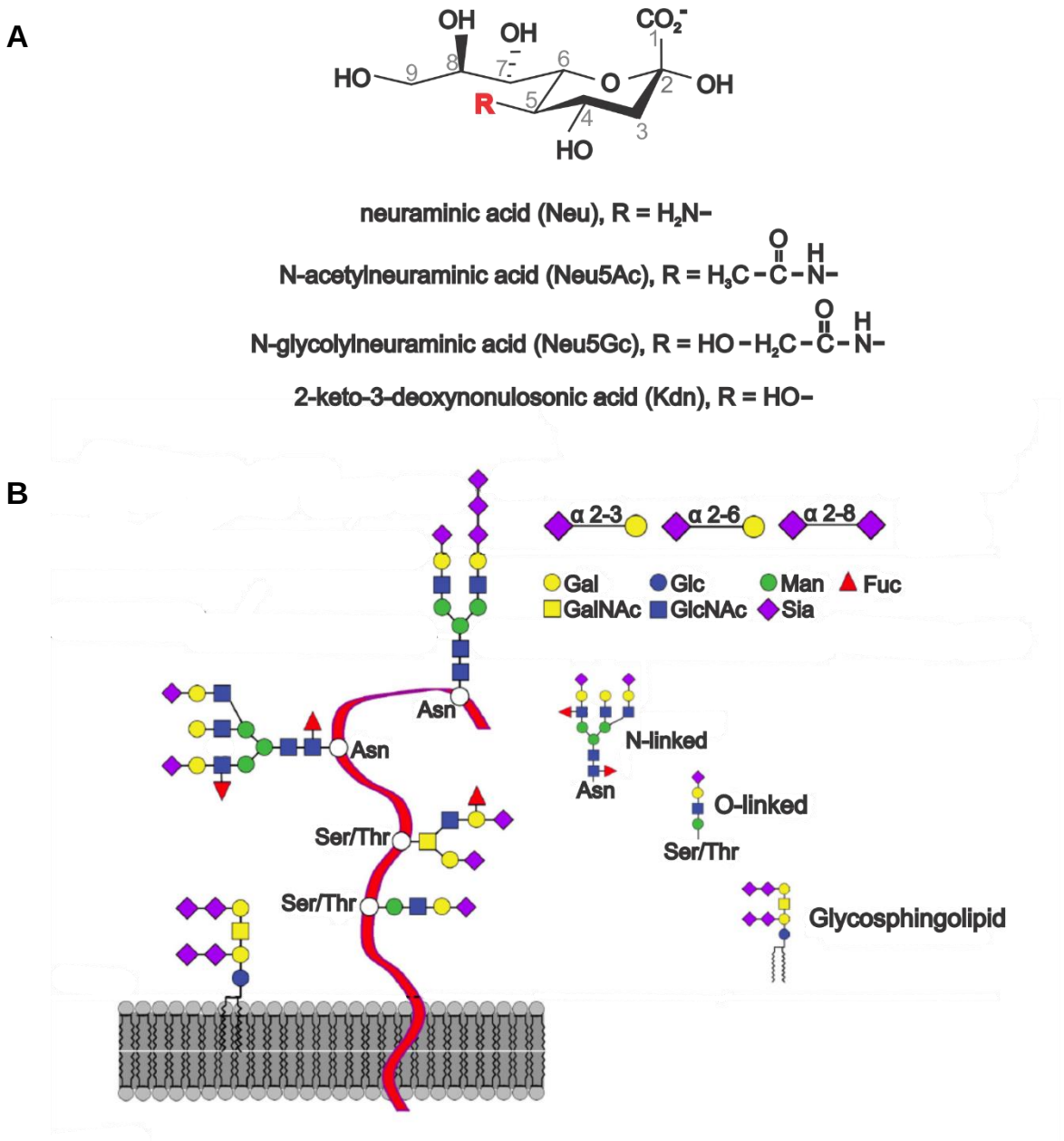

Figure 1.2. Sialic acids and schematic representation of sialoglycans. (A) Major sialic acid (Sia) backbones in mammals. Sias of animals are based on neuraminic acid (Neu), which is most often found in its N-acetyl (Neu5Ac), N-glycolyl (Neu5Gc), or on 2-keto-3-deoxy-nonulosonic acid (Kdn) forms. (B) Schematic representation of sialoglycans demonstrating the identity and arrangement of Sia underlying sugars, main linkages of Sia to its underlying sugars, and its glycan classes. Asn, asparagine; Fuc, fucose; Gal, galactose; GalNAc, N-acetylgalactosamine; Glc, glucose; GlcNAc, N-acetylglucosamine; Man, mannose; Sia, sialic acid; Ser, serine; Thr, threonine. Adapted from (Schnaar et al., 2014).

acid (diSia), oligosialic acid (oligoSia), and polysialic acid (polySia) structures, varying according to their degree of polymerization (DP) and conformation of their structures (Sato and Kitajima 2013). DiSias (DP=2) are present in both glycolipids (Merat and Dickerson, 1973) and

glycoproteins (Finne et al., 1977a). DiSia structures are abundant on brain glycolipids accounting for 16.6% of the total Sia in gangliosides of adult rat brain (Finne et al., 1977b). A large number of glycoproteins in mammals are also modified with diSia and oligoSia (DP=3-7) (Sato et al., 2000, Sato and Kitajima, 2013a, Inoko et al., 2010). Using a method based on the quantitation of the amount of 8-O-substituted neuraminic acid by methylation analysis and mass fragmentographic detection with two different m/e values, Finne et al. (1977) found that glycoproteins of brain, liver, diaphragmatic muscle, and small intestinal mucosa contain diSia (with the brain having the highest concentration, 8.5% diSia in 100% total glycopeptide bound Sia), whereas those of kidney, gastric mucosa, erythrocytes and plasma proteins were devoid of diSia. Within the rat brain, cerebral glycopeptides show a slightly higher concentration of diSia (8.8%) compared to cerebellar (7.5%) and brainstem glycopeptides (6.8%) (Finne et al., 1977b). The presence of diSia and oligoSia has also been reported in adult mouse brain by immunoprecipitation using an anti-neural cell adhesion molecule (NCAM) antibody followed by Fluorometric C7/C9 analysis. Although some oligoSia were detected on NCAM, most oligoSia residues were found located on glycoproteins other than NCAM (Sato et al., 2000). PolySia is the glycan of focus in this thesis and will be comprehensively discussed in Section 1.4 below.

Due to its external position on glycoproteins and gangliosides, located predominantly on the cells outer membrane, Sia can regulate key processes in cells and tissues through three main broad mechanisms: altering general physical and chemical characteristics, masking of biological recognition sites and direct recognition (Tiralongo, 2013). Sias have a relatively strong anionic charge which contributes to the glycoprotein secondary and tertiary structures and also to the hydration of glycoproteins (such as mucins) at the cell surface. The negative charge in combination with a bulky, hydrophilic molecule enables Sia to mask recognition sites on its underlying glycoproteins and thus prevents them from interacting with enzymes and protein receptors on other cells, regulating intracellular communication (for review see (Schauer, 1985)). On the contrary, Sias can allow recognition by a receptor protein (a lectin) and therefore act as a ligand or counter-receptor for complementary Sia binding proteins (for review see (Kelm and Schauer, 1997)).

1.3. Major brain glycoconjugates and sialoglycans

Glycoconjugates in the CNS are dominated by glycolipids, constituting more than 80% of glycoconjugates in the brain (Figure 1.3). More than half of the brain's conjugate saccharides, accounting for 1.9% of the brain's total fresh weight, are two major myelin glycolipids: galactosylceramide and its 3-O-sulphated form sulphatide (Schnaar, 2005, Norton and Poduslo, 1973). The second main class of glycolipids are gangliosides, which are enriched on neurons and carry about 25% of the glycoconjugates in the brain (Schnaar, 2005, Tettamanti et al., 1973). Although numerous ganglioside structures have been identified in different tissues and organisms, adult mammalian brain gangliosides are dominated by just four closely related structures (GM1, GD1a, GD1b, and GT1b) that altogether account for 94-97% of gangliosides in the adult human brain and 92% in the adult rat brain (Tettamanti et al., 1973, Svennerholm and Fredman, 1980). Glycoproteins carry less than 20% of the brain's total conjugate saccharides, and the majority of these glycoproteins are N-linked oligosaccharides. The remaining 2% of brain's glycoconjugates are proteoglycans (Margolis et al., 1976, Schnaar, 2005).

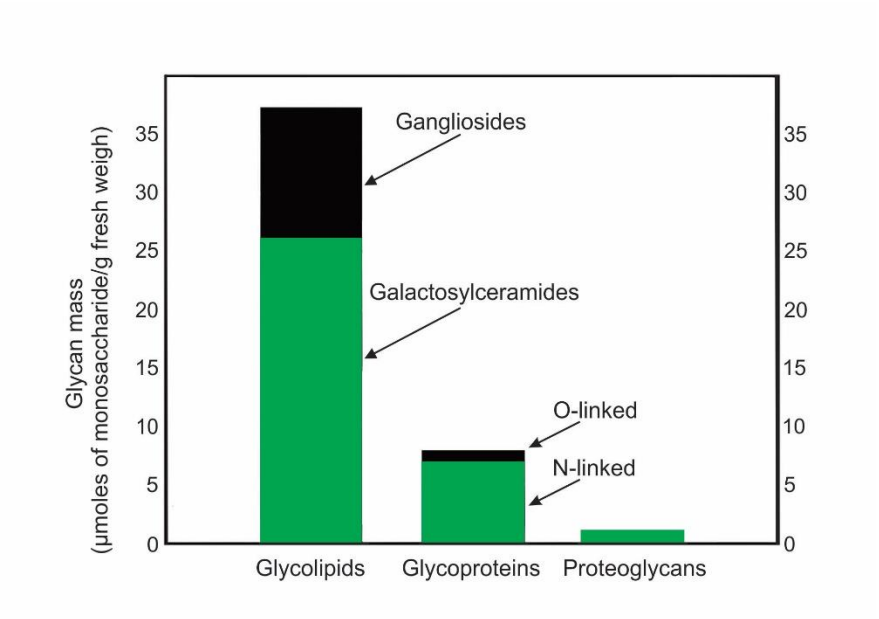

Figure 1.3. Glycan mass in the adult rat brain. The mass of principal monosaccharides (μmol/g fresh brain wt) for each glycan class and subclass were calculated. 1- Galactosylceramide and sulphatide together account for 19.4 mg/g brain fresh wt, with galactosylceramide constituting 76% (by weight). Galactosylceramide represents about 20.3 μmol galactosylceramide and 5.8 μmol sulphatide/g fresh wt. 2- Ganglioside represent 11.2 μmol monosaccharide/g fresh wt. 3-Glycoproteins represent about 7.8 μmol monosaccharide/g fresh wt, of which, O-linked glycoproteins represent 0.88 μmol/g fresh wt. 4- Proteoglycans represent 0.89 μmol/g fresh wt. Adapted from (Schnaar, 2005).

Sias in many tissues are most abundant on N-and O-linked glycoproteins, whereas in the vertebrate brain gangliosides are the primary carriers of Sia containing about 75% of the brain's Sia (Schnaar et al., 2014, Schnaar, 2004). However, still a large number of brain glycoproteins are sialylated. Large-scale proteomic profiling in the adult mouse brain identified at least 140 sialylated glycoproteins including a large number of synapse-associated proteins (Xie et al., 2016). A major protein-bound sialoglycan in the brain which is of specific interest here is polysialic acid (Schnaar et al., 2014).

1.4. Polysialic acid

1.4.1. Chemistry

Polysialic acid (polySia) is a long linear homopolymer of Sias with a DP of 8 or higher (Figure 1.4). Polymerized Sias show structural diversity that originates from differences in the Sia backbone components (Neu5Ac, Neu5Gc, or KDN), modifications (acetylation, sulphation, methylation, lactylation and lactonization), the type of intersialyl linkage (α2,5Oglycolyl, α2,8, α2,9 and α2,8/9), and the DP, which varies from 8 to 400 (Sato and Kitajima, 2013a).

PolySia was originally identified as a polysaccharide in gram-negative bacteria (*Escherichia coli* K235) and was named colominic acid (Barry and Goebel, 1957). The structure of this bacterial polySia was reported as α2,8-linked polyNeu5Ac with a DP greater than 200. PolySia has also been found in capsular polysaccharides of some other gram negative bacteria including *Neisseria meningitides* serogroups B and C (α2,8- and α2,9-linked polyNeu5Ac, respectively), *Mannheimia haemolytica* A2 and *Moraxella nonliquefaciens* (α2,8-polyNeu5Ac), and *Escherichia coli* K92 (α2,8- and α2,9-linkages) (Willis and Whitfield, 2013, Bhattacharjee et al., 1975). In addition to some bacterial strains, polySia is expressed in Echinoderm such as sea urchin egg jelly (α2,5Oglycolyl-linked Neu5Gc) and salmonid fish egg (Inoue and Iwasaki, 1978, Kitazume et al., 1994).

In mammals, polySia was originally identified by Finne in the developing brain in 1982 (Finne, 1982). In vertebrates, the term polySia describes α2,8-linked Sia chains with a DP reaching 90 Sia residues or higher (Figure 1.4) (Schnaar et al., 2014, Sato and Kitajima, 2013a, Galuska et al., 2008).

1.4.1.1. Biosynthesis of mammalian polySia

In mammals, polySia is produced in the Golgi formation by polysialyltransferases (polySTs) ST8SiaII and ST8SiaIV (formerly named STX and PST, respectively) (Eckhardt et al., 1995, Kojima et al., 1995, Livingston and Paulson, 1993, Nakayama et al., 1995, Scheidegger et al., 1995). These two enzymes, which are type II transmembrane glycoproteins, mainly reside in the trans-Golgi compartment and share about 60% similarity at the amino acid sequence level in mice (Harduin-Lepers et al., 2001, Harduin-Lepers et al., 2005, Scheidegger et al., 1995). Using cytidine 5'-monophosphate (CMP)-activated sialic acid as a donor (Sellmeier et al., 2015), ST8SiaII and ST8SiaIV synthesize polySia by the addition of chains of α2,8-linked Sia to α2,3- or α2,6-sialylated complex type at the termini of both acceptor N- and O-linked glycans (Mühlenhoff et al., 1996b,

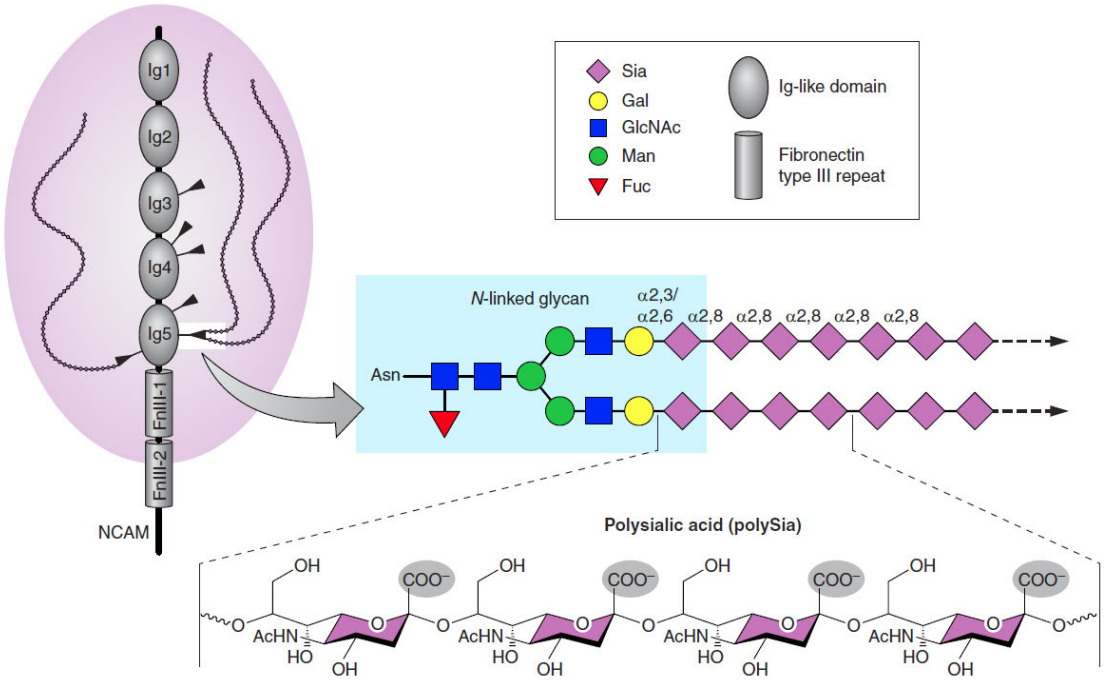

Figure 1.4. Schematic representation of polysialic acid (polySia) and polysialylated NCAM. The extracellular domain of NCAM consists of five IgG-like domains (Ig1 to Ig5) and two fibronectin type III repeats (FnIII-1 and FnIII-2). NCAM has six N-glycosylation sites (showed by black arrowheads on Ig3, Ig4, and Ig5), of which only two sites in the 5th IgG like domain can be polysialylated by the addition of a homopolymer of α2,8-linked sialic acid (Sia) residues to an acceptor N-glycan terminating with Sia in α2,3 or α2,6 linkages. On NCAM, polySia chains form polyanions (negatively charged carboxylate groups are highlighted with grey spheres) with a large hydrophilic capacity. The large hydration shell (has been shown with a pink sphere surrounding polySia-NCAM) formed by polySia on its carrier molecules including NCAM significantly increases the volume of its carrier molecule and therefore decreases its binding abilities. Asn, asparagine; Fuc, fucose; Gal, galactose; GlcNAc, N-acetylglucosamine; Man, mannose. From (Schnaar et al., 2014).

Kojima et al., 1996, Sato and Kitajima, 2013a, Liedtke et al., 2001). Remarkably, both polySTs display substrate preferences. For instance, whereas NCAM can be polysialylated by both ST8SiaII and ST8SiaIV, neuropilin-2 is exclusively polysialylated by ST8SiaIV, and the synaptic cell adhesion molecule 1 is exclusively polysialylated by ST8SiaII, at least in the cell types evaluated so far (Galuska et al., 2010, Rollenhagen et al., 2012, Rollenhagen et al., 2013).

In mice, the expression of both polyST mRNAs is first detected at embryonic day 8 as evaluated using in situ hybridization (Ong et al., 1998). Prenatally and immediately after birth, the level of ST8SiaII mRNA is significantly higher than that of ST8SiaIV. Consistent with the reduced polySia expression from postnatal to adult life, ST8SiaII mRNA level reduces significantly between postnatal days 5–11, while ST8SiaIV transcript level only gradually declines, reaching a 5-fold higher transcript level than ST8SiaII at postnatal day 21 and this level persists in the adult brain. In keeping, the abundant expression of ST8SiaII protein in the neonatal mouse brain shifts to a predominant expression of ST8SiaIV in adult brain (Ong et al., 1998, Hildebrandt et al., 1998, Oltmann-Norden et al., 2008). In humans, similar to rodents, there is an age-dependent decrease of ST8SiaII expression from birth to adulthood in the dorsolateral prefrontal cortex, as shown by microarray and qPCR data. From neonate and infant groups (up to the age of one year) to the age group of toddlers and children (up to 13 years of age), mRNA levels decreased by almost 50%. Like rodents, this marked decline was followed by a gradual decrease from teenagers to adults, who finally retain only 8% of the neonatal level (McAuley et al., 2012, Schnaar et al., 2014).

The expression of the polySTs is independently regulated at the transcriptional level in a tissue-specific fashion, with an overlapping expression pattern (Angata et al., 1997, Hildebrandt et al., 1998, Ong et al., 1998). For instance, in the adult human brain, Nakayama et al. (1995) found ST8SiaIV transcripts mainly in thalamus, subthalamic nucleus, substantia nigra, and cerebral cortex (Nakayama et al., 1995). In another study on the adult brain by Angata et al. (1997), ST8SiaIV transcripts were identified mainly in the amygdala, subthalamic nucleus, cerebral cortex, occipital lobe, and moderately in hippocampus, whereas ST8SiaII transcripts were more prominent in hippocampus, medulla oblongata, and putamen and were moderately present in subthalamic nucleus, cerebral cortex, amygdala, and cerebellum (Angata et al., 1997). The higher expression of ST8SiaII transcripts found in the medulla oblongata by Angata et al. (1997) contradicts the study of Eckhardt et al. (2000), in which western blot analysis revealed a striking reduction in polySia level (almost undetectable) in the medulla oblongata of adult ST8SiaIV knockout mice (Eckhardt

et al., 2000). However, this could be due to the species differences (rat vs mouse) or because there may not be a direct correlation between the level of polyST transcripts and polySia expression. Despite some differences overall, these studies highlight the fact that expression of polySTs varies in different brain regions.

Based on *in vitro* experiments, Angata et al. (2002) suggested that ST8SiaIV was a more efficient enzyme than ST8SiaII, was able to synthesize longer polySia chains on NCAM, and was able to extend chains initiated by ST8SiaII. ST8SiaII, on the other hand, could synthesize shorter polySia chains but could not extend polySia chains generated by ST8SiaIV (Angata et al., 2002). In 2006, *in vivo* analysis performed on mice (postnatal day 1), differing only in the allelic combinations of ST8SiaII and ST8SiaIV, showed that only ~50% of the total NCAM pool was polysialylated in ST8SiaII knockout mice, whereas ST8SiaIV knockout mice showed no differences compared with wild type animals demonstrating almost complete polysialylation of the NCAM pool (Galuska et al., 2006). Both enzymes were able individually to synthesise polySia chains of approximately 90 units in length and a reduction in longer polySia chains was detected in the absence of either enzyme (Galuska et al., 2008). These data demonstrate the dominance of ST8SiaII during development, and confirmed the suggestion by Angata et al. (2002) that the polySTs work synergistically to produce longer polySia chains. However, as mentioned earlier in this section, ST8SiaIV is the main polyST in the adult brain (Ong et al., 1998, Hildebrandt et al., 1998, Oltmann-Norden et al., 2008).

1.4.1.2. Enzymatic degradation of polySia

Sias are removed from sialoglycans via the enzymatic actions of a group of glycoside hydrolase enzymes referred to sialidases/neuraminidases (NEU). Four endogenous sialidases have been identified in mammals, designated as NEU1- NEU4, differing mainly in their substrate specificity, subcellular localization, and tissue distribution (for review see (Giacopuzzi et al., 2012, Miyagi and Yamaguchi, 2012, Monti et al., 2010)).

Although endogenous NEUs remove Sia, whether they have a role in the *in vivo* cleavage of polySia is largely unknown. Some recent evidence suggests that NEU1 and NEU4 may be involved in polySia degradation under physiological conditions (Sumida et al., 2015, Takahashi et al., 2012, Sajo et al., 2016). NEU1 is primarily found in lysosomes, where it catabolizes sialylated glycoconjugates (Seyrantepe et al., 2003, Pshezhetsky and Hinek, 2011). However, after

inflammatory stimuli, such as that induced by T-cell activation or lipopolysaccharide (LPS) activation, part of NEU1 migrated to the plasma membrane (Nan et al., 2007), a location consistent with altering expression of polySia. *In vitro,* endogenous NEU1 was secreted as an exovesicular component and was probably involved in the rapid clearance of polySia after LPS stimulation of Ra2 microglial cells or Neuro2A neuroblastoma cells co-cultured with Ra2 cells, supporting the idea that NEU1 was involved in the polySia degradation (Sumida et al., 2015). In keeping with this, the shedding of polySia was also rescued by chemical suppression of NEU1 using GSC-649, a Sia analogue, or by NEU1 knockdown (Sumida et al., 2015). In addition, the knockdown of NEU1 in newly generated hippocampal granule cells *in vivo* increased the presence of polySia on these cells (Sajo et al., 2016).

Murine sialidase NEU4, primarily expressed in the brain, also degraded polySia in sialidase *in vitro* assays, on NCAM-Fc chimera (the extracellular domain of mouse NCAM fused to the Fc part of human immunoglobulin G), on endogenous NCAM in developing mouse brain as well as in neuroblastoma cells co-transfected with ST8SiaIV gene (Takahashi et al., 2012). Additionally, in mouse embryonic hippocampal primary neurons, the expression of endogenous NEU4 decreased during neuronal differentiation which correlated with a decrease in polySia expression (Takahashi et al., 2012).

However, studies by Sumida et al. (2015) and Takahashi et al. (2012) have been performed *in vitro* using cell culture techniques. Although the study by Sajo et al. (2016) provides some evidence that NEU1 plays a role in polySia degradation *in vivo*, it is still unclear whether NEU1/4 cleaves polySia in a cell type- and tissue-specific manner or whether these NEUs are the only endogenous molecules involved in polySia degradation under physiological conditions *in vivo*.

As the identity of endogenous polySia cleaving enzymes remain mainly unknown, experiments commonly rely on bacterially or bacteriophage derived exo- and endosialidases. Exosialidases (neuraminidase, NEU) are hydrolases that chop off Sia from galactose or galactosamine in α2,3 or α2,6 linkages, or from α2,8-linked to another Sia in a wide range of glycan structures (exo-acting). In contrast, the endosialidase (endo-N-acetylneuraminidase, endoN) is a bacteriophage-borne sialidase which only cleaves α2,8-glycosidically linked Sia (Neu5Ac or Neu5Gc) polymers. EndoN cleaves 5-8 Sia residues at a time (Stummeyer et al., 2005, Jakobsson et al., 2012, Taylor, 1996,

Pelkonen et al., 1989, Sato and Kitajima, 2013a). Due to its substrate specificity towards polySia, endoN is particularly useful as a tool to investigate the functional role of polySia.

1.4.1.3. Carriers of polySia

Mammalian polysialylation is a highly protein specific glycosylation event (for review see (Bhide et al., 2016, Colley, 2010, Colley et al., 2014, Bhide and Colley, 2016)) influencing only a select group of glycoproteins (Table 1.1). The major and best studied carrier of polySia in the vertebrate is NCAM (Mühlenhoff et al., 2013, Schnaar et al., 2014) as brains of NCAM knockout neonatal mice were shown to be almost negative for polySia (Cremer et al., 1994). NCAM, a member of the immunoglobulin (Ig) superfamily of adhesion molecules, was described as a cell surface glycoprotein with cell-cell binding properties about 40 years ago (Rutishauser et al., 1976). A few years later, remarkable differences in the molecular weight of NCAM (~ 200 to 250 kilodalton (kDa) in the embryonic form compared to two distinct bands of 150 and 180 kDa in the adult) and its Sia content were found. After treatment with neuraminidase, these differences were no longer evident (Rothbard et al., 1982). Concurrently the presence of polySia in glycoproteins of developing rat brain was described by Finne et al. (Finne, 1982), and about one year later the occurrence of polySia on NCAM (polySia-NCAM also termed embryonic NCAM) was shown in mice forebrain using gas liquid chromatography (Finne et al., 1983). At least 20–30 different NCAM isoforms can be transcribed from a single copy gene by alternative splicing and post-translational modifications. The three main isoforms of NCAM are NCAM 180, 140, and 120 differing in their molecular mass (hence 180, 140 and 120), intracellular domains (NCAM 180 and 140), and in their means of attachment to the cell membrane (NCAM 120) (Bonfanti and Theodosis, 2009). NCAM 180 and NCAM 120 are expressed mainly in neurons and glia, respectively, while NCAM-140 is expressed in both cell types (Noble et al., 1985, Nybroe et al., 1985, Korshunova and Mosevitsky, 2010). NCAM 120 is almost entirely found in lipid raft fractions, while NCAM 140 and NCAM 180 are both raft- and non-raft-associated (Niethammer et al., 2002, Leshchyns' ka et al., 2003, He and Meiri, 2002). The extracellular domains of these three NCAM isoforms are identical and contain five N-terminal Ig-homology modules followed by two fibronectin type III-like repeats closest to the membrane (Figure 1.4) (Soroka et al., 2010, Nielsen et al., 2010). NCAM also exists in a secreted form generated by co-expression of a small exon called SEC-exon in the mRNA. This small exon contains a stop codon and gives rise to a truncated extracellular part of NCAM with a molecular weight around 115 kD (Gower et al., 1988, Walmod et al., 2004). Soluble

Table 1.1. Known polySia-containing glycoproteins. Occurrence indicates where these glycoproteins were found. N- and/or O- linkage shows whether polysialylation was found on N- or O-linked glycan chains.

Career protein	Occurrence	N- and/or O-linkage	PolySTs involved
NCAM	- Neurons and glia in the CNS - Extraneural tissues during development and in the adult in cells of the immune system, lung, testis, sperm, placenta and liver.	N-linked	ST8SiaII and ST8SiaIV
The voltage- sensitive Na channel α subunits	- Electrophorus electricus electroplax - The rat brain	N-linked (James and Agnew, 1987)	Unknown
SynCAM 1	- Proteoglycan NG2 positive cells in the neonatal mouse brain	O-linked	ST8SiaII
NRP-2	- Human dendritic cells - Macrophages cultured from peritoneal exudate - Stem cell- and brain-derived murine microglia - Cultured human THP-1 macrophages	O-linked	ST8SiaIV
CCR7	- Mature DCs (mouse and human)	N- and O-linked	ST8SiaIV
ESL-1	- Stem cell- and brain-derived murine microglia - Human THP-1 macrophages	Unknown	ST8SiaIV
CD36	- Human and mouse milk	O-linked	Unknown
PolySTs	- COS-1, CHO, or Lec2 CHO cells transfected with ST8SiaII or ST8SiaIV cDNA	N-linked	ST8SiaII and ST8SiaIV

forms of NCAM also exist (Walmod et al., 2004), which arise by the enzymatic excision of NCAM-120 from its GPI anchor (He et al., 1986) or by the proteolytic cleavage of the extracellular part of NCAM (Hinkle et al., 2006). These have been identified in rat brain, cerebrospinal fluid, and plasma and they can be polysialylated (Olsen et al., 1993, Krog et al., 1992, Piras et al., 2015).

NCAM is extensively glycosylated in the ER and Golgi compartments with N-glycosylation being the primary modification (Gascon et al., 2007). NCAM has at least six potential N-linked glycosylation sites (Liedtke et al., 2001, Albach et al., 2004) including one in the Ig3 module, two in the Ig4 module, and three in the Ig5 module (Figure 1.4) (Liedtke et al., 2001). The unique feature of NCAM glycosylation compared to other cell adhesion molecules is its potential N-glycosylation with polySia which attaches exclusively to a highly variable di-, tri-, or tetra-antennary core glycan at the fifth (Asn 439) and sixth (Asn 468) sites in the Ig5 module (Figure 1.4) (von der Ohe et al., 2002, Nielsen et al., 2010, Kudo et al., 1996, Liedtke et al., 2001). Both polySTs can synthesize polySia on NCAM (Nelson et al., 1995, Mühlenhoff et al., 1996b, Kojima et al., 1996, Liedtke et al., 2001).

Ubiquitously expressed on the cell surface of neurons and glia (Noble et al., 1985), NCAM proteins interact with each other in cell membranes by cis- or trans-interactions and therefore NCAM was classified as a key regulator of cell adhesion in the CNS (Rutishauser et al., 1982, Gascon et al., 2007). In addition, a number of heterophilic extracellular interacting partners of NCAM have been identified (Nielsen et al., 2010). In the developing CNS, NCAM is involved in numerous processes such as neurite outgrowth, cell migration, stabilization of cell–cell contacts, and synapse formation, whereas in higher order brain regions of the adult CNS NCAM appears to contribute to synaptic plasticity, learning, and memory (for review see (Büttner and Horstkorte, 2010, Maness and Schachner, 2007, Walmod et al., 2004, Hildebrandt and Dityatev, 2013)). Modification of NCAM with polySia significantly influences its biophysical properties and therefore its extracellular homophilic and heterophilic interactions by disrupting the adhesive properties of NCAM (Hildebrandt et al., 2010), which is discussed in section 1.4.3.1. Appropriate cell adhesion and communication is crucial for development and nervous system plasticity. Although many cell adhesion molecules are involved, NCAM is conspicuous due to its developmentally regulated switch in glycosylation pattern (Hildebrandt et al., 2010).

Although the majority of polySia is attached to NCAM, polySTs also polysialylate some other proteins. Mild acid hydrolysis and endoN treatment of glycan substituents on the voltage-sensitive sodium channels from Electrophorus electricus electroplax led to a reduction in molecular weight, suggesting that these channels carry polySia (James and Agnew, 1987). In fact, the presence of Sia, diSia, oligoSia, or polySia was later indicated as treatment of sodium channel α subunits in both the electroplax and rat brain with a neuraminidase which cleaves Sia with α2,3-, α2,6-, and α2,8-linkages, reduced their apparent molecular mass by 55 and 20 kDa respectively (Gordon et al., 1988). The presence of polySia on these channels in rat brain was further confirmed by an immunoprecipitation of polySia with a monoclonal antibody 735 directed against polySia (mAb 735). The blot of immunoprecipitates showed the presence of not only NCAM but also the voltage sensitive sodium channel α subunit isolated with polySia (Zuber et al., 1992). Removal of Sias with neuraminidase significantly lessened the conductivity of the channel (Scheuer et al., 1988, Recio-Pinto et al., 1990), indicating polySia may modulate voltage-dependent gating (Nowycky et al., 2014).

The synaptic cell adhesion molecule 1 (SynCAM 1), an Ig domain–containing protein with six potential N-glycosylation and several putative O-glycosylation sites is another polySia bearing

protein (Biederer et al., 2002). SynCAM 1 plays a role in various intercellular junctions by mediating Ca^{2+} independent cell adhesion through homo- and heterophilic interactions (Biederer et al., 2002, Furuno et al., 2005, Shingai et al., 2003, Wakayama et al., 2007). Using affinity chromatography followed by mass spectrometry, a fraction of SynCAM 1 was identified as a polySia carrier in the $NCAM^{-/-}$ neonatal mouse brain. Treatment of isolated PolySia-SynCAM 1 with N-glycosidase F, an enzyme that specifically cleaves N-glycans, followed by MALDI-TOF mass spectrometry analyses showed that polysialylation occurred at the third N-glycosylation site. SynCAM 1 polysialylation, which is exclusively mediated by ST8SiaII, is cell type specific and was found limited to proteoglycan NG2 positive cells and only in the developing brain (Rollenhagen et al., 2012, Galuska et al., 2010). The polysialylation eliminated homophilic binding of this protein (Galuska et al., 2010).

Another polySia carrier is neuropilin-2 (NRP-2), a transmembrane glycoprotein receptor for semaphorins and vascular endothelial growth factors associated with axon guidance and angiogenesis (Pellet-Many et al., 2008). Similar to SynCAM 1, NRP-2 demonstrates a cell type specific polysialylation and despite the expression of NRP-2 in several tissues including the brain, lymphatic, blood vessels, several muscle types organs, and diverse tumour cells (Pellet-Many et al., 2008, Parker et al., 2012), polysialylation has so far only been demonstrated on the surface of human dendritic cells (DCs) of the immune system (Curreli et al., 2007), on macrophages cultured from peritoneal exudate (Stamatos et al., 2014), stem cell- and brain-derived murine microglia, and cultured human THP-1 macrophages (Werneburg et al., 2016). On the surface of human dendritic cells, NRP-2 was polysialylated on its O-linked glycan chains (Curreli et al., 2007). Removal of polySia stimulated dendritic cell-induced activation of T lymphocytes (Curreli et al., 2007). In a recent study, a Golgi-restricted expression of polySia on SynCAM 1 and NRP-2 was observed in NG2 cells and microglia respectively from glial cultures of wild-type and $NCAM^{-/-}$ mice. Depolarization of NG2 cells and LPS stimulation of microglia led to the translocation of polySia from the Golgi to the cell surface (Werneburg et al., 2015).

The C–C chemokine receptor type 7 (CCR7) involved in immunity, has also been recently identified as a second polySia carrier on the surface of mature DCs (Kiermaier et al., 2016). PolySia was attached to both the N- and O-linked glycans of CCR7, because suppression of either N- or O-glycosylation did not fully abolish polysialylation of CCR7. To validate that CCR7 is

polysialylated in mature DCs, cell-surface levels of polySia in CCR7-deficient and control DCs were analysed using a flow cytometry and reduced polysialylation was seen on CCR7-deficient cells. Polysialylation of CCR7 is necessary for the recognition of the CCR7 ligand CCL21 and thus polySia modulates dendritic cell trafficking controlled by CCR7 (Kiermaier et al., 2016).

E-selectin ligand-1 (ESL-1) is a polysialylated protein identified by co-immunoprecipitation followed by mass spectrometry analysis. Stem cell- and brain-derived murine microglia, as well as human THP-1 macrophages, maintain intracellular pools of Golgi-confined polysialylated ESL-1 and NRP-2 which are quickly released in response to proinflammatory activation by LPS (Werneburg et al., 2016). ESL-1 and NRP-2 are polysialylated by the polysialyltransferase ST8SiaIV (Werneburg et al., 2016). The function of polySia on ESL-1 is still unclear.

The CD36 scavenger receptor is a glycoprotein which contains polySia on its O-linked glycan chain(s) in human and mouse milk. (Yabe et al., 2003). In addition, polySTs themselves, can undergo autopolysialylation (Close and Colley, 1998, Mühlenhoff et al., 1996a). Although NCAM is the major polySia carrier, due to the cell specific origin of the polysialylation a range of other proteins may be polysialylated both in the periphery and in different regions of the CNS.

1.4.1.4. Binding molecules of polySia

Carbohydrate-binding proteins (lectins) (for review see (Gabius et al., 2016)) can influence neuronal processes through glycan-involving interactions (for review see (Higuero et al., 2016)). Cell surface localization and selective expression of Sias on the outermost branches of glycoproteins and glycolipids make them well suited to interact or bind to proteins (Schnaar et al., 2014). However, currently only a small number of molecules have been reported as binding partners of polySia (Table 1.2).

Three binding partners appear to have a direct interaction with polySia, demonstrated using *in vitro* and *ex vivo* techniques (Mishra et al., 2010, Theis et al., 2013, Watzlawik et al., 2015). The most comprehensive studies performed by Mishra et al. (2010) and Theis et al. (2013) identified histone H1 and myristoylated alanine-rich C kinase substrate (MARCKS) respectively.

Table 1.2. Binding partners of polySia. Techniques employed indicates methods used to investigate the interaction of polySia with each interacting partner.

Interacting partner	Functional consequences of the interaction	Techniques employed	Investigation of physical interaction
Histone H1	Promoted neuritogenesis, process formation, and proliferation of Schwann cells, as well as migration of neural precursor cells *in vitro*.	*In vitro* and *ex vivo*	Yes
Myristoylated alanine-rich C kinase substrate (MARCKS)	Enhanced neurite outgrowth *in vitro.*		
HIgM12	Mediated HIgM12 binding and cell attachment in a neurite outgrowth assay.		
Chemokine (C-C motif) ligand 21 (CCL21)	PolySia removal led to a decrease in the CCL21-directed migration on mature DCs. Enzymatic removal of polySia also negatively affected CCL21-mediated ERK activation in DC cultures.	*In vitro*	
Brain-derived neurotrophic factor (BDNF)	Following polySia removal, BDNF was released at higher levels than those from non-treated cells		
Fibroblast growth factor-2 (FGF2)	Inhibited FGF2-stimulated cell growth		
Catecholamines such as dopamine (DA)	PolySia on NCAM was involved in the AKT signalling via DA		
Heparan sulphate proteoglycans (HSPGs)	Enhanced the interaction of HSPGs with NCAM		No
α-amino-3-hydroxy-5-methyl-4-isoxazole propionate (AMPA) receptors	Prolonged the open channel time of AMPA receptors		
NR2B subunit-containing N-methyl-D-aspartate (NMDA) receptors	Inhibited NMDA receptor currents	*In vitro and ex vivo*	

Both studies employed affinity chromatography on homogenates of mice brains, followed by mass spectrometry to identify the binding partner and then used a variety of *in vitro* and *ex vivo* (co-immunoprecipitation using brain homogenates) techniques to confirm the interaction. Functional studies were also performed. The interaction of histone H1 with polySia promoted neuritogenesis, process formation, and proliferation of Schwann cells, as well as migration of neural precursor cells *in vitro*. Similar to polySia which enhances regeneration after injury of the peripheral nervous system (Papastefanaki et al., 2007, Marino et al., 2009, Mehanna et al., 2010), *in vivo* application of histone H1 improved functional recovery, axon regrowth, and precision of re-innervation of the motor branch in adult mice having femoral nerve injury (Mishra et al., 2010). However, it is still unclear whether the observed functions of histone H1 were polySia dependent or not. This issue could have been addressed by functional study after enzymatic removal of polySia. Regarding the

interactions between polySia and MARCKS, *in vitro* application of the effector domain of MARCKS (MARCKS-ED peptide) enhanced neurite outgrowth from cultured hippocampal neurons. Such neurite enhancement was abolished after endoN treatment, indicating that the peptide-triggered neurite outgrowth relies on polySia (Theis et al., 2013). In addition, in a more recent study, polySia attached to NCAM was found as an antigen for the IgM antibody HIgM12 (Watzlawik et al., 2015). Double labelling experiments showed virtually identical patterns of labelling with HIgM12 and anti-polySia antibodies particularly on glial fibrillary acidic protein (GFAP)-positive astrocytes but also in a range of cells extracted from forebrain regions. As with the polySia antibody, HIgM12 was not able to detect any GFAP-positive astrocyte in endoNF treated cultures or after modification of polySia from the NCAM protein core via acid-catalysed lactonization, indicating that polySia is crucial for binding of HIgM12 to brain cells including astrocytes. Interestingly, no interaction was found between mAb HIgM12 antibody and polySia attached to SynCAM 1 in embryonic or postnatal periods. PolySia-NCAM mediated HIgM12 binding and cell attachment in a neurite outgrowth assay (Watzlawik et al., 2015). As mentioned earlier these three studies used *ex vivo* along with *in vitro* techniques to identify or confirm polySia interacting partners. In *in vitro* techniques, an interaction as well as detection of an interaction between interacting partners occurs outside their normal biological context, whereas, in *ex vivo* studies, the detection of an interaction happens *in vitro*, but the interaction itself takes place in an *in vivo* (i.e. living organism) environment (Xing et al., 2016). Therefore, interactions identified using an *ex vivo* techniques have a higher possibility of occurring in an *in vivo* environment compared to those identified using *in vitro* techniques.

In a second group of studies, direct binding of polySia and postulated partners including chemokine (C-C motif) ligand 21 (CCL21), brain-derived neurotrophic factor (BDNF), fibroblast growth factor-2 (FGF2), and catecholamines such as dopamine (DA) were identified using only *in vitro* approaches (Bax et al., 2009, Kanato et al., 2008, Ono et al., 2012, Isomura et al., 2011).

CCL21 is a ligand for CCR7 (a carrier of polySia described in Section 1.4.1.3). Bax et al. (2009) first suggested that CCL21 may be an interacting partner of polySia as endoN treatment led to a decrease in the CCL21-directed migration on mature DCs (Bax et al., 2009). It appears that polySia releases CCL21 from an autoinhibited state by interacting with its C terminus (Kiermaier et al., 2016). Enzymatic removal of polySia negatively affects CCL21-mediated extracellular signal-

regulated kinase (ERK) activation in DC cultures (Hjortø et al., 2016); however, whether these effects are due to protein binding or carrying remains to be determined.

BDNF (Kanato et al., 2008) and FGF2 (Ono et al., 2012) were originally identified as interacting partners of polySia using biochemical approaches including gel filtration, horizontal native-PAGE, and surface plasmon resonance methods (Kanato et al., 2008, Ono et al., 2012, Hane et al., 2015). Recently, Sumida et al. (2015) showed that after exogenous sialidase or endoN treatment of a group of polySia expressing cells, BDNF was released at higher levels than those from non-treated cells, indicating that cell-surface polySia chains bind to and hold endogenous BDNF molecules which are released upon removal of polySia (Sumida et al., 2015). Functional studies on polySia expressing cells displayed inhibition of FGF2-stimulated cell growth in the presence of polySia (Ono et al., 2012).

The specific binding between polySia and catecholamine neurotransmitters, including DA, was demonstrated by frontal affinity chromatography (FAC) analyses (Isomura et al., 2011). The interaction of polySia and DA was impaired using a mutated ST8SiaII (STX(G421A))-derived polySia-NCAM which has a lower amount of polySia (7.7% compared to 100% in wild type) on NCAM with a shorter chain length compared to wild type ST8SiaII-drived polySia. DA activates AKT signalling (Tan et al., 2008) and studies in the presence of endoN showed that DA stimulation led to a reduction in AKT activation (phosphorylation), indicating that polySia on NCAM was involved in the AKT signalling via DA (Isomura et al., 2011). Although an interaction of polySia with CCL21, BDNF, FGF2, and DA was confirmed using multiple *in vitro* approaches, interactions that occur under *in vitro* conditions may not occur under physiological conditions *in vivo*.

Heparan sulphate proteoglycans (HSPGs) (Storms and Rutishauser, 1998), α-amino-3-hydroxy-5-methyl-4-isoxazole propionate (AMPA) receptors (Vaithianathan et al., 2004), and NR2B subunit-containing N-methyl-D-aspartate (NMDA) receptors (Hammond et al., 2006) have been suggested as potential binding partners only because polySia alters the function of the proteins; however, investigation of physical interaction has not taken place. PolySia enhances the interaction of HSPGs with NCAM (Storms and Rutishauser, 1998) as reduced adhesion to the HSPGs was detected when cells expressing polySia-NCAM were pretreated with endoN. However, it remains unclear whether polySia actually binds to HSPGs or indirectly modulates an NCAM HSPG interaction.

Evidence of polySia interaction with glutamate receptors AMPA (Vaithianathan et al., 2004) or NMDA receptors (Hammond et al., 2006) are based on evidence obtained from a few electrophysiological recordings in cultured neurons and single channel recordings of affinity-purified receptors in reconstituted lipid bilayers. PolySia prolonged the open channel time of AMPA receptors (Vaithianathan et al., 2004) and inhibited NMDA receptor currents (Hammond et al., 2006). Enzymatic removal of polySia in both cases inhibited these effects. In agreement, impaired long-term potentiation *ex vivo* was associated with elevated transmission through GluN2B-NMDARs in the hippocampal CA1 region of adult NCAM-deficient mice (Kochlamazashvili et al., 2010). The acute elimination of polySia by endoNF in brain slices consistently enhanced GluN2B-mediated Ca^{2+} transients in CA1 pyramidal neurons, and this could be reversed by the application of colominic acid (Kochlamazashvili et al., 2010). However, it is unknown whether the influence of polySia in AMPA and NMDA receptors is due to direct binding of these receptors with polySia or is due to indirect effects such as the interaction of polySia with a lipid membrane near these receptors that could modify the configuration of these receptors and, therefore, indirectly influence ligand binding. Further experiments such as co-immunoprecipitation/affinity chromatography followed by western blot or ELISA are required to investigate the potential physical interaction between polySia or polySia-NCAM with these receptors.

Although the distribution of polySia has been described in specific regions of the CNS, only two studies (Theis et al., 2013, Mishra et al., 2010) have investigated its interactions in the brain and both of these have been performed in mouse where much less is known regarding polySia distribution. The interaction was identified both in the developing brain where polySia is abundant as well as in the adult brain. However, whether polySia in all CNS regions where its expression is high in the adult demonstrates the same interactions or even interacting partners is still an open question.

1.4.2. Anatomy of polySia in the adult CNS

PolySia is expressed in extraneural tissues during development and in the adult in cells of the immune system (Curreli et al., 2007, Drake et al., 2008, Stamatos et al., 2014), lung (Ulm et al., 2013), testis (Simon et al., 2013), sperm (Simon et al., 2013), placenta (Hromatka et al., 2013) and

liver (Tsuchiya et al., 2014). Since the focus of this thesis is the CNS, only the anatomy of polySia in the CNS will be discussed here.

1.4.2.1. Developmental regulation of polySia in the CNS

In vertebrates, polySia expression is spatio-temporally regulated (Rutishauser, 2008), and polySia is most widespread in the CNS during the embryonic and early neonatal period (Sato and Kitajima, 2013b, Mühlenhoff et al., 2009). In the mouse embryo, polySia immunoreactivity (ir) was first detected at embryonic day 9 using immunohistochemistry (Ong et al., 1998) and expression reached maximal prenatally (Ong et al., 1998, Kurosawa et al., 1997). Quantification of the total amount of polySia in the mouse brain by DMB-HPLC analysis showed that after birth, the polySia level remained high during the first postnatal week, before a rapid drop between postnatal days 9–17 to about 30% of the level at birth and the level of polySia further declined in the adult to almost 10% of the highest level (Figure 1.5) (Oltmann-Norden et al., 2008, Mühlenhoff et al., 2009).

Interestingly, a similar developmental expression pattern of polySia has been described in the human prefrontal cortex (Cox et al., 2009). PolySia-NCAM was quantified with western blotting using anti-polySia antibody in human postmortem prefrontal cortex of 42 individuals ranging in age from fetal (mid-gestation) to early adulthood (25 years old). The expression level was significantly higher in the fetal samples compared to that of all postnatal samples ($P<0.001$), ranging

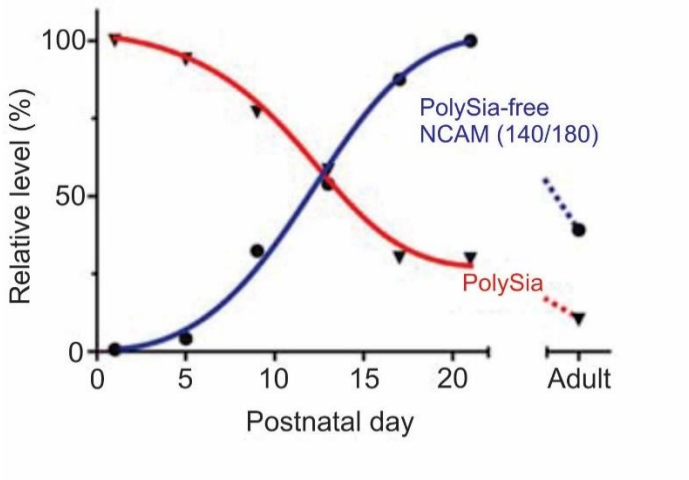

Figure 1.5. Developmental regulation of polysialylation in the mouse brain after birth. The red and blue curves indicate postnatal down-regulation of polySia and associated up-regulation of polySia-free NCAM-140/180, respectively. From (Mühlenhoff et al., 2009).

from 5-fold higher compared to the 0–12-month group to more than 30-fold higher compared to the adult group.

In the brain, almost 95% of NCAM isoforms 140 and 180 are polysialylated at birth (postnatal day 1). After birth the appearance of polySia-free NCAM increases, which is aligned with the reduction in the polySia level (Figure 1.5). In contrast, the vast majority of NCAM-120 is not polysialylated. Expression of NCAM-120 starts at postnatal day 5, followed by a huge up-regulation correlated with the down-regulation of polySia (Oltmann-Norden et al., 2008). It is curious, however, that the ratio of polySia-free NCAM to total NCAM in many regions of the adult CNS which express polySia is not yet known.

1.4.2.2. Cell types of the CNS associated with polySia

In the embryonic brain, the vast majority of polySia positive cells are the neuronal lineage (Blass-Kampmann et al., 1994). In both normal developing and adult nervous system, the largest number of cell types expressing polySia-NCAM are neurons (Bonfanti, 2006). It appears that most, if not all, neurons show positive polySia staining at some stage of differentiation (Bonfanti, 2006).

In the adult, ultrastructural and immunolabelling studies demonstrated a strong expression of polySia in migrating neuroblasts arising from the neurogenic niches of the anterior subventricular zone (Bonfanti and Theodosis, 1994, Rousselot and Nottebohm, 1995, Kornack and Rakic, 2001, Ponti et al., 2006) and early postmitotic granular cell precursors in the subgranular zone of the hippocampal dentate gyrus (Seki and Arai, 1991b, Seki, 2002a, Seri et al., 2004, Seki et al., 2007) in various mammals including but not limited to mice, rats, rabbits and macaque monkeys.

So far, three specific groups of neurons have been reported to show prominent polySia-ir. These include immature neurons mostly found in layer II of the paleocortex and to a small extent in layers II and III of the mammalian neocortex (Gómez-Climent et al., 2008, Gomez-Climent et al., 2010). These cells co-express doublecortin, a marker of immature nerve cells, but lack neuronal nuclear antigen (NeuN), a marker for mature neurons (Nacher et al., 2002, Nacher et al., 2001). Studies in rodents and cats demonstrated that most of these neurons have been generated during embryogenesis and preserve their immature neuronal phenotype into adulthood (Gómez-Climent et al., 2008, Varea et al., 2011). The number of polySia-positive immature neurons decreases significantly with age (Varea et al., 2009, Abrous et al., 1997).

The second type are polySia-positive neurons that express NeuN and hence are mature neurons. Double immunostaining with interneuron markers, principally glutamic acid decarboxylase-67 (GAD67), the GABA biosynthetic enzyme, calbindin, somatostatin, or parvalbumin (depending on the cortical area under consideration) and anti-polySia antibody (anti-Men B; Clone 2-2B) has demonstrated that many are inhibitory interneurons. This delineation has only been demonstrated in higher brain areas, including the amygdala (Gilabert-Juan et al., 2011, Varea et al., 2012), the prefrontal cortex (Varea et al., 2007, Varea et al., 2005, Gómez-Climent et al., 2011), nongranule cells of hippocampus, deep layers of paleocortex (Gómez-Climent et al., 2011), the subtriangular septal zone, and the septum (Foley et al., 2003). In addition, in the adult mouse (Gilabert-Juan et al., 2011) and human amygdala (Varea et al., 2012), the prefrontal cortex, nongranule cells of hippocampus, and deep layers of paleocortex (Gómez-Climent et al., 2011), none of the polySia expressing somata analysed co-expressed Ca^{2+}/calmodulin-dependent protein kinase II (CAMKII), a marker of excitatory neurons, and no polySia expressing puncta expressed in the neuropil showed vesicular glutamate transporter type 1 (VGLUT-1)-ir (Varea et al., 2012).

In the adult rat and human medial prefrontal cortex (mPFC), virtually all polySia labelled cells showed NeuN-ir (Varea et al., 2007, Varea et al., 2005). Only rare GFAP immunoreactive processes showed faint polySia labelling and the labelling was not found on oligodendroglia. About 35% of polySia immunoreactive neurons expressed GAD67 (Varea et al., 2005). PolySia-ir was also seen in interneuron populations labelled with calbindin, parvalbumin, and somatostatin; however, there were some differences between rat and human in the percentages of interneurons labelled with these markers (Varea et al., 2007, Varea et al., 2005). Similarly, all polysialylated cells in the subtriangular septal zone and the triangular septum expressed NeuN with many co-expressing GAD67 along with vasoactive intestinal peptide (Foley et al., 2003).

Although these studies identified polysialylated inhibitory neurons in the areas mentioned, we cannot conclude that polySia is not expressed on excitatory interneurons. The identity of the neurochemical codes of polysialylated neurons has been explored in very few brain regions that express polySia. Further studies using multiple markers in different polySia expressing brain regions would determine whether or not polySia is associated with the same cell type (neurons/glia), only inhibitory neurons, and/or in neurons with specific neurochemical codes (which likely define function).

The third group of polySia positive neurons in the adult brain are mature neurons expressing polySia only on their processes (Schnaar et al., 2014). These have been found in hippocampus in mossy fibres of dentate gyrus granule cells (Seki and Arai, 1993a) and on axons and dendrites of pyramidal cells in the CA1 region (O'Connell et al., 1997, Becker et al., 1996).

Glial cells may also be polysialylated although this expression seems to vary within different brain areas and under different physiological and pathological/experimental conditions (Bonfanti, 2006, Schnaar et al., 2014). Astrocytes do not appear to express polySia under normal conditions; however, polysialylated astrocytes have been found in the adult hypothalamo-neurohypophysial system (Theodosis et al., 1991, Theodosis et al., 1999, Kiss et al., 1993, Kaur et al., 2002, Shen et al., 1999). Ultrastructural analysis showed polySia-ir associated with astrocytic cell bodies and in particular their processes that surround the surface of non-immunoreactive supraoptic neurons (Theodosis et al., 1991, Theodosis et al., 1999). In addition, ultrastructural observations in the neurohypophysis (posterior pituitary), a highly polysialylated brain region, demonstrated surface labelling of all neurosecretory axons as well as pituicytes (neurohypophysial astrocytes) (Theodosis et al., 1999, Theodosis et al., 1991, Kiss et al., 1993). Unlike the relatively uniform staining on nerve fibres (Kiss et al., 1993), polySia-ir on glial surfaces was uneven, detected on glial surfaces facing neuronal elements but not at contact sites between pituicytes (Kiss et al., 1993). Furthermore, in the adult rat during the proestrous phase, immunofluorescence staining of the gonadotropin-releasing hormone (GnRH) neurosecretory system, demonstrated that polySia was closely associated with axon terminals of GnRH neurons as well as glial processes in the median arcuate nucleus (Kaur et al., 2002, Parkash and Kaur, 2005). Electron microscopy of the adult mouse suprachiasmatic nucleus showed that polySia-ir was associated with neuronal (in somas, dendrites, and unmyelinated axons) and glial membranes, particularly on fine astrocytic processes adjacent to synapses (Shen et al., 1999, Shen et al., 1997). Such a glial association was also seen in the radial glia-like tanycytes of the ependymal layer of the third ventricular wall, which sends processes into hypothalamus (Bolborea et al. 2011).

PolySia is expressed on reactive astrocytes, activated as a result of different insults in the brain and spinal cord (La Salle et al., 1992a, Nomura et al., 2000). An animal model of status epilepticus in which rats were treated with kainic acid (glutamate agonist) showed a strong polySia expression associated with glial cells (corresponding approximately to the reactive gliosis identified by a GFAP marker) in the hippocampus for up to 12 weeks following kainic acid administration (La

Salle et al., 1992a). Similarly a model of Parkinson's disease induced by 6-hydroxydopamine lesion of the substantia nigra induced polySia expression on reactive astrocytes (Nomura et al., 2000). A range of glia appeared to express polySia in a demyelinating model of adult mouse spinal cord including on oligodendrocyte precursors, reactive astrocytes and Schwann cells (Oumesmar et al., 1995). Direct injury of the spinal cord caused expression of polySia in the glial scar and in the surrounding region (Camand et al., 2004).

Gómez-Climent et al. (2011) used anti-OX42 antibody in the adult cerebral cortex and found that microglial cells were polySia negative (Gómez-Climent et al., 2011). However, more recently as discussed in section 1.4.1.3, a Golgi-restricted expression of polySia on SynCAM 1, NRP-2, and ESL-1 glycoproteins was found in brain-derived murine microglia, obtained from postnatal cerebral cortices (Werneburg et al., 2016, Werneburg et al., 2015).

Thus, polySia in adult has been demonstrated on distinct populations of neurons throughout the CNS, in some glia, most commonly in reactive astrocytes associated with both GFAP labelling of proximal processes but also with fine astrocytic processes, and in Golgi of microglia; however, polySia has not been found on mature oligodendrocytes although it is expressed by oligodendrocyte pre-progenitors (Bonfanti, 2006). With respect to oligodendrocyte, labelling experiments using immunoelectron microscopy have showed that in the hippocampal mossy fibre layer (Seki and Arai, 1991b), the fimbria (Seki and Arai, 1993a), the superficial layer of dorsal horn (Seki and Arai, 1993a), and the sciatic nerve (Figarella-Branger et al., 1990), polySia was only found in unmyelinated and not myelinated axons. Additional work is required to investigate whether polySia has a uniform cellular association within all areas of the CNS in which it is expressed. While distinct areas of the adult CNS maintain a distinct pattern of polySia expression (Bonfanti, 2006), exploration of the brainstem and much of the spinal cord which have received little attention may reveal any consistent patterns of labelling with respect to cell type.

1.4.2.3. Distribution of polySia in the adult CNS

PolySia is widespread in the CNS during brain development (for review see (Hildebrandt and Dityatev, 2013, Seki and Arai, 1993a, Bonfanti, 2006)); however, its expression in the adult is the topic of focus here. PolySia expression in the adult CNS is restricted to distinct areas including those that maintain neurogenic capacity, such as the subventricular zone, the granule cell layer of the hippocampus, and the olfactory bulb or regions that undergo physiological plasticity, including

regions of the hypothalamus, the entorhinal–hippocampal complex, regions of the thalamus, the habenular nuclei, the mesencephalic central grey, the lateral geniculate nucleus, and the dorsal laminae of the spinal cord (Rutishauser, 2008). The distribution of polySia in the higher brain regions including but not limited to the olfactory system, cortex, hypothalamus, visual system, striatum and amygdala have been investigated in several studies (for review see (Seki and Arai, 1993a, Bonfanti, 2006, Bonfanti et al., 1992)). Here we focus on the known distribution of this sugar in the brainstem and spinal cord.

1.4.2.3.1. Spinal cord

In the adult rat spinal cord, polySia is expressed in the superficial laminae of the dorsal horn (Seki and Arai, 1993b, Bonfanti et al., 1992), around the central canal associated with cell bodies and processes of scattered neurons (Seki and Arai, 1993b, Bonfanti et al., 1992), in the lateral spinal nucleus defined in bundles of fine fibres (Seki and Arai, 1993b), and in the most dorsal part of the anterior median fissure largely in groups of fine fibres (Seki and Arai, 1993b) or axon bundles (Stoeckel et al., 2003). The polySia positive bundles of the anterior median fissure also showed immunolabelling for GABA or GAD, suggesting some at least arose from inhibitory interneurons (Stoeckel et al., 2003). This polySia expression pattern is maintained from cervical to sacral levels (Seki and Arai, 1993b, Bonfanti et al., 1992). In addition, some isolated polySia positive cells with an astrocytic morphology throughout the peripheral white matter were observed (Bonfanti et al., 1992). PolySia staining was also found on some cerebrospinal fluid-contacting neurons (CSFcNs), co-expressing GAD (Seki and Arai, 1993b, Stoeckel et al., 2003).

In the adult mouse spinal cord, polySia expression has been found in the superficial laminae of the dorsal horn (El Maarouf et al., 2005, Oumesmar et al., 1995), the most dorsal part of the anterior median fissure (Oumesmar et al., 1995), around the central canal (El Maarouf et al., 2005), and in the dorsal funiculus (El Maarouf et al., 2005) at the thoracic and/or lumbar level but its distribution is not comprehensively described.

1.4.2.3.2. Brainstem

In the adult rat brainstem, polySia-ir is highly expressed in the dorsal vagal complex, including the nucleus of the solitary tract (NTS), the area postrema, and the dorsal motor nucleus of the vagus (Seki and Arai, 1993a, Bonfanti et al., 1992). This expression was found throughout the rostrocaudal axis of the adult rat (Bouzioukh et al., 2001a). PolySia expression has also been

reported in a few other regions including in the raphe pallidus nucleus, the pyramidal tract (Seki and Arai, 1993a), the lateral and medial parts of the parabrachial nucleus (Bonfanti et al., 1992, Seki and Arai, 1993a), and in mesencephalic trigeminal nucleus (Bonfanti et al., 1992).

Unusually the human brainstem has been more comprehensively investigated with respect to the distribution of polySia (Quartu et al., 2008, Quartu et al., 2010). Immunohistochemistry on the postmortem brainstem of adult human showed polySia-ir mainly at the level of the medulla oblongata and pons but rarely in the mesencephalon (Quartu et al., 2008). PolySia staining was present in the spinal trigeminal nucleus but was virtually absent in the principal and mesencephalic nuclei. Moreover, at caudal level of the medulla oblongata, very mild to moderate immunostaining in central reticular and lateral reticular nuclei was found. More rostrally at the level of the pyramidal decussation, the gracile, external cuneate, and commissural nuclei displayed a moderate polySia staining. PolySia labelling was also present in the dorsal vagal complex, the vestibular and cochlear nuclei, the intercalatus and prepositus hypoglossi, the paramedian reticular, the raphe obscurus, the gigantocellular, the central reticular, the intermediate reticular, and the lateral reticular nuclei labelling neuronal cell bodies and processes with mainly a peripheral immunoreactivity suggestive of membrane labelling. The olivary complex showed a diffuse staining in the neuropil with some small cell bodies. A diffuse mild staining was found in the locus coeruleus neuropil in between polySia negative pigmented neurons. The caudal pontine, gigantocellular, parvocellular, reticular tegmental, and oral pontine reticular nuclei contained sparse neuronal cell bodies with membrane labelling and rare punctate and filamentous elements. Labelled nerve fibres were observed throughout the medial longitudinal fasciculus, the medial lemniscus and the lateral lemniscus. The pontine nuclei showed a dense labelling (Quartu et al., 2008).

In Bonfanti's description of the distribution of polySia-ir in the adult rat (Bonfanti et al., 1992), no mention was made of labelling of the spinal trigeminal nucleus; however, curiously described labelling in the mesencephalic trigeminal nucleus in contrast to this being a polySia negative region in human (Quartu et al., 2008). A detailed comparison of the distribution across species is needed. The distribution of polySia in the mouse brainstem or for that matter the brainstem of other animals has not been described.

The distribution of polySia in the dorsal horn, spinal trigeminal nucleus, and trigeminal ganglion that will be the focus of this thesis are found in section 1.5.5 and 1.6.1 respectively.

1.4.3. Roles and mechanisms of polySia functions in the CNS

PolySia in the developing brain is involved in a variety of important neurological functions such as neurite outgrowth, cell migration, axonal guidance and branching, neuronal pathfinding, lamination of mossy fibres, and synapse formation as reviewed by several papers (Hildebrandt and Dityatev, 2013, Bonfanti, 2006, Brusés and Rutishauser, 2001, Schnaar et al., 2014). Despite multiple functions of polySia in the developing CNS, in adults only neurogenesis and plasticity have been suggested (Gascon et al., 2007), and these will be discussed in section 1.4.3.2.

1.4.3.1. Mechanisms of action of polySia

Due to the negative charge derived from the carboxyl group of Sia, polySia has a bulky polyanionic nature leading to an enormous hydration volume (Sato and Kitajima, 2013a, Rutishauser, 2008,

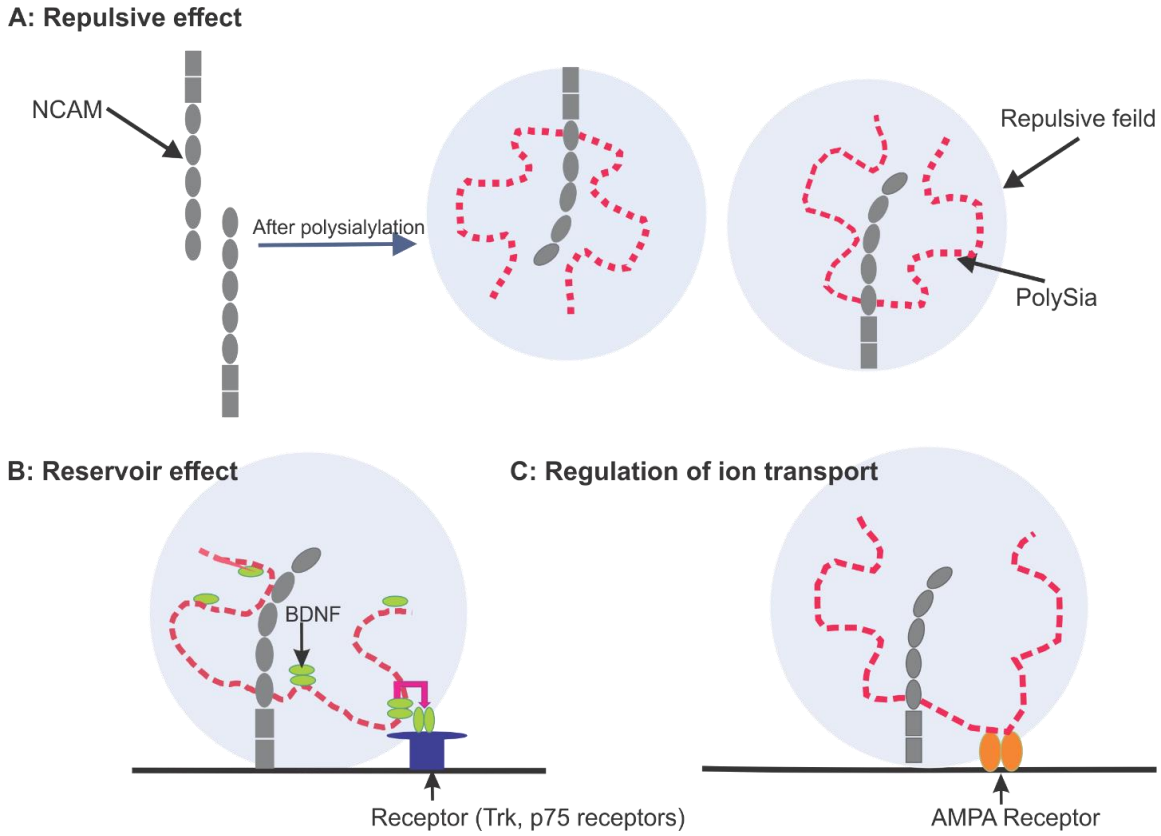

Figure 1.6. Mechanisms of action of polySia. (A) Repulsive effect. Due to the bulky polyanionic nature of polySia, a large hydration shell (has been shown with a light grey sphere surrounding polySia-NCAM) is formed on the polysialylated surface resulting in a repulsive field on the cell surface. (B) Reservoir or retain effect. PolySia on NCAM directly binds to several biologically active molecules such as BDNF. (C) Regulation of ion transport. PolySia-NCAM interacts with some ion channels, such as AMPA receptors, and regulates their opening and closing and thus controls ion transport. Adapted from (Sato and Kitajima, 2013b).

Gascon et al., 2007). As a result of this unusual hydrophilic capacity, polysialylation increases the size of its carrier molecules and enhances repulsive forces on the polysialylated surface of apposing polysialylated membranes (Figure 1.6A) (Yang et al., 1992). The removal of polySia in cell culture caused a significant decrease (25%) in the number of trapped ferritin molecules per micrometre between apposed membranes of endoN treated cells compared to non-treated ones (Yang et al., 1992). In addition, the binding of monoclonal antibodies to NCAM was altered by different ion concentrations indicating the effect of this highly charged sugar on the association of NCAM with other proteins at the cell surface (Yang et al., 1994). Therefore, polySia works as an anti-adhesive molecule, weakening cell-cell or/and cell-matrix interactions.

Recently a new mechanism of action has been suggested for polySia, which is based on its attractive force (Hane et al., 2012, Sato et al., 2010, Sato and Kitajima, 2013a). PolySia can bind and act as a reservoir for specific bioactive molecules such as BDNF and DA and through this reservoir effect can either reduce or increase interactions at receptors (Figure 1.6B). For instance, polySia's interaction with BDNF (discussed in Section 1.4.1.4) results in a complex formation where both molecules migrate toward the receptor. The migration is explained by the affinities of BDNF toward polySia and BDNF receptors. The KD of BDNF to polySia, as calculated by surface plasmon resonance, is about 10^{-9} M (Hane et al., 2012, Sato et al., 2010), whereas the KD to BDNF receptors (TrkB and p75NTR) is 10^{-12} and 10^{-10} M, respectively. Therefore, BDNF in BDNF-polySia complexes would move toward BDNF receptors due to its stronger affinity toward these receptors compared to polySia. Then, BDNF binds to its receptors and polySia dissociates (Sato and Kitajima, 2013a). This reservoir effect of polySia is suggested to be an indicator of how this sugar participates in the regulation of neural function (Sato and Kitajima, 2013a, Sato and Kitajima, 2013b). However, this mechanism is based only on the results of *in vitro* experiments and so far there is no evidence to confirm whether this type of interaction occurs *in vivo*.

PolySia can also regulate the activity of ion channels (Figure 1.6C) (Sato and Kitajima, 2013b). PolySia on NCAM can modulate the activity of glutamatergic receptors including AMPA and NMDA receptors (discussed in Section 1.4.1.4 and Section 1.4.3.2.2 of this chapter).

1.4.3.2. Functions of polySia in the adult CNS

1.4.3.2.1. PolySia and adult neurogenesis

One form of adult plasticity comprises the employment of newly produced neurons into functional circuits (Gascon et al., 2010). In the mammalian brain, this process of "rejuvenation" of existing circuits happens in two distinct areas: the subventricular zone of the lateral ventricle (Alvarez-Buylla et al., 2000) and the subgranular zone of dentate gyrus in the hippocampus (Kempermann and Gage, 2000). Progenitor cells originate from the subventricular zone of the lateral ventricle and migrate rostrally to the olfactory bulb using the rostral migratory stream (Luskin et al., 1997), where they differentiate mainly into interneurons (Zigova et al., 1998). These cells express polySia, required for efficient migration (Angata et al., 2007, Weinhold et al., 2005), during their rostral migration (Ono et al., 1994, Hu et al., 1996). However, the functional role of polySia is incompletely understood (Gascon et al., 2010). Loss of polySia in ST8SiaII, ST8SiaIV double-knockout mice led to the migration deficit of neuroblasts in the rostral migratory stream as well as a reduction in size of olfactory bulbs (Angata et al., 2007, Weinhold et al., 2005), and the mutation of NCAM or removal of polySia also had similar effects (Ono et al., 1994, Cremer et al., 1994, Tomasiewicz et al., 1993). Furthermore, polySia cleavage by endoN injection into the rostral migratory stream of adult mice led to premature differentiation, suggesting that polySia removal stimulates differentiation of newly generated neurons (Petridis et al., 2004). Similar to the subventricular zone of the lateral ventricle, a conspicuous polySia expression is associated with neurogenesis of the subgranular zone of dentate gyrus of the adult hippocampus (Seki and Arai, 1993c, Seki and Arai, 1991) and this polySia-positive microenvironment is believed to support the neurogenic niche (Seki, 2002b). PolySia also appears to play a role in survival of newly generated neurons *in vitro* as removal of polySia using endoN in cortical cultures from newborn rats radically reduces the number of newly generated neurons (Vutskits et al., 2006).

1.4.3.2.2. PolySia and synaptic plasticity

Synaptic plasticity is the biological process by which synapses are modified in structure and function resulting in changes in synaptic strength, in response to various stimuli or environmental conditions (Gaiarsa et al., 2002). These alterations in synaptic properties include a range of synaptic modifications from subtle changes in the efficacy of synaptic transmission to distinct structural reorganization of connections (Gascon et al., 2007). The classical models for studying activity-

dependent synaptic plasticity particularly in neurons of higher brain regions are long-term potentiation (LTP) and long-term depression (LTD), representing an increase and a decrease in synaptic strength respectively (Gaiarsa et al., 2002) although in some brain regions plasticity is not represented in this way (Barnett et al., 2016).

PolySia is involved in synaptic plasticity in the hippocampus which has a structure well suited for studies on synaptic function. This role arises from work on both the developing and adult CNS. A series of experiments performed by Muller et al. (Muller et al., 1996) on CA1 hippocampal slice cultures of 7-day-old neonatal rats, maintained for 10–20 days, showed high expression polySia-NCAM. Theta burst stimulation of different cultures systematically induced robust potentiation, whereas the stimulation of the cultures after enzymatic digestion of polySia with endoN, induced only a transient potentiation with no lasting LTP. Likewise, a slowly decaying form of LTP was obtained after theta burst stimulation of CA1 hippocampal slices obtained from 3–4-month-old NCAM-deficient mice, expressing less than 5% of wild-type polySia, as opposed to a robust potentiation of the EPSP slope in control mice (Muller et al., 1996). In another series of experiments, Muller et al. used a series of low frequency stimulations that failed to induce LTD in the endoN treated cultures, whereas the stimulation produced a lasting depression of synaptic efficacy in non-endoN treated cultures (Muller et al., 1996). In agreement with Muller et al. findings, local injections of endoN into the hippocampus of adult rats impaired spatial memory, which relies heavily on plasticity in the hippocampus. In the same study, tetanic stimulation of endoN treated CA1 hippocampal slices of the adult rats failed to induce LTP, again suggesting a role for polySia in induction of LTP and thus in synaptic plasticity (Becker et al., 1996).

Studies using mice deficient in ST8SiaII or ST8SiaIV further provided useful tools in determining the role of polySia in synaptic plasticity. Schaffer collateral-CA1 synapses, which were polySia positive in wild types, had impaired LTP and LDP in the adult ST8SiaIV mutants (Eckhardt et al., 2000). In contrast, theta burst stimulation of Schaffer collateral-CA1 of ST8SiaII knockout and wild type adult mice did not show any significant difference on short term potentiation and LTP (Angata et al., 2004), indicating that LTP in the CA1 region requires polySia synthesized by ST8SiaIV rather than ST8SiaII. LTP at CA3 synapses was also undisturbed in the ST8SiaII mutants (Angata et al., 2004), and knockout of ST8SiaIV had no effect on the LTP in the CA3 synapses of the adult mice, although polySia expression was significantly reduced in the mutant (Eckhardt et al., 2000). Together these data suggest that the role of polySia differs in the CA1 compared to the

CA3 region. Similarly, although the dentate gyrus in wild type mice shows polySia expression, LTP impairment at synapses of the perforant path was not detected in either of the polyST single-knockout mice *in vivo* (Stoenica et al., 2006). However, the author has not provided any information regarding the expression level of polySia in the dentate gyrus of each polyST single-knockout mice compared to the wild type. Therefore, polySia is not either required to keep LTP in the dentate gyrus or the remaining polyST makes enough polySia to maintain LTP unchanged. Investigating LTP alterations after enzymatic removal of polySia from CA3 and the dentate gyrus of adult wild type animals would address this issue.

PolySia may modulate induction of CA1 LTP through regulating the activity of glutamate receptors possibly both AMPA and NMDA type (Hammond et al., 2006, Vaithianathan et al., 2004). Since polySia potentiates opening of AMPA receptors (Vaithianathan et al., 2004), it was hypothesized that a direct interaction of polySia with the extracellular domain of LTP-mediating receptors may affect activity of the receptors (Hildebrandt and Dityatev, 2013). This hypothesis was supported by a study in which diminished LTP in CA1 region in hippocampal slices from NCAM deficient mice was restored through application of colominic acid or extracellular domains of polySia-NCAM fused to the Fc portion of human immunoglobulin (polySia-NCAM-Fc), but not with application of NCAM (NCAM-Fc) (Senkov et al., 2006).

Consistent with data suggesting that polySia inhibits activation of GluN2B (also called NR2B)-containing NMDA receptors at low concentrations of glutamate in primary hippocampal cultures (Hammond et al., 2006), isolation of NMDA receptor-mediated currents in hippocampal slices in NCAM deficient mice, which have a very low level of polySia, showed an increased GluN2B-mediated transmission in CA3-CA1 synapses (Kochlamazashvili et al., 2010). In addition, acute removal of polySia with endoNF treatment enhanced GluN2B-mediated Ca^{2+} signalling in CA1 pyramidal cells (Kochlamazashvili et al., 2010). Inhibition of extrasynaptic GluN2B-containing receptors using the GluN2B-selective antagonist Ro 25-6981 restored long term potentiation and abrogated contextual fear memory in polySia-NCAM-deficient mice (Kochlamazashvili et al., 2010).

Since the role of polySia in synaptic plasticity has been mainly studied in hippocampus, more evidence is required to comprehensively assess this role at different CNS sites that express abundant polySia in the adult.

1.4.3.2.3. PolySia and morphological plasticity

PolySia appears to also play a role in morphological plasticity (Bonfanti and Theodosis, 2009), in which plasticity is not limited to synaptic alterations, but also involves structural changes to neuronal and glial cell surfaces (Bonfanti, 2006). The evidence comes mainly from the adult hypothalamo-neurohypophysial system. In response to specific physiological/experimental manipulations such as parturition, chronic dehydration, or lactation the number and morphology of neurosecretory axons and terminals as well as remodelling of associated glia occurs (Theodosis et al., 2006, Theodosis and MacVicar, 1996, Theodosis and Poulain, 1993). Ultrastructural analyses of dissected neurohypophysis tissues from adult rats incubated with hyperosmotic medium or isoprenaline *in vitro* showed a significant enhancement in the neurovascular contact as the proportion of basic lamina next to nerve terminals was doubled, primarily due to an increased number of terminals. In contrast, a decrease in gliovascular contact was detected. This morphology was reversed after agonist washout. *In vitro* removal of polySia from the neurohypophysis tissue of adult rats with endoN prevented both stimulation-related induction and reversal of axonal and glial changes (Monlezun et al., 2005).

Under stimulated conditions, the oxytocin magnocellular neurons show hypertrophy with shorter dendrites with fewer branches but larger ramifying axons. The neurons have more synapses, glial coverage is significantly decreased and the surfaces of oxytocin somata and dendrites are directly and extensively juxtaposed (Theodosis et al., 2006, Theodosis, 2002). In accordance with the *in vitro* results obtained by Monlezun et al. (2005), *in vivo* digestion of polySia via microinjection of endoN close to the hypothalamic magnocellular nuclei showed no apparent withdrawal of astrocytic processes nor any increase in synaptic contacts usually induced by lactation and dehydration demonstrating that cell surface polySia in the adult hypothalamo-neurohypophysial system is indispensable to its capacity for activity-dependent morphological (neuronal–glial) and synaptic plasticity (Theodosis et al., 1999). Likewise, after *in vivo* blockade or enzymatic removal of polySia in the arcuate nucleus, morphological changes that were normally induced by 17β-estradiol did not occur (Hoyk et al., 2001).

The mechanisms by which polySia permits morphological changes remain elusive. Due to its anti-adhesive property discussed in section 1.4.3.1, polySia expression on cell surfaces weakens adhesion between polysialylated cells, which might lead to the detachment of cells from their

neighbours or from the extracellular matrix which may permit morphological modification upon stimulation. The second possible mechanism is that polySia may activate intracellular signals causing astrocytic shape changes and/or synapse formation that are modified by certain stimuli (Theodosis et al., 2008).

1.4.3.3. Functions altered after removal/induced expression of polySia

Manipulating polySia levels has been used frequently to investigate functions modulated by polySia. The most common methods of manipulating polySia level is its reduction or removal using enzymes or NCAM/polySTs knockout animals, described in Sections 1.4.3.2.2 and 1.4.3.2.3. However, some functional effects have been investigated by inducing expression of the glycan.

After lesion, axons of the adult mammalian CNS fail to regenerate due mainly to the non-permissive nature of the CNS environment (Schwab, 2004, Filbin, 2003, David and Aguayo, 1981). The ability of polySia to potentially regulate plasticity has made it an attractive target for therapeutic approaches to improve the repair of the damaged adult nervous system due to injury or disease (Rutishauser, 2008). A few groups have used virally mediated gene delivery techniques to induce polySia expression by targeting polySTs, leading to a sustained expression of this glycan (Zhang et al., 2007a, Zhang et al., 2007b, El Maarouf et al., 2006, Ghosh et al., 2012, Luo et al., 2011).

After spinal cord injury, axonal regeneration is inhibited due to a physical barrier effect and biological hindrance owing to the glial scar that is formed (Liuzzi and Lasek, 1987, Silver and Miller, 2004). PolySia is temporally up-regulated by astrocytes in the glial scar and this up-regulation is spatially correlated with axonal sprouting (Camand et al., 2004, Dusart et al., 1999, Emery et al., 2000, Szele and Chesselet, 1996). Induced expression of polySia via up-regulating ST8SiaIV in and around lesion cavity of the dorsal column (Zhang et al., 2007a) and across the dorsal root entry zone, dorsal root, and dorsal horn (Zhang et al., 2007b) increased polySia expression associated mainly with GFAP positive astrocytes and to a lesser extent oligodendrocytes and neurons. This induced expression resulted in significant axonal regeneration in the adult rat spinal cord. Similarly, in the adult mouse, engineered induction of polySia expression in astrocytes (using a cytomegalovirus (CMV) promoter encoding ST8SiaIV) caudal to the spinal cord lesion site in the right corticospinal tract, promoted the regeneration of axons (El Maarouf et al., 2006).

Myelin inhibits axonal regeneration after injury to the adult mammalian CNS (Filbin, 2003, Schwab, 2004). The disappearance of polySia-ir on developing axons coincides with the beginning of myelination (Hekmat et al., 1990, Seki and Arai, 1993b). In addition, *in vitro* data indicated that down-regulation of polySia promotes differentiation of oligodendrocyte precursor into mature oligodendrocytes (Decker et al., 2000). Therefore, overexpression of polySia using a PLP dependent ST8SiaIV transgenic mouse was used to study the role of polySia in myelination. Interestingly, in this transgenic animal there was a delay of myelin formation (Fewou et al., 2007, Franceschini et al., 2004), suggesting that induced polySia expression might be used to promote axonal regeneration after injury.

These studies focused on the effect of induced polySia expression on injured CNS repair; however, there is no information available as to whether the induced polySia expression can rescue any deficiency associated by its disturbed expression *in vivo*. Furthermore, the functional effect of polySia overexpression on areas expressing it either abundantly or at lower levels remains unknown.

The main focus of this thesis will be on three regions in the CNS: the dorsal horn of the spinal cord, the spinal trigeminal nucleus (and its sensory ganglia that provides afferent input) which have abundant expression of polySia, as well as the rostral ventrolateral medulla which has a much lower abundance of polySia (as shown in Chapter 2).

1.5. Anatomy and general functions of the dorsal horn of the spinal cord

The spinal cord is a long tubular bundle of nervous tissue that extends from the brainstem in the CNS (Figure 1.7A). The spinal cord dorsal horn is a major zone of the CNS in which sensory information is received, integrated, and conveyed to higher levels of the CNS (Perl, 1984, Crossman, 2016).

1.5.1. Organization of the dorsal horn

The dorsal horn is located in the grey matter of the spinal cord at all levels (Crossman, 2016). In 1952, Rexed divided the grey matter of the spinal cord into a series of parallel layers (lamina I to X) on the basis of cytoarchitecture of Nissl stained sections from the cat spinal cord. The layers are numbered sequentially from dorsal to ventral, with the dorsal horn constituting the first 6 laminae (Figure 1.7B) (Rexed, 1952). This organizational scheme has been widely accepted for mouse

(Sidman et al., 1971) and rat (Molander et al., 1984, George and Charles, 2007), the most commonly used laboratory species.

Laminae I-IV are located most dorsally. Many complex polysynaptic reflex paths (ipsilateral, contralateral, interasegmental, and intersegmental) as well as many long ascending fibres to the higher CNS levels originate from these layers (Schoenen and Faull, 2004). Lamina I (lamina marginalis) is a thin layer at the dorsolateral tip of the dorsal horn comprising loosely packed neuropil with coarse and fine nerve fibres and a low density of neurons (Schoenen and Faull, 2004). Lamina II, originally termed substantia gelatinosa (Cervero and Iggo, 1980, Rolando, 1824), is much larger and has a high neuronal density, consisting of densely packed small neurons with only

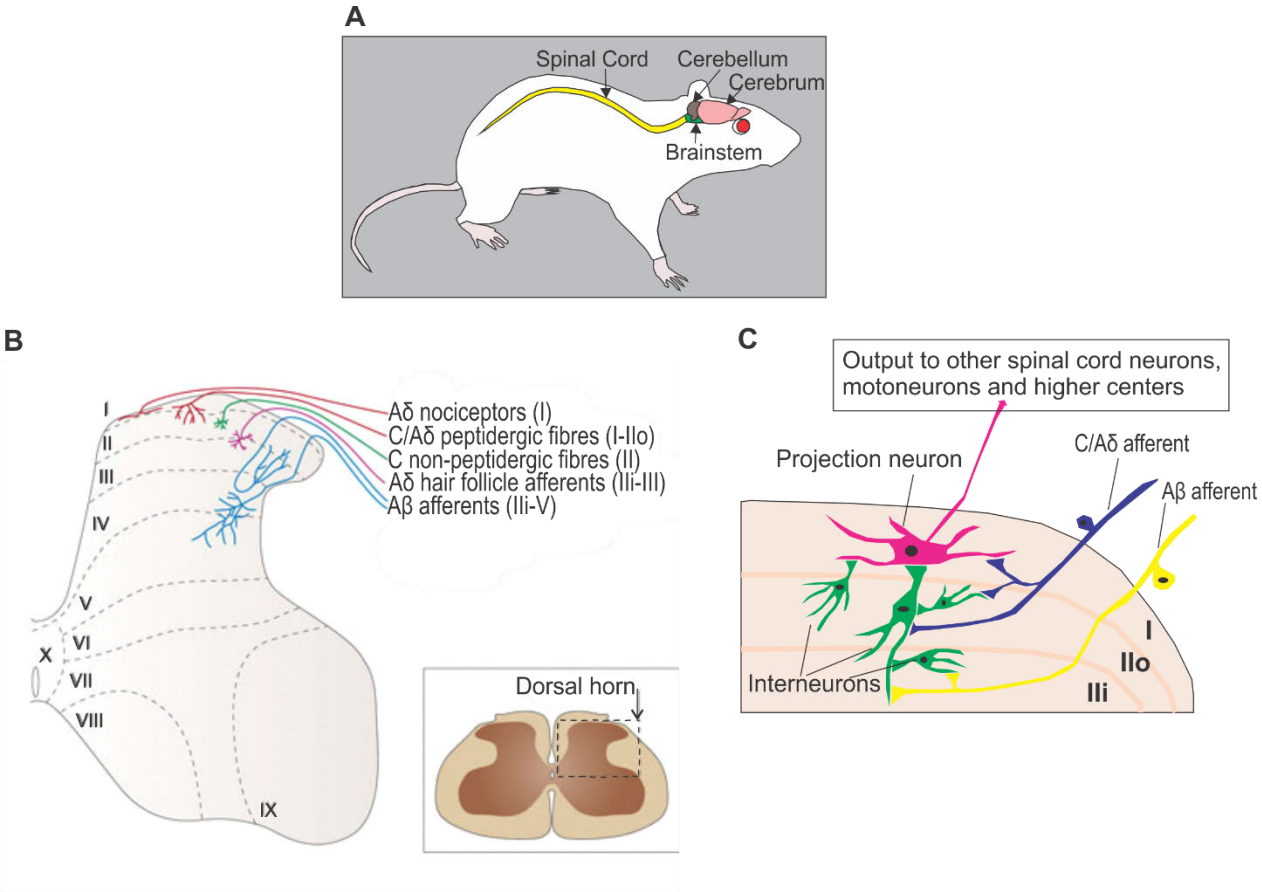

Figure 1.7. Dorsal horn, its afferent input and neurons. (A) Schematic representation of the spinal cord and brainstem in rats. (B) Dorsal horn constitutes Laminae I-VI of the spinal cord based on Rexed laminar organization, as shown in the selected box. Primary afferents innervate the dorsal horn in an orderly way with Aδ nociceptors end mainly in lamina I, peptidergic primary afferents (C fibres and some Aδ fibres) ending in lamina I/IIo (IIo: lamina II outer layers), and non-peptidergic terminating in lamina II. Aδ hair follicle afferents innervate between lamina II and lamina III, while Aβ afferents terminate mostly in lamina III–V, with some extension into lamina IIi (IIi: lamina II inner layers). From (Todd, 2010). (C) Schematic representation of neurons of the spinal cord: interneurons, projection neurons, and their input and output.

some larger neurons (Willis and Coggeshall, 2004, Schoenen and Faull, 2004). It is virtually devoid of myelinated fibres unlike the adjacent laminae (Schoenen and Faull, 2004, Crossman, 2016) which together with a high density of neurons results in a 'gelatinous' appearance (Willis and Coggeshall, 2004). Lamina III contains myelinated fibres and somata that are larger and is less closely packed compared to lamina II. Lamina IV is a thick, loosely packed, heterogeneous area filled by fibres. Neuronal somata in Lamina IV are variable in size and shape (Crossman, 2016, Schoenen and Faull, 2004). Laminae V-VI are located at the base of the dorsal horn with lamina V having a mixed cell population and lamina VI comprising a medial region of small densely packed neurons and a lateral region two-third consisting of larger somata (Crossman, 2016).

1.5.2. Input to the dorsal horn

Signals related to nociception, pain, temperature, and other somatosensory functions are initially transmitted to the spinal cord dorsal horn by primary afferent fibres from neurons located in the dorsal root ganglia, via the dorsal roots (Crossman, 2016, Perl, 1984, Perl, 1992, Zeilhofer et al., 2012). The primary afferent fibres are categorized into three groups (Aβ, Aδ, and C fibres) according to their peripheral target sites (cutaneous, articular and visceral afferents), conduction velocity (proportionate to their size and myelination), response properties (including sensory modalities and the intensity of stimulus required to activate them) and neurochemical phenotype (such as peptide expression). These characteristics are interconnected because the majority of large myelinated cutaneous afferents (Aβ fibres) are fast-conducting and low-threshold mechanoreceptors which react to touch or hair movement, while many of small-diameter fine myelinated afferents (Aδ fibres) and unmyelinated afferents (C fibres) are primarily nociceptors or thermoreceptors (Todd, 2010). In rats about 80% of cutaneous primary afferents are likely to be unmyelinated (Lynn, 1984).

The primary afferents terminate in a lamina-dependent pattern based on their functional group, with laminae I-IV being the main site of termination of cutaneous primary afferent terminals (Schoenen and Faull, 2004, Crossman, 2016). Aβ fibres mainly innervate laminae (IIi–V), while nociceptive and thermoreceptive Aδ and C fibres terminate in lamina I and a large area of lamina II, except for its most ventral part (Figure 1.7B) (Light and Perl, 1979, Todd, 2010).

All classes of primary afferent fibres use glutamate as their primary fast transmitter and therefore cause an excitatory response at second-order neurons (De Biasi and Rustioni, 1988, West et al.,

2015, Battaglia and Rustioni, 1988). Moreover, dorsal root afferent fibres contain a range of molecules including substance P, calcitonin gene-related peptide (CGRP), bombesin, vasoactive intestinal peptides, cholecystokinin, somatostatin, dynorphin, and angiotensin II. These molecules are known or are predicted to play a neurotransmitter or neuromodulator role (Crossman, 2016). Nociceptive C fibres can be categorized mainly into peptidergic and non-peptidergic fibres. Peptidergic C fibres express neuropeptides such as substance P (Lawson et al., 1997) and CGRP (Millan, 1999), whereas non-peptidergic fibres express c-Ret and neurotrophin receptor, which can bind to isolectin-B4 and express Mas-related G-protein coupled receptor member D (Snider and McMahon, 1998). These two classes innervate different zones with peptidergic C fibres terminating in lamina I/IIo (IIo: lamina II outer layers) and non-peptidergic innervating lamina II (Figure 1.7B) (Todd, 2010, Lorenzo et al., 2008). In adult rats, about half of the lumbar dorsal root ganglion cells that give rise to C fibres are reported to be peptidergic (Michael et al., 1997).

1.5.3. Neurons of the dorsal horn

In the dorsal horn, neurons are classified into two categories: those with axons remaining in the spinal cord, called interneurons, and projection neurons whose axons are sent to the white matter of the spinal cord to innervate mainly higher CNS regions (Figure 1.7C) (Todd, 2015).

1.5.3.1. Interneurons

The incoming information from primary afferent fibres including nociceptive input is processed by complex circuits involving excitatory and inhibitory interneurons (Todd, 2010). Almost all neurons in lamina II and most in lamina I and lamina III are local interneurons which can be excitatory (glutamatergic) or inhibitory (Todd, 2010). The inhibitory interneurons use GABA and/or glycine as their main neurotransmitter. In adult rat, about 25%, 30% and 40-45% of neurons in laminae I, II and III, respectively showed GABA-ir (Todd and Sullivan, 1990, Polgar et al., 2003). Glycine exists at high levels in many lamina III neurons and to a lower extent in lamina I and lamina II neurons with its expression limited mainly to cells showing GABA-ir (Polgar et al., 2003, Todd and Sullivan, 1990). Reliable immunocytochemical markers for glutamatergic interneurons are difficult; however, many excitatory neurons in the dorsal horn including laminae I-III express vesicular glutamate transporter 2 (VGLUT2) (Todd et al., 2003, Maxwell et al., 2007, Polgar et al., 2003). Maintaining the balance between excitation and inhibition is essential to preserve normal

sensory function and altering this balance can result in inflammatory or neuropathic pain (Todd, 2010).

1.5.3.2. Projection neurons

Information is conveyed to projection neurons for transmission to multiple brain areas. Projection neurons are mainly present in lamina I and dispersed throughout lamina III–VI, with very few found in lamina II at least at lumbar levels (Todd, 2010, Al-Khater et al., 2008, Spike et al., 2003). Quantitative retrograde tracing studies in the adult rat suggest that in the fourth lumbar segment, projection neurons account for about 5% of lamina I neurons, of which approximately 80% demonstrated neurokinin 1 receptor (NK1R)-ir (Spike et al., 2003, Todd et al., 2000, Al-Khater et al., 2008) and are activated by noxious stimuli (Salter and Henry, 1991). Although interneurons are the major postsynaptic target for primary afferents (Dahlhaus et al., 2005, Todd et al., 2002, Naim et al., 1997, Ikeda et al., 2003), and innervate projection neurons, projection neurons in lamina I and lamina III are also innervated by peptidergic primary afferents, most of which contain substance P (Figure 1.7C) (Todd et al., 2002, Naim et al., 1997).

Retrograde (Almarestani et al., 2007, Hylden et al., 1989, Spike et al., 2003, Todd et al., 2000) and anterograde (Gauriau and Bernard, 2004, Slugg and Light, 1994, Bernard et al., 1995) tracing studies have demonstrated that the major supraspinal areas innervated by lamina I projection neurons are the caudal ventrolateral medulla, the NTS, the lateral parabrachial area, the periaqueductal grey matter, and specific regions in the thalamus.

1.5.4. Plasticity of the dorsal horn

The dorsal horn and in particular superficial lamina of the dorsal spinal cord can undergo activity dependent synaptic plasticity under physiological, inflammatory, or injury-induced conditions (Woolf and Salter, 2000, Thompson Haskell et al., 2002, Dubner and Ruda, 1992, Luo et al., 2014). Following injury, primary afferent input is altered and many A fibres (Liu et al., 2000, Govrin-Lippmann and Devor, 1978) and C fibres (Hulse et al., 2010) develop spontaneous activity. Moreover, nerve injury modifies the pattern of expression of neurotransmitters/neuromodulators such as CGRP within the afferent neurons (Shehab and Atkinson, 1986, Wakisaka et al., 1992, Obata et al., 2006). Plasticity within the dorsal horn neurons (Ikeda et al., 2006, Latremoliere and Woolf, 2009, Sandkühler, 2009) can serve to modulate incoming somatosensory inputs following

repetitive nociceptive input, and thus can alter the processing and propagation of the information to higher CNS regions.

Trains of primary afferent discharge following repetitive nociceptive stimulation of C fibres at low frequencies evoke increasing levels of activation in the dorsal horn in a phenomenon known as 'wind up' (Woolf and Salter, 2000, Luo et al., 2014) that plays a key role in hypersensitivity. Wind-up is a form of short-term synaptic plasticity as when the stimulus is removed, the activation disappears (Woolf and Salter, 2000, Luo et al., 2014, Mendell and Wall, 1965, Mendell, 1966). In contrast, central sensitization is a state where the facilitation of input outlasts the stimulus such that repetitive C fibre input following deep and continuous noxious stimulation produces excitability in flexor reflex, an increase in spontaneous activity, a reduction in threshold for activation by a peripheral stimulus, a rise in receptive field size, and new responses to normally innocuous Aβ fibre inputs (Woolf, 1983, Latremoliere and Woolf, 2009). Central sensitization leads to hyperalgesia and allodynia (Sandkühler, 2009).

In addition some activity-dependent synaptic modifications with similarity to cortical LTP have also found in the dorsal horn (Latremoliere and Woolf, 2009). Brief high-frequency electrical stimulation of primary afferents produced a LTP or a LTD of fast (monosynaptic and polysynaptic) EPSPs in a large number of neurons in laminae I-III of lumbosacral spinal cord. LTP and LTD were observed in both the AMPA and the NMDA receptor-mediated components (Randic et al., 1993).

In addition to the activity dependent plasticity, the dorsal horn shows intrinsic plasticity, which means long-lasting changes in membrane excitability (Sandkühler, 2009), resulting from continuous noxious stimulation. This could alter the active and passive membrane properties regulating the input-output relationship of neurons (Sandkühler, 2009).

1.5.5. PolySia in the dorsal horn

Within the dorsal horn, a dense intercellular staining of polySia was reported filling the neuropil in bundles of fine fibres and on cell membranes in the superficial laminae (lamina I and II) (Seki and Arai, 1993b, El Maarouf et al., 2005, Bonfanti et al., 1992), but also on some fibres terminating in the lamina III (El Maarouf et al., 2005). The localization of polySia with regard to primary afferents, interneurons, and projection neurons are not well understood. The polySia positive cells in lamina II were considered interneurons only based on their localization, size, and shape and

length of their immunolabelled fibres without any double labelling with interneuron markers (El Maarouf et al., 2005). The C fibre presynaptic elements were reported to lack polySia based on double labelling of polySia and fluorescent wheat germ agglutinin, used to label projections of C fibres to lamina II of dorsal spinal cord, suggesting that polySia is expressed on the targets for C fibres but not on the C fibre presynaptic elements.

Removal of polySia from the spinal cord of healthy mice via intrathecal injection of endoN did not alter function measured as thermal or mechanical sensitivity (El Maarouf et al., 2005). Thus, the role of polySia in the dorsal horn of the spinal cord under normal conditions is unknown. Under conditions of chronic injury and pain, nociceptive C terminals in lamina II are lost leading to a reduced thermal hyperalgesia. Interestingly, experimental removal of polySia with endoN in a mouse model of neuropathic pain prevented this loss of nociceptive C fibres exacerbating hyperalgesia which was maintained for weeks (El Maarouf et al., 2005). This suggests that following injury, polySia may inhibit NCAM's actions to alleviate thermal hyperalgesia, even though mechanical hyperalgesia was not altered further suggesting an association only with specific types of afferent input (C fibres).

Unilateral cervical dorsal rhizotomy (cutting dorsal rootlets carrying sensory input) led to the expression of polySia in laminae III–IX of the adult rat spinal cord 24 h after lesion. polySia-ir appeared in neurons scattered in laminae III–IX, both ipsi- and contralateral to lesion, which was followed by later immunoreactivity in activated astrocytes of the grey matter and dorsal funiculus ipsilateral to the lesion (Bonfanti et al., 1996). Similarly, six weeks after dorsal column transection followed by injection of lentiviral virus encoding GFP, a moderate increase in polySia-ir around the lesion cavity was observed that was associated with a subpopulation of $GFAP^+$ astrocytes (Zhang et al., 2007a).

These data warrant further investigation to explain what polySia does under control conditions and the cellular mechanisms or mediators it modifies under conditions of 'wind up" in order to understand the impact of this sugar in altering neurotransmission in the CNS. Furthermore, nothing is known about potential interacting partners of polySia in the spinal cord.

1.6. The trigeminal ganglion and spinal trigeminal nucleus

The sensory information including mechanical, thermal, chemical, and proprioceptive information from orofacial structures (most of the head, including the face and teeth) is conveyed to the

trigeminal nuclei in the brainstem through the trigeminal nerve (Figure 1.8A) (Iwata et al., 2011, Bereiter et al., 2000, Hanani, 2005). This nerve has three peripheral branches: the ophthalmic, maxillary, and mandibular divisions. The first two divisions are purely sensory, while the mandibular division is both motor and sensory. These branches converge within the posterior aspect of the cavernous sinus forming the sensory trigeminal ganglion (Figure 1.8A-C) (Iwata et al., 2011).

The trigeminal (semilunar or Gasserian) ganglion (TG) is the sensory ganglion of the trigeminal nerve containing the cell bodies of most trigeminal primary afferents of the three divisions of the trigeminal nerve and is situated at the base of the brain (Figure 1.8B and C) (Kapila et al., 1984, Sessle, 2005a). Apart from cell bodies, the TG contains associated nerve fibres as well as fibres originating from cells elsewhere that pass through or terminate within the ganglion (Lazarov, 2002). Three discrete categories of TG neurons based on cell size include small cells (20–30 µm) related to cutaneous branches, medium-sized cells (30–50 µm) related to corneal afferents, and large-sized cells (50–80 µm) related to oral and perioral branches, including the tooth pulp (Marfurt, 1981, Sugimoto et al., 1986). TG neurons have been further classified to Aα/β, Aδ, and

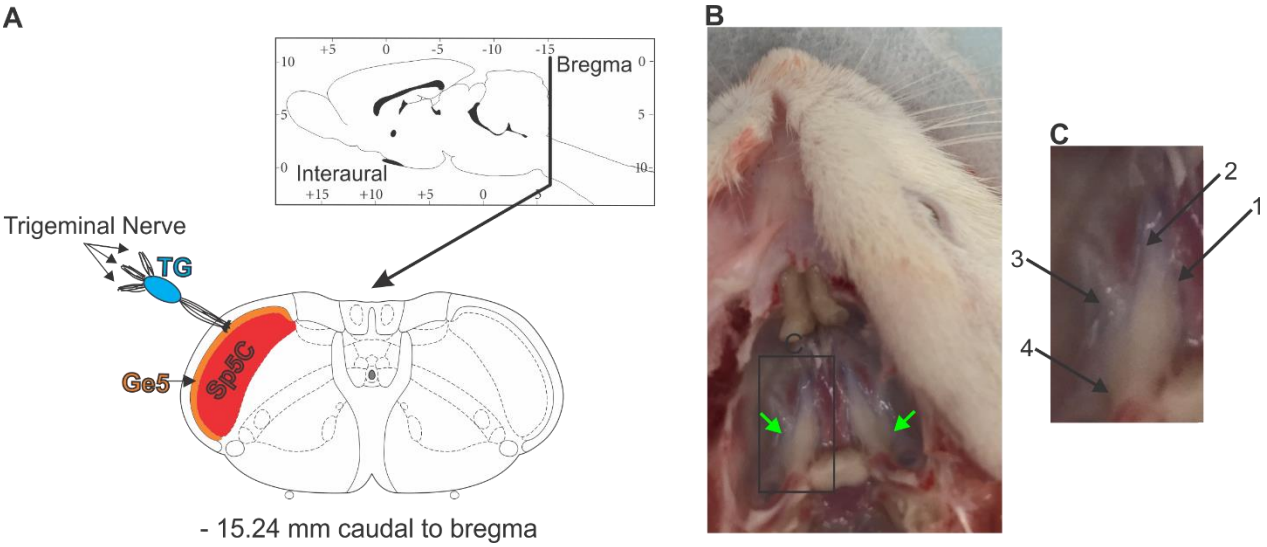

Figure 1.8. The trigeminal ganglion and spinal trigeminal nucleus. (A) A coronal section of the brainstem showing the location of trigeminal ganglion (TG; blue), the spinal trigeminal nucleus caudalis (Sp5C; red and orange), and gelatinous layer of the caudal spinal trigeminal nucleus (Ge5; orange). (B) shows a dorsal view of the rat skull following the bone and brain removal to display the location of the trigeminal ganglion (green arrows). (C) The magnified image of the box indicated in B demonstrating the location of 3 divisions of the trigeminal ganglion. Arrows 1 and 2 show ophthalmic and maxillary branches respectively, while arrow 3 points to the cell bodies of the primary afferent neurons with axons in the mandibular division. Arrow 4 points to the trigeminal nerve root heading towards the brainstem.

C fibres (for review see (Dubner and Bennett, 1983)). The medium- to large-sized TG neurons have conduction velocities in the Aβ and Aδ groups, representing low-threshold mechanoreceptors (the Aβ category) and low-threshold mechanoreceptors, thermoreceptors, and nociceptors (the Aδ category). The small ganglion cells with a conduction velocity matching the C category are thought to be nociceptive (Lawson, 1992). Trigeminal nerve injury or orofacial inflammation alters the excitability and molecular expression of TG neurons, which in turn changes information processing in their innervating neurons and therefore causes hypersensitivities to nociception (Takeda et al., 2005, Takeda et al., 2006, Takeda et al., 2011).

TG somata are surrounded by an envelope of satellite glial cells (SGCs) (Lazarov, 2002, Hanani, 2005). SGCs directly affect neuronal activity by regulating the microenvironment in the ganglion (Hanani, 2005, Pannese et al., 2003). There is an increasing number of studies suggesting that SGCs may play an important role in orofacial sensory disorders following trigeminal nerve injury or orofacial inflammation (Takeda et al., 2011, K. Gunjigake et al., 2009, Katagiri et al., 2012, Takeda et al., 2009).

Sensory information is conveyed by the central axonal branches of TG neurons to the brainstem, where they ascend or descend in the trigeminal spinal tract, and then enter the trigeminal brainstem sensory nuclear complex (Sessle, 1987, Sessle, 2005a), composed of the main sensory nucleus and the spinal trigeminal nucleus (Sessle, 2000). The spinal trigeminal nucleus is a long nucleus extending down from the pons to the spinal cord as far as the second cervical root ultimately merging with the lamina II of the spinal cord (Grant, 2005). It is subdivided into three subnuclei from rostral to caudal: oralis, interpolaris, and caudalis. The focus in this thesis is the spinal trigeminal nucleus caudalis (Sp5C) (Figure 1.8A).

The Sp5C extends from the obex to the first cervical root and merges with the dorsal horn. This nucleus, which is regarded an upward extension of the dorsal horn, has several morphologically distinct classes of neurons and a laminated structure similar to that of the dorsal horn of the spinal cord (Sessle, 2000, Gobel et al., 1981, Bereiter et al., 2000, Sessle, 1987). It is divided into three regions: subnucleus marginalis corresponding to lamina I of the spinal cord dorsal horn, subnucleus gelatinosus corresponding to laminae II and III (Figure 1.8A), and subnuclei magnocellularis (lamina IV) (Grant, 2005). Most C and Aδ fibres from different craniofacial tissues terminate in Sp5C (Tashiro et al., 1984, Sessle, 2000, Pajot et al., 2000, DaSilva and DosSantos, 2012). Afferent

fibres are arranged dorsoventrally within the spinal tract, with all three trigeminal nerve divisions innervating the Sp5C (Shigenaga et al., 1986, Grant, 2005, Haines, 2015).

The signals from second-order neurons of the Sp5C are relayed to the somatosensory cortex through the thalamus (Lazarov, 2002, Sessle, 2005a). The subnucleus caudalis has been implicated in orofacial nociceptive mechanisms on the basis of clinical, behavioural, anatomical, immunocytochemical, and electrophysiological findings (for review see (Dubner and Bennett, 1983, Sessle, 2000, Sessle, 2005b, Bereiter et al., 2000)).

1.6.1. PolySia in the trigeminal ganglion and spinal trigeminal nucleus

In the adult human TG, polySia expression was detected in neuronal perikarya, nerve fibres, pericellular networks, and satellite and Schwann cells. Intense cytoplasmic staining and positive pericellular fibre networks were also reported. Positive neurons were mostly small- and medium-sized, accounting for almost 6% of the total ganglionic population (Quartu et al., 2008).

PolySia-ir in the trigeminal nucleus of the adult human was found restricted to the substantia gelatinosa of Sp5C on the surface of neuronal cell bodies and processes (Quartu et al., 2008). PolySia distribution is not described in the TG or Sp5C of any other species to our knowledge. Furthermore, nothing is known regarding partners and function of polySia in these regions.

1.7. The rostral ventrolateral medulla

The rostral ventrolateral medulla (RVLM) in the rat is located in the medulla of the brainstem ventral to the nucleus ambiguus, lateral to the inferior olive, medial to the spinal trigeminal tract, and caudal and ventral to the inferior pole of facial nucleus, within the region about 1 mm caudal to the facial nucleus (Figure 1.9) (Goodchild and Moon, 2009). The RVLM lies immediately adjacent to major sites generating and maintaining respiratory rhythm and depth known as the pre-Bötzinger and Bötzinger regions (Stornetta et al., 2003, Kanjhan et al., 1995). Other neurons play a role in sensory and motor control (Stornetta et al., 2013, Ludlow, 2015). The RVLM plays a crucial role in the tonic and reflex regulation of arterial blood pressure (AP) and sympathetic vasomotor tone. Inhibition of cells on the surface of the brain overlying the RVLM in anaesthetized animals with GABA or glycine resulted in a significant fall in blood pressure (Feldberg and Guertzenstein, 1976, Guertzenstein and Silver, 1974). Using stereotaxic mapping, chemical inhibition of the RVLM in anaesthetized animals generated falls in blood pressure and sympathetic

nerve activity (SNA) (Ross et al., 1984, Willette et al., 1983b). In contrast, excitation of the RVLM by electrical or chemical stimulation caused profound increases in the blood pressure and the SNA innervating cardiovascular organs including blood vessels, heart, and adrenal medulla (Ross et al., 1984, Willette et al., 1983a, Goodchild et al., 1982, McAllen, 1986). These data suggest neurons within the RVLM set and maintain the level of sympathetic nerve activity which sets the level of blood pressure.

1.7.1. The RVLM neurons

The RVLM neurons, crucial for the generation of sympathetic tone, project to sympathetic preganglionic neurons (SPNs) and demonstrate a discharge pattern very similar to that of SPNs (Dampney, 1994b, Spyer, 1994, Sun, 1996). The activity of these cells, called 'RVLM presympathetic neurons' correlated with that of sympathetic nerves using techniques such as spike-triggered averaging or coherence analysis (Montano et al., 1996, Barman and Gebber, 1997). Extracellular recording of these bulbospinal neurons showed that these neurons were spontaneously active with a basal activity, found to be inversely correlated to blood pressure and acutely sensitive to pharmacologically stimulated changes in AP (Brown and Guyenet, 1984, Brown and Guyenet, 1985). These barosensitive neurons are mainly found at the rostral pole of the RVLM (Verberne et al., 1999b). The bulbospinal neurons of the RVLM are excitatory neurons, as most express mRNA for VGLUT2 (Stornetta et al., 2002, Stornetta and Guyenet, 1999) and therefore it is believed that their sympathoexcitatory effect is mainly mediated by glutamatergic transmission (Deuchars et al., 1995, Morrison, 2003). A group of bulbospinal neurons, accounting for approximately 70% of the

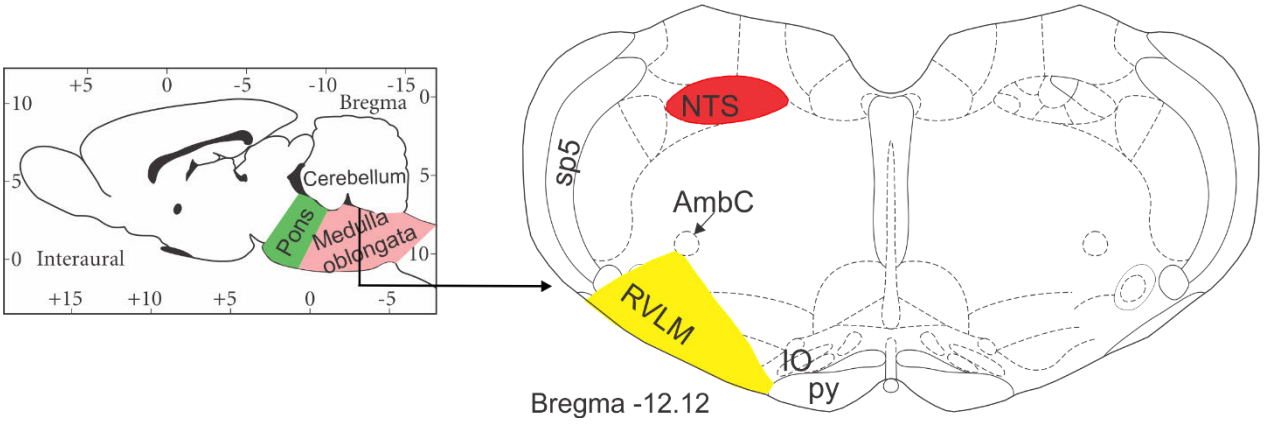

Figure 1.9. The rostral ventrolateral medulla (RVLM). A coronal section of the rat brainstem showing the location of the RVLM. AmbC, ambiguus nucleus, compact part; IO, inferior olive; NTS, nucleus of solitary tract; py, pyramidal tract; Sp5, spinal trigeminal tract.

RVLM bulbospinal neurons are C1 neurons. These neurons that have the capacity to synthesize adrenaline (Phillips et al., 2001) occupy the region that spatially overlaps with the RVLM pressor area (Schreihofer and Guyenet, 1997, Schreihofer et al., 2000, Guyenet, 2006, Sartor and Verberne, 2003). Optogenetic activation of C1 neurons generates a sympathoexcitatory effect (Abbott et al., 2009) suggesting they significantly contribute to the regulation of the blood pressure (for review see (Guyenet et al., 2013)). Although targeted stimulation of C1 neurons of the RVLM led to the marginal increase in the blood pressure (Abbott et al., 2009), selective neurotoxic lesions of the C1 cells with saporin conjugates (Madden et al., 2006, Madden and Sved, 2003) showed that the activity of C1 neurons are not essential for setting basal blood pressure indicating that non-C1 (non-catecholaminergic presympathetic) neurons of the RVLM may be sufficient to maintain basal sympathetic tone and blood pressure.

1.7.2. The RVLM and blood pressure control

Acute changes in arterial blood pressure are detected by baroreceptors on the wall of the aortic arch and carotid sinus (McMullan et al., 2009). Baroreceptor afferents drive second-order excitatory neurons of the NTS (Zhang and Mifflin, 1998) that send excitatory input to GABAergic neurons of the caudal ventrolateral medulla (CVLM) (Schreihofer and Guyenet, 2002, Bailey et al., 2006). GABAergic neurons in the CVLM drive inhibitory input to RVLM neurons leading to important baroreflex-mediated changes in presympathetic RVLM neuronal activity, SNA and AP (Verberne et al., 1999b, Schreihofer and Guyenet, 1997, Schreihofer and Guyenet, 2003, Schreihofer and Guyenet, 2002). C1 neurons participate in baroreflex mediated function (Madden et al., 2006, Schreihofer et al., 2000).

1.7.3. The RVLM and hypoxia

Hypoxia stimulates reflex changes in respiration (increased ventilation) and sympathetic activity to increase blood oxygen levels and re-distribute blood flow and thus protect vital organs such as brain, heart, and kidneys. The sympathetic adjustments generated by acute mild hypoxia (sympathetic chemoreflex) are initiated by activation of arterial chemoreceptors located in the carotid and aortic bodies while severe hypoxia also has a direct effect on the brainstem (Chalmers et al., 1967, Sun and Reis, 1994, Downing et al., 1963, Fukuda et al., 1989). Peripheral chemoreceptor activation by carotid sinus stimulation or intra-arterial cyanide showed profound activation of vertebral, splanchnic, lumbar, and renal SNA (Koganezawa and Terui, 2007,

Miyawaki et al., 1996), whereas cardiac SNA was depressed (Koganezawa and Terui, 2007, Kollai et al., 1978). In both cases (acute mild and severe hypoxia), the RVLM plays an important role in the responses generated. Most RVLM bulbospinal barosensitive neurons demonstrate strong activation as a result of carotid body stimulation (cyanide or brief hypoxia) (Reis et al., 1994, Koshiya et al., 1993, Sun, 1996). In line with this observation, the vast majority of C1 neurons express Fos in conscious mammals exposed to hypoxia (Erickson and Millhorn, 1994, Hirooka et al., 1997), while the sympathoexcitatory response caused by carotid body stimulation is blocked after selective lesions of the C1 neurons (Schreihofer and Guyenet, 2000).

Cerebral ischemia can lead to a neurogenic increase in AP. This increase is independent of the carotid bodies and is largely mediated by the activation of the barosensitive neurons of the RVLM; however, it is accepted that at some point all neurons are sensitive to hypoxia (Dampney and Moon, 1980, Sun and Reis, 1994, Dampney et al., 1979).

In addition to being sensitive to baroreceptor and chemoreceptor reflexes, bulbospinal neurons of the RVLM are sensitive to other stimuli such as hypercapnia (Koganezawa and Paton, 2014, Koshiya et al., 1993, Wakai et al., 2015), somatosympathetic reflexes (Shahid et al., 2012), glucoprivation (Verberne and Sartor, 2010), osmolarity (Stocker et al., 2008), temperature (McAllen and May, 1994), and body position (Sugiyama et al., 2011). However, C1 neurons may not be crucial in the cardiovascular response to hypercapnia (Wenker et al., 2017, Marina et al., 2011).

1.7.4. Synaptic input to the RVLM

The main sources of synaptic input to RVLM presympathetic neurons include the CVLM, area postrema, the NTS, dorsal motor nucleus of vagus, midline raphe, caudal midline medulla, retrotrapezoid nucleus, the lateral parabrachial nucleus, cuneiform nucleus, the Kolliker-Fuse nucleus, lateral periaqueductal grey, and multiple hypothalamic nuclei (such as paraventricular nucleus) (Dampney et al., 1987, Carrive et al., 1988, Koshiya and Guyenet, 1996, Horiuchi et al., 1999, Sun and Spyer, 1991, Verberne et al., 1999a, Potas and Dampney, 2003, Dempsey et al., 2017).

Currently, only the CVLM (Schreihofer and Guyenet, 2002, Sved et al., 2000) and caudal pressor area (Horiuchi and Dampney, 2002) are known to provide tonic inhibitory input to the RVLM neurons.

1.7.5. Axonal projection of RVLM neurons

Retrograde tracing experiments (Ross et al., 1981, Goodchild et al., 1984, Blessing et al., 1981) and antidromic activation of RVLM neurons (Lipski et al., 1995, Lipski, 1981, Brown and Guyenet, 1985) demonstrated that many RVLM neurons project to the intermediolateral cell column of the thoracic spinal cord. Barosensitive presympathetic RVLM neurons innervate vasoconstrictor SPNs monosynaptically in the thoracic and lumbar spinal cord (Strack et al., 1989, Oshima et al., 2008).

The RVLM also contains neurons, concentrated in the caudal half of the RVLM (600-800 μm behind facial nucleus), projecting to higher brain regions including the paraventricular and supraoptic nucleus of the hypothalamus and amygdala (Sawchenko and Swanson, 1982, Petrov et al., 1993, Tucker et al., 1987, Verberne et al., 1999b).

1.7.6. PolySia in the RVLM

PolySia expression in the RVLM was not specifically described by studies investigating polySia expression within the brainstem of human (Quartu et al., 2008) or rat (Bonfanti et al., 1992, Seki and Arai, 1993a), thus is presumed to express little if any polySia.

1.8. Aims of this thesis

The expression of polySia is restricted to specific areas of the adult CNS. Unlike many studies performed on higher brain regions, far less attention has been paid to the distribution and functions of this sugar within the brainstem, spinal cord, and peripheral ganglia. Therefore, our initial aim (**Chapter 2**) was to investigate the distribution of polySia within the brainstem, spinal cord, and TG of the adult rat, one of the most commonly used rodent research models. The relationship of polySia with different cell types (neurons, astrocytes, and oligodendrocytes) in three sensory regions that we found to show high polySia expression was studied. The association of polySia with a) primary afferents and interneurons and b) presynaptic elements in the dorsal horn was explored. In the TG, the association of polySia with neurons, satellite glial cells, and Schwann cells was examined. Then, the distribution of polySia in the adult rat brainstem and spinal cord was compared with that of the adult mouse, another commonly used rodent research model, especially as the use of genetically engineered mice is becoming commonplace (Vandamme, 2014). In the final part of this chapter, polySia expression was compared using two most commonly used polySia antibodies, mAb 735 and mAb 5324.

Despite the high expression of polySia in some regions of the spinal cord such as the dorsal horn or brainstem such as the Sp5C, few studies have investigated its function within these areas, and no study has looked for interacting partners of the glycan. This is important as this information may assist us with identifying functions associated with polySia. Thus our second aim (**Chapter 3**) was to identify interacting partners of polySia within the dorsal horn of the adult rat utilising co-immunoprecipitation combined with western blotting and/or mass spectrometry and confocal microscopy. We then investigated whether these binding partners were limited to the dorsal horn or were common in different regions including the intermediolateral cell column of the spinal cord and the Sp5C of the brainstem. Finally, we sought to determine whether these interacting partners were species specific by examining whether similar partners with polySia could be identified in the mouse dorsal horn.

PolySia removal by enzymatic treatment or genetic knockout has been used to study functions modified *in vivo* and *in vitro*, mainly performed on higher order brain regions. Likewise, in our laboratory, removal of polySia from the NTS, where second-order neurons receive visceral afferent sensory input from stretch receptors of the aortic arch and carotid sinus, via endoN microinjection resulted in sympathoexcitation (Bokiniec et al., 2017). The information from the NTS is transmitted to the RVLM to mediate excitatory reflex responses and the level of vasomotor tone, but the level of polySia expression is low (see Chapter 2). We sought to determine whether overexpression of polySia would alter functions dictated by the NTS and RVLM. Therefore, we used a lentiviral vector in the NTS and RVLM neurons (**Chapter 4**) to drive the expression of ST8SiaIV, the main enzyme responsible for polySia synthesis in the adult mammals. Then, we examined the effects of polySia overexpression in the cardiorespiratory functions generated by the RVLM.

Finally, in **Chapter 5**, we summarized the major findings of the studies described and provided ideas for future studies.

Chapter 2 : Polysialic acid distribution within the spinal cord, brainstem, and trigeminal ganglion

Abstract

Polysialic acid (polySia), a large cell surface glycan widely expressed in the developing nervous system, exhibits a discrete expression pattern within the adult brain, often associated with sites showing plasticity. The expression and cellular localization of polySia is commonly described in higher brain regions of the adult rat and mouse whereas limited evidence regarding its distribution in the other regions of the central nervous system and in the peripheral nervous system is available. Therefore, the aims were to examine the distribution and cellular localization of polySia in the adult rat brainstem, spinal cord, and trigeminal ganglion and then compare these with the adult mouse using immunohistochemistry and confocal microscopy. Finally, we compared the distribution of labelling using two commonly used polySia antibodies–mAb 735 and mAb 5324.

Our results demonstrate numerous, yet specific sites expressing polySia immunoreactivity (ir) throughout the rodent brainstem. We extended the previous findings describing polySia-ir in the spinal cord by demonstrating polySia labelling also in the intermediolateral cell column around many sympathetic preganglionic neurons and further described polySia expression in the trigeminal ganglion of the adult rat. We found that polySia-ir was not localized with large astrocytic processes or oligodendrocytes in the spinal trigeminal nucleus, the nucleus of solitary tract, and the spinal cord, while it was found associated mainly with neurons and fine astrocytic processes, confirmed by ultrastructural analyses. Within the spinal cord dorsal horn, some inhibitory neurons showed polySia-ir, whereas calcitonin gene-related peptide (CGRP) expressing primary afferent fibres were not associated with polySia-ir. Comparing the expression of polySia in rats and mice demonstrated mostly common patterns with only a few regions such as the spinal cord dorsal horn differing between species. Moreover, similar distributions of polySia-ir was found for both antibodies in most regions evaluated.

2.1. Introduction

Polysialic acid (polySia) is a large cell surface glycan mainly found as a post-translational modification of the neural cell adhesion molecule (NCAM) in the mammalian brain (Hildebrandt et al. 2008). Due to its large hydrated volume, polySia can produce a physical hindrance between apposing cell membranes thus weakening intercellular adhesion (Rutishauser, 2008, Johnson et al., 2005). PolySia is abundantly expressed in the developing nervous system (Sunshine et al., 1987), where it is involved in neuronal migration, nerve branching and fasciculation (Landmesser et al., 1990, Doherty et al., 1990), synaptogenesis, and plasticity (Kiss and Rougon, 1997, El Maarouf and Rutishauser, 2003). In the adult brain, polySia expression is significantly reduced, although discrete expression patterns have been found in specific areas of the central nervous system (such as the olfactory cortex, hippocampus, and hypothalamus) postulated to retain neurogenic capacity or maintain a capability for plasticity throughout life (Rutishauser, 2008, Bonfanti, 2006, Seki and Arai, 1993a). Studies in the adult brain have focused mainly on the localization and distribution of polySia in higher brain regions such as the cerebral cortex (Miragall et al., 1988, Aaron and Chesselet, 1989, Seki and Arai, 1993c, Theodosis et al., 1991, Chung et al., 1991, Kiss et al., 1993, Dhúill et al., 1999) where altered expression of the sugar is associated with altered learning and memory (Becker et al., 1996, Fox et al., 2000), chronic stress (Pham et al., 2003, Sandi et al., 2003), and neuropathological conditions such as schizophrenia (Barbeau et al., 1995), epilepsy (Mikkonen et al., 1998), and Alzheimer's disease (Mikkonen et al., 1999). The distribution of polySia in the brainstem and spinal cord has been briefly described only using an antibody against polySia attached to NCAM (anti-Men B; mAb 5324) in rat (Bonfanti et al., 1992, Seki and Arai, 1993b, Seki and Arai, 1993a) and human (brainstem only) (Quartu et al., 2010, Quartu et al., 2008). Detailed descriptions of the expression of the sugar in the rat and mouse lower brain regions are very limited.

In addition, the cellular and subcellular localization of polySia in the brainstem and spinal cord remain poorly understood. In some higher brain regions of the adult such as in cerebral cortex and medial prefrontal cortex, virtually all polySia labelled cells studied were reported to be mature neurons (Varea et al., 2005, Varea et al., 2007, Gómez-Climent et al., 2011) with a considerable proportion reported to be inhibitory interneurons (Gilabert-Juan et al., 2011, Varea et al., 2012, Varea et al., 2007). Moreover, in some forebrain regions, polySia is associated with immature

neurons (Gómez-Climent et al., 2008, Gomez-Climent et al., 2010). While most astrocytes appear to not express polySia under normal conditions, polysialylated astrocytes have been found in some brain regions including the highly specialized hypothalamo-neurohypophysial system (Theodosis and Poulain, 1993).

The first aim of this chapter was to describe the distribution and cellular localization of polySia in the brainstem, spinal cord, and primary sensory neurons, specifically those of the trigeminal ganglion, of the adult rat using the monoclonal antibody 735 directed against polySia (mAb 735). We then compared the distribution of polySia immunoreactivity (ir) in the brainstem and spinal cord of the adult rat and adult mouse. Finally, we compared the distribution of immunoreactivity using mAb 735 with that of the only commercially available polySia antibody, mAb 5324. The study has been performed using immunohistochemistry combined with confocal microscopy, electron microscopy, and western blotting.

2.2. Materials and methods

2.2.1. Animals

All experimental procedures were approved by the Macquarie University Animal Ethics Committee (reference number ARA 2014/041 and 2015/040) and conducted in accordance with the Australian Code of Practice for the Care and Use of Animals for Scientific Purposes. Experiments were performed on male Sprague Dawley rats (14–20 weeks old) and male C57BL/6J mice (8-12 weeks old) from the Animal Resources Centre, Perth, Western Australia.

2.2.2. Antibodies

Table 2.1 details the antibodies used. Endosialidase N (endoN) and mAb 735 were kindly provided by Professor Rita Gerardy-Schahn (Hannover Medical School, Hannover, Germany) with all other antibodies commercially sourced as indicated.

2.2.3. Tissue collection for western blotting

The method used was adapted from our previous work (Bokiniec et al., 2017). Animals were deeply anaesthetized using sodium pentobarbitone (80mg/kg). When reflex testing of corneal and paw withdrawal to pain evoked no response, the heart was punctured and the brain, spinal cord, and trigeminal ganglia were removed as rapidly as possible (brain within 3-4 min and the spinal cord within 7-9 min). These tissues were then placed in ice cold cryoprotectant solution (876 mM sucrose, 500 µm polyvinylpyrrolidone, 76.7 mM Na_2HPO_4, 26.6 mM NaH_2PO_4, 5mM ethylene glycol) and were cooled on dry ice before being transferred to a -80 C degree freezer for preservation until dissection. The brain and spinal cord were dissected into 2 mm coronal segments on dry ice using a brain matrix or manual cutting. The spinal cord was dissected such that the dorsal section containing laminae I-IV of the dorsal horn was isolated. Similarly, the trigeminal nucleus caudalis (Sp5C) and adjacent regions were isolated. To extract the brain region containing the nucleus of solitary tract (NTS), a 2 mm rostrocaudal region of the brainstem was isolated as described previously (Damanhuri et al., 2012). Care was taken not to allow the tissue to defrost during dissection.

Table 2.1. Details of primary and secondary antibodies used.

Primary antibody	**Cat # and Company**	**Species and mono/polyclonal**	**Reference/Publication**	**Dilution**
Anti-Calcitonin Gene-Related Peptide (CGRP)	C8198, Sigma-Aldrich	Rabbit, poly	(Brumovsky et al., 2011)	IHC* 1:12000
Anti-Choline Acetyltransferase (ChAT)	AB144P, Merck Millipore	Goat, poly	(Hinrichs and Llewellyn-Smith, 2009)	IHC 1:1000
Anti-EAAT2	Ab41621, Abcam	Rabbit, poly	(Li et al., 2013)	IHC 1:1000
Anti-GAPDH	Ab9485, Abcam	Rabbit, poly	(Dion et al., 2017)	WB* 1:5000
Anti-Glial Fibrillary Acidic Protein (GFAP)	G9269, Sigma-Aldrich	Rabbit, poly	(Gargini et al., 2007)	IHC 1:500
Anti-Glutamine Synthetase	G2781, Sigma-Aldrich	Rabbit, poly	(Hoehme et al., 2017)	IHC 1:3000
Anti-Myelin Basic Protein (mbp)	ab40390, Abcam	Rabbit, poly	(Makar et al., 2015)	IHC 1:1000
Anti-NeuN [EPR12763] - Neuronal Marker	ab177487, Abcam	Rabbit, mono	(Larsson, 2017) (Luan et al., 2016)	IHC 1:1000 1:2000 for TG sections
Anti-Polysialic Acid-NCAM, clone 2-2B	MAB5324, Merck Millipore	Mouse, mono	(Watzlawik et al., 2015)	IHC 1:1000
Endosialidase N (endoN; 2 mg/ml)	NA	NA		WB 1 µl/40µg protein
Anti-GAD65+GAD67 (0.5 mg/ml)	A01437, GenScript	Rabbit, poly	NA	IHC 1:67
Monoclonal IgG2a antibody 735 against polySia (mAb 735; 2 mg/ml)	NA	Mouse, mono		WB: 1:2000, EM: 1:2000 IHC: 1:4000 slide mounted & 1:16000 free floating sections
Somatostatin Receptor 2A (SSTR2A)	SS-870, Biotrend	Guinea pig, poly	(Bou Farah et al., 2016)	IHC 1:1000
Synaptophysin 1	101 002, Synaptic Systems	Rabbit, poly	(Bhattacharya et al., 2017) (Binotti et al., 2015) (Jahn et al., 1985)	IHC 1:500
Secondary antibody	**Cat # and Company**	**Species**		**Dilution**
Alexa Fluor® 488 AffiniPure Donkey Anti-Rabbit IgG (H+L)	711-545-152, Jackson ImmunoResearch	Donkey		IHC: 1:500
Anti-Mouse IgG (H+L) Secondary Antibody, HRP conjugate	Invitrogen	Goat		WB 1:5000
Anti-Rabbit IgG H&L (HRP)	ab6721, Abcam	Goat		WB 1:3300
Biotin-SP donkey anti-mouse IgG	715-065-150, Jackson ImmunoResearch Laboratories	Donkey		EM: 1:500

Table 2.1. (continued)

Primary antibody	Cat # and Company	Species and mono/polyclonal	Reference/Publication	Dilution
Cy3-conjugated donkey anti-mouse IgG	715-165-151, Jackson ImmunoResearch Laboratories	Mouse		IHC: 1:500 for TG sections
Donkey anti-Goat IgG (H+L) Cross-Adsorbed Secondary Antibody, Alexa Fluor 488	A-11055, Thermo Fisher Scientific	Donkey		IHC 1:500
Donkey anti-Mouse IgG (H+L) Highly Cross-Adsorbed Secondary Antibody, Alexa Fluor 555	A-31570, Thermo Fisher Scientific	Donkey		IHC 1:500
Goat anti-Guinea Pig IgG (H+L) Highly Cross-Adsorbed Secondary Antibody, Alexa Fluor 488	A-11073, , Thermo Fisher Scientific	Goat		IHC 1:500

IHC*; immunohistochemistry, WB*; western blotting

2.2.4. Tissue homogenization and western blotting

The samples were lysed in 10 µl/mg ice cold lysis buffer containing 50 mM Tris-HCl (pH 8), 150 mM NaCl, 4 mM EDTA, 1% (v/v) Triton X-100, and 1% (v/v) protease inhibitor cocktail (Sigma–Aldrich, NSW, Australia). Lysates were homogenized for 3 cycles at 5 speed, each cycle lasting for 20 s using a FastPrep-24 instrument (MP Biomedicals, NSW, Australia). Ceramic beads and detergent insoluble materials were removed by two rounds of centrifugation at 13200 RPM for 5 and 30 min respectively, at 4 °C. Supernatants were collected and protein concentrations were obtained using a BCA (bicinchoninic acid) assay kit according to the manufacturer's instructions (Pierce, Thermo Fisher Scientific, VIC, Australia). For removal of polySia, supernatant fractions containing 40 µg protein were incubated with endoN (1 µg) or neuraminidase α(2→3,6,8,9) (0.001 U/µl in 50 M sodium acetate, pH=5) for 1 h at 37°C. Western blot analysis was carried out as described previously with some modifications (Galuska et al., 2006). In brief, samples (containing 40 µg protein) and Precision Plus Protein Western C standards (Bio-Rad, NSW, Australia) were separated by sodium dodecyl sulphate–polyacrylamide gel electrophoresis (SDS–PAGE) under reducing conditions. Any kD™ Mini-PROTEAN® TGX Stain-Free protein gels (Bio-Rad, NSW, Australia) and 10x Tris/Glycine/SDS running buffer (Bio-Rad, NSW, Australia) were used. Proteins were transferred to a nitrocellulose membrane (Bio-Rad, NSW, Australia) by semi-dry method. The membrane was blocked with 5% (w/v) skim milk in Tris-buffered saline containing 0.1% Tween-20 (TBST, 20 mM Tris-HCl, pH 7.5, 150 mM NaCl, 0.1% (v/v) Tween-20) for 1 h at RT, then washed with TBST, 3×5 min. Membranes were probed with primary antibodies (diluted in 5% (w/v) skim milk in TBST) overnight at 4 °C. This was followed by three washes in TBST (3×5 min), and 1-h room temperature incubation with secondary antibodies. The membranes were washed with TBST, 3×5 min and visualized with enhanced chemiluminescence (ECL) using a Bio-Rad ChemiDoc XRS chemiluminescence detector.

2.2.5. Immunohistochemistry

The method used was adapted from Dempsey et al. (Dempsey et al., 2015). Male rats or mice were deeply anaesthetized using sodium pentobarbital (100 mg/kg i.p). Once pinch failed to elicit a pain withdrawal reflex, rats were perfused transcardially with 400 ml and mice with 30 ml ice-cold Dulbecco's modified Eagle medium (pH 7.4, Sigma-Aldrich, Australia), followed by the same volume of ice-cold 4% paraformaldehyde in 0.1 M phosphate buffer (pH 7.4, Sigma-Aldrich,

Australia). The brains, spinal cords, and trigeminal ganglia were then removed and post-fixed overnight.

2.2.5.1. Slide mounted immunohistochemistry

The post-fixed tissue was then cryoprotected in 30% sucrose in phosphate-buffered saline (PBS) for 24 h and placed in OCT compound (Tissue-Tek®, Sakura Finetek, USA). The tissue was cut using a cryostat (CM1950; Leica, NSW, Australia) into coronal sections 15 µm thick, and mounted onto Superfrost Plus slides (Thermo Fisher Scientific, VIC, Australia). The permeabilization step was performed by incubation with 0.3% (v/v) Triton X-100 in Tris (10 mM)-phosphate (10 mM) buffered saline (TPBS, pH 7.4) for 15 min at RT. Sections were blocked in 10% (v/v) goat or donkey serum or both in TPBS containing 0.3% (v/v) Triton X-100, and then probed with primary antibodies (Table 2.1) overnight at 4 °C, followed by four-hour incubation at RT. As controls, several sections from each sample were incubated without primary antibodies. All sections were then incubated with fluorescently conjugated secondary antibodies overnight at 4 °C. Both primary and secondary incubations were followed by washing with TPBS, 3×15 min. Nuclei were stained using 4,6-diamidino-2- phenylindole (DAPI, #62248, Thermo Fisher Scientific, VIC, Australia). Slides were mounted using Dako Fluorescent mounting medium (Dako, Australia) and analysed using a Zeiss upright microscope (Axio Imager Z.2, Germany) using ZEN 2012 imaging software (Zeiss, Germany). Mosaic images of each coronal spinal cord section were taken at 10x magnification. High power images were captured with a Leica confocal microscope (Leica TCS SP5X; Leica Microsystems, NSW, Australia) using Leica Application Suite Advanced Fluorescence software (LAS AF; Leica, Germany) and analysed using the ImageJ plugin Fiji (Schindelin et al., 2012). Data presented are representative of five independent experiments.

2.2.5.2. Free floating sections

Free floating sections were used to study the distribution of polySia in the adult rat and mouse brainstem using both mAb 735 and mAb 5324. The post-fixed tissue was cryoprotected in cryoprotectant solution (see Section 2.2.3) for 24 h, cut into coronal sections (40 µm thick) using a vibrating microtome (Leica VT 1200S, NSW, Australia). Sections were permeabilized in 50% (v/v) ethanol for 30 min at RT and washed in TPBS (pH 7.4), 3×30 min. Sections were incubated with mAb 735 or mAb 5324 antibody diluted in 10 % (v/v) normal horse serum in TPBS for 48 h at 4 °C. Several sections from each sample were stained without primary antibody to test whether

other detection reagents could cause a signal even if the primary antibody was absent. Sections were washed, 3×30 min and then incubated with a fluorescent conjugated secondary antibody overnight at 4 °C. Sections were washed, 3×30 min with TPBS, mounted onto glass slides using Dako Fluorescent mounting medium (Dako, Australia), and visualized using a Zeiss upright microscope (Axio Imager Z.2, Germany). Mosaic images of each coronal brainstem section were acquired at 10x magnification using ZEN 2012 imaging software (Zeiss, Germany). Data presented are representative of three independent experiments. The level of polySia labelling in different regions of mosaic images was visually classified into very light, light, moderate, and dense.

2.2.6. Electron Microscopy

2.2.6.1. Tissue Processing

The method used was based on that by Llewellyn-Smith et al. (Llewellyn-Smith et al., 2005). Three male Sprague-Dawley rats (8-10 weeks of age) were transcardially perfused under sodium pentobarbital anaesthesia with DMEM/Ham's F12 tissue culture medium (Sigma D-8900; St Louis, MO, USA). This was followed by perfusion fixation with 4% formaldehyde and 0.3% glutaraldehyde (Electron Microscopy Sciences, Hatfield, PA, USA) in 0.1 M phosphate buffer (pH 7.4). The lower percentage of glutaraldehyde, 0.3%, was used to facilitate immunolabelling for polySia. The medulla was dissected from each brain and post-fixed overnight in the same fixative. Coronal sections of 50 µm thickness were cut the following day using a vibrating microtome (Leica VT 1200S, NSW, Australia).

2.2.6.2. Immunohistochemistry

All steps were performed at room temperature with sections undergoing constant agitating. Free-floating sections were permeabilized in 50% ethanol for 3 h and washed in phosphate buffer. Sections were blocked using 10% normal horse serum in phosphate buffer containing 10 mM Tris, 0.9% NaCl and 0.05% merthiolate (TPBSm) for 30 min. They were then incubated with mAb 735 diluted in 10% normal horse serum in TPBSm for 7 days. After washing sections were incubated in biotinylated secondary antibody, diluted in 1% normal horse serum in TPBSm for 4 days. Sections were washed and incubated for a further 4 days in ExtrAvidin-Peroxidase (1:1500, Sigma-Aldrich, #E2886). Immunoreactivity for polySia was revealed by nickel-intensified 3,3'-diaminobenzidine (DAB) reaction using glucose oxidase to determine peroxidase activity as previously described (Llewellyn-Smith et al., 2005). Briefly, sections were washed with TPBSm

and exposed to 1 ml pre-incubation solution for 10 min, with an additional 1 ml of pre-incubation solution containing 2 µl glucose oxidase added to each pot, giving a final glucose oxidase dilution of 1:1000. Sections were reacted for 30 min (or until a strong but specific signal was detected) and halted with several washes with TPBSm. As controls, several sections from each sample were stained without primary antibody. Sections were washed with 0.1 M phosphate buffer, fixed in 0.5% osmium tetroxide for 60 min. After washing with distilled H_2O sections were stained *en bloc* with aqueous uranyl acetate (1%) for 30 min, protected from light. Sections were then dehydrated through graded series of acetone and infiltrated with 1:1 solution of absolute acetone and medium grade EPON resin. This was followed by overnight incubation in 100% resin. Resin was periodically changed over 2 days before sections were flat embedded between glass slides and ACLAR plastic film and polymerized at 60 °C for 48 h. Regions of the lateral trigeminal nucleus were dissected using a scalpel blade and mounted onto flat blank blocks. Ultrathin sections (60 nm) were cut using a diamond knife (Diatome, USA) attached to an ultramicrotome (Ultracut, Leica, Heerbrugg, Switzerland). Sections were then collected onto copper 200 mesh grids. Selected grids were post stained with 2% uranyl acetate followed by Reynold's lead citrate, then imaged using a JEOL transmission electron microscope (JEM-1400, JEOL, Tokyo, Japan). Micrographs were acquired using Digital Micrograph Software (Gatan, USA), and digitally optimized for brightness and contrast using the ImageJ plugin Fiji (Schindelin et al., 2012).

2.3. Results

2.3.1. PolySia distribution within the adult rat CNS using mAb 735 antibody

2.3.1.1. PolySia distribution within the brainstem of the adult rat

The distribution of polySia-ir was examined in the adult rat throughout the medulla oblongata and pons (n=3) from bregma level -15.96 to -9 mm. All polySia positive regions are depicted in Figure 2.1. At all levels examined, the nucleus of solitary tract (NTS), dorsal motor nucleus of vagus (10N), area postrema (AP), and dorsal tegmental nucleus (DTg) showed intense labelling.

In the trigeminal brainstem sensory nuclear complex extending through the medulla and pons, intense polySia-ir was found only in the spinal trigeminal nucleus caudalis (Sp5C) located caudally (bregma -15.96 to 13.92). Labelling was limited to the superficial layer comprising the substantia gelatinosa. Occasional labelling was present within the spinal trigeminal tract (sp5) limited to processes (bregma -14.16 and -13.68 in Figure 2.1).

All polySia labelled regions in the adult rat as well as the relative labelling intensity are shown in Table 2.2.

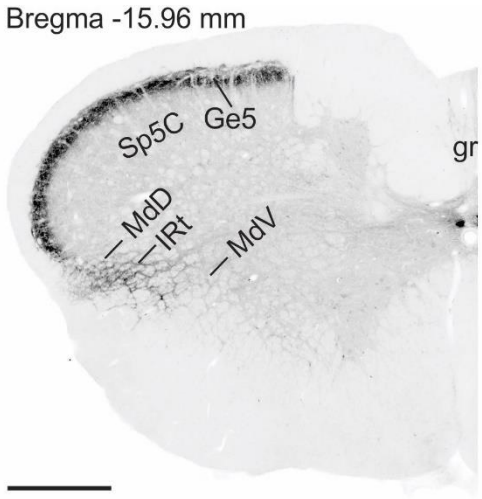
Bregma -15.96 mm
Sp5C
Ge5
gr
MdD
IRt
MdV

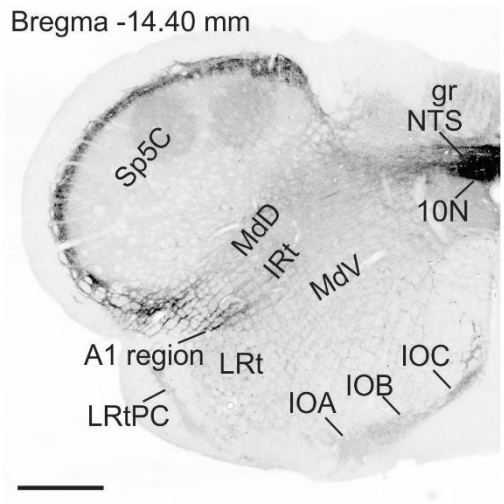
Bregma -14.40 mm
gr
NTS
Sp5C
10N
MdD
IRt
MdV
A1 region
LRt
IOC
IOB
IOA
LRtPC

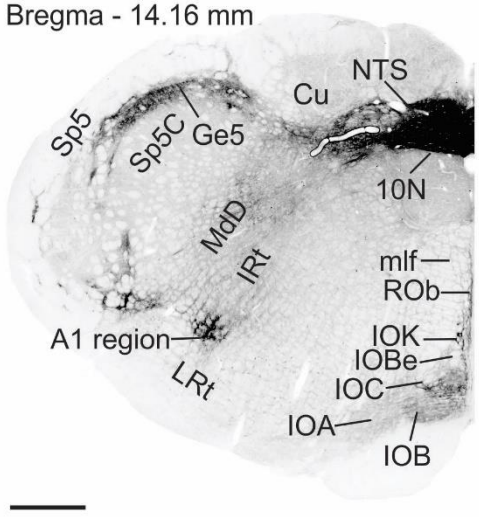
Bregma - 14.16 mm
NTS
Cu
Sp5
Sp5C
Ge5
10N
MdD
IRt
mlf
ROb
A1 region
IOK
IOBe
LRt
IOC
IOA
IOB

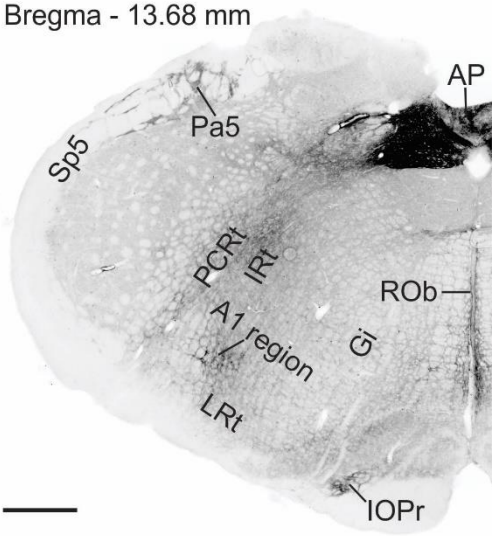
Bregma - 13.68 mm
AP
Pa5
Sp5
PCRt
IRt
ROb
A1 region
Gi
LRt
IOPr

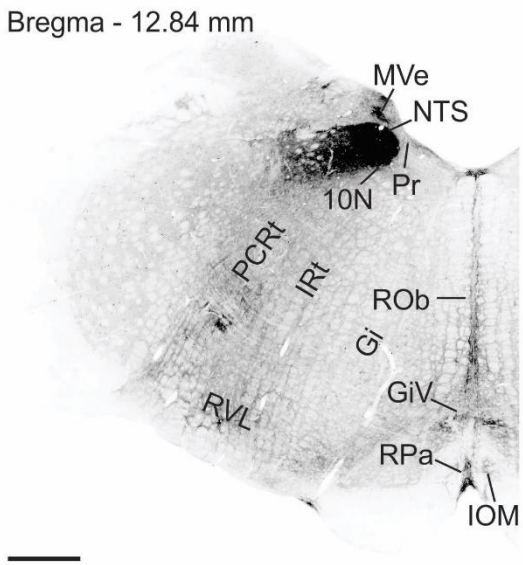
Bregma - 12.84 mm
MVe
NTS
Pr
10N
PCRt
IRt
ROb
Gi
GiV
RVL
RPa
IOM

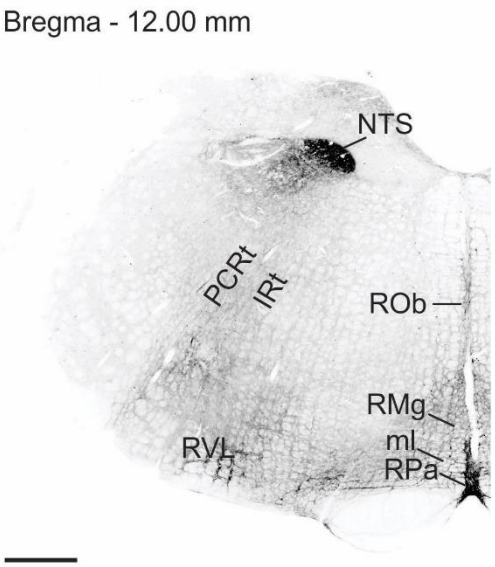
Bregma - 12.00 mm
NTS
PCRt
IRt
ROb
RMg
RVL
ml
RPa

Bregma - 11.76 mm

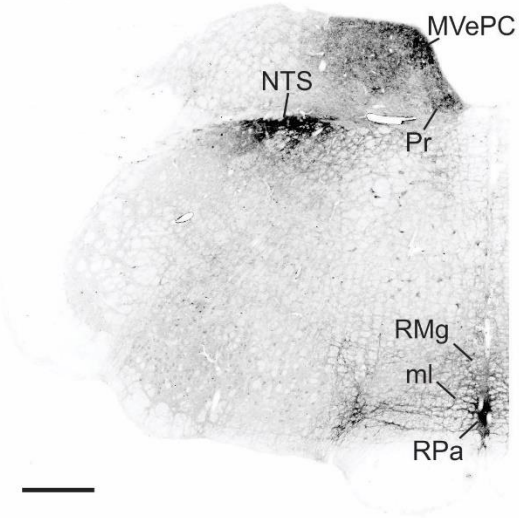

Bregma - 11.04 mm

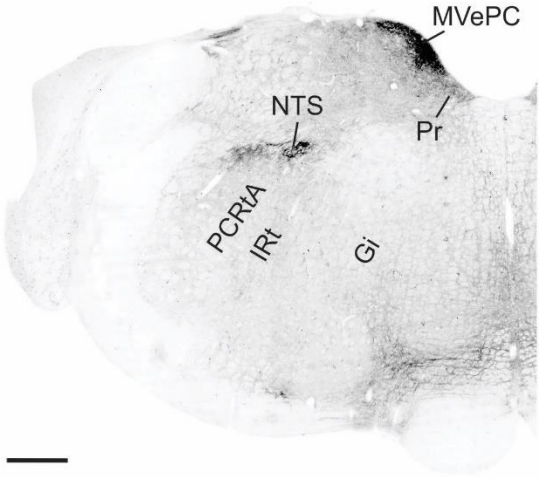

Bregma - 10.68 mm

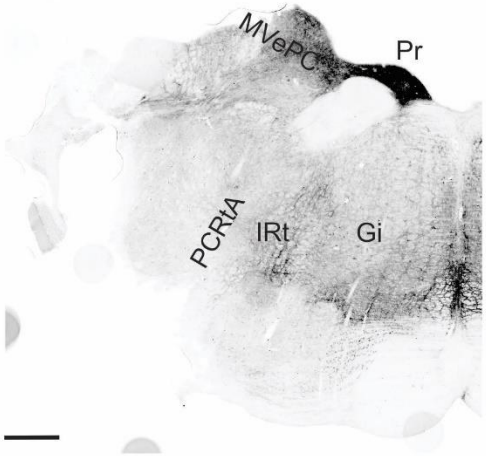

Bregma - 10.32 mm

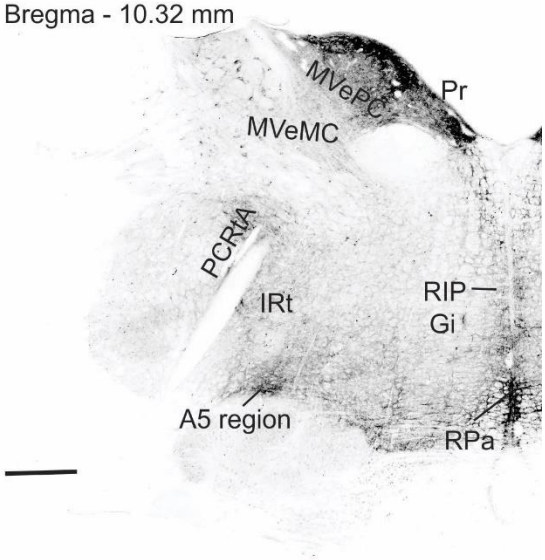

Bregma - 9.60 mm

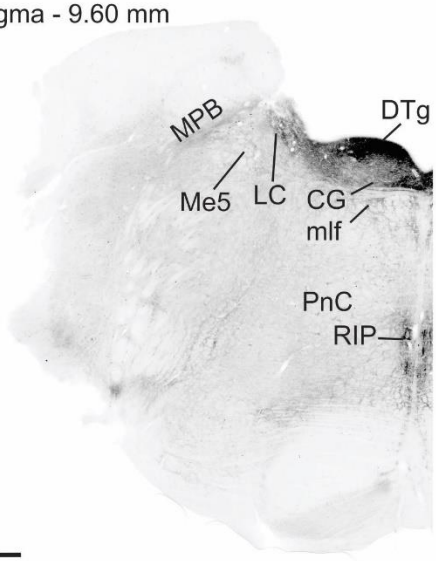

Bregma - 9 mm

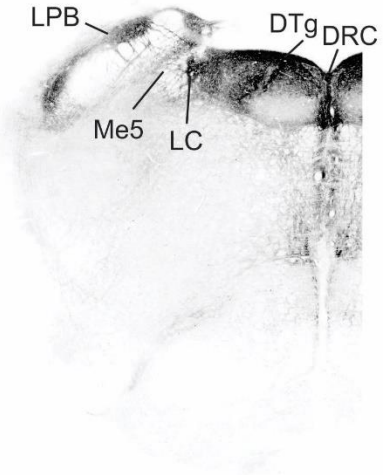

Figure 2.1. PolySia distribution in the adult rat medulla oblongata and pons shown by labelling using mAb 735, bregma levels -15.96 to -9.00 mm. 10N, dorsal motor nucleus of the vagus; AP, area postrema; CG, central grey of pons; Cu, cuneate nucleus; DRC, dorsal raphe nucleus, caudal part; DTg, dorsal tegmental nucleus; Ge5, gelatinous layer of the spinal trigeminal nucleus caudalis; Gi, gigantocellular reticular nucleus; GiV, gigantocellular reticular nucleus, ventral; gr, gracile fasciculus; IOA, inferior olive, subnucleus A of medial nucleus; IOB, inferior olive, subnucleus B of medial nucleus; IOBe, inferior olive, beta subnucleus; IOC, inferior olive, subnucleus C of medial nucleus; IOK, inferior olive, cap of Kooy of the medial nucleus; IOM, inferior olive, medial nucleus; IOPr, inferior olive, principal nucleus; IRt, intermediate reticular nucleus; LC, locus coeruleus; LPB, lateral parabrachial nucleus; LRt, lateral reticular nucleus; LRtPC, lateral reticular nucleus, parvicellular part; MdD, medullary reticular nucleus, dorsal part; MdV, medullary reticular nucleus, ventral part; Me5, mesencephalic trigeminal nucleus; ml, medial lemniscus; mlf, the medial longitudinal fasciculus; MPB, medial parabrachial nucleus; MVe, medial vestibular nucleus; MVeMC, medial vestibular nucleus, magnocellular part; MVePC, medial vestibular nucleus, parvicellular part; NTS, nucleus of solitary tract; Pa5, paratrigeminal nucleus; PCRt, parvicellular reticular nucleus; PCRtA, parvicellular reticular nucleus, alpha part; PnC, pontine reticular nucleus, caudal part; Pr, prepositus nucleus; RIP, raphe interpositus nucleus; RMg, raphe magnus nucleus,; ROb, raphe obscurus nucleus; RPa, raphe pallidus nucleus; RVL, rostroventrolateral reticular nucleus; Sp5, spinal trigeminal tract; Sp5C, spinal trigeminal nucleus caudalis. Scale bars = 500 μm.

Table 2.2. PolySia immunoreactive regions in the adult rat medulla oblongata and pons. *, **, ***, and **** represent very light, light, moderate, and dense labelling. # represents regions showing variable expression levels rostrocaudally - the peak expression is indicated. Bregma indicates the first level in Figure 2.1 that staining appears.

Region	Abbreviation	Intensity	Bregma
The area where the A1 cells are located	A1 region	****#	-14.40
Area postrema	AP	****	-13.68
Cuneate nucleus	Cu	*	-14.16
Central grey of pons	CG	***#	-9.60
Dorsal motor nucleus of vagus	10 N	****	-14.40
Dorsal raphe nucleus	DRC	****	-9.00
Dorsal tegmental nucleus	DTg	****	-9.60
Spinal trigeminal nucleus caudalis-gelatinous layer	Sp5C	****	-15.96
Gigantocellular reticular nucleus	Gi	**#	-13.68
Gigantocellular reticular nucleus, ventral	GiV	**	-12.84
Gracile fasciculus[c]	gr	*#	-15.96
Inferior olive complex	IOA, IOB, IOBe, IOC, IOK, IOM, IOPr	**#	-14.40
Intermediate reticular nucleus	IRt	**	-15.96
Lateral parabrachial nucleus	LPB	**	-9.00
Lateral reticular nucleus	LRt	*	-14.40
Lateral reticular nucleus, parvicellular part	LRtPC	*	-14.40
Locus coeruleus	LC	**	-9.60
Medial lemniscus[c]	ml	*	-12.00
Medial longitudinal fasciculus[c]	mlf	**#	-14.16
Medial parabrachial nucleus	MPB	*	-9.60
Medial vestibular nucleus	MVe, MVePC, MVeMC	****#	-12.84
Medullary reticular nucleus, dorsal	MdD	**#	-15.96
Medullary reticular nucleus, ventral	MdV	*#	-15.96
Mesencephalic trigeminal nucleus	Me5	*##	-9.60
Nucleus of solitary tract	NTS	****	-15.96
Paratrigeminal nucleus	Pa5	*	-13.68
Parvicellular reticular nucleus	PCRt	**	-13.68
Parvicellular reticular nucleus, alpha part	PCRtA	**	-11.04
Pontine reticular nucleus, caudal part	PnC	**#	-9.60
Prepositus nucleus	Pr	****#	-12.84
Raphe nucleus interpositus	RIP	***#	-10.32
Raphe nucleus magnus	RMg	**#	-12.00
Raphe nucleus obscurus	ROb	**#	-14.16
Raphe nucleus pallidus	RPa	****#	-12.84
Rostroventrolateral reticular nucleus	RVL	**#	-12.00
Spinal trigeminal tract[c]	Sp5	*#	-14.16

c indicates regions where polySia-ir was found restricted to some fibres.

2.3.1.1.1. Cellular distribution of labelling in three regions with high polySia abundance

A high expression of polySia was found in several regions (Figure 2.2A), three of which including the nucleus of solitary tract (NTS), gelatinous layer of the spinal trigeminal nucleus caudalis (Sp5C), and the area where the A1 cells were located (A1 region) were further examined using confocal microscopy (Figure 2.2B-D). In all three regions, polySia-ir was found in the neuropil and enveloped somata.

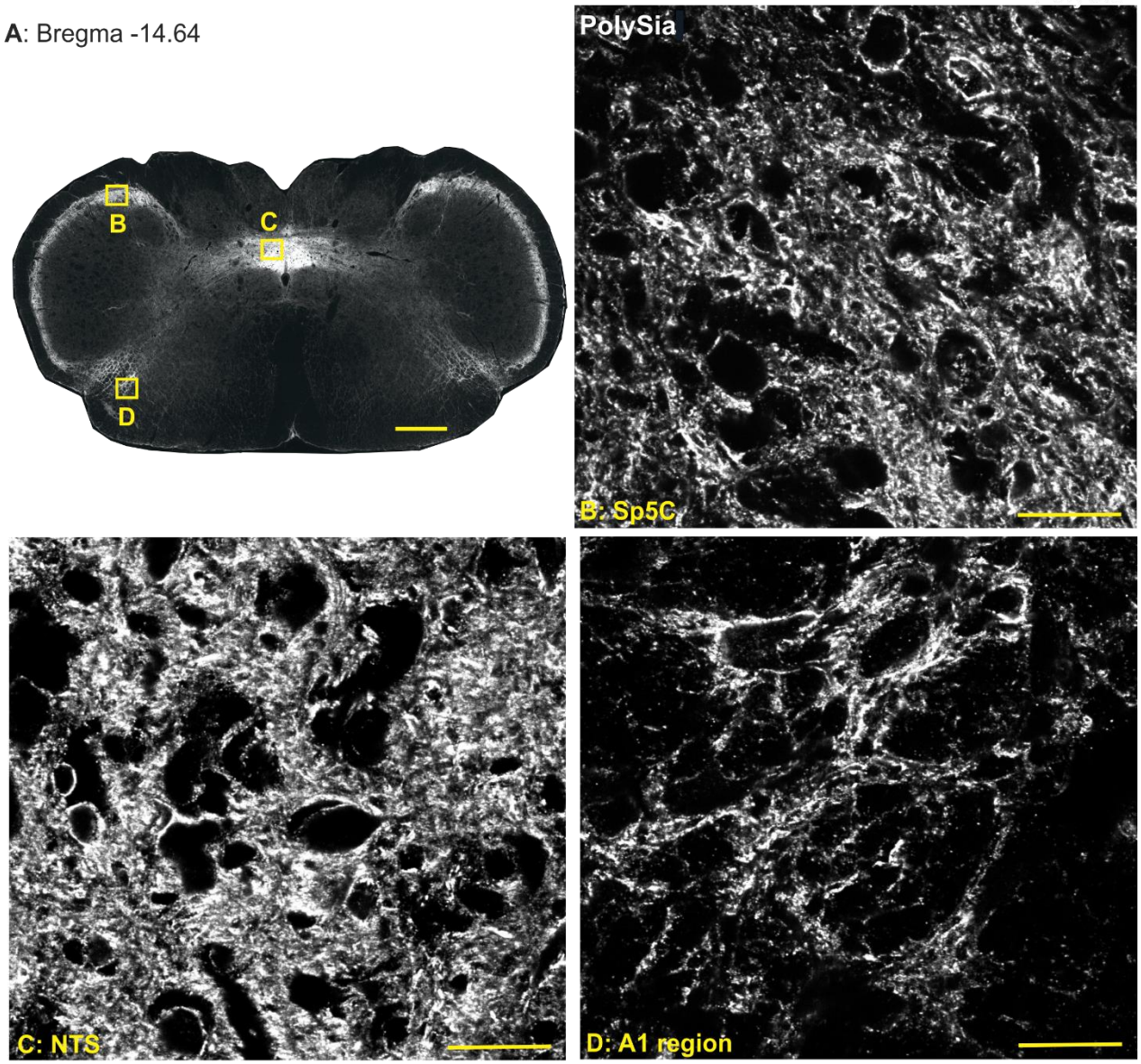

Figure 2.2. PolySia is expressed in neuropil and surrounds cells. (A) A coronal section of the brainstem (bregma -14.64) showing polySia-ir (white). (B, C, and D) are confocal images of boxes in A showing polySia-ir in the spinal trigeminal nucleus caudalis (Sp5C), the nucleus of solitary tract (NTS), and the area where the A1 cells are located (A1 region), respectively. Scale bars = 500 µm in A and = 20 µm in B, C, and D.

2.3.1.2. PolySia distribution within the adult rat spinal cord

Within the spinal cord, polySia-ir was present mainly in the grey matter. The strongest immunoreactivity was found in the superficial laminae of the dorsal horn (DH; Figure 2.3A and B) filling the neuropil between cell bodies and encircling many somata (Figure 2.3B). Such a dense labelling pattern makes it difficult to differentiate between cell surfaces and intercellular staining.

A comparatively lower level of labelling density was seen in the dorsal part of the lateral funiculus including the lateral spinal nucleus and surrounding regions (LF; Figure 2.3A and C). Punctate labelling was present mainly associated with processes (Figure 2.3C).

The lateral horn (LH; Figure 2.3A and D) also showed dense polySia labelling that appeared to coat neurons in the region and fibres which tracked laterally (Figure 2.3D). An intense polySia-ir was also seen around the central canal, most abundantly at the dorsal surface (CC; Figure 2.3A and E) coating some cells and processes (Figure 2.3E). A moderate to strong density of staining was observed in the dorsomedial part of the ventral funiculus towards the anterior median fissure (F; Figure 2.3A). Some isolated immunoreactive cells were detected in the white matter (Figure 2.3A).

More than 80% of sympathetic preganglionic neurons (SPNs) occupy the intermediolateral cell column (IML), contained within the lateral horn (Llewellyn-Smith, 2009), so we sought to determine whether the polySia labelling here was associated with SPNs. We double labelled rat spinal cord sections (n=5) using mAb 735 and an antibody against choline acetyltransferase (ChAT), a marker of cholinergic SPNs. Anti-ChAT labelling was present in both lateral horn as well as ventral horn where it labels motoneurons (data not shown). Within the IML polySia labelling was consistently associated with characteristic nests of SPNs (Figure 2.4A and B). Although quantification was not possible, confocal imaging revealed that many SPNs (3 out of 4) were coated or enveloped with polySia-ir (Figure 2.4C). PolySia also stains the neuropil between and around SPNs.

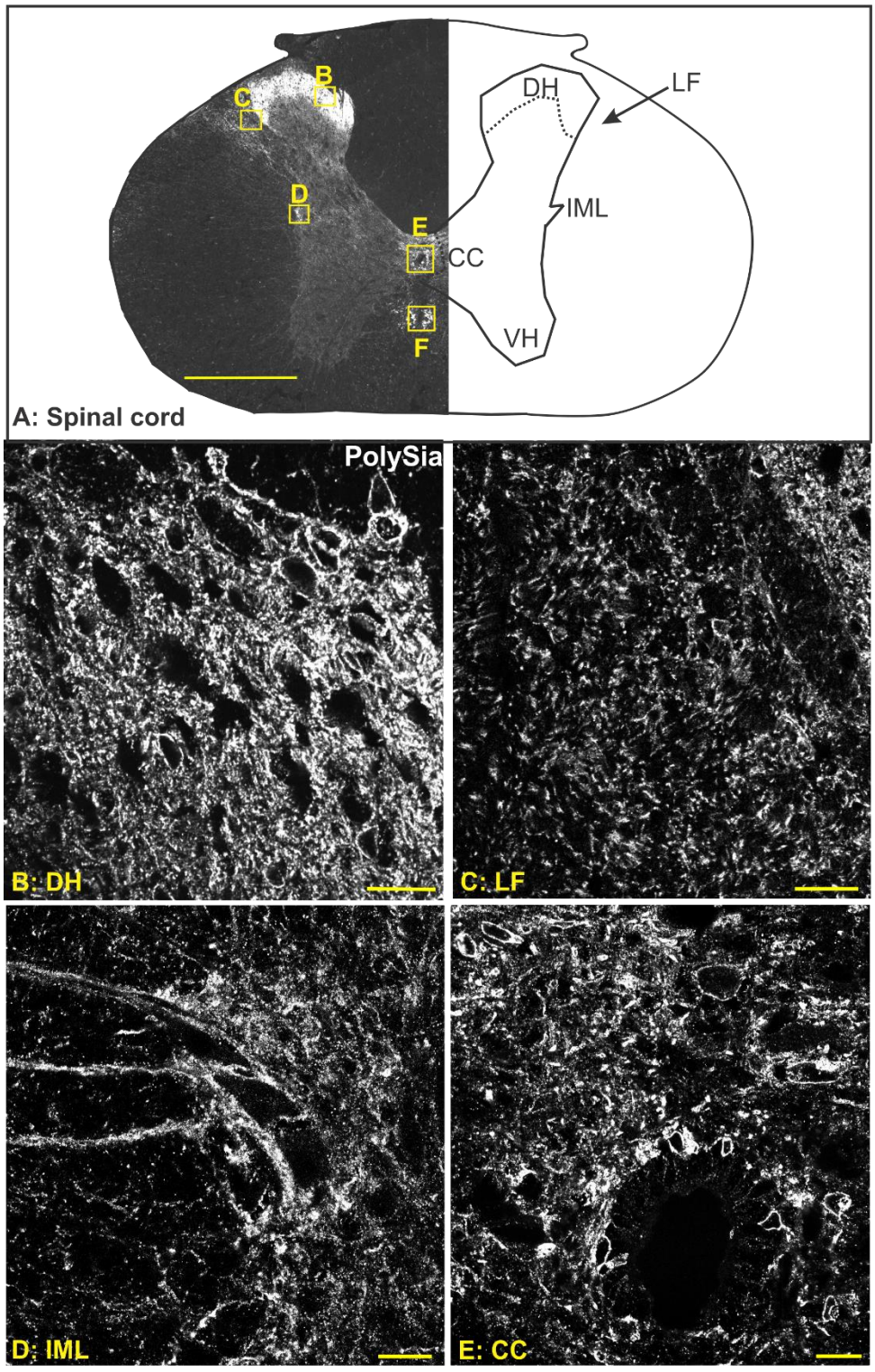

Figure 2.3. Distribution of polySia in the spinal cord of the adult rat. (A) A coronal section of the thoracic spinal cord showing polySia-ir in the superficial laminae of the dorsal horn (DH: B), the upper dorsal portion of the lateral funiculus (LF: C), the intermediolateral cell column (IML: D), around the central canal (CC: E), and the ventral funiculus towards the anterior median fissure (F). (B), (C), (D), and (E) are confocal images. Scale bars = 500 μm in A and = 20 μm in B, C, D, and E.

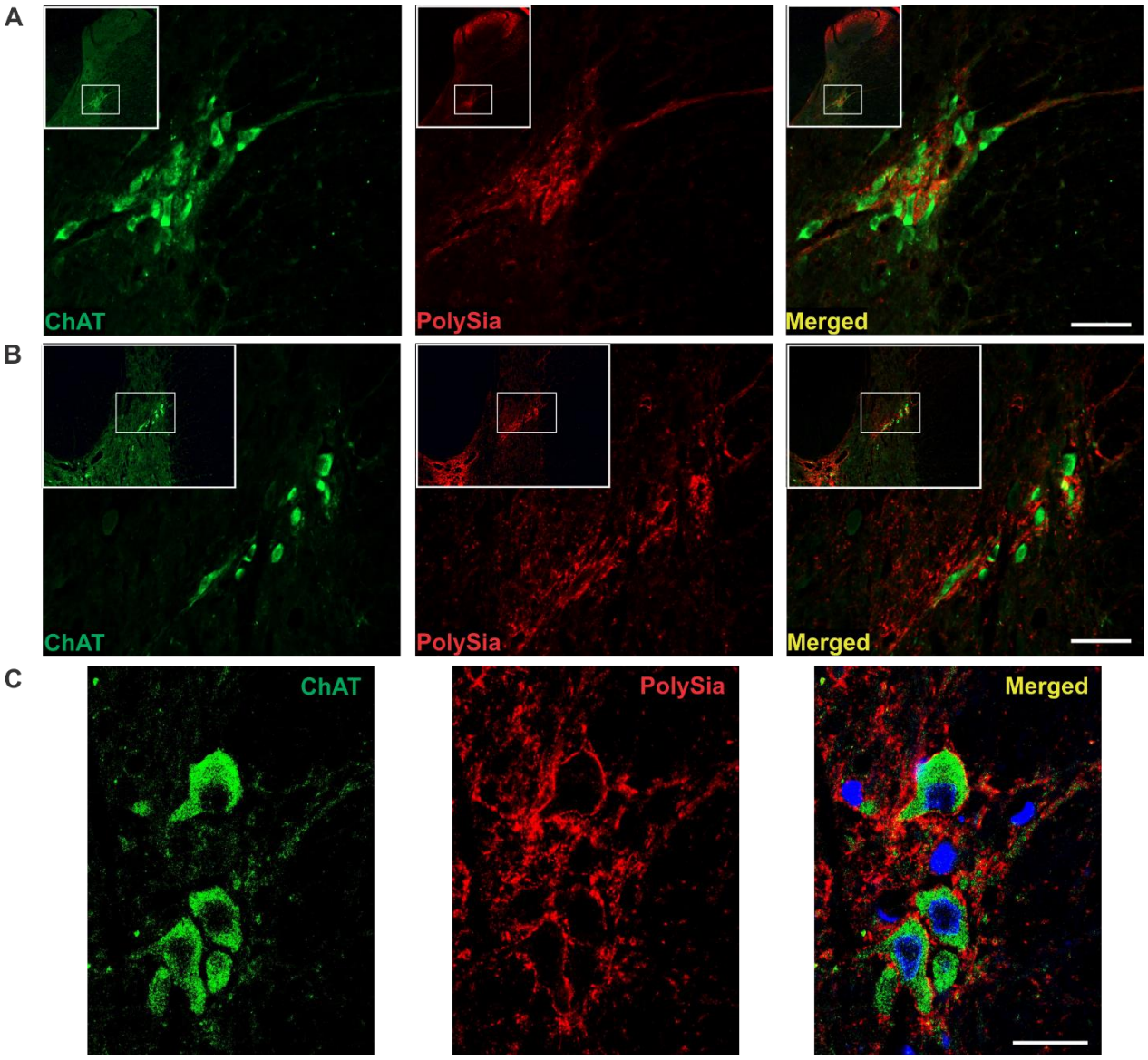

Figure 2.4. PolySia is expressed on and around sympathetic preganglionic neurons (SPNs). (A) and (B) PolySia-ir is present around ChAT immunoreactive SPNs in the intermediolateral horn (IML). (C) A confocal image of polySia in IML showing the expression of polySia on cell surfaces of some SPNs and in the neuropil between and around SPNs. The images were captured from three different rats. ChAT is a marker of SPNs. Nuclei were stained with DAPI (blue). Scale bars = 50 µm in A and B and = 20 µm in C.

2.3.1.3. PolySia in the spinal cord, trigeminal nucleus, and nucleus of solitary tract—is it associated with glia?

Glial cells comprise oligodendrocytes that can be labelled using antibodies against myelin basic protein (MBP) (Sternberger et al., 1978), astrocytes distinguished using antibodies against glial fibrillary acidic protein (GFAP) (Sofroniew and Vinters, 2010), and microglia (not targeted in this study). Combining Mab 735 with anti-MBP that labels mature oligodendrocytes showed no double labelling in any region of the spinal cord, the trigeminal nucleus caudalis, or the nucleus of solitary tract. Areas showing high expression of polySia in fact displayed low or very low expression of MBP: the dorsal horn (DH) (Figure 2.5A), trigeminal nucleus caudalis (Sp5C) (Figure 2.5B-C), and the nucleus of solitary tract (NTS) (Figure 2.5D). Confocal microscopy in the superficial layers of the dorsal spinal cord (Figure 2.5E) further demonstrated that oligodendrocytes were not associated with polySia.

Similarly, double labelling using mAb 735 antibody together with anti-GFAP, did not show colocalization (Figure 2.6A-D). Very rarely minor instances of co-labelling were observed (Figure 2.6Bii). However, GFAP only labels the large process of astrocytes that express intermediate filaments so astrocytic fine cellular processes cannot be visualized (Wilhelmsson et al., 2004). To visualize fine astrocytic processes an antibody to excitatory amino acid transporter 2 (EAAT2) was used (Rothstein et al., 1994, Chaudhry et al., 1995). Figure 2.7 shows some colocalisation of polySia with EAAT2 in the Sp5C of the adult rat. However, polySia was also found closely apposed to EAAT2 but much polySia was not associated with EAAT2. Similar results were also observed in the NTS (data not shown).

Thus, polySia was not associated with oligodendrocytes and any colocalization with astrocytes was restricted to fine processes.

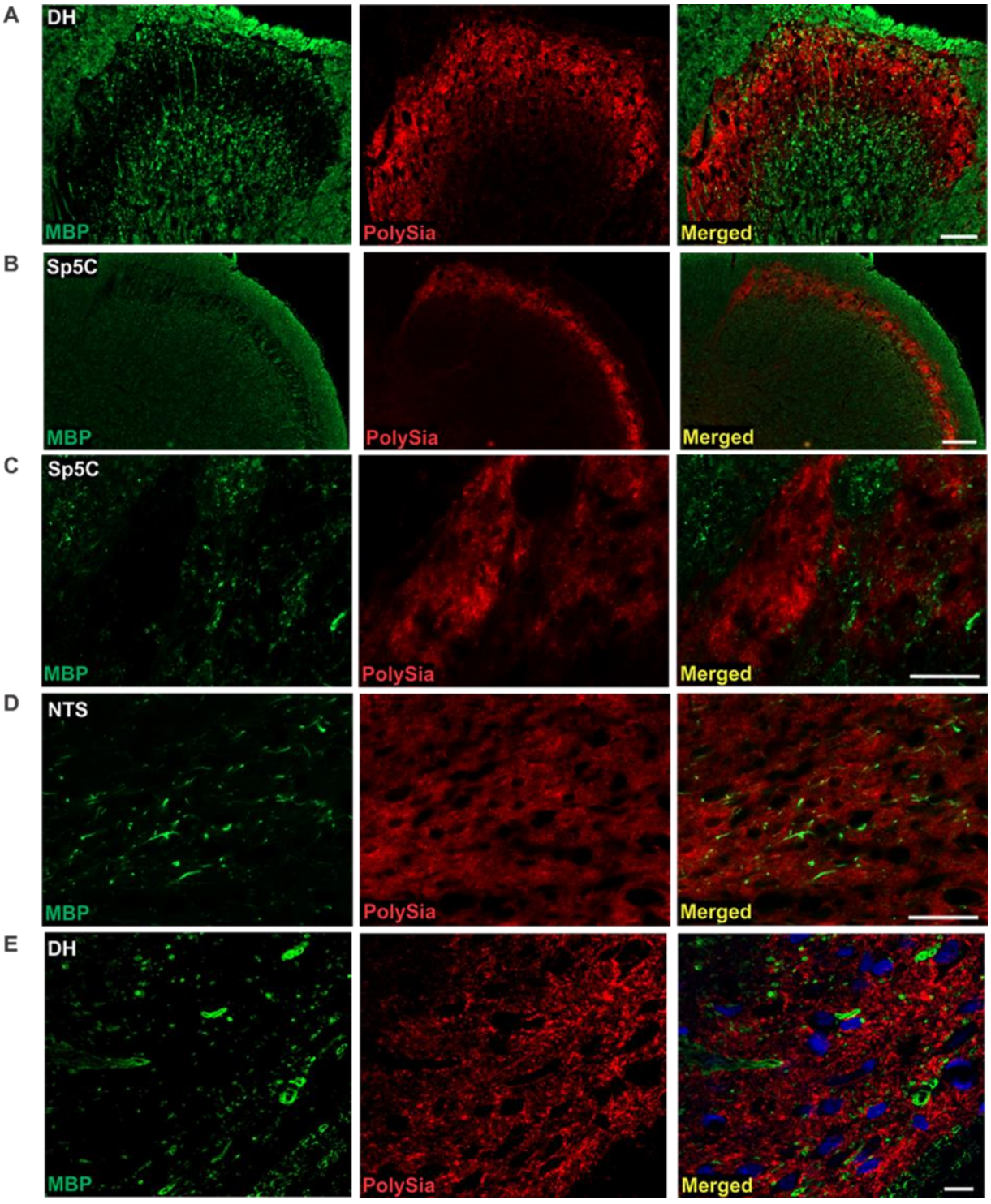

Figure 2.5. PolySia-ir did not colocalize with MBP-ir. (A) the dorsal horn, DH; (B) the trigeminal nucleus caudalis, Sp5C; (C) the trigeminal nucleus caudalis, Sp5C; (D) the nucleus of solitary tract, NTS, and (E) a confocal image of superficial dorsal horn of the adult rat. Nuclei were stained with DAPI (blue). Scale bars = 100 μm in A, = 200 μm in B, = 50 μm in C and D, and = 10 μm in E.

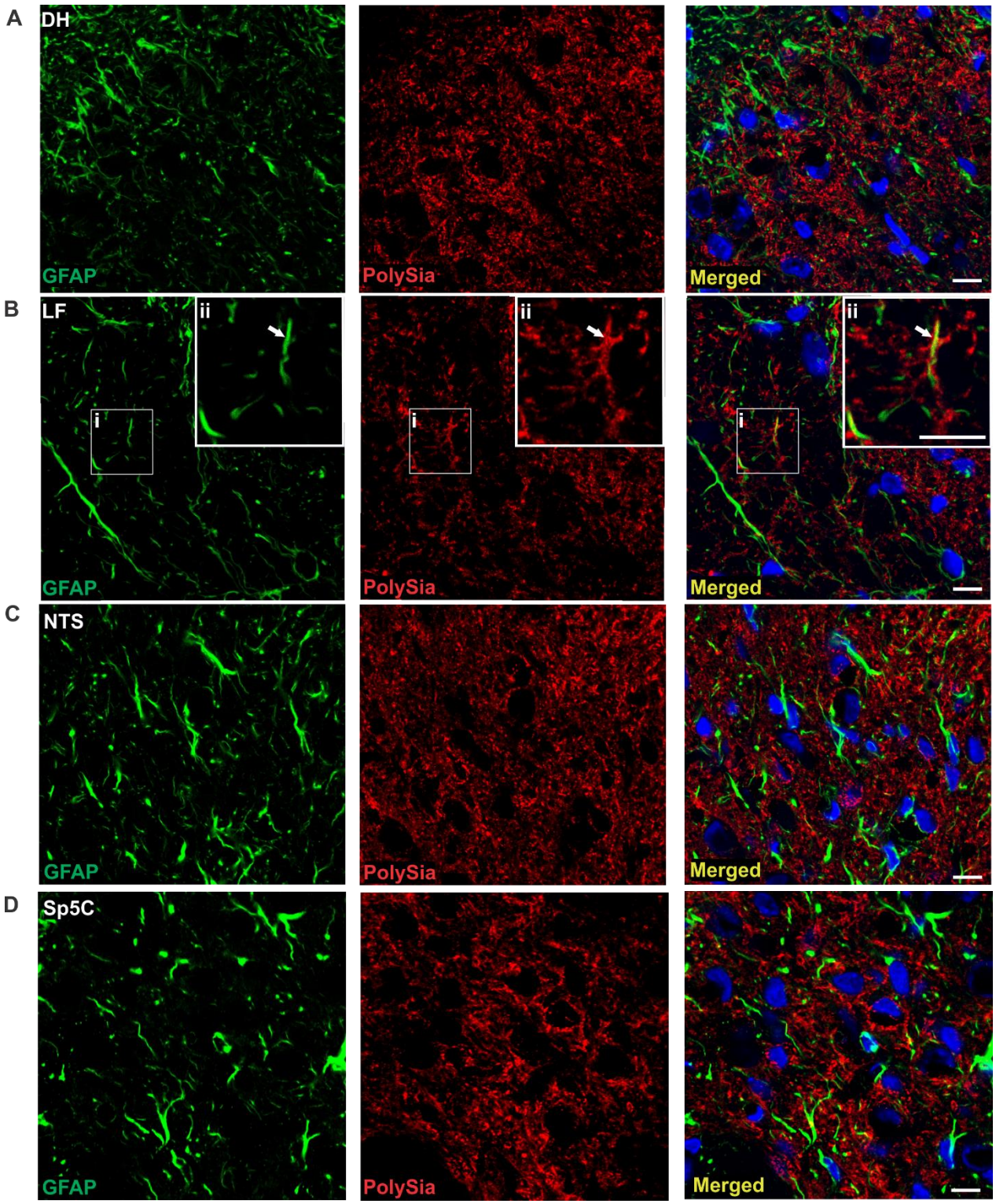

Figure 2.6. PolySia-ir very rarely colocalized with GFAP-ir. (A) the dorsal horn, DH; (B) lateral funiculus, LF; (C) the nucleus of solitary tract, NTS; and (D) trigeminal nucleus caudalis, Sp5C. (Bii) is the magnified image of Bi box displaying rare instances of co-labelling. These are all confocal images. Nuclei were stained with DAPI (blue). The arrow indicates a rare instance of colocalization. Scale bars = 10 µm.

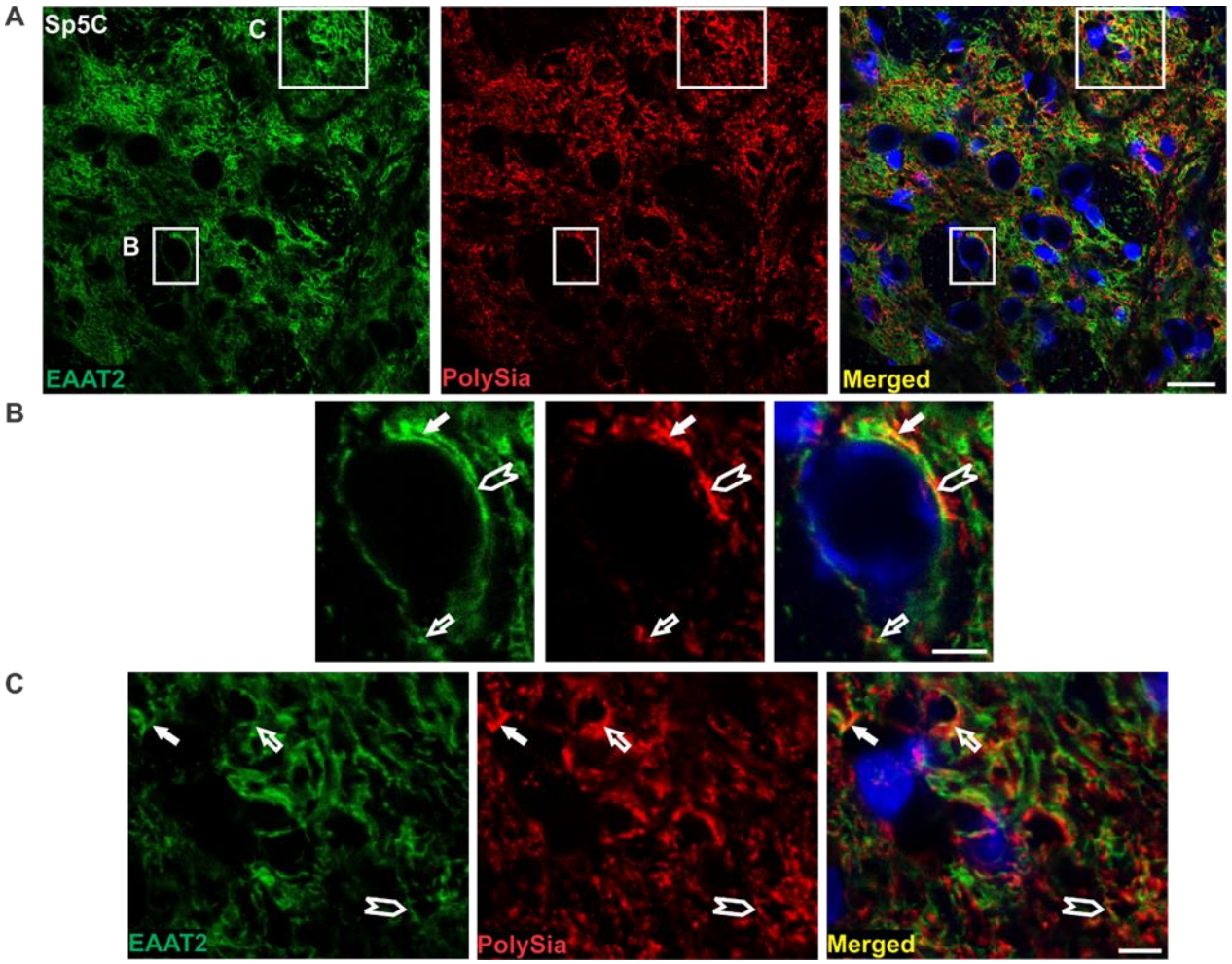

Figure 2.7. PolySia-ir partially colocalized with EAAT2-ir. (A) A confocal image showing some double labelling of polySia and EAAT2 in the trigeminal nucleus caudalis (Sp5C) in the adult rat. (B) and (C) Magnified images of the boxes indicated in A. Nuclei were stained with DAPI (blue). Arrows indicate examples of colocalization. Scale bars = 20 µm in A and = 5 µm in B and C.

We next investigated the type of neurons associated with polySia in laminae I-II of the dorsal horn. Although antibodies against GABA or the GABA synthetic enzyme, glutamic acid decarboxylase (GAD), are commonly used in higher brain regions to label inhibitory interneurons (Gilabert-Juan et al., 2011, Varea et al., 2012, Shumyatsky et al., 2002), an anti-GAD65+67 antibody in the spinal cord showed only punctate terminal labelling with the strongest immunoreactivity in in lamina I-III (Figure 2.8A). No cell body staining was observed as described previously (Mackie et al., 2003). PolySia-ir was rarely associated with GAD65+67-ir (Figure 2.8B).

The somatostatin receptor type 2A **(**SSTR2A) (Olias et al., 2004) is exclusively found on inhibitory interneurons in lamina I and lamina II of the dorsal horn (Todd et al., 1998), so we used this as a

marker of some inhibitory neurons in the region and found some SSTR2A positive cells are associated with polySia-ir, an example of which is highlighted in Figure 2.8C and D.

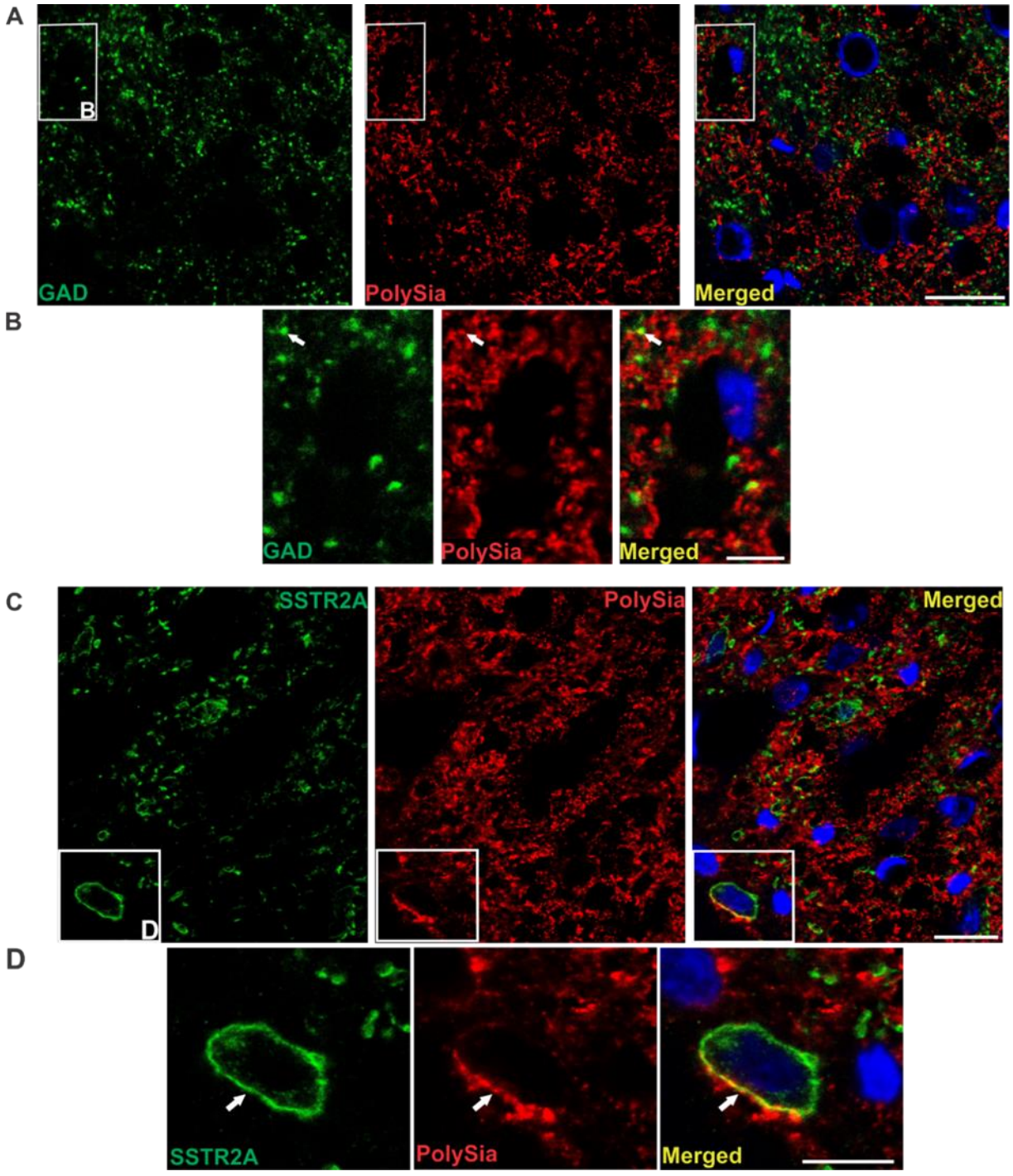

Figure 2.8. PolySia was found associated with some inhibitory interneurons. (A): PolySia-ir was rarely colocalized with GAD65+67-ir (GAD). (C) PolySia-ir was found on some neurons expressing SSTR2A. (B) and (D) magnified images of the boxes indicated in (A) and (C) respectively. Nuclei were stained with DAPI (blue). Arrows indicate examples of colocalization. Scale bars = 20 µm in A and C and = 5 µm in B and D.

Primary afferent fibres (C and Aδ fibres) are the only source of calcitonin gene-related peptide (CGRP; the most frequently occurring peptide in sensory neurons (Ju et al., 1987)) in the dorsal horn (Chung et al., 1988, Traub et al., 1989, Gibson et al., 1984), and thus to investigate potential localization of polySia on afferent fibres we used CGRP. Very little colocalization with polySia in the superficial laminae of the dorsal horn was found (Figure 2.9A and B).

Synaptophysin, a marker of the presynaptic density, showed a wide expression throughout the grey matter of the spinal cord as well as in the lateral spinal nucleus. Double staining for polySia and synaptophysin indicated some colocalization in the superficial laminae of the dorsal horn, around the central canal, and also in the intermediolateral horn (Figure 2.10A). Confocal microscopy confirmed partial colocalization of polySia with synaptophysin in lamina I (Figure 2.10B and C) and in the intermediolateral cell column (Figure 2.10D and E).

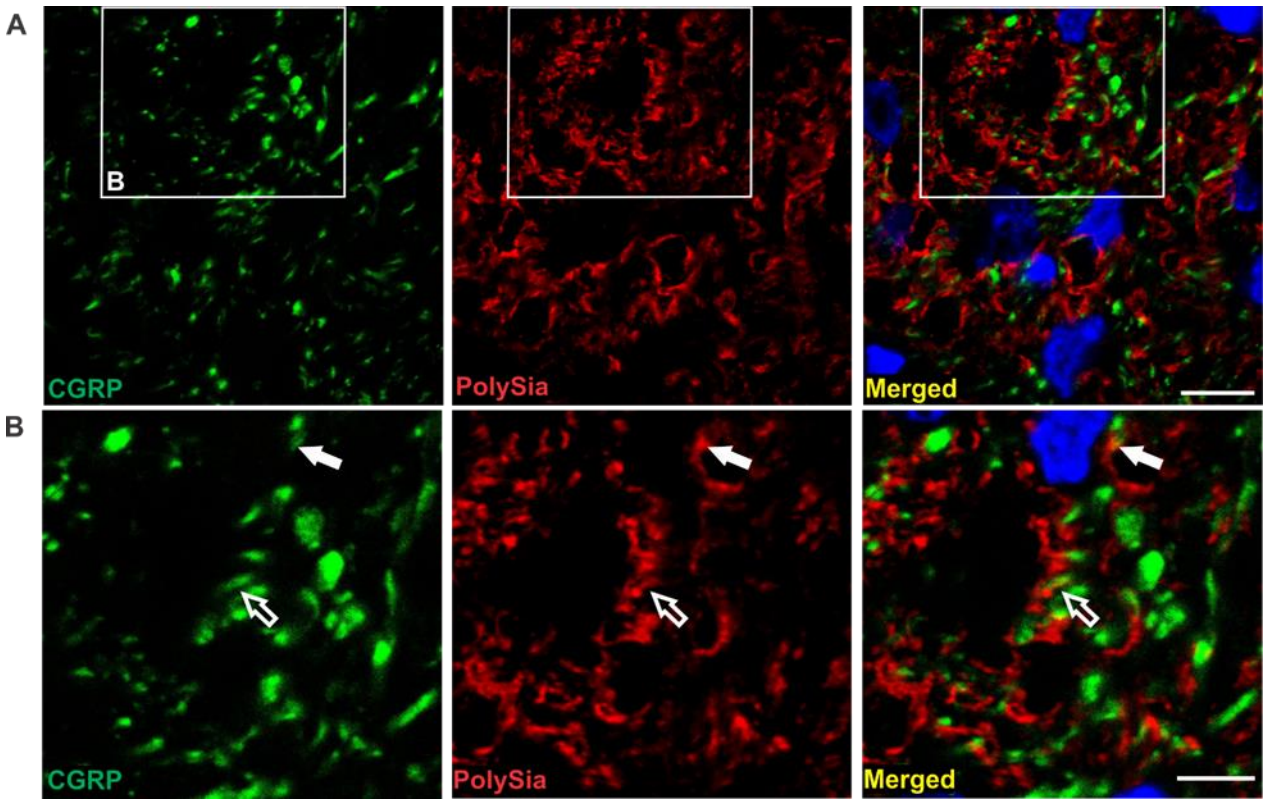

Figure 2.9. Very little polySia-ir was colocalized with CGRP-ir in the dorsal horn of the adult rat. (A) A confocal image showing little double labelling of polySia and CGRP in the superficial laminae. (B) The magnified image of the box in A. Nuclei were stained with DAPI (blue). Arrows indicate examples of colocalization. Scale bars = 10 µm in A and = 5 µm in B.

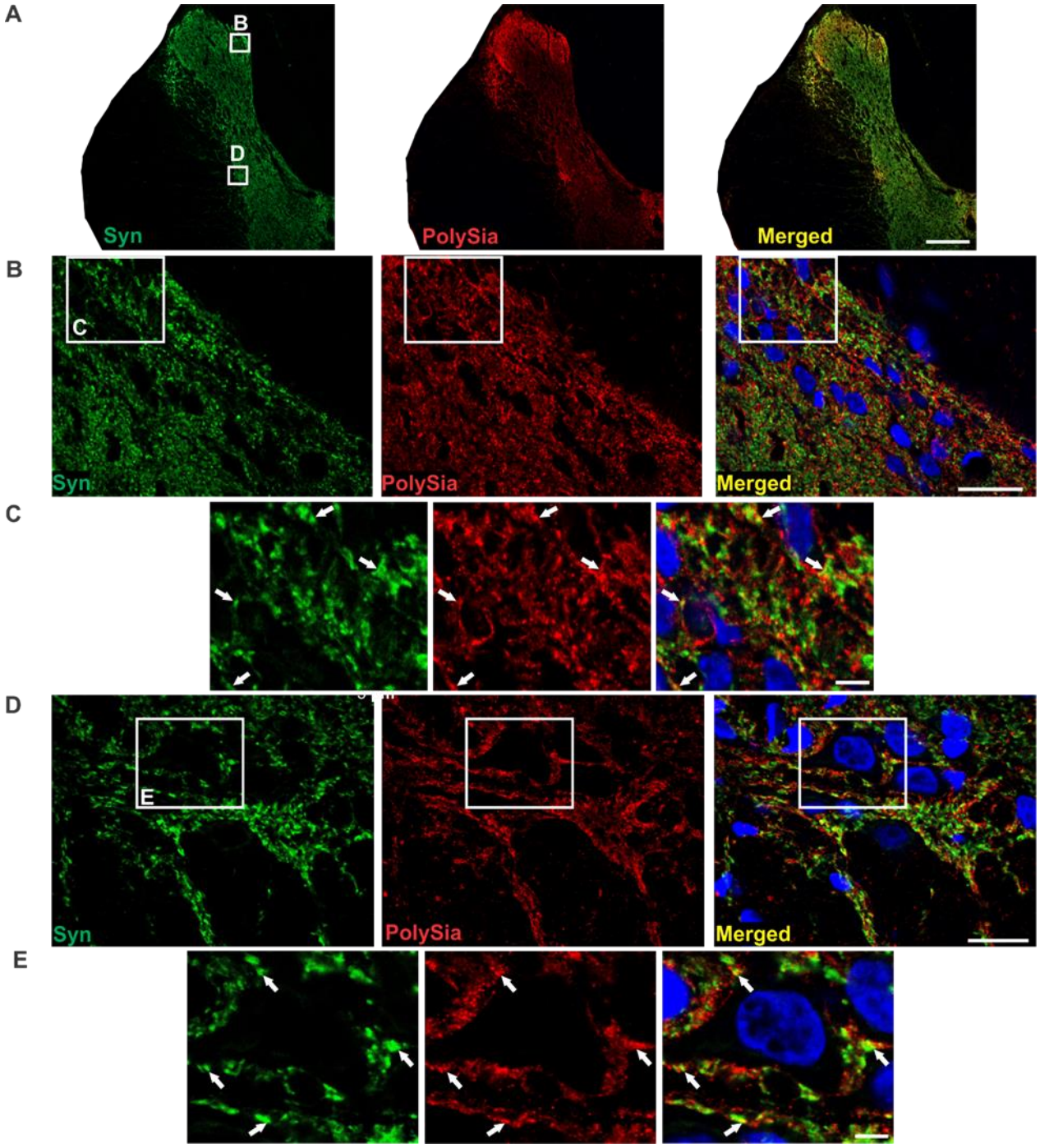

Figure 2.10. PolySia-ir was partially colocalized with synaptophysin (Syn)-ir in the spinal cord of the adult rat. (A) Synaptophysin-ir is widely expressed throughout the grey matter of the spinal cord and in the lateral funiculus and appears to colocalize with polySia-ir. (B) and (D) Confocal images of boxes indicated in A from the superficial laminae of the dorsal horn and intermediolateral cell column, respectively. (C) and (E) Magnified images of the boxes indicated in B and D, respectively. Nuclei were stained with DAPI (blue). Arrows indicate examples of colocalization. Scales bars = 200 µm in A, = 20 µm in B and D, and = 5 µm in C and E.

To gain further insight as to the exact location of polySia in the major regions examined, two were selected for examination at the ultrastructural level. Ultrastructural analysis by electron microscopy in the NTS and Sp5C demonstrated polySia labelling in the space around neuronal cell bodies, fibres and dendrites (Figure 2.11A and 2.12.A and B). The ultrastructural location also showed polySia present in or on the fine processes of astrocytes that lack GFAP (consistent with the result

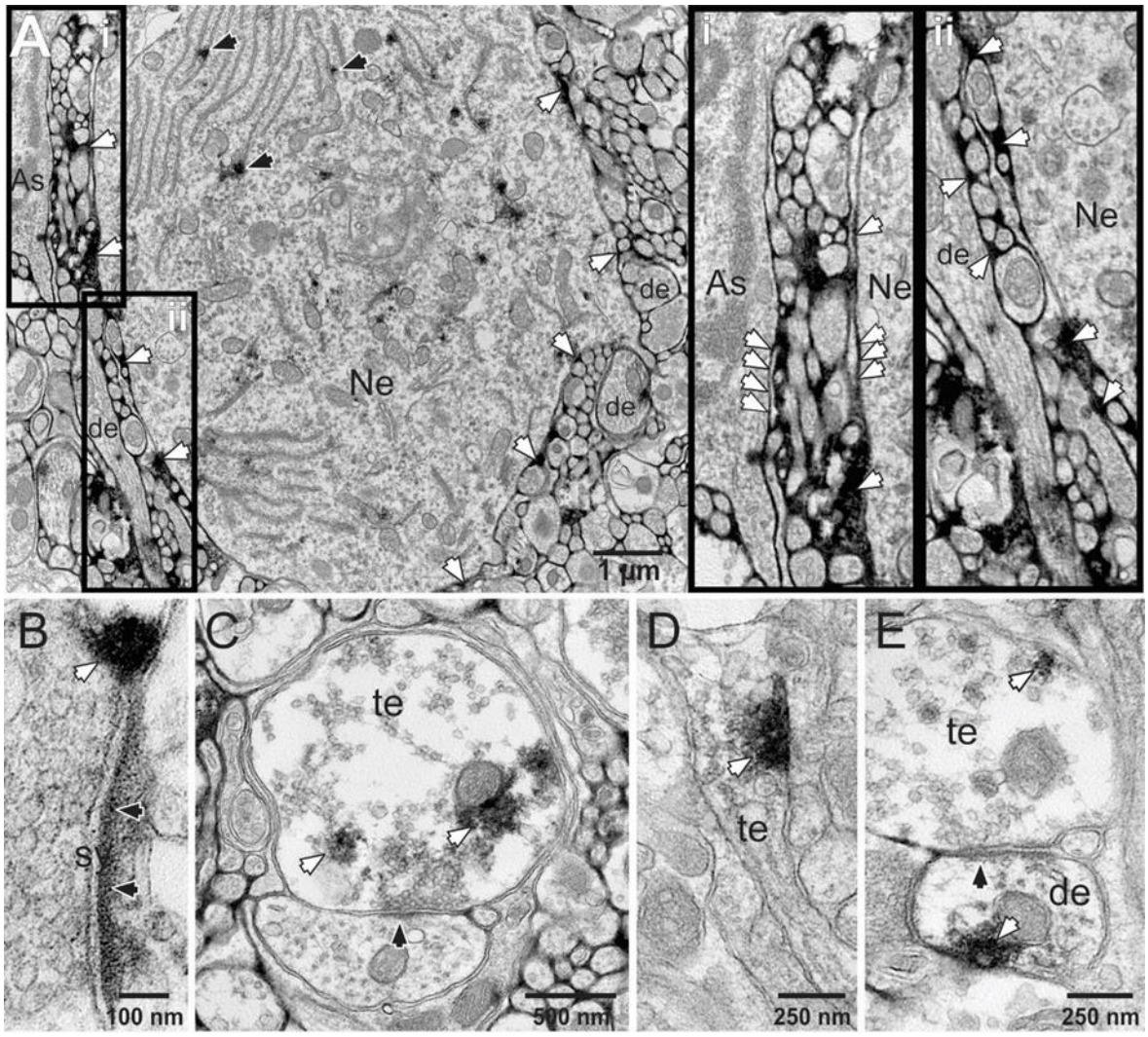

Figure 2.11. Ultrastructural analysis showed polySia-ir in the nucleus of solitary tract (NTS). (A) PolySia-ir (white arrows) surrounded neuronal soma (Ne), proximal dendrites (de) and fine neuronal processes consistent with expression in fine processes of astrocytes (As) (white arrows). PolySia-ir was also found in the rough endoplasmic reticulum and/or Golgi apparatus of some neurons (black arrows). (Ai) PolySia-ir occurred along the exterior surface of the plasma membrane of some astrocytic (As) and neuronal (Ne) soma (white arrows) indicating its presence in the extracellular space. (Aii) Dendrites (de) and axons were sheathed by polySia labelling. (B) PolySia-ir (white arrows) was found adjacent to some synapses (sy) likely in astrocytic processes, as a tripartite synapse. (C-E) PolySia-ir was found within some dendrites (de) and axon terminals (te) of neurons. Black arrows indicate post-synaptic densities.

observed in Figures 2.6 and 2.7) and/or within the extracellular space adjacent to plasma membranes (Figure 2.11Ai and ii and 2.12.A). The labelling pattern was also consistent with the polySia-ir that surrounded some cell bodies identified by light or confocal microscopy (Figure 2.2 and 2.3). In the NTS, polySia-ir was also found on the rough endoplasmic reticulum and/or Golgi apparatus evident in some neuronal cell bodies (Figure 2.11A) where it may be produced before being transported extracellularly to the cell surface (as described in the hypothalamus (Theodosis et al., 1999)). PolySia-ir was also present adjacent to some synapses and in a subset of dendrites and axon terminals (Figure 2.11B-E and 2.12C-G), consistent with the close association and partial colocalization of polySia and synaptophysin revealed using immunofluorescence (Figure 2.10).

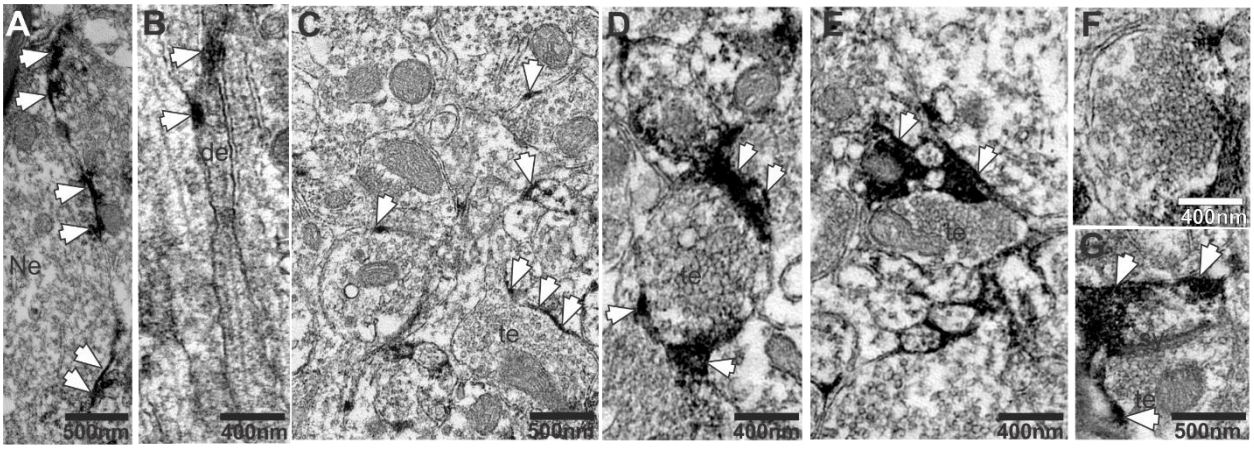

Figure 2.12. Ultrastructural analysis showed polySia-ir in the trigeminal nucleus caudalis (Sp5C). (A) PolySia-ir occurred along the exterior surface of the plasma membrane of some neuronal (Ne) soma (white arrows) consistent with expression in fine processes of astrocytes and/or within the extracellular space adjacent to plasma membranes. (B) Dendrites (de) were sheathed by polySia labelling. (C-F) PolySia-ir (white arrows) surrounding neuronal terminals (te) consistent with expression in fine processes of astrocytes (white arrows). (G) PolySia-ir (white arrows) was found adjacent to some synapses (sy) likely in astrocytic processes. White arrows indicate examples of polySia-ir.

2.3.2. PolySia distribution within the adult rat trigeminal ganglion using mAb 735 antibody

In addition to examining central sites, we also decided to examine the distribution of polySia in the adult rat trigeminal ganglion (TG) as this provides input to the Sp5C that has abundant expression of polySia and a description of labelling in human tissue is available (Quartu et al., 2008). Within the rat trigeminal ganglia, polySia was present on some cell surfaces (Figure 2.13A and B) and fibres (Figure 2.13B). The intensity of polySia staining varied between cells, with some cells demonstrating a dense ring of polySia on their surface, whereas some cells showed little if any labelling.

Double labelling longitudinal sections of TG with mAb 735 and anti-NeuN (Vit et al., 2006), anti-glutamine synthetase (GS; (Gunjigake et al., 2009)) and anti-MBP (Eftekhari et al., 2010) were used to investigate the association of polySia with neurons, satellite glial cells (SGCs) and Schwann cells (and myelin), respectively. TG neurons are classified into three discrete categories based on cell size including small cells (20–30 µm), medium-sized cells (30–50 µm), and large-sized cells (50–80 µm) (see Chapter 1) (Marfurt, 1981, Sugimoto et al., 1986). PolySia-ir was found on small-, medium-, and large-sized neurons labelled with anti-NeuN. However, polySia was associated with some but not all neurons (Figure 2.14A an B). Figure 2.14C confirms that neurons in TG are surrounded by SGCs labelled with anti-GS, as previously described (Lazarov, 2002, Hanani, 2005). Some SGCs were coated with polySia-ir.

The MBP antibody stained the myelin sheath of nerve fibres. Although polySia-ir was found on some fibres, no colocalisation of polySia-ir was seen with MPB-ir as in the CNS regions examined (Figure 2.14D). Also we did not detect polySia-ir on Schwann cells.

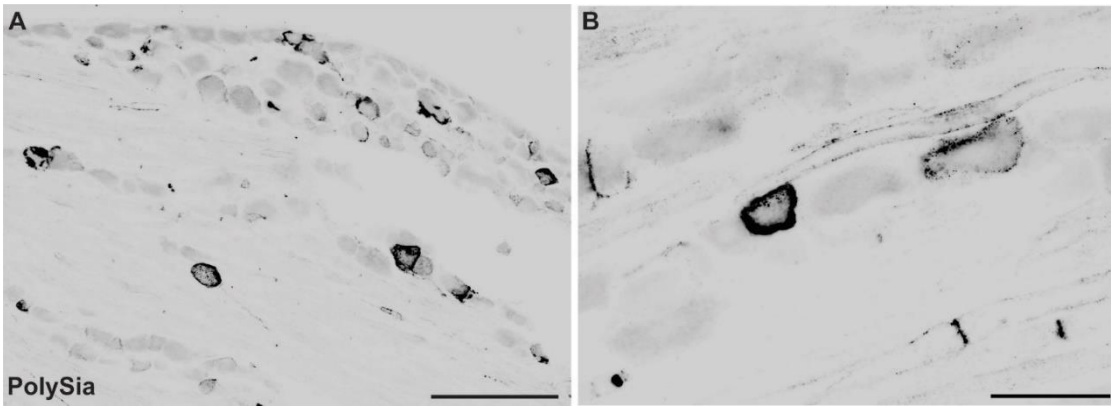

Figure 2.13. PolySia-ir was found on some cell surfaces and fibers of trigeminal ganglia of the adult rat. (A) and (B) PolySia-ir in two individual rats. Scale bars = 200 in A and = 50 µm in B.

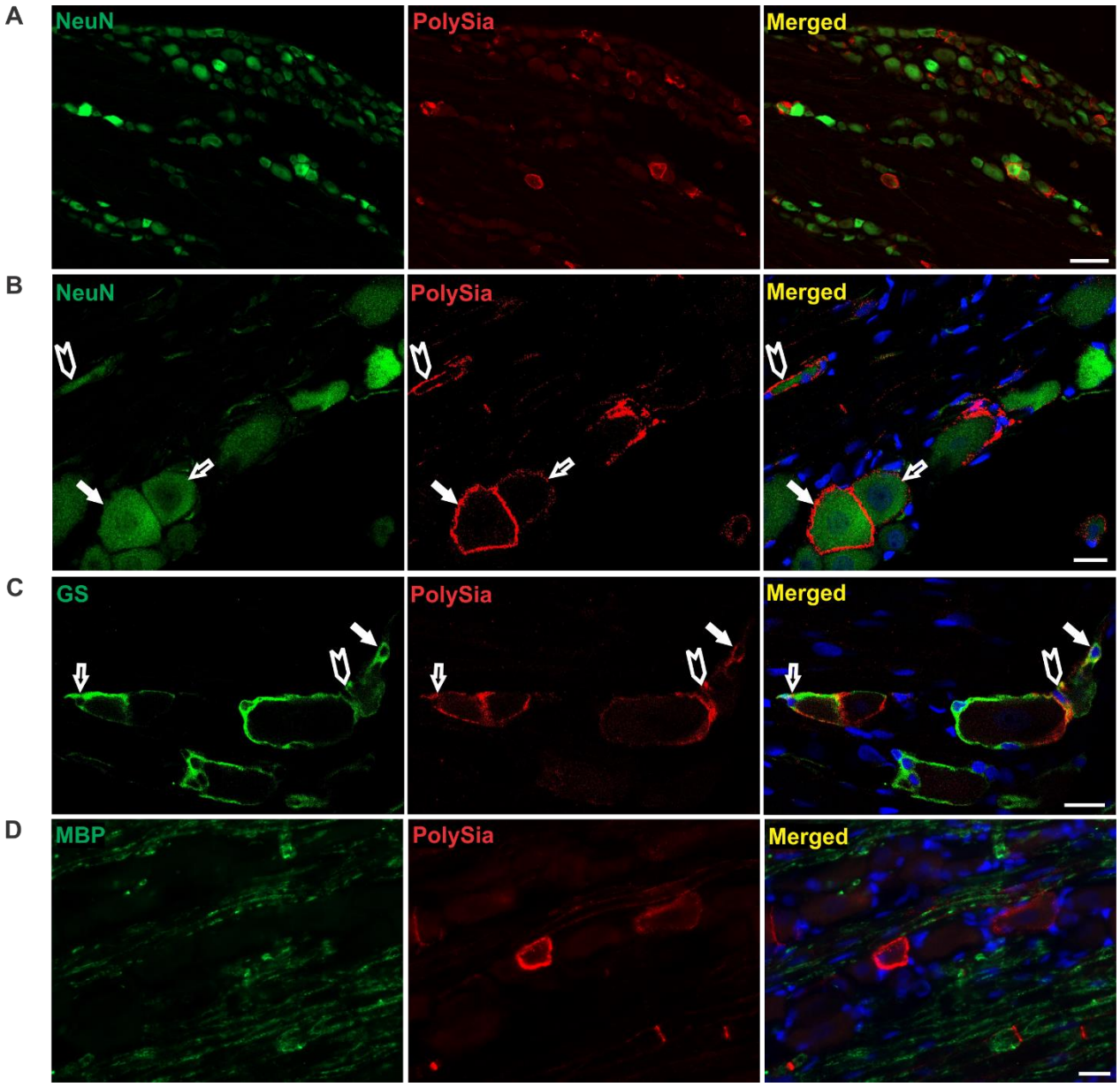

Figure 2.14. Cellular localization of polySia in the adult rat trigeminal ganglion. (A) and (B) Double staining of longitudinal trigeminal ganglion sections with mAb 735 and anti-NeuN showing polySia-ir on the surface of some neurons. (C) PolySia-ir was found on some satellite glial cells stained with anti-GS antibody but not associated with MBP (D). Scale bars = 100 µm in A and = 20 µm in B-D.

2.3.3. Investigating the specificity of mAb 735 and mAb 5324 antibodies against polySia

Three regions with high expression of polySia i.e. DH, Sp5C, and NTS, as well as TG were used in western blotting experiments to confirm whether mAb 735 used to detect polySia-ir as shown above is polySia specific (Figure 2.15A). After probing the blot against mAb 735, a band around 250 kDa was observed in all samples (Figure 2.15A). The band almost or completely disappeared in samples pretreated with NEU or endoN, that are exo- and endosialidases respectively, with endoN specific for polySia. However, a band around 150 kDa was detected in TG samples. This

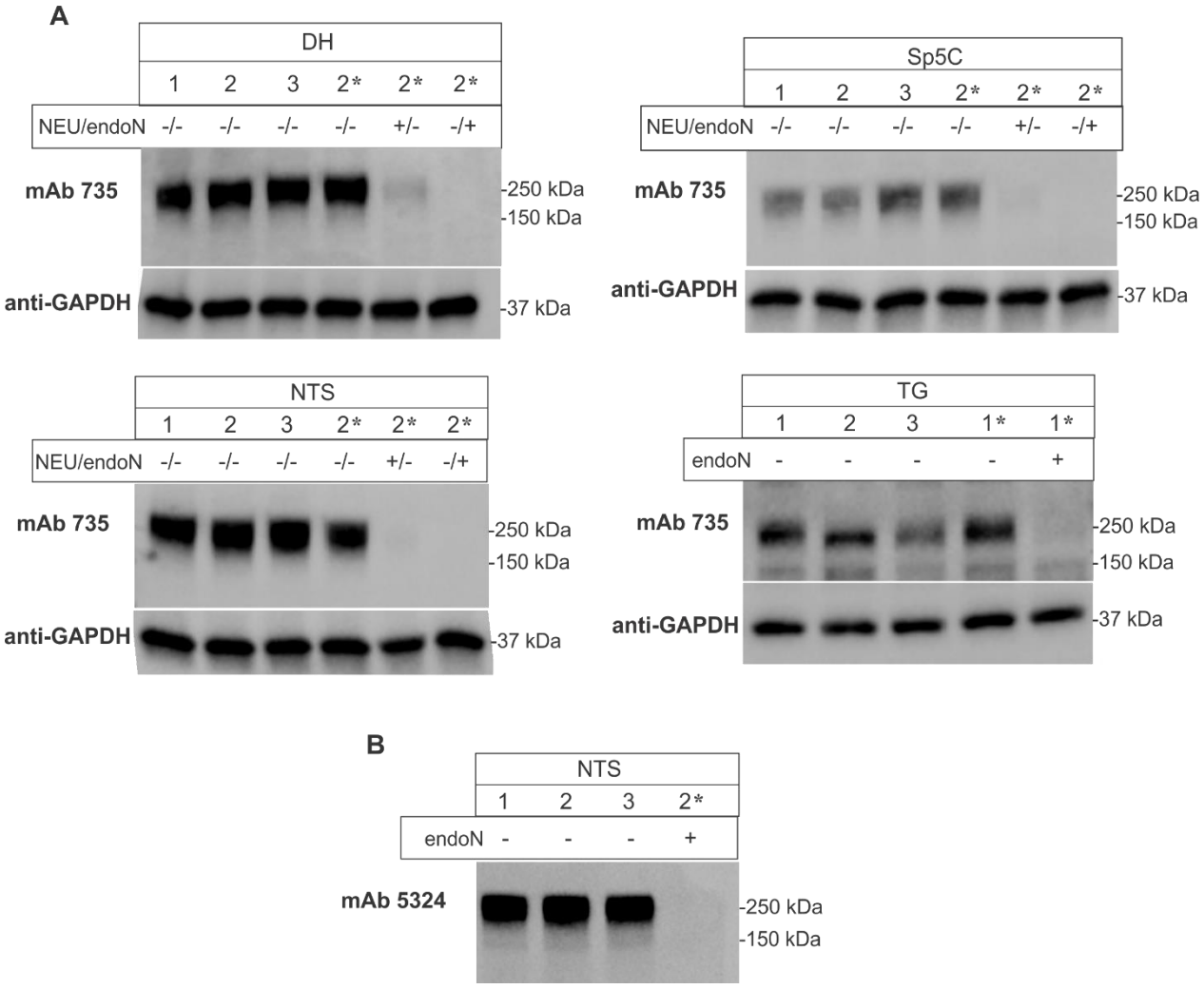

Figure 2.15. Western blot of extracts of the superficial layers of the dorsal horn (DH), trigeminal nucleus caudalis (Sp5C), nucleus of solitary tract (NTS), and trigeminal ganglion (TG) in the adult rat using mAb 735 (A) or mAb 5324 antibody (B). A band around 250 kDa was observed in all samples demonstrating polySia. The band almost or completely disappeared in neuraminidase (NEU) or endoN treated samples. Anti-GAPDH was used as a loading control. 1-3 represent the number of replicates. *: heated at 37 °C for 1 h.

band was also detected in the same samples pretreated with endoN suggesting that in the TG samples, the antibody might also bind to a non-polySia antigen.

Similarly, using mAb 5324 antibody, a band around 250 kDa was detected in the NTS samples which completely disappeared in the sample pretreated with endoN (Figure 2.15B).

2.3.4. PolySia expression in the rat vs. mouse brainstem and spinal cord

Next, we investigated whether the pattern of polySia distribution in the adult rat brainstem and spinal cord (n=3) was similar to that of the adult mouse (n=3) using mAb 735. Due to significant differences in the size of brainstem in the rat and mouse, matching sections were not always available. Overall, the pattern of polySia distribution in the brainstem of the adult mouse was similar to that seen in rat. All polySia labelled regions in rat also showed labelling in mouse (Figure 2.16); however, some differences in the intensity of polySia labelling were evident. Labelling within the gracile fasciculus (Figure 2.16A and B), medullary reticular nucleus, dorsal part (MdD), and the rostroventrolateral reticular nucleus (RVL) (Figure 2.16C and D) were more intense in mouse compared to rat. Moreover, the ventral part of Sp5C showed more intensity than its dorsal part in mouse compared to rat.

In contrast, in the spinal cord, the labelling differences between mouse and rat were quite distinct (Figure 2.17). Although polySia-ir was commonly found in the superficial layers of the dorsal horn (DH), the dorsal part of the lateral funiculus (LF), lateral horn (LH), around the central canal (CC), and in the dorsomedial part of the ventral funiculus towards the anterior median fissure (F) stark differences in the precise distribution in the dorsal horn were observed. In rat, both lamina I and lamina II showed high expression levels of polySia-ir (Figure 2.17A and C). In mouse however dense labelling was restricted to lamina II with significantly less labelling present in lamina I. This difference persisted in both thoracic and lumbar spinal cord (Figure 2.17B and D). In addition, the rat dorsal horn was densely labelled whereas there was less labelling around the central canal region, but in mouse this intensity pattern was reversed (Figure 2.17).

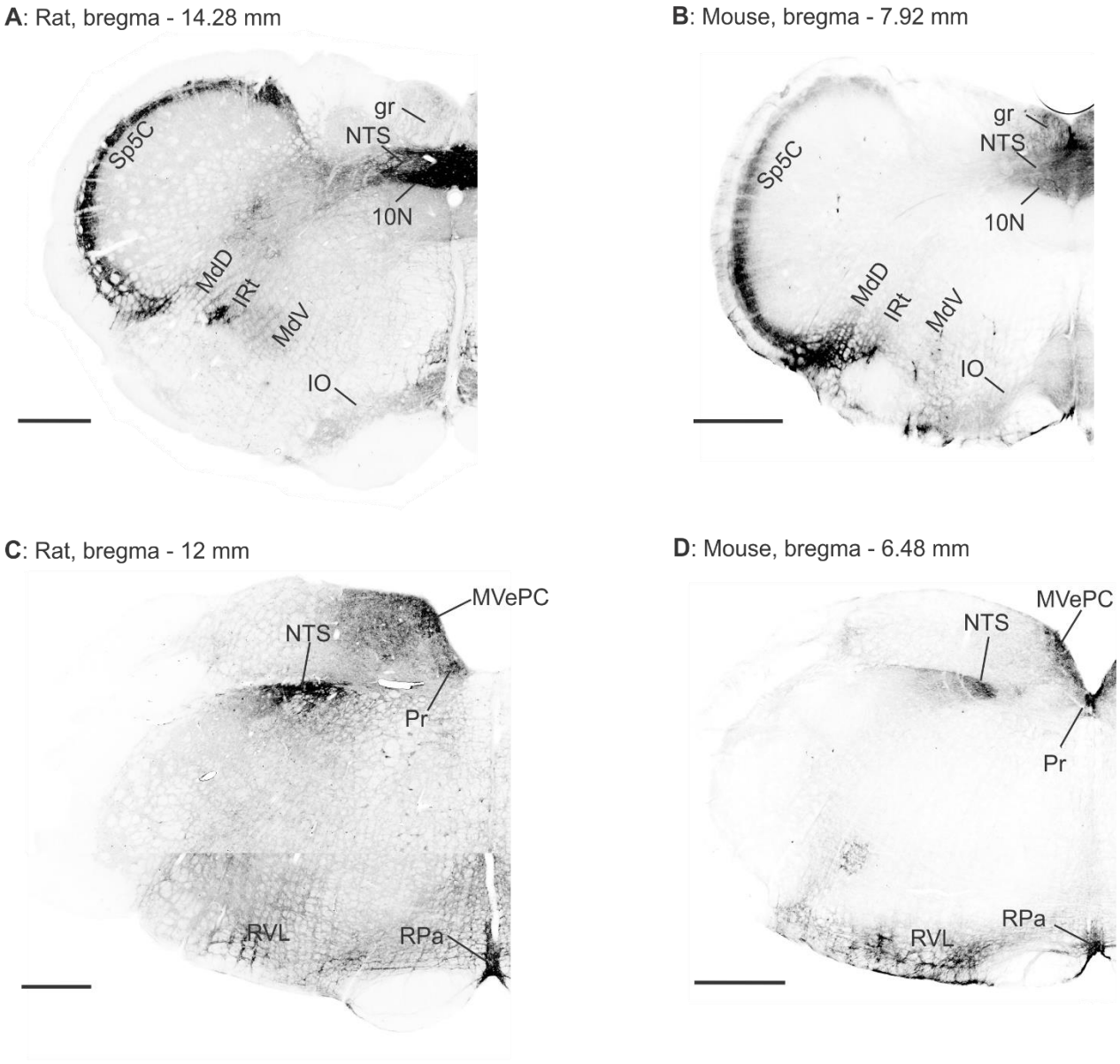

Figure 2.16. Comparison of polySia distribution between rat and mouse brainstem. (A) and (C) show polySia expression in the adult rat, whereas (B) and (D) show polySia expression in similar levels of the adult mouse in A and C, respectively. 10N, dorsal motor nucleus of vagus; gr, gracile fasciculus; IO, inferior olive; IRt, intermediate reticular nucleus; MdD, medullary reticular nucleus, dorsal part; MdV, medullary reticular nucleus, ventral part; MVePC, medial vestibular nucleus, parvicellular part; NTS, nucleus of the solitary tract; Pr, prepositus nucleus; RPa, raphe pallidus nucleus; RVL, rostroventrolateral reticular nucleus; Sp5C, spinal trigeminal nucleus, caudal part. Scale bars = 500 µm.

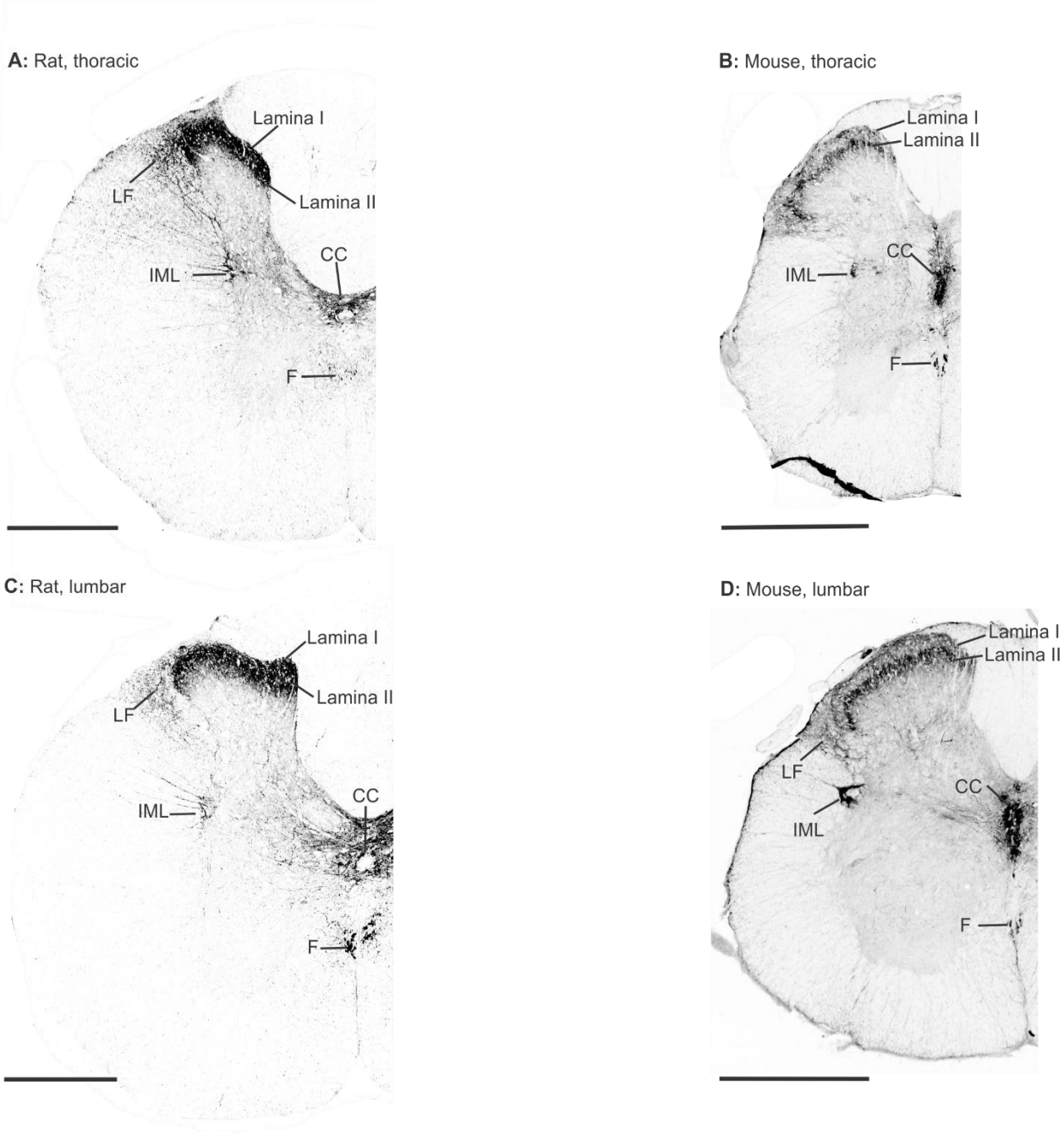

Figure 2.17. Comparison of polySia distribution between rat and mouse spinal cord at the thoracic and lumbar levels. (A) and (C) display polySia-ir in the adult rat with (B) and (D) showing polySia-ir in the adult mouse. Lamina I and II, the superficial laminae in the dorsal horn; LF, the lateral funiculus; IML, intermediolateral cell column; CC, around the central canal; F, the ventral funiculus towards the anterior median fissure. Scale bars = 500 µm.

2.3.5. Comparison of polySia distribution pattern in two most widely used polySia antibodies—mAb 735 and mAb 5324

The description of polySia labelling so far has been based on labelling using Mab 735 which as seen in Figure 2.15 (western blotting) detects polySia. However a range of antibodies have been used previously to investigate polySia so we next decided to compare and contrast labelling of mAb 735 (n=3) with mAb 5324 (n=3), an antibody reported to recognize oligo/polySia (DP≥4) (Sato and Kitajima, 2013a). The distribution of polySia in the adult rat brainstem (bregma -9 to -15.96) (Figure 2.18) and spinal cord (Figure 2.19) was compared using both antibodies. As can be seen in Figure 2.18A-D, patterns of labelling were very similar in the dorsal motor nucleus of the vagus (10N), the spinal trigeminal nucleus caudalis (Sp5C), Inferior olive complex (IO), intermediate reticular nucleus (IRt), medullary reticular nucleus, dorsal part, (MdD), parvicellular reticular nucleus (PCRt), raphe obscurus nucleus (ROb), and the nucleus of solitary tract (NTS). However, some very subtle differences were detected. While gracile fasciculus in the adult rat stained with mAb 735 showed only very mild expression of polySia in some fibres and in some coronal sections, this staining was more evident with mAb 5324 (Figure 2.18A and B). Mab 5324 also showed considerably higher levels of labelling of the ventral surface compared to mAb 735 (Figure 2.18A and C). These minor differences were consistently present in all samples examined (n=3).

All areas of the spinal cord labelled by mAb 735 were also labelled by mAb 5324 (Figure 2.19 A and B); however, with mAb 735 the intensity of labelling in lamina I-II of the dorsal horn was comparatively higher than the intensity in the other regions, whereas with mAb 5324 this difference was less evident.

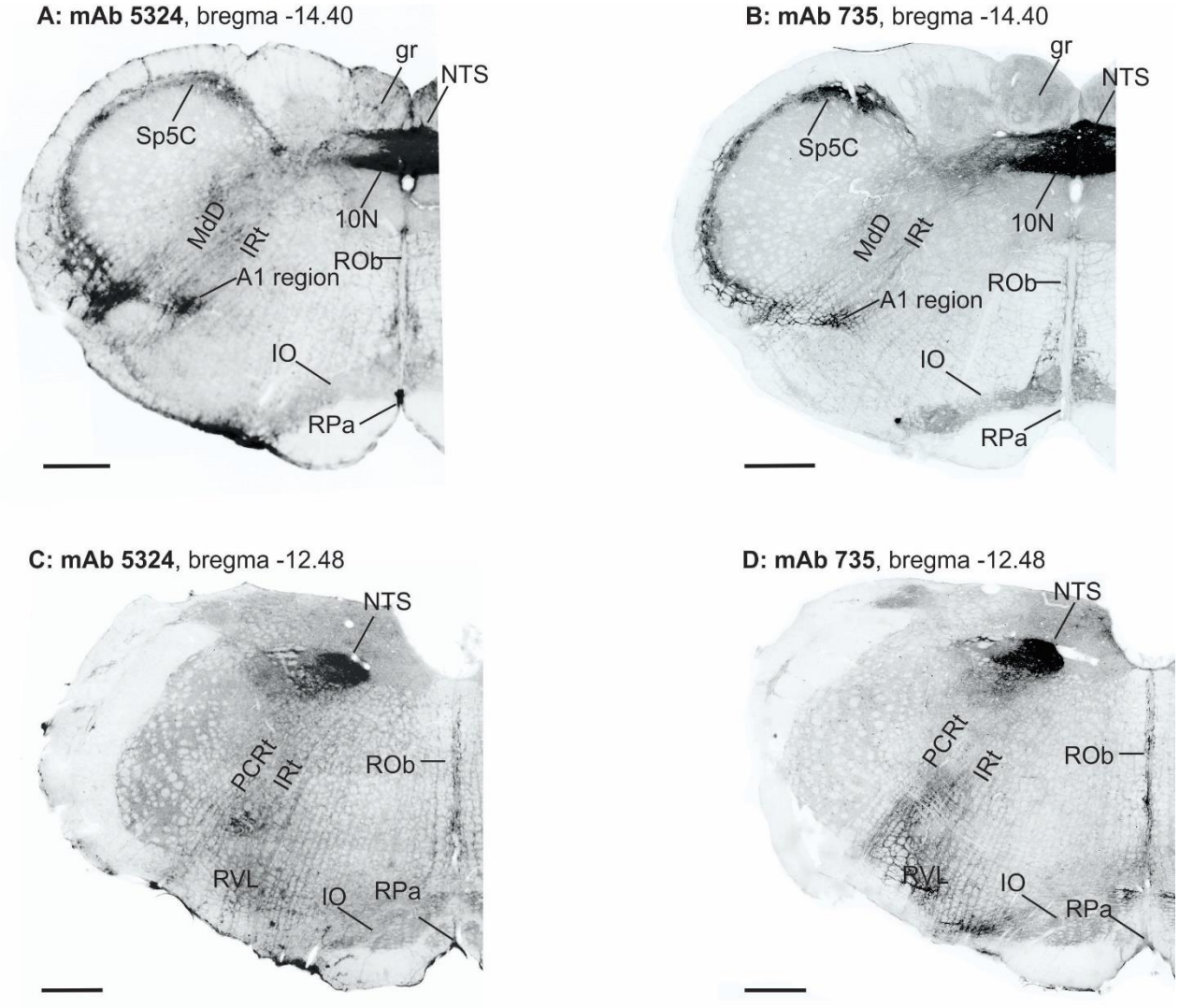

Figure 2.18. Comparison of mAb 5324 and mAb 735 anti-polySia antibodies in the brainstem of the adult rat. (A) and (C) show polySia staining in the coronal sections of the brainstem labelled with mAb 5324, while (B) and (D) show similar sections labelled with mAb 735. Both antibodies produced similar pattern of labelling in most regions studied. 10N, Dorsal motor nucleus of the vagus; IO, Inferior olive complex; IRt, intermediate reticular nucleus; MdD, medullary reticular nucleus, dorsal part; NTS, nucleus of solitary tract; PCRt, parvicellular reticular nucleus; ROB, raphe obscurus nucleus; RPa, raphe pallidus nucleus; RVL, rostroventrolateral reticular nucleus; Sp5C, spinal trigeminal nucleus caudalis. Scale bars = 500 μm.

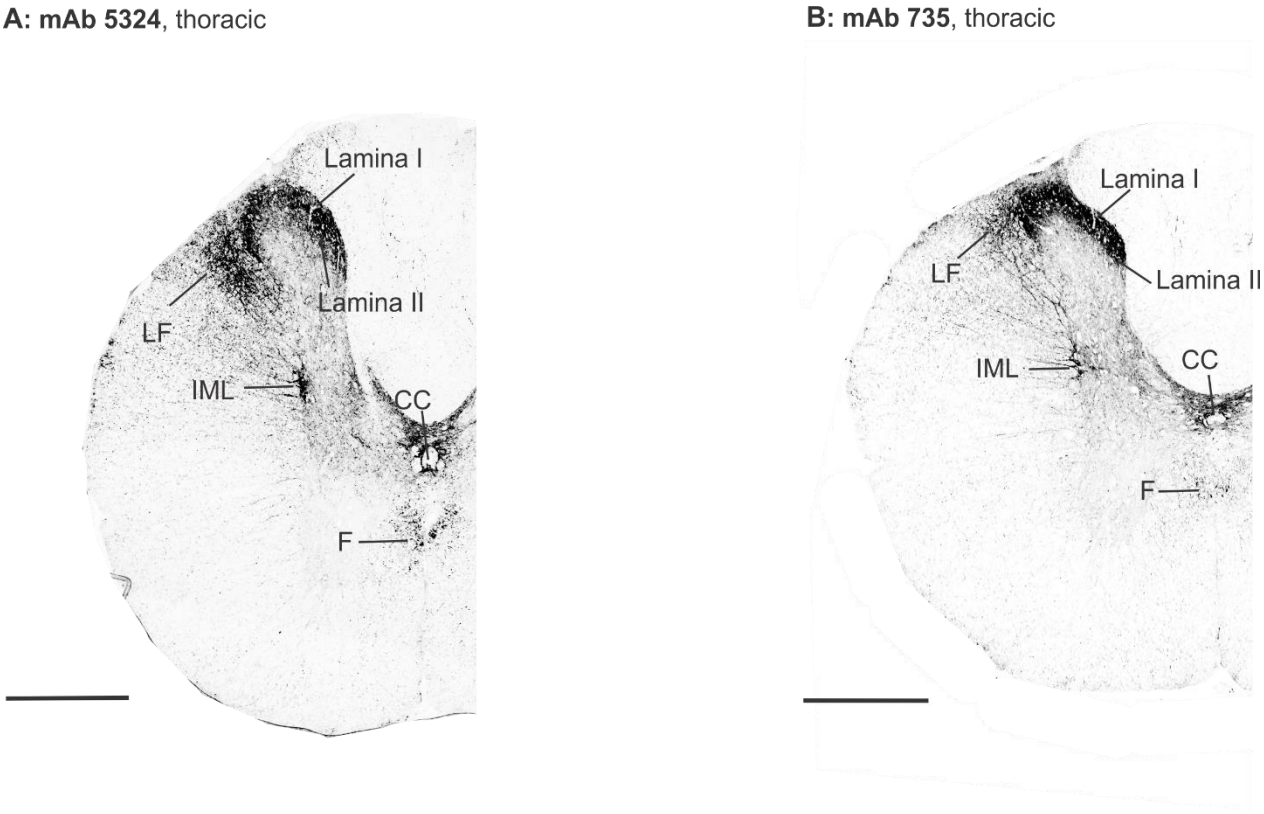

Figure 2.19. PolySia labelling in the adult rat thoracic spinal cord using mAb 5324 (A) and mAb 735 (B). A similar pattern of labelling was seen however intensity differences are evident in Laminae I and II. Lamina I and II, the superficial laminae in the dorsal horn; LF, the lateral funiculus; IML, intermediolateral cell column; CC, around the central canal; F, the ventral funiculus towards the anterior median fissure. Scale bars = 500 μm.

2.4. Discussion

We have confirmed the findings of earlier studies regarding the distribution of polySia in the adult rat brainstem and spinal cord. We have also extended these findings by identifying several new polySia expressing regions including the IML, where polySia-ir enveloped many sympathetic preganglionic neurons and demonstrated within 5 CNS regions--the dorsal horn, IML, lateral funiculus, Sp5C and NTS--polySia was not associated with GFAP positive astrocytic processes or oligodendrocytes. Within the superficial laminae of the dorsal horn, some association of polySia was seen with inhibitory interneurons and presynaptic densities labelled with synaptophysin, whereas little if any association was found between polySia and CGRP, labelling sensory afferents. Within the Sp5C and NTS, some polySia was found associated with fine processes of astrocytes (that are not GFAP positive) identified by EAAT2-ir. Ultrastructural analysis of both the NTS and Sp5C confirmed the results shown by light and confocal microscopy revealing that neurons were enveloped by polySia, expressed predominantly in or on the fine processes of astrocytes and within the extracellular space. Within the trigeminal ganglion of the adult rat, polySia-ir was found around some neurons and some satellite cells. Mostly, common patterns of polySia labelling were seen between rat and mouse CNS with the biggest differences seen within the spinal cord dorsal horn. Finally, comparison of the two most common polySia antibodies within the lower brain regions demonstrated similar patterns of immunolabelling.

Together these data indicate that in the brainstem and spinal cord of rodents, polySia is likely associated with excitatory and inhibitory neurons as well as astrocytes, is found on membranes or in the extracellular space and near synapses where it could influence synaptic function.

2.4.1. Distribution of polySia in the adult rat

The distribution of polySia in the adult rodent brain has been investigated previously (for review see (Seki and Arai, 1993a, Bonfanti, 2006, Bonfanti et al., 1992, Hildebrandt and Dityatev, 2013)); however, the studies have focused predominantly on higher brain regions. Only three studies (Bonfanti et al., 1992, Seki and Arai, 1993a, Bouzioukh et al., 2001) have described the distribution of polySia immunoreactivity in the rat brainstem performed using anti-Men B antibody (mAb 5324). PolySia expression was described in a limited number of regions including the dorsal vagal complex, the raphe pallidus nucleus, the pyramidal tract, in the lateral and medial parts of the parabrachial nucleus, and in the mesencephalic trigeminal nucleus. Our results confirm the

presence of polySia in all these regions, except for the pyramidal tract which was not labelled in our study. Our data suggest that polySia expression is not limited to these regions as immunoreactivity was also detected in the other regions of the brainstem (see Table 2.2). Notably, the pattern of polySia-ir we described in the adult rat brainstem is similar to that described in the adult human brainstem (Quartu et al., 2008, Quartu et al., 2010). Some differences were noted. We did not detect immunoreactivity in the external cuneate or the hypoglossal nucleus, while polySia labelling in rat was present in A1 region, raphe pallidus nucleus, rostroventrolateral reticular nucleus, and mesencephalic trigeminal nucleus, not described in the human study. In addition, the area postrema was densely labelled in our study, whereas moderate diffuse immunostaining was described in the human study (Quartu et al., 2008). Whether these differences are truly species specific requires a detailed comparison. PolySia expression in the better studied higher brain regions appears to be indicative of cells undergoing structural or synaptic plasticity (for review see (Bonfanti, 2006, Hildebrandt and Dityatev, 2013)). Whether such functions are associated with polySia labelling in rat brainstem regions requires further study.

The polySia distribution we observed in the rat spinal cord also confirms and extends previous findings (Seki and Arai, 1993b, Bonfanti et al., 1992). Most significantly we showed for the first time polySia-ir in the IML, specifically associated with many, but not all, SPNs. SPNs innervate, by way of postganglionic neurons, a diverse range of functionally distinct targets including, but not limited to, blood vessels and the heart (Llewellyn-Smith, 2011), brown and white adipose tissue (Bamshad et al., 1998, Bamshad et al., 1999), and the adrenal medulla (Edwards et al., 1996, Morrison and Cao, 2000). SPNs such as those innervating the heart and blood vessels are tonically driven by supraspinal sites such as the rostral ventrolateral medulla (Guyenet, 2006). It would be interesting to know if the tonically active SPNs are those associated with polySia as this would be in keeping with the idea that polySia is linked to plasticity. Such an association would not be surprising as the NTS, dorsal horn, and trigeminal nucleus which are also constantly receiving viscera- or somatosensory input from the periphery (Bokiniec et al., 2017, Kalia and Sullivan, 1982, Leak et al., 1988) also express high levels of polySia. Potentially we could raise the hypothesis that high expression of polySia is associated with brain regions that receive continuous synaptic input.

Within the selected regions of the brainstem (Sp5C and NTS) and spinal cord examined, we did not detect any polySia expression on myelinated axons which is in keeping with the result of a previous immunoelectron microscopic observation in which polySia labelling was found to be

restricted to unmyelinated axons in the superficial layer of the dorsal horn of the adult rat (Seki and Arai, 1993a) and mouse (Oumesmar et al., 1995). This is also in keeping with the finding during development that down-regulation of polySia was required for myelination of axons (Charles et al., 2000, Fewou et al., 2007).

We found some colocalization of polySia with synaptophysin in the dorsal horn, suggestive of a synaptic or presynaptic location of polySia. Similarly, partial colocalization of polySia with synaptophysin was reported in the rat cerebral (Gómez-Climent et al., 2011) and medial prefrontal cortex (Varea et al., 2005) and the human amygdala (Varea et al., 2012). In the dorsal vagal complex (Bouzioukh et al., 2001a) and the NTS (Bokiniec et al., 2017), however, a close apposition of the vast majority of polySia positive dots with synaptophysin positive terminals and not their colocalization was found, suggesting that the localization of polySia may vary at synapses in different brain regions.

No association of polySia with GFAP in the Sp5C, NTS, and spinal cord was found. This is in line with the finding of Bouzioukh et al. (2001a) in the dorsal vagal complex, indicating that proximal dendrites of astrocytes at least in the regions examined do not express polySia (Bouzioukh et al., 2001a). Similar results were found in the studies on higher brain regions where polySia-ir was not found in the GFAP positive structures in the adult rodent cerebral cortex (Gómez-Climent et al., 2011) and the adult mouse and human mPFC (Varea et al., 2005). However, we have shown for the first time association of polySia with fine astrocytic processes in the two selected regions (the Sp5C and NTS) using an anti-EAAT2 antibody. Our ultrastructural analysis showed polySia expression at sites that influence neurotransmission: in the extracellular space and intricate processes of astrocytes that envelop neurons and synapses, as well as in some dendrites and axon terminals, consistent with our EAAT2/polySia and synaptophysin/polySia double labelling. Supporting our finding of polySia expression in the fine distal processes of astrocytes, blocking microtubular function in the neurosecretory hypothalamus caused accumulation of polySia in astrocyte cell bodies (Theodosis et al., 1999, Theodosis et al., 2008). Expression around neurons found here is consistent with previous studies in the hippocampus, striatum, and cortex where polySia was linked with synaptic plasticity (Uryu et al., 1999, Hildebrandt and Dityatev, 2013, Eckhardt et al., 2000, Muller et al., 1996). Expression of polySia in the ER/Golgi found in the NTS is expected as polySia is posttranslationally added to its acceptors in the Golgi compartment (Eckhardt et al., 1995, Scheidegger et al., 1995). It would be interesting to investigate polySia

carriers in the Golgi of the NTS as recently a Golgi-confined expression of polySia on carriers other than NCAM was found. These polysialylated proteins were transiently recruited to the cell surface in response to stimuli (Werneburg et al., 2016, Werneburg et al., 2015).

Within the spinal cord dorsal horn, dorsal root afferent fibres contain a range of molecules with most peptidergic C fibres expressing CGRP (Crossman, 2016), and the lack of association of CGRP with polySia indicates that these unmyelinated fibres are unaltered by polysialylation. In line with this, C fibre presynaptic elements were reported to lack polySia based on double labelling of polySia and fluorescent wheat germ agglutinin, used to label projections to lamina II of the dorsal spinal cord (El Maarouf et al., 2005).

In contrast, polySia-ir was found on inhibitory neurons revealed using SSTR2A. El Maarouf et al. (2005) described polySia positive cells in lamina II as interneurons based on their localization and morphology (size, shape, and length of immunolabelled fibres) using confocal microscopy (El Maarouf et al., 2005), though there was no experimental evidence confirming this. In addition, studies on cortical areas, including the adult human and rat prefrontal cortex (Varea et al., 2007, Varea et al., 2005), the adult human and mouse amygdala (Gilabert-Juan et al., 2011, Varea et al., 2012), and the subtriangular septal zone and the triangular septum (Foley et al., 2003) have demonstrated that many polySia positive neurons were inhibitory using interneuron markers, principally GAD67. However, GAD labelling in the spinal cord, except for the ventral horn, labels predominantly terminals (Mackie et al., 2003) despite GABA being the primary inhibitory neurotransmitter in the dorsal horn of the spinal cord (Todd and Maxwell, 2000). GAD mRNA labelling by in situ hybridization (Deuchars et al., 2005) or GAD67-GFP (or mCherry) knock-in mice (Gotts et al., 2016) would be required to demonstrate GABAergic cell bodies. Further examination using different markers against GABA and glycine, such as neuropeptide Y and parvalbumin, as well as glutamatergic interneuron markers, such as vesicular glutamate transporter 2 (Todd et al., 2003, Maxwell et al., 2007, Polgar et al., 2003) would be useful to determine the level of polySia associated with different interneuron cell types within the dorsal horn. In addition, whether polySia is always expressed in the same subgroups of interneurons retaining it constantly or whether it is temporarily expressed on different subgroups of interneurons depending on synaptic activity is unclear. Furthermore, the functional role of polySia on inhibitory neurons of the dorsal horn remains to be examined. In the adult cerebral cortex, polySia positive interneurons received less synaptic input compared to polySia negative ones and demonstrated less dendritic arborization

and spine density suggesting that polySia in the cerebral cortex is a negative regulator of connectivity of interneurons and may be involved in the structural plasticity of inhibitory cortical networks (Gómez-Climent et al., 2011). In keeping with this, polySia removal was associated with a transient increase in dendritic spines of hippocampal interneurons (Guirado et al., 2013). Does polySia expression allow interneurons of the dorsal horn to remodel the structure of their neurites and synaptic contacts? Does it alter receptor conformations or change NCAM signalling pathways in these neurons? These questions need to be addressed in future studies.

The distribution of polySia in the adult rat trigeminal ganglion was similar to that of human for neurons and SGCs (Quartu et al., 2008) although we did not find any cytoplasmic labelling described by Quartu et al. (2008) in some neurons. Moreover, we did not identify polySia-ir in Schwann cells. It is possible that polySia expression on the cell surface of neurons and around SGCs surrounding neurons play a role in signalling and plasticity by interrupting transducing intracellular signals between neurons and their surrounding glia (Gu et al., 2010, Suadicani et al., 2010) due to the hydrated large volume of polySia (Rutishauser, 2008). However functional evidence is required.

Overall, our results regarding the distribution of polySia in the adult rat show that rodents can be good models for humans when it comes to polySia investigations in brainstem regions and trigeminal ganglion due to similarity in the polySia positive structures, facilitating potential rat-human scale-up procedures.

2.4.2. Comparison of polySia distribution in the adult rat and mouse

Surprisingly, the distribution of polySia within the adult mouse brainstem has been poorly investigated. Genetically modified (transgenic, knockout, conditional knockout, or knock-in) mice are used extensively in research particularly as animal models to study human development, diseases, and disorders (Cho et al., 2009). This includes a significant number of studies where polySia function was investigated (see Chapter 1). This deficit in knowledge led us to examine the distribution of polySia in the mouse brainstem and spinal cord. A similar distribution pattern was seen between mouse and rat brainstem with only few differences in the intensity of labelling. Differences were more apparent in the spinal cord, particularly in lamina I of the dorsal horn, where much less labelling was present in mouse compared to rat. These differences raise a question as to whether polySia functions differently in the dorsal horn of rat and mouse or whether the differences

reflect functional rearrangements within mouse or are due to variations in signalling or plasticity. A functional study using a patch-clamp technique is suggested to look at 2nd order neurons with and without enzymatic removal of polySia to determine how the sugar alters transmission in the dorsal horn of rats and mice (Bokiniec et al., 2017).

2.4.3. Comparison of mAb 735 and mAb 5324

Several anti-polySia antibodies have been developed including but not limited to 12E3, 5A5, 2-2B (mAb 5324; anti-Men B), polyclonal Ab H.46, and mAb 735. Comprehensive examination of the immunospecificity of these anti-polySia antibodies using an ELISA based approach revealed that these antibodies recognized different Sia chain lengths (Sato et al., 1995) with only H.46 (currently unavailable) and mAb 735 being specific only towards polySia (DP≥11 and DP≥8, respectively) (Sato and Kitajima, 2013a). However, mAb 5324 is currently the only commercially available polySia antibody which was also used in most studies describing polySia distribution including those investigated the brainstem and spinal cord (Bonfanti et al., 1992, Quartu et al., 2008, Quartu et al., 2010). Anti-polySia mAb 5324 (Rougon et al., 1986) is an IgM antibody reported to recognize oligo/polySia (DP≥4), while anti-polySia mAb 735 (Frosch et al., 1985) is an IgG2a antibody reported to recognize polySia (Sato and Kitajima, 2013a).

The presence of oligoSia has been reported in the adult mouse brain with most oligoSia residues located on glycoproteins other than NCAM (Sato et al., 2000). Therefore, one might expect to see labelling differences between mAb 735 and mAb 5324. However, the labelling was similar in most areas examined, suggesting that either both antibodies only recognize polySia or the level of oligoSia in the brainstem and spinal cord is quite low, or oligoSia is present only in the regions expressing polySia. It is also possible that mAb 5324 only recognizes polySia on NCAM as described previously (Bonfanti et al., 1992); however, no strong evidence is available to confirm this. Interestingly, when homogenized samples from the superficial DH and NTS were pretreated with endoN, no band was observed in the blot probed with mAb 5324 (Figure 2.15B), further indicating that either the sample lacked oligoSia or the antibody only recognizes polySia or oligo/polySia-NCAM.

2.5. Conclusion

Our data expands previous studies and shows that polySia is expressed in discrete regions of the central and peripheral nervous system of adult rats, which might be indicative of the capacity of

polySia to structurally and/or functionally alter neuronal function particularly at sites which receive continuous input including sensory information. Furthermore, the expression of polySia on fine processes of astrocytes in the Sp5C and NTS or inhibitory interneurons of the dorsal spinal cord, found in this study, may have important implications on the structure and physiology of these cells and may help us to understand the etiology of certain disorders associated with alteration of astrocytes or inhibitory networks. Finally, the similarity of polySia expression in the rat, mouse, and human brainstem indicates that rats and mice are appropriate animal models for polySia study in humans. This conservation could also indicate the importance of polySia in modulating function in the areas that express this sugar.

Chapter 3 : Identification of polysialic acid interacting partners in the dorsal horn of rat and mouse and the trigeminal nucleus of rat

Abstract

Polysialic acid (polySia) is a large cell surface glycan attached predominantly to the neural cell adhesion molecule (NCAM) in the mammalian brain. PolySia has a discrete expression pattern which is restricted to specific regions of the adult central nervous system (CNS), postulated to exhibit synaptic plasticity. In the lower brain and spinal cord, the interacting partners, function, and mechanisms of action of polySia are poorly understood. The aim of this study was to determine interacting partners of polySia initially in the dorsal horn of the spinal cord of adult Sprague Dawley rats using co-immunoprecipitation (IP) followed by label-free liquid chromatography tandem mass spectrometry analyses. Thirteen proteins were identified as potential binding partners of polySia. Five of these candidates: receptor expression-enhancing protein 5 (REEP5), guanine nucleotide-binding protein G(o) subunit alpha (GNOA1), sodium/potassium-transporting ATPase subunit alpha-2 (ATP1A2), sodium/potassium-transporting ATPase subunit alpha-3 (ATP1A3), and clathrin heavy chain (CLTC) were selected for further investigation using co-IP and reverse co-IP followed by western blot analyses and further validated as potential binding partners of polySia. Colocalization of polySia with ATP1A2 and GNAO1 at the cell surface, neuropil and fine fibres of the dorsal horn and dorsolateral funiculus was detected using confocal microscopy. Co-labelling was also detected in dorsolateral funiculus between polySia and REEP5. Two other regions in the brainstem and spinal cord were also explored in order to determine whether the same interactions were present in different brain regions. Co-IP of polySia from trigeminal nucleus caudalis followed by western blot analyses of REEP5 and GNAO1 and immunostaining of this region with REEP5, GNAO1, and ATP1A2 confirmed their polySia interaction status. Immunostaining of the intermediolateral cell column (IML) showed colocalization of polySia with ATP1A2, GNAO1, and REEP5 suggesting that polySia may have similar actions within functionally different regions of the adult rat CNS. Furthermore, we examined whether the same potential binding of polySia with REEP5, GNAO1, ATP1A2, and ATP1A3 detected in rat were also present in mouse. Similar interactions were seen between the four binding proteins and polySia in the mouse dorsal horn. However, ATP1A2, GNAO1, and REEP5 also showed partial colocalization with NCAM and thus we have not yet determined if the interaction is with polySia, NCAM, or both. Overall, our data suggest that in multiple species polySia may have the same or similar roles. This result may also extend to humans as some evidence suggests that similar brainstem regions exhibit high expression

levels of polySia. The findings of this study greatly extend the list of potential interacting partners of polySia expanding the functional role of sugar in the adult nervous system.

3.1. Introduction

Polysialic acid (polySia) is a long linear homopolymer of sialic acid, linked via α2,8-glycosidic bonds in the mammalian brain (Finne, 1982, Mühlenhoff et al., 1998). This large cell surface glycan is predominantly attached to the neural cell adhesion molecule (NCAM) in vertebrates (Bonfanti and Theodosis, 2009) and due to its highly hydrated and negatively charged structure acts as a negative regulator of the adhesive properties and binding abilities of NCAM (Brusés and Rutishauser, 2001, Hildebrandt et al., 2010, Yang et al., 1992, Yang et al., 1994). Glycosylation with this unusual carbohydrate has also been described on a limited number of other mammalian proteins including the α subunit of the voltage-dependent sodium channel (James and Agnew, 1987, Zuber et al., 1992), the synaptic cell adhesion molecule 1 (SynCAM 1) (Galuska et al., 2010), neuropilin-2 (NRP-2) (Curreli et al., 2007), the C–C chemokine receptor type 7 (CCR7) (Kiermaier et al., 2016), E-selectin ligand-1 (Werneburg et al., 2016), CD36 scavenger receptor in human milk (Yabe et al., 2003), and the polysialyltransferases (polySTs) which polysialylate NCAM and other molecules (Mühlenhoff et al., 1996a, Close and Colley, 1998).

PolySia is widely expressed during central nervous system (CNS) development where it modulates dynamic cell interactions such as neurite outgrowth, cell migration, axonal guidance and branching, neuronal pathfinding, and synapse formation (Hildebrandt and Dityatev, 2013, Bonfanti, 2006, Brusés and Rutishauser, 2001, Schnaar et al., 2014). However, in the adult, polySia has a discrete expression pattern where high levels of expression are restricted to specific areas of the CNS (as described in Chapter 2) associated at least in higher order brain regions with high levels of synaptic plasticity and likely synaptic throughput (Eckhardt et al., 2000, Dityatev et al., 2004, Rutishauser, 2008, Bonfanti and Theodosis, 2009, Kochlamazashvili et al., 2010).

PolySia on the cell surface is located on the outermost branches of glycosylated NCAM or the other glycoproteins making it a suitable target for binding proteins (Schnaar et al., 2014). Despite this, only a small number of molecules have been reported as binding partners of this sugar: the gonadal hormone estradiol (Garcia-Segura et al.,1995), heparan sulphate proteoglycans (Storms and Rutishauser, 1998), brain-derived neurotrophic factor (BDNF) (Muller et al., 2000), AMPA receptors (Vaithianathan et al., 2004), NR2B subunit-containing NMDA receptors (Hammond et al., 2006), chemokine (C-C motif) ligand 21 (Bax et al., 2009, Kiermaier et al., 2016), histone H1 (Mishra et al., 2010), dopamine (Isomura et al., 2011), fibroblast growth factor 2 (FGF2) (Ono et

al., 2012), myristoylated alanine-rich C kinase substrate (MARCKS) (Theis et al., 2013), and HIgM12 monoclonal antibody (Watzlawik et al., 2015). These interacting partners have been identified mainly using artificial or recombinant systems or using tissue extracted from higher brain regions. The objective here was to identify potential binding partners in the spinal cord and areas of the phylogenetically primitive brainstem that also express high levels of polySia.

The dorsal horn of the spinal cord is a major sensory centre of the CNS in which information from the periphery is received, integrated, and transmitted to local centres or higher levels of the CNS (Perl, 1984, Crossman, 2016). The superficial dorsal horn exhibits considerable activity-dependent synaptic plasticity following inflammation and tissue and/or nerve injury (Woolf and Salter, 2000, Thompson Haskell et al., 2002, Dubner and Ruda, 1992, Luo et al., 2014, Gerber et al., 2000) and expresses abundant polySia (Bonfanti et al., 1992, El Maarouf et al., 2005, Seki and Arai, 1993b) (see Chapter 2). Our first aim therefore was to determine potential binding partners of polySia in the dorsal horn of the spinal cord since abundant polySia in a large enough accessible region was required for mass spectrometry analysis. It was difficult to isolate intermediolateral cell column of the spinal cord (IML), a novel polySia positive area found in Chapter 2, and too many animals would be sacrificed for inclusion of the nucleus of solitary tract or rostral ventrolateral medulla (the initial targets for Chapter 4).

Next we asked whether similar binding partners are found in different regions of the lower brainstem and spinal cord by determining whether binding partners identified in the dorsal horn are also binding partners of polySia in the spinal trigeminal nucleus caudalis (Sp5C) and IML. Both Sp5C and the IML express considerable levels of polySia in the adult rat (see Chapter 2) but mediate very different functions: Sp5C receives sensory information related to pain and temperature, via the trigeminal ganglion, from the face (Sessle, 1987, Sessle, 2000), whereas the IML contains about 80% of sympathetic preganglionic neurons (SPNs), the major source of sympathetic outflow to the periphery (Llewellyn-Smith, 2011). Finally, we sought to determine whether binding partners of polySia identified in the dorsal horn were common across species by comparing our findings in rat with those in mouse spinal cord. We identified and compared binding partners utilising co-immunoprecipitation followed by mass spectrometry, western blotting, and immunohistochemistry combined with confocal microscopy.

3.2. Materials and methods

3.2.1. Animals

All experimental procedures were approved by the Macquarie University Animal Ethics Committee (reference number ARA 2014/041 and 2015/040) and conducted in accordance with the Australian Code of Practice for the Care and Use of Animals for Scientific Purposes. Animals were housed under constant 12 h light/dark cycles and allowed standard rat chow and libitum. Experiments were performed on male Sprague Dawley rats (12-20 weeks old) and male C57BL/6J mice (8-12 weeks old) from the Animal Resources Centre, Perth, Western Australia.

3.2.2. Antibodies

Table 3.1 details the antibodies used. Monoclonal antibody 735 directed against polySia (mAb 735), endosialidase NF (endoNF), and monoclonal antibody H28 against NCAM were kindly provided by Professor Rita Gerardy-Schahn (Hannover Medical School, Hannover, Germany) with all other antibodies commercially sourced as indicated.

3.2.3. Tissue collection for western blotting and immunoprecipitation analysis

Animals were deeply anaesthetized using sodium pentobarbitone (80mg/kg i.p.). When reflex testing of paw withdrawal to pain evoked no response the heart was punctured and the brain and spinal cord removed as rapidly as possible (brain within 3-4 min and the spinal cord within 7-9 min). These tissues were placed in cryoprotectant solution (876 mM sucrose, 500 µm polyvinylpyrrolidone, 76.7 mM disodium monophosphate (Na_2HPO_4), 26.6 mM sodium diphosphate (NaH_2PO_4), 5mM ethylene glycol) and cooled on dry ice before being transferred to a -80 C degree freezer for preservation until dissection. The brain and spinal cord were dissected into 2 mm coronal segments on dry ice using a brain matrix or manual cutting. The spinal cord was dissected as shown in Figure 3.1 with the dorsalmost section of the spinal cord containing laminae I-IV being termed the dorsal horn (DH) for this analysis. Similarly, the trigeminal nucleus caudalis (Sp5C) and adjacent regions (Figure 3.1) were also isolated and this sample is called Sp5C. Care was taken not to allow the tissue to defrost during dissection.

Table 3.1. Details of primary and secondary antibodies used.

Primary antibody	**Cat # and Company**	**Species**	**Reference/Publication**	**Dilution**
Anti-ATP1A2	16836-1-AP, Proteintech Group	Rabbit	(Liu et al., 2017)	IHC* 1:2000 WB* 1:1600 IP* 19.5 µl
Anti-Clathrin heavy chain	ab21679, Abcam	Mouse	(Wiernasz et al., 2014), (Poulsen et al., 2017)	WB 1:1000 IP 3 µl
Anti-GAPDH	Ab9485, Abcam	Rabbit, poly		WB 1:5000
Anti-GNAO1	12635-1-AP, Proteintech Group	Rabbit	(Liu et al., 2014), (Zhen et al., 2016)	IHC 1:400 WB 1:600 IP 13 µl
Anti-REEP5	14643-1-AP, Proteintech Group	Rabbit	(Sharoar et al., 2016), (Chang et al., 2013)	IHC 1:100 WB 1:1000 IP 10 µl
endoNF (6.7 mg/ml)			(Stummeyer et al., 2005)	WB 2.25 µl/1 mg protein
mAb 735 (2 mg/ml)		Mouse	(Zhang et al., 2004, Frosch et al., 1985)	IHC 0.5 µl/ml WB 0.5 µl/ml IP: 1 µl/ 540µg protein (rat/mouse DH) 1 µl/ 900 µg protein (rat TN) 1.5 µl/ 730 µg protein (rat DH) 1.5 µl/ 1 mg protein (mouse DH)
Monoclonal antibody H28 against NCAM (4.45 mg/m1)		Rat	(Hirn et al., 1981)	IHC 1:8900
Sodium / potassium ATPase alpha-3 Antibody (XVIF9-G10)	MA3-915, Thermo Fisher Scientific	Mouse	(Arystarkhova and Sweadner, 1996, Edwards et al., 2013)	WB 1:1000 IP 3 µl
Secondary antibody	**Cat # and Company**	**Species**		**Dilution**
Alexa Fluor® 488 AffiniPure Donkey Anti-Rabbit IgG (H+L)	Jackson ImmunoResearch	Donkey		IHC 1:500
Anti-Mouse IgG (H+L), HRP conjugate	Invitrogen	Goat		WB 1:5000
Anti-Rabbit IgG H&L (HRP)	ab6721, Abcam	Goat		WB 1:3300
Donkey anti-Mouse IgG (H+L) Highly Cross-Adsorbed Secondary Antibody, Alexa Fluor 555	A-31570, Thermo Fisher Scientific	Donkey		IHC 1:500
Goat anti-Rat IgG (H+L) Secondary Antibody, Alexa Fluor 647 conjugate	A-21247, Thermo Fisher Scientific	Goat		IHC: 1:500

IHC*; immunohistochemistry, WB*; western blotting, IP*; immunoprecipitation

3.2.4. Tissue homogenization, western blotting, and immunoprecipitation

Tissue homogenization was carried out using a lysis buffer, described previously, with some modifications (Weinhold et al., 2005). The tissues were lysed in 10 µl/mg ice cold lysis buffer containing 50 mM Tris-HCl (pH 8), 150 mM NaCl, 4 mM EDTA, 1% (v/v) Triton X-100, and 1% (v/v) protease inhibitor cocktail (Sigma–Aldrich, NSW, Australia). Lysates were homogenized for 3 cycles at 5 speed, each cycle lasting for 20 s using a FastPrep-24 instrument (MP Biomedicals, NSW, Australia). Ceramic beads and detergent insoluble materials were removed by two rounds of centrifugation at 13,200 RPM for 5 and 30 min respectively, at 4 °C. Supernatants were collected and protein concentrations were obtained using a bicinchoninic acid (BCA) assay kit according to the manufacturer's instructions (Pierce, Thermo Fisher Scientific, VIC, Australia). For removal of polySia, a fraction of the lysate was treated with endoNF (3 h at 37 °C) before western blotting. Samples (containing approximately 10-40 µg protein) were boiled in 4X NuPAGE® LDS Sample Buffer (Invitrogen, CA, USA) at 70 °C for 10 min under reducing condition, and along with Precision Plus Protein Western C standards (Bio-Rad, NSW, Australia) were separated by sodium dodecyl sulphate–polyacrylamide gel electrophoresis (SDS–PAGE). Any kD™ Mini-PROTEAN® TGX Stain-Free protein gels (Bio-Rad) and 10x Tris/Glycine/SDS running buffer (Bio-Rad, NSW, Australia) were used. Proteins were transferred to a nitrocellulose or polyvinylidenefluoride (PVDF) membrane (Bio-Rad, NSW, Australia) by semi-dry method. The membrane was blocked

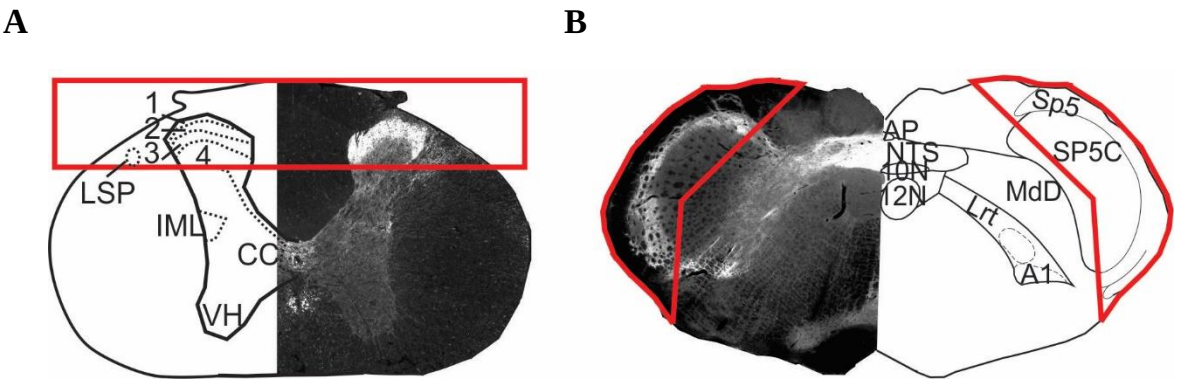

Figure 3.1. Areas of the rat spinal cord (A) and brainstem (B) dissected for analysis (red boxes). (A) The numbered regions (1-4) show the lamina of the thoracic spinal cord. The dissected region includes laminae I-IV, part of dorsolateral funiculus including the lateral spinal cord (LPS), and adjacent white matter. (B) The dissected region includes spinal trigeminal tract (Sp5), spinal trigeminal nucleus, caudal part (Sp5C), and adjacent tissues (including dorsal spinocerebellar tract, and parts of external cuneate nucleus and cuneate nucleus).

with 5% (w/v) skim milk in Tris-buffered saline containing 0.1% Tween-20 (TBST, 20 mM Tris-HCl, pH 7.5, 150 mM NaCl, 0.1% (v/v) Tween 20) for 1 h at RT, then washed with TBST, 3×5 min. Membranes were probed with primary antibodies (Table 3.1) overnight at 4 °C. This was followed by three washes in TBST (3×5 min), and 1-h room temperature incubation with secondary antibodies (Table 3.1). The membranes were washed with TBST, 3×5 min and visualized with enhanced chemiluminescence (ECL) using a Bio-Rad ChemiDoc XRS chemiluminescence detector.

Co-immunoprecipitation (IP) was performed according to the manufacturer's instructions for Dynabeads® Protein G (Life technologies) with some modifications. Briefly, Dynabeads Protein G (20-30 µg) was incubated with 2 µg of mAb 735 or with preimmune mouse IgG (negative control; #Sc-2025, Santa Cruz Biotechnology, CA, USA) for 40 min at room temperature, followed by 3 h at 4 °C. The beads were washed with 250 µl of IP lysis buffer (50 mM ice-cold Tris-HCl (pH 8) containing 150 mM NaCl, 4 mM EDTA, 1% (v/v) Triton X-100). The supernatant containing 540 µg protein (for murine samples tissues for each sample were acquired from 2 animals) was pre-cleared with Dynabeads Protein G for 1 h at 4 °C. The pre-cleared supernatant was added to the antibody-bead complex and incubated overnight at 4 °C. The complex was washed three times using IP lysis buffer, twice without Triton X-100, and finally with 20 mM Tris-HCl (pH 7.5). Elution was carried out by heating the beads in 4X NuPAGE® LDS Sample Buffer (Invitrogen, CA, USA) in Milli-Q water (1:3) containing 100 mM DTT at 70 °C for 10 min and the eluates were separated on an SDS-PAGE gel.

3.2.5 Protein identification by trypsin in-gel digestion followed by label-free liquid chromatography tandem mass spectrometry (LC-MS/MS) analysis

Approximately 75% of the eluate obtained by immunoprecipitation was used for protein identification by LC-MS/MS. Proteins were separated using Bio-Rad 4-20% mini-protein gels. The gels were stained by Coomassie Brilliant Blue G-250 (Bio-Rad) overnight and destained in 25% (v/v) methanol, and 10% (v/v) acetic acid in water for 1 h prior to in-gel digestion. The gel bands were chopped into small pieces, washed twice with 300 µl of 50% (v/v) acetonitrile (ACN) for 15 min, and shrunk with 300 µl of 100% (v/v) ACN. To the gel pieces, 60 µl of 100 mM NH_4HCO_3 was added and after 5 min, an equal volume of 100% (v/v) ACN was added. After 15 min, the liquid was discarded and the gel pieces were dried in a Speed-Vac. Reduction and alkylation were

performed in a solution of 10 mM dithiothreitol (DTT) in 100 mM NH_4HCO_3 (37 °C, 1 h) and 55 mM iodoacetamide in 100 mM NH_4HCO_3 (room temperature, 30 min, in the dark), respectively. The fractions were washed twice with 300 µl of 50% (v/v) ACN for 15 min and dehydrated with 300 µl of 100% (v/v) ACN. Then, 60 µl of 100 mM NH_4HCO_3 was added and after 5 min, an equal volume of 100% (v/v) ACN was added. After 15 min, the liquid was discarded and the gel pieces were dried in a Speed-Vac. Proteins were digested with 70 µl (5 ng/µl) Trypsin (Promega Corporation, Madison WI) in 50 mM NH_4HCO_3 overnight at 37 °C. Peptide extraction was performed twice with 100 µl of 2% (v/v) formic acid in 50% (v/v) ACN on ice. Each time after 20 min the supernatant was collected. After the second round of extraction, the supernatant was dried using a vacuum centrifuge and reconstituted to 20 µl with 1% (v/v) formic acid. Prior to the mass spectrometric analysis, samples were desalted using Zip Tip C_{18} pipette tips (Millipore, NSW, Australia) pre-activated by 10 µl of 0.1% (v/v) formic acid/ 60% (v/v) ACN solution and equilibrated with 10 µl 0.1% (v/v) formic acid solution. Samples were concentrated on Zip Tip by drawn up 20 µl of the samples from the Eppendorf tube pipetting up and down 10 times. After several washes of Zip Tips with 0.1% (v/v) formic acid, peptides were eluted with 30 µl of 0.1% (v/v) formic acid/ 60% (v/v) acetonitrile solution. The extracted peptides were dried in a vacuum centrifuge and then reconstituted in 12 µl of 0.1 % (v/v) formic acid, 10 µl of which was used for protein identification by nano-flow liquid chromatography electrospray tandem mass spectrometry (nanoLC-ESI-MS/MS) using a Q Exactive mass spectrometer coupled to an EASY nLC1000 (Thermo Fisher Scientific, Bremen, Germany). The digested peptide mixture was loaded onto a 75 µm x 100 mm C18 Halo, 2.7 µm bead size, 160 Å pore size column for reverse phase chromatography separation. Chromatography was performed on nanoLC system using a 90 min gradient (5%–90% v/v acetonitrile, 0.1% v/v formic acid) with a flow rate of 300 nl/min, and the peptides were eluted and ionized into a Q Exactive mass spectrometer. The electrospray source was fitted with an emitter tip 10 µm (New Objective, Woburn, MA) and maintained at 2.0 kV electrospray voltage. Precursor ions were selected for MS/MS fragmentation using a data-dependent "Top 10" method operating in FT-FT acquisition mode with HCD fragmentation. Data-dependent MS/MS acquisition mode consisted of a resolution of 35,000 scan acquisition and an AGC target of $1x10^6$ ions with a full mass range of 350-2000 m/z in full MS, and a MS^2 resolution of 17,500 with an AGC target of $2x10^5$ ions. Maximum injection times were set to 120 and 60 milliseconds in full MS and MS^2 respectively. The ion selection threshold for triggering MS/MS

fragmentation was set to 25,000 counts and an isolation width of 1.9 Da was used to perform HCD fragmentation with normalized collision energy of 30%.

All MS/MS spectra were searched against the Swiss-Prot Rattus proteome database (Swiss Institute of Bioinformatics) using the Mascot search engine (Matrix Sciences, UK) incorporated in the Proteome Discoverer software version 1.4.0.288 (Thermo Fisher Scientific, VIC, Australia). In the search parameters, a static modification was set for carbamidomethylation of cysteine whereas dynamic modifications were set for oxidation of methionine, N-terminal modification of glutamine and pyroglutamate, and acetyl modification on N-terminal residues. The enzyme specificity was set to trypsin and a precursor mass tolerance of 10 ppm and a fragment ion mass tolerance of 0.02 Da was used. Protein and peptide false discovery rates (FDR) was set to be < 0.01 (1% false discovery rate) for each database search and one missed cleavage was allowed. Protein identifications were validated employing a minimum of 2 peptides. The search results were exported into Microsoft Excel for quantitative analysis.

Quantitative analyses of expressed proteins were carried out with a label-free approach using spectral counting and normalized spectral abundance factor (Zybailov et al., 2006). The 2-sample unpaired t tests were run on log transformed NSAF data of a total of 3 biological replicates using the Scrappy program (Mirzaei et al., 2011, Neilson et al., 2013, Varkey et al., 2016). Proteins with a t test p-value < 0.05 were considered to be differentially expressed between eluted immunoprecipitates of mAb 735 co-IPs relative to those of the pre-immune IgG control co-IPs. In each individual comparison, only isolated proteins present in all triplicates of mAb 735 co-IP and with a total spectral count of > 5 were included in the data set. This resulted in a list of differentially expressed proteins (Mirzaei et al., 2011).

3.2.6. Reverse co-immunoprecipitations

For reverse co-IPs, Dynabeads Protein G (40 µg) were pre-bound with an anti-REEP5, ATP1A2, ATP1A3, GNAO1, or CLTC antibody (Table 3.1) or with a preimmune mouse/rabbit IgG (#Sc-2025 and #Sc-2027, Santa Cruz Biotechnology, CA, USA) as a control for 40 min at room temperature, followed by 3 h at 4 °C. Homogenized DH sample from Section 3.2.4 containing 900 µg protein (for murine samples tissues for each sample were acquired from 3 animals) was added to the antibody-beads complex after being pre-cleared with beads for 1 h at 4 °C. The washing step and elution steps were done exactly according to Section 3.2.4 with an extra step of washing with

the lysis buffer containing no Triton X-100 was added to the 5 washing steps. The eluted samples were used for western blotting analyses. Data presented are representative of three independent experiments.

3.2.7. Slide mounted immunohistochemistry

This method is described in Chapter 2 in Sections 2.2.5 and 2.2.5.1. Table 3.1 provides the details of the antibodies and dilutions used. Data presented are representative of five independent experiments.

3.3. Results

3.3.1. Identification of polySia binding proteins in the dorsal horn of the spinal cord

PolySia-specific mAb 735 (Frosch et al., 1985), extensively characterised and shown to be specific for only polySia (Loers et al., 2016, Galuska et al., 2010, Werneburg et al., 2015, Rollenhagen et al., 2012), was used for immunoprecipitation of polySia. To firstly confirm the specificity of this antibody, three samples (containing 40 µg protein) of homogenized dorsal horn (DH, n=3) were treated with endoNF, an enzyme that specifically cleaves polySia (α2,8-linked sialic acids) or were left untreated. The membranes were probed using mAb 735. A band was detected in untreated samples at around 250 kDa which was not present in endoNF-treated samples and this band was taken to be polySia (Figure 3.2A).

We next performed co-immunoprecipitation experiments on DH samples (n=3) to identify potential binding partners of polySia using mAb 735 and preimmune mouse IgG as a control. Immunoprecipitated proteins were eluted by denaturation in SDS loading buffer, and 25% of the total volume was analysed by SDS-PAGE and western blotting with mAb 735 to assess polySia binding. Analysis of the blot revealed specific and strong polySia enrichment from DH (Fig 3.2B). No polySia signal was detected in the control samples (Fig. 3.2B). The remainder of the eluate was subjected to separation using SDS-PAGE and after an in-gel trypsin digestion, the tryptic peptides were analysed by LC-MS/MS. After identification of proteins, relative quantification of enriched proteins was achieved based on spectral counts and normalized spectral abundance factor (Zybailov et al., 2006). Proteins that were not detected in the immunoprecipitate of preimmune IgG (control) IP or enriched in the immunoprecipitate of mAb 735 IP were considered as potential binding partners. We identified 14 potential polySia interacting proteins in three biological replicates using the following filtering criteria: i) a minimum of two unique peptides per identification, and ii) a protein and peptide false discovery rate (FDR) of ≤1% (Table 3.2). We selected five of the 14 candidate proteins to investigate further based on their Mascot score, percentage of coverage, and/or their potential or known functions, especially related to plasticity which is the main described function of polySia in the adult (see Chapter 1). The protein NCAM had the highest Mascot score and percentage of coverage which was not surprising and also provided validation since NCAM is the major carrier of polySia in the CNS (see Chapter 1).

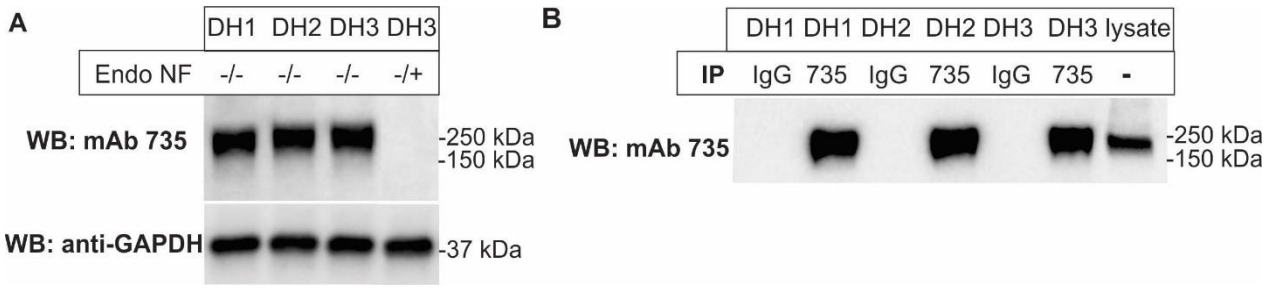

Figure 3.2. Confirmation of the specificity of monoclonal antibody 735 directed against polySia (mAb 735) and isolation of polysialylated proteins in the adult rat dorsal horn (DH). (A) Triton X-soluble DH fractions were separated by Any kD Mini-PROTEAN TGX Stain-Free Protein Gel and SDS/PAGE using 40 µg protein per lane with or without prior incubation with endoNF and immunostained with mAb 735. (B) mAb 735 was immobilized on beads and co-immunoprecipitation (IP) was performed using DH (n=3, DH1-DH3). A fraction of each eluate was immunostained with mAb 735.

Although Tubulin beta-5 chain had the highest score and percentage of coverage after NCAM, no reliable antibodies were available, limiting our ability to pursue this protein. The next four highest scoring proteins including receptor expression-enhancing protein 5 (REEP5), sodium/potassium ATPase subunits alpha 2 and alpha 3 (ATP1A2 and ATP1A3 respectively), and guanine nucleotide-binding protein G(o) subunit alpha (GNAO1) as well as clathrin heavy chain 1 (CLTC) were selected considering their importance in neuronal signalling (Isaksen and Lykke-Hartmann, 2016, Jiang et al., 1998, Vieira et al., 1996). Although ATP1A2 and ATP1A3 were identified we initially investigated only ATP1A3 due to antibody availability.

We then sought to validate the mass spectrometry results using co-IP followed by western blotting. Experiments were carried out on rat DH (n=3, with each lysate containing ~540 µg protein) using mAb 735 antibody. The eluted fractions were then analysed by western blot using antibodies specific to REEP5, GNAO1, ATP1A3, and CLTC. The antibodies detected bands corresponding to the molecular weights for REEP5 (21 kDa), GNAO1 (40 kDa), ATP1A3 (MW:110 kDa, detected band: 100 kDa), and CLTC (180 kDa) in the eluted proteins obtained by mAb 735 IP (Figure 3.3A). The results obtained were comparable to the quantitative proteomics data in that all proteins were enriched in eluates obtained from mAb 735 compared to the negative control IPs. REEP5 and CLTC (except for one replicate) were only found in the eluate following mAb 735 binding but not in the IgG control. GNAO1 and ATP1A3 protein bands were intense in the mAb 735 eluate but were still detectable in the control IgG IPs (Figure 3.3.A).

Table 3.2. Potential binding proteins detected by immunoprecipitation followed by label-free mass spectrometry. The Mascot score (probability based scoring), coverage (% of the protein identified), number of unique peptides, number of peptides, and number of peptide spectrum matches (PSMs) are the average of three independent experiments.

Accession	Gene Name	Description	Score	Coverage	# Unique Peptides	# Peptides	# PSMs	p.value
P13596	NCAM1	Neural cell adhesion molecule 1	32105.52	43.55	39	39	1216	0.003
P69897	Tubb5	Tubulin beta-5 chain	1159.8	29.5	2	12	55	3.35E-06
B2RZ37	Reep5	Receptor expression-enhancing protein 5	835.94	22.75	6	6	40	2.30E-05
P06687	Atp1a3	Sodium/potassium-transporting ATPase subunit alpha-3	610.6	15.86	5	14	31	0.011
P06686	Atp1a2	Sodium/potassium-transporting ATPase subunit alpha-2	498.88	14.35	5	14	30	0.047
P59215	Gnao1	Guanine nucleotide-binding protein G(o) subunit alpha	421.4	17.42	6	6	17	1.19E-05
P01830	Thy1	Thy-1 membrane glycoprotein	337.47	14.08	3	3	12	0.004
Q05962	Slc25a4	ADP/ATP translocase 1	332.64	23.38	6	7	16	0.021
P68255	Ywhaq	14-3-3 protein theta	326.64	16.33	2	4	13	2.03E-06
Q63198	Cntn1	Contactin-1	276.35	6.69	6	6	11	0.008
P11442	Cltc	Clathrin heavy chain 1	151.01	1.93	3	3	6	5.4E-04
P16036	Slc25a3	Phosphate carrier protein, mitochondrial	145.67	7.49	3	3	6	5.91E-05
P07340	Atp1b1	Sodium/potassium-transporting ATPase subunit beta-1	94.37	12.94	4	4	5	0.002
P47942	Dpysl2	Dihydropyrimidinase-related protein 2	69.47	2.97	2	2	4	3.17E-05

In order to determine if the detected bands in the immunoprecipitates of mAb 735 IPs were due to the interaction of the candidate proteins with polySia or due to non-specific binding of these proteins, a co-IP was performed on rat DH homogenates containing 730 µg protein with and without pretreatment with endoNF using mAb 735. All polySia was removed after endoNF treatment (Figure 3.3B). The REEP5 antibody did not detect any protein in eluates obtained either by mAb 735 or control IgG in endoNF treated samples which lacked polySia, indicating that REEP5 binding was polySia dependent (Figure 3.3C). Probing the eluates using ATP1A3 and

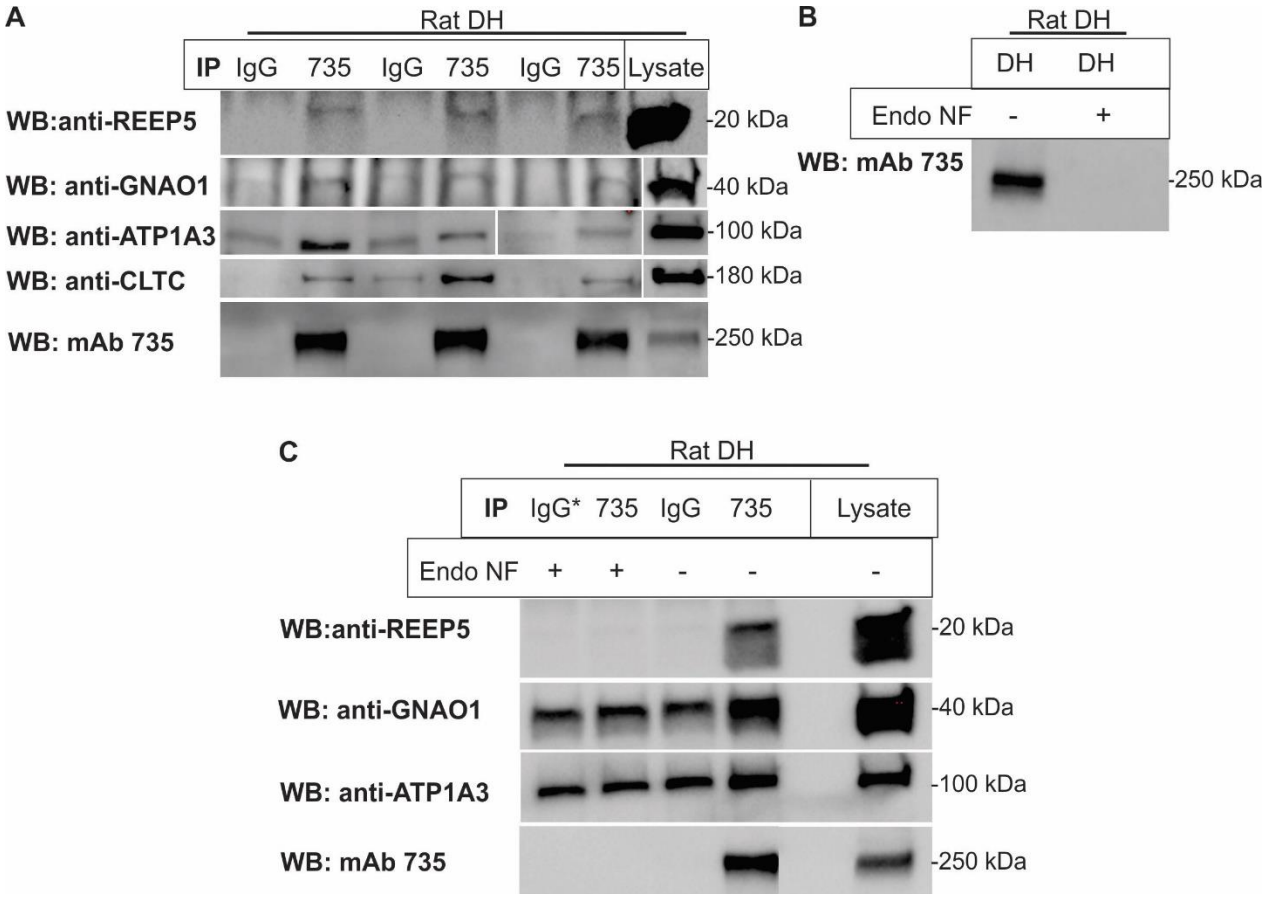

Figure 3.3. Co-immunoprecipitation (IP) followed by western blotting (WB) in adult rat dorsal horn (DH) to validate mass spectrometry results. (A) PolySia was immunoprecipitated from the homogenized DH fractions using mAb 735 antibody and the eluates were stained with anti-REEP5, anti-GNAO1, anti-ATP1A3, anti-CLTC, or mAb 735 antibodies. (B) The blot shows a fraction of endoNF treated DH (containing 30 µg protein) probed with mAb 735. PolySia was removed in the endoNF treated sample. The enzyme treated sample was used for the data shown in C. (C) Fractions of DH containing 1 mg protein were immunoprecipitated with mAb 735 before and after endoNF treatment. The immunoprecipitates were blotted against anti-REEP5, anti-ATP1A3, and anti-GNAO1 antibodies. IgG*: preimmune mouse IgG (used as control). Reduced exposure times were required for some lysate containing samples, the same membranes were imaged however.

GNAO1 antibodies showed that in both mAb 735 and control IgG immunoprecipitates of endoNF treated samples the intensity of the bands was similar between each sample and its IgG control, whereas in the samples that were not treated with endoNF, the intensity of the band was considerably higher in the eluates obtained from the sample than those of control IgG (Figure 3.3C).

3.3.2. Reverse co-immunoprecipitation verified the association of polySia with REEP5, GNAO1, ATP1A2, ATP1A3, and CLTC

Due to the non-specific binding of ATP1A3 and GNAO1 detected in the control IgG eluates in the co-IP experiments using mAb 735, any interaction of polySia with these proteins was considered as secondary targets for further validation. Therefore, in order to verify the interactions, a reverse co-IP on homogenized DH tissue of the adult rat was performed. Anti-REEP5, GNAO1, ATP1A2, ATP1A3, and CLTC antibodies were each immobilized on beads and after IP, the eluates were probed using mAb 735 antibody (Figure 3.4). To control for non-specific protein interactions, the preimmune mouse or rabbit IgG were used as controls appropriate for each antibody species. Western blot analysis of eluates showed a polySia band around 250 kDa in the resulting immunoprecipitates of REEP5, GNAO1, ATP1A2, ATP1A3, or CLTC IPs detected using mAb 735. This band was not detectable in the control IgG eluates (Figure 3.4).

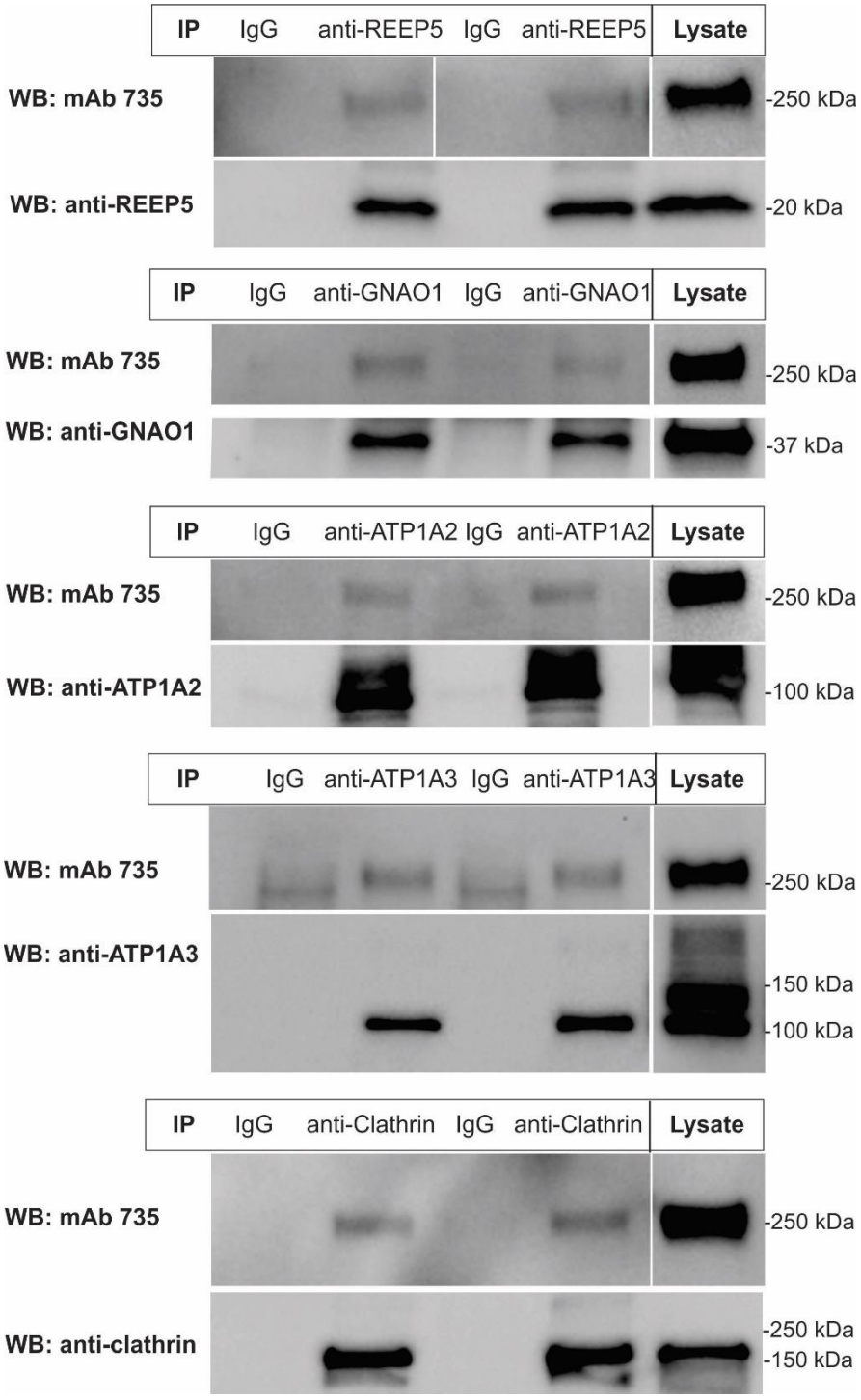

Figure 3.4. Interaction of polySia with REEP5, GNAO1, ATP1A2, ATP1A3, and CLTC by reverse co-immunoprecipitation (IP), followed by immunoblotting (WB). Dorsal horn fractions (DH) of adult rat were used for immunoprecipitation experiments using anti-REEP5, anti-GNAO1, anti-ATP1A2, anti-ATP1A3, or anti-clathrin antibodies. The isolated proteins were immunostained with mAb 735. Reduced exposure times were required for some lysate containing samples, the same membranes were imaged however.

3.3.3. Colocalization of ATP1A2, GNAO1, and REEP5 with polySia in the rat dorsal horn and dorsolateral funiculus

Next, the distribution of polySia and the candidate binding proteins were explored using confocal microscopy and dual label immunofluorescence in coronal sections of the adult rat DH using antibodies against polySia (mAb 735), ATP1A2, GNAO1, or REEP5. PolySia immunoreactivity (ir) was present at high levels in the superficial laminae of the dorsal horn, and comparatively lower in the dorsolateral funiculus including the lateral spinal cord (Figure 3.5A). Dense punctate staining was present in the neuropil with neuronal somata being immunonegative (Figure 3.5B-D) as described in Chapter 2. These results are in agreement with findings of previous studies in which distribution of polySia in the dorsal horn of adult rat has been described (Bonfanti et al., 1992).

ATP1A2-ir was present throughout the grey matter of the spinal cord and less abundantly in the dorsolateral funiculus, with some labelling also in the adjacent white matter (Figure 3.5A). Immunoreactivity was present in the neuropil and appeared to envelope somata (Figure 3.5B-C). ATP1A2-ir displayed some colocalization with polySia-ir with structures in the neuropil and on the cell surface of some neurons in the superficial laminae of the dorsal horn (Figure 3.5B-C). In the dorsolateral funiculus, some polySia was co-labelled with ATP1A2 mainly in bundles of fine fibres and to a lower extent on some cell membranes (Figure 3.5D).

Similar to the distribution of polySia, GNAO1-ir was highly expressed in the superficial layers of the dorsal horn as described previously (Worley et al., 1986). GNAO1-ir was also detectable in some regions of dorsolateral funiculus adjacent to the dorsal horn. The remaining white matter was largely immunonegative (Figure 3.6A). PolySia partially colocalized with GNAO1 in the superficial laminae of the dorsal horn and dorsolateral funiculus (Figure 3.6B and C). Colocalization was present in the neuropil and on some cell membranes.

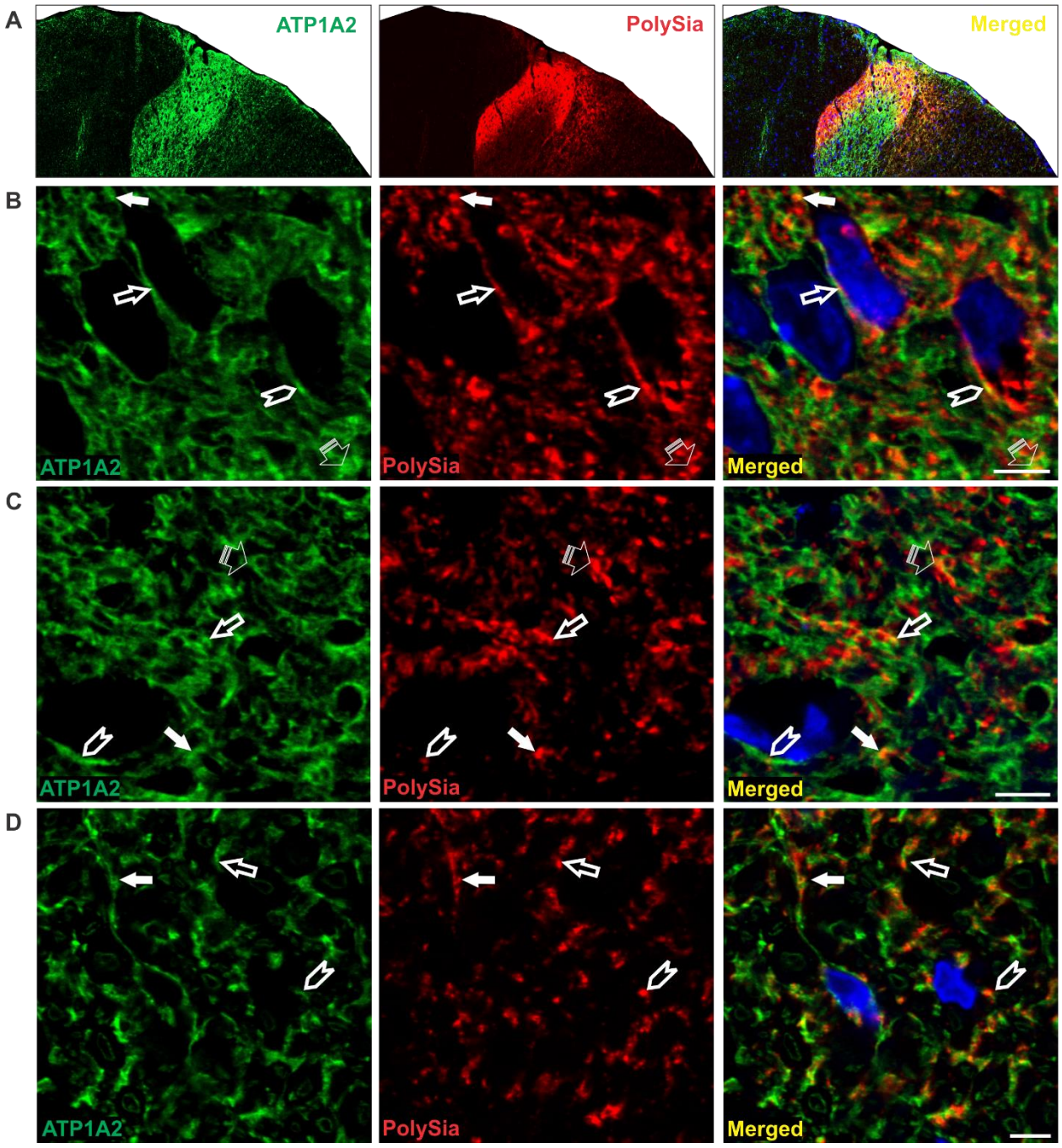

Figure 3.5. ATP1A2-ir (green) and polySia-ir (red) partially colocalized (yellow) at the cell surface of some cells and in the neuropil of the adult rat spinal cord. Nuclei were stained with DAPI (blue). (A) Distribution of ATP1A2-ir and polySia-ir in the dorsal hon. (B) and (C) The superficial laminae of the dorsal horn of two biological replicates, and (D) The dorsolateral funiculus. Arrows indicate examples of colocalization. Scale bars = 5 µm.

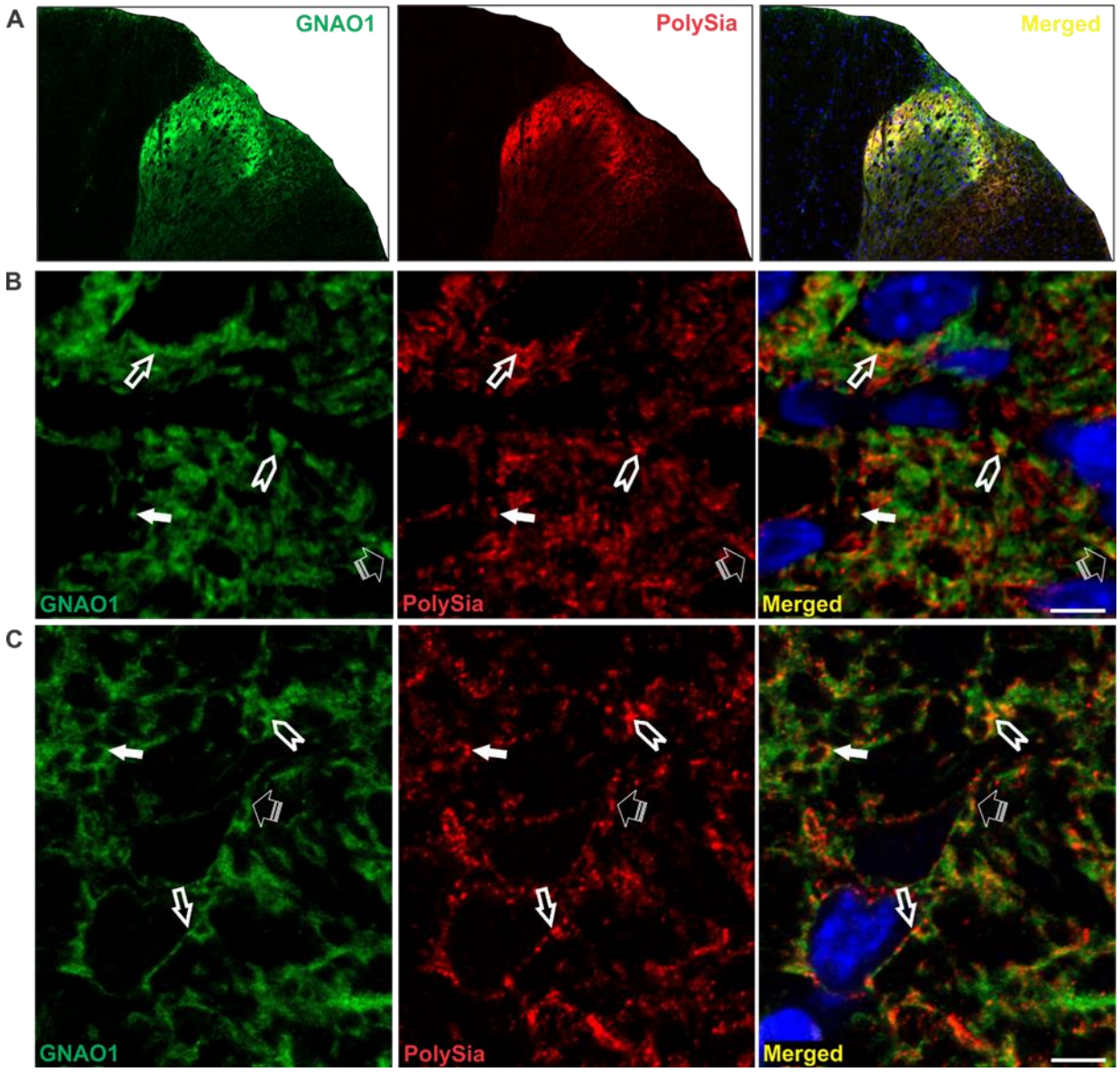

Figure 3.6. GNAO1-ir (green) and polySia-ir (red) partially colocalized (yellow) at the cell surface of some cells and in the neuropil of the adult rat spinal cord. Nuclei were stained with DAPI (blue). (A) Distribution of GNAO1-ir and polySia-ir in the dorsal horn. (B) The superficial laminae of the dorsal horn. (C) The dorsolateral funiculus. Arrows indicate examples of colocalization. Scale bars = 5 µm.

REEP5-ir was present in both white and grey matter of the spinal cord (Fig. 3.7A). Within the superficial laminae of the dorsal horn, the background staining made it difficult to assess potential co-labelling of this protein with polySia (Fig. 3.7Ai). Western blot analysis performed on the superficial laminae of the dorsal horn and Sp5C showed staining of multiple bands by this polyclonal antibody, which may indicate dimerization or non-specific binding (Figure 3.7B). This, however, is the most commonly used antibody for REEP5 (see Table 3.1).

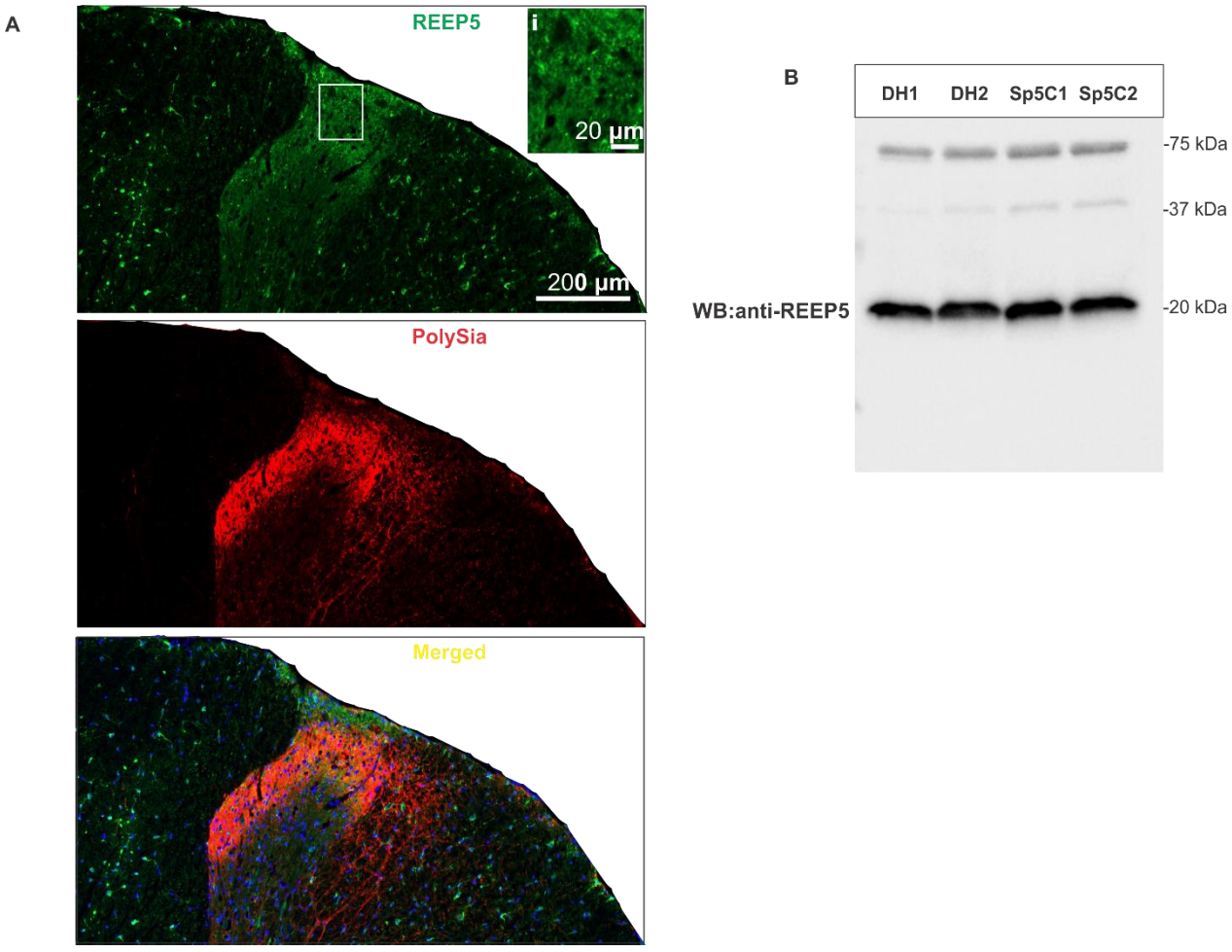

Figure 3.7. Labelling using the anti-REEP5 antibody may indicate dimerization or non-specific binding. (A) Distribution of REEP5- and polySia-ir in the dorsal horn. (Ai) The magnified image of the box in A. (B) Western blot images of the superficial laminae of the adult rat dorsal horn (DH) and trigeminal nucleus caudalis (Sp5C) probed using the anti-REEP5 antibody. Additional bands were detected in addition to the expected band (21 kDa) which may represent dimerization.

In the white matter including dorsolateral funiculus, the anti-REEP5 antibody appeared to label neuronal somata and processes (Figure 3.8A-D). Nevertheless, some colocalization between REEP5 and polySia was detected (Figure 3.8A-C) in the dorsolateral funiculus which appeared to be mainly in processes. Occasional colocalization was also found in the posterior funiculus, where some polySia expression was found (Figure 3.8D).

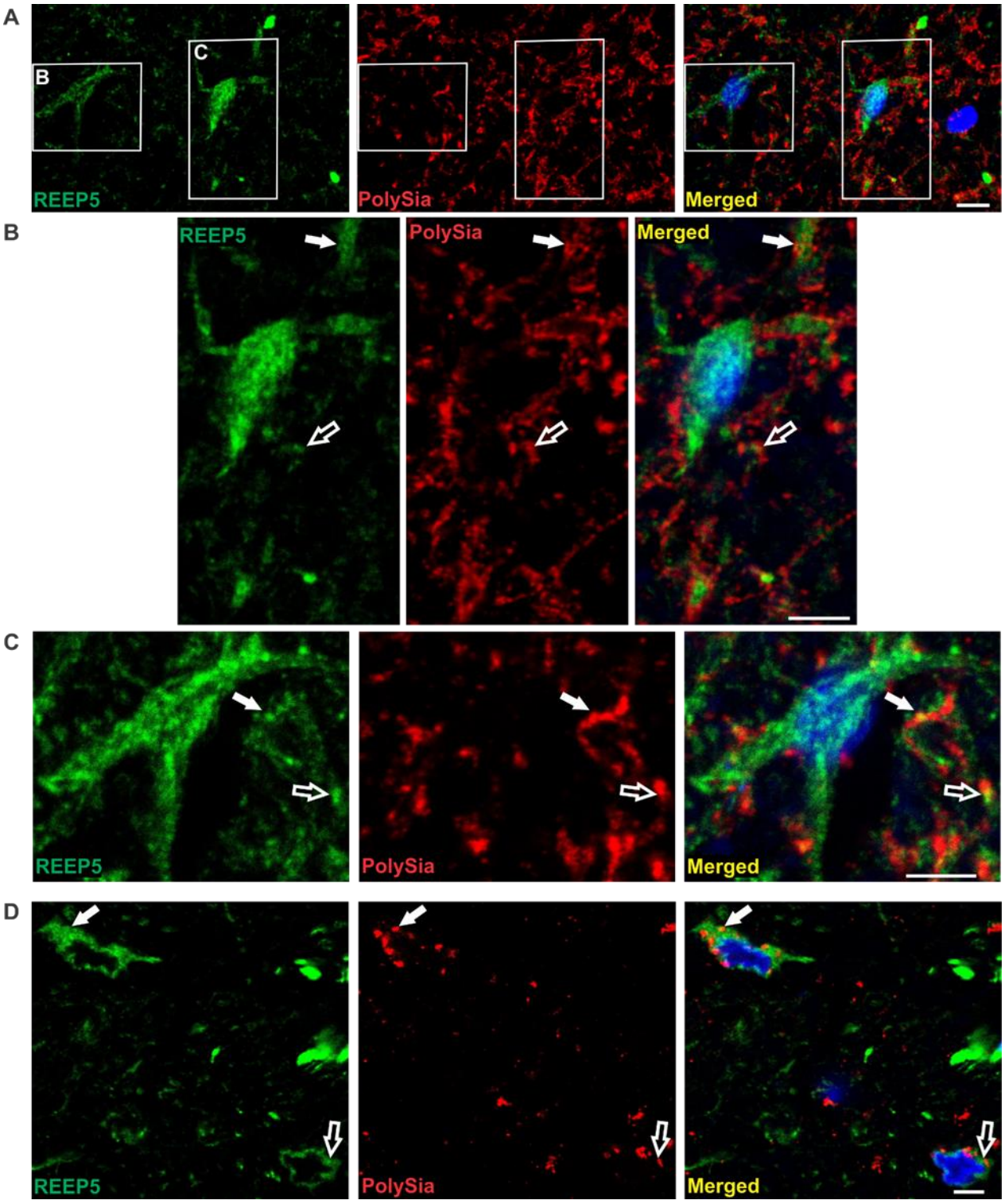

Figure 3.8. Some colocalization of REEP5- and polySia-ir was observed in the rat spinal cord. Nuclei were stained with DAPI (blue). (A) shows some colocalization of REEP5-ir (green) and polySia-ir (red) in the dorsolateral funiculus. (B) and (C) show magnified images of the boxes indicated in the panel A. (D) shows partial co-labelling of REEP5 with polySia in the posterior funiculus (dorsal white column). Arrows indicate examples of colocalization. Scale bar = 10 µm in A and = 5 µm in B, C, and D.

3.3.4. PolySia colocalized/interacted with the same binding partners in the IML and Sp5C as in the dorsal horn

To determine whether the same binding partners of polySia are present in different brain regions, we investigated both the Sp5C and IML of the adult rat using immunoprecipitation and/or immunohistochemical confocal analyses as both these regions also expressed abundant polySia (see Chapter 2). Homogenized Sp5C samples were used for immunoprecipitation experiments using mAb 735. The immunoprecipitates were probed using anti-REEP5 and GNAO1 antibodies. Figure 3.9A shows that REEP5 and GNAO1 co-immunoprecipitated with mAb 735 antibody but were absent (REEP5) or notably lower (GNAO1) in the IgG control. Double labelling immunofluorescent confocal images showed partial co-labelling of polySia with ATP1A2 (Figure 3.9B) and GNAO1 (Figure 3.9C) in the neuropil and on some cell surfaces in the Sp5C. Confocal analysis of immunostained coronal sections of the adult rat spinal cord showed partial colocalization of polySia with ATP1A2 (Figure 3.10A) and GNAO1 (Figure 3.10B) in the IML. REEP5 staining in the IML showed limited colocalization between polySia and REEP5 in all replicates.

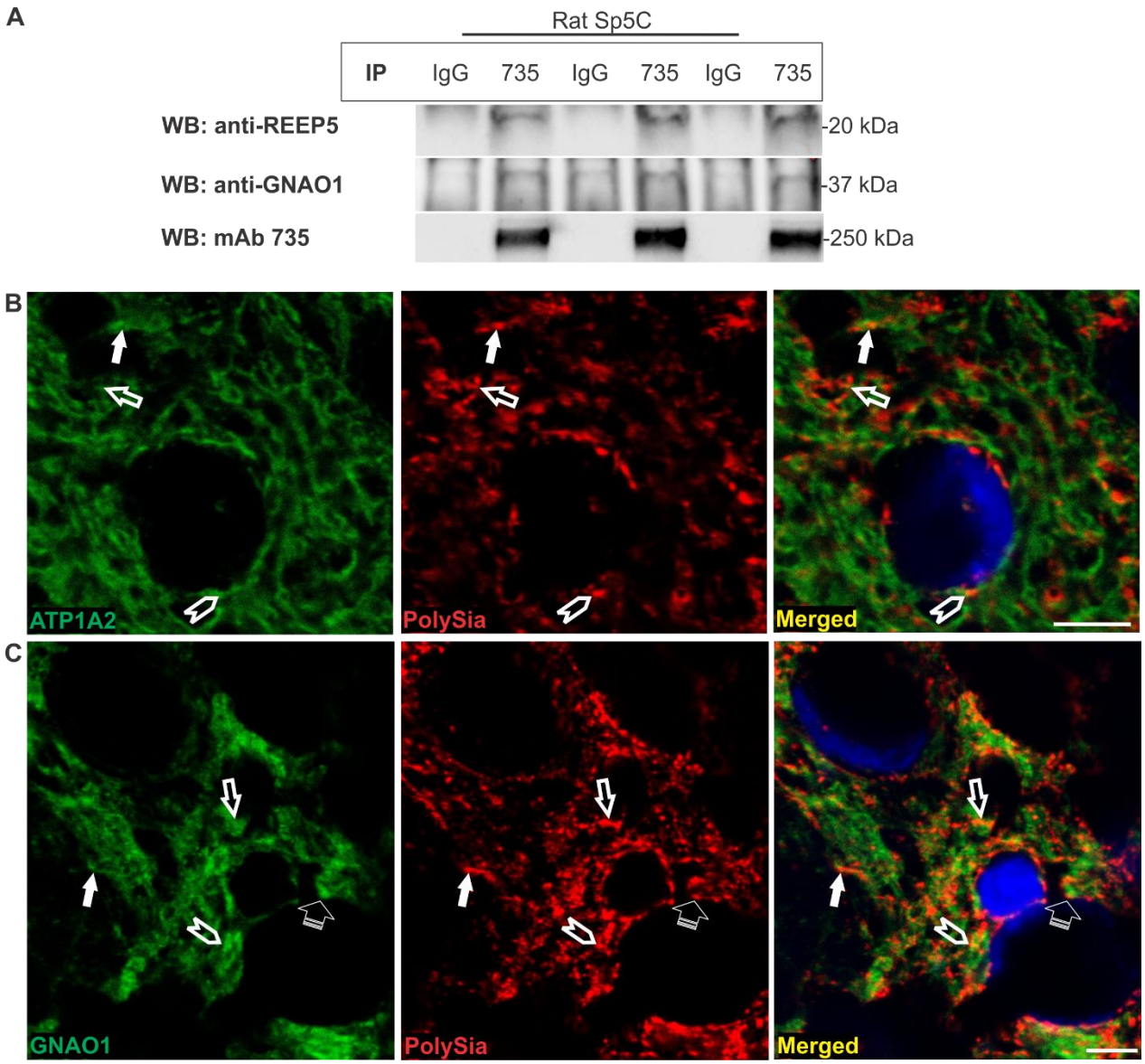

Figure 3.9. Interaction of ATP1A2, GNAO1, or REEP5 with polySia in the adult rat trigeminal nucleus caudalis (Sp5C). Nuclei were stained with DAPI (blue). (A) Immunoprecipitation of polySia in the Sp5C using mAb 735 and probing the blots against anti-REEP5 or GNAO1 antibody. (B) and (C) PolySia-ir (red) with ATP1A2- and GNAO1-ir (green) respectively. Arrows indicate examples of colocalization of polySia and each of the candidate partners. Scale bars = 5 µm.

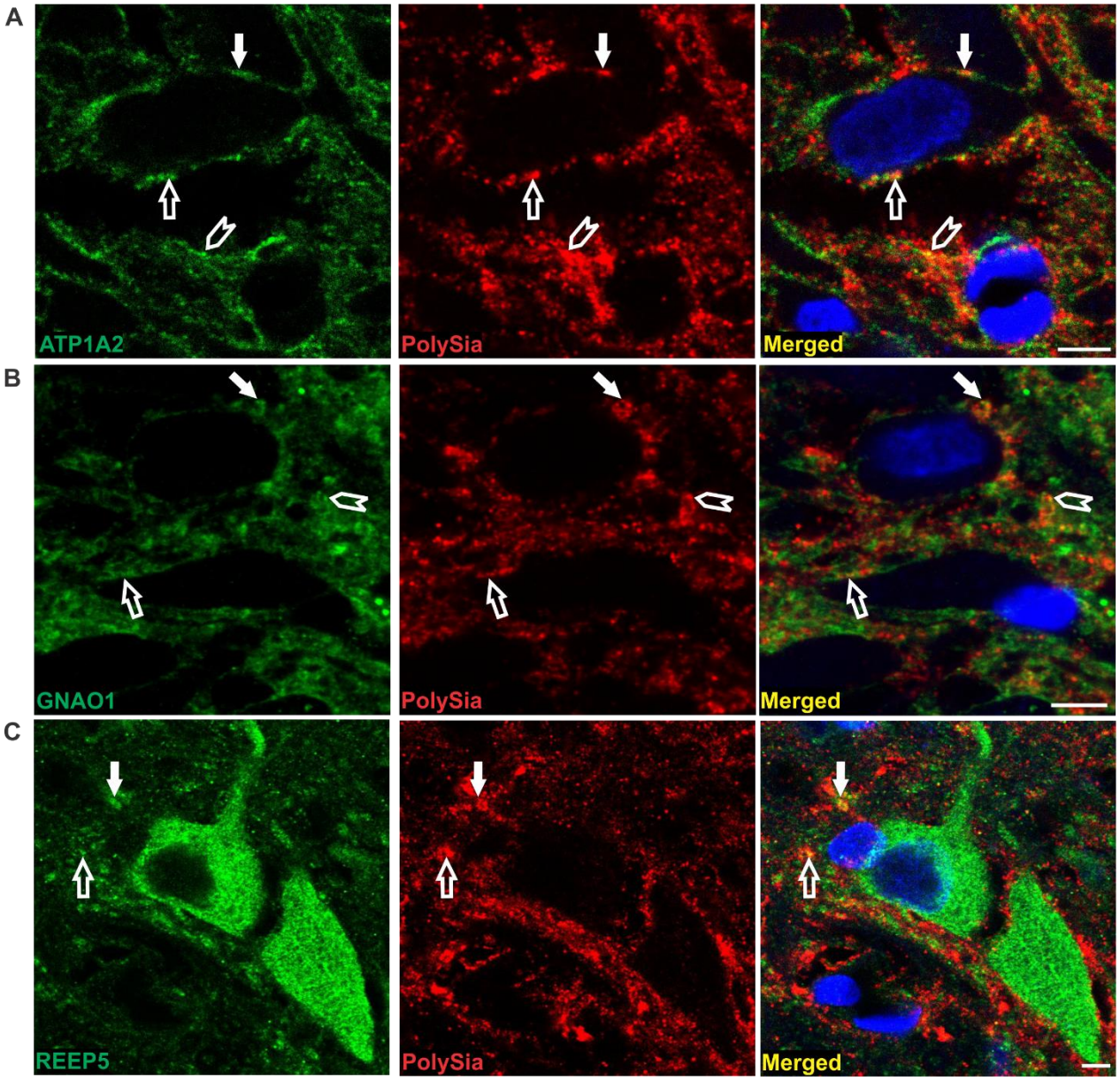

Figure 3.10. In the intermediolateral cell column (IML) of the spinal cord of the adult rat polySia-ir partially colocalized with ATP1A2-, GNAO1-, and REEP5-ir. Nuclei were stained with DAPI (blue)**.** (A), (B), and (C) PolySia-ir (red) with ATP1A2-, GNAO1-, and REEP5-ir (green), respectively. Arrows indicate examples of colocalization. Scale bars = 5 µm.

3.3.5. Binding partners identified in the rat dorsal horn were similar in the mouse dorsal horn

Next, we determined whether the same binding partners were present in the dorsal horn of the spinal cord of the mouse using mAb 735 IPs. Immunoblotting of immunoprecipitated proteins detected bands corresponding to REEP5, GNAO1, and ATP1A3 (Fig. 3.11A). Similar to the rat, REEP5 protein was only detected in the mAb 735 IP and not control IgG IP. GNAO1 and ATP1A3 proteins were seen both in mAb 735 and control IgG IPs, but notably, higher levels of these proteins were present in mAb 735 IP than in control IgG IP.

Further confirmation was performed using immunohistochemical and confocal analyses on coronal sections of the mouse spinal cord which also showed results similar to that of rat for GNAO1, ATP1A2 and REEP5 (Fig. 3.11B-D). Partial colocalization of polySia-ir with ATP1A2- and GNAO1-ir were observed on the cell surfaces and in the neuropil of the dorsal horn (Fig. 3.11B and C) and on the fibres of dorsolateral funiculus (data not shown). Some colocalization of polySia-ir with REEP5-ir was found in the dorsolateral funiculus (Fig. 3.11D).

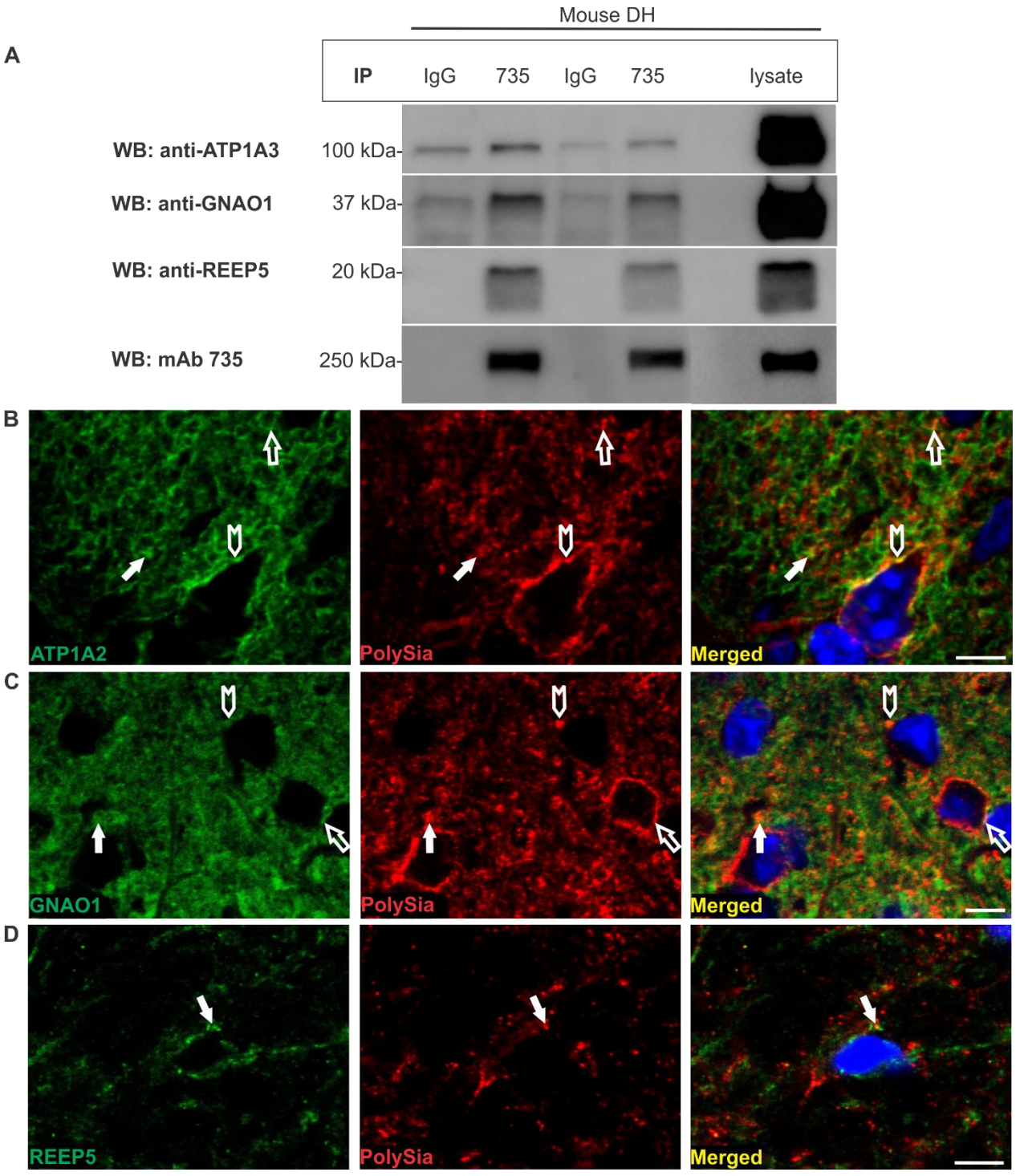

Figure 3.11. Interaction of ATP1A2, ATP1A3, GNAO1, or REEP5 with polySia in the adult mouse dorsal horn (DH). Nuclei were stained with DAPI (blue). (A) Immunoprecipitation of polySia in the DH fractions using mAb 735 and probing the blots against anti-REEP5, GNAO1, and ATP1A3 antibodies. (B) and (C) PolySia-ir (red) with ATP1A2- and GNAO1-ir (green), respectively in the dorsal horn. (C) PolySia-ir (red) with REEP5-ir (green) in the dorsolateral funiculus. Arrows indicate examples of colocalization. Scale bar = 5 µm.

3.3.6. NCAM partially colocalized with GNAO1, ATP1A2, and REEP5

As the majority of polySia is bound by NCAM in the brain (Schnaar et al., 2014), our next aim was to determine whether the interaction between the newly identified proteins was in fact a protein-protein (candidate: NCAM) rather than with polySia itself. This study could not be performed with our rat samples as the commercially available antibodies against NCAM in this species are unreliable (data not shown) so this study was conducted only using mouse tissue.

Double labelling of NCAM with ATP1A2 and GNAO1 showed partial colocalization of NCAM with these two proteins (Figure 3.12A-B) in the neuropil and on some cell surfaces in the dorsal horn of the adult rat, similar to that seen with polySia-ir. Double labelling of NCAM with REEP5 only showed some colocalization in the mouse dorsolateral funiculus (Figure 3.12C). However, this association would be expected due to the association of polySia and NCAM.

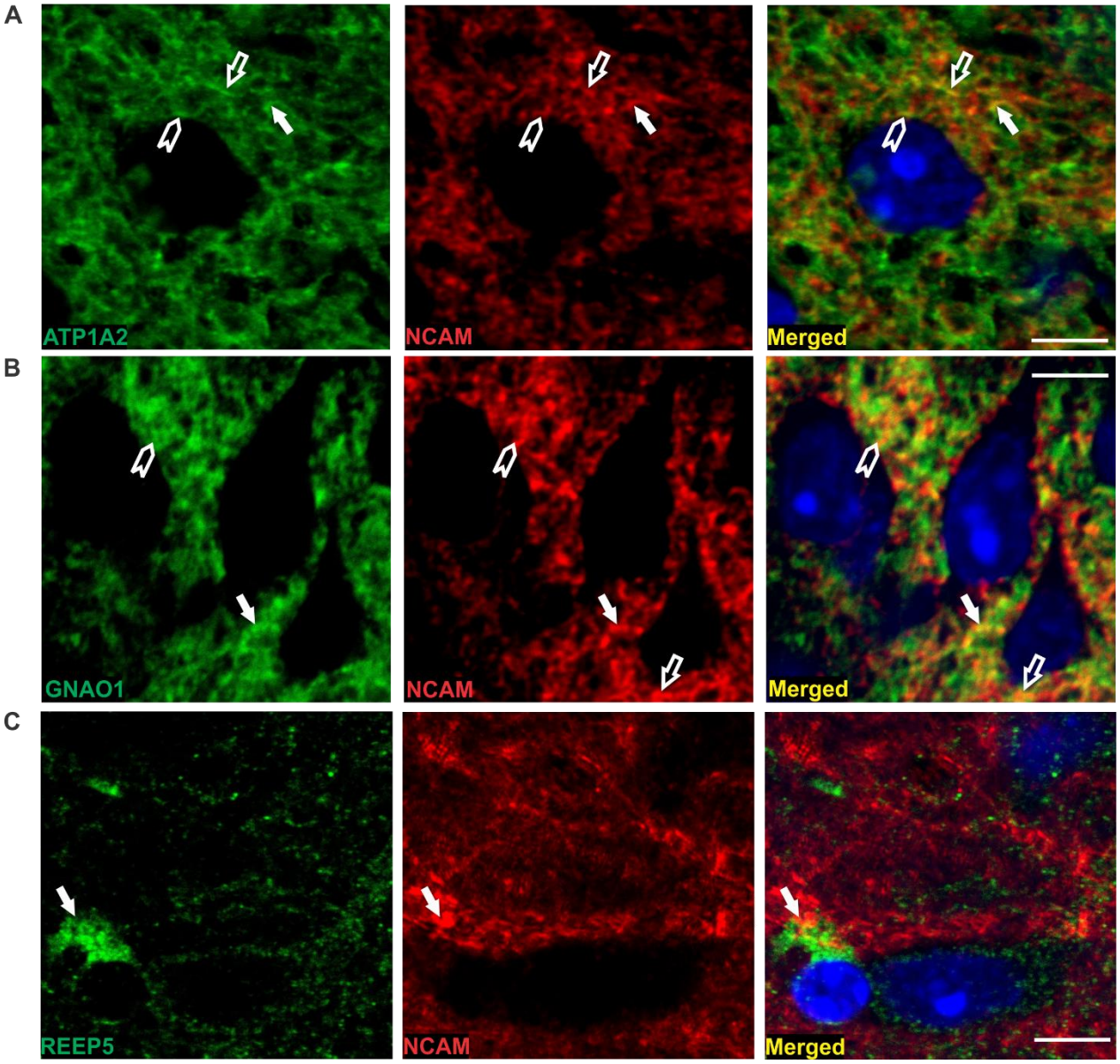

Figure 3.12. NCAM-ir showed partial colocalization with GNAO1-, ATP1A2-, and REEP5-ir in the mouse dorsal horn and dorsolateral funiculus. Nuclei were stained with DAPI (blue). (A) and (B) NCAM-ir (red) with ATP1A2- and GNAO1-ir (green), respectively in the dorsal horn. (C) NCAM-ir (red) with REEP5-ir (green) in the dorsolateral funiculus. Arrows indicate examples of colocalization. Scale bars = 5 µm.

3.4. Discussion

PolySia is involved in cell-cell communication and plasticity (Rutishauser, 2008); however, not much is known about its interacting partners, particularly in the brainstem and spinal cord. Therefore, we sought to explore which proteins bind to polySia initially in the spinal cord. Thirteen novel proteins were identified as potential interactors with polySia in the dorsal horn of adult rat. Comprehensive analysis of five of these proteins (ATP1A2, ATP1A3, GNAO1, REEP5, and CLTC) using co-IP and reverse co-IP followed by western blotting and colocalization analysis provided further evidence that these proteins interact with polySia. Three of these candidate proteins ATP1A2, GNAO1, and REEP5 were also potential interacting partners of polySia in two other functionally distinct CNS regions – the trigeminal nucleus caudalis and the intermediolateral nucleus, demonstrating these interactions were not region-specific. Finally, we demonstrated that the interactions of polySia with four proteins ATP1A2, ATP1A3, GNAO1, and REEP5 were not species-specific as they were present in the dorsal horn of both mouse and rat. ATP1A2, GNAO1, and REEP5 also showed partial colocalization with NCAM, the major polySia carrier, in the dorsal horn, and thus we have not yet determined if the interaction is with polySia alone or NCAM or both. However, these data add significantly to the list of potential interacting proteins of polySia.

3.4.1. Identification of 13 putative binding partners of polySia

We identified 13 novel potential interacting proteins of polySia (Figure 3.13). Most of these proteins are involved in or postulated to impact neuronal signalling implying that polySia could influence such signalling. For example, a role in plasticity could be associated with polySia's potential interaction with 14-3-3θ as 14-3-3 proteins are involved in signal transduction (Berg et al., 2003) with 14-3-3θ up-regulated after injury at least in motoneurons (Namikawa et al., 1998) or down-regulated with increased climbing fibre activity in the cerebellum, associated with changes in GABA receptor expression (Qian et al., 2012). Another isoform, 14-3-3β, has been detected in immunoprecipitates from brain membrane fractions using anti-NCAM antibodies (Ramser et al., 2010), indicating an interaction of NCAM with this protein. Although the study showed an indirect effect of this protein on NCAM neurite outgrowth through binding to specific binding motif of αII spectrin, the presence of 14-3-3β in the eluates obtained from NCAM IP could be either due to its interactions with NCAM or with polySia, present on NCAM in discrete regions of the adult brain (see Chapter 1). 14-3-3 proteins are mainly found in the cytoplasmic compartment (Fu et al., 2000)

and thus might interact with cytoplasmic domain of NCAM. However, they can also be detected at the plasma membrane and in intracellular organelles such as the Golgi apparatus (Fu et al., 2000) where they might interact with the extracellular domain of NCAM and polySia. 14-3-3 proteins have two asparagine sites (Asn-Xaa-Ser/Thr) in their peptide sequence for potential N-linked glycosylation (Ichimura et al., 1988), but these asparagine residues appeared not to be glycosylated as the protein did not stain for carbohydrate (Boston et al., 1982). However, in a more recent study (Di Domenico et al., 2010) three members of this family (14-3-3ϵ, 14-3-3γ, and 14-3-3ζ) were isolated with lectin affinity chromatography on hippocampus using wheat germ agglutinin which selectively binds to terminal N-acetylglucosamine (O-GlcNAc) and sialic acid moieties (characteristic of O-linked glycosylation), indicating that 14-3-3 proteins could be glycosylated (Di Domenico et al., 2010).

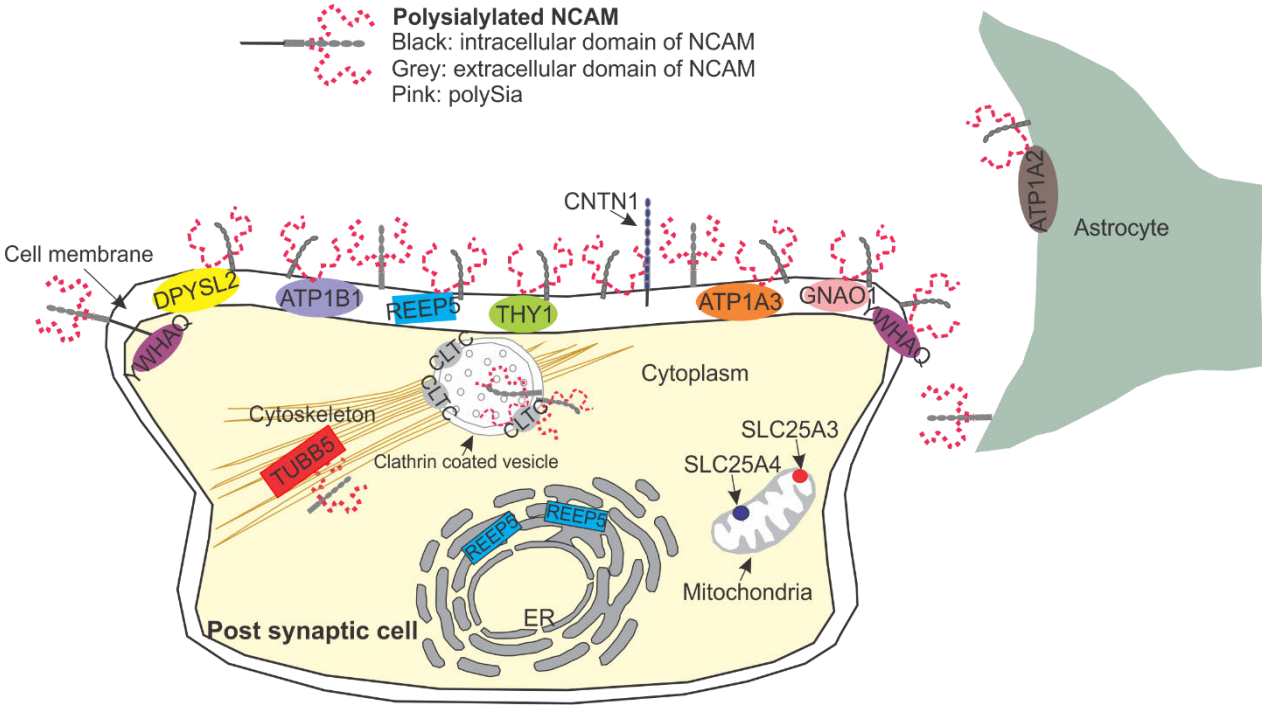

Figure 3.13. Overview depicting the potential interaction of polySia with potential interacting partners in a post synaptic neuron and astrocyte. The majority of these proteins are localized to cell membranes where the interaction is estimated to occur. However, it is unclear how polySia might interact with mitochondrial proteins (SLC25A3 and SLC25A4) or TUBB5. ATP1A2, sodium/potassium-transporting ATPase subunit alpha-2; ATP1A3, sodium/potassium-transporting ATPase subunit alpha-3; ATP1B1, sodium/potassium-transporting ATPase subunit beta-1; CLTC, clathrin heavy chain 1; CNTN1, contactin-1; DPYSL2, dihydropyrimidinase-related protein 2; ER, endoplasmic reticulum; GNAO1, guanine nucleotide-binding protein G(o) subunit alpha; REEP5, receptor expression-enhancing protein 5; SLC25A3, phosphate carrier protein, mitochondrial; SLC25A4, ADP/ATP translocase 1; TUBB5, tubulin beta-5 chain; THY1, thy-1 membrane glycoprotein; YWHAQ, 14-3-3 protein theta.

Contactin-1 on the other hand is a GPI-anchored cell recognition molecule, involved in signalling between axons and myelinating glial cells (Bhat et al., 2001) indicating that the influence of polySia is likely not restricted to neurons. Contactin-1 is a glycoprotein from the family of cell adhesion molecules which contains 6 IgC2 domains and 4 FNIII repeats (Milev et al., 1996) and has been found on the cell surface, where the majority of polySia is found (see Chapter 1), as well as in the secretion from cells (Ruegg et al., 1989, Xenaki et al., 2011, Gennarini et al., 1991). Some evidence suggests that contactin-1 acts as a lectin-like neuronal receptor, binds to CD24 glycoprotein, and can mediate Lewis x-dependent CD24-induced effects on neurite outgrowth (Lieberoth et al., 2009), though no evidence of interaction of this glycoprotein with Sia or polySia is available. Partial colocalization of contactin-1 with NCAM was observed in some regions such as in the spinal cord and dorsal root ganglion (Milev et al., 1996), suggesting an interaction between NCAM and this protein.

Dihydropyrimidinase-related protein 2 (DPYSL2) perhaps more commonly known as collapsing response mediator protein 2 is a signalling protein that alters neurotransmission via neurotransmitter release through interaction with presynaptic CaV and NaV channels as well as interactions with NMDA receptors and also functions as a microtubule binding protein involved in vesicle trafficking (Quach et al., 2004, Kawano et al., 2005, Brittain et al., 2009, Dustrude et al., 2016). NCAM is not described in the interactome of DPYSL2 (Martins-de-Souza et al., 2015) but DPYSL2 can be O-glycosylated (Khanna et al., 2012).

Tubulin beta-5 chain (TUBB5), a structural component of microtubules integral for intracellular transport, potentially alters signalling by vesicle trafficking (Wilson and González-Billault, 2015). TUBB5 is involved in the generation and migration of neurons within the embryonic mouse cortex and its perturbation disturbs the morphological transitions of neurons into the cortical plate (Breuss et al., 2012). PolySia also functions in cell migration as progenitors born in the subventricular zone express high levels of polySia (for review see (El Maarouf and Rutishauser, 2010)) suggesting an interaction in the cortex during development. Perturbations to TUBB5 in mouse postnatal (P17) cerebral cortical neurons also alters the numbers and shapes of dendritic spines (Ngo et al., 2014) suggesting a potential role in plasticity in line with influences of polySia. Although not much data is available beta tubulin is glycosylated with sialyloligosaccharides (Hino et al., 2003, Song and Brady, 2015). β-tubulin was isolated by immunoaffinity chromatography via immobilizing

intracellular domains of rat NCAM 140 and NCAM 180, indicating an interaction of cytoplasmic domain of NCAM with this protein (Büttner et al., 2003).

The main focus of this study were the five proteins REEP5, sodium potassium ATPase subunits (ATP1A2 and ATP1A3), GNAO1, and CLTC that are described below in more detail.

REEP5 is a member of the REEP (DP1) family that shape the tubular endoplasmic reticulum (ER) where they are highly enriched and ubiquitously expressed in all mammals (Shibata et al., 2008, Voeltz et al., 2006, Björk et al., 2013). Although some studies indicate that REEP family proteins enhance G protein-coupled receptor (GPCR) trafficking or increase its functional expression (Saito et al., 2004, Behrens et al., 2006), their role in signalling is not well studied. REEP1, 2 and 6 are involved in signalling through GPCRs (Ilegems et al., 2010, Björk et al., 2013), with REEP2 found recruiting sweet receptors into lipid rafts thereby improving GPCR signalling (Ilegems et al., 2010). Single cell analysis showed that REEP1, 2, and 6 affect ER cargo capacity of specific GPCRs and thus their surface expression (Björk et al., 2013). Therefore, it is possible that an interaction of cell surface polySia with REEP5 could alter GPCR expression and therefore influence cell signalling and plasticity. Specifically REEP5 appears to directly interact with the GPCR CXCR1 altering endocytosis at least in some cell lines (Park et al., 2016b). REEP proteins are however localized predominantly to ER (Björk et al., 2013). As we have demonstrated that polySia is found on the Golgi/ER in neurons at the ultrastructural level, a role for polySia in modifying ER cargo capacity is possible. Additional experiments are required to determine the exact location of REEP5 and study how the interaction with polySia occurs.

Three subunits of the sodium/potassium ATPase were found to interact with polySia in the present study. The sodium/potassium ATPase is a plasma membrane protein comprising four α and three β subunits regulating intracellular Na^+ and K^+ concentrations (Geering, 2006, Skou and Esmann, 1992). The electrochemical gradient produced by the sodium/potassium ATPase maintains the osmotic balance of the cell as well as the resting membrane and excitable properties of neurons, indicating its integral role in neuronal transmission. This pump is also involved in transporting some neurotransmitters across the plasma membrane (Blanco and Mercer, 1998) including glutamate where both uptake and transporters are directly coupled to α1-α3 subunits of the sodium/potassium ATPase at least in rat cerebellum (Rose et al., 2009). α1 and α3 subunits also interacts with NMDA receptors (Akkuratov et al., 2015) and ouabain (a cardiotonic steroid which

is a specific ligand of sodium/potassium ATPase) caused a reduction in the levels of NMDA receptors, an effect likely mediated by the α3 subunit (Akkuratov et al., 2015). PolySia on the other hand also modulates glutamate signalling by restraining activity of extrasynaptic GluN2B-containing NMDA receptors (Hammond et al., 2006) and facilitating activity of a subset of AMPA receptors (Vaithianathan et al., 2004). Since the direct interaction of polySia with these receptors has not been shown, it is possible that polySia affects these receptors through its interaction with subunits α2 or α3 of ATPase as identified in our study. Curiously the function of the non-catalytic ATP1B1 subunit is not known; however, it does have three asparagine sites which could be glycosylated unlike the α2 and α3 subunits (Blanco and Mercer, 1998, Vagin et al., 2005). In line with this the β2 subunit of sodium/potassium ATPase, also known as AMOG (Gloor et al., 1990), actually carries 30% of its molecular weight as oligomannosidic glycans (Fahrig et al., 1990) and has been found to interact directly with NCAM (Horstkorte et al., 1993). Our mass spectrometry data detected only ATP1A2, ATP1A3, and ATP1B1 as potential interacting partners of polySia and not ATP1B2 suggesting that these three subunits do interact with polySia, while AMOG interacts with NCAM, or it is possible that we did not detect ATP1B2 due to its oligomannosidic glycans.

GNAO1 encodes for one of three subtypes of the Gαo subunit, the most abundant G protein in the brain (Huff et al., 1985, Neer et al., 1984, Exner et al., 1999) with high abundance in neurons (Jiang et al., 1998). Ligand binding at GPCRs activates G proteins catalysing the exchange of GDP for GTP on the α subunit separating the α subunit and βγ subunits which activate downstream effectors such as adenylyl cyclases, phospholipases, and ion channels (Hepler and Gilman, 1992, Neer, 1995). It appears that most GPCR exhibit N-linked glycosylation with some sites important in receptor and G-protein coupling (Wheatley and Hawtin, 1999, Ray et al., 1998, Chen et al., 2010); however, whether polysialylation of GPCRs occurs is unclear. Nevertheless, GNAO1 is a signalling protein in line with the idea that polySia is involved in plasticity. Pertussis toxin which inhibits Gi and Go proteins prevents NCAM-mediated neuritogenesis in E7 neurons which is dependent upon the presence of polySia (Doherty et al., 1992, Doherty et al., 1991, Sandig et al., 1994) suggesting an interaction between Gi/o proteins, NCAM, and polySia. The organization of this interaction remains to be determined with our data suggesting that an interaction between Go and polySia exists. It is interesting to note that Gαo also interacts with ganglioside GD3, a sialic

acid-containing glycosphingolipids (Yuyama et al., 2007) further emphasizing the potential for sialic acid containing sugars to modify functions of signalling G proteins.

Clathrin is involved in neurotransmission and signal transduction via clathrin-mediated endocytosis (CME) of some proteins, especially GPCRs, the most abundant signalling molecules in the CNS (Vieira et al., 1996) (for review see (McMahon and Boucrot, 2011, Sorkin and Von Zastrow, 2009)). Application of chlorpromazine, used as an inhibitor of clathrin-related endocytosis (Daniel et al., 2015), increased polySia expression on the cell surface of human neuroblastoma cells, and this effect was decreased by the addition of brefeldin A, which inhibits the recycling pathway (Eaton et al., 2000), suggesting that the regulated clathrin-related endocytosis system was involved in the polySia expression (Abe et al., 2017). In line with this, the surface of clathrin-coated vesicles showed immunoreactivity for polySia which colocalized with clathrin-ir (Minana et al., 2001). Moreover, in the same study, NCAM was found to be associated with clathrin when NCAM was immunoprecipitated (with an anti-NCAM antibody) in cultured cortical neurons and proliferating astrocytes which were immunoreactive for polySia, as well as in differentiating astrocytes lacking polySia-ir (Minana et al., 2001). Since clathrin was found associated with NCAM even in astrocyte cultures which were polySia negative, it remains unclear whether there is any direct interaction between polySia and clathrin. However, recently a role was suggested for another important member of sialoglycans, gangliosides in CME (Rodriguez-Walker et al., 2015), further suggesting that polySia might be associated with clathrin or affect its function. An increased endocytosis of transferrin, the archetypical cargo for CME, was found in cells containing gangliosides with high levels of sialylation (Rodriguez-Walker et al., 2015).

Therefore, the signalling functions of these potential interacting partners are in line with postulated function of polySia in signalling and plasticity in the adult higher order brain regions (Eckhardt et al., 2000, Dityatev et al., 2004, Rutishauser, 2008, Bonfanti and Theodosis, 2009, Kochlamazashvili et al., 2010).

3.4.2. Are interacting proteins region or species specific?

To the best of our knowledge, this is the first description of interacting partners of polySia in the dorsal horn of the spinal cord demonstrating that GNAO1, ATP1A2, ATP1A3, REEP5, and CLTC may interact with polySia. It is curious that these proteins have not been detected as binding partners of polySia in studies of higher brain regions (Mishra et al., 2010, Theis et al., 2013) or via

in vitro examination (Kanato et al., 2008, Storms and Rutishauser, 1998, Vaithianathan et al., 2004, Isomura et al., 2011, Ono et al., 2012, Hammond et al., 2006) particularly as most of these proteins are highly abundant throughout the CNS. However, in both studies which utilised tissue from higher brain regions, only the part of the gel containing protein bands visible by silver staining in the sample but not the control (with a molecular weight of 50 and 70 kDa (Theis et al., 2013) or 30 kDa (Mishra et al., 2010)) was analysed by mass spectrometry. Since none of the five binding partners identified and verified in the current study has a similar molecular weight, they may have simply been present at lower levels or just not detected in the previous studies despite the fact that silver staining is quite sensitive. It is also possible that these proteins were absent in the eluates from previous studies due to the differences in sample preparation. This perhaps is more likely as we did not detect histone H1 (Mishra et al., 2010) or MARCKS (Theis et al., 2013) in our mass spectrometry data. Histone H1 was only detected in Triton X-100 insoluble fractions and in the post synaptic density but not in Triton X-100 soluble fractions of brain (Mishra et al., 2010). Similarly, we did not find interacting proteins identified using *in vitro* preparations or artificial setups such as BDNF (Kanato et al., 2008). It is possible that we could not detect these proteins due to size (BDNF is only 14 kDa), sample preparation and analysis, or due to the potential non-stable (transient) interactions (Wetie et al., 2014) between polySia and these partners, resulting in the separation of the binding partner from polySia isolated on the beads. Furthermore, it should be noted that proteins may interact differently between *in vitro* and *in vivo* systems (Berggård et al., 2007).

Our study shows the value of quantitative proteomics for identifying interacting partners in biological complexes. Using NSAF values, we were able to eliminate many contaminants by comparing the level of protein abundance between samples and an equal number of negative controls. More importantly, we were able to identify proteins that are quantitatively enriched in the samples over the negative controls. Immunoprecipitation studies which did not use quantitative approaches (Mishra et al., 2010, Theis et al., 2013), only chose proteins that were absent in controls. If we were to take this approach, we would not have considered ATP1A2 and ATP1A3 even though we provided further evidence that these are likely binding partners of polySia.

Our study shows that when similar techniques of analysis are used to determine binding partners for polySia in different CNS regions they appear similar, at least for the lower brainstem and spinal cord. We demonstrated that GNAO1, ATP1A2, and REEP5 which are potential interacting partners

for polySia in the dorsal horn and trigeminal nucleus are also likely partners of polySia in in the intermediolateral cell column. To our knowledge no other studies have compared binding partners from different regions. This result may also extend to humans as some evidence suggests that similar brainstem regions exhibit high expression levels of polySia (Quartu et al., 2008). It remains a possibility that the binding partners of polySia in primitive brainstem regions may be different to those found in higher brain regions; however, this requires comprehensive and comparative analysis.

We were also able to compare the potential binding partners identified across different species by comparing the dorsal horn in mouse with that of rat and the same partners were identified. This seems to make sense as polySia is abundant in the dorsal horn of both mouse and rat even though its distribution does differ slightly (see Chapter 2).

3.4.3. Protein-protein or carbohydrate-protein interaction?

Since more than 95% of polySia is located on NCAM (Cremer et al., 1994, Schnaar et al., 2014), isolation of polySia leads to isolation of NCAM as found in our mass spectrometry data. Therefore, the potential binding partners identified here may interact with polySia, NCAM, or both. As mentioned above, there is some evidence that tubulin β, clathrin, and contactin-1 interact or might interact with NCAM (Büttner et al., 2003, Minana et al., 2001, Milev et al., 1996). However, being an interacting partner of NCAM does not preclude a direct interaction of polySia with the potential binding partners or involvement of polySia in heterophilic interactions of NCAM with those interacting proteins. For instance, evidence shows heterophilic interactions between heparin sulphate proteoglycans (HSPGs) and NCAM through NCAM Ig domain 2 (Storms et al., 1996, Murray and Jensen, 1992). PolySia can augment this interaction *in vitro*, although it remains unclear whether polySia directly binds to HSPGs or indirectly modulates an NCAM/HSPG interaction (Storms and Rutishauser, 1998). Another example is fibroblast growth factor 2 (FGF2) that binds to the second fibronectin type III repeat (FGL peptide) and/or the first FN3 (BCL motif) of NCAM (Kiselyov et al., 2005, Jacobsen et al., 2008). PolySia also directly binds to the growth factor FGF2, though the interaction has been demonstrated only *in vitro* (Ono et al., 2012).

Our final series of data showed partial colocalization of ATP1A2, GNAO1, and REEP5 also with NCAM using confocal microscopy. However, this evidence requires further validation as NCAM, ATP1A2, and GNAO1 are all abundantly expressed within the CNS so the chance of random

colocalization is high. In addition, since polySia is a posttranslational modification of NCAM, due to its proximity to NCAM, double labelling of both polySia and NCAM with these proteins would be expected. Further experiments are required (see Chapter 5) to investigate the direct interaction of the potential interacting partners with polySia and/or NCAM.

It remains a possibility that these potential interacting partners might be found in the immunoprecipitates of mAb 735 IPs due to their interaction with a protein that interacts with polySia and/or NCAM. This issue can be addressed by approaches such ELISA and BIACORE analysis or by immunofluorescent staining to investigate colocalization of polySia with these proteins as we did for ATP1A2, GNAO1, and REEP5 proteins.

3.4.4. Limitations of the study

When dissecting tissue from the spinal cord and brainstem, it was not possible to isolate only dorsal horn or trigeminal nucleus caudalis so each sample contained adjacent tissues. To some extent this limitation was addressed by looking at the colocalization of binding partners with polySia. We were able to assess only some of the proteins detected by mass spectrometry, so it is important that all proteins identified are assessed to determine the region where colocalization occurs.

Another major limitation is antibody specificity. Although mAb 735 is well characterised to isolate polySia, commercially available antibodies were used for identification of potential binding partners and these have variable levels of characterisation. Western blot analysis using REEP5 antibody of brain tissue showed multiple bands, suggesting that the antibody may bind non-specifically (for example to other REEP isoforms). Although we tried several NCAM antibodies that were supposed to detect the rat version of NCAM (# ab9018, Abcam; # GTX19782, GeneTex; and # MAB310, Merck Millipore), none were able to detect the three NCAM isoforms preventing further investigation of NCAM interacting with the binding partners identified here in this species; therefore, the interaction of NCAM with GNAO1, REEP1, and ATP1A2 could only be investigated in mouse.

It is also clear that it is difficult to detect transient interactions using co-IP (Xing et al., 2016). *In vivo*, many interactions involved in intracellular and intercellular signalling, especially cell surface interactions, are dynamic and transient because their function needs dynamic change between interacting and not interacting (Wetie et al., 2014, Schreiber et al., 2009). Although this issue could

have been addressed by utilising cross-linking methods (Wetie et al., 2014), this would require significant amounts of antibody that were not available.

Moreover, polySia, ATP1A2, and GNAO1 are all abundantly expressed within the CNS and thus some colocalization seen could arise from random association.

Finally, there is a possibility that some of the identified potential binding proteins in this study are in fact carriers of polySia rather than interacting partners. As discussed in section 3.4.1, some of the identified putative interacting partners, such as ATP1B1 and contactin-1 are glycoproteins though there is no evidence that they are polysialylated. Contactin-1, for example, contains both Ig domains and FNIII repeats (Milev et al., 1996). In NCAM, the first FNIII repeat is the polyST recognition site and docking site for the polysialylation of two N-linked glycans in the adjacent Ig domain (Close et al., 2003). This raises a possibility that contactin-1 may be polysialylated. In case of REEP5, ATP1A2, ATP1A3 and CLTC, no evidence is present that these proteins are glycosylated. In addition, treatment of samples with endoN did not result in any shift in their expected molecular weights in western blotting (data not shown), suggesting that these proteins are not polysialylated. However, using NetOGlyc 4.0 Server (Steentoft et al., 2013) showed 3, 1, 1, and 5 predicted glycosylation sites for ATP1A2, ATP1A3, GNAO1, and CLTC respectively based on their sequence. Whether any of these predicted sites are glycosylated or not requires further examination.

Our data do show a discrepancy with respect to GNAO1 with the mass spectrometry data showing an absence of GNAO1 in the control; however, after co-IP followed by western blotting a GNAO1 band was detected in the control. This discrepancy could be explained by loss of GNAO1 during sample preparation for mass spectrometry (such as peptide loss during ZipTip) indicating perhaps the amount of GNAO1 in the control eluates was probably below the detection limit of the MS instrument used.

3.5. Conclusion

This study has successfully identified potential binding proteins of polySia in the dorsal horn of the spinal cord of adult rats, the first such investigation. The co-immunoprecipitation followed by label-free proteomics approach identified 13 potential binding partners of polySia, five of which were validated using co-IP and/or immunohistochemical analysis. Most proteins identified were associated with neuronal signalling and plasticity, the major known function of polySia in the adult

CNS. We also demonstrated that these interactions were similar in different spinal cord and brainstem regions and showed that polySia interaction with these proteins was not species-specific. Functional testing of polySia interactions with the putative binding partners would determine the potential contribution of these proteins to polySia in plasticity or contribution of polySia to the role of these proteins. Elucidation of interacting partners of polySia with already known functions can provide novel insights into fundamental aspects of the function of polySia in the dorsal horn of the spinal cord. Moreover, it will help to identify new mechanisms of action of polySia and understand how polySia is implicated in plasticity and/or signalling. Understanding polySia–protein interactions can also help to clarify the pathophysiology and development of some diseases associated with changes in the expression of polySia.

Chapter 4 : Viral vector induced expression of polysialic acid in the rostral ventrolateral medulla: expression pattern and cardiorespiratory effects

Abstract

Polysialic acid (polySia), a large cell surface glycan, is mainly found as a posttranslational modification of the neural cell adhesion molecule in the mammalian brain. PolySia is synthesised mainly by polysialyltransferase ST8SiaIV (PST) in the adult brain. In some higher brain regions that exhibit high polySia expression such as the hippocampus and hypothalamus, polySia modulates plasticity. However, its functional role in the lower brain regions is poorly studied. The nucleus of solitary tract (NTS) is a primary relay centre of visceral sensory information. We recently demonstrated that the enzymatic removal of polySia in the NTS resulted in sympathoexcitation. Thus our initial aim was to overexpress polySia in the NTS using a lentiviral vector driving the expression of PST along with mCherry and GFP reporters (LV/PST) and determine the effects on neural transmission. However, injection of LV/PST failed to adequately express ST8SiaIV. Therefore, our objective moved to examine the effect of induced expression of polySia in the rostral ventrolateral medulla (RVLM), which receives input from the NTS and is involved in the basal and reflex control of cardiorespiratory function. A control lentiviral vector driving the expression of GFP reporter (LV/GFP) was also used. Using LV/PST, we were able to overexpress polySia in the RVLM as polySia immunoreactivity (ir) in the injected side was higher than in the non-injected side. Moreover, polySia-ir was significantly more distinct on neurons expressing the reporters in the LV/PST than the LV/GFP group. However, polySia overexpression was found in LV/GFP group, although it was significantly lower than in LV/PST group. To determine if tissue damage caused this overexpression, astrocyte morphology and expression were examined as previous studies have described induced polySia expression by reactive astrocytes following injury. However, very little colocalization of polySia with mildly reactive astrocytes was found. Animals bilaterally injected with LV/PST and LV/GFP or naïve animals were used for physiological experiments as unilateral manipulation would be compensated by the unmanipulated side. Nevertheless, no significant change was found in the LV/PST group in the baseline level or function of cardiorespiratory reflexes examined. Only a minor change was seen in the baroreceptor function showing a significant elevation of the lower plateau, possibly due to an increase in non-barosensitive sympathetic activity. To investigate whether LV/PST influenced a population of neurons with cardiorespiratory function, the number of the reporter expressing C1 neurons was assessed. Overall, our results suggest that either polySia expression does not alter the

cardiorespiratory functions of the RVLM or the increased polySia level was not enough or did not target a large enough population of neurons with cardiorespiratory functions to alter function.

4.1. Introduction

Nearly all cells are covered by a dense coat of cell surface carbohydrates, termed glycans, which are usually attached to underlying proteins or lipids (Rambourg and Leblond, 1967, Varki, 2007). Glycans are developmentally regulated, usually change in response to environmental situations (for review see (Ohtsubo and Marth, 2006, Taylor and Drickamer, 2011)), and can cause disease when genetically deficient (for review see (Freeze, 2006)). In mammals, terminal components of glycoproteins and glycolipids are often sialic acids (Cohen and Varki, 2010), a family of sugars with a nine-carbon backbone (Varki, 2007) that can be found as a monomer, dimer, oligomer, or polymer (polysialic acid) (Sato and Kitajima, 2013a). Within the mammalian central nervous system (CNS), polysialic acid (polySia) is a group of sialoglycans that is of particular interest (Schnaar et al., 2014). PolySia is predominantly attached to the neural cell adhesion molecule (NCAM) (Cremer et al., 1994) and due to its highly hydrated and negatively charged structure acts as a negative regulator of the adhesive properties and binding abilities of NCAM (Yang et al., 1994, Yang et al., 1992, Brusés and Rutishauser, 2001, Hildebrandt et al., 2010).

PolySia in mammals is synthesised by polysialyltransferases (polySTs) ST8SiaII and ST8SiaIV (also named STX and PST, respectively) (Eckhardt et al., 1995, Kojima et al., 1995, Livingston and Paulson, 1993, Nakayama et al., 1995, Scheidegger et al., 1995), primarily present in the trans-Golgi compartment (Harduin-Lepers et al., 2001, Harduin-Lepers et al., 2005, Scheidegger et al., 1995). The expression of the polySTs is individually regulated at the transcriptional level in a tissue-specific fashion, with an overlapping expression pattern (Angata et al., 1997, Hildebrandt et al., 1998, Ong et al., 1998). Overall, ST8SiaII is the main enzyme in the developing brain, whereas ST8SiaIV is the main polyST in the adult CNS (Ong et al., 1998, Hildebrandt et al., 1998, Oltmann-Norden et al., 2008).

PolySia has been found to modulate several functions (McCall et al., 2013, Becker et al., 1996, Muller et al., 1996), studied mainly in the higher brain regions. For instance, in the hippocampus, one of the main regions with abundant expression of polySia (Bonfanti, 2006), altering the expression of polySia altered memory formation caused by a reduction in long term potentiation (Muller et al., 1996, Becker et al., 1996, Eckhardt et al., 2000, Angata et al., 2004). PolySia removal resulted in phase resetting of the circadian clock in the suprachiasmatic nucleus (Fedorkova et al., 2002, Prosser et al., 2003), increased vulnerability to excitotoxic stimuli due to induced dendritic

expansion in CA3 pyramidal neurons (McCall et al., 2013), and increased thermal hyperalgesia in the spinal cord associated with neuropathic pain (El Maarouf et al., 2005) demonstrating that perturbing polySia alters neurotransmission.

The function of polySia within the brainstem has been poorly investigated. The nucleus of solitary tract (NTS), located in the dorsal brainstem, is a major integrative centre of viscerosensory information and receives constant synaptic input from peripheral cardiovascular, respiratory, and gastrointestinal sensors as well as descending input from higher brain regions to regulate several homeostatic reflexes (Pilowsky and Goodchild, 2002, Guyenet, 2006, Andresen and Paton, 2011, Browning and Travagli, 2014). Increasing sensory activity within the NTS, which at baseline exhibits abundant polySia expression (see Chapter 2), decreased polySia levels (Bouzioukh et al., 2001). In keeping with this data, enzymatic removal of polySia in the NTS in our laboratory resulted in sympathoexcitation (Bokiniec et al., 2017). In this chapter, our initial aim was to induce polySia expression in the NTS using a lentiviral vector in order to examine the effects of polySia overexpression in the cardiorespiratory functions generated by this region. However, we were only ever able to induce very poor expression of the fluorescent reporter so we changed our target to a downstream site regulated by the NTS, the rostral ventrolateral medulla (RVLM).

Sensory input from the NTS regulates cardiorespiratory outflows via the RVLM (Koshiya and Guyenet, 1996, Aicher et al., 1996) which is located within the ventral medulla extending about 1mm caudal to the pole of the facial nucleus (Goodchild and Moon, 2009). The RVLM plays a crucial role in the tonic and reflex regulation of arterial blood pressure (AP) as chemical inhibition of cells in the region results in falls in sympathetic nerve activity (SNA) and blood pressure (Feldberg and Guertzenstein, 1976, Guertzenstein and Silver, 1974, Ross et al., 1984), while electrical or chemical stimulation of the RVLM evokes increases in the activity of sympathetic nerves innervating vasomotor organs including blood vessels, the heart, and the adrenal medulla (Ross et al., 1984, Willette et al., 1983a, Goodchild et al., 1982, McAllen, 1986). Cardiovascular and respiratory reflexes dependent upon neurons in the RVLM include the baroreceptor and von Bezold-Jarisch reflexes as well as the responses generated by peripheral and to some extent central chemoreceptor reflexes amongst others (Verberne and Guyenet, 1992, Guyenet, 2006, Wakai et al., 2015, Guyenet, 2000). For example, most RVLM bulbospinal barosensitive neurons demonstrate strong activation as a result of carotid body stimulation by cyanide or brief hypoxia (peripheral chemoreceptor reflex) (Reis et al., 1994, Koshiya et al., 1993, Sun, 1996). Adjacent to

the RVLM are key respiratory centres responsible for the generation and rhythm of breathing: the Bötzinger and pre-Bötzinger regions (Sun et al., 1998, Smith et al., 1991, Stornetta et al., 2003). Unlike the NTS, the RVLM and adjacent regions have a low expression of polySia and therefore our aim was firstly to determine if it is possible to overexpress polySia in the region and then determine whether this overexpression alters functions generated by the region. We attempted to induce expression of polySia within the RVLM using lentiviral vectors (LV) carrying the ST8SiaIV (hereafter is referred to PST) gene and functionally examined baseline cardiorespiratory functions and cardiorespiratory reflex functions.

4.2. Materials and methods

4.2.1. Animals

All experimental procedures were approved by the Macquarie University Animal Ethics Committee (Animal Research Authorities: 2015/041) and conducted in accordance with the Australian Code of Practice for the Care and Use of Animals for Scientific Purposes. Animals were housed under constant 12 h light/dark cycles and allowed standard rat chow ad libitum. Experiments were performed on male Sprague Dawley rats (12-20 weeks old, n = 51) from the Animal Resources Centre, Perth, Western Australia.

4.2.2. Vectors

A lentiviral vector that drives the expression of PST (ST8SiaIV) and contains 2 reporters, mCherry and GFP, was manufactured by sub-cloning a plasmid containing the coding region of mouse PST from pcDNA3/mPST into a lentiviral backbone under the control of human (h) synapsin (Syn) promoter, hereafter is referred to as LV/PST. The plasmid was kindly made and provided by Dr. Xuenong Bo (UCL, UK), who used this virus to induce polySia expression in the spinal cord (as yet unpublished) and the viral vector was made at Salk Vector Core with a titre of 7.9×10^9 IU/ml. Green fluorescent protein (GFP) was used as a reporter molecule for PST gene expression. The plasmid also has a Syn_mCherry reporter sequence. Thus the vector sequence was pRRL_Syn_PST-GFP_Syn-mCherry.

In order to examine whether the brain injection itself and/or the lentivirus induced polySia expression, a control lentiviral vector under the control of human synapsin was used that only contained the GFP reporter and was manufactured by SignaGen Laboratories (MD, USA) with a titre of 2.23×10^9 IU/ml and hereafter is referred to as LV/GFP.

4.2.3. Stereotaxic microinjection of vectors

Adult male SD rats were anaesthetized with a mixture of ketamine (75mg/kg; Parnell Laboratories, Australia) and medetomidine (0.75 mg/kg; Pfizer Animal health, Australia) and were administered with prophylactic antibiotics (100 mg/kg cephazolin sodium, i.m.; Mayne Pharma, Australia) and analgesia (2.5-10 mg/kg carprofen, s.c.; Norbrook Pharmaceuticals, Australia). The hind paw was firmly pinched to check for a lack of reflexes ensuring the animal was anaesthetized. The rats' head and left cheek were shaved and swabbed with 10% povidone-iodine solution (Betadine TM, Mayne

Pharma, Australia). Anaesthetic depth was checked frequently by monitoring motor and respiratory responses to noxious pinching of hindpaws, and if required at any time, additional dose of ketamine (7.5 mg/kg i.p.) was administered. Rats were transferred to a heated pad on a stereotaxic frame and placed in the skull flat position. The skin was opened, with a midline incision along the skull. An approximately 4 mm diameter hole was made in the occipital bone 2 mm lateral to midline over the RVLM. The dura was cut with a 26G needle so the cerebellum was exposed. The left facial nucleus, an anatomical landmark for the rostral extent of the RVLM, was mapped by antidromic facial field potentials evoked by using a borosilicate pipette filled with viral vector in PBS and a silver wire, as previously described (Dempsey et al., 2015). The caudal pole of the facial nucleus was determined. 300 nl of LV/PST or LV/GFP was microinjected 200-300 µm caudal to the caudal pole of the facial nucleus at a depth of 200 µm deeper than the most ventral position at which facial field potentials could still be detected. After the injection, the pipette was left in position for approximately 5 min prior to its slow withdrawal. Wounds were irrigated using sterile saline, covered with oxidized cellulose haemostat and closed with suture clips. In some animals (n=23), the injection was performed unilaterally (RVLM left side), whereas in the animals used for electrophysiological recordings the injection was performed bilaterally. Anaesthesia was reversed with the administration of atipamezole (0.4 mg/kg, s.c.; Pfizer Animal Health, Australia). Rats were closely monitored during recovery until they were awake and active. Then, they were transferred to the home cage in the PC2 laboratories at the Faculty of Medicine and Health Sciences (Macquarie University) with twice-daily monitoring for three days post-microinjection, followed by a twice-weekly monitoring. Some animals were used to determine that a four- to five-week period post injection was required for optimal expression and from this point animals were either used for electrophysiological recordings or euthanized and perfused.

4.2.4. Electrophysiological recordings

After 4-5 weeks, rats that had received bilateral microinjections were anaesthetized with urethane (1.3 g/kg, i.p. 10% solution in 0.9% saline; Sigma-Aldrich, Australia). Depth of anaesthesia was assessed at regular intervals during the experiment by monitoring autonomic responses to noxious pinching of hindpaws. If the pinch evoked changes in arterial pressure (AP) or respiratory rate, 10% of the initial dose of urethane (i.v.) was administered. Core temperature (rectal temperature) was maintained between 36.5 and 37.1°C by a thermostatically regulated heating pad (Harvard Apparatus, Holliston, MA, USA). The right femoral artery and vein were cannulated for measuring

AP and the administration of drugs and saline respectively. A tracheostomy was performed by inserting a 14G catheter into the trachea to permit artificial oxygen-enriched (100% oxygen) ventilation (Ugo Basile, SRL, Italy). The end-tidal CO_2 was maintained between 3.5-4.5% (Capstar-100, CWE Inc., USA). Rats were placed in a stereotaxic frame and the left splanchnic nerve, used for the measurement of sympathetic outflow, was isolated dorsally by a retroperitoneal approach as described previously (Burke et al., 2008). The left phrenic nerve, used for the measurement of central inspiratory function, was isolated using a dorsal subscapular approach. After isolation of the nerves, they were cut distally to exclude afferent transmission and prepared for recording. The nerve recording was performed from the phrenic nerve, and splanchnic sympathetic nerve using handmade bipolar silver wire electrodes as described previously (Burke et al., 2008). Nerve recordings were amplified (×10000; CWE Inc., Ardmore, USA), band pass filtered (0.1-3 kHz), sampled at 5 kHz (1401, Cambridge Electronic Design (CED) Ltd, UK) and recorded using Spike 2 software (version 6.2, CED, Ltd, Cambridge, UK). Core temperatures and end-trial CO_2 were sampled at 2 kHz.

A stabilization period of 30 min was allowed. To evoke the von Bezold-Jarisch reflex, rats were injected with phenylbiguanide (PBG; 10 µg/kg, i.v. bolus) allowing at least 10 min between injections to avoid tachyphylaxis. Rats were then paralysed with pancuronium bromide (0.8 mg/kg, i.v. every 60 min) and the vagi were cut bilaterally to eradicate synchronization of the artificial ventilation and phrenic nerve activity (PNA) via input from pulmonary stretch afferents (Morrison, 1999). To assess baroreceptor function, phenylephrine, a vasoconstrictor agent, (PE; 20 µg/kg in 0.1 ml 0.9% saline, i.v. bolus) and sodium nitroprusside, a vasodilator agent, (SNP; 20 µg/kg in 0.1 ml 0.9% saline, i.v. bolus) were administered separately to load or unload the baroreceptor reflex respectively. The activation of central and peripheral chemoreceptors was induced via application of 2 min of 5% CO_2 (in O_2, hypercapnia) and 1 min of 10% O_2 (in nitrogen, hypoxia), directly to the inspiratory tube of the ventilator that normally provided oxygen-enriched room air. Intermittent hypoxia was generated by cyclic hypoxic events repeating the 10% O_2 for 1 min followed by 100% O_2 for 5 min to induce hypoxia a total of 5 times. The response to the acute intermittent hypoxia (AIH) was recorded for 30 min after which a final 1 min hypoxic challenge was administered.

4.2.5. Perfusion, tissue collection, and immunohistochemistry

All viral vector injected rats were perfused 4-5 weeks post-injection and almost all bilateral injected animals were subjected to the electrophysiology experiments just described. The rats were then either euthanized with an overdose of sodium pentobarbitone (100 mg/kg, i.p. or i.v.) or if already anaesthetized sacrificed using 3M KCl (i.v.) or 1 ml urethane (i.v.) prior to intracardiac perfusion as described in Section 2.2.5. Brains were removed and post-fixed overnight. The tissue was then cut into coronal sections (50 µm thick) using a vibrating microtome (Leica VT 1200S, NSW, Australia) and sections were kept in cryoprotectant solution (see Chapter 2) for 24 h, before being transferred to -20 °C.

For the immunohistochemistry experiment, free-floating sections were washed with 0.3% (v/v) Triton X-100 in Tris (10 mM)-phosphate (10 mM) buffered saline (TPBS, pH 7.4), 3×30 min at room temperature. Sections were then blocked in 10% (v/v) donkey serum in TPBS containing 0.3% (v/v) Triton X-100 for 1 hour at room temperature, and incubated with primary antibodies (monoclonal antibody 735 directed against polySia (mAb 735) 0.5 µg/ml, anti-GFP antibody Abcam 1:500, mouse anti-tyrosine hydroxylase (TH) T1299 Sigma Aldrich 1:1000, and anti-glial fibrillary acidic protein (GFAP) G9269 Sigma-Aldrich 1:500), diluted in 10 % normal horse serum in TPBS containing 0.3% (v/v) Triton X-100 for 48 hours at 4 °C. Sections were washed with TPBS, 3×30 min at room temperature and then were incubated in fluorescent conjugated secondary antibodies (Alexa Fluor 647-AffiniPure donkey anti-mouse IgG #715-165-151 and Alexa Fluor® 488 AffiniPure Donkey Anti-Rabbit IgG (H+L) # 711-545-152, Jackson ImmunoResearch 1:500) overnight at 4 °C. Sections were washed, 3×30 min with TPBS, mounted onto glass slides using Dako Fluorescent mounting medium (Dako, Australia), and visualized using a Zeiss upright microscope (Axio Imager Z.2, Germany). Images were acquired using ZEN 2012 imaging software (Zeiss, Germany). Mosaic images of each coronal brainstem section were acquired at 20x magnification. High power images were captured with a Leica confocal microscope (Leica TCS SP5X; Leica Microsystems, NSW, Australia) using Leica Application Suite Advanced Fluorescence software (LAS AF; Leica, Germany) and analysed using the ImageJ plugin Fiji (Schindelin et al., 2012).

4.2.6. Criteria for selecting animals for further analysis

A number of unilateral injections were performed: LV/PST (n=18) and LV/GFP (n=5). However, only injections that were located within the RVLM (see below), showed a good coverage, and a good expression of mCherry (for LV/PST) or GFP (for LV/GFP) were selected for further analyses. The same criteria used for animals injected bilaterally; however, these criteria were assessed in both sides and animals with only one good injection site were also rejected.

4.2.7. Data analysis

To measure mCherry, GFP, and polySia fluorescence in each unilaterally LV/PST or LV/GFP injected animal, tile images of two single brainstem sections containing the RVLM (using a Zeiss upright microscope as discussed in section 4.2.5) were used. Using ImageJ plugin Fiji (Schindelin et al., 2012), an outline was drawn around the fluorescent reporter positive regions and the mean grey value of fluorescence was measured in all three channels (mCherry, GFP, and polySia immunoreactivity). The same area on the contralateral side was then measured. For background levels a site on each side of the pyramidal tract that was label free was measured and deducted from the mean grey value of the injected and uninjected side for each channel. The results are presented as fold increase in the injected side (mean grey value of injected/non-injected side). All statistical analysis (unpaired 2-sided Student's t-test and one-way ANOVA) were performed using Prism (version 7.02, GraphPad Software, CA, USA).

Data for all electrophysiological experiments were analysed offline using Spike2 software. The baseline measurements were taken immediately preceding the 1st SNP response when the animal was paralysed and ventilated. Peak values for all outflows were calculated as the maximal change observed in comparison with the baseline values (5 minutes of stable data before each drug administration or stimulus challenge). Instantaneous heart rate (HR) was obtained from the AP signal by measuring the frequency per minute. Mean arterial pressure (MAP) was derived by smoothing the pressure waveform (using a 1 s time constant). Splanchnic and phrenic nerve recordings were rectified and smoothed using 1 second averages. Phrenic nerve frequency (PNf) was obtained from phrenic nerve activity and was derived by calculating the duration between the onset of phrenic nerve bursting. Phrenic nerve amplitude (PNamp) was calculated from the peak value of bursting through each cycle. To remove noise level from the nerve recording, the level of activity was subtracted after cutting the nerve. Thus parameters measured were MAP (mmHg), HR

(bpm), SNA (either as µV for baseline or % change for all challenges), PNf (bursts per min) and PNamp (µV for baseline or % change for all challenges).

To measure barosensitivity, MAP and rectified SNA responses to phenylephrine and sodium nitroprusside were assessed. Sympathetic baroreflex function curves were generated during the peak active phases of bolus intravenous injections of PE and SNP. Non-linear regression analysis was used to fit normalized SNA values against MAP to a four-parameter sigmoid logistic function curve (version 7.02, GraphPad Prism Software, CA, USA):

$Y=P1+(P2-P1/(1+10^{[P3-x].p4}))$

Y is SNA, P1 is the bottom plateau, P2 is the top plateau, P3 is MAP halfway between the top and bottom plateau, x is MAP, and P4 is the steepness of the curve. Maximal gain was obtained from the first derivative of the logistic function curve (G_{max}; gain at MAP_{50}).

To examine von Bezold-Jarisch reflex, peak values observed in HR, MAP, and SNA were calculated in response to PBG.

To assess chemosensitivity, peak values observed in MAP, HR, PNf, PNamp, and SNA were calculated in response to peripheral (hypoxia) and central (hypercapnia) chemoreceptor challenge compared to 1 min baseline prior to stimulus.

Responses were compared in LV/PST, LV/GFP, and Naïve rats and examined using one-way ANOVA. For multiple comparisons, Tukey's test was applied. $P < 0.05$ was considered significant. Symbols are indicated as $P < 0.05$ (*), $P < 0.01$ (**), $P < 0.001$ (***), and $P < 0.0001$ (****). All values were calculated using PRISM (version 7.02, GraphPad Software, CA, USA).

4.2.8. Counting C1 neurons

The number of C1 neurons expressing mCherry reporter was counted in five RVLM sections (at 120 µm intervals) 0–480 µm caudal to the caudal pole of the facial nucleus (bregma -12.48 to -12, n=4) and this was divided by the total number of C1 neurons in all five sections.

4.3. Results

4.3.1. The injection of LV/PST did not result in mCherry or GFP expression in the NTS

A lentiviral vector containing PST cDNAs (LV/PST) which expresses PST, mCherry, and GFP under synapsin promoter, a neuron-specific promoter (Hioki et al., 2007), was injected into the NTS in 8 animals. All animals showed very poor expression of the fluorescent reporters, an example is shown in Figure 4.1A. Even using a more ventral injection site closer to the dorsal motor nucleus of vagus (DMV) did not improve the labelling in either NTS or DMV (Figure 4.1B - one of the best expression levels obtained). However, some mCherry expression was present outside of these regions (Figure 4.1B). Using multiple smaller injection sites similarly did not improve labelling. Labelling was consistently poor to non-existent in the NTS.

4.3.2. Induced expression of polySia in the RVLM after viral delivery of PST cDNAs unilaterally

In order to determine whether we could obtain overexpression of polySia in the RVLM, we used the same vector (LV/PST) and a control vector (LV/GFP) for unilateral injections in the RVLM. These injections resulted in a more consistent expression; however, a number of animals were rejected as they did not meet the selection criteria (see Section 4.2.6). Figure 4.2A and B show the dorsoventral and mediolateral extent of unilateral injection sites in all animals that met the criteria where reporter expression covered part or all of the RVLM (n=8). Figure 4.2C and D show the

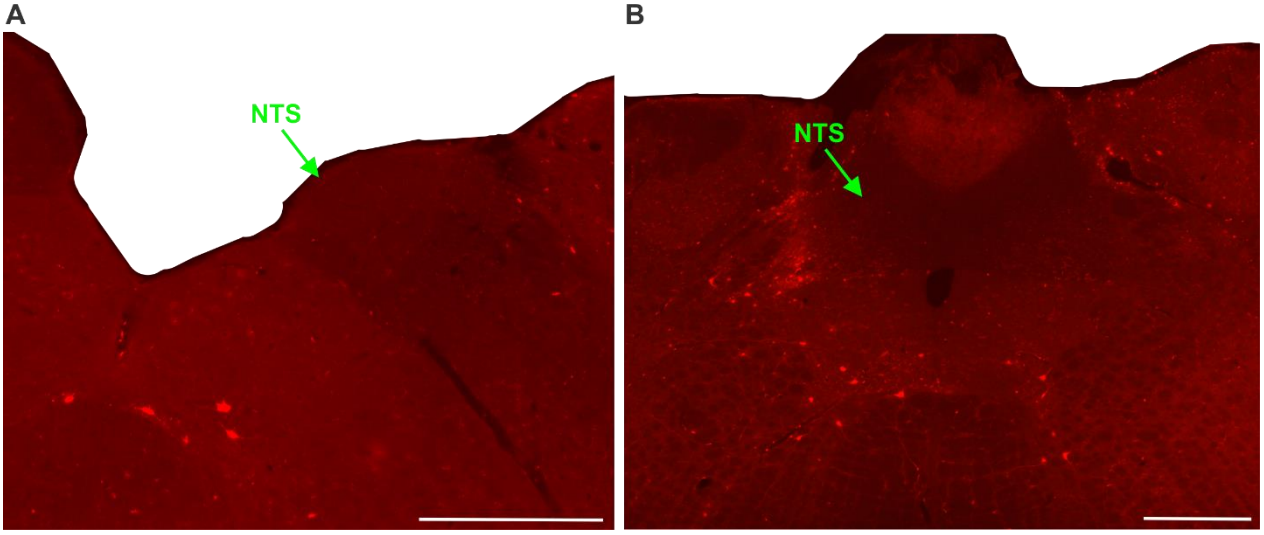

Figure 4.1. Very poor expression of mCherry was found in the NTS 4-5 weeks post-injection of LV/PST. (A) and (B) show mCherry expression in two different rats. Scale bars = 500 µm.

rostrocaudal extent of these unilateral injection sites. For the LV/PST injected group (n=5), these sites varied from -11.88 to -13.08 mm from bregma with all injection sites covering -12 to -12.12 mm (Figure 4.2A and C). In rats injected unilaterally with LV/GFP (n=3), the rostrocaudal extent varied from -12 to -12.96 with all three injections covering -12.24 to -12.36 mm from bregma.

An example of a unilateral injection site indicated by fluorescent reporter labelling and immunofluorescence for polySia (using mAb 735) together with its contralateral non-injected side is shown in Figure 4.3A and B. Both mCherry and GFP labelled neurons can be clearly seen on the injected side but not on the non-injected side (Figure 4.3B). PolySia-ir was clearly more intense on the injected side (Figure 4.3A and B). Using LV/GFP a similar pattern was seen where GFP expression was seen on the injected side only (Figure 4.3C).

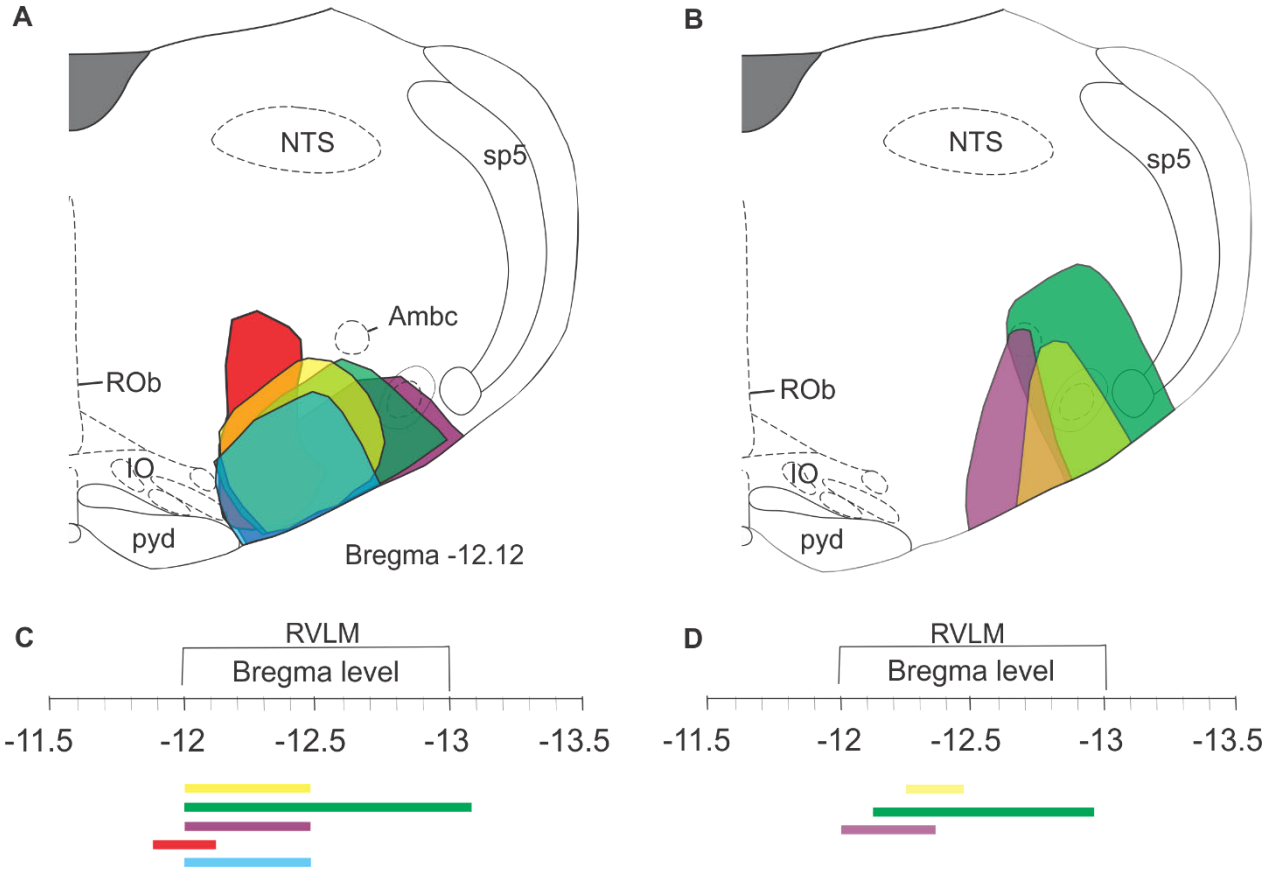

Figure 4.2. Lentiviral vector (LV/PST and LV/GFP) injection sites targeting the RVLM in unilateral injections of the adult rat. (A) and (B) The right coronal hemisections show schematically the spread of injection sites in the RVLM of animals injected unilaterally with the lentiviral vector containing PST cDNAs (LV/PST, n=5) and without PST cDNAs (LV/GFP, n=3) respectively. (C) and (D) show the rostrocaudal extents of the injection sites in LV/PST and LV/GFP transduced animals, respectively.

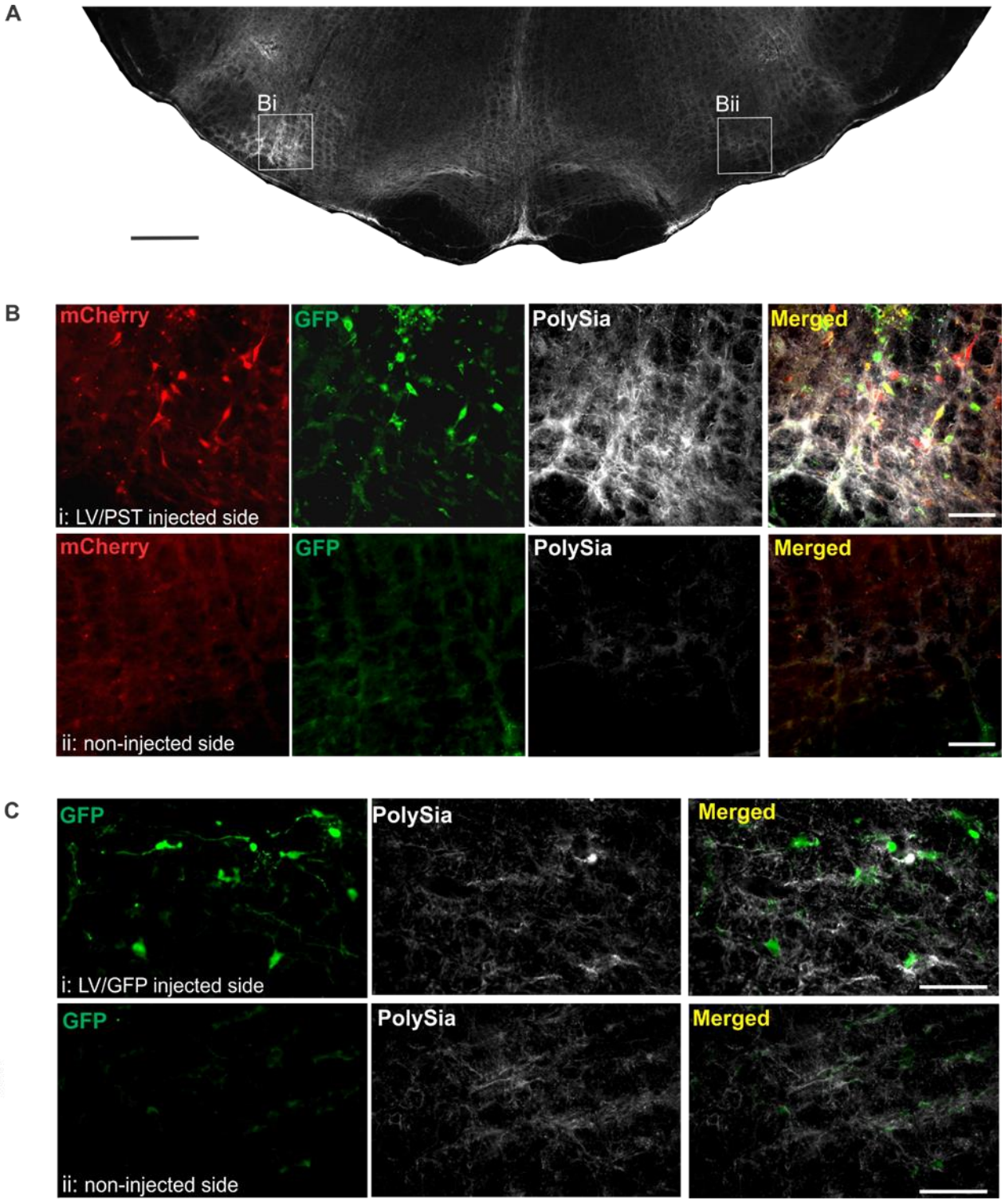

Figure 4.3. Induced expression of polySia in the RVLM after injection of LV/PST. (A) A coronal brainstem section through the RVLM (bregma -12.12) from a rat injected with LV/PST showing mCherry-ir (red), GFP-ir (green), and polySia-ir (white). (B) shows images from Bi and Bii indicated in A depicting injected and contralateral non-injected sides, respectively. Similarly, Ci shows the expression of GFP- and polySia-ir in the RVLM after LV/GFP injection compared to its contralateral non-injected side, Cii. Scale bars = 500 µm in A and = 100 µm in B and C.

However, it was clear that in some LV/GFP animals some polySia expression was also induced on the injected side (Figure 4.3C). Nevertheless, the expression appeared to be less intense in the LV/GFP animals compared to the LV/PST injected ones (Figure 4.3B and C).

In order to assess the level of polySia overexpression measured by immunoreactivity, we compared the mean grey value of GFP- and polySia-ir from unilaterally LV/PST injected rats (n=5) with those of unilaterally LV/GFP transduced animals (n=3) (Figure 4.4A). The data revealed that the induced expression of polySia in the LV/PST injected rats was variable but as a group was significantly higher than that of LV/GFP group, whereas there was no significant difference in the expression of GFP between these two groups. Figure 4.4A also shows that in the LV/PST injected animals the expression of mCherry is significantly higher than that of GFP (although similarly variable). However, comparison of polySia-ir in LV/GFP injected rats with that of naïve rats (n=3) also showed a significant increase in polySia expression in LV/GFP rats. It is also clear that there is much less variability in the polySia expression in naïve animals.

Green fluorescent protein (GFP) in the LV/PST vector is used as a reporter molecule (Chalfie et al., 1994, Soboleski et al., 2005) for PST gene expression and therefore its expression is taken to indicate the expression of PST. However, in our experiments it was clear that animals with a higher expression of mCherry and GFP did not always show a higher level of polySia-ir despite being treated identically. Figure 4.4B shows an example of this in a rat unilaterally injected with LV/PST. Although more expression of mCherry and GFP is seen in the injection side of this rat compared to the rat depicted in Figure 4.3B, less expression of polySia is seen (Figure 4.4B) and this is also confirmed by the graph (Figure 4.4A; red (represents 4.3B) vs. green (represents 4.4B)). Nevertheless, both animals showed polySia overexpression. Similarly, from each of these examples it is evident that some cells express both mCherry and GFP, whilst others express only GFP or mCherry.

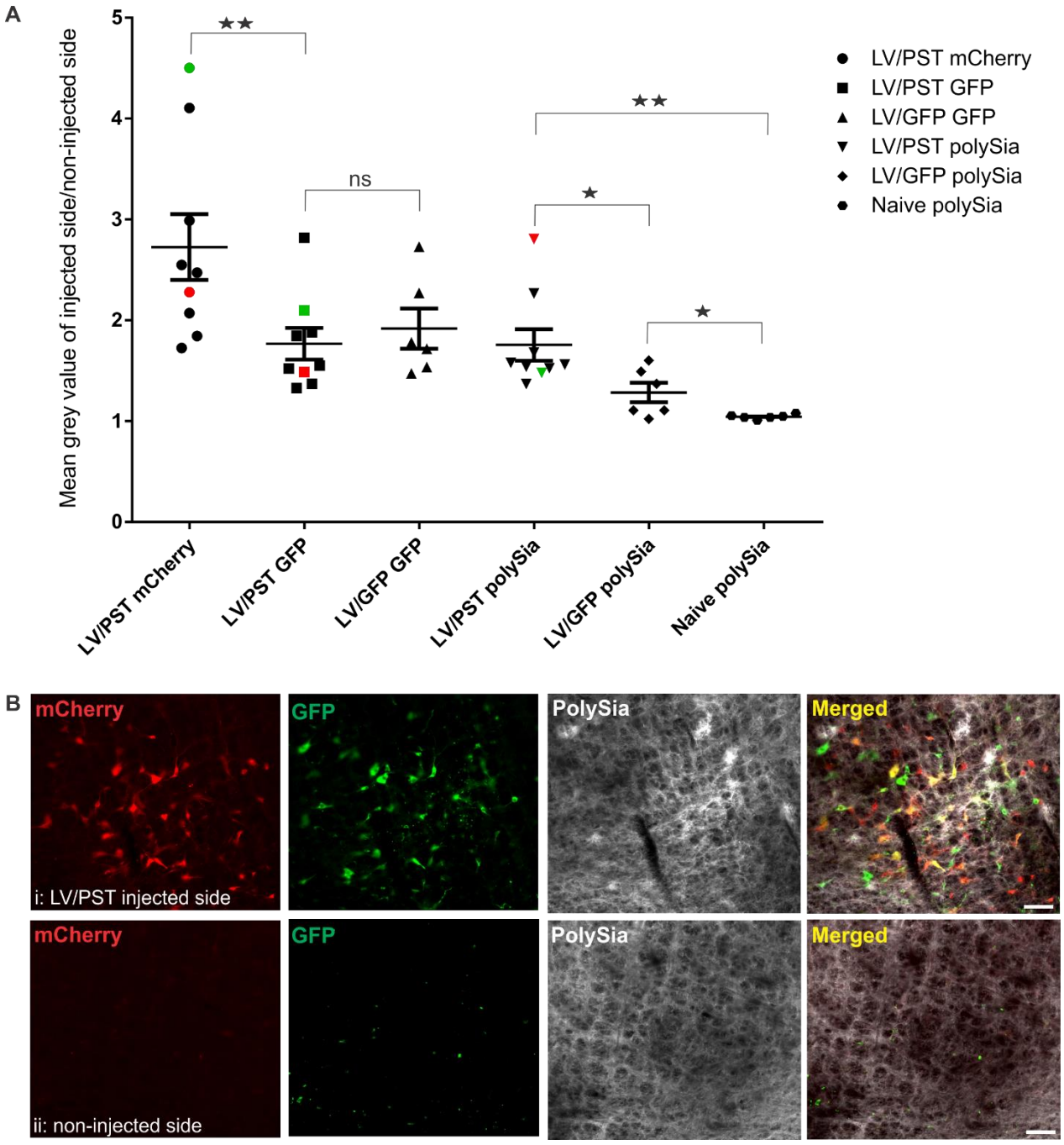

Figure 4.4. PolySia expression was significantly higher in the LV/PST injected rats compared to the LV/GFP injected and naïve animals. (A) The graph shows the fold change of mCherry-, GFP-, and polySia-ir in the injected sides compared to the non-injected sides in the LV/PST, LV/GFP, and naïve animals. (Bi) and (Bii) show mCherry-ir (red), GFP-ir (green), polySia-ir (white), and merged image (yellow) in the injected and non-injected sides of an LV/PST transduced animal respectively, demonstrating viral vector-induced expression of polySia. (Bi) also shows that some GFP and mCherry were colocalized (yellow), while some were expressed individually in different neurons. Scale bars = 100 µm.

As seen in Chapter 2, polySia-ir was often seen encircling or surrounding neurons in polySia abundant regions such the NTS and spinal trigeminal nucleus caudalis. In order to further assess the level of polySia expression in the RVLM, confocal microscopy was used to compare expression on mCherry and GFP positive cells in LV/PST and LV/GFP injected animals. In LV/PST transduced animals in some mCherry and GFP positive cells, a very dense ring polySia was very obvious (Figure 4.5A and D). In the others, although a distinct ring was not evident, neuronal morphology could be distinguished based on the intensity of polySia (Figure 4.5B and D). However, in GFP expressing cells of LV/GFP transduced animals, although some occasional rings

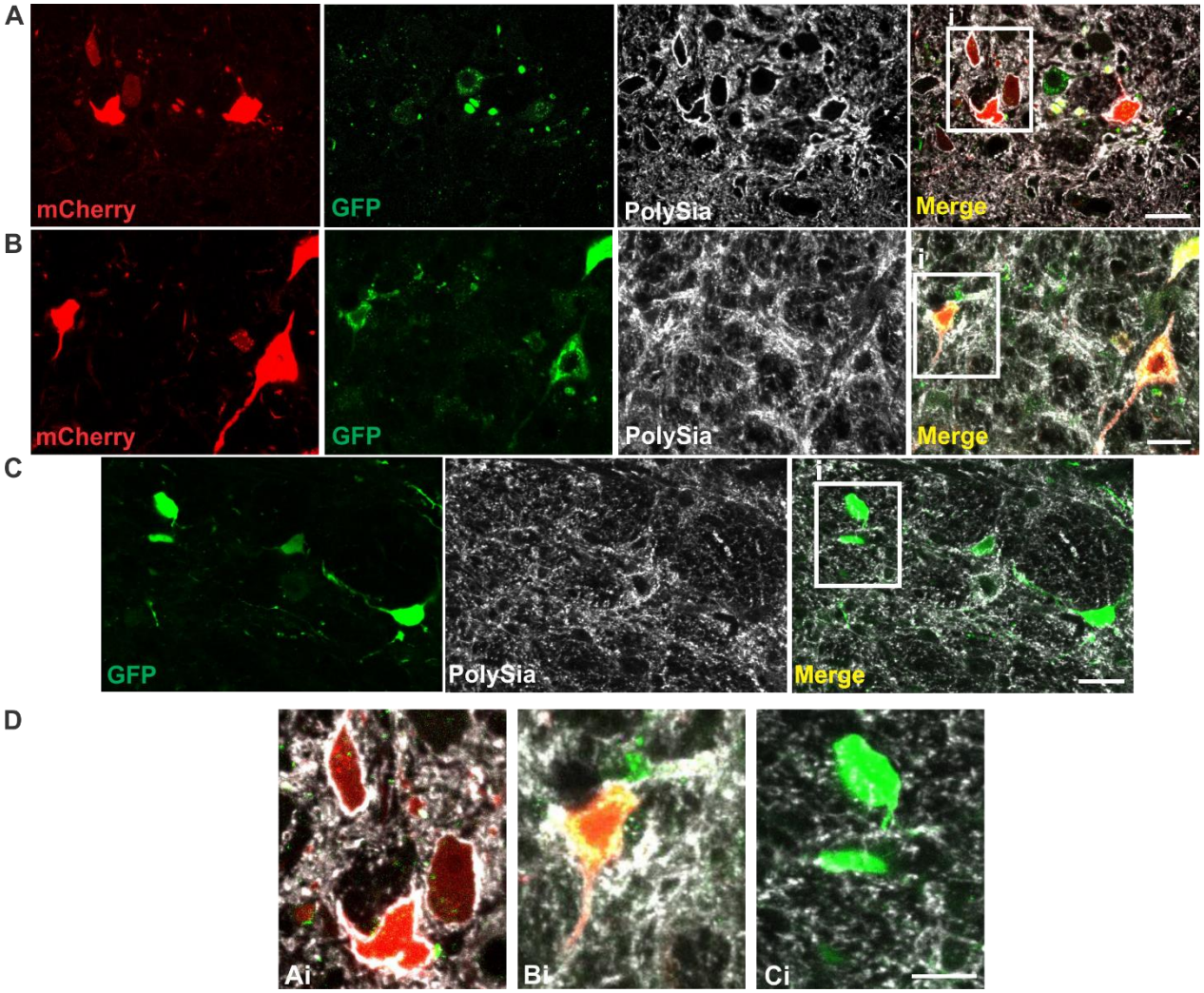

Figure 4.5. PolySia-ir enveloping mCherry or GFP positive cells was more distinct in LV/PST than LV/GFP transduced animals. (A) shows rings of polySia-ir enveloping mCherry and GFP positive cells in LV/PST injected animals. (B) PolySia positive cells were more distinct due to higher expression of polySia in LV/PST injected animals. (C) The majority of GFP positive cells in LV/GFP injected animals did not show a ring of polySia-ir or distinct polySia expression. (D) Magnified images of the boxes indicated in A-C. Scale bars = 25 µm in A-C and = 12 µm in D.

were found, the majority of the cell bodies did not show rings or the rings were not as distinct (Figure 4.5C and D).

4.3.3. Little polySia-ir in the RVLM was associated with GFAP-ir in astrocytes

In order to determine if injury due to injection could cause up-regulation of polySia expression, we assessed astrocytes within the RVLM by looking at the expression of GFAP-ir. Injury can cause activated astrocytes and these were found to be associated with polySia in and around the site of injury (La Salle et al., 1992a, Nomura et al., 2000). In all animals examined, some evidence of activated astrocytes was found as a mild increase in the intensity of GFAP labelling was seen in astrocytes in the mCherry and GFP positive regions compared to the same region of the non-injected side. Also, some animals showed morphological changes in some astrocytes such as elongated processes. An example (one of the worse cases) is shown in Figure 4.6A-B. To determine if the level of colocalization of polySia with GFAP increased from naïve animals (see Chapter 2) where no colocalization was seen, confocal microscopy was used. Although little colocalization was found (Figure 4.6C-D), the expression of polySia was not predominantly associated with GFAP immunoreactive astrocytic processes (Fig. 4.6B-C).

4.3.4. Bilateral injections of LV/PST and LV/GFP for physiology studies

Following injection of viral vectors, conduct of electrophysiological experiments followed by perfusion and tissue processing, and assessment of vector labelling, six animals with bilateral injections of LV/PST and four with LV/GFP met our criteria (see Section 4.2.6), an example of the injection sites in each group is shown in Figure 4.7A and B. All injection sites covered the RVLM or part of the RVLM (Figure 4.7C and D) with the majority of the injections (except for one) in the LV/PST covering at least 300 µm from 600 µm rostral to the facial nucleus, as demonstrated by the expression of mCherry reporter (Figure 4.7E). In LV/GFP induced animals, at least 500 µm out of the first 600 µm rostral RVLM showed expression of the lentivirus, as demonstrated by the expression of GFP reporters (Figure 4.7F).

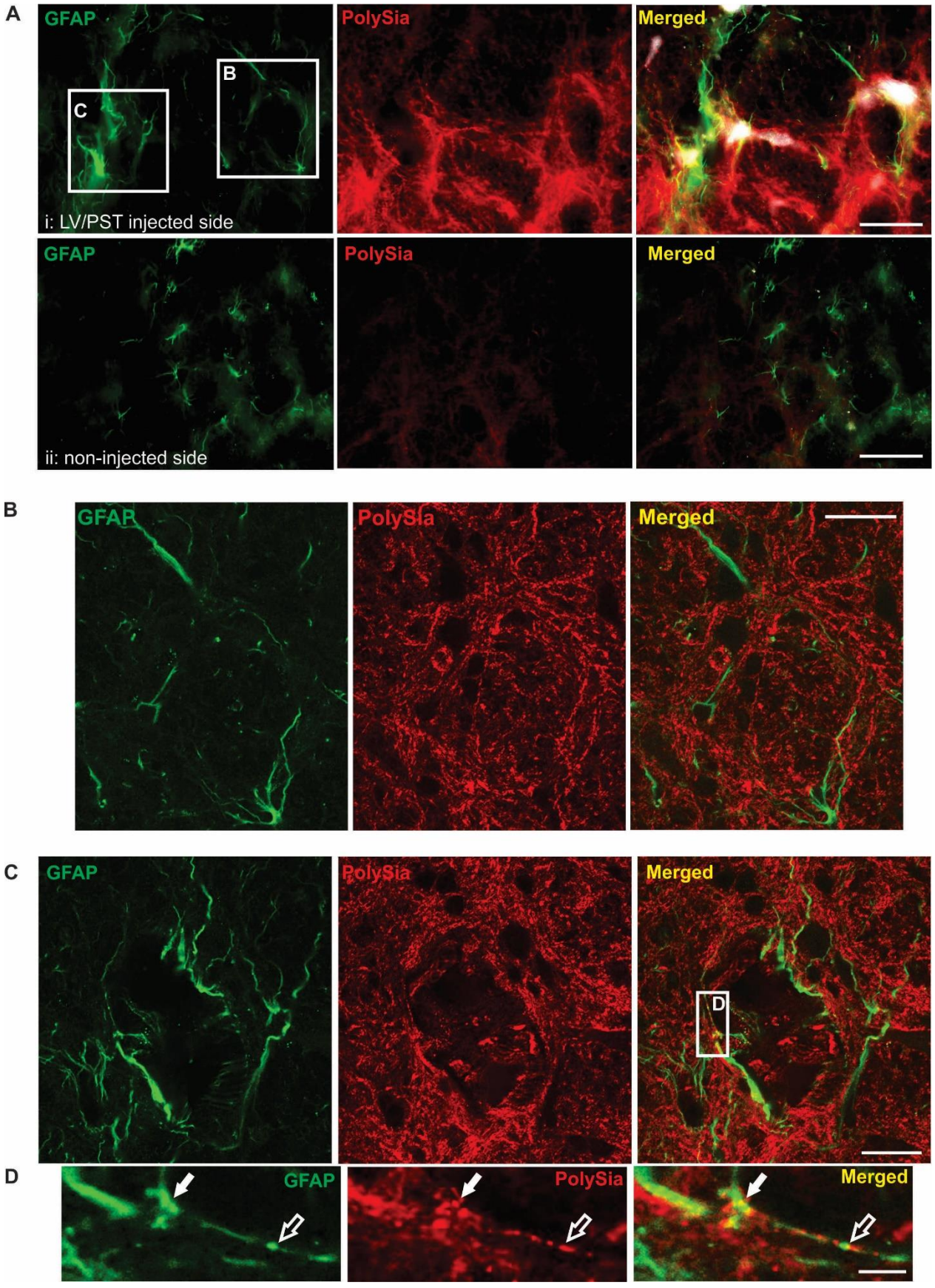
A
GFAP
PolySia
Merged
B
C
i: LV/PST injected side
GFAP
PolySia
Merged
ii: non-injected side
B
GFAP
PolySia
Merged
C
GFAP
PolySia
Merged
D
D
GFAP
PolySia
Merged

Figure 4.6. Few GFAP positive astrocytic processes in the LV/PST injected sites colocalized with polySia. (A) shows the expression of GFAP-ir (green) and polySia-ir (red) and their merged image (yellow) in the injected (Ai) and non-injected side (Aii) of an LV/PST transduced animal. (B) and (C) Confocal images of boxes in A. (D) The box in C showing an example of colocalization of GFAP and polySia. Arrows indicate colocalization. Scale bars = 50 μm in A and B, = 20 μm in C, and = 5 μm in D.

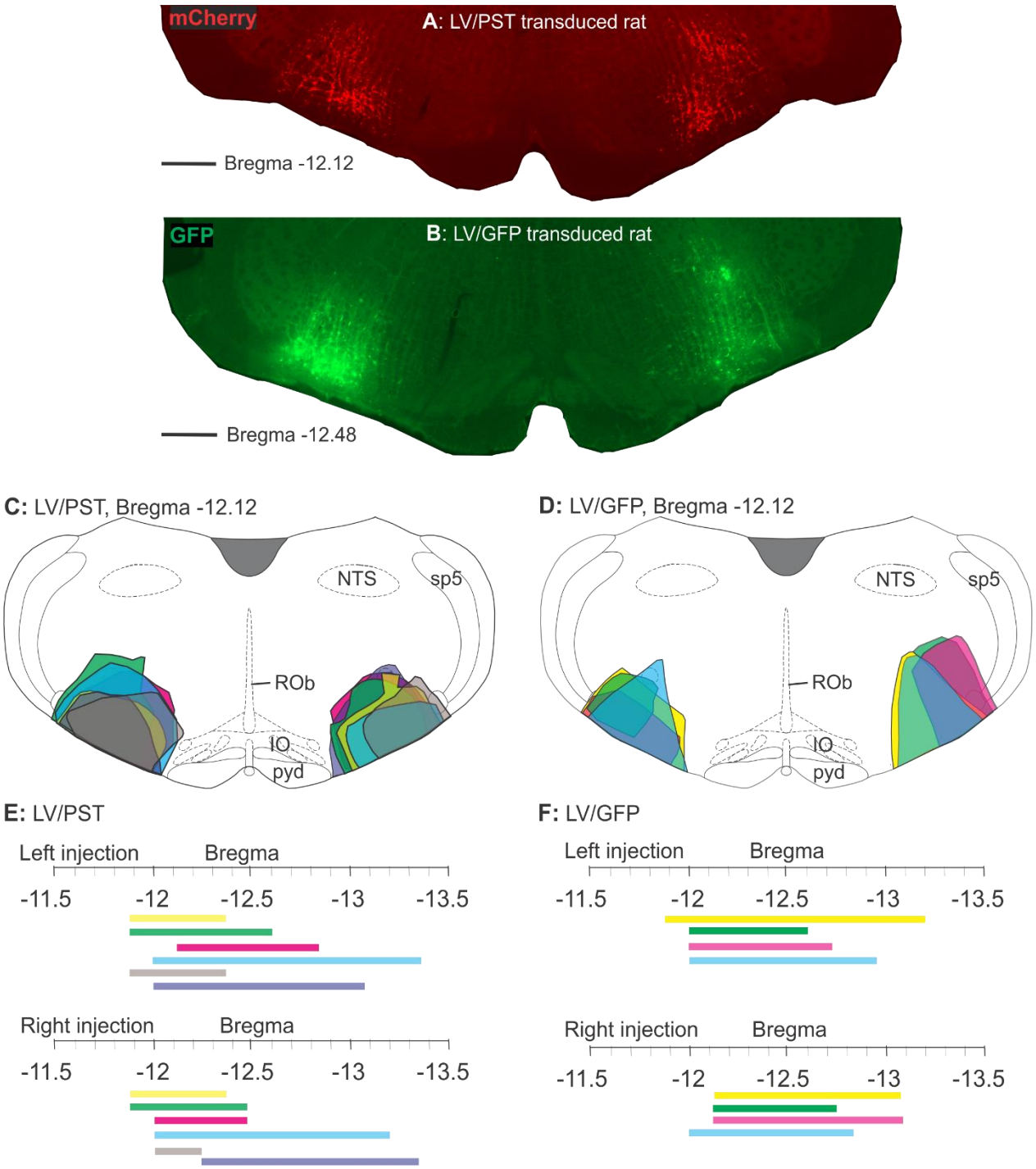

Figure 4.7. Bilateral injection sites of LV/PST (n=6) and LV/GFP (n=4) targeting the RVLM of the adult rat. (A) and (B) Coronal sections showing the mCherry (red) or GFP (green) expression respectively 4-5 weeks post injection. (C) and (D) show schematically the spread of injection sites in the RVLM. (E) and (F) show the rostrocaudal extent of the injection sites. Scale bars= 500 µm.

4.3.5. C1 neurons: how many in the RVLM are transfected with LV/PST?

The RVLM neurons that are most directly associated with the control of blood pressure and the cardiorespiratory reflexes are the bulbospinal neurons that innervate sympathetic preganglionic neurons monosynaptically, about 70% of which are C1 neurons (Schreihofer and Guyenet, 1997, Brown and Guyenet, 1985, Ross et al., 1984). Therefore, we investigated the number of the reporter (mCherry) expressing C1 neurons in the RVLM using an antibody against tyrosine hydroxylase (TH, a marker of C1 neurons (Phillips et al., 2001)). In four animals injected bilaterally with LV/PST, an average of 32 ± 4.2% of TH neurons were double labelled with mCherry, an example of which is shown in Figure 4.8A and B.

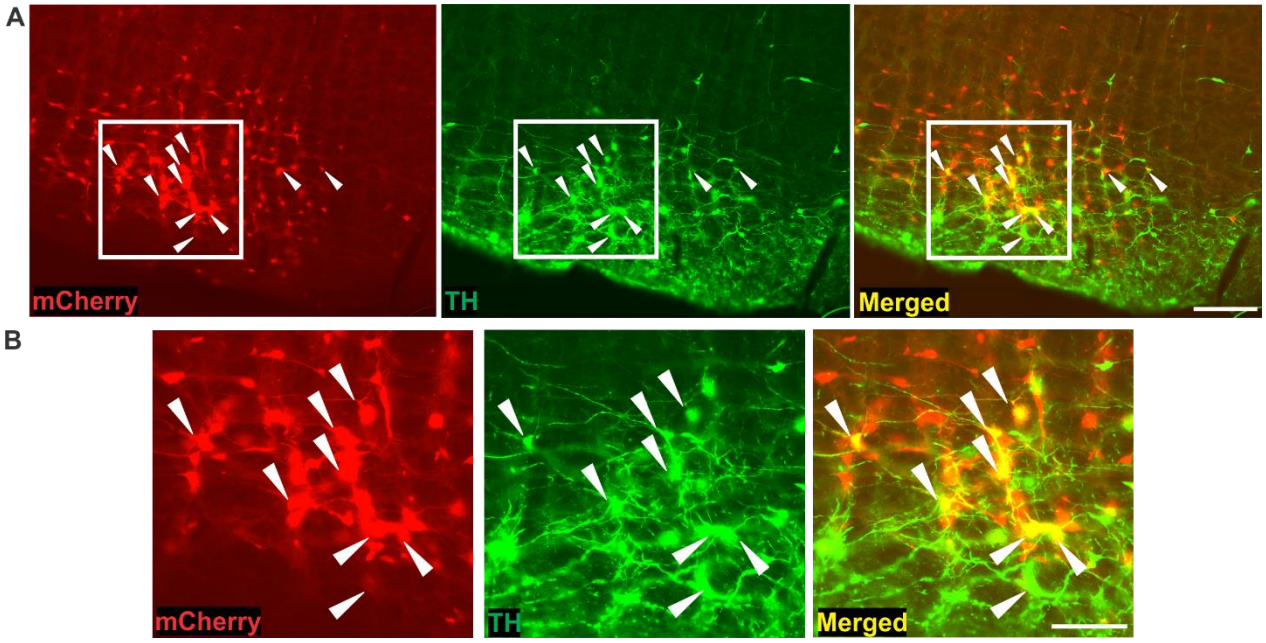

Figure 4.8. Some C1 neurons were transfected with LV/PST in the RVLM. (A) Some C1 neurons, labelled with anti-tyrosine hydroxylase (TH, green), were transfected with LV/PST (mCherry, red), shown by arrow heads. (B) The magnified image of the box indicated in A. Scale bars = 200 µm in A and = 100 µm in B.

4.3.6. Physiology results

In order to determine whether overexpression of polySia in the RVLM influenced the function of neurons in the region, baseline cardiovascular and respiratory variables and cardiorespiratory reflex function were compared in three groups of adult rats: LV/PST injected, LV/GFP injected, and naïve. Naïve animals were included to enable comparison with bilaterally vector injected animals. Only animals that fitted the criteria outlined in Section 4.2.6 were included in the analysis.

4.3.6.1. Baseline

Baseline levels of MAP, HR, SNA, and PNf were determined in LV/PST, LV/GFP, and naïve animals that were paralysed, vagotomised, and artificially ventilated (after PBG administration, see below) (Table 4.1). No significant differences were seen between the groups except, PNf was curiously higher in LV/GFP animals compared to the other two groups.

Table 4.1. Baseline Measurements

Treatment group	MAP (mmHg)	HR (beats per min)	SNA (uV)	PNf (bursts per min)
LV/PST (n=6)	98.4 ± 5.0	466 ± 14.5	2.55 ± 0.25	41.1 ± 3.2
LV/GFP (n=4)	93.2 ± 7.2	428 ± 26.3	2.53 ± 0.42	60.2 ± 7.6 *
Naïve control (n=4)	108.6 ± 4.7	454 ± 15.5	2.47 ± 0.78	39.3 ± 4.4

The * indicates PNf in LV/GFP is significantly ($P < 0.05$, *) different to the other two treatment groups.

4.3.6.2. Bezold-Jarisch Reflex

The von Bezold-Jarisch reflex is a vagally mediated chemoreflex (Salo et al., 2007) so this reflex function was assessed prior to cutting the vagi. A representative example of the responses evoked in a naïve animal by PBG (i.v.) is shown in Figure 4.9A. A bradycardic, hypotensive response together with sympathoinhibition was seen accompanied by hypopnea (Figure 4.9A). The grouped data are shown in Figure 4.9B-C. The heart rate effect was bradycardia with some animals in all groups exhibiting arrhythmia rather than bradycardia (Figure 4.9B). However, no significant differences were seen between the treatment groups.

4.3.6.3. Sympathetic baroreflex

The administration of phenylephrine and SNP induced rises and falls in AP generating reflex decreases and increases in SNA respectively as described previously (Tallapragada et al., 2016). From these data sympathetic baroreflex function curves were constructed. Comparison of these

curves do not show any significant changes in gain or upper plateau in all three treatment groups however in the LV/PST group the lower plateau was consistently increased compared to the other two groups (P value LV/GFP vs. LV/PST= 0.001 and P value naïve vs. LV/PST= 0.005) (Figure 4.10).

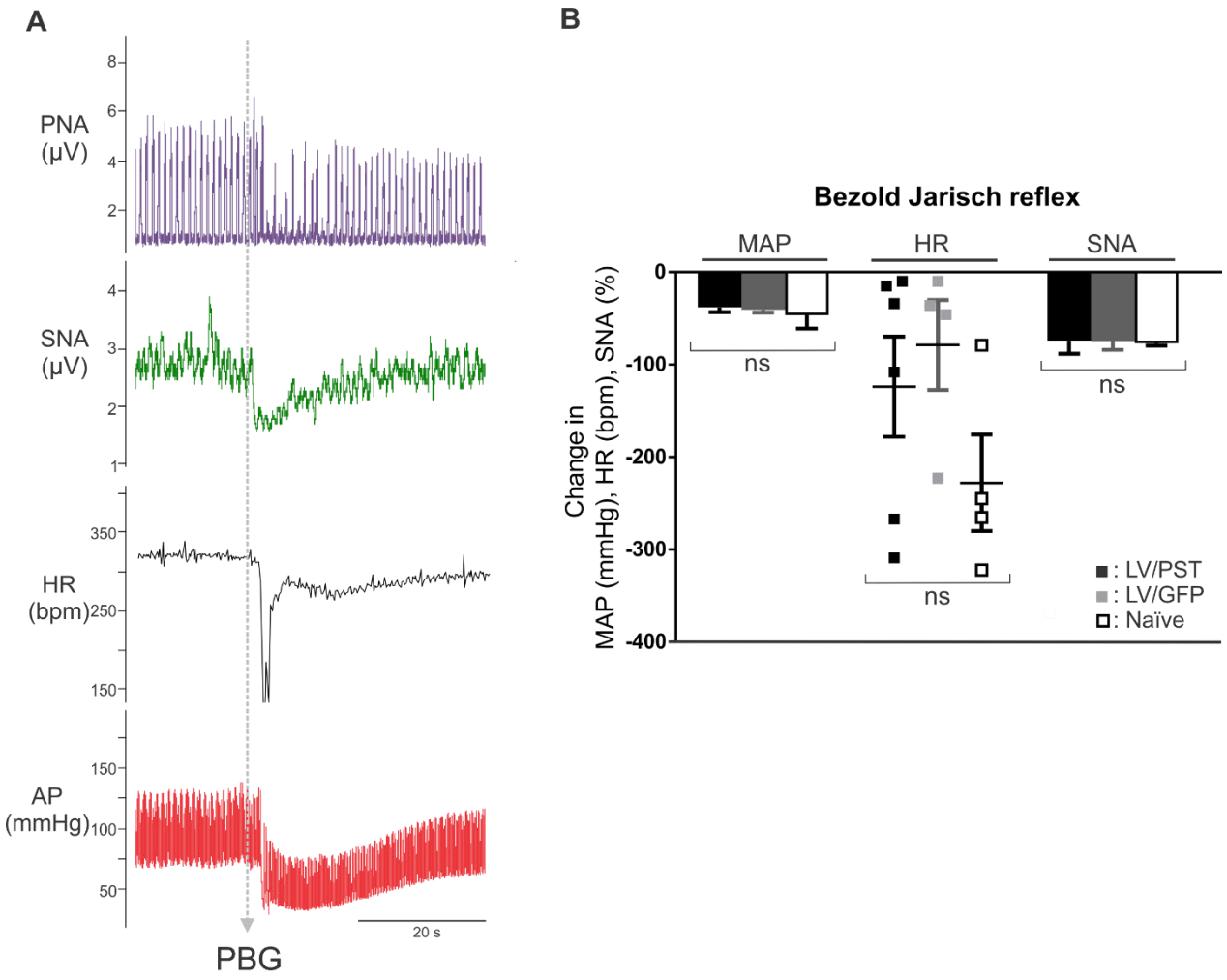

C

Treatment group	Change in MAP (mmHg)	Change in HR (beats per min)	Change in SNA (%)	Change in PNA
LV/PST (n=6)	-38.1 ± 5.2	-123.8 ± 54.1	-73.9 ± 14.5	Hypopnea to apnea
LV/GFP (n=4)	-40.6 ± 3.2	-78.8 ± 48.7	-74.6 ± 9.6	Hypopnea to apnea
Naïve control (n=4)	-46.8 ± 14.2	-227.9 ± 52.2	-76.9 ± 2.6	Hypopnea to apnea

Figure 4.9. Bezold-Jarisch Reflex. (A) A representative example of integrated phrenic (PNA) and sympathetic (SNA) nerve and cardiovascular (heart rate (HR) and arterial pressure (AP)) responses to phenylbiguanide (PBG). (B) and (C) show changes in MAP, HR, SNA and PNA (only C) after the administration of PBG in LV/PST, LV/GFP, and naïve treatment groups.

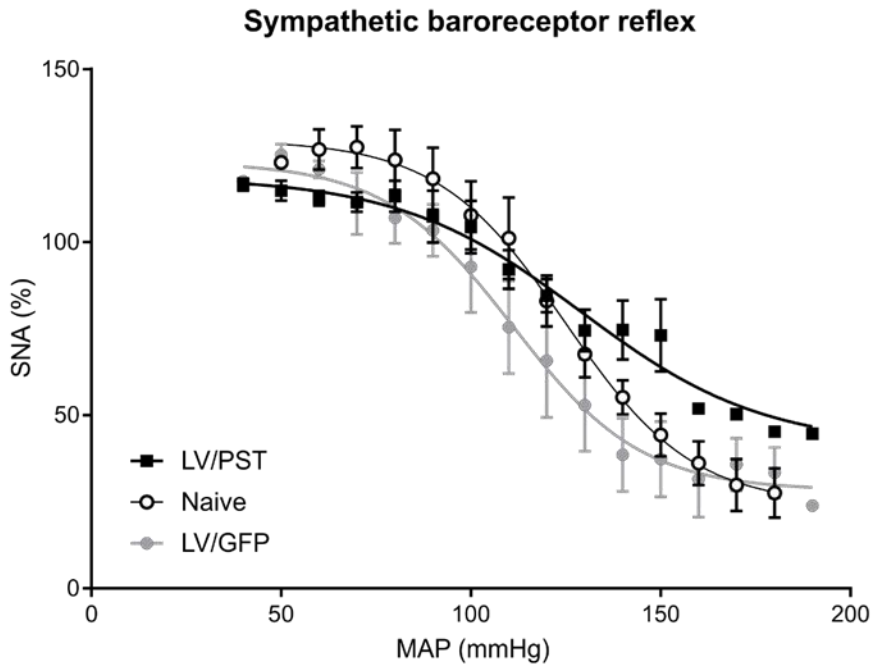

Figure 4.10. Baroreceptor function curves in LV/PST, LV/GFP, and naïve groups of rats. In the LV/PST group the lower plateau was consistently elevated (P value LV/GFP vs. LV/PST= 0.001 and naïve vs. LV/PST= 0.005).

4.3.6.4. Responses to hypercapnia

An example of the response to 5% CO_2 in oxygen for two minutes in a naïve rat is shown in Figure 4.11A. Hypercapnia resulted in a very modest increase in MAP, HR, SNA, and PNf, but the PNamp increased by about 40%. Grouped data are shown in Figure 4.11B with no significant difference in the responses observed between the three treatment groups.

4.3.6.5. Responses to hypoxia

A representative example to the response to 1 min of 10% oxygen in nitrogen is shown in Figure 4.12A. Large increases in HR, SNA and both PNf and PNamp were generated with variable increases in AP evident. The grouped data are shown in Figure 4.12B with no significant differences evident between the treatment groups.

As polySia in higher brain regions is thought to be important in plasticity (Rutishauser, 2008, Gascon et al., 2010, Hildebrandt and Dityatev, 2013), we assessed response evoked by acute intermittent hypoxia (30 min after 5 sequential episodes of hypoxia). We assessed whether there were differences in baseline measurements 30 min after the final challenge and then whether the

responses to a final hypoxic challenge were altered. An example response is shown in Figure 4.13A from a naïve animal. The grouped data are shown in Figure 4.13B. An increase in baseline SNA and PNA is evident at 30 min post the 5^{th} challenge only in LV/PST transduced group (4.13C and D) with no significant difference in the responses between the first and final hypoxic challenge (4.12B and 4.13B). However, no significant differences were found among the treatment groups.

A

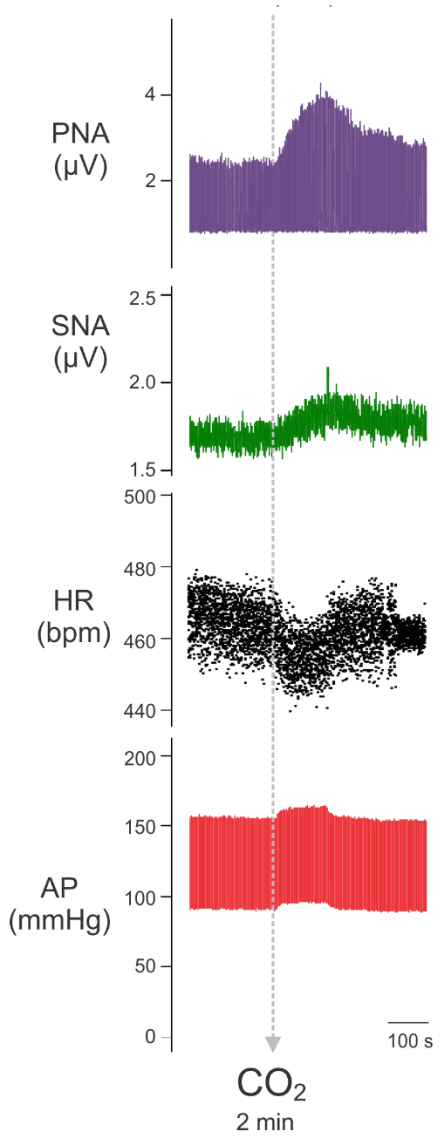

B

Treatment group	Change in MAP (mmHg)	Change in HR (beats per min)	Change in SNA (%)	Change in PNf (bursts per min)	Change in PNamp (%)
LV/PST (n=6)	10.3 ± 2.3	-4.8 ± 2.7	10.2 ± 1.4	14.1 ± 4.1	39.8 ±12.5
LV/GFP (n=4)	7.7 ± 3.9	-10.5 ± 5.3	15.1 ± 1.7	1.3 ± 10.3	34.7 ± 6.4
Naïve control (n=4)	16.4 ± 6.1	-7.0 ± 1.9	18.4 ± 5.0	8.2 ± 1.4	45.7 ± 15.2

No significant difference was found among the three groups for all outflows measured.

Figure 4.11. Response to hypercapnia. (A) A representative example of the cardiovascular (heart rate (HR) and arterial pressure (AP)), sympathetic (SNA), and phrenic nerve (PNA) responses to exposure to 5% CO_2 for 2 min. (B) The table shows changes in MAP, HR, SNA and PNf (phrenic nerve frequency) and PNamp (phrenic nerve amplitude) after hypercapnia in LV/PST, LV/GFP, and naïve groups of rats.

A

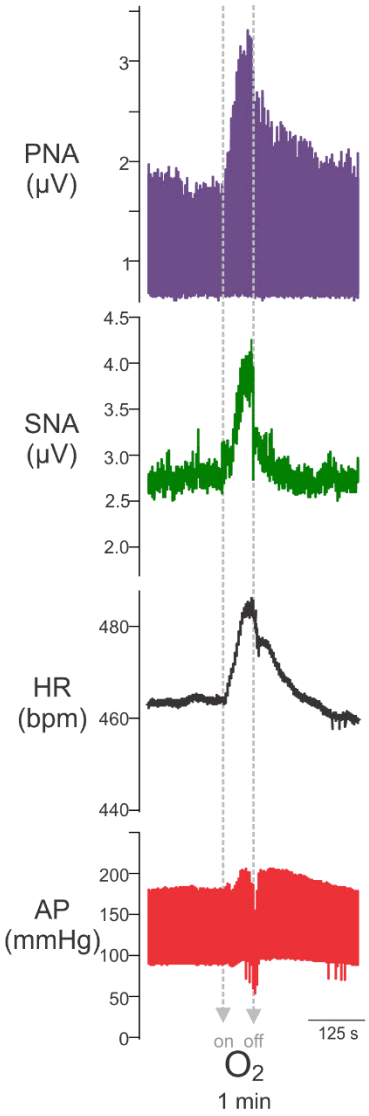

B

Treatment group*	Change in MAP (mmHg)	Change in HR (beats per min)	Change in SNA (%)	Change in PNf (bursts per min)	Change in PNamp (%)
LV/PST (n=6)	18.2 ± 5.1	30.8 ± 3.7	70.9 ± 7.6	27.7 ± 4.0	82.8 ± 7.5
LV/GFP (n=4)	8.0 ± 3.9	32.6 ± 11.4	85.1 ± 31.8	47.2 ± 9.3	116.1 ± 15.3
Naïve control (n=4)	12.8 ± 7.1	28.7 ± 7.5	95.8 ± 30.1	28.7 ± 7.9	99.8 ± 27.3

* No significant difference was found among the three groups for all outflows measured.

Figure 4.12: Response to hypoxia. (A) A representative example of cardiovascular (heart rate (HR) and arterial pressure (AP)), sympathetic (SNA), and phrenic nerve (PNA) responses to exposure to 10% O_2 for 1 min. (B) The table shows changes in MAP, HR, SNA and PNf (phrenic nerve frequency) and PNamp (phrenic nerve amplitude) after hypoxia in LV/PST, LV/GFP, and naïve groups of rats.

A

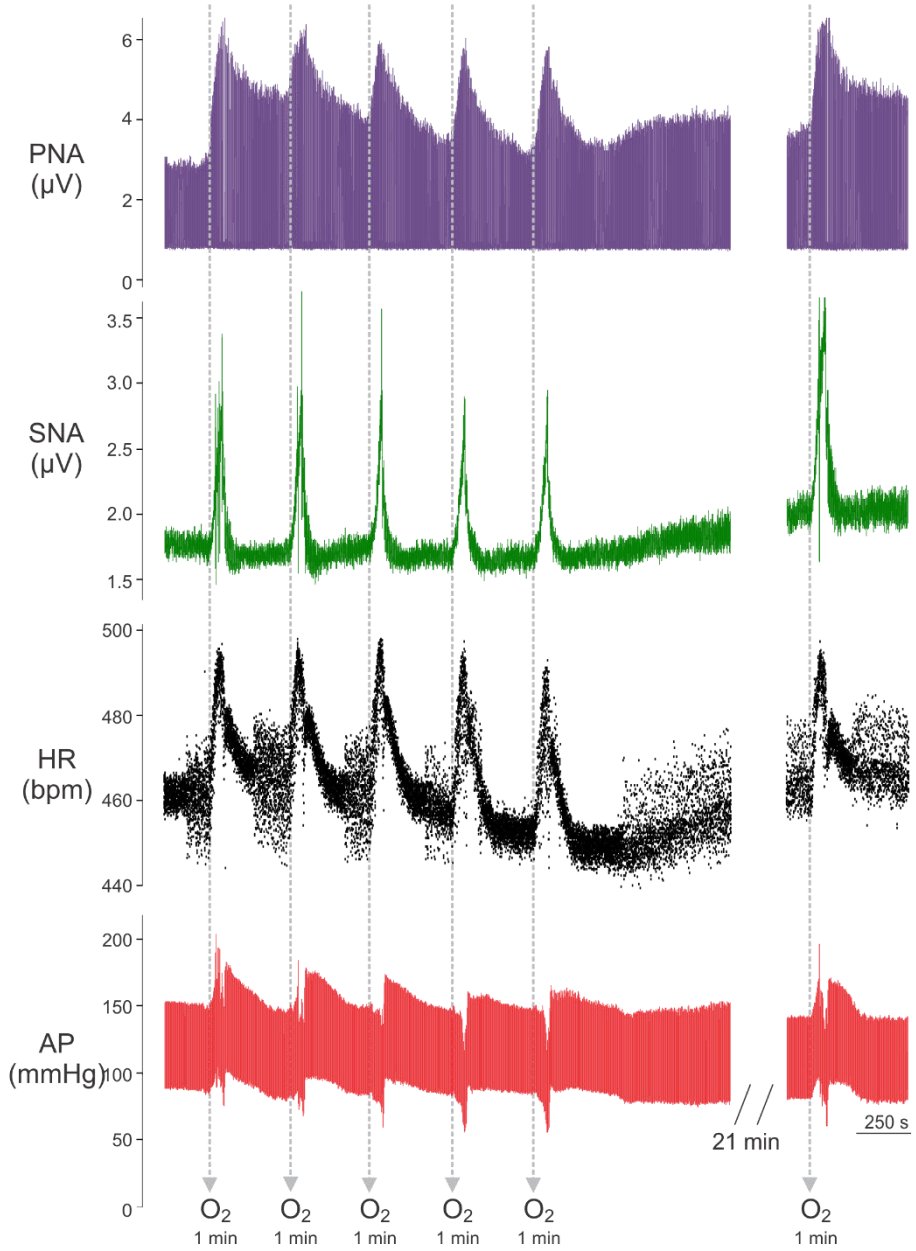

B

Treatment group	Change in MAP (mmHg)	Change in HR (beats per min)	Change in SNA (%)	Change in PNf (bursts per min)	Change in PNamp (%)
LV/PST (n=6)	13.0 ± 5.0	28.2 ± 5.1	51.9 ± 5.0	26.5 ± 5.1	66.0 ± 9.2
LV/GFP (n=4)	16.5 ± 6.8	29.1 ± 6.3	73.4 ± 9.6	46.5 ± 7.9	87.5 ± 7.3
Naïve control (n=4)	18.1 ± 7.0	27.1 ± 6.8	84.8 ± 25.3	26.6 ± 7.3	82.1 ±17.1

No significant difference was found among the three groups for all outflows measured.

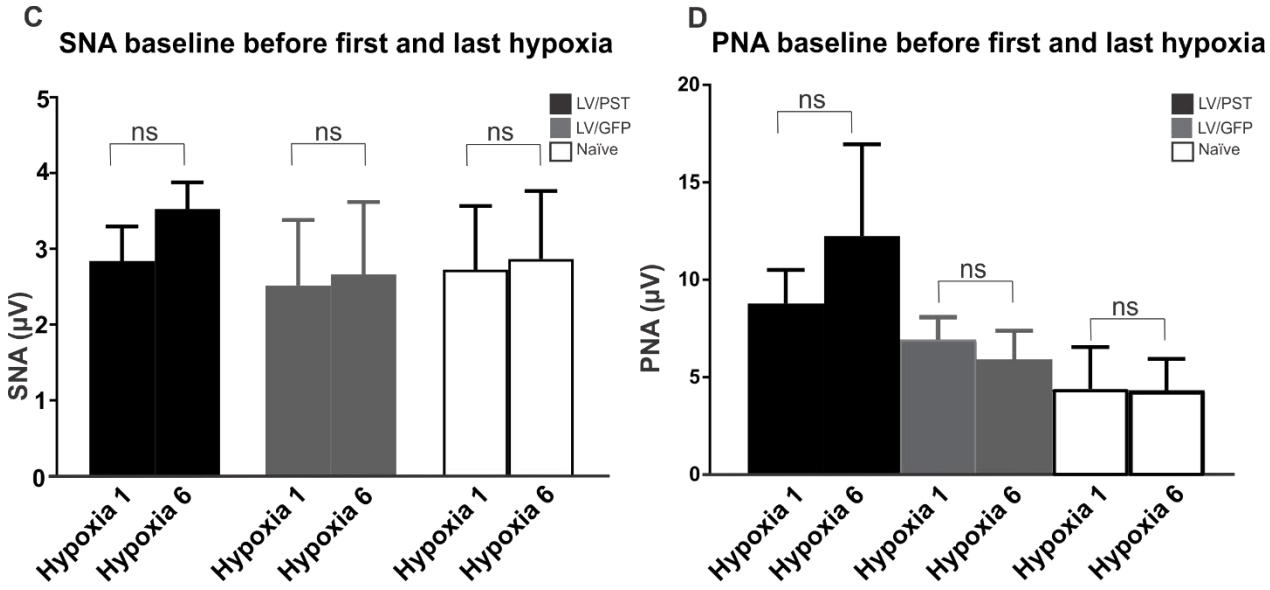

Figure 4.13: Acute intermittent hypoxia. (A) A representative example of the cardiovascular (heart rate (HR) and arterial pressure (AP)), sympathetic (SNA), and phrenic nerve (PNA) responses to exposure to acute intermittent hypoxia. (B) The table shows changes in MAP, HR, SNA and PNf (phrenic nerve frequency), and PNamp (phrenic nerve amplitude) after the last episode of hypoxia (hypoxia stimulus #6), in LV/PST, LV/GFP, and naïve groups of rats. (C) and (D) Changes in SNA and PNamp baselines respectively before and after 6 cycles of hypoxia.

4.4. Discussion

The aim of this study was firstly to induce polySia expression in the RVLM of adult rats using lentiviral vectors carrying polyST ST8SiaIV (PST) gene and a neuron specific promoter. Neuronal expression of the promoter was present and there was little evidence of other cell type labelling. In unilateral LV/PST injected animals, an increased expression of polySia was found compared to the uninjected side; however, the induced expression level was variable. In the LV/PST group, mCherry and GFP positive cells were surrounded by a ring of polySia-ir or showed distinctively higher levels of polySia compared to most GFP positive cells in LV/GFP transduced animals, further confirming induced expression of polySia. Staining with anti-GFAP showed a slightly increased labelling intensity on the injected sides, suggestive of mildly activated astrocytes. However, little colocalization of activated astrocytes with polySia was found, suggesting they were not responsible for the increase in polySia expression. Although LV/PST animals showed an increased expression of polySia in the RVLM, labelling in the LV/GFP group was also slightly greater than in naïve animals, suggesting that the injection itself or injury may increase polySia expression. A subset rats injected bilaterally in the RVLM with LV/PST or LV/GFP and naïve rats were available for physiological studies. The data analyses demonstrated no differences in cardiovascular and respiratory parameters at baseline. We tested a number of cardiorespiratory reflexes (Bezold-Jarisch reflex, responses to hypercapnia, hypoxia, and acute intermittent hypoxia) which are integrated within the RVLM and surrounding regions but again found no differences between treatment groups. Only baroreceptor function was seemingly altered with gain being unaffected but with a significant elevation of the lower plateau, perhaps suggestive of an increase in non-barosensitive sympathetic drive. Apart from this small and singular effect our data suggest a few possibilities either that the level of polySia expression present did not alter function or was not enhanced to a great enough level or did not target enough of a population of neurons with a specific function.

4.4.1. Limitations of the study

Although 51 animals (n=8 in the NTS and n=43 in the RVLM) were injected unilaterally or bilaterally with viral vectors, more than half of the transduced animals were rejected due to the injection being off-target, poor mCherry expression, or due to overt damage. This resulted in a small sample size within the groups and some variability particularly of injection site extent with

groups. This small sample size may explain the increased PNf baseline in the LV/GFP group compared to the other two groups as it is difficult to explain why the control virus could have such an effect. It is also possible although unlikely that the vagotomy in two of these animals was incomplete as this would result in a higher PNf as respiratory frequency would be linked to ventilator frequency. Due to the duration of the experiments (about 6 weeks per animal) we were unable to increase the sample sizes in the time of candidature.

4.4.2. Little expression of the reporter genes in the NTS of the LV/PST transduced group

We initially used LV/PST to overexpress polySia in the NTS; however, little to no reporter labelling was seen in these animals. Physical hindrance associated with the superficial location (see Chapter 2) and morphology of the NTS and associated regions, leakage up the pipette tract, high cerebrospinal fluid (CSF) flow associated with the adjacent area postrema, and vascular structure of the NTS might have caused dilution and washout of the injected vectors even before being taken up by neurons (Shaver et al., 1991, Gross et al., 1991, Gross et al., 1986). It is also possible that transcription or translation were suboptimal. Some transgenes, although effectively transcribed into mRNAs, are degraded preceding translation by microRNA-mediated mechanisms (El-Shamayleh et al., 2016) which are known to be differentially expressed within the CNS (Bak et al., 2008, He et al., 2007, Olsen et al., 2009). Thus it is possible that some microRNAs in the NTS repressed the translation of mRNAs transcribed from the transgene.

4.4.3. Induced expression of polySia in the RVLM

In contrast to the NTS, rats injected with LV/PST in the RVLM showed induced expression of polySia in regions demonstrating the expression of reporters. However, this expression level was variable and not always correlated with a higher expression of the reporters. Although all animals were injected with equal volumes of the lentiviral vectors, they showed different expression levels of the mCherry reporter. This might be at least partly due to the speed of injection, some leakage or blockage of the delivery pipette, or some variations within the injection sites. It is also likely that some variability is due to differences in translation processes in subregions of the RVLM; however, this could be examined by measuring the ST8SiaIV mRNA levels in these animals using PCR techniques (Yin et al., 2016). mCherry in LV/PST was used as an indicator of whether the transgenes were taken up by neurons; consequently, variations in the expression of the reporter in

different animals may indicate different amounts of transgene uptake by neurons which can lead to variable levels of ST8SiaIV and therefore alterations in polySia expression.

However, a higher expression of both mCherry and GFP was not always associated with a higher expression of polySia as some animals with a lower expression of reporters showed higher induced expression of polySia. This could be due to other parameters rather than ST8SiaIV involved in polySia synthesis. To make polySia, polySTs need a cytidine 5'-monophosphate (CMP) –activated sialic acid as a donor (Sellmeier et al., 2015) and an α2,3- or α2,6-sialylated complex type at the termini of both acceptor N- and O-linked glycans (Mühlenhoff et al., 1996b, Kojima et al., 1996, Sato and Kitajima, 2013a, Liedtke et al., 2001) which in the CNS is usually NCAM (Cremer et al., 1994). Therefore, differences seen might be due to variability in the levels of polySia donor or acceptor in this region among these animals. Moreover, changes in endocytosis/exocytosis rates might have also contributed to the variation of polySia expression on the cell surface (Abe et al., 2017). In keeping with our data, in the piglet brain during postnatal development (postnatal day 3 and 38), no correlation was found between the level of mRNA coding for polySTs (ST8SiaII and ST8SiaIV) and the expression level of polySia in all nine brain regions (including the brainstem) examined, suggesting that the cellular abundance of polySTs in these regions is regulated at the level of translation/post-translation, and not at the level of transcription (Wang et al., 2017). In summary, we were unable to achieve highly reproducible polySia overexpression likely due to multiple factors, in addition to virally induced abundance of ST8SiaIV, that are involved in polySia synthesis.

While some cells showed expression of both mCherry and GFP, some only expressed GFP or mCherry. Since the plasmid construct had both hSyn-PST-GFP and hSyn-mCherry, all transduced neurons should have incorporated these reporters into their DNA equally. However, since each reporter was attached separately to the hSyn promoter, differences in transcription and translations could occur.

4.4.4. Did injury contribute to the induced polySia expression?

Temporary expression or up-regulation of polySia post-injury has been reported in glial scars and their surrounding region by several studies (Camand et al., 2004, Dusart et al., 1999, Emery et al., 2000, Miller et al., 1994, Zhang et al., 1995, La Salle et al., 1992a). After injury of Purkinje Cells (Dusart et al., 1999), the kainate-induced hippocampal lesion model (La Salle et al., 1992b), and

hemisection of the mouse spinal cord (Camand et al., 2004), polySia expression was reported on reactive astrocytes for up to a year (Camand et al., 2004) or 18 months (Dusart et al., 1999), whereas following lateral fluid percussion brain injury of moderate severity (Emery et al., 2000) and ipsilateral entorhinal cortex lesion (Miller et al., 1994), increased expression of polySia was found on neurons including their processes. PolySia expression on both neurons and activated astrocytes were also reported after peripheral nerve grafts implanted into the thalamus of adult rats (Zhang et al., 1995) and following unilateral cervical dorsal rhizotomy (Bonfanti et al., 1996). However, in all the above mentioned studies, a moderate to severe injury was induced. In contrast, in our experiment, there was no such injury evident, as lesions in the RVLM would have resulted in a significant fall in AP and SNA (Feldberg and Guertzenstein, 1976, Guertzenstein and Silver, 1974, Ross et al., 1984) which did not occur at baseline. In keeping with this, we saw only a slightly increased labelling intensity of astrocytes and only some astrocytes had a mildly activated morphology on the injected sides, indicating that the injury was neither moderate nor severe. We found little colocalization of polySia with the mildly reactive astrocytes, suggesting that in the LV/PST animals the induced expression of polySia was not due to increased expression by activated astrocytes. However, it remains unclear as to whether some up-regulation of polySia level observed in LV/GFP induced animals was due to the contribution of some damaged neurons as reported by the studies above or due to the small sample size of unilaterally injected LV/GFP animals (n=3) as a small sample size reduces the chance of detecting a true effect (Button et al., 2013). It should be emphasized that regardless of contribution or lack of contribution of injury to the polySia overexpression, the expression of ST8SiaIV still remains the main contributor to this increase since a significant difference in polySia-ir was observed between LV/PST and LV/GFP transduced groups.

4.4.5. PolySia overexpression did not alter cardiovascular and respiratory responses evoked by chemoreceptor and baroreceptor stimuli

In a previous study, removal of polySia in the NTS increased sympathetic nerve activity, indicating that polySia alterations change sympathetic outflow (Bokiniec et al., 2017). Sensory input from the NTS regulates cardiorespiratory outflows through the RVLM (Koshiya and Guyenet, 1996, Aicher et al., 1996) and thus we investigated the effect of polySia up-regulation on cardiorespiratory functions of the RVLM. Using our data from unilateral injections of LV/PST we assumed, in our bilaterally injected animals that where we saw expression of fluorescent reporters we would have

elevated levels of polySia and thus firstly determined whether this altered baseline cardiorespiratory variables. The baseline data measured was in line with previous studies (Salo et al., 2007, Edwards and Paton, 2000) so either overexpression of polySia did not alter these variables or compensatory mechanisms were activated to maintain homeostasis. We then tested four cardiorespiratory reflexes in order to assess whether homeostatic reflexes were altered by overexpression of polySia.

4.4.5.1. Bezold–Jarisch reflex

The Bezold–Jarisch reflex is a vagally mediated reflex generated by activation of cardiopulmonary afferents likely by metabolites resulting from cardiac ischemia (Aviado and Aviado, 2001, Campagna and Carter, 2003, Salo et al., 2007). Its first relay in the brain is the NTS and it is thought to share or possibly parallel medullary pathways similar to the baroreceptor reflex (Verberne and Guyenet, 1992, Sartor and Verberne, 2007). The RVLM however is a critical synaptic relay in mediating the sympathoinhibitory component of the Bezold–Jarisch reflex (Verberne and Guyenet, 1992, Vayssettes-Courchay et al., 1997, Salo et al., 2007). The apnea and hypopnea, bradycardia, hypotension, and the sympathoinhibition are characteristic responses evoked by PBG (Salo et al., 2007, Verberne and Guyenet, 1992, Zhang et al., 2006, Moreira et al., 2007). Bradycardic arrhythmia we observed in some animals of our study was not directly reported in these studies. However, similar profound decreases in HR were similarly reported (Edwards and Paton, 2000, Salo et al., 2007). Although overexpression of polySia in the LV/PST animals was seen, no differences in the reflex function evoked by PBG was found.

4.4.5.2. Responses to hypercapnia, hypoxia, and acute intermittent hypoxia

Hypercapnia activates central chemoreceptors likely present with in the retrotrapezoid nucleus (Guyenet et al., 2010). Elevations in brain CO_2 resulted in the activation of the RVLM neurons demonstrated by Fos labelling (Wakai et al., 2015) and increased the activity of RVLM neurons and the sympathetic nerve discharge (Moreira et al., 2006). It is thought that RVLM sympathoexcitatory neurons likely receive input directly or indirectly from the retrotrapezoid nucleus (Moreira et al., 2006). Increased MAP, SNA, and PNamp found in all three groups of our study are characteristic responses to hypercapnia, described previously (Fukuda et al., 1989, Moreira et al., 2006, Powell et al., 1998). A relatively modest response was seen as only 5% CO_2 was used. Increasing CO_2 evokes larger responses in SNA and PNA (Moreira et al., 2006). Despite

increased polySia levels in the RVLM of the LV/PST group, no differences were seen in the responses to hypercapnia among the three treatment groups.

In contrast, hypoxia activates peripheral chemoreceptors located in the carotid and aortic bodes which in turn send signals to the RVLM mainly via the NTS (Powell et al., 1998, Prabhakar, 2006, Guyenet, 2000). It should be noted that all cells are sensitive to hypoxia, but a 1 min exposure is unlikely to activate cell based activity. Exposure to brief hypoxic stimuli in our study increased HR, SNA, PNf, and PNamp as reported by previous studies (Hsieh et al., 2008, Fukuda et al., 1989, Wakai et al., 2015). We saw a mild increase in arterial pressure (From 8.0 ± 3.9 to 18.2 ± 5.1), whereas another study reported unchanged levels of arterial pressure (Fukuda et al., 1989). However, PNAmp and to a lower extent SNA and PNf are the characteristic responses to hypoxia investigated in most papers (Baker-Herman and Mitchell, 2008). We saw no differences in response to hypoxia in our three treatment groups.

AIH activates a form of respiratory plasticity by generating long-term facilitation (LTF), in which respiratory motor activity progressively increases, even after the stimuli have ceased and blood gases have returned to normal (Baker et al., 2001, Mitchell et al., 2001). AIH also evokes similar plasticity in SNA likely by increasing respiratory modulation of sympathetic nerve activity (Dick et al., 2007, Xing and Pilowsky, 2010). Considering the role of polySia in plasticity (see Chapter 1) and neurotransmission (Bokiniec et al., 2017), it was interesting to investigate whether polySia contributes to this facilitation. In anaesthetized and vagotomised rats, AIH leads to an increased levels of SNA (Dick et al., 2007, Xing and Pilowsky, 2010) and respiratory-related nerve burst amplitude (PNamp) with variable effects on burst frequency (Baker-Herman and Mitchell, 2008, Mahamed and Mitchell, 2008, MacFarlane and Mitchell, 2008, Dick et al., 2007). There are multiple AIH protocols described (Fletcher, 2000, Baker-Herman and Mitchell, 2008) with effects on multiple systems and these appear highly sensitive to variation. No protocols are described which are preceded by other stimulus so our data may be confounded by the diverse preceding stimuli or the fact that we used a 6 cycle as opposed to the commonly described 10 cycle hypoxia (Xing and Pilowsky, 2010). This was evident as we did not see any change in SNA and PNA in our naïve or LV/GFP groups. Interestingly, in line with previous data (Xing and Pilowsky, 2010, Dick et al., 2007), an increase at SNA and PNA baselines was found only in LV/PST group after 30 min, although this did not reach significance. Therefore, it is possible that polySia may have contributed to LTF in these animals but more data is required.

4.4.5.3. Sympathetic baroreceptor curve

Baroreceptors work to oppose any change in arterial pressure on a beat by beat basis by altering sympathetic nerve activity to the heart and blood vessels and parasympathetic drive to the heart (Nichols et al., 2006, Guyenet, 2006, Mancia et al., 1986, Karemaker and Strackee, 1987). Although polySia removal in the NTS enhanced sympathetic outflow (Bokiniec et al., 2017) which is mainly generated in the RVLM, we saw no change in SNA after induced expression of polySia in the RVLM. The only significant change in all the reflexes we tested was an elevation of the lower plateau of the baroreceptor reflex function curve in the LV/PST group, possibly generated by an increase in non-barosensitive sympathetic drive.

4.4.6. PolySia and functions of the RVLM

Both sympathoexcitatory neurons and cell groups responsible for generating and maintaining respiratory rhythm are located within the region defined in this study as the RVLM (Guyenet, 2006, Guyenet, 2000); however, we saw no significant changes in functions associated with them in any of our three treatment groups apart a singular effect in baroreflex function. These findings therefore suggest a few possibilities: 1) the level of polySia expression present did not alter the functions measured, 2) polySia expression was not enhanced enough to affect functions, 3) polySia expression did not target enough of a population of neurons that drive a specific function, or 4) any changes evoked were compensated for. The latter possibility is unlikely as although we may not have detected changes in SNA or PNA at baseline, we most likely would have detected compensation as we measured sensitive homeostatic reflex function.

4.4.6.1. Did we target the right category of neurons with cardiorespiratory functions?

The location of C1 neurons in the RVLM spatially overlaps with the RVLM pressor area (Goodchild et al., 1984) and these neurons, although show low activity under normoxia, play an important role in driving sympathoexcitatory effects of the RVLM as elimination of most C1 neurons with the immunotoxin anti-dopamine β-hydroxylase-saporin (anti-DβH-Sap) severely attenuated the sympathetic baroreflex (Schreihofer and Guyenet, 2000). Many RVLM C1 neurons also demonstrate strong activation as a result of carotid body stimulation (peripheral chemoreceptor reflex) (Reis et al., 1994, Koshiya et al., 1993, Sun, 1996). In line with this, most C1 neurons expressed Fos in conscious mammals exposed to hypoxia (Erickson and Millhorn, 1994, Hirooka et al., 1997), while the sympathoexcitatory response evoked by carotid body stimulation is virtually

eliminated after selective lesions of C1 neurons (Schreihofer and Guyenet, 2000). In this study, we used a neuron specific promoter (synapsin) with stronger preference in excitatory neurons (Yaguchi et al., 2013, Nathanson et al., 2009, Dittgen et al., 2004) as the majority of RVLM bulbospinal neurons, and in particular C1 neurons, express mRNA for vesicular glutamate transporter 2 and thus are excitatory neurons (Stornetta and Guyenet, 1999, Stornetta et al., 2002). Still we only found the expression of the mCherry reporter in an average of 32 ± 4% of C1 neurons, indicating that about 70% were not probably affected. Whether such a change is adequate to influence cardiorespiratory function of the RVLM needs to be further investigated.

4.4.6.2. Was the level of polySia induced enough to change functions investigated?

Removal of polySia within the NTS affected sympathetic outflow; however, the NTS has abundant polySia (Bokiniec et al., 2017). In contrast, in the animals unilaterally injected with LV/PST, except in one case where an increase of ~2.5 times was found in polySia-ir (in the injected side compared to the uninjected one), in the other cases a range of 1.4- to 1.7-fold increase was measured, and thus the question is whether or not this difference was large enough to see a change in function. Was this level of increase large enough at the cellular level to influence adhesive properties on the polysialylated surface or heterophilic bindings of its carriers (Yang et al., 1994, Yang et al., 1992)? Alternatively, polySia may affect the activity of ion channels important in function of RVLM such as AMPA (Vaithianathan et al., 2004) and NMDA (Hammond et al., 2006) receptors. Nevertheless, no firm conclusions can be made from the data presented here as more data is required particularly in animals showing higher and more consistent levels of overexpression of polySia, particularly in C1 neurons.

4.5. Conclusion

In summary, we induced expression of polySia in the RVLM of the adult rat using a lentiviral vector driving the expression of polyST ST8SiaIV, the primarily polyST in the adult CNS. PolySia-ir was more distinct around many reporter expressing neurons in LV/PST transduced animals compared to the control ones and showed a significant increase in the LV/PST injected versus uninjected side. This overexpression, however, did not alter cardiorespiratory functions of the RVLM (in particular Bezold–Jarisch reflex and response to hypercapnia and hypoxia) with only a minor change in the lower plateau of the baroreceptor curve. Not targeting enough of C1 neurons as well as not inducing enough expression of polySia could be potential contributors to not altering

cardiorespiratory function. More data however is required before any concrete conclusions can be made.

Chapter 5 : Synthesis and future directions

Every living cell has a dense and complex coat of an array of glycans (Varki, 2011) which are integral parts of the extracellular matrix (Fuster and Esko, 2005). Changes in glycosylation states in the central nervous system (CNS) are commonly associated with disease states (for review see (Abou-Abbass et al., 2016)). Polysialic acid (polySia), a long homopolymer composed of more than eight sialic acids (Schauer, 2009), is of particular interest (Schnaar et al., 2014) as its expression in the adult CNS is restricted to discrete regions that exhibit synaptic plasticity including the hippocampus, cortex, and hypothalamus (Bonfanti, 2006, Bonfanti et al., 1992, Hildebrandt and Dityatev, 2013). These higher brain regions have provided the major focus of polySia investigation (Miragall et al., 1988, Aaron and Chesselet, 1989, Seki and Arai, 1993c, Theodosis et al., 1991, Chung et al., 1991, Kiss et al., 1993, Dhúill et al., 1999) and altered expression of the sugar has been found associated with conditions of altered learning and memory (Becker et al., 1996, Fox et al., 2000), chronic stress (Pham et al., 2003, Sandi et al., 2003) and neuropathological conditions such as schizophrenia (Barbeau et al., 1995), epilepsy (Mikkonen et al., 1998), and Alzheimer's disease (Mikkonen et al., 1999). In contrast the distribution, interacting partners, and function of polySia in the brainstem and spinal cord are poorly understood.

Chapter 2

A detailed investigation of the distribution of polySia in the medulla and pons of the adult rat identified over 30 polySia positive regions with dense polySia immunoreactivity (ir) consistently observed in the A1 region, area postrema, dorsal motor nucleus of vagus, dorsal raphe nucleus, caudal part, dorsal tegmental nucleus, medial vestibular nucleus, nucleus of solitary tract (NTS), prepositus nucleus, and spinal trigeminal nucleus caudalis (Sp5C). Within the spinal cord, we extended previous studies by identifying polySia expression in the intermediolateral cell column (IML) consistently surrounding sympathetic preganglionic neurons (SPNs) within their complex nest like structures. Within the Sp5C, NTS, and spinal cord no association was found between polySia and the large processes of astrocytes or oligodendrocytes using GFAP and MBP as cell type markers, respectively. In the NTS and Sp5C, there was however some association of polySia with fine astrocytic processes. Within the superficial laminae of the spinal cord dorsal horn where a dense labelling was seen, polySia-ir was present on some inhibitory interneurons expressing SSTR2A, whereas CGRP expressing afferent fibres expressed little to no polySia, suggesting that polySia is not localized to peptidergic C fibres. PolySia-ir was associated, though not often colocalized, with a marker of the presynaptic density, synaptophysin, suggesting a synaptic

localization. Within two regions (NTS and Sp5C), ultrastructural examination provided concrete evidence that polySia was present in or on the fine processes of astrocytes and/or within the extracellular space adjacent to plasma membranes as well as adjacent to some synapses and in a subset of dendrites and axon terminals, consistent with the close association of polySia with EAAT2 and synaptophysin revealed using immunofluorescence. Within the trigeminal ganglion of the adult rat, polySia expression was found around neurons and satellite glia cells. Comparing the polySia expression in rats and mice demonstrated mainly common patterns of expression. Only in some areas was the distribution different such as in the spinal cord dorsal horn. Finally, comparison of two of the most commonly used polySia antibodies – mAb 735 and mAb 5324 – showed a similar pattern of expression in the brainstem and spinal cord.

Does the expression of polySia in numerous regions of the brainstem found in this study indicate that polySia in the brainstem could be as, or even more, important as in higher brain regions even though its functions are largely unknown? PolySia expression in the higher brain regions is postulated to be associated with plasticity (Rutishauser, 2008, Gascon et al., 2007) so it would be interesting to see if it exerts a similar function in the more primitive brainstem and spinal cord. This could be achieved by removal of polySia in regions that show abundant expression. This is demonstrated by a study I participated in during my PhD candidature (see Appendices) (Bokiniec et al., 2017). Here we showed that removal of polySia from the NTS region reduced neurotransmission indicating that normal levels of polySia facilitate afferent transmission through the nucleus. The medial vestibular nucleus, prepositus nucleus, and dorsal tegmental nucleus which similarly showed dense polySia labelling, form part of the head direction circuit, as lesions of these regions disturb this circuit (Bassett et al., 2007, Muir et al., 2009, Butler and Taube, 2015, Stackman and Taube, 1997). Head direction neurons fire at a steady rate when the animal's head is facing in the cell's "preferred firing direction" with the firing decreasing back to baseline rates when the animal's head turns away from the preferred direction (Taube, 2007). Whether polySia plays a role in the directional activity of these neurons is unclear. This could be investigated in transgenic mice lacking polySia to see whether they show any deficit in their head direction circuit. ST8SiaII, ST8SiaIV double-knockout mice show progressive hydrocephalus, growth retardation, deficits in brain wiring as well as severe developmental deficits with more than 80% dying within 4 weeks after birth (Weinhold et al., 2005) and therefore would likely not be usable. However, $NCAM^{-/-}$ mice which show significant deficits in polySia but not the severe neurological deficiencies seen

in the polysialyltransferase (polyST) double-knockouts could be useful to explore the role of polySia (Weinhold et al., 2005, Cremer et al., 1994, Hildebrandt et al., 2009). Such a study could also be used to determine whether the vast majority of polySia in these regions is found associated with neural cell adhesion molecule (NCAM) as indicated in higher brain regions (Cremer et al., 1994). Alternatively, enzymatic removal of polySia could be used to investigate acute effects of polySia alteration on this circuit as in the study described in Appendices. The ideal solution would be to use a conditional knockout (Zhang et al., 2012, Skarnes et al., 2011) in which only neurons in these three regions could be manipulated to not express polySia.

We identified for the first time that SPNs in the IML were surrounded by polySia-ir. SPNs innervating cardiovascular fibres such as those supplying the heart and blood vessels receive continuous tonic input from sympathetic premotor neurons in the rostral ventrolateral medulla (RVLM), whereas SPNs ultimately innervating brown adipose tissue (Morrison and Cao, 2000), sweat glands, or muscles responsible for piloerection (for review see (Iriki and Simon, 2012)) are silent at normal body temperature or under basal conditions. It is clear that sensory regions of the spinal cord and medulla such as the dorsal horn and Sp5C as well as the NTS receive tonic input and exhibit abundant polySia so whether expression of polySia is associated with neurons receiving tonic input, at least in the brainstem and spinal cord remains to be determined. Furthermore, whether polySia is only associated with SPNs that receive constant input or with 'silent' SPNs also remains unknown. This issue could be investigated using selective stimulation of the SPNs and then studying the chemical codes of types of neurons activated using a marker such as c-Fos, pCREB, and Arc. Activation of the RVLM which provides tonic excitatory input (Dampney et al., 2003) related to peripheral vasculature, organ perfusion pressure (Brown and Guyenet, 1985, Pilowsky and Goodchild, 2002), resting level of arterial pressure (Dampney, 1994a, Guyenet, 2006), and the sympathoadrenal response to glucoprivation (Ritter et al., 2011, Ritter et al., 2001, Madden et al., 2006) would provide some selectivity of input. Alternatively activating silent populations of SPNs such as those innervating brown fat could be achieved using cold exposure to activate cold defence pathways (Morrison, 2011).

There is one piece of evidence to suggest that the expression of polySia in the NTS is dynamic and controlled by synaptic activity (Bouzioukh et al., 2001). Electrical stimulation of vagal afferents (30 Hz, 15 min) innervating the polySia rich nucleus of solitary tract resulted in a 30% decrease in polySia expression 15 min after stimulation, measured by western blotting (Bouzioukh et al., 2001).

In a similar manner sensory input including mechanical, thermal, chemical and proprioceptive information from orofacial structures (most of the head, including the face and teeth) is constantly conveyed to the trigeminal nucleus in the brainstem via the trigeminal ganglia (Iwata et al., 2011, Bereiter et al., 2000, Hanani, 2005). We have demonstrated that both Sp5C and trigeminal ganglion (TG) express polySia-ir. Therefore, it would be interesting to increase afferent drive to investigate the potential alterations in polySia expression level. Such stimulation could be achieved by noxious stimuli such as pinching (Strassman and Vos, 1993) or the injection of the Complete Freund's Adjuvant (CFA) (Villa et al., 2010) as these methods have been shown to activate neurons and/or glia in the TG and Sp5C.

We found polySia-ir around both satellite glial cells (SGCs) and neurons of TG. However, the labelling was faint or very faint around some cells making it difficult at times to examine whether the labelling was associated with neurons or its surrounding glia. To determine how much polySia is associated with glia or neurons, colchicine administration could be used. Colchicine is a drug used to block cell transport and induces a rapid blockade of recently generated substances from the rough endoplasmic reticulum to the Golgi and from the Golgi to the cell surface (Malaisse and Orci, 1978, Alonso, 1988). Theodosis et al. (1999) used tissues from animals that had been treated with colchicine and observed an increase in polySia labelling in the cytoplasm of astrocytic cell bodies and processes as well as in the cytoplasm of neuronal somata in the magnocellular nuclei (Theodosis et al., 1999).

Chapter 3

Our aim here was to identify interacting partners of polySia initially in the dorsal horn of the spinal cord of adult rats using co-immunoprecipitation (IP) followed by a proteomics approach resulting in thirteen proteins identified as potential binding partners of polySia. Five of these candidates: receptor expression-enhancing protein 5 (REEP5), guanine nucleotide-binding protein G(o) subunit alpha (GNOA1), sodium/potassium-transporting ATPase subunit alpha-2 (ATP1A2), sodium/potassium-transporting ATPase subunit alpha-3 (ATP1A3), and clathrin heavy chain (CLTC) were further validated as potential binding partners of polySia. Colocalization of polySia-ir with ATP1A2- and GNAO1-ir at the cell surface, neuropil and fine fibres of the dorsal horn and dorsolateral funiculus was detected using confocal microscopy. Some co-labelling was also detected in dorsolateral funiculus between polySia and REEP5. The interaction of polySia with

GNAO1, ATP1A2, and REEP5 was also examined in Sp5C and IML and their polySia interaction status were confirmed, suggesting that similar interactions occur in functionally different parts of the CNS. We also showed that the interactions identified in the rat spinal cord dorsal horn similarly occurred in the mouse dorsal horn. Together, these data expand the rather short current list of potential interacting partners of polySia and may help to provide insight on the functional role this sugar has within the areas studied. PolySia may play a role in neuronal signalling as more than half of the potential partners identified are involved in signalling and these common signalling functions appear to be present in multiple brain regions and in different species.

As noted in this chapter, polySia is predominantly attached to NCAM in vertebrates (Bonfanti and Theodosis, 2009) and thus it is possible that some of the potential partners identified in this study interact with NCAM rather than polySia or even possibly both. The most direct studies to confirm the identified interactions would be by ELISA using polySia-NCAM or NCAM fused to Fc portion of human immunoglobulin (PolySia-NCAM-Fc or NCAM-Fc) (Mishra et al., 2010, Theis et al., 2013) or by immunoaffinity/immunoprecipitation experiments with anti-NCAM antibodies using ST8SiaII, ST8SiaIV double-knockout animals (Angata et al., 2007, Weinhold et al., 2005) (however, note lack of viability above). Alternatively, immunoprecipitation, in the absence or presence of endoN, using an antibody against each interacting partner could be performed and immunoprecipitates could be probed against NCAM antibodies (Theis et al., 2013). If immunoprecipitates from untreated samples show larger amounts of NCAM compared to those of endoN treated samples, the interaction would most probably be with polySia and not with NCAM.

The mechanisms by which polySia may affect these interacting partners and the functional consequences of the interaction need to be investigated. Functional studies could be performed *in vivo* by manipulating polySia level either through enzymatic removal of polySia by endoN or using transgenic mice lacking both ST8SiaII and ST8SiaIV (Angata et al., 2007, Weinhold et al., 2005) or NCAM (Cremer et al., 1994) to seek potential alterations in the activity of these binding partners. Alternatively, an *in vitro* system using isolated cells (Kanato et al., 2008) or artificial systems (Hammond et al., 2006, Vaithianathan et al., 2004) could be employed. An increase in polySia level *in vivo* or *in vitro* might also alter the function of its interacting partners. This could be done via induced expression of polySia by ST8SiaII and/or ST8SiaIV (see Chapter 4), the application of colominic acid, a bacterially derived polySia (Hammond et al., 2006), or polySia mimetics, although currently their functional effects are primarily tested in recovery after the CNS injury

(Bushman et al., 2014, Mehanna et al., 2010, Loers et al., 2017). The advantage of using these polySia mimetics is that unlike polySia which is cleaved *in vivo* by neuraminidases and sialidases (Sumida et al., 2015, Takahashi et al., 2012, Sajo et al., 2016), the mimetics cannot be cleaved (Loers et al., 2017).

Another question to tackle is whether polySia expression is influenced by the activity of these protein partners? This could be investigated via inhibiting (or decreasing) (Skou, 1990), or increasing the activity of these proteins and then examining potential alterations in polySia levels. In case of the ATPase pump, ouabain or oligomycin could be used as their application inhibits the activity of the pump or decreases the transport rate of Na^+ respectively (Skou, 1990, Urayama and Sweadner, 1988, Edwards et al., 2013). In contrast, during intense neuronal activity caused by suprathreshold synaptic stimulation, the concentration of sodium in dendrites and spines can increase radically (Rose and Konnerth, 2001), and the rapid clearance of intracellular sodium is primarily attributed to ATP1A3 (Azarias et al., 2013), mainly localized to neuronal processes (Bøttger et al., 2011) and dendritic spines (Blom et al., 2016, Kim et al., 2007). The recovery of intracellular sodium levels after intense neuronal activity thus requires increased ATP1A3 activity (Azarias et al., 2013). Interestingly, high frequency stimulation of the solitary tract reduced polySia expression (Bouzioukh et al., 2001b, Bouzioukh et al., 2001a) and polySia removal in the NTS increased NMDA dependent neuronal transmission (see Appendices). These data suggest that glycan, and in particular, polySia could optimize the activity of ATP1A3 during intense neuronal firing.

Moreover, to examine the effect of the activity of these proteins on the expression levels of polySia, polySia expression could be studied in the human or animal diseases/disorders associated with mutations or alterations in the activity and/or expression levels of these proteins. For example, polySia expression was up-regulated in some hippocampal areas such as the dentate gyrus, CA1 subfield, and the entorhinal cortex in Alzheimer's disease patients (Mikkonen et al., 1999) as well as in CA1 and DG subfields after acute administration of amyloid β (Limón et al., 2011, Mikkonen et al., 1999). In contrast, the activity of Na^+, K^+-ATPase was significantly lower in the brains of patients with Alzheimer´s disease than in the brains of normal controls (Liguri et al., 1990), suggesting a potential interaction of polySia with Na^+, K^+-ATPase might inhibit the activity of this pump. Such associations could further be examined as there are well described mutations in

ATP1A3 that cause three neurological disorders: Rapid Onset Dystonia Parkinsonism (RDP), Alternating Hemiplegia of Childhood (AHC), and Cerebellar ataxia, areflexia, pes cavus, optic atrophy, and sensorineural hearing loss (CAPOS) (Holm and Lykke-Hartmann, 2016) and polySia expression could be evaluated in the phenotypically accurate animal models available. Similarly, whether or not polySia dysfunctions described in schizophrenia (Castillo-Gómez et al., 2016) could be associated with neuronal signalling deficits caused by the protein partners described (Goldstein et al., 2006) could also be evaluated. Although wildly speculative, schizophrenic patients exhibit disturbances in polySia (Arai et al., 2006, Barbeau et al., 1995) and these changes may be evident in regions important in cardiovascular control which could alter neuronal transmission (Bokiniec et al., 2017), potentially providing the missing link explaining why there is such an increased cardiovascular mortality in schizophrenic patients (Westman et al., 2017).

Chapter 4

Induced expression of polySia has been demonstrated by a few groups both *in vitro* and *in vivo* (Zhang et al., 2007b, Zhang et al., 2007c, Franceschini et al., 2004, El Maarouf et al., 2006). However, these studies induced polySia expression mainly in and around an injury site and were focused on CNS repair mechanisms. Removal of polySia in the NTS of anaesthetized rats, in our laboratory, reduced AMPA receptor dependent signalling and increased sympathetic nerve activity, indicating that polySia is required for the normal transmission of information through the NTS (Bokiniec et al., 2017). Following these findings, our aim was to determine the effect of polySia overexpression in the NTS; however, in all animals tested little to no expression of the virus was seen. The NTS is one of the main sources of synaptic input to the RVLM presympathetic neurons (Dampney et al., 1982, Ross et al., 1985, Koshiya and Guyenet, 1996). As opposed to the NTS which shows high polySia expression, the RVLM shows relatively little polySia-ir (see Chapter 2) and thus we sought to investigate the effect of increasing polySia content within the RVLM. Using a viral based approach, induced expression of polySia in and around the site of injection was observed in all animals that received a unilateral injection of the virus encoding ST8SiaIV (LV/PST). These expression levels were higher compared to the contralateral non-injected side. Although the injection of the control virus lacking ST8SiaIV gene (LV/GFP) did result in some polySia expression, the expression was significantly lower than that of LV/PST transduced animals. The RVLM plays a crucial role in the tonic and reflex regulation of arterial blood pressure (AP) and sympathetic vasomotor tone (Feldberg and Guertzenstein, 1976, Guertzenstein and

Silver, 1974, Ross et al., 1984, Goodchild et al., 1982) as well as in regulation of respiration (Reis et al., 1994, Koshiya et al., 1993, Sun, 1996, Schreihofer and Guyenet, 2000). However, in the animals where polySia was overexpressed in the RVLM, no changes in baseline variables of cardiorespiratory function were altered. A range of cardiorespiratory reflexes are mediated by and integrated in the RVLM (Pilowsky and Goodchild, 2002, Guyenet, 2006). However, no difference was observed in cardiovascular and respiratory functions associated with the von Bezold-Jarisch reflex and the response to hypoxia or hypercapnia in LV/PST injected animals compared to LV/GFP transduced or naïve rats. The only difference found with respect to baroreceptor function was that the lower plateau of the baroreceptor curve elevated in LV/PST animals although the gain was unchanged. One explanation could be that sympathetic activity independent of baroreceptor function was elevated by polySia overexpression however no differences were seen in overall baseline activity. Whether the lack of a major difference was due to low level of overexpression of polySia in the LV/PST injected animals or these reflexes are not affected by polySia overexpression in the RVLM requires significantly more investigation. Despite a considerable number of animals injected with LV/PST virus, regulating the level of polySia expression was not uniform and we need to better understand how this can be better controlled. We certainly cannot conclude that induced expression of polySia in the RVLM does not alter cardiorespiratory function, still ensuring this is an important question.

In vivo injection of a purified polyST from Neisseria meningitidis (PST_{Nm}) and its donor substrate cytidine 5'-monophosphate–activated sialic acid (CMP-Neu5Ac) was used to, and did, induce high levels of polySia expression in different adult brain regions, including the cerebral cortex, striatum, and spinal cord. This expression was very rapid occurring in less than 2.5 h post injection, reached a plateau level by 6 h and reduced within a few weeks (El Maarouf et al., 2012). PST_{Nm} could be used to overexpress polySia in the NTS and RVLM since it generated abundant polySia expression in the brain regions in the study performed by El Maarouf et al. (El Maarouf et al., 2012). However, unlike viral delivery of the vertebrate ST8SiaII/ST8SiaIV genes where the majority of polySia is made on NCAM (Cremer et al., 1994), although PST_{Nm} was able to add polySia to NCAM, it mainly added polySia to other cell surface proteins (El Maarouf et al., 2012). Therefore, induced polySia might exert different effects on the function of the injected regions as polySia expression on these proteins might affect their signalling pathways as it does for NCAM (for review see (Schnaar et al., 2014)). Basically we need to better understand how polySia expression is

controlled, whether it is present in both neurons and glia and what proteins it is associated with in every brain region in which it is expressed.

Final thoughts

Our understanding of the distribution and function of polySia at the cellular and tissue level have radically progressed over the past two decades. We know that polySia contributes to brain development, function, health, and disease studied mainly in higher brain regions. Here we investigated the distribution of polySia within the brainstem, spinal cord, and trigeminal ganglion. We also found polySia interacting partners in the dorsal horn and studied potential functions in the RVLM. Nevertheless, there are still important areas that require further investigation including, but not limited to, the potential role and partners of polySia in the many polySia positive regions identified in this study and the influence of polySia in the function of identified binding partners and in particular in their signalling pathways. Furthermore, studying polySia alterations in disease/disorders associated with mutation or alterations of these partners may open new avenues of future research. Recently, new tools and techniques has emerged in the field of glycobiology such as new enzymatic tools allowing faster and more efficient release of glycans from proteins and glycolipids, new fluorescent labelling reagents with the ability to more quickly label N-glycans and enhance sensitivity in mass spectrometry, intrabodies against ST8SiaII and ST8SiaIV resulting in a knock-down in polySia level, and high-throughput analytical workflows that can expand the applicability of glycomics to large sample sets (Albrecht et al., 2016, Stöckmann et al., 2015, Somplatzki et al., 2017, Lauber et al., 2015). These rapid developments are profoundly enhancing our understanding of how glycans and in particular polySia may contribute to brain morphogenesis, development, and function, which in turn may enhance our understanding of human physiology and pathology.

References

AARON, L. & CHESSELET, M.-F. 1989. Heterogeneous distribution of polysialylated neuronal-cell adhesion molecule during post-natal development and in the adult: an immunohistochemical study in the rat brain. *Neuroscience,* 28**,** 701-710.

ABBOTT, S. B., STORNETTA, R. L., FORTUNA, M. G., DEPUY, S. D., WEST, G. H., HARRIS, T. E. & GUYENET, P. G. 2009. Photostimulation of retrotrapezoid nucleus phox2b-expressing neurons in vivo produces long-lasting activation of breathing in rats. *Journal of Neuroscience,* 29**,** 5806-5819.

ABE, C., NISHIMURA, S., MORI, A., NIIMI, Y., YANG, Y., HANE, M., KITAJIMA, K. & SATO, C. 2017. Chlorpromazine Increases the Expression of Polysialic Acid (PolySia) in Human Neuroblastoma Cells and Mouse Prefrontal Cortex. *International Journal of Molecular Sciences,* 18**,** 1123.

ABOU-ABBASS, H., ABOU-EL-HASSAN, H., BAHMAD, H., ZIBARA, K., ZEBIAN, A., YOUSSEF, R., ISMAIL, J., ZHU, R., ZHOU, S. & DONG, X. 2016. Glycosylation and other PTMs alterations in neurodegenerative diseases: Current status and future role in neurotrauma. *Electrophoresis,* 37**,** 1549-1561.

ABROUS, D., MONTARON, M., PETRY, K., ROUGON, G., DARNAUDERY, M., LE MOAL, M. & MAYO, W. 1997. Decrease in highly polysialylated neuronal cell adhesion molecules and in spatial learning during ageing are not correlated. *Brain research,* 744**,** 285-292.

AEBI, M., BERNASCONI, R., CLERC, S. & MOLINARI, M. 2010. N-glycan structures: recognition and processing in the ER. *Trends in biochemical sciences,* 35**,** 74-82.

AICHER, S. A., SARAVAY, R. H., CRAVO, S., JESKE, I., MORRISON, S. F., REIS, D. J. & MILNER, T. A. 1996. Monosynaptic projections from the nucleus tractus solitarii to C1 adrenergic neurons in the rostral ventrolateral medulla: comparison with input from the caudal ventrolateral medulla. *Journal of Comparative Neurology,* 373**,** 62-75.

AKKURATOV, E. E., LOPACHEVA, O. M., KRUUSMÄGI, M., LOPACHEV, A. V., SHAH, Z. A., BOLDYREV, A. A. & LIU, L. 2015. Functional interaction between Na/K-ATPase and NMDA receptor in cerebellar neurons. *Molecular neurobiology,* 52**,** 1726-1734.

AL-KHATER, K. M., KERR, R. & TODD, A. J. 2008. A quantitative study of spinothalamic neurons in laminae I, III, and IV in lumbar and cervical segments of the rat spinal cord. *Journal of Comparative Neurology,* 511**,** 1-18.

ALBACH, C., DAMOC, E., DENZINGER, T., SCHACHNER, M., PRZYBYLSKI, M. & SCHMITZ, B. 2004. Identification of N-glycosylation sites of the murine neural cell adhesion molecule NCAM by MALDI-TOF and MALDI-FTICR mass spectrometry. *Analytical and bioanalytical chemistry,* 378**,** 1129-1135.

ALBRECHT, S., VAINAUSKAS, S., STÖCKMANN, H., MCMANUS, C., TARON, C. H. & RUDD, P. M. 2016. Comprehensive profiling of glycosphingolipid glycans using a novel broad specificity endoglycoceramidase in a high-throughput workflow. *Analytical chemistry,* 88**,** 4795-4802.

ALMARESTANI, L., WATERS, S., KRAUSE, J., BENNETT, G. & RIBEIRO-DA-SILVA, A. 2007. Morphological characterization of spinal cord dorsal horn lamina I neurons projecting to the parabrachial nucleus in the rat. *Journal of Comparative Neurology,* 504**,** 287-297.

ALONSO, G. 1988. Effects of colchicine on the intraneuronal transport of secretory material prior to the axon: a morphofunctional study in hypothalamic neurosecretory neurons of the rat. *Brain research,* 453**,** 191-203.

ALVAREZ-BUYLLA, A., HERRERA, D. G. & WICHTERLE, H. 2000. The subventricular zone: source of neuronal precursors for brain repair. *Progress in brain research,* 127**,** 1-11.

ANDRESEN, M. C. & PATON, J. 2011. The nucleus of the solitary tract: processing information from viscerosensory afferents. *Central regulation of autonomic functions***,** 23-46.

ANGATA, K., HUCKABY, V., RANSCHT, B., TERSKIKH, A., MARTH, J. D. & FUKUDA, M. 2007. Polysialic acid-directed migration and differentiation of neural precursors are essential for mouse brain development. *Molecular and cellular biology,* 27**,** 6659-6668.

ANGATA, K., LONG, J. M., BUKALO, O., LEE, W., DITYATEV, A., WYNSHAW-BORIS, A., SCHACHNER, M., FUKUDA, M. & MARTH, J. D. 2004. Sialyltransferase ST8Sia-II assembles a subset of polysialic acid that directs hippocampal axonal targeting and promotes fear behavior. *Journal of Biological Chemistry,* 279**,** 32603-32613.

ANGATA, K., NAKAYAMA, J., FREDETTE, B., CHONG, K., RANSCHT, B. & FUKUDA, M. 1997. Human STX polysialyltransferase forms the embryonic form of the neural cell adhesion molecule Tissue-specific expression, neurite outgrowth, and chromosomal localization in comparison with another polysialyltransferase, PST. *Journal of Biological Chemistry,* 272**,** 7182-7190.

ANGATA, K., SUZUKI, M. & FUKUDA, M. 2002. ST8Sia II and ST8Sia IV Polysialyltransferases Exhibit Marked Differences in Utilizing Various Acceptors Containing Oligosialic Acid and Short Polysialic Acid THE BASIS FOR COOPERATIVE POLYSIALYLATION BY TWO ENZYMES. *Journal of Biological Chemistry,* 277**,** 36808-36817.

ANGATA, T. & VARKI, A. 2002. Chemical diversity in the sialic acids and related α-keto acids: an evolutionary perspective. *Chemical reviews,* 102**,** 439-470.

APWEILER, R., HERMJAKOB, H. & SHARON, N. 1999. On the frequency of protein glycosylation, as deduced from analysis of the SWISS-PROT database. *Biochimica et Biophysica Acta (BBA)-General Subjects,* 1473**,** 4-8.

ARAI, M., YAMADA, K., TOYOTA, T., OBATA, N., HAGA, S., YOSHIDA, Y., NAKAMURA, K., MINABE, Y., UJIKE, H. & SORA, I. 2006. Association between polymorphisms in the promoter region of the sialyltransferase 8B (SIAT8B) gene and schizophrenia. *Biological psychiatry,* 59**,** 652-659.

ARYSTARKHOVA, E. & SWEADNER, K. J. 1996. Isoform-specific Monoclonal Antibodies to Na, K-ATPase α Subunits EVIDENCE FOR A TISSUE-SPECIFIC POST-TRANSLATIONAL MODIFICATION OF THE α SUBUNIT. *Journal of Biological Chemistry,* 271**,** 23407-23417.

AVIADO, D. M. & AVIADO, D. G. 2001. The Bezold-Jarisch Reflex. *Annals of the New York Academy of Sciences,* 940**,** 48-58.

AZARIAS, G., KRUUSMÄGI, M., CONNOR, S., AKKURATOV, E. E., LIU, X.-L., LYONS, D., BRISMAR, H., BROBERGER, C. & APERIA, A. 2013. A specific and essential role for Na, K-ATPase α3 in neurons co-expressing α1 and α3. *Journal of Biological Chemistry,* 288**,** 2734-2743.

BAILEY, T. W., HERMES, S. M., ANDRESEN, M. C. & AICHER, S. A. 2006. Cranial visceral afferent pathways through the nucleus of the solitary tract to caudal ventrolateral medulla or paraventricular hypothalamus: target-specific synaptic reliability and convergence patterns. *Journal of Neuroscience,* 26**,** 11893-11902.

BAK, M., SILAHTAROGLU, A., MØLLER, M., CHRISTENSEN, M., RATH, M. F., SKRYABIN, B., TOMMERUP, N. & KAUPPINEN, S. 2008. MicroRNA expression in the adult mouse central nervous system. *Rna,* 14**,** 432-444.

BAKER-HERMAN, T. L. & MITCHELL, G. S. 2008. Determinants of frequency long-term facilitation following acute intermittent hypoxia in vagotomized rats. *Respiratory physiology & neurobiology,* 162**,** 8-17.

BAKER, T., FULLER, D., ZABKA, A. & MITCHELL, G. 2001. Respiratory plasticity: differential actions of continuous and episodic hypoxia and hypercapnia. *Respiration physiology,* 129**,** 25-35.

BAMSHAD, M., AOKI, V. T., ADKISON, M. G., WARREN, W. S. & BARTNESS, T. J. 1998. Central nervous system origins of the sympathetic nervous system outflow to white adipose tissue. *American Journal of Physiology-Regulatory, Integrative and Comparative Physiology,* 275**,** R291-R299.

BAMSHAD, M., SONG, C. K. & BARTNESS, T. J. 1999. CNS origins of the sympathetic nervous system outflow to brown adipose tissue. *American Journal of Physiology-Regulatory, Integrative and Comparative Physiology,* 276**,** R1569-R1578.

BARBEAU, D., LIANG, J. J., ROBITALILLE, Y., QUIRION, R. & SRIVASTAVA, L. K. 1995. Decreased expression of the embryonic form of the neural cell adhesion molecule in schizophrenic brains. *Proceedings of the National Academy of Sciences,* 92**,** 2785-2789.

BARMAN, S. M. & GEBBER, G. L. 1997. Subgroups of rostral ventrolateral medullary and caudal medullary raphe neurons based on patterns of relationship to sympathetic nerve discharge and axonal projections. *Journal of Neurophysiology,* 77**,** 65-75.

BARNETT, W. H., ABDALA, A. P., PATON, J. F., RYBAK, I. A., ZOCCAL, D. B. & MOLKOV, Y. I. 2016. Chemoreception and neuroplasticity in respiratory circuits. *Experimental neurology,* 287**,** 153-164.

BARRY, G. T. & GOEBEL, W. F. 1957. Colominic acid, a substance of bacterial origin related to sialic acid. *Nature,* 179**,** 206.

BASSETT, J. P., TULLMAN, M. L. & TAUBE, J. S. 2007. Lesions of the tegmentomammillary circuit in the head direction system disrupt the head direction signal in the anterior thalamus. *Journal of Neuroscience,* 27**,** 7564-7577.

BATTAGLIA, G. & RUSTIONI, A. 1988. Coexistence of glutamate and substance P in dorsal root ganglion neurons of the rat and monkey. *Journal of Comparative Neurology,* 277**,** 302-312.

BAX, M., VAN VLIET, S. J., LITJENS, M., GARCÍA-VALLEJO, J. J. & VAN KOOYK, Y. 2009. Interaction of polysialic acid with CCL21 regulates the migratory capacity of human dendritic cells. *PLoS One,* 4**,** e6987.

BECKER, C., ARTOLA, A., GERARDY-SCHAHN, R., BECKER, T., WELZL, H. & SCHACHNER, M. 1996. The polysialic acid modification of the neural cell adhesion molecule is involved in spatial learning and hippocampal long-term potentiation. *Journal of neuroscience research,* 45**,** 143-152.

BEHRENS, M., BARTELT, J., REICHLING, C., WINNIG, M., KUHN, C. & MEYERHOF, W. 2006. Members of RTP and REEP gene families influence functional bitter taste receptor expression. *Journal of Biological Chemistry,* 281**,** 20650-20659.

BEREITER, D. A., HIRATA, H. & HU, J. W. 2000. Trigeminal subnucleus caudalis: beyond homologies with the spinal dorsal horn. *Pain,* 88**,** 221-224.

BERG, D., HOLZMANN, C. & RIESS, O. 2003. 14-3-3 proteins in the nervous system. *Nature Reviews Neuroscience,* 4**,** 752-762.

BERGGÅRD, T., LINSE, S. & JAMES, P. 2007. Methods for the detection and analysis of protein–protein interactions. *Proteomics,* 7**,** 2833-2842.

BERNARD, J. F., DALLEL, R., RABOISSON, P., VILLANUEVA, L. & BARS, D. L. 1995. Organization of the efferent projections from the spinal cervical enlargement to the parabrachial area and periaqueductal graye. A PHA-L study in the rat. *Journal of Comparative Neurology,* 353**,** 480-505.

BHAT, M. A., RIOS, J. C., LU, Y., GARCIA-FRESCO, G. P., CHING, W., MARTIN, M. S., LI, J., EINHEBER, S., CHESLER, M. & ROSENBLUTH, J. 2001. Axon-glia interactions and the domain organization of myelinated axons requires neurexin IV/Caspr/Paranodin. *Neuron,* 30**,** 369-383.

BHATTACHARJEE, A. K., JENNINGS, H., KENNY, C. P., MARTIN, A. & SMITH, I. 1975. Structural determination of the sialic acid polysaccharide antigens of Neisseria meningitidis serogroups B and C with carbon 13 nuclear magnetic resonance. *Journal of Biological Chemistry,* 250**,** 1926-1932.

BHATTACHARYA, S., HERRERA-MOLINA, R., SABANOV, V., AHMED, T., ISCRU, E., STÖBER, F., RICHTER, K., FISCHER, K.-D., ANGENSTEIN, F. & GOLDSCHMIDT, J. 2017. Genetically induced retrograde amnesia of associative memories after neuroplastin ablation. *Biological psychiatry,* 81**,** 124-135.

BHIDE, G. P. & COLLEY, K. J. 2016. Sialylation of N-glycans: mechanism, cellular compartmentalization and function. *Histochemistry and Cell Biology,* 147(2)**,** 149-174.

BHIDE, G. P., FERNANDES, N. R. & COLLEY, K. J. 2016. Sequence requirements for neuropilin-2 recognition by ST8SiaIV and polysialylation of its O-glycans. *Journal of Biological Chemistry,* 291**,** 9444-9457.

BIEDERER, T., SARA, Y., MOZHAYEVA, M., ATASOY, D., LIU, X., KAVALALI, E. T. & SÜDHOF, T. C. 2002. SynCAM, a synaptic adhesion molecule that drives synapse assembly. *Science,* 297**,** 1525-1531.

BINOTTI, B., PAVLOS, N. J., RIEDEL, D., WENZEL, D., VORBRÜGGEN, G., SCHALK, A. M., KÜHNEL, K., BOYKEN, J., ERCK, C. & MARTENS, H. 2015. The GTPase Rab26 links synaptic vesicles to the autophagy pathway. *Elife,* 4**,** e05597.

BJÖRK, S., HURT, C. M., HO, V. K. & ANGELOTTI, T. 2013. REEPs are membrane shaping adapter proteins that modulate specific G protein-coupled receptor trafficking by affecting ER cargo capacity. *PLoS One,* 8**,** e76366.

BLANCO, G. & MERCER, R. W. 1998. Isozymes of the Na-K-ATPase: heterogeneity in structure, diversity in function. *American Journal of Physiology-Renal Physiology,* 275**,** F633-F650.

BLASS-KAMPMANN, S., REINHARDT-MAELICKE, S., KINDLER-RÖHRBORN, A., CLEEVES, V. & RAJEWSKY, M. 1994. In vitro differentiation of E-N-CAM expressing rat neural precursor cells isolated by FACS during prenatal development. *Journal of neuroscience research,* 37**,** 359-373.

BLESSING, W. W., GOODCHILD, A. K., DAMPNEY, R. & CHALMERS, J. P. 1981. Cell groups in the lower brain stem of the rabbit projecting to the spinal cord, with special reference to catecholamine-containing neurons. *Brain research,* 221**,** 35-55.

BLOM, H., BERNHEM, K. & BRISMAR, H. 2016. Sodium pump organization in dendritic spines. *Neurophotonics,* 3**,** 041803-041803.

BOKINIEC, P., SHAHBAZIAN, S., MCDOUGALL, S. J., BERNING, B. A., CHENG, D., LLEWELLYN-SMITH, I. J., BURKE, P. G., MCMULLAN, S., MÜHLENHOFF, M., HILDEBRANDT, H., BRAET, F., CONNOR, M., PACKER, N. H. & GOODCHILD, A. K. 2017. Polysialic acid regulates sympathetic outflow by facilitating information transfer within the nucleus of the solitary tract. *Journal of Neuroscience***,** 0200-17.

BONFANTI, L. 2006. PSA-NCAM in mammalian structural plasticity and neurogenesis. *Progress in neurobiology,* 80**,** 129-164.

BONFANTI, L., MERIGHI, A. & THEODOSIS, D. 1996. Dorsal rhizotomy induces transient expression of the highly sialylated isoform of the neural cell adhesion molecule in neurons and astrocytes of the adult rat spinal cord. *Neuroscience,* 74**,** 619-623.

BONFANTI, L., OLIVE, S., POULAIN, D. & THEODOSIS, D. 1992. Mapping of the distribution of polysialylated neural cell adhesion molecule throughout the central nervous system of the adult rat: an immunohistochemical study. *Neuroscience,* 49**,** 419-436.

BONFANTI, L. & THEODOSIS, D. 1994. Expression of polysialylated neural cell adhesion molecule by proliferating cells in the subependymal layer of the adult rat, in its rostral extension and in the olfactory bulb. *Neuroscience,* 62**,** 291-305.

BONFANTI, L. & THEODOSIS, D. T. 2009. **Polysialic acid and activity-dependent synapse remodeling**. *Cell adhesion & migration,* 3**,** 43-50.

BORGHGRAEF, P., MENUET, C., THEUNIS, C., LOUIS, J. V., DEVIJVER, H., MAURIN, H., SMET-NOCCA, C., LIPPENS, G., HILAIRE, G. & GIJSEN, H. 2013. Increasing brain protein O-GlcNAc-ylation mitigates breathing defects and mortality of Tau. P301L mice. *PLoS One,* 8**,** e84442.

BOSTON, P. F., JACKSON, P. & THOMPSON, R. 1982. Human 14-3-3 Protein: Radioimmunoassay, Tissue Distribution, and Cerebrospinal Fluid Levels in Patients with Neurological Disorders. *Journal of neurochemistry,* 38**,** 1475-1482.

BØTTGER, P., TRACZ, Z., HEUCK, A., NISSEN, P., ROMERO-RAMOS, M. & LYKKE-HARTMANN, K. 2011. Distribution of Na/K-ATPase alpha 3 isoform, a sodium-potassium P-

type pump associated with rapid-onset of dystonia parkinsonism (RDP) in the adult mouse brain. *Journal of Comparative Neurology,* 519**,** 376-404.
BOU FARAH, L., BOWMAN, B. R., BOKINIEC, P., KARIM, S., LE, S., GOODCHILD, A. K. & MCMULLAN, S. 2016. Somatostatin in the rat rostral ventrolateral medulla: Origins and mechanism of action. *Journal of Comparative Neurology,* 524**,** 323-342.
BOUZIOUKH, F., TELL, F., JEAN, A. & ROUGON, G. 2001. NMDA receptor and nitric oxide synthase activation regulate polysialylated neural cell adhesion molecule expression in adult brainstem synapses. *The Journal of Neuroscience,* 21**,** 4721-4730.
BREUSS, M., HENG, J. I.-T., POIRIER, K., TIAN, G., JAGLIN, X. H., QU, Z., BRAUN, A., GSTREIN, T., NGO, L. & HAAS, M. 2012. Mutations in the β-tubulin gene TUBB5 cause microcephaly with structural brain abnormalities. *Cell reports,* 2**,** 1554-1562.
BRITTAIN, J. M., PIEKARZ, A. D., WANG, Y., KONDO, T., CUMMINS, T. R. & KHANNA, R. 2009. An atypical role for collapsin response mediator protein 2 (CRMP-2) in neurotransmitter release via interaction with presynaptic voltage-gated calcium channels. *Journal of Biological Chemistry,* 284**,** 31375-31390.
BROWN, D. & GUYENET, P. G. 1984. Cardiovascular neurons of brain stem with projections to spinal cord. *American Journal of Physiology-Regulatory, Integrative and Comparative Physiology,* 247**,** R1009-R1016.
BROWN, D. & GUYENET, P. G. 1985. Electrophysiological study of cardiovascular neurons in the rostral ventrolateral medulla in rats. *Circulation Research,* 56**,** 359-369.
BROWN, J. R., CRAWFORD, B. E. & ESKO, J. D. 2007. Glycan antagonists and inhibitors: a fount for drug discovery. *Critical reviews in biochemistry and molecular biology,* 42**,** 481-515.
BROWNING, K. N. & TRAVAGLI, R. A. 2014. Central nervous system control of gastrointestinal motility and secretion and modulation of gastrointestinal functions. *Comprehensive Physiology*.
BRUMOVSKY, P. R., ROBINSON, D. R., LA, J. H., SEROOGY, K. B., LUNDGREN, K. H., ALBERS, K. M., KIYATKIN, M. E., SEAL, R. P., EDWARDS, R. H. & WATANABE, M. 2011. Expression of vesicular glutamate transporters type 1 and 2 in sensory and autonomic neurons innervating the mouse colorectum. *Journal of Comparative Neurology,* 519**,** 3346-3366.
BRUSÉS, J. L. & RUTISHAUSER, U. 2001. Roles, regulation, and mechanism of polysialic acid function during neural development. *Biochimie,* 83**,** 635-643.
BURKE, P. G., LI, Q., COSTIN, M. L., MCMULLAN, S., PILOWSKY, P. M. & GOODCHILD, A. K. 2008. Somatostatin 2A receptor-expressing presympathetic neurons in the rostral ventrolateral medulla maintain blood pressure. *Hypertension,* 52**,** 1127-1133.
BUSHMAN, J., MISHRA, B., EZRA, M., GUL, S., SCHULZE, C., CHAUDHURY, S., RIPOLL, D., WALLQVIST, A., KOHN, J. & SCHACHNER, M. 2014. Tegaserod mimics the neurostimulatory glycan polysialic acid and promotes nervous system repair. *Neuropharmacology,* 79**,** 456-466.
BUTLER, W. N. & TAUBE, J. S. 2015. The nucleus prepositus hypoglossi contributes to head direction cell stability in rats. *Journal of Neuroscience,* 35**,** 2547-2558.
BÜTTNER, B. & HORSTKORTE, R. 2010. Intracelluar ligands of NCAM. *Structure and Function of the Neural Cell Adhesion Molecule NCAM.* Springer.
BÜTTNER, B., KANNICHT, C., REUTTER, W. & HORSTKORTE, R. 2003. The neural cell adhesion molecule is associated with major components of the cytoskeleton. *Biochemical and biophysical research communications,* 310**,** 967-971.
BUTTON, K. S., IOANNIDIS, J. P., MOKRYSZ, C., NOSEK, B. A., FLINT, J., ROBINSON, E. S. & MUNAFÒ, M. R. 2013. Power failure: why small sample size undermines the reliability of neuroscience. *Nature Reviews Neuroscience,* 14**,** 365-376.
CAMAND, E., MOREL, M. P., FAISSNER, A., SOTELO, C. & DUSART, I. 2004. Long-term changes in the molecular composition of the glial scar and progressive increase of serotoninergic fibre sprouting after hemisection of the mouse spinal cord. *European Journal of Neuroscience,* 20**,** 1161-1176.

CAMPAGNA, J. A. & CARTER, C. 2003. Clinical relevance of the Bezold-Jarisch reflex. *ANESTHESIOLOGY-PHILADELPHIA THEN HAGERSTOWN-*, 98**,** 1250-1260.
CARRIVE, P., BANDLER, R. & DAMPNEY, R. 1988. Anatomical evidence that hypertension associated with the defence reaction in the cat is mediated by a direct projection from a restricted portion of the midbrain periaqueductal grey to the subretrofacial nucleus of the medulla. *Brain research,* 460**,** 339-345.
CASTILLO-GÓMEZ, E., VAREA, E., BLASCO-IBÁÑEZ, J. M., CRESPO, C. & NACHER, J. 2016. Effects of Chronic Dopamine D2R Agonist Treatment and Polysialic Acid Depletion on Dendritic Spine Density and Excitatory Neurotransmission in the mPFC of Adult Rats. *Neural plasticity,* 2016.
CERVERO, F. & IGGO, A. 1980. The substantia gelatinosa of the spinal cord. *Brain,* 103**,** 717-772.
CHALFIE, M., TU, Y., EUSKIRCHEN, G., WARD, W. W. & PRASHER, D. C. 1994. Green fluorescent protein as a marker for gene expression. *Science***,** 802-805.
CHALMERS, J., KORNER, P. & WHITE, S. W. 1967. The relative roles of the aortic and carotid sinus nerves in the rabbit in the control of respiration and circulation during arterial hypoxia and hypercapnia. *The Journal of physiology,* 188**,** 435.
CHANG, J., LEE, S. & BLACKSTONE, C. 2013. Protrudin binds atlastins and endoplasmic reticulum-shaping proteins and regulates network formation. *Proceedings of the National Academy of Sciences,* 110**,** 14954-14959.
CHARLES, P., HERNANDEZ, M., STANKOFF, B., AIGROT, M., COLIN, C., ROUGON, G., ZALC, B. & LUBETZKI, C. 2000. Negative regulation of central nervous system myelination by polysialylated-neural cell adhesion molecule. *Proceedings of the National Academy of Sciences,* 97**,** 7585-7590.
CHAUDHRY, F. A., LEHRE, K. P., VAN LOOKEREN CAMPAGNE, M., OTTERSEN, O. P., DANBOLT, N. C. & STORM-MATHISEN, J. 1995. Glutamate transporters in glial plasma membranes: highly differentiated localizations revealed by quantitative ultrastructural immunocytochemistry. *Neuron,* 15**,** 711-720.
CHEN, Q., MILLER, L. J. & DONG, M. 2010. Role of N-linked glycosylation in biosynthesis, trafficking, and function of the human glucagon-like peptide 1 receptor. *American Journal of Physiology-Endocrinology and Metabolism,* 299**,** E62-E68.
CHO, A., HARUYAMA, N. & KULKARNI, A. B. 2009. Generation of transgenic mice. *Current protocols in cell biology***,** 19-11.
CHOU, H.-H., HAYAKAWA, T., DIAZ, S., KRINGS, M., INDRIATI, E., LEAKEY, M., PAABO, S., SATTA, Y., TAKAHATA, N. & VARKI, A. 2002. Inactivation of CMP-N-acetylneuraminic acid hydroxylase occurred prior to brain expansion during human evolution. *Proceedings of the National Academy of Sciences,* 99**,** 11736-11741.
CHRISTIANSON, H. C. & BELTING, M. 2014. Heparan sulfate proteoglycan as a cell-surface endocytosis receptor. *Matrix Biology,* 35**,** 51-55.
CHUNG, K., LEE, W. & CARLTON, S. 1988. The effects of dorsal rhizotomy and spinal cord isolation on calcitonin gene-related peptide-labeled terminals in the rat lumbar dorsal horn. *Neuroscience letters,* 90**,** 27-32.
CHUNG, W. W., LAGENAUR, C. F., YAN, Y. & LUND, J. S. 1991. Developmental expression of neural cell adhesion molecules in the mouse neocortex and olfactory bulb. *Journal of Comparative Neurology,* 314**,** 290-305.
CLOSE, B. E. & COLLEY, K. J. 1998. In vivo autopolysialylation and localization of the polysialyltransferases PST and STX. *Journal of Biological Chemistry,* 273**,** 34586-34593.
CLOSE, B. E., MENDIRATTA, S. S., GEIGER, K. M., BROOM, L. J., HO, L.-L. & COLLEY, K. J. 2003. The minimal structural domains required for neural cell adhesion molecule polysialylation by PST/ST8Sia IV and STX/ST8Sia II. *Journal of Biological Chemistry,* 278**,** 30796-30805.
COHEN, M. & VARKI, A. 2010. The sialome—far more than the sum of its parts. *Omics: a journal of integrative biology,* 14**,** 455-464.

COLLEY, K. J. 2010. Structural basis for the polysialylation of the neural cell adhesion molecule. *Structure and Function of the Neural Cell Adhesion Molecule NCAM.* Springer.
COLLEY, K. J., KITAJIMA, K. & SATO, C. 2014. Polysialic acid: Biosynthesis, novel functions and applications. *Critical reviews in biochemistry and molecular biology,* 49**,** 498-532.
COSKUN, Ü., GRZYBEK, M., DRECHSEL, D. & SIMONS, K. 2011. Regulation of human EGF receptor by lipids. *Proceedings of the National Academy of Sciences,* 108**,** 9044-9048.
COX, E. T., BRENNAMAN, L. H., GABLE, K. L., HAMER, R. M., GLANTZ, L. A., LAMANTIA, A.-S., LIEBERMAN, J. A., GILMORE, J. H., MANESS, P. F. & JARSKOG, L. F. 2009. Developmental regulation of neural cell adhesion molecule in human prefrontal cortex. *Neuroscience,* 162**,** 96-105.
CREMER, H., LANGE, R., CHRISTOPH, A., PLOMANN, M., VOPPER, G., ROES, J., BROWN, R., BALDWIN, S., KRAEMER, P., SCHEFF, S., BARTHELS, D., RAJEWSKY, K. & WILLIE, W. 1994. Inactivation of the N-CAM gene in mice results in size reduction of the olfactory bulb and deficits in spatial learning. *Nature,* 367**,** 455-459.
CROSSMAN, A. R. 2016. Spinal cord: internal organisation. *In:* STANDRING, S. (ed.) *Gray's anatomy: the anatomical basis of clinical practice*

41 ed.: Elsevier Health Sciences.
CURRELI, S., ARANY, Z., GERARDY-SCHAHN, R., MANN, D. & STAMATOS, N. M. 2007. Polysialylated neuropilin-2 is expressed on the surface of human dendritic cells and modulates dendritic cell-T lymphocyte interactions. *Journal of Biological Chemistry,* 282**,** 30346-30356.
DAHLHAUS, A., RUSCHEWEYH, R. & SANDKÜHLER, J. 2005. Synaptic input of rat spinal lamina I projection and unidentified neurones in vitro. *The Journal of physiology,* 566**,** 355-368.
DAMANHURI, H. A., BURKE, P. G., ONG, L. K., BOBROVSKAYA, L., DICKSON, P. W., DUNKLEY, P. R. & GOODCHILD, A. K. 2012. Tyrosine hydroxylase phosphorylation in catecholaminergic brain regions: a marker of activation following acute hypotension and glucoprivation. *PLoS One,* 7**,** e50535.
DAMPNEY, R. 1994a. Functional organization of central pathways regulating the cardiovascular system. *Physiological reviews,* 74**,** 323-364.
DAMPNEY, R. 1994b. The subretrofacial vasomotor nucleus: anatomical, chemical and pharmacological properties and role in cardiovascular regulation. *Progress in neurobiology,* 42**,** 197-227.
DAMPNEY, R., CZACHURSKI, J., DEMBOWSKY, K., GOODCHILD, A. & SELLER, H. 1987. Afferent connections and spinal projections of the pressor region in the rostral ventrolateral medulla of the cat. *Journal of the autonomic nervous system,* 20**,** 73-86.
DAMPNEY, R., GOODCHILD, A., ROBERTSON, L. & MONTGOMERY, W. 1982. Role of ventrolateral medulla in vasomotor regulation: a correlative anatomical and physiological study. *Brain research,* 249**,** 223-235.
DAMPNEY, R. & MOON, E. A. 1980. Role of ventrolateral medulla in vasomotor response to cerebral ischemia. *American Journal of Physiology-Heart and Circulatory Physiology,* 239**,** H349-H358.
DAMPNEY, R. A., KUMADA, M. & REIS, D. J. 1979. Central neural mechanisms of the cerebral ischemic response. *Circ. Res,* 44**,** 48-62.
DAMPNEY, R. A., POLSON, J. W., POTTS, P. D., HIROOKA, Y. & HORIUCHI, J. 2003. Functional organization of brain pathways subserving the baroreceptor reflex: studies in conscious animals using immediate early gene expression. *Cellular and molecular neurobiology,* 23**,** 597-616.
DANIEL, J. A., CHAU, N., ABDEL-HAMID, M. K., HU, L., VON KLEIST, L., WHITING, A., KRISHNAN, S., MAAMARY, P., JOSEPH, S. R. & SIMPSON, F. 2015. Phenothiazine-Derived Antipsychotic Drugs Inhibit Dynamin and Clathrin-Mediated Endocytosis. *Traffic,* 16**,** 635-654.
DASILVA, A. & DOSSANTOS, M. 2012. The role of sensory fiber demography in trigeminal and postherpetic neuralgias. *Journal of dental research,* 91**,** 17-24.
DAVID, S. & AGUAYO, A. J. 1981. Axonal elongation into peripheral nervous system "bridges" after central nervous system injury in adult rats. *Science,* 214**,** 931-933.

DE BIASI, S. & RUSTIONI, A. 1988. Glutamate and substance P coexist in primary afferent terminals in the superficial laminae of spinal cord. *Proceedings of the National Academy of Sciences,* 85**,** 7820-7824.

DECKER, L., AVELLANA-ADALID, V., NAIT-OUMESMAR, B., DURBEC, P. & BARON-VAN EVERCOOREN, A. 2000. Oligodendrocyte precursor migration and differentiation: combined effects of PSA residues, growth factors, and substrates. *Molecular and Cellular Neuroscience,* 16**,** 422-439.

DEMPSEY, B., LE, S., TURNER, A., BOKINIEC, P., RAMADAS, R., BJAALIE, J. G., MENUET, C., NEVE, R., ALLEN, A. M., GOODCHILD, A. K. & MCMULLAN, S. 2017. Mapping and analysis of the connectome of sympathetic premotor neurons in the rostral ventrolateral medulla of the rat using a volumetric brain atlas. *Frontiers in Neural Circuits,* 11.

DEMPSEY, B., TURNER, A. J., LE, S., SUN, Q. J., FARAH, L. B., ALLEN, A. M., GOODCHILD, A. K. & MCMULLAN, S. 2015. Recording, labeling, and transfection of single neurons in deep brain structures. *Physiological reports,* 3**,** e12246.

DEUCHARS, S. A., MILLIGAN, C. J., STORNETTA, R. L. & DEUCHARS, J. 2005. GABAergic neurons in the central region of the spinal cord: a novel substrate for sympathetic inhibition. *Journal of Neuroscience,* 25**,** 1063-1070.

DEUCHARS, S. A., MORRISON, S. F. & GILBEY, M. P. 1995. Medullary-evoked EPSPs in neonatal rat sympathetic preganglionic neurones in vitro. *The Journal of physiology,* 487**,** 453.

DHÚILL, N., CAOIMHE, M., FOX, G. B., PITTOCK, S. J., O'CONNELL, A. W., MURPHY, K. J. & REGAN, C. M. 1999. Polysialylated neural cell adhesion molecule expression in the dentate gyrus of the human hippocampal formation from infancy to old age. *Journal of neuroscience research,* 55**,** 99-106.

DI DOMENICO, F., OWEN, J. B., SULTANA, R., SOWELL, R. A., PERLUIGI, M., CINI, C., CAI, J., PIERCE, W. M. & BUTTERFIELD, D. A. 2010. The wheat germ agglutinin-fractionated proteome of subjects with Alzheimer's disease and mild cognitive impairment hippocampus and inferior parietal lobule: Implications for disease pathogenesis and progression. *Journal of neuroscience research,* 88**,** 3566-3577.

DICK, T. E., HSIEH, Y. H., WANG, N. & PRABHAKAR, N. 2007. Acute intermittent hypoxia increases both phrenic and sympathetic nerve activities in the rat. *Experimental physiology,* 92**,** 87-97.

DION, F., DUMAYNE, C., HENLEY, N., BEAUCHEMIN, S., ARIAS, E. B., LEBLOND, F. A., LESAGE, S., LEFRANÇOIS, S., CARTEE, G. D. & PICHETTE, V. 2017. Mechanism of insulin resistance in a rat model of kidney disease and the risk of developing type 2 diabetes. *PloS one,* 12**,** e0176650.

DITTGEN, T., NIMMERJAHN, A., KOMAI, S., LICZNERSKI, P., WATERS, J., MARGRIE, T. W., HELMCHEN, F., DENK, W., BRECHT, M. & OSTEN, P. 2004. Lentivirus-based genetic manipulations of cortical neurons and their optical and electrophysiological monitoring in vivo. *Proceedings of the National Academy of Sciences,* 101**,** 18206-18211.

DITYATEV, A., DITYATEVA, G., SYTNYK, V., DELLING, M., TONI, N., NIKONENKO, I., MULLER, D. & SCHACHNER, M. 2004. Polysialylated neural cell adhesion molecule promotes remodeling and formation of hippocampal synapses. *The Journal of neuroscience,* 24**,** 9372-9382.

DOHERTY, P., ASHTON, S. V., MOORE, S. E. & WALSH, F. S. 1991. Morphoregulatory activities of NCAM and N-cadherin can be accounted for by G protein-dependent activation of L-and N-type neuronal Ca 2+ channels. *Cell,* 67**,** 21-33.

DOHERTY, P., COHEN, J. & WALSH, F. S. 1990. Neurite outgrowth in response to transfected N-CAM changes during development and is modulated by polysialic acid. *Neuron,* 5**,** 209-219.

DOHERTY, P., SKAPER, S. D., MOORE, S. E., LEON, A. & WALSH, F. S. 1992. A developmentally regulated switch in neuronal responsiveness to NCAM and N-cadherin in the rat hippocampus. *Development,* 115**,** 885-892.

DOWNING, S. E., MITCHELL, J. H. & WALLACE, A. G. 1963. Cardiovascular responses to ischemia, hypoxia, and hypercapnia of the central nervous system. *American Journal of Physiology--Legacy Content,* 204**,** 881-887.

DRAKE, P. M., NATHAN, J. K., STOCK, C. M., CHANG, P. V., MUENCH, M. O., NAKATA, D., READER, J. R., GIP, P., GOLDEN, K. P. & WEINHOLD, B. 2008. Polysialic acid, a glycan with highly restricted expression, is found on human and murine leukocytes and modulates immune responses. *The Journal of Immunology,* 181**,** 6850-6858.

DUBNER, R. & BENNETT, G. J. 1983. Spinal and trigeminal mechanisms of nociception. *Annual review of neuroscience,* 6**,** 381-418.

DUBNER, R. & RUDA, M. 1992. Activity-dependent neuronal plasticity following tissue injury and inflammation. *Trends in neurosciences,* 15**,** 96-103.

DUSART, I., MOREL, M. P., WEHRLÉ, R. & SOTELO, C. 1999. Late axonal sprouting of injured Purkinje cells and its temporal correlation with permissive changes in the glial scar. *Journal of Comparative Neurology,* 408**,** 399-418.

DUSTRUDE, E. T., MOUTAL, A., YANG, X., WANG, Y., KHANNA, M. & KHANNA, R. 2016. Hierarchical CRMP2 posttranslational modifications control NaV1. 7 function. *Proceedings of the National Academy of Sciences***,** 201610531.

EATON, B. A., HAUGWITZ, M., LAU, D. & MOORE, H.-P. H. 2000. Biogenesis of regulated exocytotic carriers in neuroendocrine cells. *Journal of Neuroscience,* 20**,** 7334-7344.

ECKHARDT, M., BUKALO, O., CHAZAL, G., WANG, L., GORIDIS, C., SCHACHNER, M., GERARDY-SCHAHN, R., CREMER, H. & DITYATEV, A. 2000. Mice deficient in the polysialyltransferase ST8SiaIV/PST-1 allow discrimination of the roles of neural cell adhesion molecule protein and polysialic acid in neural development and synaptic plasticity. *The Journal of Neuroscience,* 20**,** 5234-5244.

ECKHARDT, M., MÜHLENHOFF, M., BETHE, A., KOOPMAN, J., FROSCH, M. & GERARDY-SCHAHN, R. 1995. Molecular characterization of eukaryotic polysialyltransferase-1. *Nature,* 373(6516)**,** 715.

EDRI-BRAMI, M., ROSENTAL, B., HAYOUN, D., WELT, M., ROSEN, H., WIRGUIN, I., NEFUSSY, B., DRORY, V. E., PORGADOR, A. & LICHTENSTEIN, R. G. 2012. Glycans in sera of amyotrophic lateral sclerosis patients and their role in killing neuronal cells. *PloS one,* 7**,** e35772.

EDWARDS, E. & PATON, J. F. 2000. Glutamate stimulation of raphe pallidus attenuates the cardiopulmonary reflex in anaesthetised rats. *Autonomic Neuroscience,* 82**,** 87-96.

EDWARDS, I. J., BRUCE, G., LAWRENSON, C., HOWE, L., CLAPCOTE, S. J., DEUCHARS, S. A. & DEUCHARS, J. 2013. Na+/K+ ATPase α1 and α3 isoforms are differentially expressed in α-and γ-motoneurons. *Journal of Neuroscience,* 33**,** 9913-9919.

EDWARDS, S., ANDERSON, C., SOUTHWELL, B. & MCALLEN, R. 1996. Distinct preganglionic neurons innervate noradrenaline and adrenaline cells in the cat adrenal medulla. *Neuroscience,* 70**,** 825-832.

EFTEKHARI, S., SALVATORE, C. A., CALAMARI, A., KANE, S. A., TAJTI, J. & EDVINSSON, L. 2010. Differential distribution of calcitonin gene-related peptide and its receptor components in the human trigeminal ganglion. *Neuroscience,* 169**,** 683-696.

EL-SHAMAYLEH, Y., NI, A. M. & HORWITZ, G. D. 2016. Strategies for targeting primate neural circuits with viral vectors. *Journal of neurophysiology,* 116**,** 122-134.

EL MAAROUF, A., KOLESNIKOV, Y., PASTERNAK, G. & RUTISHAUSER, U. 2005. Polysialic acid-induced plasticity reduces neuropathic insult to the central nervous system. *Proceedings of the National Academy of Sciences of the United States of America,* 102**,** 11516-11520.

EL MAAROUF, A., PETRIDIS, A. K. & RUTISHAUSER, U. 2006. Use of polysialic acid in repair of the central nervous system. *Proceedings of the National Academy of Sciences,* 103**,** 16989-16994.

EL MAAROUF, A. & RUTISHAUSER, U. 2003. Removal of polysialic acid induces aberrant pathways, synaptic vesicle distribution, and terminal arborization of retinotectal axons. *Journal of Comparative Neurology,* 460**,** 203-211.

EL MAAROUF, A. & RUTISHAUSER, U. 2010. Use of PSA-NCAM in repair of the central nervous system. *Structure and Function of the Neural Cell Adhesion Molecule NCAM*. Springer.
EL MAAROUF, A., YAW, D. M.-L., LINDHOUT, T., PEARSE, D. D., WAKARCHUK, W. & RUTISHAUSER, U. 2012. Enzymatic engineering of polysialic acid on cells in vitro and in vivo using a purified bacterial polysialyltransferase. *Journal of Biological Chemistry,* 287**,** 32770-32779.
EMERY, D. L., RAGHUPATHI, R., SAATMAN, K. E., FISCHER, I., GRADY, M. S. & MCINTOSH, T. K. 2000. Bilateral growth-related protein expression suggests a transient increase in regenerative potential following brain trauma. *Journal of Comparative Neurology,* 424**,** 521-531.
ERICKSON, J. T. & MILLHORN, D. E. 1994. Hypoxia and electrical stimulation of the carotid sinus nerve induce fos-like immunoreactivity within catecholaminergic and serotoninergic neurons of the rat brainstem. *Journal of Comparative Neurology,* 348**,** 161-182.
EXNER, T., JENSEN, O. N., MANN, M., KLEUSS, C. & NÜRNBERG, B. 1999. Posttranslational modification of Gαo1 generates Gαo3, an abundant G protein in brain. *Proceedings of the National Academy of Sciences,* 96**,** 1327-1332.
FAHRIG, T., SCHMITZ, B., WEBER, D., KÜCHERER-EHRET, A., FAISSNER, A. & SCHACHNER, M. 1990. Two monoclonal antibodies recognizing carbohydrate epitopes on neural adhesion molecules interfere with cell interactions. *European Journal of Neuroscience,* 2**,** 153-161.
FEDORKOVA, L., RUTISHAUSER, U., PROSSER, R., SHEN, H. & GLASS, J. D. 2002. Removal of polysialic acid from the SCN potentiates nonphotic circadian phase resetting. *Physiology & behavior,* 77**,** 361-369.
FELDBERG, W. & GUERTZENSTEIN, P. 1976. Vasodepressor effects obtained by drugs acting on the ventral surface of the brain stem. *The Journal of physiology,* 258**,** 337-355

FERNANDEZ-VALDIVIA, R., TAKEUCHI, H., SAMARGHANDI, A., LOPEZ, M., LEONARDI, J., HALTIWANGER, R. S. & JAFAR-NEJAD, H. 2011. Regulation of mammalian Notch signaling and embryonic development by the protein O-glucosyltransferase Rumi. *Development,* 138**,** 1925-1934.
FEWOU, S. N., RAMAKRISHNAN, H., BÜSSOW, H., GIESELMANN, V. & ECKHARDT, M. 2007. Down-regulation of polysialic acid is required for efficient myelin formation. *Journal of Biological Chemistry,* 282**,** 16700-16711.
FIGARELLA-BRANGER, D., NEDELEC, J., PELLISSIER, J., BOUCRAUT, J., BIANCO, N. & ROUGON, G. 1990. Expression of various isoforms of neural cell adhesive molecules and their highly polysialylated counterparts in diseased human muscles. *Journal of the neurological sciences,* 98**,** 21-36.
FILBIN, M. T. 2003. Myelin-associated inhibitors of axonal regeneration in the adult mammalian CNS. *Nature Reviews Neuroscience,* 4**,** 703-713.
FINNE, J. 1982. Occurrence of unique polysialosyl carbohydrate units in glycoproteins of developing brain. *Journal of Biological Chemistry,* 257**,** 11966-11970.
FINNE, J., FINNE, U., DEAGOSTINI-BAZIN, H. & GORIDIS, C. 1983. Occurrence of α2–8 linked polysialosyl units in a neural cell adhesion molecule. *Biochemical and biophysical research communications,* 112**,** 482-487.
FINNE, J., KRUSIUS, T. & RAUVALA, H. 1977a. Occurrence of disialosyl groups in glycoproteins. *Biochemical and biophysical research communications,* 74**,** 405-410.
FINNE, J., KRUSIUS, T., RAUVALA, H. & HEMMINKI, K. 1977b. The disialosyl group of glycoproteins. *European Journal of Biochemistry,* 77**,** 319-323.
FLETCHER, E. C. 2000. Effect of episodic hypoxia on sympathetic activity and blood pressure. *Respiration physiology,* 119**,** 189-197.
FOLEY, A. G., RØNN, L. C., MURPHY, K. J. & REGAN, C. M. 2003. Distribution of polysialylated neural cell adhesion molecule in rat septal nuclei and septohippocampal pathway: transient

increase of polysialylated interneurons in the subtriangular septal zone during memory consolidation. *Journal of neuroscience research,* 74**,** 807-817.
FOX, G. B., FICHERA, G., BARRY, T., O'CONNELL, A. W., GALLAGHER, H. C., MURPHY, K. J. & REGAN, C. M. 2000. Consolidation of passive avoidance learning is associated with transient increases of polysialylated neurons in layer II of the rat medial temporal cortex. *Journal of neurobiology,* 45**,** 135-141.
FRANCESCHINI, I., VITRY, S., PADILLA, F., CASANOVA, P., THAM, T. N., FUKUDA, M., ROUGON, G., DURBEC, P. & DUBOIS-DALCQ, M. 2004. Migrating and myelinating potential of neural precursors engineered to overexpress PSA-NCAM. *Molecular and Cellular Neuroscience,* 27**,** 151-162.
FREEZE, H. H. 2006. Genetic defects in the human glycome. *Nature Reviews Genetics,* 7**,** 537-551.
FROSCH, M., GÖRGEN, I., BOULNOIS, G. J., TIMMIS, K. N. & BITTER-SUERMANN, D. 1985. NZB mouse system for production of monoclonal antibodies to weak bacterial antigens: isolation of an IgG antibody to the polysaccharide capsules of Escherichia coli K1 and group B meningococci. *Proceedings of the National Academy of Sciences,* 82**,** 1194-1198.
FU, H., SUBRAMANIAN, R. R. & MASTERS, S. C. 2000. 14-3-3 proteins: structure, function, and regulation. *Annual review of pharmacology and toxicology,* 40**,** 617-647.
FUKUDA, Y., SATO, A., SUZUKI, A. & TRZEBSKI, A. 1989. Autonomic nerve and cardiovascular responses to changing blood oxygen and carbon dioxide levels in the rat. *Journal of the autonomic nervous system,* 28**,** 61-74.
FURUNO, T., ITO, A., KOMA, Y.-I., WATABE, K., YOKOZAKI, H., BIENENSTOCK, J., NAKANISHI, M. & KITAMURA, Y. 2005. The spermatogenic Ig superfamily/synaptic cell adhesion molecule mast-cell adhesion molecule promotes interaction with nerves. *The Journal of Immunology,* 174**,** 6934-6942.
FUSTER, M. M. & ESKO, J. D. 2005. The sweet and sour of cancer: glycans as novel therapeutic targets. *Nature Reviews Cancer,* 5**,** 526-542.
GABIUS, H.-J., MANNING, J., KOPITZ, J., ANDRÉ, S. & KALTNER, H. 2016. Sweet complementarity: the functional pairing of glycans with lectins. *Cellular and Molecular Life Sciences,* 73**,** 1989-2016.
GAIARSA, J.-L., CAILLARD, O. & BEN-ARI, Y. 2002. Long-term plasticity at GABAergic and glycinergic synapses: mechanisms and functional significance. *Trends in neurosciences,* 25**,** 564-570.
GALUSKA, S. P., GEYER, R., GERARDY-SCHAHN, R., MÜHLENHOFF, M. & GEYER, H. 2008. Enzyme-dependent variations in the polysialylation of the neural cell adhesion molecule (NCAM) in vivo. *Journal of Biological Chemistry,* 283**,** 17-28.
GALUSKA, S. P., OLTMANN-NORDEN, I., GEYER, H., WEINHOLD, B., KUCHELMEISTER, K., HILDEBRANDT, H., GERARDY-SCHAHN, R., GEYER, R. & MÜHLENHOFF, M. 2006. Polysialic acid profiles of mice expressing variant allelic combinations of the polysialyltransferases ST8SiaII and ST8SiaIV. *Journal of Biological Chemistry,* 281**,** 31605-31615.
GALUSKA, S. P., ROLLENHAGEN, M., KAUP, M., EGGERS, K., OLTMANN-NORDEN, I., SCHIFF, M., HARTMANN, M., WEINHOLD, B., HILDEBRANDT, H. & GEYER, R. 2010. Synaptic cell adhesion molecule SynCAM 1 is a target for polysialylation in postnatal mouse brain. *Proceedings of the National Academy of Sciences,* 107**,** 10250-10255.
GARGINI, C., TERZIBASI, E., MAZZONI, F. & STRETTOI, E. 2007. Retinal organization in the retinal degeneration 10 (rd10) mutant mouse: a morphological and ERG study. *Journal of Comparative Neurology,* 500**,** 222-238.
GARNER, O. B., YUN, T., PERNET, O., AGUILAR, H. C., PARK, A., BOWDEN, T. A., FREIBERG, A. N., LEE, B. & BAUM, L. G. 2015. Timing of galectin-1 exposure differentially modulates Nipah virus entry and syncytium formation in endothelial cells. *Journal of virology,* 89**,** 2520-2529.

GASCON, E., VUTSKITS, L. & KISS, J. Z. 2007. Polysialic acid–neural cell adhesion molecule in brain plasticity: from synapses to integration of new neurons. *Brain research reviews,* 56**,** 101-118.
GASCON, E., VUTSKITS, L. & KISS, J. Z. 2010. The role of PSA-NCAM in adult neurogenesis. *Structure and Function of the Neural Cell Adhesion Molecule NCAM.* Springer.
GAURIAU, C. & BERNARD, J. F. 2004. A comparative reappraisal of projections from the superficial laminae of the dorsal horn in the rat: the forebrain. *Journal of Comparative Neurology,* 468**,** 24-56.
GEERING, K. 2006. FXYD proteins: new regulators of Na-K-ATPase. *American Journal of Physiology-Renal Physiology,* 290**,** F241-F250.
GENNARINI, G., DURBEC, P., BONED, A., ROUGON, G. & GORIDIS, C. 1991. Transfected F3/F11 neuronal cell surface protein mediates intercellular adhesion and promotes neurite outgrowth. *Neuron,* 6**,** 595-606.
GEORGE, P. & CHARLES, W. 2007. The rat brain in stereotaxic coordinates. *Qingchuan Zhuge translate. People's Medical Publishing House, Beijing,* 32.
GERBER, G., YOUN, D.-H., HSU, C., ISAEV, D. & RANDIĆ, M. 2000. Spinal dorsal horn synaptic plasticity: involvement of group I metabotropic glutamate receptors. *Progress in brain research,* 129**,** 115-134.
GHOSH, M., TUESTA, L. M., PUENTES, R., PATEL, S., MELENDEZ, K., EL MAAROUF, A., RUTISHAUSER, U. & PEARSE, D. D. 2012. Extensive cell migration, axon regeneration, and improved function with polysialic acid-modified Schwann cells after spinal cord injury. *Glia,* 60**,** 979-992.
GIACOPUZZI, E., BRESCIANI, R., SCHAUER, R., MONTI, E. & BORSANI, G. 2012. New insights on the sialidase protein family revealed by a phylogenetic analysis in metazoa. *PloS one,* 7**,** e44193.
GIBSON, S., POLAK, J., BLOOM, S., SABATE, I., MULDERRY, P., GHATEI, M., MCGREGOR, G., MORRISON, J., KELLY, J. & EVANS, R. 1984. Calcitonin gene-related peptide immunoreactivity in the spinal cord of man and of eight other species. *Journal of Neuroscience,* 4**,** 3101-3111.
GILABERT-JUAN, J., CASTILLO-GOMEZ, E., PÉREZ-RANDO, M., MOLTÓ, M. D. & NACHER, J. 2011. Chronic stress induces changes in the structure of interneurons and in the expression of molecules related to neuronal structural plasticity and inhibitory neurotransmission in the amygdala of adult mice. *Experimental neurology,* 232**,** 33-40.
GLOOR, S., ANTONICEK, H., SWEADNER, K. J., PAGLIUSI, S., FRANK, R., MOOS, M. & SCHACHNER, M. 1990. The adhesion molecule on glia (AMOG) is a homologue of the b-subunit of the Na, K-ATPase. *J. Cell Biol,* 110**,** 165-174.
GOBEL, S., HOCKFIELD, S. & RUDA, M. 1981. Anatomical similarities between medullary and spinal dorsal horns. *Oral-facial sensory and motor functions.* Quintessence Tokyo.
GOLDSTEIN, I., LEVY, T., GALILI, D., OVADIA, H., YIRMIYA, R., ROSEN, H. & LICHTSTEIN, D. 2006. Involvement of Na+, K+-ATPase and endogenous digitalis-like compounds in depressive disorders. *Biological psychiatry,* 60**,** 491-499.
GOMEZ-CLIMENT, M., GUIRADO, R., VAREA, E. & NACHER, J. 2010. " Arrested development". Immature, but not recently generated, neurons in the adult brain. *Archives italiennes de biologie,* 148**,** 159-172.
GÓMEZ-CLIMENT, M. Á., CASTILLO-GÓMEZ, E., VAREA, E., GUIRADO, R., BLASCO-IBÁÑEZ, J. M., CRESPO, C., MARTÍNEZ-GUIJARRO, F. J. & NÁCHER, J. 2008. A population of prenatally generated cells in the rat paleocortex maintains an immature neuronal phenotype into adulthood. *Cerebral cortex,* 18**,** 2229-2240.
GÓMEZ-CLIMENT, M. Á., GUIRADO, R., CASTILLO-GÓMEZ, E., VAREA, E., GUTIERREZ-MECINAS, M., GILABERT-JUAN, J., GARCÍA-MOMPÓ, C., VIDUEIRA, S., SANCHEZ-MATAREDONA, D. & HERNÁNDEZ, S. 2011. The polysialylated form of the neural cell adhesion molecule (PSA-NCAM) is expressed in a subpopulation of mature cortical interneurons characterized by reduced structural features and connectivity. *Cerebral cortex,* 21**,** 1028-1041.

GOODCHILD, A., DAMPNEY, R. & BANDLER, R. 1982. A method for evoking physiological responses by stimulation of cell bodies, but not axons of passage, within localized regions of the central nervous system. *Journal of neuroscience methods,* 6**,** 351-363.
GOODCHILD, A., MOON, E., DAMPNEY, R. & HOWE, P. 1984. Evidence that adrenaline neurons in the rostral ventrolateral medulla have a vasopressor function. *Neuroscience letters,* 45**,** 267-272.
GOODCHILD, A. K. & MOON, E. A. 2009. Maps of cardiovascular and respiratory regions of rat ventral medulla: focus on the caudal medulla. *Journal of chemical neuroanatomy,* 38**,** 209-221.
GORDON, D., MERRICK, D., WOLLNER, D. A. & CATTERALL, W. A. 1988. Biochemical properties of sodium channels in a wide range of excitable tissues studied with site-directed antibodies. *Biochemistry,* 27**,** 7032-7038.
GOTTS, J., ATKINSON, L., YANAGAWA, Y., DEUCHARS, J. & DEUCHARS, S. A. 2016. Co-expression of GAD67 and choline acetyltransferase in neurons in the mouse spinal cord: A focus on lamina X. *Brain research,* 1646**,** 570-579.
GOVRIN-LIPPMANN, R. & DEVOR, M. 1978. Ongoing activity in severed nerves: source and variation with time. *Brain research,* 159**,** 406-410.
GOWER, H. J., BARTON, C. H., ELSOM, V. L., THOMPSON, J., MOORE, S. E., DICKSON, G. & WALSH, F. S. 1988. Alternative splicing generates a secreted form of N-CAM in muscle and brain. *Cell,* 55**,** 955-964.
GRANT, L. T. 2005. The trigeminal nerve and its central connections. *In:* MILLER, N. R., WALSH, F. B. & HOYT, W. F. (eds.) *Walsh and Hoyt's clinical neuro-ophthalmology.* 6 ed. Philadelphia Lippincott Williams & Wilkins.
GROSS, P. M., SPOSITO, N. M., PETTERSEN, S. E. & FENSTERMACHER, J. D. 1986. Differences in function and structure of the capillary endothelium in gray matter, white matter and a circumventricular organ of rat brain. *Journal of Vascular Research,* 23**,** 261-270.
GROSS, P. M., WALL, K. M., WAINMAN, D. S. & SHAVER, S. W. 1991. Subregional topography of capillaries in the dorsal vagal complex of rats: II. Physiological properties. *Journal of comparative neurology,* 306**,** 83-94.
GU, Y., CHEN, Y., ZHANG, X., LI, G.-W., WANG, C. & HUANG, L.-Y. M. 2010. Neuronal soma–satellite glial cell interactions in sensory ganglia and the participation of purinergic receptors. *Neuron glia biology,* 6**,** 53-62.
GUERTZENSTEIN, P. & SILVER, A. 1974. Fall in blood pressure produced from discrete regions of the ventral surface of the medulla by glycine and lesions. *The Journal of Physiology,* 242**,** 489-503.
GUIRADO, R., PEREZ-RANDO, M., SANCHEZ-MATARREDONA, D., CASTILLO-GÓMEZ, E., LIBERIA, T., ROVIRA-ESTEBAN, L., VAREA, E., CRESPO, C., BLASCO-IBÁÑEZ, J. M. & NACHER, J. 2013. The dendritic spines of interneurons are dynamic structures influenced by PSA-NCAM expression. *Cerebral cortex,* 24**,** 3014-3024.
GUNJIGAKE, K. K., GOTO, T., NAKAO, K., KOBAYASHI, S. & YAMAGUCHI, K. 2009. Activation of satellite glial cells in rat trigeminal ganglion after upper molar extraction. *Acta histochemica et cytochemica,* 42**,** 143-149.
GUYENET, P. G. 2000. Neural structures that mediate sympathoexcitation during hypoxia. *Respiration physiology,* 121**,** 147-162.
GUYENET, P. G. 2006. The sympathetic control of blood pressure. *Nature Reviews Neuroscience,* 7**,** 335-346.
GUYENET, P. G., STORNETTA, R. L. & BAYLISS, D. A. 2010. Central respiratory chemoreception. *Journal of Comparative Neurology,* 518**,** 3883-3906.
GUYENET, P. G., STORNETTA, R. L., BOCHORISHVILI, G., DEPUY, S. D., BURKE, P. G. & ABBOTT, S. B. 2013. C1 neurons: the body's EMTs. *American Journal of Physiology-Regulatory, Integrative and Comparative Physiology,* 305**,** R187-R204.
GUZMAN-ARANGUEZ, A. & ARGÜESO, P. 2010. Structure and biological roles of mucin-type O-glycans at the ocular surface. *The ocular surface,* 8**,** 8-17.

HAINES, D. E. 2015. Brainstem. *In:* STANDRING, S. (ed.) *Gray's anatomy: the anatomical basis of clinical practice.* Elsevier Health Sciences.

HAMMOND, M. S., SIMS, C., PARAMESHWARAN, K., SUPPIRAMANIAM, V., SCHACHNER, M. & DITYATEV, A. 2006. Neural cell adhesion molecule-associated polysialic acid inhibits NR2B-containing N-methyl-D-aspartate receptors and prevents glutamate-induced cell death. *Journal of Biological Chemistry,* 281**,** 34859-34869.

HANANI, M. 2005. Satellite glial cells in sensory ganglia: from form to function. *Brain research reviews,* 48**,** 457-476.

HANE, M., MATSUOKA, S., ONO, S., MIYATA, S., KITAJIMA, K. & SATO, C. 2015. Protective effects of polysialic acid on proteolytic cleavage of FGF2 and proBDNF/BDNF. *Glycobiology,* 25.10**,** 1112-1124.

HANE, M., SUMIDA, M., KITAJIMA, K. & SATO, C. 2012. Structural and functional impairments of polysialic acid (polySia)-neural cell adhesion molecule (NCAM) synthesized by a mutated polysialyltransferase of a schizophrenic patient. *Pure and Applied Chemistry,* 84**,** 1895-1906.

HARDUIN-LEPERS, A., MOLLICONE, R., DELANNOY, P. & ORIOL, R. 2005. The animal sialyltransferases and sialyltransferase-related genes: a phylogenetic approach. *Glycobiology,* 15**,** 805-817.

HARDUIN-LEPERS, A., VALLEJO-RUIZ, V., KRZEWINSKI-RECCHI, M.-A., SAMYN-PETIT, B., JULIEN, S. & DELANNOY, P. 2001. The human sialyltransferase family. *Biochimie,* 83**,** 727-737.

HE, H.-T., BARBET, J., CHAIX, J.-C. & GORIDIS, C. 1986. Phosphatidylinositol is involved in the membrane attachment of NCAM-120, the smallest component of the neural cell adhesion molecule. *The EMBO journal,* 5**,** 2489.

HE, Q. & MEIRI, K. F. 2002. Isolation and characterization of detergent-resistant microdomains responsive to NCAM-mediated signaling from growth cones. *Molecular and Cellular Neuroscience,* 19**,** 18-31.

HE, X., ZHANG, Q., LIU, Y. & PAN, X. 2007. Cloning and identification of novel microRNAs from rat hippocampus. *Acta biochimica et biophysica Sinica,* 39**,** 708-714.

HEKMAT, A., BITTER-SUERMANN, D. & SCHACHNER, M. 1990. Immunocytological localization of the highly polysialylated form of the neural cell adhesion molecule during development of the murine cerebellar cortex. *Journal of Comparative Neurology,* 291**,** 457-467.

HEPLER, J. R. & GILMAN, A. G. 1992. G proteins. *Trends in biochemical sciences,* 17**,** 383-387.

HIGUERO, A. M., DÍEZ-REVUELTA, N. & ABAD-RODRÍGUEZ, J. 2016. The sugar code in neuronal physiology. *Histochemistry and Cell Biology***,** 1-11.

HILDEBRANDT, H., BECKER, C., MÜRAU, M., GERARDY-SCHAHN, R. & RAHMANN, H. 1998. Heterogeneous expression of the polysialyltransferases ST8Sia II and ST8Sia IV during postnatal rat brain development. *Journal of neurochemistry,* 71**,** 2339-2348.

HILDEBRANDT, H. & DITYATEV, A. 2013. Polysialic acid in brain development and synaptic plasticity. *SialoGlyco Chemistry and Biology I.* Springer.

HILDEBRANDT, H., MÜHLENHOFF, M. & GERARDY-SCHAHN, R. 2010. Polysialylation of NCAM. *Structure and Function of the Neural Cell Adhesion Molecule NCAM.* Springer.

HILDEBRANDT, H., MÜHLENHOFF, M., OLTMANN-NORDEN, I., RÖCKLE, I., BURKHARDT, H., WEINHOLD, B. & GERARDY-SCHAHN, R. 2009. Imbalance of neural cell adhesion molecule and polysialyltransferase alleles causes defective brain connectivity. *Brain,* 132**,** 2831-2838.

HINO, M., KIJIMA-SUDA, I., NAGAI, Y. & HOSOYA, H. 2003. Glycosylation of the alpha and beta tubulin by sialyloligosaccharides. *Zoological science,* 20**,** 709-715.

HINRICHS, J. M. & LLEWELLYN-SMITH, I. J. 2009. Variability in the occurrence of nitric oxide synthase immunoreactivity in different populations of rat sympathetic preganglionic neurons. *Journal of Comparative Neurology,* 514**,** 492-506.

HIOKI, H., KAMEDA, H., NAKAMURA, H., OKUNOMIYA, T., OHIRA, K., NAKAMURA, K., KURODA, M., FURUTA, T. & KANEKO, T. 2007. Efficient gene transduction of neurons by lentivirus with enhanced neuron-specific promoters. *Gene therapy,* 14**,** 872-882.
HIRN, M., PIERRES, M., DEAGOSTINI-BAZIN, H., HIRSCH, M. & GORIDIS, C. 1981. Monoclonal antibody against cell surface glycoprotein of neurons. *Brain research,* 214**,** 433-439.
HIROOKA, Y., POLSON, J., POTTS, P. & DAMPNEY, R. 1997. Hypoxia-induced Fos expression in neurons projecting to the pressor region in the rostral ventrolateral medulla. *Neuroscience,* 80**,** 1209-1224.
HJORTØ, G. M., LARSEN, O., STEEN, A., DAUGVILAITE, V., BERG, C., FARES, S., HANSEN, M., ALI, S. & ROSENKILDE, M. M. 2016. Differential CCR7 targeting in dendritic cells by three naturally occurring CC-chemokines. *Frontiers in Immunology*, 7.
HOEHME, S., FRIEBEL, A., HAMMAD, S., DRASDO, D. & HENGSTLER, J. G. 2017. Creation of Three-Dimensional Liver Tissue Models from Experimental Images for Systems Medicine. *In:* STOCK, P. & CHRIST, B. (eds.) *Hepatocyte Transplantation: Methods and Protocols.* New York, USA: Humana Press.
HOLM, T. H. & LYKKE-HARTMANN, K. 2016. Insights into the pathology of the α3 Na+/K+-ATPase ion pump in neurological disorders; lessons from animal models. *Frontiers in Physiology,* 7.
HORIUCHI, J. & DAMPNEY, R. 2002. Evidence for tonic disinhibition of RVLM sympathoexcitatory neurons from the caudal pressor area. *Autonomic Neuroscience,* 99**,** 102-110.
HORIUCHI, J., POTTS, P., POLSON, J. & DAMPNEY, R. 1999. Distribution of neurons projecting to the rostral ventrolateral medullary pressor region that are activated by sustained hypotension. *Neuroscience,* 89**,** 1319-1329.
HORSTKORTE, R., SCHACHNER, M., MAGYAR, J. P., VORHERR, T. & SCHMITZ, B. 1993. The fourth immunoglobulin-like domain of NCAM contains a carbohydrate recognition domain for oligomannosidic glycans implicated in association with L1 and neurite outgrowth. *The Journal of cell biology,* 121**,** 1409-1421.
HOYK, Z., PARDUCZ, A. & THEODOSIS, D. 2001. The highly sialylated isoform of the neural cell adhesion molecule is required for estradiol-induced morphological synaptic plasticity in the adult arcuate nucleus. *European Journal of Neuroscience,* 13**,** 649-656.
HROMATKA, B. S., DRAKE, P. M., KAPIDZIC, M., STOLP, H., GOLDFIEN, G. A., SHIH, I.-M. & FISHER, S. J. 2013. Polysialic acid enhances the migration and invasion of human cytotrophoblasts. *Glycobiology,* 23**,** 593-602.
HSIEH, Y.-H., DICK, T. E. & SIEGEL, R. E. 2008. Adaptation to hypobaric hypoxia involves GABAA receptors in the pons. *American Journal of Physiology-Regulatory, Integrative and Comparative Physiology,* 294**,** R549-R557.
HU, H., TOMASIEWICZ, H., MAGNUSON, T. & RUTISHAUSER, U. 1996. The role of polysialic acid in migration of olfactory bulb interneuron precursors in the subventricular zone. *Neuron,* 16**,** 735-743.
HUFF, R. M., AXTON, J. M. & NEER, E. 1985. Physical and immunological characterization of a guanine nucleotide-binding protein purified from bovine cerebral cortex. *Journal of Biological Chemistry,* 260**,** 10864-10871.
HULSE, R., WYNICK, D. & DONALDSON, L. F. 2010. Intact cutaneous C fibre afferent properties in mechanical and cold neuropathic allodynia. *European Journal of Pain,* 14**,** 565. e1-565. e10.
HYLDEN, J. L., ANTON, F. & NAHIN, R. L. 1989. Spinal lamina I projection neurons in the rat: collateral innervation of parabrachial area and thalamus. *Neuroscience,* 28**,** 27-37.
ICHIMURA, T., ISOBE, T., OKUYAMA, T., TAKAHASHI, N., ARAKI, K., KUWANO, R. & TAKAHASHI, Y. 1988. Molecular cloning of cDNA coding for brain-specific 14-3-3 protein, a protein kinase-dependent activator of tyrosine and tryptophan hydroxylases. *Proceedings of the National Academy of Sciences,* 85**,** 7084-7088.
IKEDA, H., HEINKE, B., RUSCHEWEYH, R. & SANDKÜHLER, J. 2003. Synaptic plasticity in spinal lamina I projection neurons that mediate hyperalgesia. *Science,* 299**,** 1237-1240.

IKEDA, H., STARK, J., FISCHER, H., WAGNER, M., DRDLA, R., JÄGER, T. & SANDKÜHLER, J. 2006. Synaptic amplifier of inflammatory pain in the spinal dorsal horn. *Science,* 312**,** 1659-1662.
ILEGEMS, E., IWATSUKI, K., KOKRASHVILI, Z., BENARD, O., NINOMIYA, Y. & MARGOLSKEE, R. F. 2010. REEP2 enhances sweet receptor function by recruitment to lipid rafts. *The Journal of Neuroscience,* 30**,** 13774-13783.
INOKO, E., NISHIURA, Y., TANAKA, H., TAKAHASHI, T., FURUKAWA, K., KITAJIMA, K. & SATO, C. 2010. Developmental stage-dependent expression of an α2, 8-trisialic acid unit on glycoproteins in mouse brain. *Glycobiology,* 20**,** 916-928.
INOUE, S. & IWASAKI, M. 1978. Isolation of a novel glycoprotein from the eggs of rainbow trout: occurrence of disialosyl groups on all carbohydrate chains. *Biochemical and biophysical research communications,* 83**,** 1018-1023.
IRIKI, M. & SIMON, E. 2012. Differential control of efferent sympathetic activity revisited. *The Journal of Physiological Sciences,* 62**,** 275-298.
ISAKSEN, T. J. & LYKKE-HARTMANN, K. 2016. Insights into the Pathology of the α2-Na+/K+-ATPase in Neurological Disorders; Lessons from Animal Models. *Frontiers in physiology,* 7.
ISOMURA, R., KITAJIMA, K. & SATO, C. 2011. Structural and functional impairments of polysialic acid by a mutated polysialyltransferase found in schizophrenia. *Journal of Biological Chemistry,* 286**,** 21535-21545.
IWATA, K., IMAMURA, Y., HONDA, K. & SHINODA, M. 2011. Physiological mechanisms of neuropathic pain: the orofacial region. *Int Rev Neurobiol,* 97**,** 227-250.
JACOBSEN, J., KISELYOV, V., BOCK, E. & BEREZIN, V. 2008. A peptide motif from the second fibronectin module of the neural cell adhesion molecule, NCAM, NLIKQDDGGSPIRHY, is a binding site for the FGF receptor. *Neurochemical research,* 33**,** 2532-2539.
JAHN, R., SCHIEBLER, W., OUIMET, C. & GREENGARD, P. 1985. A 38,000-dalton membrane protein (p38) present in synaptic vesicles. *Proceedings of the National Academy of Sciences,* 82**,** 4137-4141.
JAKOBSSON, E., SCHWARZER, D., JOKILAMMI, A. & FINNE, J. 2012. Endosialidases: versatile tools for the study of polysialic acid. *SialoGlyco Chemistry and Biology II.* Springer.
JAMES, W. M. & AGNEW, W. S. 1987. Multiple oligosaccharide chains in the voltage-sensitive Na channel from Electrophorus electricus: evidence for α-2, 8-linked polysialic acid. *Biochemical and biophysical research communications,* 148**,** 817-826.
JIANG, M., GOLD, M. S., BOULAY, G., SPICHER, K., PEYTON, M., BRABET, P., SRINIVASAN, Y., RUDOLPH, U., ELLISON, G. & BIRNBAUMER, L. 1998. Multiple neurological abnormalities in mice deficient in the G protein Go. *Proceedings of the National Academy of Sciences,* 95**,** 3269-3274.
JOHNSON, C. P., FUJIMOTO, I., RUTISHAUSER, U. & LECKBAND, D. E. 2005. Direct evidence that neural cell adhesion molecule (NCAM) polysialylation increases intermembrane repulsion and abrogates adhesion. *Journal of Biological Chemistry,* 280**,** 137-145.
JU, G., HÖKFELT, T., BRODIN, E., FAHRENKRUG, J., FISCHER, J., FREY, P., ELDE, R. & BROWN, J. 1987. Primary sensory neurons of the rat showing calcitonin gene-related peptide immunoreactivity and their relation to substance P-, somatostatin-, galanin-, vasoactive intestinal polypeptide-and cholecystokinin-immunoreactive ganglion cells. *Cell and tissue research,* 247**,** 417-431.
K. GUNJIGAKE, K., GOTO, T., NAKAO, K., KOBAYASHI, S. & YAMAGUCHI, K. 2009. Activation of satellite glial cells in rat trigeminal ganglion after upper molar extraction. *Acta histochemica et cytochemica,* 42**,** 143-149.
KALIA, M. & SULLIVAN, J. M. 1982. Brainstem projections of sensory and motor components of the vagus nerve in the rat. *Journal of Comparative Neurology,* 211**,** 248-264.
KANATO, Y., KITAJIMA, K. & SATO, C. 2008. Direct binding of polysialic acid to a brain-derived neurotrophic factor depends on the degree of polymerization. *Glycobiology,* 18**,** 1044-1053.

KANJHAN, R., LIPSKI, J., KRUSZEWSKA, B. & RONG, W. 1995. A comparative study of pre-sympathetic and Bötzinger neurons in the rostral ventrolateral medulla (RVLM) of the rat. *Brain research,* 699**,** 19-32.

KAPILA, A., CHAKERES, D. W. & BLANCO, E. 1984. The Meckel cave: computed tomographic study. Part I: Normal anatomy; Part II: Pathology. *Radiology,* 152**,** 425-433.

KAREMAKER, J. & STRACKEE, J. 1987. Hemodynamic fluctuations and baroreflex sensitivity in humans: a beat-to-beat model. *American Journal of Physiology-Heart and Circulatory Physiology,* 253**,** H680-H689.

KATAGIRI, A., SHINODA, M., HONDA, K., TOYOFUKU, A., SESSLE, B. J. & IWATA, K. 2012. Satellite glial cell P2Y 12 receptor in the trigeminal ganglion is involved in lingual neuropathic pain mechanisms in rats. *Molecular pain,* 8**,** 1.

KAUR, G., HEERA, P. K. & SRIVASTAVA, L. K. 2002. Neuroendocrine plasticity in GnRH release during rat estrous cycle: correlation with molecular markers of synaptic remodeling. *Brain research,* 954**,** 21-31.

KAWANO, Y., YOSHIMURA, T., TSUBOI, D., KAWABATA, S., KANEKO-KAWANO, T., SHIRATAKI, H., TAKENAWA, T. & KAIBUCHI, K. 2005. CRMP-2 is involved in kinesin-1-dependent transport of the Sra-1/WAVE1 complex and axon formation. *Molecular and cellular biology,* 25**,** 9920-9935.

KELM, S. & SCHAUER, R. 1997. Sialic acids in molecular and cellular interactions. *International review of cytology,* 175**,** 137-240.

KEMPERMANN, G. & GAGE, F. H. Neurogenesis in the adult hippocampus. Neural Transplantation in Neurodegenerative Disease: Current Status and New Directions: Novartis Foundation Symposium 231, 2000. Wiley Online Library, 220-241.

KHANNA, R., WILSON, S. M., BRITTAIN, J. M., WEIMER, J., SULTANA, R., BUTTERFIELD, A. & HENSLEY, K. 2012. Opening Pandora's jar: a primer on the putative roles of CRMP2 in a panoply of neurodegenerative, sensory and motor neuron, and central disorders. *Future neurology,* 7**,** 749-771.

KIERMAIER, E., MOUSSION, C., VELDKAMP, C. T., GERARDY-SCHAHN, R., DE VRIES, I., WILLIAMS, L. G., CHAFFEE, G. R., PHILLIPS, A. J., FREIBERGER, F. & IMRE, R. 2016. Polysialylation controls dendritic cell trafficking by regulating chemokine recognition. *Science,* 351**,** 186-190.

KIM, J. H., SIZOV, I., DOBRETSOV, M. & VON GERSDORFF, H. 2007. Presynaptic Ca2+ buffers control the strength of a fast post-tetanic hyperpolarization mediated by the α3 Na+/K+-ATPase. *Nature neuroscience,* 10**,** 196-205.

KISELYOV, V. V., SOROKA, V., BEREZIN, V. & BOCK, E. 2005. Structural biology of NCAM homophilic binding and activation of FGFR. *Journal of neurochemistry,* 94**,** 1169-1179.

KISS, J. Z. & ROUGON, G. 1997. Cell biology of polysialic acid. *Current opinion in neurobiology,* 7**,** 640-646.

KISS, J. Z., WANG, C. & ROUGON, G. 1993. Nerve-dependent expression of high polysialic acid neural cell adhesion molecule in neurohypophysial astrocytes of adult rats. *Neuroscience,* 53**,** 213-221.

KITAZUME, S., KITAJIMA, K., INOUE, S., TROY, F., CHO, J.-W., LENNARZ, W. J. & INOUE, Y. 1994. Identification of polysialic acid-containing glycoprotein in the jelly coat of sea urchin eggs. Occurrence of a novel type of polysialic acid structure. *Journal of Biological Chemistry,* 269**,** 22712-22718.

KJELLÉN, L. & LINDAHL, U. 1991. Proteoglycans: structures and interactions. *Annual review of biochemistry,* 60**,** 443-475.

KOCHLAMAZASHVILI, G., SENKOV, O., GREBENYUK, S., ROBINSON, C., XIAO, M.-F., STUMMEYER, K., GERARDY-SCHAHN, R., ENGEL, A. K., FEIG, L. & SEMYANOV, A. 2010. Neural cell adhesion molecule-associated polysialic acid regulates synaptic plasticity and learning by restraining the signaling through GluN2B-containing NMDA receptors. *The Journal of Neuroscience,* 30**,** 4171-4183.

KOGANEZAWA, T. & PATON, J. F. 2014. Intrinsic chemosensitivity of rostral ventrolateral medullary sympathetic premotor neurons in the in situ arterially perfused preparation of rats. *Experimental physiology,* 99**,** 1453-1466.
KOGANEZAWA, T. & TERUI, N. 2007. Differential responsiveness of RVLM sympathetic premotor neurons to hypoxia in rabbits. *American Journal of Physiology-Heart and Circulatory Physiology,* 292**,** H408-H414.
KOJIMA, N., TACHIDA, Y., YOSHIDA, Y. & TSUJI, S. 1996. Characterization of Mouse ST8Sia II (STX) as a Neural Cell Adhesion Molecule-specific Polysialic Acid Synthase REQUIREMENT OF CORE α1, 6-LINKED FUCOSE AND A POLYPEPTIDE CHAIN FOR POLYSIALYLATION. *Journal of Biological Chemistry,* 271**,** 19457-19463.
KOJIMA, N., YOSHIDA, Y., KUROSAWA, N., LEE, Y.-C. & TSUJI, S. 1995. Enzymatic activity of a developmentally regulated member of the sialyltransferase family (STX): evidence for α2, 8-sialyltransferase activity toward N-linked oligosaccharides. *FEBS letters,* 360**,** 1-4.
KOLLAI, M., KOIZUMI, K. & BROOKS, C. M. 1978. Nature of differential sympathetic discharges in chemoreceptor reflexes. *Proceedings of the National Academy of Sciences,* 75**,** 5239-5243.
KORNACK, D. R. & RAKIC, P. 2001. The generation, migration, and differentiation of olfactory neurons in the adult primate brain. *Proceedings of the National Academy of Sciences,* 98**,** 4752-4757.
KORNFELD, R. & KORNFELD, S. 1980. Structure of glycoproteins and their oligosaccharide units. *In:* LENNARZ, W. (ed.) *The biochemistry of glycoproteins and proteoglycans.* 1st ed. New York Plenum Press.
KORSHUNOVA, I. & MOSEVITSKY, M. 2010. Role of the growth-associated protein GAP-43 in NCAM-mediated neurite outgrowth. *Structure and Function of the Neural Cell Adhesion Molecule NCAM.* Springer.
KOSHIYA, N. & GUYENET, P. 1996. NTS neurons with carotid chemoreceptor inputs arborize in the rostral ventrolateral medulla. *American Journal of Physiology-Regulatory, Integrative and Comparative Physiology,* 270**,** R1273-R1278.
KOSHIYA, N., HUANGFU, D. & GUYENET, P. G. 1993. Ventrolateral medulla and sympathetic chemoreflex in the rat. *Brain research,* 609**,** 174-184.
KROG, L., OLSEN, M., DALSEG, A. M., ROTH, J. & BOCK, E. 1992. Characterization of soluble neural cell adhesion molecule in rat brain, CSF, and plasma. *Journal of neurochemistry,* 59**,** 838-847.
KUDO, M., KITAJIMA, K., INOUE, S., SHIOKAWA, K., MORRIS, H. R., DELL, A. & INOUE, Y. 1996. Characterization of the major core structures of the α2→ 8-linked polysialic acid-containing glycan chains present in neural cell adhesion molecule in embryonic chick brains. *Journal of Biological Chemistry,* 271**,** 32667-32677.
KUROSAWA, N., YOSHIDA, Y., KOJIMA, N. & TSUJI, S. 1997. Polysialic acid synthase (ST8Sia II/STX) mRNA expression in the developing mouse central nervous system. *Journal of neurochemistry,* 69**,** 494-503.
LA SALLE, G. L. G., ROUGON, G. & VALIN, A. 1992a. The embryonic form of neural cell surface molecule (E-NCAM) in the rat hippocampus and its reexpression on glial cells following kainic acid-induced status epilepticus. *The Journal of neuroscience,* 12**,** 872-882.
LA SALLE, G. L. G., ROUGON, G. & VALIN, A. 1992b. The embryonic form of neural cell surface molecule (E-NCAM) in the rat hippocampus and its reexpression on glial cells following kainic acid-induced status epilepticus. *Journal of Neuroscience,* 12**,** 872-882.
LANDMESSER, L., DAHM, L., TANG, J. & RUTISHAUSER, U. 1990. Polysialic acid as a regulator of intramuscular nerve branching during embryonic development. *Neuron,* 4**,** 655-667.
LARSSON, M. 2017. Pax2 is persistently expressed by GABAergic neurons throughout the adult rat dorsal horn. *Neuroscience letters,* 638**,** 96-101.
LATREMOLIERE, A. & WOOLF, C. J. 2009. Central sensitization: a generator of pain hypersensitivity by central neural plasticity. *The Journal of Pain,* 10**,** 895-926.

LAUBER, M. A., YU, Y.-Q., BROUSMICHE, D. W., HUA, Z., KOZA, S. M., MAGNELLI, P., GUTHRIE, E., TARON, C. H. & FOUNTAIN, K. J. 2015. Rapid preparation of released N-glycans for HILIC analysis using a labeling reagent that facilitates sensitive fluorescence and ESI-MS detection. *Analytical chemistry,* 87**,** 5401-5409.

LAWSON, S., CREPPS, B. & PERL, E. 1997. Relationship of substance P to afferent characteristics of dorsal root ganglion neurones in guinea-pig. *The Journal of physiology,* 505**,** 177-191.

LAWSON, S. N. 1992. Morphological and biochemical cell types of sensory neurons. *In:* SCOTT, S. A. (ed.) *Sensory neurons: diversity, development and plasticity. Oxford University Press, New York.* New York: Oxford University Press.

LAZAROV, N. E. 2002. Comparative analysis of the chemical neuroanatomy of the mammalian trigeminal ganglion and mesencephalic trigeminal nucleus. *Progress in neurobiology,* 66**,** 19-59.

LEAK, J., MENETREY, D. & DE POMMERY, J. 1988. Neuropeptides in long ascending spinal tract cells in the rat: evidence for parallel processing of ascending information. *Neuroscience,* 24**,** 195-207.

LESHCHYNS' KA, I., SYTNYK, V., MORROW, J. S. & SCHACHNER, M. 2003. Neural cell adhesion molecule (NCAM) association with PKCβ2 via βI spectrin is implicated in NCAM-mediated neurite outgrowth. *The Journal of cell biology,* 161**,** 625-639.

LI, D., HÉRAULT, K., SILM, K., EVRARD, A., WOJCIK, S., OHEIM, M., HERZOG, E. & ROPERT, N. 2013. Lack of evidence for vesicular glutamate transporter expression in mouse astrocytes. *Journal of Neuroscience,* 33**,** 4434-4455.

LIEBEROTH, A., SPLITTSTOESSER, F., KATAGIHALLIMATH, N., JAKOVCEVSKI, I., LOERS, G., RANSCHT, B., KARAGOGEOS, D., SCHACHNER, M. & KLEENE, R. 2009. Lewisx and α2, 3-sialyl glycans and their receptors TAG-1, Contactin, and L1 mediate CD24-dependent neurite outgrowth. *Journal of Neuroscience,* 29**,** 6677-6690.

LIEDTKE, S., GEYER, H., WUHRER, M., GEYER, R., FRANK, G., GERARDY-SCHAHN, R., ZÄHRINGER, U. & SCHACHNER, M. 2001. Characterization of N-glycans from mouse brain neural cell adhesion molecule. *Glycobiology,* 11**,** 373-384.

LIGHT, A. R. & PERL, E. 1979. Spinal termination of functionally identified primary afferent neurons with slowly conducting myelinated fibers. *Journal of Comparative Neurology,* 186**,** 133-150.

LIGURI, G., TADDEI, N., NASSI, P., LATORRACA, S., NEDIANI, C. & SORBI, S. 1990. Changes in Na+, K+-ATPase, Ca 2+-ATPase and some soluble enzymes related to energy metabolism in brains of patients with Alzheimer's disease. *Neuroscience letters,* 112**,** 338-342.

LIMÓN, I. D., RAMÍREZ, E., DÍAZ, A., MENDIETA, L., MAYORAL, M. Á., ESPINOSA, B., GUEVARA, J. & ZENTENO, E. 2011. Alteration of the sialylation pattern and memory deficits by injection of Aβ (25–35) into the hippocampus of rats. *Neuroscience letters,* 495**,** 11-16.

LIPSKI, J. 1981. Antidromic activation of neurones as an analytic tool in the study of the central nervous system. *Journal of neuroscience methods,* 4**,** 1-32.

LIPSKI, J., KANJHAN, R., KRUSZEWSKA, B. & SMITH, M. 1995. Barosensitive neurons in the rostral ventrolateral medulla of the rat in vivo: morphological properties and relationship to C1 adrenergic neurons. *Neuroscience,* 69**,** 601-618.

LIS, H. & SHARON, N. 1993. Protein glycosylation. Structural and functional aspects. *European Journal of Biochemistry,* 218**,** 1-27.

LIU, C.-N., WALL, P. D., BEN-DOR, E., MICHAELIS, M., AMIR, R. & DEVOR, M. 2000. Tactile allodynia in the absence of C-fiber activation: altered firing properties of DRG neurons following spinal nerve injury. *Pain,* 85**,** 503-521.

LIU, X., SHEN, Y., XIE, J., BAO, H., CAO, Q., WAN, R., XU, X., ZHOU, H., HUANG, L. & XU, Z. 2017. A mutation in the CACNA1C gene leads to early repolarization syndrome with incomplete penetrance: A Chinese family study. *PloS one,* 12**,** e0177532.

LIU, Z., ZHANG, J., WU, L., LIU, J. & ZHANG, M. 2014. Overexpression of GNAO1 correlates with poor prognosis in patients with gastric cancer and plays a role in gastric cancer cell proliferation and apoptosis. *International journal of molecular medicine,* 33**,** 589-596.

LIUZZI, F. J. & LASEK, R. J. 1987. Astrocytes block axonal regeneration in mammals by activating the physiological stop pathway. *Science,* 237**,** 642-645.
LIVINGSTON, B. D. & PAULSON, J. 1993. Polymerase chain reaction cloning of a developmentally regulated member of the sialyltransferase gene family. *Journal of Biological Chemistry,* 268**,** 11504-11507.
LLEWELLYN-SMITH, I. J. 2009. Anatomy of synaptic circuits controlling the activity of sympathetic preganglionic neurons. *Journal of chemical neuroanatomy,* 38**,** 231-239.
LLEWELLYN-SMITH, I. J. 2011. Sympathetic Preganglionic Neurons. *In:* LLEWELLYN-SMITH, I. J. & VERBERNE, A. J. (eds.) *Central regulation of autonomic functions.* second ed. New York: Oxford University Press.
LLEWELLYN-SMITH, I. J., DICARLO, S. E., COLLINS, H. L. & KEAST, J. R. 2005. Enkephalin-immunoreactive interneurons extensively innervate sympathetic preganglionic neurons regulating the pelvic viscera. *Journal of Comparative Neurology,* 488**,** 278-289.
LOERS, G., ASTAFIEV, S., HAPIAK, Y., SAINI, V., MISHRA, B., GUL, S., KAUR, G., SCHACHNER, M. & THEIS, T. 2017. The polysialic acid mimetics idarubicin and irinotecan stimulate neuronal survival and neurite outgrowth and signal via protein kinase C. *Journal of Neurochemistry*.
LOERS, G., SAINI, V., MISHRA, B., GUL, S., CHAUDHURY, S., WALLQVIST, A., KAUR, G. & SCHACHNER, M. 2016. Vinorelbine and epirubicin share common features with polysialic acid and modulate neuronal and glial functions. *Journal of neurochemistry,* 136**,** 48-62.
LORENZO, L. E., RAMIEN, M., ST LOUIS, M., DE KONINCK, Y. & RIBEIRO-DA-SILVA, A. 2008. Postnatal changes in the Rexed lamination and markers of nociceptive afferents in the superficial dorsal horn of the rat. *Journal of Comparative Neurology,* 508**,** 592-604.
LUAN, G., GAO, Q., ZHAI, F., CHEN, Y. & LI, T. 2016. Upregulation of HMGB1, toll-like receptor and RAGE in human Rasmussen's encephalitis. *Epilepsy research,* 123**,** 36-49.
LUDLOW, C. L. 2015. Central nervous system control of voice and swallowing. *Journal of clinical neurophysiology: official publication of the American Electroencephalographic Society,* 32**,** 294.
LUO, C., KUNER, T. & KUNER, R. 2014. Synaptic plasticity in pathological pain. *Trends in neurosciences,* 37**,** 343-355.
LUO, J., BO, X., WU, D., YEH, J., RICHARDSON, P. M. & ZHANG, Y. 2011. Promoting survival, migration, and integration of transplanted Schwann cells by over-expressing polysialic acid. *Glia,* 59**,** 424-434.
LUSKIN, M. B., ZIGOVA, T., SOTERES, B. J. & STEWART, R. R. 1997. Neuronal progenitor cells derived from the anterior subventricular zone of the neonatal rat forebrain continue to proliferatein vitroand express a neuronal phenotype. *Molecular and Cellular Neuroscience,* 8**,** 351-366.
LYNN, B. 1984. Effect of neonatal treatment with capsaicin on the numbers and properties of cutaneous afferent units from the hairy skin of the rat. *Brain research,* 322**,** 255-260.
MACFARLANE, P. & MITCHELL, G. 2008. Respiratory long-term facilitation following intermittent hypoxia requires reactive oxygen species formation. *Neuroscience,* 152**,** 189-197.
MACKIE, M., HUGHES, D., MAXWELL, D., TILLAKARATNE, N. & TODD, A. 2003. Distribution and colocalisation of glutamate decarboxylase isoforms in the rat spinal cord. *Neuroscience,* 119**,** 461-472.
MADDEN, C. J., STOCKER, S. D. & SVED, A. F. 2006. Attenuation of homeostatic responses to hypotension and glucoprivation after destruction of catecholaminergic rostral ventrolateral medulla neurons. *American Journal of Physiology-Regulatory, Integrative and Comparative Physiology,* 291**,** R751-R759.
MADDEN, C. J. & SVED, A. F. 2003. Cardiovascular regulation after destruction of the C1 cell group of the rostral ventrolateral medulla in rats. *American Journal of Physiology-Heart and Circulatory Physiology,* 285**,** H2734-H2748.
MAHAMED, S. & MITCHELL, G. S. 2008. Simulated apnoeas induce serotonin-dependent respiratory long-term facilitation in rats. *The Journal of physiology,* 586**,** 2171-2181.

MAKAR, T. K., GERZANICH, V., NIMMAGADDA, V. K., JAIN, R., LAM, K., MUBARIZ, F., TRISLER, D., IVANOVA, S., WOO, S. K. & KWON, M. S. 2015. Silencing of Abcc8 or inhibition of newly upregulated Sur1-Trpm4 reduce inflammation and disease progression in experimental autoimmune encephalomyelitis. *Journal of neuroinflammation,* 12**,** 210.

MALAISSE, W. & ORCI, L. 1978. The role of the cytoskeleton in pancreatic B-cell function. *Methods and achievements in experimental pathology,* 9**,** 112-136.

MANCIA, G., PARATI, G., POMIDOSSI, G., CASADEI, R., DI RIENZO, M. & ZANCHETTI, A. 1986. Arterial baroreflexes and blood pressure and heart rate variabilities in humans. *Hypertension,* 8**,** 147-153.

MANESS, P. F. & SCHACHNER, M. 2007. Neural recognition molecules of the immunoglobulin superfamily: signaling transducers of axon guidance and neuronal migration. *Nature neuroscience,* 10**,** 19-26.

MARFURT, C. F. 1981. The somatotopic organization of the cat trigeminal ganglion as determined by the horseradish peroxidase technique. *The Anatomical Record,* 201**,** 105-118.

MARGOLIS, R., PRETI, C., LAI, D. & MARGOLIS, R. 1976. Developmental changes in brain glycoproteins. *Brain research,* 112**,** 363-369.

MARINA, N., ABDALA, A. P., KORSAK, A., SIMMS, A. E., ALLEN, A. M., PATON, J. F. & GOURINE, A. V. 2011. Control of sympathetic vasomotor tone by catecholaminergic C1 neurones of the rostral ventrolateral medulla oblongata. *Cardiovascular research,* 91**,** 703-710.

MARINO, P., NORREEL, J.-C., SCHACHNER, M., ROUGON, G. & AMOUREUX, M.-C. 2009. A polysialic acid mimetic peptide promotes functional recovery in a mouse model of spinal cord injury. *Experimental neurology,* 219**,** 163-174.

MARTH, J. D. & GREWAL, P. K. 2008. Mammalian glycosylation in immunity. *Nature Reviews Immunology,* 8**,** 874-887.

MARTINS-DE-SOUZA, D., CASSOLI, J. S., NASCIMENTO, J. M., HENSLEY, K., GUEST, P. C., PINZON-VELASCO, A. M. & TURCK, C. W. 2015. The protein interactome of collapsin response mediator protein-2 (CRMP2/DPYSL2) reveals novel partner proteins in brain tissue. *PROTEOMICS-Clinical Applications,* 9**,** 817-831.

MAXWELL, D. J., BELLE, M. D., CHEUNSUANG, O., STEWART, A. & MORRIS, R. 2007. Morphology of inhibitory and excitatory interneurons in superficial laminae of the rat dorsal horn. *The Journal of physiology,* 584**,** 521-533.

MCALLEN, R. 1986. Action and specificity of ventral medullary vasopressor neurones in the cat. *Neuroscience,* 18**,** 51-59.

MCALLEN, R. & MAY, C. 1994. Effects of preoptic warming on subretrofacial and cutaneous vasoconstrictor neurons in anaesthetized cats. *The Journal of physiology,* 481**,** 719.

MCAULEY, E. Z., SCIMONE, A., TIWARI, Y., AGAHI, G., MOWRY, B. J., HOLLIDAY, E. G., DONALD, J. A., WEICKERT, C. S., MITCHELL, P. B. & SCHOFIELD, P. R. 2012. Identification of sialyltransferase 8B as a generalized susceptibility gene for psychotic and mood disorders on chromosome 15q25-26. *PloS one,* 7**,** e38172.

MCCALL, T., WEIL, Z. M., NACHER, J., BLOSS, E. B., EL MAAROUF, A., RUTISHAUSER, U. & MCEWEN, B. S. 2013. Depletion of polysialic acid from neural cell adhesion molecule (PSA-NCAM) increases CA3 dendritic arborization and increases vulnerability to excitotoxicity. *Experimental neurology,* 241**,** 5-12.

MCMAHON, H. T. & BOUCROT, E. 2011. Molecular mechanism and physiological functions of clathrin-mediated endocytosis. *Nature reviews Molecular cell biology,* 12**,** 517-533.

MCMULLAN, S., DICK, T. E., FARNHAM, M. M. & PILOWSKY, P. M. 2009. Effects of baroreceptor activation on respiratory variability in rat. *Respiratory physiology & neurobiology,* 166**,** 80-86.

MEHANNA, A., JAKOVCEVSKI, I., ACAR, A., XIAO, M., LOERS, G., ROUGON, G., IRINTCHEV, A. & SCHACHNER, M. 2010. Polysialic acid glycomimetic promotes functional recovery and plasticity after spinal cord injury in mice. *Molecular Therapy,* 18**,** 34-43.

MENDELL, L. M. 1966. Physiological properties of unmyelinated fiber projection to the spinal cord. *Experimental neurology,* 16**,** 316-332.
MENDELL, L. M. & WALL, P. D. 1965. Responses of single dorsal cord cells to peripheral cutaneous unmyelinated fibres. *Nature,* 206**,** 97-99.
MERAT, A. & DICKERSON, J. 1973. The effect of development on the gangliosides of rat and pig brain. *Journal of neurochemistry,* 20**,** 873-880.
MICHAEL, G., AVERILL, S., NITKUNAN, A., RATTRAY, M., BENNETT, D., YAN, Q. & PRIESTLEY, J. 1997. Nerve growth factor treatment increases brain-derived neurotrophic factor selectively in TrkA-expressing dorsal root ganglion cells and in their central terminations within the spinal cord. *The Journal of neuroscience,* 17**,** 8476-8490.
MIKKONEN, M., SOININEN, H., KÄLVIÄINEN, R., TAPIOLA, T., YLINEN, A., VAPALAHTI, M., PALJÄRVI, L. & PITKÄNEN, A. 1998. Remodeling of neuronal circuitries in human temporal lobe epilepsy: increased expression of highly polysialylated neural cell adhesion molecule in the hippocampus and the entorhinal cortex. *Annals of neurology,* 44**,** 923-934.
MIKKONEN, M., SOININEN, H., TAPIOLA, T., ALAFUZOFF, I. & MIETTINEN, R. 1999. Hippocampal plasticity in Alzheimer's disease: changes in highly polysialylated NCAM immunoreactivity in the hippocampal formation. *European Journal of Neuroscience,* 11**,** 1754-1764.
MILEV, P., MAUREL, P., HÄRING, M., MARGOLIS, R. K. & MARGOLIS, R. U. 1996. TAG-1/axonin-1 is a high-affinity ligand of neurocan, phosphacan/protein-tyrosine phosphatase-ζ/β, and N-CAM. *Journal of Biological Chemistry,* 271**,** 15716-15723.
MILLAN, M. J. 1999. The induction of pain: an integrative review. *Progress in neurobiology,* 57**,** 1-164.
MILLER, P., STYREN, S., LAGENAUR, C. & DEKOSKY, S. 1994. Embryonic neural cell adhesion molecule (N-CAM) is elevated in the denervated rat dentate gyrus. *Journal of Neuroscience,* 14**,** 4217-4225.
MINANA, R., DURAN, J., TOMAS, M., RENAU-PIQUERAS, J. & GUERRI, C. 2001. Neural cell adhesion molecule is endocytosed via a clathrin-dependent pathway. *European Journal of Neuroscience,* 13**,** 749-756.
MIRAGALL, F., KADMON, G., HUSMANN, M. & SCHACHNER, M. 1988. Expression of cell adhesion molecules in the olfactory system of the adult mouse: presence of the embryonic form of N-CAM. *Developmental biology,* 129**,** 516-531.
MIRZAEI, M., SOLTANI, N., SARHADI, E., PASCOVICI, D., KEIGHLEY, T., SALEKDEH, G. H., HAYNES, P. A. & ATWELL, B. J. 2011. Shotgun proteomic analysis of long-distance drought signaling in rice roots. *Journal of proteome research,* 11**,** 348-358.
MISHRA, B., VON DER OHE, M., SCHULZE, C., BIAN, S., MAKHINA, T., LOERS, G., KLEENE, R. & SCHACHNER, M. 2010. Functional role of the interaction between polysialic acid and extracellular histone H1. *The Journal of Neuroscience,* 30**,** 12400-12413.
MITCHELL, G. S., BAKER, T. L., NANDA, S. A., FULLER, D. D., ZABKA, A. G., HODGEMAN, B. A., BAVIS, R. W., MACK, K. J. & OLSON, E. 2001. Invited review: Intermittent hypoxia and respiratory plasticity. *Journal of Applied Physiology,* 90**,** 2466-2475.
MIYAGI, T. & YAMAGUCHI, K. 2012. Mammalian sialidases: physiological and pathological roles in cellular functions. *Glycobiology,* 22**,** 880-896.
MIYAWAKI, T., MINSON, J., ARNOLDA, L., LLEWELLYN-SMITH, I., CHALMERS, J. & PILOWSKY, P. 1996. AMPA/kainate receptors mediate sympathetic chemoreceptor reflex in the rostral ventrolateral medulla. *Brain research,* 726**,** 64-68.
MOLANDER, C., XU, Q. & GRANT, G. 1984. The cytoarchitectonic organization of the spinal cord in the rat. I. The lower thoracic and lumbosacral cord. *Journal of Comparative Neurology,* 230**,** 133-141.
MONLEZUN, S., OUALI, S., POULAIN, D. A. & THEODOSIS, D. T. 2005. Polysialic acid is required for active phases of morphological plasticity of neurosecretory axons and their glia. *Molecular and Cellular Neuroscience,* 29**,** 516-524.

MONTANO, N., GNECCHI-RUSCONE, T., PORTA, A., LOMBARDI, F., MALLIANI, A. & BARMAN, S. M. 1996. Presence of vasomotor and respiratory rhythms in the discharge of single medullary neurons involved in the regulation of cardiovascular system. *Journal of the autonomic nervous system,* 57**,** 116-122.

MONTI, E., BONTEN, E., D'AZZO, A., BRESCIANI, R., VENERANDO, B., BORSANI, G., SCHAUER, R. & TETTAMANTI, G. 2010. Sialidases in vertebrates: a family of enzymes tailored for several cell functions. *Advances in carbohydrate chemistry and biochemistry,* 64**,** 403-479.

MOREIRA, T. S., TAKAKURA, A. C., COLOMBARI, E. & GUYENET, P. G. 2006. Central chemoreceptors and sympathetic vasomotor outflow. *The Journal of physiology,* 577**,** 369-386.

MOREIRA, T. S., TAKAKURA, A. C., COLOMBARI, E. & GUYENET, P. G. 2007. Activation of 5-hydroxytryptamine type 3 receptor-expressing C-fiber vagal afferents inhibits retrotrapezoid nucleus chemoreceptors in rats. *Journal of neurophysiology,* 98**,** 3627-3637.

MOREMEN, K. W. & MOLINARI, M. 2006. N-linked glycan recognition and processing: the molecular basis of endoplasmic reticulum quality control. *Current opinion in structural biology,* 16**,** 592-599.

MOREMEN, K. W., TIEMEYER, M. & NAIRN, A. V. 2012. Vertebrate protein glycosylation: diversity, synthesis and function. *Nature reviews Molecular cell biology,* 13**,** 448-462.

MORRISON, S. F. 1999. RVLM and raphe differentially regulate sympathetic outflows to splanchnic and brown adipose tissue. *American Journal of Physiology-Regulatory, Integrative and Comparative Physiology,* 276**,** R962-R973.

MORRISON, S. F. 2003. Glutamate transmission in the rostral ventrolateral medullary sympathetic premotor pathway. *Cellular and molecular neurobiology,* 23**,** 761-772.

MORRISON, S. F. 2011. 2010 Carl Ludwig Distinguished Lectureship of the APS Neural Control and Autonomic Regulation Section: central neural pathways for thermoregulatory cold defense. *Journal of applied physiology,* 110**,** 1137-1149.

MORRISON, S. F. & CAO, W.-H. 2000. Different adrenal sympathetic preganglionic neurons regulate epinephrine and norepinephrine secretion. *American Journal of Physiology-Regulatory, Integrative and Comparative Physiology,* 279**,** R1763-R1775.

MÜHLENHOFF, M., ECKHARDT, M., BETHE, A., FROSCH, M. & GERARDY-SCHAHN, R. 1996a. Autocatalytic polysialylation of polysialyltransferase-1. *The EMBO Journal,* 15**,** 6943.

MÜHLENHOFF, M., ECKHARDT, M., BETHE, A., FROSCH, M. & GERARDY-SCHAHN, R. 1996b. Polysialylation of NCAM by a single enzyme. *Current Biology,* 6**,** 1188-1191.

MÜHLENHOFF, M., ECKHARDT, M. & GERARDY-SCHAHN, R. 1998. Polysialic acid: three-dimensional structure, biosynthesis and function. *Current opinion in structural biology,* 8**,** 558-564.

MÜHLENHOFF, M., OLTMANN-NORDEN, I., WEINHOLD, B., HILDEBRANDT, H. & GERARDY-SCHAHN, R. 2009. Brain development needs sugar: the role of polysialic acid in controlling NCAM functions. *Biological chemistry,* 390**,** 567-574.

MÜHLENHOFF, M., ROLLENHAGEN, M., WERNEBURG, S., GERARDY-SCHAHN, R. & HILDEBRANDT, H. 2013. Polysialic acid: versatile modification of NCAM, SynCAM 1 and neuropilin-2. *Neurochemical research,* 38**,** 1134-1143.

MUIR, G. M., BROWN, J. E., CAREY, J. P., HIRVONEN, T. P., DELLA SANTINA, C. C., MINOR, L. B. & TAUBE, J. S. 2009. Disruption of the head direction cell signal after occlusion of the semicircular canals in the freely moving chinchilla. *Journal of Neuroscience,* 29**,** 14521-14533.

MULLER, D., DJEBBARA-HANNAS, Z., JOURDAIN, P., VUTSKITS, L., DURBEC, P., ROUGON, G. & KISS, J. Z. 2000. Brain-derived neurotrophic factor restores long-term potentiation in polysialic acid-neural cell adhesion molecule-deficient hippocampus. *Proceedings of the National Academy of Sciences,* 97**,** 4315-4320.

MULLER, D., WANG, C., SKIBO, G., TONI, N., CREMER, H., CALAORA, V., ROUGON, G. & KISS, J. Z. 1996. PSA–NCAM is required for activity-induced synaptic plasticity. *Neuron,* 17**,** 413-422.

MURRAY, B. A. & JENSEN, J. J. 1992. Evidence for heterophilic adhesion of embryonic retinal cells and neuroblastoma cells to substratum-adsorbed NCAM. *The Journal of cell biology,* 117**,** 1311-1320.

NACHER, J., ALONSO-LLOSA, G., ROSELL, D. & MCEWEN, B. 2002. PSA-NCAM expression in the piriform cortex of the adult rat. Modulation by NMDA receptor antagonist administration. *Brain research,* 927**,** 111-121.

NACHER, J., CRESPO, C. & MCEWEN, B. S. 2001. Doublecortin expression in the adult rat telencephalon. *European Journal of Neuroscience,* 14**,** 629-644.

NAIM, M., SPIKE, R. C., WATT, C., SHEHAB, S. A. & TODD, A. J. 1997. Cells in laminae III and IV of the rat spinal cord that possess the neurokinin-1 receptor and have dorsally directed dendrites receive a major synaptic input from tachykinin-containing primary afferents. *The Journal of neuroscience,* 17**,** 5536-5548.

NAKAYAMA, J., FUKUDA, M. N., FREDETTE, B., RANSCHT, B. & FUKUDA, M. 1995. Expression cloning of a human polysialyltransferase that forms the polysialylated neural cell adhesion molecule present in embryonic brain. *Proceedings of the National Academy of Sciences,* 92**,** 7031-7035.

NAMIKAWA, K., SU, Q., KIRYU-SEO, S. & KIYAMA, H. 1998. Enhanced expression of 14-3-3 family members in injured motoneurons. *Molecular brain research,* 55**,** 315-320.

NAN, X., CARUBELLI, I. & STAMATOS, N. M. 2007. Sialidase expression in activated human T lymphocytes influences production of IFN-γ. *Journal of leukocyte biology,* 81**,** 284-296.

NATHANSON, J. L., YANAGAWA, Y., OBATA, K. & CALLAWAY, E. M. 2009. Preferential labeling of inhibitory and excitatory cortical neurons by endogenous tropism of adeno-associated virus and lentivirus vectors. *Neuroscience,* 161**,** 441-450.

NEER, E. J. 1995. Heterotrimeric C proteins: organizers of transmembrane signals. *Cell,* 80**,** 249-257.

NEER, E. J., LOK, J. & WOLF, L. 1984. Purification and properties of the inhibitory guanine nucleotide regulatory unit of brain adenylate cyclase. *Journal of Biological Chemistry,* 259**,** 14222-14229.

NEILSON, K. A., KEIGHLEY, T., PASCOVICI, D., COOKE, B. & HAYNES, P. A. 2013. Label-free quantitative shotgun proteomics using normalized spectral abundance factors. *Proteomics for Biomarker Discovery***,** 205-222.

NELSON, R. W., BATES, P. A. & RUTISHAUSER, U. 1995. Protein determinants for specific polysialylation of the neural cell adhesion molecule. *Journal of Biological Chemistry,* 270**,** 17171-17179.

NGO, L., HAAS, M., QU, Z., LI, S. S., ZENKER, J., TENG, K. S. L., GUNNERSEN, J. M., BREUSS, M., HABGOOD, M. & KEAYS, D. 2014. TUBB5 and its disease-associated mutations influence the terminal differentiation and dendritic spine densities of cerebral cortical neurons. *Human molecular genetics,* 23**,** 5147-5158.

NICHOLS, D. G., GREELEY, W. J., LAPPE, D. G., UNGERLEIDER, R. M., CAMERON, D. E., SPEVAK, P. J. & WETZEL, R. C. 2006. *Critical Heart Disease in Infants and Children E-Book*, Elsevier Health Sciences.

NIELSEN, J., KULAHIN, N. & WALMOD, P. S. 2010. Extracellular protein interactions mediated by the neural cell adhesion molecule, NCAM: heterophilic interactions between NCAM and cell adhesion molecules, extracellular matrix proteins, and viruses. *Structure and function of the neural cell adhesion molecule NCAM.* Springer.

NIETHAMMER, P., DELLING, M., SYTNYK, V., DITYATEV, A., FUKAMI, K. & SCHACHNER, M. 2002. Cosignaling of NCAM via lipid rafts and the FGF receptor is required for neuritogenesis. *J Cell Biol,* 157**,** 521-532.

NOBLE, M., ALBRECHTSEN, M., MØLLERT, C., LYLES, J., BOCK, E., GORIDIS, C., WATANABE, M. & RUTISHAUSER, U. 1985. Glial cells express N-CAM/D2-CAM-like polypeptides in vitro. *Nature,* 316**,** 725-728.

NOMURA, T., YABE, T., ROSENTHAL, E. S., KRZAN, M. & SCHWARTZ, J. P. 2000. PSA-NCAM distinguishes reactive astrocytes in 6-OHDA-lesioned substantia nigra from those in the striatal terminal fields. *Journal of neuroscience research,* 61**,** 588-596.

NORTON, W. & PODUSLO, S. 1973. Myelination in rat brain: changes in myelin composition during brain maturation. *Journal of neurochemistry,* 21**,** 759.

NOWYCKY, M. C., WU, G. & LEDEEN, R. W. 2014. Glycobiology of ion transport in the nervous system. *Glycobiology of the Nervous System.* Springer.

NYBROE, O., ALBRECHTSEN, M., DAHLIN, J., LINNEMANN, D., LYLES, J. M., MDLLER, C. J. & BOCK, E. 1985. Biosynthesis of the Neural Cell Adhesion Characterization of Polypeptide C. *The Journal of cell biology,* 101**,** 2310-2315.

O'CONNELL, A. W., FOX, G. B., BARRY, T., MURPHY, K. J., FICHERA, G., FOLEY, A. G., KELLY, J. & REGAN, C. M. 1997. Spatial learning activates neural cell adhesion molecule polysialylation in a corticohippocampal pathway within the medial temporal lobe. *Journal of neurochemistry,* 68**,** 2538-2546.

OBATA, K., YAMANAKA, H., KOBAYASHI, K., DAI, Y., MIZUSHIMA, T., KATSURA, H., FUKUOKA, T., TOKUNAGA, A. & NOGUCHI, K. 2006. The effect of site and type of nerve injury on the expression of brain-derived neurotrophic factor in the dorsal root ganglion and on neuropathic pain behavior. *Neuroscience,* 137**,** 961-970.

OHTSUBO, K. & MARTH, J. D. 2006. Glycosylation in cellular mechanisms of health and disease. *Cell,* 126**,** 855-867.

OLIAS, G., VIOLLET, C., KUSSEROW, H., EPELBAUM, J. & MEYERHOF, W. 2004. Regulation and function of somatostatin receptors. *Journal of neurochemistry,* 89**,** 1057-1091.

OLSEN, L., KLAUSEN, M., HELBOE, L., NIELSEN, F. C. & WERGE, T. 2009. MicroRNAs show mutually exclusive expression patterns in the brain of adult male rats. *PloS one,* 4**,** e7225.

OLSEN, M., KROG, L., EDVARDSEN, K., SKOVGAARD, L. & BOCK, E. 1993. Intact transmembrane isoforms of the neural cell adhesion molecule are released from the plasma membrane. *Biochemical Journal,* 295**,** 833-840.

OLTMANN-NORDEN, I., GALUSKA, S. P., HILDEBRANDT, H., GEYER, R., GERARDY-SCHAHN, R., GEYER, H. & MÜHLENHOFF, M. 2008. Impact of the polysialyltransferases ST8SiaII and ST8SiaIV on polysialic acid synthesis during postnatal mouse brain development. *Journal of Biological Chemistry,* 283**,** 1463-1471.

ONG, E., NAKAYAMA, J., ANGATA, K., REYES, L., KATSUYAMA, T., ARAI, Y. & FUKUDA, M. 1998. Developmental regulation of polysialic acid synthesis in mouse directed by two polysialyltransferases, PST and STX. *Glycobiology,* 8**,** 415-424.

ONO, K., TOMASIEWICZ, H., MAGNUSON, T. & RUTISHAUSER, U. 1994. N-CAM mutation inhibits tangential neuronal migration and is phenocopied by enzymatic removal of polysialic acid. *Neuron,* 13**,** 595-609.

ONO, S., HANE, M., KITAJIMA, K. & SATO, C. 2012. Novel regulation of fibroblast growth factor 2 (FGF2)-mediated cell growth by polysialic acid. *Journal of Biological Chemistry,* 287**,** 3710-3722.

OSHIMA, N., KUMAGAI, H., ONIMARU, H., KAWAI, A., PILOWSKY, P. M., IIGAYA, K., TAKIMOTO, C., HAYASHI, K., SARUTA, T. & ITOH, H. 2008. Monosynaptic excitatory connection from the rostral ventrolateral medulla to sympathetic preganglionic neurons revealed by simultaneous recordings. *Hypertension Research,* 31**,** 1445.

OUMESMAR, B. N., VIGNAIS, L., DUHAMEL-CLÉRIN, E., AVELLANA-ADALID, V., ROUGON, G. & EVERCOOREN, A. 1995. Expression of the highly polysialylated neural cell adhesion molecule during postnatal myelination and following chemically induced demyelination of the adult mouse spinal cord. *European Journal of Neuroscience,* 7**,** 480-491.

PAJOT, J., PELISSIER, T., SIERRALTA, F., RABOISSON, P. & DALLEL, R. 2000. Differential effects of trigeminal tractotomy on Aδ-and C-fiber-mediated nociceptive responses. *Brain research,* 863**,** 289-292.

PANNESE, E., LEDDA, M., CHERKAS, P., HUANG, T. & HANANI, M. 2003. Satellite cell reactions to axon injury of sensory ganglion neurons: increase in number of gap junctions and formation of bridges connecting previously separate perineuronal sheaths. *Anatomy and embryology,* 206**,** 337-347.

PAPASTEFANAKI, F., CHEN, J., LAVDAS, A. A., THOMAIDOU, D., SCHACHNER, M. & MATSAS, R. 2007. Grafts of Schwann cells engineered to express PSA-NCAM promote functional recovery after spinal cord injury. *Brain,* 130**,** 2159-2174.

PARK, A.-M., HAGIWARA, S., HSU, D. K., LIU, F.-T. & YOSHIE, O. 2016a. Galectin-3 plays an important role in innate immunity to gastric infection by Helicobacter pylori. *Infection and immunity,* 84**,** 1184-1193.

PARK, C. R., YOU, D.-J., PARK, S., MANDER, S., JANG, D.-E., YEOM, S.-C., OH, S.-H., AHN, C., LEE, S. H. & SEONG, J. Y. 2016b. The accessory proteins REEP5 and REEP6 refine CXCR1-mediated cellular responses and lung cancer progression. *Scientific Reports,* 6.

PARKASH, J. & KAUR, G. 2005. Neuronal-glial plasticity in gonadotropin-releasing hormone release in adult female rats: role of the polysialylated form of the neural cell adhesion molecule. *Journal of endocrinology,* 186**,** 397-409.

PARKER, M. W., GUO, H.-F., LI, X., LINKUGEL, A. D. & VANDER KOOI, C. W. 2012. Function of members of the neuropilin family as essential pleiotropic cell surface receptors. *Biochemistry,* 51**,** 9437-9446.

PASZEK, M. J., DUFORT, C. C., ROSSIER, O., BAINER, R., MOUW, J. K., GODULA, K., HUDAK, J. E., LAKINS, J. N., WIJEKOON, A. C. & CASSEREAU, L. 2014. The cancer glycocalyx mechanically primes integrin-mediated growth and survival. *Nature,* 511**,** 319-325.

PELKONEN, S., PELKONEN, J. & FINNE, J. 1989. Common cleavage pattern of polysialic acid by bacteriophage endosialidases of different properties and origins. *Journal of virology,* 63**,** 4409-4416.

PELLET-MANY, C., FRANKEL, P., JIA, H. & ZACHARY, I. 2008. Neuropilins: structure, function and role in disease. *Biochemical Journal,* 411**,** 211-226.

PERL, E. R. 1984. Pain and nociception. *In:* I, D.-S. (ed.) *Handbook of physiology. The nervous system.* Bethesda, MD: American Physiological Society.

PERL, E. R. 1992. Function of dorsal root ganglion neurons: an overview. *In:* SCOTT, S. A. (ed.) *Sensory neurons: diversity, development, and plasticity*

Ney York, USA: Oxford University Press

PETRIDIS, A. K., EL MAAROUF, A. & RUTISHAUSER, U. 2004. Polysialic acid regulates cell contact-dependent neuronal differentiation of progenitor cells from the subventricular zone. *Developmental dynamics,* 230**,** 675-684.

PETROV, T., KRUKOFF, T. L. & JHAMANDAS, J. H. 1993. Branching projections of catecholaminergic brainstem neurons to the paraventricular hypothalamic nucleus and the central nucleus of the amygdala in the rat. *Brain research,* 609**,** 81-92.

PHAM, K., NACHER, J., HOF, P. R. & MCEWEN, B. S. 2003. Repeated restraint stress suppresses neurogenesis and induces biphasic PSA-NCAM expression in the adult rat dentate gyrus. *European Journal of Neuroscience,* 17**,** 879-886.

PHILLIPS, J. K., GOODCHILD, A. K., DUBEY, R., SESIASHVILI, E., TAKEDA, M., CHALMERS, J., PILOWSKY, P. M. & LIPSKI, J. 2001. Differential expression of catecholamine biosynthetic enzymes in the rat ventrolateral medulla. *Journal of Comparative Neurology,* 432**,** 20-34.

PILOWSKY, P. M. & GOODCHILD, A. K. 2002. Baroreceptor reflex pathways and neurotransmitters: 10 years on. *Journal of hypertension,* 20**,** 1675-1688.

PINHO, S. S. & REIS, C. A. 2015. Glycosylation in cancer: mechanisms and clinical implications. *Nature Reviews Cancer,* 15**,** 540-555.

PIRAS, F., SCHIFF, M., CHIAPPONI, C., BOSSU, P., MÜHLENHOFF, M., CALTAGIRONE, C., GERARDY-SCHAHN, R., HILDEBRANDT, H. & SPALLETTA, G. 2015. Brain structure,

cognition and negative symptoms in schizophrenia are associated with serum levels of polysialic acid-modified NCAM. *Translational psychiatry,* 5**,** e658.
POLGAR, E., HUGHES, D., RIDDELL, J., MAXWELL, D., PUSKAR, Z. & TODD, A. 2003. Selective loss of spinal GABAergic or glycinergic neurons is not necessary for development of thermal hyperalgesia in the chronic constriction injury model of neuropathic pain. *Pain,* 104**,** 229-239.
PONTI, G., AIMAR, P. & BONFANTI, L. 2006. Cellular composition and cytoarchitecture of the rabbit subventricular zone and its extensions in the forebrain. *Journal of Comparative Neurology,* 498**,** 491-507.
POTAS, J. R. & DAMPNEY, R. A. 2003. Sympathoinhibitory pathway from caudal midline medulla to RVLM is independent of baroreceptor reflex pathway. *American Journal of Physiology-Regulatory, Integrative and Comparative Physiology,* 284**,** R1071-R1078.
POULSEN, E. T., IANNUZZI, F., RASMUSSEN, H. F., MAIER, T. J., ENGHILD, J. J., JØRGENSEN, A. L. & MATRONE, C. 2017. An Aberrant Phosphorylation of Amyloid Precursor Protein Tyrosine Regulates Its Trafficking and the Binding to the Clathrin Endocytic Complex in Neural Stem Cells of Alzheimer's Disease Patients. *Frontiers in Molecular Neuroscience,* 10.
POWELL, F., MILSOM, W. & MITCHELL, G. 1998. Time domains of the hypoxic ventilatory response. *Respiration physiology,* 112**,** 123-134.
PRABHAKAR, N. R. 2006. O2 sensing at the mammalian carotid body: why multiple O2 sensors and multiple transmitters? *Experimental physiology,* 91**,** 17-23.
PROSSER, R. A., RUTISHAUSER, U., UNGERS, G., FEDORKOVA, L. & GLASS, J. D. 2003. Intrinsic role of polysialylated neural cell adhesion molecule in photic phase resetting of the mammalian circadian clock. *Journal of Neuroscience,* 23**,** 652-658.
PSHEZHETSKY, A. V. & HINEK, A. 2011. Where catabolism meets signalling: neuraminidase 1 as a modulator of cell receptors. *Glycoconjugate journal,* 28**,** 441-452.
QIAN, Z., MICORESCU, M., YAKHNITSA, V. & BARMACK, N. H. 2012. Climbing fiber activity reduces 14-3-3-θ regulated GABA A receptor phosphorylation in cerebellar Purkinje cells. *Neuroscience,* 201**,** 34-45.
QUACH, T. T., DUCHEMIN, A.-M., ROGEMOND, V., AGUERA, M., HONNORAT, J., BELIN, M.-F. & KOLATTUKUDY, P. E. 2004. Involvement of collapsin response mediator proteins in the neurite extension induced by neurotrophins in dorsal root ganglion neurons. *Molecular and Cellular Neuroscience,* 25**,** 433-443.
QUARTU, M., SERRA, M. P., BOI, M., IBBA, V., MELIS, T. & DEL FIACCO, M. 2008. Polysialylated-neural cell adhesion molecule (PSA-NCAM) in the human trigeminal ganglion and brainstem at prenatal and adult ages. *BMC neuroscience,* 9**,** 108.
QUARTU, M., SERRA, M. P., BOI, M., MELIS, T., AMBU, R. & DEL FIACCO, M. 2010. Brain-derived neurotrophic factor (BDNF) and polysialylated-neural cell adhesion molecule (PSA-NCAM): codistribution in the human brainstem precerebellar nuclei from prenatal to adult age. *Brain research,* 1363**,** 49-62.
RAMBOURG, A. & LEBLOND, C. 1967. Electron microscope observations on the carbohydrate-rich cell coat present at the surface of cells in the rat. *The Journal of cell biology,* 32**,** 27.
RAMSER, E. M., BUCK, F., SCHACHNER, M. & TILLING, T. 2010. Binding of αII spectrin to 14-3-3β is involved in NCAM-dependent neurite outgrowth. *Molecular and Cellular Neuroscience,* 45**,** 66-74.
RANDIC, M., JIANG, M. & CERNE, R. 1993. Long-term potentiation and long-term depression of primary afferent neurotransmission in the rat spinal cord. *The Journal of neuroscience,* 13**,** 5228-5241.
RAPPORT, M. M. 1981. Introduction to the biochemistry of gangliosides. *In:* RAPPORT, M. M. & GORIO, A. (eds.) *Gangliosides in neurological and neuromuscular function, development, and repair.* Raven Press (ID).

RAY, K., CLAPP, P., GOLDSMITH, P. K. & SPIEGEL, A. M. 1998. Identification of the sites of N-linked glycosylation on the human calcium receptor and assessment of their role in cell surface expression and signal transduction. *Journal of Biological Chemistry,* 273**,** 34558-34567.

RECIO-PINTO, E., THORNHILL, W. B., DUCH, D. S., LEVINSON, S. R. & URBAN, B. W. 1990. Neuraminidase treatment modifies the function of electroplax sodium channels in planar lipid bilayers. *Neuron,* 5**,** 675-684.

REIS, D. J., GOLANOV, E. V., RUGGIERO, D. A. & SUN, M.-K. 1994. Sympatho-excitatory neurons of the rostral ventrolateral medulla are oxygen sensors and essential elements in the tonic and reflex control of the systemic and cerebral circulations. *Journal of hypertension. Supplement: official journal of the International Society of Hypertension,* 12**,** S159-80.

REXED, B. 1952. The cytoarchitectonic organization of the spinal cord in the cat. *Journal of Comparative Neurology,* 96**,** 415-495.

RITTER, S., BUGARITH, K. & DINH, T. T. 2001. Immunotoxic destruction of distinct catecholamine subgroups produces selective impairment of glucoregulatory responses and neuronal activation. *Journal of Comparative Neurology,* 432**,** 197-216.

RITTER, S., LI, A.-J., WANG, Q. & DINH, T. T. 2011. Minireview: The value of looking backward: the essential role of the hindbrain in counterregulatory responses to glucose deficit. *Endocrinology,* 152**,** 4019-4032.

RODRIGUEZ-WALKER, M., VILCAES, A. A., GARBARINO-PICO, E. & DANIOTTI, J. L. 2015. Role of plasma-membrane-bound sialidase NEU3 in clathrin-mediated endocytosis. *Biochemical Journal,* 470**,** 131-144.

ROLANDO, L. 1824. *Ricerche anatomiche sulla struttura del midollo spinale,* dalla Stamperia Reale.

ROLLENHAGEN, M., BUETTNER, F. F., REISMANN, M., JIRMO, A. C., GROVE, M., BEHRENS, G. M., GERARDY-SCHAHN, R., HANISCH, F.-G. & MÜHLENHOFF, M. 2013. Polysialic acid on neuropilin-2 is exclusively synthesized by the polysialyltransferase ST8SiaIV and attached to mucin-type o-glycans located between the b2 and c domain. *Journal of Biological Chemistry,* 288**,** 22880-22892.

ROLLENHAGEN, M., KUCKUCK, S., ULM, C., HARTMANN, M., GALUSKA, S. P., GEYER, R., GEYER, H. & MÜHLENHOFF, M. 2012. Polysialylation of the synaptic cell adhesion molecule 1 (SynCAM 1) depends exclusively on the polysialyltransferase ST8SiaII in vivo. *Journal of Biological Chemistry,* 287**,** 35170-35180.

ROSE, C. R. & KONNERTH, A. 2001. NMDA receptor-mediated Na+ signals in spines and dendrites. *Journal of Neuroscience,* 21**,** 4207-4214.

ROSE, E. M., KOO, J. C., ANTFLICK, J. E., AHMED, S. M., ANGERS, S. & HAMPSON, D. R. 2009. Glutamate transporter coupling to Na, K-ATPase. *The Journal of Neuroscience,* 29**,** 8143-8155.

ROSS, C. A., ARMSTRONG, D., RUGGIERO, D., PICKEL, V., JOH, T. & REIS, D. 1981. Adrenaline neurons in the rostral ventrolateral medulla innervate thoracic spinal cord: a combined immunocytochemical and retrograde transport demonstration. *Neuroscience letters,* 25**,** 257-262.

ROSS, C. A., RUGGIERO, D. A., PARK, D. H., JOH, T. H., SVED, A. F., FERNANDEZ-PARDAL, J., SAAVEDRA, J. M. & REIS, D. J. 1984. Tonic vasomotor control by the rostral ventrolateral medulla: effect of electrical or chemical stimulation of the area containing C1 adrenaline neurons on arterial pressure, heart rate, and plasma catecholamines and vasopressin. *Journal of Neuroscience,* 4**,** 474-494.

ROSS, C. A., RUGGIERO, D. A. & REIS, D. J. 1985. Projections from the nucleus tractus solitarii to the rostral ventrolateral medulla. *Journal of Comparative Neurology,* 242**,** 511-534.

ROTHBARD, J., BRACKENBURY, R., CUNNINGHAM, B. A. & EDELMAN, G. M. 1982. Differences in the carbohydrate structures of neural cell-adhesion molecules from adult and embryonic chicken brains. *J Biol Chem,* 257**,** 11064-11069.

ROTHSTEIN, J. D., MARTIN, L., LEVEY, A. I., DYKES-HOBERG, M., JIN, L., WU, D., NASH, N. & KUNCL, R. W. 1994. Localization of neuronal and glial glutamate transporters. *Neuron,* 13**,** 713-725.

ROUGON, G., DUBOIS, C., BUCKLEY, N., MAGNANI, J. L. & ZOLLINGER, W. 1986. A monoclonal antibody against meningococcus group B polysaccharides distinguishes embryonic from adult N-CAM. *The Journal of cell biology,* 103**,** 2429-2437.

ROUSSELOT, P. & NOTTEBOHM, F. 1995. Expression of polysialylated N-CAM in the central nervous system of adult canaries and its possible relation to function. *Journal of Comparative Neurology,* 356**,** 629-640.

RUEGG, M. A., STOECKLI, E. T., KUHN, T. B., HELLER, M., ZUELLIG, R. & SONDEREGGER, P. 1989. Purification of axonin-1, a protein that is secreted from axons during neurogenesis. *The EMBO journal,* 8**,** 55.

RUTISHAUSER, U. 2008. Polysialic acid in the plasticity of the developing and adult vertebrate nervous system. *Nature Reviews Neuroscience,* 9**,** 26-35.

RUTISHAUSER, U., HOFFMAN, S. & EDELMAN, G. M. 1982. Binding properties of a cell adhesion molecule from neural tissue. *Proceedings of the National Academy of Sciences,* 79**,** 685-689.

RUTISHAUSER, U., THIERY, J.-P., BRACKENBURY, R., SELA, B.-A. & EDELMAN, G. M. 1976. Mechanisms of adhesion among cells from neural tissues of the chick embryo. *Proceedings of the National Academy of Sciences,* 73**,** 577-581.

SÁEZ-VALERO, J., BARQUERO, M., MARCOS, A., MCLEAN, C. & SMALL, D. 2000. Altered glycosylation of acetylcholinesterase in lumbar cerebrospinal fluid of patients with Alzheimer's disease. *Journal of Neurology, Neurosurgery & Psychiatry,* 69**,** 664-667.

SÁEZ-VALERO, J., SBERNA, G., MCLEAN, C. A. & SMALL, D. H. 1999. Molecular isoform distribution and glycosylation of acetylcholinesterase are altered in brain and cerebrospinal fluid of patients with Alzheimer's disease. *Journal of neurochemistry,* 72**,** 1600-1608.

SAITO, H., KUBOTA, M., ROBERTS, R. W., CHI, Q. & MATSUNAMI, H. 2004. RTP family members induce functional expression of mammalian odorant receptors. *Cell,* 119**,** 679-691.

SAJO, M., SUGIYAMA, H., YAMAMOTO, H., TANII, T., MATSUKI, N., IKEGAYA, Y. & KOYAMA, R. 2016. Neuraminidase-dependent degradation of polysialic acid is required for the lamination of newly generated neurons. *PloS one,* 11**,** e0146398.

SALO, L. M., WOODS, R. L., ANDERSON, C. R. & MCALLEN, R. M. 2007. Nonuniformity in the von Bezold-Jarisch reflex. *American Journal of Physiology-Regulatory, Integrative and Comparative Physiology,* 293**,** R714-R720.

SALTER, M. W. & HENRY, J. 1991. Responses of functionally identified neurones in the dorsal horn of the cat spinal cord to substance P, neurokinin A and physalaemin. *Neuroscience,* 43**,** 601-610.

SANDI, C., MERINO, J. J., CORDERO, M. I., KRUYT, N. D., MURPHY, K. J. & REGAN, C. M. 2003. Modulation of hippocampal NCAM polysialylation and spatial memory consolidation by fear conditioning. *Biological psychiatry,* 54**,** 599-607.

SANDIG, M., RAO, Y. & SIU, C.-H. 1994. The homophilic binding site of the neural cell adhesion molecule NCAM is directly involved in promoting neurite outgrowth from cultured neural retinal cells. *Journal of Biological Chemistry,* 269**,** 14841-14848.

SANDKÜHLER, J. 2009. Models and mechanisms of hyperalgesia and allodynia. *Physiological reviews,* 89**,** 707-758.

SARTOR, D. M. & VERBERNE, A. J. 2003. Phenotypic identification of rat rostroventrolateral medullary presympathetic vasomotor neurons inhibited by exogenous cholecystokinin. *Journal of Comparative Neurology,* 465**,** 467-479.

SARTOR, D. M. & VERBERNE, A. J. 2007. The role of NMDA and non-NMDA receptors in the NTS in mediating three distinct sympathoinhibitory reflexes. *Naunyn-Schmiedeberg's archives of pharmacology,* 376**,** 241-252.

SATO, C., FUKUOKA, H., OHTA, K., MATSUDA, T., KOSHINO, R., KOBAYASHI, K., TROY, F. A. & KITAJIMA, K. 2000. Frequent Occurrence of Pre-existing α2→ 8-Linked Disialic and Oligosialic Acids with Chain Lengths Up to 7 Sia Residues in Mammalian Brain Glycoproteins PREVALENCE REVEALED BY HIGHLY SENSITIVE CHEMICAL METHODS AND ANTI-

DI-, OLIGO-, AND POLY-Sia ANTIBODIES SPECIFIC FOR DEFINED CHAIN LENGTHS. *Journal of Biological Chemistry,* 275**,** 15422-15431.
SATO, C. & KITAJIMA, K. 2013a. Disialic, oligosialic and polysialic acids: distribution, functions and related disease. *Journal of biochemistry,* 154**,** 115-136.
SATO, C. & KITAJIMA, K. 2013b. Impact of structural aberrancy of polysialic acid and its synthetic enzyme ST8SIA2 in schizophrenia. *Frontiers in cellular neuroscience,* 7**,** 61.
SATO, C., KITAJIMA, K., INOUE, S., SEKI, T., TROY, F. A. & INOUE, Y. 1995. Characterization of the antigenic specificity of four different anti-(α2→ 8-linked polysialic acid) antibodies using lipid-conjugated oligo/polysialic acids. *Journal of Biological Chemistry,* 270**,** 18923-18928.
SATO, C., YAMAKAWA, N. & KITAJIMA, K. 2010. Chapter ten-Measurement of Glycan-Based Interactions by Frontal Affinity Chromatography and Surface Plasmon Resonance. *Methods in enzymology,* 478**,** 219-232.
SAWCHENKO, P. & SWANSON, L. 1982. The organization of noradrenergic pathways from the brainstem to the paraventricular and supraoptic nuclei in the rat. *Brain Research Reviews,* 4**,** 275-325.
SCHAUER, R. 1985. Sialic acids and their role as biological masks. *Trends in Biochemical Sciences,* 10**,** 357-360.
SCHAUER, R. 2000. Achievements and challenges of sialic acid research. *Glycoconjugate journal,* 17**,** 485-499.
SCHAUER, R. 2009. Sialic acids as regulators of molecular and cellular interactions. *Current opinion in structural biology,* 19**,** 507-514.
SCHEIDEGGER, E. P., STERNBERG, L. R., ROTH, J. & LOWE, J. B. 1995. A human STX cDNA confers polysialic acid expression in mammalian cells. *Journal of Biological Chemistry,* 270**,** 22685-22688.
SCHEUER, T., MCHUGH, L., TEJEDOR, F. & CATTERALL, W. FUNCTIONAL-PROPERTIES OF NEURAMINIDASE-TREATED RAT-BRAIN SODIUM-CHANNELS. BIOPHYSICAL JOURNAL, 1988. BIOPHYSICAL SOCIETY 9650 ROCKVILLE PIKE, BETHESDA, MD 20814-3998, A541-A541.
SCHINDELIN, J., ARGANDA-CARRERAS, I., FRISE, E., KAYNIG, V., LONGAIR, M., PIETZSCH, T., PREIBISCH, S., RUEDEN, C., SAALFELD, S. & SCHMID, B. 2012. Fiji: an open-source platform for biological-image analysis. *Nature methods,* 9**,** 676-682.
SCHNAAR, R. L. 2004. Glycolipid-mediated cell–cell recognition in inflammation and nerve regeneration. *Archives of biochemistry and biophysics,* 426**,** 163-172.
SCHNAAR, R. L. 2005. Brain glycolipids: insights from genetic modifications of biosynthetic enzymes. *Neuroglycobiology. Oxford University Press, New York***,** 95-113.
SCHNAAR, R. L., GERARDY-SCHAHN, R. & HILDEBRANDT, H. 2014. Sialic acids in the brain: gangliosides and polysialic acid in nervous system development, stability, disease, and regeneration. *Physiological Reviews,* 94**,** 461-518.
SCHNAAR, R. L., SUZUKI, A. & STANLEY, P. 2009. Glycosphingolipids. *In:* VARKI A, C. R., ESKO JD, ET AL. (ed.) *Essentials of Glycobiology.* second ed. New York: Cold Spring Harbor Laboratory Press.
SCHOENEN, J. & FAULL, R. L. 2004. Spinal cord: cyto-and chemoarchitecture. *The human nervous system.* 2 ed. California, USA: Elsevier Academic Press.
SCHREIBER, G., HARAN, G. & ZHOU, H.-X. 2009. Fundamental aspects of protein− protein association kinetics. *Chemical reviews,* 109**,** 839-860.
SCHREIHOFER, A. M. & GUYENET, P. G. 1997. Identification of C1 presympathetic neurons in rat rostral ventrolateral medulla by juxtacellular labeling in vivo. *Journal of Comparative Neurology,* 387**,** 524-536.
SCHREIHOFER, A. M. & GUYENET, P. G. 2000. Sympathetic reflexes after depletion of bulbospinal catecholaminergic neurons with anti-DβH-saporin. *American Journal of Physiology-Regulatory, Integrative and Comparative Physiology,* 279**,** R729-R742.

SCHREIHOFER, A. M. & GUYENET, P. G. 2002. The baroreflex and beyond: control of sympathetic vasomotor tone by GABAergic neurons in the ventrolateral medulla. *Clinical and experimental pharmacology and physiology,* 29**,** 514-521.
SCHREIHOFER, A. M. & GUYENET, P. G. 2003. Baro-activated neurons with pulse-modulated activity in the rat caudal ventrolateral medulla express GAD67 mRNA. *Journal of neurophysiology,* 89**,** 1265-1277.
SCHREIHOFER, A. M., STORNETTA, R. L. & GUYENET, P. G. 2000. Regulation of sympathetic tone and arterial pressure by rostral ventrolateral medulla after depletion of C1 cells in rat. *The Journal of Physiology,* 529**,** 221-236.
SCHWAB, M. E. 2004. Nogo and axon regeneration. *Current opinion in neurobiology,* 14**,** 118-124.
SEKI, T. 2002a. Expression patterns of immature neuronal markers PSA-NCAM, CRMP-4 and NeuroD in the hippocampus of young adult and aged rodents. *Journal of neuroscience research,* 70**,** 327-334.
SEKI, T. 2002b. Hippocampal adult neurogenesis occurs in a microenvironment provided by PSA-NCAM-expressing immature neurons. *Journal of neuroscience research,* 69**,** 772-783.
SEKI, T. & ARAI, Y. 1991. The persistent expression of a highly polysialylated NCAM in the dentate gyrus of the adult rat. *Neuroscience research,* 12**,** 503-513.
SEKI, T. & ARAI, Y. 1993a. Distribution and possible roles of the highly polysialylated neural cell adhesion molecule (NCAM-H) in the developing and adult central nervous system. *Neuroscience research,* 17**,** 265-290.
SEKI, T. & ARAI, Y. 1993b. Highly polysialylated NCAM expression in the developing and adult rat spinal cord. *Developmental brain research,* 73**,** 141-145.
SEKI, T. & ARAI, Y. 1993c. Highly polysialylated neural cell adhesion molecule (NCAM-H) is expressed by newly generated granule cells in the dentate gyrus of the adult rat. *Journal of Neuroscience,* 13**,** 2351-2358.
SEKI, T., NAMBA, T., MOCHIZUKI, H. & ONODERA, M. 2007. Clustering, migration, and neurite formation of neural precursor cells in the adult rat hippocampus. *Journal of Comparative Neurology,* 502**,** 275-290.
SELLMEIER, M., WEINHOLD, B. & MÜNSTER-KÜHNEL, A. 2015. CMP-Sialic Acid Synthetase: the point of constriction in the sialylation pathway. *Top. Curr. Chem,* 366**,** 139-167.
SENKOV, O., SUN, M., WEINHOLD, B., GERARDY-SCHAHN, R., SCHACHNER, M. & DITYATEV, A. 2006. Polysialylated neural cell adhesion molecule is involved in induction of long-term potentiation and memory acquisition and consolidation in a fear-conditioning paradigm. *The Journal of neuroscience,* 26**,** 10888-109898.
SERI, B., GARCÍA-VERDUGO, J. M., COLLADO-MORENTE, L., MCEWEN, B. S. & ALVAREZ-BUYLLA, A. 2004. Cell types, lineage, and architecture of the germinal zone in the adult dentate gyrus. *Journal of Comparative Neurology,* 478**,** 359-378.
SESSLE, B. 1987. Invited review: the neurobiology of facial and dental pain: present knowledge, future directions. *Journal of Dental Research,* 66**,** 962-981.
SESSLE, B. 2005a. Peripheral and central mechanisms of orofacial pain and their clinical correlates. *Minerva anestesiologica,* 71**,** 117-136.
SESSLE, B. J. 2000. Acute and chronic craniofacial pain: brainstem mechanisms of nociceptive transmission and neuroplasticity, and their clinical correlates. *Critical Reviews in Oral Biology & Medicine,* 11**,** 57-91.
SESSLE, B. J. 2005b. Trigeminal central sensitization. *Reviews in Analgesia,* 8**,** 85-102.
SEYRANTEPE, V., POUPETOVA, H., FROISSART, R., ZABOT, M. T., MAIRE, I. & PSHEZHETSKY, A. V. 2003. Molecular pathology of NEU1 gene in sialidosis. *Human mutation,* 22**,** 343-352.
SHAHID, I. Z., RAHMAN, A. A. & PILOWSKY, P. M. 2012. Orexin A in rat rostral ventrolateral medulla is pressor, sympatho-excitatory, increases barosensitivity and attenuates the somato-sympathetic reflex. *British journal of pharmacology,* 165**,** 2292-2303.

SHAROAR, M., SHI, Q., GE, Y., HE, W., HU, X., PERRY, G., ZHU, X. & YAN, R. 2016. Dysfunctional tubular endoplasmic reticulum constitutes a pathological feature of Alzheimer's disease. *Molecular psychiatry,* 21**,** 1263-1271.

SHAVER, S. W., PANG, J. J., WALL, K. M., SPOSITO, N. M. & GROSS, P. M. 1991. Subregional topography of capillaries in the dorsal vagal complex of rats: I. Morphometric properties. *Journal of comparative neurology,* 306**,** 73-82.

SHEHAB, S. & ATKINSON, M. 1986. Vasoactive intestinal polypeptide (VIP) increases in the spinal cord after peripheral axotomy of the sciatic nerve originate from primary afferent neurons. *Brain research,* 372**,** 37-44.

SHEN, H., GLASS, J. D., SEKI, T. & WATANABE, M. 1999. Ultrastructural analysis of polysialylated neural cell adhesion molecule in the suprachiasmatic nuclei of the adult mouse. *The Anatomical Record,* 256**,** 448-457.

SHEN, H., WATANABE, M., TOMASIEWICZ, H., RUTISHAUSER, U., MAGNUSON, T. & GLASS, J. D. 1997. Role of neural cell adhesion molecule and polysialic acid in mouse circadian clock function. *The Journal of neuroscience,* 17**,** 5221-5229.

SHIBATA, Y., VOSS, C., RIST, J. M., HU, J., RAPOPORT, T. A., PRINZ, W. A. & VOELTZ, G. K. 2008. The reticulon and DP1/Yop1p proteins form immobile oligomers in the tubular endoplasmic reticulum. *Journal of Biological Chemistry,* 283**,** 18892-18904.

SHIGENAGA, Y., CHEN, I., SUEMUNE, S., NISHIMORI, T., NASUTION, I., YOSHIDA, A., SATO, H., OKAMOTO, T., SERA, M. & HOSOI, M. 1986. Oral and facial representation within the medullary and upper cervical dorsal horns in the cat. *Journal of Comparative Neurology,* 243**,** 388-408.

SHINGAI, T., IKEDA, W., KAKUNAGA, S., MORIMOTO, K., TAKEKUNI, K., ITOH, S., SATOH, K., TAKEUCHI, M., IMAI, T. & MONDEN, M. 2003. Implications of nectin-like molecule-2/IGSF4/RA175/SgIGSF/TSLC1/SynCAM1 in cell-cell adhesion and transmembrane protein localization in epithelial cells. *Journal of Biological Chemistry,* 278**,** 35421-35427.

SHUMYATSKY, G. P., TSVETKOV, E., MALLERET, G., VRONSKAYA, S., HATTON, M., HAMPTON, L., BATTEY, J. F., DULAC, C., KANDEL, E. R. & BOLSHAKOV, V. Y. 2002. Identification of a signaling network in lateral nucleus of amygdala important for inhibiting memory specifically related to learned fear. *Cell,* 111**,** 905-918.

SIDMAN, R. L., ANGEVINE, J. B. & PIERCE, E. T. 1971. Atlas of the mouse brain and spinal cord.

SILVER, J. & MILLER, J. H. 2004. Regeneration beyond the glial scar. *Nature Reviews Neuroscience,* 5**,** 146-156.

SILVEYRA, M. X., CUADRADO-CORRALES, N., MARCOS, A., BARQUERO, M. S., RÁBANO, A., CALERO, M. & SÁEZ-VALERO, J. 2006. Altered glycosylation of acetylcholinesterase in Creutzfeldt–Jakob disease. *Journal of neurochemistry,* 96**,** 97-104.

SIMON, P., BÄUMNER, S., BUSCH, O., RÖHRICH, R., KAESE, M., RICHTERICH, P., WEHREND, A., MÜLLER, K., GERARDY-SCHAHN, R. & MÜHLENHOFF, M. 2013. Polysialic acid is present in mammalian semen as a post-translational modification of the neural cell adhesion molecule NCAM and the polysialyltransferase ST8SiaII. *Journal of Biological Chemistry,* 288**,** 18825-18833.

SKARNES, W. C., ROSEN, B., WEST, A. P., KOUTSOURAKIS, M., BUSHELL, W., IYER, V., MUJICA, A. O., THOMAS, M., HARROW, J. & COX, T. 2011. A conditional knockout resource for the genome-wide study of mouse gene function. *Nature,* 474**,** 337-342.

SKOU, J. 1990. The energy coupled exchange of Na+ for K+ across the cell membrane. *FEBS letters,* 268**,** 314-324.

SKOU, J. C. & ESMANN, M. 1992. The na, k-atpase. *Journal of bioenergetics and biomembranes,* 24**,** 249-261.

SLUGG, R. M. & LIGHT, A. R. 1994. Spinal cord and trigeminal projections to the pontine parabrachial region in the rat as demonstrated with Phaseolus vulgaris leucoagglutinin. *Journal of Comparative Neurology,* 339**,** 49-61.

SMITH, J. C., ELLENBERGER, H. H., BALLANYI, K., RICHTER, D. W. & FELDMAN, J. L. 1991. Pre-Bötzinger complex: a brainstem region that may generate respiratory rhythm in mammals. *Science (New York, NY),* 254**,** 726.
SNIDER, W. D. & MCMAHON, S. B. 1998. Tackling pain at the source: new ideas about nociceptors. *Neuron,* 20**,** 629-632.
SOBOLESKI, M. R., OAKS, J. & HALFORD, W. P. 2005. Green fluorescent protein is a quantitative reporter of gene expression in individual eukaryotic cells. *The FASEB journal,* 19**,** 440-442.
SOFRONIEW, M. V. & VINTERS, H. V. 2010. Astrocytes: biology and pathology. *Acta neuropathologica,* 119**,** 7-35.
SOMPLATZKI, S., MÜHLENHOFF, M., KRÖGER, A., GERARDY-SCHAHN, R. & BÖLDICKE, T. 2017. Intrabodies against the Polysialyltransferases ST8SiaII and ST8SiaIV inhibit Polysialylation of NCAM in rhabdomyosarcoma tumor cells. *BMC biotechnology,* 17**,** 42.
SONG, Y. & BRADY, S. T. 2015. Post-translational modifications of tubulin: pathways to functional diversity of microtubules. *Trends in cell biology,* 25**,** 125-136.
SORKIN, A. & VON ZASTROW, M. 2009. Endocytosis and signalling: intertwining molecular networks. *Nature reviews Molecular cell biology,* 10**,** 609-622.
SOROKA, V., KASPER, C. & POULSEN, F. M. 2010. Structural biology of NCAM. *Structure and Function of the Neural Cell Adhesion Molecule NCAM.* Springer.
SPIKE, R., PUSKAR, Z., ANDREW, D. & TODD, A. 2003. A quantitative and morphological study of projection neurons in lamina I of the rat lumbar spinal cord. *European Journal of Neuroscience,* 18**,** 2433-2448.
SPIRO, R. G. 2002. Protein glycosylation: nature, distribution, enzymatic formation, and disease implications of glycopeptide bonds. *Glycobiology,* 12**,** 43R-56R.
SPYER, K. 1994. Annual review prize lecture. Central nervous mechanisms contributing to cardiovascular control. *The Journal of Physiology,* 474**,** 1-19.
STACKMAN, R. W. & TAUBE, J. S. 1997. Firing properties of head direction cells in the rat anterior thalamic nucleus: dependence on vestibular input. *Journal of Neuroscience,* 17**,** 4349-4358.
STAMATOS, N. M., ZHANG, L., JOKILAMMI, A., FINNE, J., CHEN, W. H., EL-MAAROUF, A., CROSS, A. S. & HANKEY, K. G. 2014. Changes in polysialic acid expression on myeloid cells during differentiation and recruitment to sites of inflammation: role in phagocytosis. *Glycobiology,* 24**,** 864-879.
STEENTOFT, C., VAKHRUSHEV, S. Y., JOSHI, H. J., KONG, Y., VESTER-CHRISTENSEN, M. B., KATRINE, T., SCHJOLDAGER, B., LAVRSEN, K., DABELSTEEN, S. & PEDERSEN, N. B. 2013. Precision mapping of the human O-GalNAc glycoproteome through SimpleCell technology. *The EMBO journal,* 32**,** 1478-1488.
STERNBERGER, N. H., ITOYAMA, Y., KIES, M. W. & WEBSTER, H. D. 1978. Myelin basic protein demonstrated immunocytochemically in oligodendroglia prior to myelin sheath formation. *Proceedings of the National Academy of Sciences,* 75**,** 2521-2524.
STOCKER, S. D., OSBORN, J. L. & CARMICHAEL, S. P. 2008. Forebrain osmotic regulation of the sympathetic nervous system. *Clinical and Experimental Pharmacology and Physiology,* 35**,** 695-700.
STÖCKMANN, H., O'FLAHERTY, R., ADAMCZYK, B., SALDOVA, R. & RUDD, P. 2015. Automated, high-throughput serum glycoprofiling platform. *Integrative Biology,* 7**,** 1026-1032.
STOECKEL, M. E., UHL-BRONNER, S., HUGEL, S., VEINANTE, P., KLEIN, M. J., MUTTERER, J., FREUND-MERCIER, M. J. & SCHLICHTER, R. 2003. Cerebrospinal fluid-contacting neurons in the rat spinal cord, a γ-aminobutyric acidergic system expressing the P2X2 subunit of purinergic receptors, PSA-NCAM, and GAP-43 immunoreactivities: Light and electron microscopic study. *Journal of Comparative Neurology,* 457**,** 159-174.
STOENICA, L., SENKOV, O., GERARDY-SCHAHN, R., WEINHOLD, B., SCHACHNER, M. & DITYATEV, A. 2006. In vivo synaptic plasticity in the dentate gyrus of mice deficient in the

neural cell adhesion molecule NCAM or its polysialic acid. *European Journal of Neuroscience,* 23**,** 2255-2264.
STORMS, S. D., KIM, A. C., TRAN, B.-H. T., COLE, G. J. & MURRAY, B. A. 1996. NCAM-mediated adhesion of transfected cells to agrin. *Cell Communication & Adhesion,* 3**,** 497-509.
STORMS, S. D. & RUTISHAUSER, U. 1998. A role for polysialic acid in neural cell adhesion molecule heterophilic binding to proteoglycans. *Journal of Biological Chemistry,* 273**,** 27124-27129.
STORNETTA, R. L. & GUYENET, P. G. 1999. Distribution of glutamic acid decarboxylase mRNA-containing neurons in rat medulla projecting to thoracic spinal cord in relation to monoaminergic brainstem neurons. *Journal of Comparative Neurology,* 407**,** 367-380.
STORNETTA, R. L., MACON, C. J., NGUYEN, T. M., COATES, M. B. & GUYENET, P. G. 2013. Cholinergic neurons in the mouse rostral ventrolateral medulla target sensory afferent areas. *Brain Structure and Function,* 218**,** 455-475.
STORNETTA, R. L., ROSIN, D. L., WANG, H., SEVIGNY, C. P., WESTON, M. C. & GUYENET, P. G. 2003. A group of glutamatergic interneurons expressing high levels of both neurokinin-1 receptors and somatostatin identifies the region of the pre-Bötzinger complex. *Journal of Comparative Neurology,* 455**,** 499-512.
STORNETTA, R. L., SEVIGNY, C. P. & GUYENET, P. G. 2002. Vesicular glutamate transporter DNPI/VGLUT2 mRNA is present in C1 and several other groups of brainstem catecholaminergic neurons. *Journal of Comparative Neurology,* 444**,** 191-206.
STRACK, A., SAWYER, W., HUGHES, J., PLATT, K. & LOEWY, A. 1989. A general pattern of CNS innervation of the sympathetic outflow demonstrated by transneuronal pseudorabies viral infections. *Brain research,* 491**,** 156-162.
STRASSMAN, A. M. & VOS, B. P. 1993. Somatotopic and laminar organization of fos-like immunoreactivity in the medullary and upper cervical dorsal horn induced by noxious facial stimulation in the rat. *Journal of Comparative Neurology,* 331**,** 495-516.
STROUS, G. J. & DEKKER, J. 1992. Mucin-type glycoproteins. *Critical reviews in biochemistry and molecular biology,* 27**,** 57-92.
STUMMEYER, K., DICKMANNS, A., MÜHLENHOFF, M., GERARDY-SCHAHN, R. & FICNER, R. 2005. Crystal structure of the polysialic acid–degrading endosialidase of bacteriophage K1F. *Nature structural & molecular biology,* 12**,** 90-96.
SUADICANI, S. O., CHERKAS, P. S., ZUCKERMAN, J., SMITH, D. N., SPRAY, D. C. & HANANI, M. 2010. Bidirectional calcium signaling between satellite glial cells and neurons in cultured mouse trigeminal ganglia. *Neuron glia biology,* 6**,** 43-51.
SUGIMOTO, T., TAKEMURA, M., SAKAI, A. & ISHIMARU, M. 1986. Cell size analysis of trigeminal primary afferent neurons comprizing individual peripheral branches of the rat mandibular nerve. *Experimental neurology,* 93**,** 565-573.
SUGIYAMA, Y., SUZUKI, T. & YATES, B. J. 2011. Role of the rostral ventrolateral medulla (RVLM) in the patterning of vestibular system influences on sympathetic nervous system outflow to the upper and lower body. *Experimental brain research,* 210**,** 515-527.
SUMIDA, M., HANE, M., YABE, U., SHIMODA, Y., PEARCE, O. M., KISO, M., MIYAGI, T., SAWADA, M., VARKI, A. & KITAJIMA, K. 2015. Rapid trimming of cell surface polysialic acid (PolySia) by exovesicular sialidase triggers release of preexisting surface neurotrophin. *Journal of Biological Chemistry,* 290**,** 13202-13214.
SUN, M.-K. 1996. Pharmacology of reticulospinal vasomotor neurons in cardiovascular regulation. *Pharmacological Reviews,* 48**,** 465-494.
SUN, M.-K. & REIS, D. J. 1994. Central neural mechanisms mediating excitation of sympathetic neurons by hypoxia. *Progress in neurobiology,* 44**,** 197-219.
SUN, M. & SPYER, K. 1991. GABA-mediated inhibition of medullary vasomotor neurones by area postrema stimulation in rats. *The Journal of physiology,* 436**,** 669.
SUN, Q.-J., GOODCHILD, A. K., CHALMERS, J. P. & PILOWSKY, P. M. 1998. The pre-Bötzinger complex and phase-spanning neurons in the adult rat. *Brain research,* 809**,** 204-213.

SUNSHINE, J., BALAK, K., RUTISHAUSER, U. & JACOBSON, M. 1987. Changes in neural cell adhesion molecule (NCAM) structure during vertebrate neural development. *Proceedings of the National Academy of Sciences,* 84**,** 5986-5990.

SVED, A. F., ITO, S. & MADDEN, C. J. 2000. Baroreflex dependent and independent roles of the caudal ventrolateral medulla in cardiovascular regulation. *Brain research bulletin,* 51**,** 129-133.

SVENNERHOLM, L. & FREDMAN, P. 1980. A procedure for the quantitative isolation of brain gangliosides. *Biochimica et Biophysica Acta (BBA)-Lipids and Lipid Metabolism,* 617**,** 97-109.

SZELE, F. G. & CHESSELET, M. F. 1996. Cortical lesions induce an increase in cell number and PSA-NCAM expression in the subventricular zone of adult rats. *Journal of Comparative Neurology,* 368**,** 439-454.

TAKAHASHI, K., MITOMA, J., HOSONO, M., SHIOZAKI, K., SATO, C., YAMAGUCHI, K., KITAJIMA, K., HIGASHI, H., NITTA, K. & SHIMA, H. 2012. Sialidase NEU4 hydrolyzes polysialic acids of neural cell adhesion molecules and negatively regulates neurite formation by hippocampal neurons. *Journal of Biological Chemistry,* 287**,** 14816-14826.

TAKEDA, M., TAKAHASHI, M. & MATSUMOTO, S. 2009. Contribution of the activation of satellite glia in sensory ganglia to pathological pain. *Neuroscience & Biobehavioral Reviews,* 33**,** 784-792.

TAKEDA, M., TAKAHASHI, M., NASU, M. & MATSUMOTO, S. 2011. Peripheral inflammation suppresses inward rectifying potassium currents of satellite glial cells in the trigeminal ganglia. *Pain,* 152**,** 2147-2156.

TAKEDA, M., TANIMOTO, T., IKEDA, M., NASU, M., KADOI, J., SHIMA, Y., OHTA, H. & MATSUMOTO, S. 2005. Temporomandibular joint inflammation potentiates the excitability of trigeminal root ganglion neurons innervating the facial skin in rats. *Journal of neurophysiology,* 93**,** 2723-2738.

TAKEDA, M., TANIMOTO, T., IKEDA, M., NASU, M., KADOI, J., YOSHIDA, S. & MATSUMOTO, S. 2006. Enhanced excitability of rat trigeminal root ganglion neurons via decrease in A-type potassium currents following temporomandibular joint inflammation. *Neuroscience,* 138**,** 621-630.

TALLAPRAGADA, V. J., HILDRETH, C. M., BURKE, P. G., RALEY, D. A., HASSAN, S. F., MCMULLAN, S. & GOODCHILD, A. K. 2016. Tonically active cAMP-dependent signaling in the ventrolateral medulla regulates sympathetic and cardiac vagal outflows. *Journal of Pharmacology and Experimental Therapeutics,* 356**,** 424-433.

TAN, H.-Y., NICODEMUS, K. K., CHEN, Q., LI, Z., BROOKE, J. K., HONEA, R., KOLACHANA, B. S., STRAUB, R. E., MEYER-LINDENBERG, A. & SEI, Y. 2008. Genetic variation in AKT1 is linked to dopamine-associated prefrontal cortical structure and function in humans. *The Journal of clinical investigation,* 118**,** 2200-2208.

TASHIRO, T., HIGO, S. & MATSUYAMA, T. 1984. Soma size comparison of the trigeminal ganglion cells giving rise to the ascending and descending tracts: a horseradish peroxidase study in the cat. *Experimental neurology,* 84**,** 37-46.

TAUBE, J. S. 2007. The head direction signal: origins and sensory-motor integration. *Annu. Rev. Neurosci.,* 30**,** 181-207.

TAYLOR, G. 1996. Sialidases: structures, biological significance and therapeutic potential. *Current opinion in structural biology,* 6**,** 830-837.

TAYLOR, M. E. & DRICKAMER, K. 2011. *Introduction to glycobiology,* Oxford university press.

TETTAMANTI, G., BONALI, F., MARCHESINI, S. T. & ZAMBOTTI, V. 1973. A new procedure for the extraction, purification and fractionation of brain gangliosides. *Biochimica et Biophysica Acta (BBA)-Lipids and Lipid Metabolism,* 296**,** 160-170.

THEIS, T., MISHRA, B., VON DER OHE, M., LOERS, G., PRONDZYNSKI, M., PLESS, O., BLACKSHEAR, P. J., SCHACHNER, M. & KLEENE, R. 2013. Functional role of the interaction between polysialic acid and myristoylated alanine-rich C kinase substrate at the plasma membrane. *Journal of Biological Chemistry,* 288**,** 6726-6742.

THEODOSIS, D. & POULAIN, D. 1993. Activity-dependent neuronal-glial and synaptic plasticity in the adult mammalian hypothalamus. *Neuroscience,* 57**,** 501-535.
THEODOSIS, D. T. 2002. Oxytocin-secreting neurons: a physiological model of morphological neuronal and glial plasticity in the adult hypothalamus. *Frontiers in neuroendocrinology,* 23**,** 101-135.
THEODOSIS, D. T., BONHOMME, R., VITIELLO, S., ROUGON, G. & POULAIN, D. A. 1999. Cell surface expression of polysialic acid on NCAM is a prerequisite for activity-dependent morphological neuronal and glial plasticity. *The Journal of neuroscience,* 19**,** 10228-10236.
THEODOSIS, D. T. & MACVICAR, B. 1996. Neurone-glia interactions in the hypothalamus and pituitary. *Trends in neurosciences,* 19**,** 363-367.
THEODOSIS, D. T., POULAIN, D. A. & OLIET, S. H. 2008. Activity-dependent structural and functional plasticity of astrocyte-neuron interactions. *Physiological reviews,* 88**,** 983-1008.
THEODOSIS, D. T., ROUGON, G. & POULAIN, D. A. 1991. Retention of embryonic features by an adult neuronal system capable of plasticity: polysialylated neural cell adhesion molecule in the hypothalamo-neurohypophysial system. *Proceedings of the National Academy of Sciences,* 88**,** 5494-5498.
THEODOSIS, D. T., TRAILIN, A. & POULAIN, D. A. 2006. Remodeling of astrocytes, a prerequisite for synapse turnover in the adult brain? Insights from the oxytocin system of the hypothalamus. *American Journal of Physiology-Regulatory, Integrative and Comparative Physiology,* 290**,** R1175-R1182.
THOMPSON HASKELL, G., MAYNARD, T. M., SHATZMILLER, R. A. & LAMANTIA, A. S. 2002. Retinoic acid signaling at sites of plasticity in the mature central nervous system. *Journal of Comparative Neurology,* 452**,** 228-241.
TIRALONGO, J. 2013. Introduction to sialic acid structure, occurance, biosynthetis and function. *In:* TIRALONGO, J. & MARTINEZ-DUNCKER, I. (eds.) *Sialobiology: Structure, Biosynthesis and Function. Sialic Acid Glycoconjugates in Health and Disease.* IL, USA: Bentham Science Publishers.
TODD, A., HUGHES, D., POLGAR, E., NAGY, G., MACKIE, M., OTTERSEN, O. & MAXWELL, D. 2003. The expression of vesicular glutamate transporters VGLUT1 and VGLUT2 in neurochemically defined axonal populations in the rat spinal cord with emphasis on the dorsal horn. *European Journal of Neuroscience,* 17**,** 13-27.
TODD, A. & MAXWELL, D. 2000. GABA in the mammalian spinal cord. *In:* MARTIN, D. L. & OLSEN, R. W. (eds.) *GABA in the nervous system: the view at fifty years.* Philadelphia, PA, USA: Lippincott Williams and Wilkins.
TODD, A., SPIKE, R. & POLGAR, E. 1998. A quantitative study of neurons which express neurokinin-1 or somatostatin sst 2a receptor in rat spinal dorsal horn. *Neuroscience,* 85**,** 459-473.
TODD, A. J. 2010. Neuronal circuitry for pain processing in the dorsal horn. *Nature Reviews Neuroscience,* 11**,** 823-836.
TODD, A. J. 2015. Plasticity of inhibition in the spinal cord. *Pain Control.* Springer.
TODD, A. J., MCGILL, M. M. & SHEHAB, S. A. 2000. Neurokinin 1 receptor expression by neurons in laminae I, III and IV of the rat spinal dorsal horn that project to the brainstem. *European Journal of Neuroscience,* 12**,** 689-700.
TODD, A. J., PUSKÁR, Z., SPIKE, R. C., HUGHES, C., WATT, C. & FORREST, L. 2002. Projection neurons in lamina I of rat spinal cord with the neurokinin 1 receptor are selectively innervated by substance p-containing afferents and respond to noxious stimulation. *The Journal of neuroscience,* 22**,** 4103-4113.
TODD, A. J. & SULLIVAN, A. C. 1990. Light microscope study of the coexistence of GABA-like and glycine-like immunoreactivities in the spinal cord of the rat. *Journal of Comparative Neurology,* 296**,** 496-505.
TODESCHINI, A. R. & HAKOMORI, S.-I. 2008. Functional role of glycosphingolipids and gangliosides in control of cell adhesion, motility, and growth, through glycosynaptic microdomains. *Biochimica et Biophysica Acta (BBA)-General Subjects,* 1780**,** 421-433.

TOMASIEWICZ, H., ONO, K., YEE, D., THOMPSON, C., GORIDIS, C., RUTISHAUSER, U. & MAGNUSON, T. 1993. Genetic deletion of a neural cell adhesion molecule variant (N-CAM-180) produces distinct defects in the central nervous system. *Neuron,* 11**,** 1163-1174.

TRAUB, R. J., SOLODKIN, A. & RUDA, M. 1989. Calcitonin gene-related peptide immunoreactivity in the cat lumbosacral spinal cord and the effects of multiple dorsal rhizotomies. *Journal of Comparative Neurology,* 287**,** 225-237.

TSUCHIYA, A., LU, W. Y., WEINHOLD, B., BOULTER, L., STUTCHFIELD, B. M., WILLIAMS, M. J., GUEST, R. V., MINNIS-LYONS, S. E., MACKINNON, A. C. & SCHWARZER, D. 2014. Polysialic acid/neural cell adhesion molecule modulates the formation of ductular reactions in liver injury. *Hepatology,* 60**,** 1727-1740.

TUCKER, D. C., SAPER, C. B., RUGGIERO, D. A. & REIS, D. J. 1987. Organization of central adrenergic pathways: I. Relationships of ventrolateral medullary projections to the hypothalamus and spinal cord. *Journal of Comparative Neurology,* 259**,** 591-603.

ULM, C., SAFFARZADEH, M., MAHAVADI, P., MÜLLER, S., PREM, G., SABOOR, F., SIMON, P., MIDDENDORFF, R., GEYER, H. & HENNEKE, I. 2013. Soluble polysialylated NCAM: a novel player of the innate immune system in the lung. *Cellular and molecular life sciences,* 70**,** 3695-3708.

URAYAMA, O. & SWEADNER, K. J. 1988. Ouabain sensitivity of the alpha 3 isozyme of rat Na, K-ATPase. *Biochemical and biophysical research communications,* 156**,** 796-800.

URYU, K., BUTLER, A. K. & CHESSELET, M. F. 1999. Synaptogenesis and ultrastructural localization of the polysialylated neural cell adhesion molecule in the developing striatum. *J Comp Neurol,* 405**,** 216-32.

VAGIN, O., TURDIKULOVA, S. & SACHS, G. 2005. Recombinant addition of N-glycosylation sites to the basolateral Na, K-ATPase β1 subunit results in its clustering in caveolae and apical sorting in HGT-1 cells. *Journal of Biological Chemistry,* 280**,** 43159-43167.

VAITHIANATHAN, T., MATTHIAS, K., BAHR, B., SCHACHNER, M., SUPPIRAMANIAM, V., DITYATEV, A. & STEINHAÜSER, C. 2004. Neural cell adhesion molecule-associated polysialic acid potentiates α-amino-3-hydroxy-5-methylisoxazole-4-propionic acid receptor currents. *Journal of Biological Chemistry,* 279**,** 47975-47984.

VANDAMME, T. F. 2014. Use of rodents as models of human diseases. *Journal of Pharmacy and Bioallied Sciences,* 6**,** 2.

VAREA, E., BELLES, M., VIDUEIRA, S., BLASCO-IBAÑEZ, J. M., CRESPO, C., PASTOR, Á. M. & NACHER, J. 2011. PSA-NCAM is expressed in immature, but not recently generated, neurons in the adult cat cerebral cortex layer II. *Frontiers in neuroscience,* 5**,** 17.

VAREA, E., CASTILLO-GÓMEZ, E., GÓMEZ-CLIMENT, M. Á., BLASCO-IBÁÑEZ, J. M., CRESPO, C., MARTÍNEZ-GUIJARRO, F. J. & NÀCHER, J. 2007. PSA-NCAM expression in the human prefrontal cortex. *Journal of chemical neuroanatomy,* 33**,** 202-209.

VAREA, E., CASTILLO-GÓMEZ, E., GÓMEZ-CLIMENT, M. Á., GUIRADO, R., BLASCO-IBÁÑEZ, J. M., CRESPO, C., MARTÍNEZ-GUIJARRO, F. J. & NÁCHER, J. 2009. Differential evolution of PSA-NCAM expression during aging of the rat telencephalon. *Neurobiology of aging,* 30**,** 808-818.

VAREA, E., GUIRADO, R., GILABERT-JUAN, J., MARTÍ, U., CASTILLO-GOMEZ, E., BLASCO-IBÁÑEZ, J. M., CRESPO, C. & NACHER, J. 2012. Expression of PSA-NCAM and synaptic proteins in the amygdala of psychiatric disorder patients. *Journal of psychiatric research,* 46**,** 189-197.

VAREA, E., NACHER, J., BLASCO-IBANEZ, J., GOMEZ-CLIMENT, M., CASTILLO-GOMEZ, E., CRESPO, C. & MARTINEZ-GUIJARRO, F. 2005. PSA-NCAM expression in the rat medial prefrontal cortex. *Neuroscience,* 136**,** 435-443.

VARKEY, D., MAZARD, S., OSTROWSKI, M., TETU, S. G., HAYNES, P. & PAULSEN, I. T. 2016. Effects of low temperature on tropical and temperate isolates of marine Synechococcus. *The ISME journal,* 10**,** 1252-1263.

VARKI, A. 1993. Biological roles of oligosaccharides: all of the theories are correct. *Glycobiology,* 3**,** 97-130.
VARKI, A. 2007. Glycan-based interactions involving vertebrate sialic-acid-recognizing proteins. *Nature,* 446**,** 1023-1029.
VARKI, A. 2011. Evolutionary forces shaping the Golgi glycosylation machinery: why cell surface glycans are universal to living cells. *Cold Spring Harbor perspectives in biology,* 3**,** a005462.
VARKI, A. 2017. Biological roles of glycans. *Glycobiology,* 27**,** 3-49.
VARKI, A. & SCHAUER, R. 2009. Sialic acids. *In:* VARKI A, C. R., ESKO JD, ET AL. (ed.) *Essentials of Glycobiology.* 2nd ed. Cold Spring Harbor (NY): Cold Spring Harbor Laboratory Press.
VARKI, A. & SHARON, N. 2009. Historical Background and Overview. *In:* VARKI A, C. R., ESKO JD, ET AL. (ed.) *Essentials of Glycobiology.* 2 ed. Cold Spring Harbor (NY): Cold Spring Harbor Laboratory Press.
VAYSSETTES-COURCHAY, C., BOUYSSET, F., LAUBIE, M. & VERBEUREN, T. J. 1997. Central integration of the Bezold-Jarish reflex in the cat. *Brain research,* 744**,** 272-278.
VERBERNE, A. & GUYENET, P. G. 1992. Medullary pathway of the Bezold-Jarisch reflex in the rat. *American Journal of Physiology-Regulatory, Integrative and Comparative Physiology,* 263**,** R1195-R1202.
VERBERNE, A. J. & SARTOR, D. M. 2010. Rostroventrolateral medullary neurons modulate glucose homeostasis in the rat. *American Journal of Physiology-Endocrinology and Metabolism,* 299**,** E802-E807.
VERBERNE, A. J., SARTOR, D. M. & BERKE, A. 1999a. Midline medullary depressor responses are mediated by inhibition of RVLM sympathoexcitatory neurons in rats. *American Journal of Physiology-Regulatory, Integrative and Comparative Physiology,* 276**,** R1054-R1062.
VERBERNE, A. J., STORNETTA, R. L. & GUYENET, P. G. 1999b. Properties of C1 and other ventrolateral medullary neurones with hypothalamic projections in the rat. *The Journal of Physiology,* 517**,** 477-494.
VIEIRA, A. V., LAMAZE, C. & SCHMID, S. L. 1996. Control of EGF receptor signaling by clathrin-mediated endocytosis. *Science,* 274**,** 2086.
VILLA, G., CERUTI, S., ZANARDELLI, M., MAGNI, G., JASMIN, L., OHARA, P. T. & ABBRACCHIO, M. P. 2010. Temporomandibular joint inflammation activates glial and immune cells in both the trigeminal ganglia and in the spinal trigeminal nucleus. *Molecular pain,* 6**,** 89.
VIMR, E. R., KALIVODA, K. A., DESZO, E. L. & STEENBERGEN, S. M. 2004. Diversity of microbial sialic acid metabolism. *Microbiology and molecular biology reviews,* 68**,** 132-153.
VIT, J.-P., JASMIN, L., BHARGAVA, A. & OHARA, P. T. 2006. Satellite glial cells in the trigeminal ganglion as a determinant of orofacial neuropathic pain. *Neuron glia biology,* 2**,** 247-257.
VOELTZ, G. K., PRINZ, W. A., SHIBATA, Y., RIST, J. M. & RAPOPORT, T. A. 2006. A class of membrane proteins shaping the tubular endoplasmic reticulum. *Cell,* 124**,** 573-586.
VON DER OHE, M., WHEELER, S. F., WUHRER, M., HARVEY, D. J., LIEDTKE, S., MÜHLENHOFF, M., GERARDY-SCHAHN, R., GEYER, H., DWEK, R. A. & GEYER, R. 2002. Localization and characterization of polysialic acid–containing N-linked glycans from bovine NCAM. *Glycobiology,* 12**,** 47-63.
VUTSKITS, L., GASCON, E., ZGRAGGEN, E. & KISS, J. Z. 2006. The polysialylated neural cell adhesion molecule promotes neurogenesis in vitro. *Neurochemical research,* 31**,** 215-225.
WAKAI, J., TAKAMURA, D., MORINAGA, R., NAKAMUTA, N. & YAMAMOTO, Y. 2015. Differences in respiratory changes and Fos expression in the ventrolateral medulla of rats exposed to hypoxia, hypercapnia, and hypercapnic hypoxia. *Respiratory physiology & neurobiology,* 215**,** 64-72.
WAKAYAMA, T., SAI, Y., ITO, A., KATO, Y., KUROBO, M., MURAKAMI, Y., NAKASHIMA, E., TSUJI, A., KITAMURA, Y. & ISEKI, S. 2007. Heterophilic binding of the adhesion molecules poliovirus receptor and immunoglobulin superfamily 4A in the interaction between mouse spermatogenic and Sertoli cells. *Biology of reproduction,* 76**,** 1081-1090.

WAKISAKA, S., KAJANDER, K. & BENNETT, G. 1992. Effects of peripheral nerve injuries and tissue inflammation on the levels of neuropeptide Y-like immunoreactivity in rat primary afferent neurons. *Brain research,* 598**,** 349-352.

WALMOD, P. S., KOLKOVA, K., BEREZIN, V. & BOCK, E. 2004. Zippers make signals: NCAM-mediated molecular interactions and signal transduction. *Neurochemical research,* 29**,** 2015-2035.

WANG, B., CHEN, Y., REN, H., ZHANG, N., TROY, I. & ARTHUR, F. 2017. Biochemical Characterization and Analyses of Polysialic Acid-Associated Carrier Proteins and Genes in Piglets during Neonatal Development. *ChemBioChem*.

WATZLAWIK, J. O., KAHOUD, R. J., NG, S., PAINTER, M. M., PAPKE, L. M., ZOECKLEIN, L., WOOTLA, B., WARRINGTON, A. E., CAREY, W. A. & RODRIGUEZ, M. 2015. Polysialic acid as an antigen for monoclonal antibody HIgM12 to treat multiple sclerosis and other neurodegenerative disorders. *Journal of neurochemistry,* 134**,** 865-878.

WEIGEL, P. H. & YIK, J. H. 2002. Glycans as endocytosis signals: the cases of the asialoglycoprotein and hyaluronan/chondroitin sulfate receptors. *Biochimica et Biophysica Acta (BBA)-General Subjects,* 1572**,** 341-363.

WEINHOLD, B., SEIDENFADEN, R., RÖCKLE, I., MÜHLENHOFF, M., SCHERTZINGER, F., CONZELMANN, S., MARTH, J. D., GERARDY-SCHAHN, R. & HILDEBRANDT, H. 2005. Genetic ablation of polysialic acid causes severe neurodevelopmental defects rescued by deletion of the neural cell adhesion molecule. *Journal of Biological Chemistry,* 280**,** 42971-42977.

WENKER, I. C., ABE, C., VIAR, K. E., STORNETTA, D. S., STORNETTA, R. L. & GUYENET, P. G. 2017. Blood Pressure Regulation by the Rostral Ventrolateral Medulla in Conscious Rats: Effects of Hypoxia, Hypercapnia, Baroreceptor Denervation, and Anesthesia. *Journal of Neuroscience,* 37**,** 4565-4583.

WERNEBURG, S., BUETTNER, F. F., ERBEN, L., MATHEWS, M., NEUMANN, H., MÜHLENHOFF, M. & HILDEBRANDT, H. 2016. Polysialylation and lipopolysaccharide-induced shedding of E-selectin ligand-1 and neuropilin-2 by microglia and THP-1 macrophages. *Glia,* 64**,** 1314-1330.

WERNEBURG, S., MÜHLENHOFF, M., STANGEL, M. & HILDEBRANDT, H. 2015. Polysialic acid on SynCAM 1 in NG2 cells and on neuropilin-2 in microglia is confined to intracellular pools that are rapidly depleted upon stimulation. *Glia,* 63**,** 1240-1255.

WEST, S., BANNISTER, K., DICKENSON, A. & BENNETT, D. 2015. Circuitry and plasticity of the dorsal horn–toward a better understanding of neuropathic pain. *Neuroscience,* 300**,** 254-275.

WESTMAN, J., ERIKSSON, S., GISSLER, M., HÄLLGREN, J., PRIETO, M., BOBO, W., FRYE, M., ERLINGE, D., ALFREDSSON, L. & ÖSBY, U. 2017. Increased cardiovascular mortality in people with schizophrenia: a 24-year national register study. *Epidemiology and Psychiatric Sciences***,** 1-9.

WETIE, A. G. N., SOKOLOWSKA, I., WOODS, A. G., ROY, U., DEINHARDT, K. & DARIE, C. C. 2014. Protein–protein interactions: switch from classical methods to proteomics and bioinformatics-based approaches. *Cellular and molecular life sciences,* 71**,** 205-228.

WHEATLEY, M. & HAWTIN, S. R. 1999. Glycosylation of G-protein-coupled receptors for hormones central to normal reproductive functioning: its occurrence and role. *Human reproduction update,* 5**,** 356-364.

WIERNASZ, E., KALISZEWSKA, A., BRUTKOWSKI, W., BEDNARCZYK, J., GORNIAK, M., KAZA, B. & LUKASIUK, K. 2014. Ttyh1 protein is expressed in glia in vitro and shows elevated expression in activated astrocytes following status epilepticus. *Neurochemical research,* 39**,** 2516-2526.

WILHELMSSON, U., LI, L., PEKNA, M., BERTHOLD, C.-H., BLOM, S., ELIASSON, C., RENNER, O., BUSHONG, E., ELLISMAN, M. & MORGAN, T. E. 2004. Absence of glial fibrillary acidic protein and vimentin prevents hypertrophy of astrocytic processes and improves post-traumatic regeneration. *Journal of Neuroscience,* 24**,** 5016-5021.

WILLETTE, R., BARCAS, P., KRIEGER, A. & SAPRU, H. N. 1983a. Vasopressor and depressor areas in the rat medulla: identification by microinjection of L-glutamate. *Neuropharmacology,* 22**,** 1071-1079.
WILLETTE, R. N., KRIEGER, A., BARCAS, P. & SAPRU, H. 1983b. Medullary gamma-aminobutyric acid (GABA) receptors and the regulation of blood pressure in the rat. *Journal of Pharmacology and Experimental Therapeutics,* 226**,** 893-899.
WILLIS, L. M. & WHITFIELD, C. 2013. Structure, biosynthesis, and function of bacterial capsular polysaccharides synthesized by ABC transporter-dependent pathways. *Carbohydrate research,* 378**,** 35-44.
WILLIS, W. D. & COGGESHALL, R. E. 2004. Structure of the dorsal horn. *In:* WILLIS, W. D. & COGGESHALL, R. E. (eds.) *Sensory Mechanisms of the Spinal Cord. Primary Afferent Neurons and the Spinal Dorsal Horn.* third ed. New York, USA: Kluwer Academic/Plenum Publishers.
WILSON, C. & GONZÁLEZ-BILLAULT, C. 2015. Regulation of cytoskeletal dynamics by redox signaling and oxidative stress: implications for neuronal development and trafficking. *Frontiers in cellular neuroscience,* 9.
WONG, C.-H. 2005. Protein glycosylation: new challenges and opportunities. *The Journal of organic chemistry,* 70**,** 4219-4225.
WOOLF, C. J. 1983. Evidence for a central component of post-injury pain hypersensitivity. *Nature*.
WOOLF, C. J. & SALTER, M. W. 2000. Neuronal plasticity: increasing the gain in pain. *Science,* 288**,** 1765-1768.
WORLEY, P. F., BARABAN, J. M., VAN DOP, C., NEER, E. J. & SNYDER, S. H. 1986. Go, a guanine nucleotide-binding protein: immunohistochemical localization in rat brain resembles distribution of second messenger systems. *Proceedings of the National Academy of Sciences,* 83**,** 4561-4565.
XENAKI, D., MARTIN, I. B., YOSHIDA, L., OHYAMA, K., GENNARINI, G., GRUMET, M., SAKURAI, T. & FURLEY, A. J. 2011. F3/contactin and TAG1 play antagonistic roles in the regulation of sonic hedgehog-induced cerebellar granule neuron progenitor proliferation. *Development,* 138**,** 519-529.
XIE, R., DONG, L., DU, Y., ZHU, Y., HUA, R., ZHANG, C. & CHEN, X. 2016. In vivo metabolic labeling of sialoglycans in the mouse brain by using a liposome-assisted bioorthogonal reporter strategy. *Proceedings of the National Academy of Sciences,* 113**,** 5173-5178.
XING, S., WALLMEROTH, N., BERENDZEN, K. W. & GREFEN, C. 2016. Techniques for the analysis of protein-protein interactions in vivo. *Plant physiology,* 171**,** 727-758.
XING, T. & PILOWSKY, P. M. 2010. Acute intermittent hypoxia in rat in vivo elicits a robust increase in tonic sympathetic nerve activity that is independent of respiratory drive. *The Journal of physiology,* 588**,** 3075-3088.
YABE, U., SATO, C., MATSUDA, T. & KITAJIMA, K. 2003. Polysialic Acid in Human Milk CD36 IS A NEW MEMBER OF MAMMALIAN POLYSIALIC ACID-CONTAINING GLYCOPROTEIN. *Journal of Biological Chemistry,* 278**,** 13875-13880.
YAGUCHI, M., OHASHI, Y., TSUBOTA, T., SATO, A., KOYANO, K. W., WANG, N. & MIYASHITA, Y. 2013. Characterization of the properties of seven promoters in the motor cortex of rats and monkeys after lentiviral vector-mediated gene transfer. *Human gene therapy methods,* 24**,** 333-344.
YANG, P., MAJOR, D. & RUTISHAUSER, U. 1994. Role of charge and hydration in effects of polysialic acid on molecular interactions on and between cell membranes. *Journal of Biological Chemistry,* 269**,** 23039-23044.
YANG, P., YIN, X. & RUTISHAUSER, U. 1992. Intercellular space is affected by the polysialic acid content of NCAM. *The Journal of cell biology,* 116**,** 1487-1496.
YEN, H.-Y., LIU, Y.-C., CHEN, N.-Y., TSAI, C.-F., WANG, Y.-T., CHEN, Y.-J., HSU, T.-L., YANG, P.-C. & WONG, C.-H. 2015. Effect of sialylation on EGFR phosphorylation and resistance to tyrosine kinase inhibition. *Proceedings of the National Academy of Sciences,* 112**,** 6955-6960.

YIN, H., SONG, C.-Q., DORKIN, J. R., ZHU, L. J., LI, Y., WU, Q., PARK, A., YANG, J., SURESH, S. & BIZHANOVA, A. 2016. Therapeutic genome editing by combined viral and non-viral delivery of CRISPR system components in vivo. *Nature biotechnology,* 34**,** 328-333.

YUYAMA, K., SEKINO-SUZUKI, N., SANAI, Y. & KASAHARA, K. 2007. Translocation of activated heterotrimeric G protein Gαo to ganglioside-enriched detergent-resistant membrane rafts in developing cerebellum. *Journal of Biological Chemistry,* 282**,** 26392-26400.

YUZWA, S. A., SHAN, X., MACAULEY, M. S., CLARK, T., SKOROBOGATKO, Y., VOSSELLER, K. & VOCADLO, D. J. 2012. Increasing O-GlcNAc slows neurodegeneration and stabilizes tau against aggregation. *Nature chemical biology,* 8**,** 393-399.

ZEILHOFER, H. U., WILDNER, H. & YÉVENES, G. E. 2012. Fast synaptic inhibition in spinal sensory processing and pain control. *Physiological reviews,* 92**,** 193-235.

ZHANG, H., VUTSKITS, L., CALAORA, V., DURBEC, P. & KISS, J. Z. 2004. A role for the polysialic acid–neural cell adhesion molecule in PDGF-induced chemotaxis of oligodendrocyte precursor cells. *Journal of cell science,* 117**,** 93-103.

ZHANG, J. & MIFFLIN, S. W. 1998. Differential roles for NMDA and non-NMDA receptor subtypes in baroreceptor afferent integration in the nucleus of the solitary tract of the rat. *The Journal of Physiology,* 511**,** 733-745.

ZHANG, J., WALKER, J. F., GUARDIOLA, J. & YU, J. 2006. Pulmonary sensory and reflex responses in the mouse. *Journal of Applied Physiology,* 101**,** 986-992.

ZHANG, J., ZHAO, J., JIANG, W.-J., SHAN, X.-W., YANG, X.-M. & GAO, J.-G. 2012. Conditional gene manipulation: Cre-ating a new biological era. *Journal of Zhejiang University-Science B,* 13**,** 511-524.

ZHANG, Y., CAMPBELL, G., ANDERSON, P., MARTINI, R., SCHACHNER, M. & LIEBERMAN, A. 1995. Molecular basis of interactions between regenerating adult rat thalamic axons and Schwann cells in peripheral nerve grafts I. Neural cell adhesion molecules. *Journal of Comparative Neurology,* 361**,** 193-209.

ZHANG, Y., GHADIRI-SANI, M., ZHANG, X., RICHARDSON, P. M., YEH, J. & BO, X. 2007a. Induced expression of polysialic acid in the spinal cord promotes regeneration of sensory axons. *Molecular and Cellular Neuroscience,* 35**,** 109-119.

ZHANG, Y., ZHANG, X., WU, D., VERHAAGEN, J., RICHARDSON, P. M., YEH, J. & BO, X. 2007b. Lentiviral-mediated expression of polysialic acid in spinal cord and conditioning lesion promote regeneration of sensory axons into spinal cord. *Molecular Therapy,* 15**,** 1796-1804.

ZHANG, Y., ZHANG, X., YEH, J., RICHARDSON, P. & BO, X. 2007c. Engineered expression of polysialic acid enhances Purkinje cell axonal regeneration in L1/GAP-43 double transgenic mice. *European Journal of Neuroscience,* 25**,** 351-361.

ZHEN, J., ANTONIO, T., JACOB, J. C., GRANDY, D. K., REITH, M. E., DUTTA, A. K. & SELLEY, D. E. 2016. Efficacy of hybrid tetrahydrobenzo [d] thiazole based aryl piperazines D-264 and D-301 at D2 and D3 receptors. *Neurochemical research,* 41**,** 328-339.

ZIGOVA, T., PENCEA, V., WIEGAND, S. J. & LUSKIN, M. B. 1998. Intraventricular administration of BDNF increases the number of newly generated neurons in the adult olfactory bulb. *Molecular and Cellular Neuroscience,* 11**,** 234-245.

ZUBER, C., LACKIE, P. M., CATTERALL, W. A. & ROTH, J. 1992. Polysialic acid is associated with sodium channels and the neural cell adhesion molecule N-CAM in adult rat brain. *Journal of Biological Chemistry,* 267**,** 9965-9971.

ZYBAILOV, B., MOSLEY, A. L., SARDIU, M. E., COLEMAN, M. K., FLORENS, L. & WASHBURN, M. P. 2006. Statistical Analysis of Membrane Proteome Expression Changes in Saccharomyces c erevisiae. *Journal of proteome research,* 5**,** 2339-2347.

Appendices

ANIMAL RESEARCH AUTHORITY (ARA)

AEC Reference No.: 2014/041-5 **Date of Expiry:** 25 October 2017

Full Approval Duration: *25 October 2014 to 25 October 2017 (36 Months)*

This ARA remains in force until the Date of Expiry (unless suspended, cancelled or surrendered) **and will only be renewed upon receipt of a satisfactory Progress Report before expiry (see Approval email for submission details).**

Principal Investigator:
A/Professor Ann Goodchild
FMHS Laboratory
Macquarie University, NSW 2109
Ann.goodchild@mq.edu.au

Associate Investigators:
Phillip Wisinski-Bokiniec
Shila Shahbazian
Britt Berning
Katherine Robinson

In case of emergency, please contact:
the Principal Investigator / Associate Investigator named above
or Manager, CAF: 9850 7780 / 0428 861 163 and **Animal Welfare Officer**: 9850 7758 / 0439 497 383

The above-named are authorised by MACQUARIE UNIVERSITY ANIMAL ETHICS COMMITTEE to conduct the following research:

Title of the project: **Function and interacting partners of polysialic acid in functionally distinct regions of the central nervous system**

Purpose: **4 - Research: Human or Animal Biology**

Aims: **To: 1. Identify whether neuraminidase in the NTS is exhibiting its effects via BDNF/TRKB mechanism. 2. Identify what glycan linkages are functionally relevant in the NTS. A control region containing low levels of PSA-NCAM will also be assessed- the rostral ventrolateral medulla (RVLM) 3.Identify the binding partners of PSA in 6 areas associated with cardiovascular control and pain transmission. 4. Identify whether inflammatory pain increases PSA in trigeminal ganglia and trigeminal nucleus.**

Surgical Procedures category: 7 - Major Physiological Challenge
All procedures must be performed as per the AEC-approved protocol, unless stated otherwise by the AEC and/or AWO.

Maximum numbers approved (for the Full Approval Duration):

Species	Strain	Age/Sex/Weight	Total	Supplier/Source
02 Rattus	Sprague Dawley	6- 8 weeks/ Male	215	ARCH Perth
			215	

Location of research:

Location	*Full street address*
Central Animal Facility	Building F9A, Research Park Drive, Macquarie University, NSW 2109
FMHS Laboratory	Level 1, Clinic Building, 2 Technology Place, Macquarie University NSW 2109

Amendments approved by the AEC since initial approval:

1. **Amendment #1 -** Addition of Britt Berning as Associate Investigator (Executive approved. Ratified by AEC 20 August 2015)
2. **Amendment #2 -** Extend study currently carried only in rat to now include mice (Declined by AEC 10 December 2015).
3. **Amendment #3 -** Add Katherine Robinson as Associate Investigator (Executive approved. Ratified by AEC 19 May 2016).

Conditions of Approval: N/A

Being animal research carried out in accordance with the Code of Practice for a recognised research purpose and in connection with animals (other than exempt animals) that have been obtained from the holder of an animal suppliers licence.

Assoc. Professor Jennifer Cornish (Chair, Animal Ethics Committee) **Approval Date: 20 October 2016**

MACQUARIE University ANIMAL RESEARCH AUTHORITY (ARA)

AEC Reference No.: 2015/040-3 **Date of Expiry:** 31 July 2017

Full Approval Duration: *01 January 2016 to 31 July 2017*

This ARA remains in force until the Date of Expiry (unless suspended, cancelled or surrendered) **and will only be renewed upon receipt of a satisfactory Progress Report before expiry (see Approval email for submission details).**

Principal Investigator:
Associate Professor Ann Goodchild
Faculty of Medicine and Health Sciences
Macquarie University, NSW 2109
ann.goodchild@mq.edu.au

Associate Investigators:
Britt Berning
Anita Turner
Shila Shahbazian
Katherine Robinson

In case of emergency, please contact:
the Principal Investigator / Associate Investigator named above
or Manager, CAF: 9850 7780 / 0428 861 163 and **Animal Welfare Officer**: 9850 7758 / 0439 497 383

The above-named are authorised by MACQUARIE UNIVERSITY ANIMAL ETHICS COMMITTEE to conduct the following research:

Title of the project: **Distribution and binding partners of polysialic acid in the brainstem of mice**

Purpose: **4 - Research: Human or Animal Biology**

Aims: **1. To describe the distribution of polysialic acid in the mouse brainstem and spinal cord and compare this with our current data in rats**
2. To identify binding partners of polysialic acid in mouse dorsal horn of the spinal cord and compare these with those identified in rats.
3. To determine whether the binding partners identified in mouse require the presence of NCAM or not.

Surgical Procedures category: 2 - Animal Unconscious without Recovery

All procedures must be performed as per the AEC-approved protocol, unless stated otherwise by the AEC and/or AWO.

Maximum numbers approved (for the Full Approval Duration):

Species	Strain	Age/Weight/Sex	Total	Supplier/Source
01 - Mice	C57BL/6JArc	10-16weeks/Any/Male	93	Animal Resources Centre, Perth

Location of research:

Location	*Full street address*
Central Animal Facility	Building F9A, Research Park Drive, Macquarie University, NSW 2109
FMHS Laboratory	Level 1, F10A, 2 Technology Place, Macquarie University, NSW 2109

Amendments approved by the AEC since initial approval:
1. **Amendment #1 -** Add Katherine Robinson as Associate Investigator (Executive approved. Ratified by AEC 19 May 2016).
2. **Amendment #2 -** Extend the approved duration of the project to 31 July 2017 (Approved by AEC 07 December 2016).

Conditions of Approval: N/A

Being animal research carried out in accordance with the Code of Practice for a recognised research purpose and in connection with animals (other than exempt animals) that have been obtained from the holder of an animal suppliers licence.

Dr Karolyn White (Acting Chair, Animal Ethics Committee) **Approval Date: 07 December 2016**

MACQUARIE University ANIMAL RESEARCH AUTHORITY (ARA)

AEC Reference No.: 2015/041-3 **Date of Expiry:** 14 December 2017

Full Approval Duration: *14 December 2015 to 14 December 2017*

This ARA remains in force until the Date of Expiry (unless suspended, cancelled or surrendered) **and will only be renewed upon receipt of a satisfactory Progress Report before expiry (see Approval email for submission details).**

Principal Investigator:
Associate Professor Ann Goodchild

Faculty of Medicine and Health Sciences
Macquarie University, NSW 2109
ann.goodchild@mq.edu.au

Associate Investigators:
Britt Berning
Anita Turner
Shila Shahbazian
Simon McMullan
Katherine Robinson
Sheng Le

In case of emergency, please contact:
the Principal Investigator / Associate Investigator named above
or Manager, CAF: 9850 7780 / 0428 861 163 and **Animal Welfare Officer**: 9850 7758 / 0439 497 383

The above-named are authorised by MACQUARIE UNIVERSITY ANIMAL ETHICS COMMITTEE to conduct the following research:

Title of the project: **Overexpression of polysialic acid: method development and functional consequences**

Purpose: **4 - Research: Human or Animal Biology**

Aims:
1. **Develop a method utilising viral vectors which increases expression of polysialic acid in the brainstem**
2. **Determine where in the cell and tissue overexpression of polysialic acid is found.**
3. **Determine whether virally mediated overexpression of polysialic acid in the NTS or RVLM alters the tonic and reflex control of blood pressure**

Surgical Procedures category: 5 - Major Surgery with Recovery

All procedures must be performed as per the AEC-approved protocol, unless stated otherwise by the AEC and/or AWO.

Maximum numbers approved (for the Full Approval Duration):

Species	Strain	Age/Weight/Sex	Total	Supplier/Source
02 - Rat	Sprague Dawley	10-14 weeks/Any/Male	164	Animal Resources Centre, Perth

Location of research:

Location	*Full street address*
Central Animal Facility	Building F9A, Research Park Drive, Macquarie University, NSW 2109
Faculty of Medicine and Health Sciences	Level 1, F10A, 2 Technology Place, Macquarie University, NSW 2109

Amendments approved by the AEC since initial approval:
1. **Amendment #1 -** Add Katherine Robinson as Associate Investigator (Executive approved. Ratified by AEC 19 May 2016).
2. **Amendment #2** - Add Sheng Le as Associate Investigator (Executive approved. Ratified by AEC 07 December 2016).
3. **Amendment #3** - Extend protocol for 12 months until 14 December 2017 (Approved by AEC 07 December 2016).

Conditions of Approval: N/A

Being animal research carried out in accordance with the Code of Practice for a recognised research purpose and in connection with animals (other than exempt animals) that have been obtained from the holder of an animal suppliers licence.

Dr Karolyn White (Acting Chair, Animal Ethics Committee) **Approval Date: 07 December 2016**

Development/Plasticity/Repair

Polysialic Acid Regulates Sympathetic Outflow by Facilitating Information Transfer within the Nucleus of the Solitary Tract

Phillip Bokiniec,[1,9] Shila Shahbazian,[1] Stuart J. McDougall,[2] Britt A. Berning,[1] Delfine Cheng,[3] Ida J. Llewellyn-Smith,[4] Peter G.R. Burke,[5] Simon McMullan,[1] Martina Mühlenhoff,[6] Herbert Hildebrandt,[6] Filip Braet,[3,7] Mark Connor,[1] Nicolle H. Packer,[8] and Ann K. Goodchild[1]

[1]Department of Biomedical Sciences, Faculty of Medicine and Health Sciences, Macquarie University, Sydney, 2109 New South Wales, Australia, [2]Florey Institute of Neuroscience and Mental Health, University of Melbourne, Melbourne, 3010 Victoria, Australia, [3]School of Medical Sciences, Discipline of Anatomy and Histology, University of Sydney, Sydney, 2006 New South Wales, Australia, [4]Cardiovascular Medicine and Human Physiology, Flinders University, Adelaide, 5042 South Australia, Australia, [5]Neuroscience Research Australia, Sydney, 2031 New South Wales, Australia, [6]Institut für Zelluläre Chemie, Medizinische Hochschule Hannover, Hannover 30625, Germany, [7]Australian Centre for Microscopy and Microanalysis, University of Sydney, Sydney, 2006 New South Wales, Australia, [8]ARC Centre of Excellence in Nanoscale Biophotonics, Macquarie University, Sydney, 2109 New South Wales, Australia, and [9]Max Delbrück Center for Molecular Medicine, Robert-Roessle-Str. 10, Berlin, 13092, Germany

Expression of the large extracellular glycan, polysialic acid (polySia), is restricted in the adult, to brain regions exhibiting high levels of plasticity or remodeling, including the hippocampus, prefrontal cortex, and the nucleus of the solitary tract (NTS). The NTS, located in the dorsal brainstem, receives constant viscerosensory afferent traffic as well as input from central regions controlling sympathetic nerve activity, respiration, gastrointestinal functions, hormonal release, and behavior. Our aims were to determine the ultrastructural location of polySia in the NTS and the functional effects of enzymatic removal of polySia, both *in vitro* and *in vivo*. polySia immunoreactivity was found throughout the adult rat NTS. Electron microscopy demonstrated polySia at sites that influence neurotransmission: the extracellular space, fine astrocytic processes, and neuronal terminals. Removing polySia from the NTS had functional consequences. Whole-cell electrophysiological recordings revealed altered intrinsic membrane properties, enhancing voltage-gated K^+ currents and increasing intracellular Ca^{2+}. Viscerosensory afferent processing was also disrupted, dampening low-frequency excitatory input and potentiating high-frequency sustained currents at second-order neurons. Removal of polySia in the NTS of anesthetized rats increased sympathetic nerve activity, whereas functionally related enzymes that do not alter polySia expression had little effect. These data indicate that polySia is required for the normal transmission of information through the NTS and that changes in its expression alter sympathetic outflow. polySia is abundant in multiple but discrete brain regions, including sensory nuclei, in both the adult rat and human, where it may regulate neuronal function by mechanisms identified here.

Key words: electron microscopy; nucleus of the solitary tract; patch clamp; polysialic acid; sympathetic nerve activity; viscerosensory afferents

Significance Statement

All cells are coated in glycans (sugars) existing predominantly as glycolipids, proteoglycans, or glycoproteins formed by the most complex form of posttranslational modification, glycosylation. How these glycans influence brain function is only now beginning to be elucidated. The adult nucleus of the solitary tract has abundant polysialic acid (polySia) and is a major site of integration, receiving viscerosensory information which controls critical homeostatic functions. Our data reveal that polySia is a determinant of neuronal behavior and excitatory transmission in the nucleus of the solitary tract, regulating sympathetic nerve activity. polySia is abundantly expressed at distinct brain sites in adult, including major sensory nuclei, suggesting that sensory transmission may also be influenced via mechanisms described here. These findings hint at the importance of elucidating how other glycans influence neural function.

Introduction

The extracellular space is complex, filled with molecularly diverse matrix, a dynamic structure that influences neuronal function (Venstrom and Reichardt, 1993; Theodosis et al., 2008). This extracellular matrix is enriched in proteoglycans, as well as membrane bound glycoproteins and glycolipids commonly terminated by sialic acids, that form elaborate coats around all cells (Schnaar et al., 2014).

Polysialic acid (polySia) is a long, homopolymer composed of eight or more α2,8-linked sialic acids (Schauer, 2009; Chen and Varki, 2010). It is linked predominantly to the neural cell adhesion molecule (NCAM) and its expression is developmentally regulated (Bonfanti et al., 1992; Szele et al., 1994; Oltmann-Norden et al., 2008). In adult CNS, polySia expression is restricted to discrete regions that exhibit high levels of synaptic remodeling, including the hippocampus, cortex, and hypothalamus (Bonfanti et al., 1992; Rutishauser and Landmesser, 1996; Bonfanti, 2006; Hildebrandt and Dityatev, 2015). In these regions, polySia modulates synaptic plasticity and efficacy via a range of postulated mechanisms, including interactions with cell adhesion complexes, binding of neurotransmitter/neurotrophic substances, or via actions at glutamate receptors (Rutishauser and Landmesser, 1996; Rutishauser, 2008; Schnaar et al., 2014; Hildebrandt and Dityatev, 2015). In adults, polySia is also highly expressed in the nucleus of the solitary tract (NTS) (Bouzioukh et al., 2001a, b; Bonfanti, 2006). Despite such abundance, the precise location and function/s exerted by polySia in the NTS are unknown.

The NTS is a major integrative center receiving synaptic input from peripheral cardiovascular, respiratory, and gastrointestinal sensors as well as descending drive from higher brain centers, and is a critical relay of multiple homeostatic reflexes (Andresen and Paton, 2011; Pilowsky and Goodchild, 2002; Guyenet, 2006; Browning and Travagli, 2014). Glutamatergic viscerosensory afferents enter via the solitary tract and synapse with second-order NTS neurons (Talman et al., 1980; Appleyard et al., 2007; McDougall et al., 2009; Jin et al., 2010). Information is then relayed within the NTS or transmitted to more distal nuclei (Aicher et al., 1995; Hermes et al., 2006), driving a range of autonomic, hormonal, and behavioral responses. Plasticity occurs within the NTS, providing a beneficial adaptive mechanism acutely but chronically can be maladaptive, resulting in cardiovascular, respiratory, or gastrointestinal dysfunction (Kline, 2008; Browning and Travagli, 2010, 2014; Zoccal et al., 2014). Such plasticity is mediated by changes in presynaptic or postsynaptic excitability, via mechanisms, including quantal size, vesicle turnover, or release probability (Kline, 2008). The contribution of glycans to neurotransmission and/or plasticity in the NTS is unknown.

Only one group has investigated polySia in the NTS, demonstrating that high-frequency stimulation of the solitary tract reduced polySia expression (Bouzioukh et al., 2001a, b). Intriguingly, similar stimulation paradigms modify the effectiveness of excitatory and inhibitory synapses within the area (Miles, 1986; Glaum and Brooks, 1996; Zhou et al., 1997), resulting in increased sympathetic drive (Sun and Guyenet, 1987). Together, these data suggest that polySia in the NTS could modify neuronal function and the transfer of information to downstream networks, altering sympathetic nerve activity.

In exploring this hypothesis, we verified the distribution of polySia immunoreactivity in the adult rat NTS and described its ultrastructural location. Next, we determined the intrinsic neuronal properties and signaling mechanisms in the NTS altered by enzymatic removal of polySia, using whole-cell recordings in brain slice. Finally, we examined the consequences of this removal on sympathetic nerve activity *in vivo*. polySia was present at sites regulating information transfer: in fine astrocytic processes, the extracellular space, and axon terminals. We used multiple enzymes (neuraminidases) to desialylate glycans, including the polySia-specific enzyme, endo-*N*-acetyl-neuraminidase F (endoNF) (Stummeyer et al., 2005). Enzymatic removal of polySia within the NTS altered passive membrane properties, perturbed both high- and low-frequency viscerosensory afferent input, and increased sympathetic nerve activity. Our data indicate that, within the NTS, polySia expression is crucial for maintaining neuronal function and afferent transmission which, if altered, impacts signaling at downstream networks modifying sympathetic outflow.

Materials and Methods

Animal welfare and ethical approval

All experiments were conducted in accordance with the Australian Code of Practice for the Care and Use of Animals for Scientific Purposes and were performed with the approval of the Macquarie University Ethics Committee (Animal Research Authorities: 2012/015, 2014/019, 2014/041). Animals were housed under constant 12 h light/dark cycles and allowed standard rat chow *ad libitum*.

Immunohistochemistry

Immunohistochemical procedures were performed as previously described (Parker et al., 2013; Bou Farah et al., 2016). Male Sprague Dawley rats ($n = 4$) were anesthetized with sodium pentobarbital (80 mg/kg, i.p) and transcardially perfused with ice-cold DMEM followed by 4% PFA. Brains were removed and postfixed overnight in the same fixative. Coronal brainstem sections (40 μm) were cut using a vibrating microtome (Leica VT 1200S). Free-floating sections were permeabilized in 50% ethanol for 30 min at room temperature and washed in Tris-PBS (TPBS, 10 mM Tris, 0.9% NaCl, 0.05% thimerosal in 10 mM phosphate buffer, pH 7.4). Sections were incubated in primary antibodies (diluted in 10% normal horse serum in TPBS) against polySia (mouse Mab735, 0.1 μg/ml, RRID: AB_2619682) or synaptophysin (rabbit anti-synaptophysin, 1:500, Synaptic Systems, #101002, RRID: AB_2619681) for 48 h at 4°C. Sections were washed and then incubated in fluorescent conjugated secondaries (Cy3-conjugated donkey anti-mouse IgG, or 488-conjugated donkey anti-rabbit IgG, 1:250, Jackson ImmunoResearch Laboratories, #715-165-151, RRID: AB_2315777, and #711-545-152, RRID: AB_2313584, respectively) overnight at 4°C. Sections were washed, mounted onto glass slides using Dako mounting medium, and visualized using a Zeiss upright microscope (Axio Imager Z.2). Images were acquired using ZEN 2012 imaging software (Zeiss). High-power confocal images were visualized using a Leica confocal microscope (Leica TCS SP8) and acquired using Leica Application Software AF (Leica). All images were imported and analyzed using the ImageJ plugin Fiji (Schindelin et al., 2012).

Received Jan. 19, 2017; revised May 15, 2017; accepted May 25, 2017.

Author contributions: P.B., S.J.M., N.H.P., and A.K.G. designed research; P.B., S.S., B.A.B., D.C., I.J.L.-S., and A.K.G. performed research; M.M., H.H., F.B., and N.H.P. contributed unpublished reagents/analytic tools; P.B., B.A.B., I.J.L.-S., P.G.R.B., S.M., M.C., and A.K.G. analyzed data; P.B., S.J.M., B.A.B., I.J.L.-S., P.G.R.B., S.M., M.M., H.H., M.C., and A.K.G. wrote the paper.

P.B. is a scholar of the Australian Course in Advanced Neuroscience. This work was supported by the National Health and Medical Research Council of Australia APP1028183 and APP1030301, Australian Research Council DP120100920, and Hillcrest Foundation FR2014/0781. We thank Profs. John Bekkers and Javier Stern for helpful discussions regarding data collection and interpretation; Dr. Lama Bou-Farah for assisting in preliminary data collection; Prof. Rita Gerardy-Schahn for her valuable contribution; and Australian Microscopy and Microanalysis Research Facility (http://ammrf.org.au/) node at the University of Sydney for facilities and scientific and technical assistance.

The authors declare no competing financial interests.

Correspondence should be addressed to Dr. Ann K. Goodchild, Department of Biomedical Sciences, Faculty of Medicine and Health Sciences, Macquarie University, Sydney, 2109 New South Wales, Australia. E-mail: ann.goodchild@mq.edu.au.

DOI:10.1523/JNEUROSCI.0200-17.2017

 0270-6474/17/376559-17$15.00/0

Electron microscopy

The method for electron microscopic immunocytochemistry was slightly modified (Llewellyn-Smith et al., 2005). Male Sprague Dawley rats (n = 4, 10–12 weeks of age) were anesthetized and perfused as described above with 4% formaldehyde and 0.3% glutaraldehyde (Electron Microscopy Sciences) in 0.1 M phosphate buffer, pH 7.4. Brains were removed and postfixed overnight in same fixative. Coronal sections of the medulla were cut into 50 μm sections using a vibrating microtome (Leica VT 1200S). Free floating sections were then permeabilized in 50% ethanol for 3 h and washed briefly in phosphate buffer. Sections were blocked using 10% normal horse serum in TPBS for 30 min and subsequently incubated in primary antibody against polySia (mouse Mab735, 1 μg/ml, RRID: AB_2619682) diluted in 10% normal horse serum in TPBS for 7 d. Sections were then incubated in biotinylated anti-mouse Ig (1:500, Jackson ImmunoResearch Laboratories, #715-065-150, RRID: AB_2307438) for 4 d followed by exposure to ExtrAvidin-Peroxidase (1:1500, Sigma-Aldrich, #E2886, RRID: AB_2620165) for a further 4 d. All steps were performed at room temperature with sections washed in TPBS (3 × 30 min) following each incubation. Immunoreactivity for polySia was detected with a nickel-intensified 3,3′-DAB reaction using glucose oxidase. Sections were reacted for 30 min (or until strong signal was detected), and the reaction was halted with three washes in TPBS.

After the DAB reaction, sections were washed in 0.1 M PBS, osmicated in 0.5% osmium tetroxide, stained *en bloc* with 1% aqueous uranyl acetate, and dehydrated through a graded series of acetone solutions. Sections were then infiltrated with 1:1 acetone:medium grade EPON resin and then in 100% resin overnight. Resin was periodically changed over 2 d before sections were flat embedded between glass slides and ACLAR plastic film and polymerized at 60°C for 48 h. Regions of interest dissected using a scalpel blade and mounted onto flat blank blocks. Ultrathin sections (60 nm) were cut using a diamond knife and an ultramicrotome (Ultracut, Leica). Ultrathin sections were collected onto 200 μm mesh copper grids. Selected grids were poststained with 2% uranyl acetate and Reynold's lead citrate and imaged using a transmission electron microscope (JEM-1400, JEOL). Electron micrographs were acquired using Digital Micrograph Software (Gatan), imported to and analyzed using the ImageJ plugin Fiji (Schindelin et al., 2012).

In vitro *electrophysiology data collection and analysis*

Brainstem slice preparation. Coronal and horizontal brainstem slices were collected from male Sprague Dawley rats as described previously (Andresen and Yang, 1990; Titz and Keller, 1997). *Coronal slices*: Rats (weight: 50–250 g; mean age: P41 ± 2) were deeply anesthetized using isoflurane (5% in 100% O_2, Cenvet) and once nociceptive reflexes (hindpaw pinch) were absent, quickly decapitated. The brainstem was rapidly removed and placed in ice-cold aCSF (in mM as follows: 125 NaCl, 25 $NaHCO_3$, 3 KCl, 1.25 $NaH_2PO_4.H_2O$, 25 D-glucose, 2 $CaCl_2$, 1 $MgCl_2$, equilibrated with 95% O_2-5% CO_2). Coronal sections (300 μm) were cut using a vibrating microtome (Leica VT 1200S). Slices of the medial NTS (bregma: −13.92 to −13.56 mm) (Paxinos and Watson, 2006) were collected and placed in warm (34°C) aCSF and allowed to equilibrate for up to 60 min before recording. *Horizontal slices*: Rats (weight: 150–350 g; mean age: P56 ± 4) were deeply anesthetized using isoflurane (Cenvet, 5% in 100% O_2) and once nociceptive reflexes (hindpaw pinch) were absent, quickly decapitated. The brainstem was rapidly removed and placed in ice-cold aCSF. The cerebellum was then removed and a wedge of the ventral surface removed so as to orientate the brainstem at an angle that allows a 250-μm-thick slice to contain both the solitary tract and the nucleus. Slices were cut using a vibrating microtome (Leica VT 1200S) and placed in warm (34°C) aCSF. Slices were incubated for 60 min before recording. For "solitary tract evoked sustained current" protocol, the brainstem was initially incubated in ice-cold aCSF for 1 min, then sliced and incubated in Mg^{2+}-free aCSF for 60 min at 32°C.

Recording parameters. Slices were placed in a custom-built chamber continuously bathed in aCSF warmed to 32°C (Temperature Controller TC-324B, Warner Instruments). Submerged sections were secured with a nylon harp and superfused at a rate of 2 ml/min. All recordings were made from neurons within the intermediate NTS. Neurons were visualized using an Olympus microscope (BX51WI). Patch recording electrodes (3.5–5.5 MΩ) were pulled using a P2000 laser pipette puller (Sutter Instruments) and filled with a potassium gluconate (K-Glu) internal solution consisting of (in mM) as follows: 10 NaCl, 130 K-Glu, 11 EGTA, 10 HEPES, 1 $CaCl_2$, 2 $MgCl_2$, 2 Na_2ATP, 0.2 Na_2GTP, 0.5% biocytin, pH 7.35–7.45, 290–295 mOsm. Recording electrodes were guided using a micromanipulator (Mp-225, Sutter Instruments).

Recordings were obtained using a Multiclamp 700B patch clamp amplifier (Molecular Devices), sampled at 20 kHz, and acquired using a 1401 CED computerized acquisition system (Cambridge Electronic Design), and analyzed offline using Spike2 software (Cambridge Electronic Design). The selection criteria for usable recordings were based on neuron stability, resting membrane potentials below −45 mV upon breaking in, series resistances <25 MΩ, and input resistances >200 MΩ. Series resistances were not compensated and liquid junction potentials not corrected. Data were not further analyzed if a ≥20% change in any of the parameters mentioned above was observed.

Steady-state outward currents. Coronal slices were initially incubated in aCSF, neuraminidase (Neu; 0.01, 0.1, 1 U/ml), or endoNF (0.1, 1 μg/ml) for 60 min at room temperature before recording. In whole-cell voltage clamp (−60 mV clamped potential), membrane potentials were stepped in 10 mV intervals to determine the currents generated (−70 to 30 mV, Δ10 mV, 1000 ms step). aCSF and endoNF activated steady-state outward currents tested in the following paradigms: (1) in the recording pipette, EGTA was substituted with the calcium-chelating agent BAPTA (10 mM, Sigma-Aldrich #A4926); (2) the extracellular concentration of $CaCl_2$ was lowered to 0.1 mM; and (3) before and after superfusion of tetraethylammonium (TEA, 10 mM; Sigma-Aldrich #T2265). Steady-state outward currents were measured as the last 50 ms of the current generated at each voltage step, normalized to baseline current. Two-way ANOVA with Bonferonni's correction was used for data analysis of steady-state outward currents. Unpaired Mann–Whitney test was used for comparison between enzyme treatments.

Current evoked action potential discharge and after hyperpolarization (AHP). Coronal slices were initially incubated in either aCSF or endoNF (1 μg/ml) for 60 min at room temperature before recording. In current clamp (at resting membrane potentials), neurons were injected with depolarizing currents (10–100 pA, Δ10 pA, 500 ms per step) to evoke action potential discharge. The number of action potentials generated was then compared between endoNF and control (aCSF) treatment. The AHP was measured at the peak change in membrane potential (mV) 5 ms after termination of 100 pA current injection. AHP amplitude was then compared between endoNF and control (aCSF) treatment. Two-way ANOVA with Bonferonni correction was used for data analysis of action potential discharge. Unpaired t test was used for comparison.

Stimulus-evoked action potential generation. In horizontal slices, evoked action potential generation was investigated in previously identified monosynaptically connected neurons (described below). Action potential generation was induced by solitary tract stimulation (1 Hz, 20 stimuli) recorded in current-clamp mode. The number of action potentials generated in response to 20 stimuli (following frequency) was then compared before and 30 min after endoNF (1 μg/ml) infusion in the same neuron. The latency of action potential generation was calculated as the time between the stimulus artifact and the onset of the action potential. Paired t tests were used to compare responses.

Solitary tract evoked EPSCs and spontaneous EPSCs. A concentric bipolar stimulating electrode (200 μm outer tip diameter, Frederick Haer) was placed on the distal portion of the solitary tract rostral to the recording region. Using an Isolated Pulse stimulator (model 2100, A-M Systems), current shocks (100–800 μA; Δ50 μA) were delivered to the solitary tract every 6 s (shock duration 0.5 μs) until a compound evoked EPSC (eEPSC) was observed. The latency of eEPSCs was calculated as the time between the stimulus artifact and onset of the first eEPSC. Synaptic jitter between responses was calculated as previously described (Doyle and Andresen, 2001) and a jitter (SD <200 μs) was accepted to identify neurons connected monosynaptically. Only monosynaptically connected neurons were further analyzed. eEPSC amplitude and latency of solitary tract activation were subsequently recorded in the same neurons in the presence of aCSF and then endoNF (1 μg/ml, 30 min). Spontaneous EPSCs (sEPSCs) were recorded in the absence of stimulation. sEPSC frequencies and amplitudes were compared in the presence of aCSF and then endoNF (1 μg/ml,

30 min) in the same neuron. sEPSCs were characterized by having an amplitude >10 pA and interevent interval within 10 ms. Paired *t* tests were used to compare responses.

Solitary tract-evoked sustained current. In slices incubated and recorded in Mg^{2+}-free aCSF, we first identified monosynaptically connected neurons as described above before delivering high-frequency current shocks (50 Hz, 5–10 stimuli) to the solitary tract to evoke NMDA-mediated sustained currents as previously described (Zhao et al., 2015). The sustained current was measured as the percentage change in current 100 ms following initiation of the first stimulus in the presence of Mg^{2+}-free aCSF alone and then following endoNF (1 μg/ml, 30 min) superfusion, in the same neuron. Paired *t* tests were used to compare responses.

Miniature EPSCs (mEPSCs). mEPSCs were recorded in monosynaptically identified neurons, in the presence of the sodium channel blocker TTX (10 μM, Jomar Bioscience, #T550) and the $GABA_A$ receptor antagonist gabazine (GBZ; 25 μM, Sigma-Aldrich, #S106). Following recording of baseline mEPSCs (10 min, and until depolarizing steps injected in current clamp did not evoke action potentials), endoNF (1 μg/ml) was superfused for 30 min. The presence of glutamatergic mEPSCs was verified by infusion of the non-NMDA glutamate receptor antagonist CNQX (10 μM, Sigma-Aldrich, #C127) at the end of experimentation. mEPSC frequency was observed between single mEPSC events with amplitudes >10 pA and interevent intervals between 10 ms, expressed in 10 s bins. Paired *t* test was used for data analysis of all responses measured.

Immunohistochemical characterization of recorded neurons

Following electrophysiological experimentation, slices were incubated overnight in 4% PFA in PBS at 4°C followed by overnight incubation in cryoprotectant consisting of the following (in mM): 0.5 polyvinylpyrrolidone, 76.7 Na_2HPO_4, 26.6 NaH_2PO_4, 876 sucrose, 5 ethylene glycol. Slices were then processed for polySia immunoreactivity and recovery of recorded cells as described previously (Gogolla et al., 2006; Bou Farah et al., 2016). Briefly, free-floating sections were permeabilized using 0.5% Triton X-100 in 0.01 M PBS, overnight at 4°C. Slices were then blocked in 5% BSA in PBS for 4 h at room temperature. The antibody against polySia (mouse Mab735, 0.1 μg/ml, RRID: AB_2619682) was added and slices incubated for a 4 h at room temperature. Slices were then incubated in secondary antibody (Cy3-conjugated donkey anti-mouse IgG, 1:250, Jackson ImmunoResearch Laboratories #715-165-151, RRID: AB_2315777) and fluorophore-conjugated ExtrAvidin (ExtrAvidin-FITC, 1:500, Sigma-Aldrich #E2761, RRID: AB_2492295) for detection of the biocytin-filled cells, overnight at 4°C. Slices were washed, mounted onto glass slides using Dako mounting medium, and visualized using either a Zeiss upright microscope (Axio Imager Z.2), or Leica confocal microscope (Leica TCS SP8). Images were acquired and analyzed as described above.

In vivo *electrophysiology data collection and analysis*

Surgery and electrophysiological recordings. Male Sprague Dawley rats ($n = 26$, 10–12 weeks of age) were anesthetized with urethane (1.3 g/kg, i.p. 10% solution in saline, Sigma-Aldrich). Depth of anesthesia was assessed throughout each experiment by autonomic responses to hindpaw pinch. Core temperature was maintained between 36.5°C and 37°C by a homoeothermic heating blanket (Harvard Apparatus). The left femoral artery and vein were cannulated for measuring blood pressure and the administration of drugs and saline, respectively. The trachea was intubated to allow artificial oxygen-enriched ventilation. Rats were then paralyzed (pancuronium bromide, 0.8 mg/kg, i.v.) and ventilated with end-tidal CO_2 maintained between 3.5% and 4.5%. Animals were placed in a stereotaxic frame and the left greater splanchnic sympathetic nerve isolated, cut and prepared for recording, using bipolar silver wire electrodes as described previously (Burke et al., 2008). Nerve recordings were amplified (×10,000; CWE), bandpass filtered (0.1–3 kHz), sampled at 5 kHz (CED Micro 1401, Cambridge Electronic Design) and recorded using Spike2 software (Cambridge Electronic Design).

NTS microinjection. The dorsal surface of the medulla was exposed by removal of the occipital plate. NTS injections sites were in accordance with the location of the intermediate NTS (Paxinos and Watson, 2006). Following a 30 min baseline period, injections were made with respect to the calamus scriptorius 0.4 and 0. 8 mm rostral, 0.5 and 1.0 mm lateral, and 0.5 and 1.0 mm ventral to the dorsal surface, a total of 12 injections with a total injection volume of 800 nl. In some cases, vehicle control injections (12) were made before injection of enzymes. Following injection, responses were recorded for 60 min and at the end of experimentation rats were killed with an overdose of sodium pentobarbital (80 mg/kg, i.v.). Brains were removed and rapidly frozen to −80°C before dissection of the region containing the NTS (see below). Immunoblot was used to determine the level of enzymatic digestion of polySia. Neurograms were amplified, rectified, and smoothed (integrated splanchnic sympathetic nerve activity [sSNA], 1 s time constant). Changes were expressed as a percentage of baseline activity (100%). Time course analysis was obtained from data averaged over 5 min periods, from 5 min before microinjection to 60 min after completion of the microinjections. Data analysis was only performed after the injection period, as injection of any solution (including vehicle control) evoked fluctuations in sSNA. Peak responses were obtained at 60 min after the injection completion. Statistical analysis was performed using two-way ANOVA with Bonferonni correction. Comparison of enzymatic treatments was performed using the Mann–Whitney test.

Western blot

In vitro *tissue collection*. Coronal brain slices were collected as described above. Slices were then incubated in either aCSF, neuraminidase (0.1 U/ml, Sigma-Aldrich #N2876) or endoNF (1 μg/ml) (Stummeyer et al., 2005) for 0, 45, and 60 min at room temperature. Slices were then trimmed by removing the ventral half of the slice below the hypoglossal nucleus and the dorsal region was stored and frozen at −80°C.

In vivo *tissue collection*. To extract the brain region containing the NTS, brains were placed in an ice-cold brain matrix and a 2 mm rostrocaudal region of the brainstem was isolated as described previously (Damanhuri et al., 2012). The section was maintained frozen using dry ice and the region containing the NTS was hand cut using a scalpel blade (size 10).

Electrophoresis. Tissue was lysed using lysis buffer consisting of (in mM) as follows: 320 sucrose, 2 EDTA, 4 HEPES, and 1% SDS. Protein was extracted by incubating tissue on ice for 10 min, homogenizing with the FastPrep-24-homogenizer (MP Biomedicals) for 2 × 40 s cycles, and then centrifuged for 30 min at 13,200 rpm at 4°C. Supernatants were kept and protein concentrations determined using the BCA protein assay kit (Thermo Fisher Scientific) according to the manufacturer's instructions. Equal amounts of protein (20 μg) were loaded on a 7.5% polyacrylamide gel for electrophoresis. Proteins were then transferred onto a nitrocellulose membrane using the Trans-Blot Turbo System (Bio-Rad) and incubated in primary antibodies (diluted in 5% skim milk in PBS) against either polySia (mouse Mab735, 1 μg/ml, RRID: AB_2619682) or GAPDH (rabbit anti-GAPDH, 1:5000, abcam, #ab9485, RRID:AB_307275) overnight at 4°C. HRP-secondary antibodies (goat anti-mouse IgG H and L, 1:10,000, and goat anti-rabbit IgG H and L, 1:10,000, R&D Systems, #HAF018, RRID: AB_573130, and #HAF008, RRID: AB_357235, respectively) were incubated on the membrane at room temperature for 2 h. Chemiluminescence detection was then performed using the Bio-Rad ECL kit and imaged using the Bio-Rad ChemiDoc system. All images were imported into ImageJ for densitometric analysis and expressed as a percentage change relative to protein loading control (GAPDH). One-way ANOVA with Bonferonni correction was used for comparison between treatments.

Statistical analysis

All values are expressed as mean ± SEM. Paired or unpaired *t* tests were used as indicated. One- or two-way ANOVA tests with Bonferroni *post hoc* tests were used as indicated. Mann–Whitney tests were used to determine whether different enzymes evoked different responses in sympathetic nerve activity. Statistically significant differences were considered at $p < 0.05$. All statistical analysis was performed using GraphPad Prism 6.

Drugs, enzymes, and reagents

All drugs, enzymes and reagents, with the exception of endoNF (Stummeyer et al., 2005), or TTX (Jomar Biosciences) were purchased from Sigma-Aldrich.

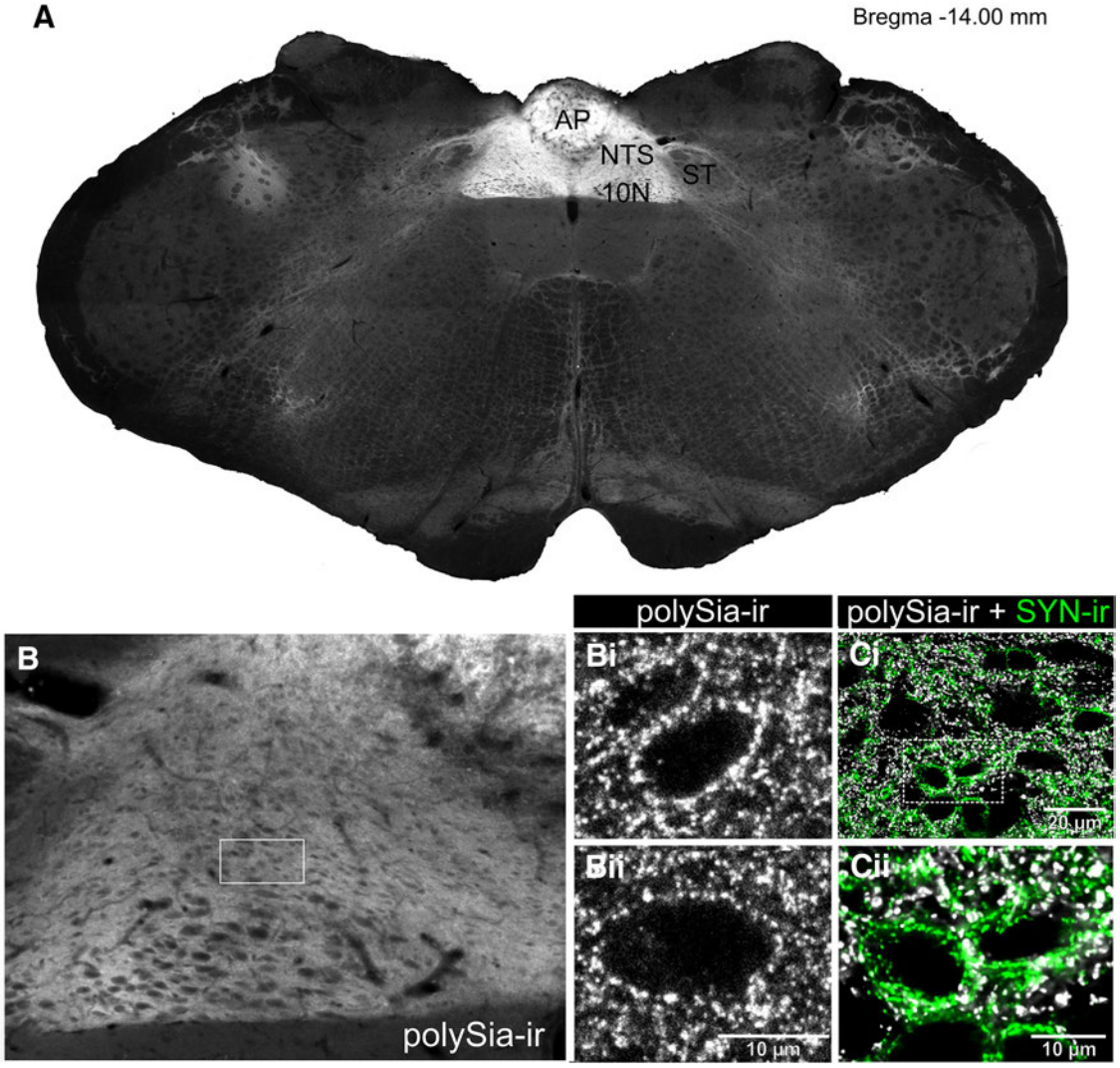

Figure 1. polySia immunoreactivity in the dorsal vagal complex. ***A***, polySia immunoreactivity (ir) is abundant in the NTS, area postrema (AP), and dorsal motor nucleus of the vagus (10N) but not the solitary tract (ST) or surrounding regions (bregma level −14.00 mm). ***B***, polySia-ir is seen throughout the NTS and dorsal motor nucleus of the vagus. ***Bi***, ***Bii***, polySia-ir puncta present throughout the neuropil and enveloping some unlabeled neurons. ***Ci***, ***Cii***, polySia-ir (white) closely apposes but rarely colocalizes with synaptophysin-ir (green) within the NTS.

Results

polySia is expressed abundantly within the neuropil of the NTS predominantly in fine astrocytic processes, the extracellular space, and apposing some synapses

In the adult brain, polySia is expressed abundantly within NTS, the adjacent area postrema, and dorsal motor nucleus of the vagus (Bonfanti et al., 1992). We confirmed these observations using the polySia specific antibody Mab735 (Frosch et al., 1985), demonstrating that a high density of expression was restricted to this, the dorsal vagal complex (Fig. 1*A*). polySia immunoreactivity (ir) was densely distributed throughout the intermediate NTS (Fig. 1*B*), as individual puncta or as punctate rings surrounding unlabeled soma (Fig. 1*Bi*,*Bii*). Similar expression patterns were evident throughout the rostrocaudal extent of the nucleus (data not shown), suggesting potential influence over all functions controlled by the NTS: respiratory (caudal), cardiorespiratory (intermediate), gastrointestinal and gustatory (rostral), and all states influenced by the region: emotional, behavioral, and autonomic (Craig, 2003).

Electron microscopic immunohistochemistry revealed dense labeling of polySia in the space around neuronal cell bodies, fibers, and dendrites (Fig. 2*A*). polySia-ir does not colocalize with GFAP-labeled astrocytes in the NTS (Bouzioukh et al., 2001a). The ultrastructural location is therefore consistent with polySia present in or on the fine processes of astrocytes that lack GFAP and/or within the extracellular space or adjacent to plasma membranes (Fig. 2*Ai*,*Aii*). The labeling pattern is consistent with the punctate rings of immunoreactivity that surround some neuronal cell bodies identified by light microscopy (Fig. 1*Bi*,*Bii*). polySia-ir was found on the rough endoplasmic reticulum and Golgi apparatus of some neuronal cell bodies (Fig. 2*A*) where it may be produced before being transported extracellularly to the cell surface (as described in the hypothalamus) (Theodosis et al., 1999). polySia-ir was also present adjacent to some synapses and in a subset of dendrites and axon terminals (Fig. 2*B–E*), consistent with the close association of polySia and synaptophysin revealed using immunofluorescence (Fig. 1*Ci*,*Cii*).

Enzymatic digestion of polySia enhances ionic currents of neurons in the NTS

To determine whether removal of sialic acids would alter the ionic conductance of NTS neurons, we first determined the time

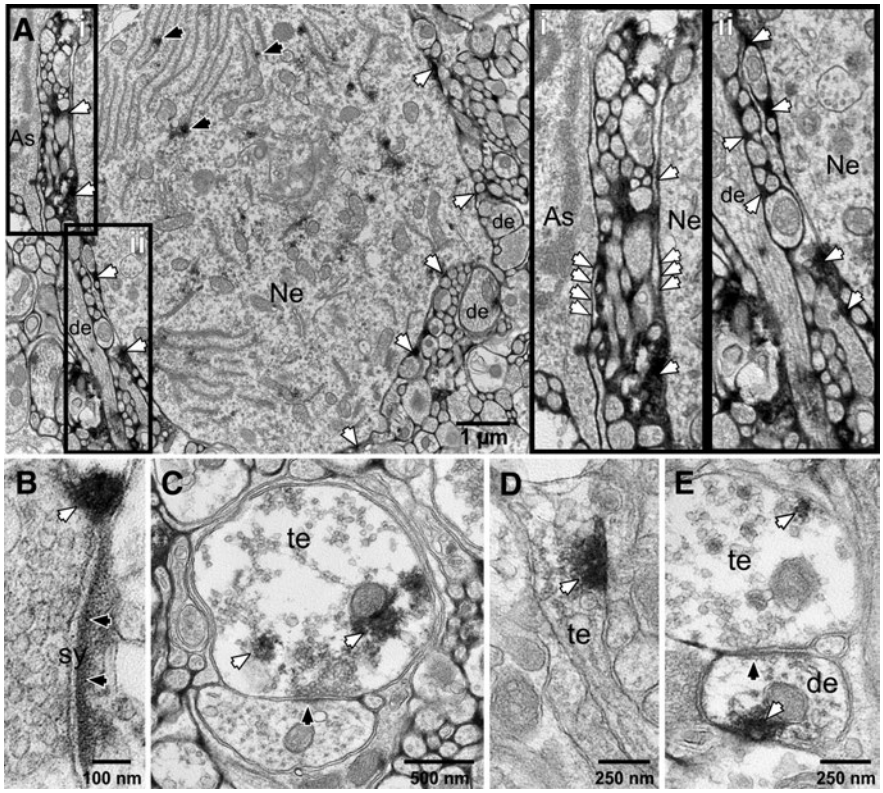

Figure 2. Ultrastructural location of polySia immunoreactivity. ***A***, Ultrastructural analysis shows polySia-ir (white arrows) surrounding neuronal soma (Ne), proximal dendrites (de), and fine neuronal processes consistent with expression in fine processes of astrocytes (As) (white arrows). polySia-ir is also found in the rough endoplasmic reticulum and Golgi apparatus of some neurons (black arrows). ***Ai***, polySia-ir occurs along the exterior surface of the plasma membrane of some astrocytic (As) and neuronal (Ne) soma (white arrows) indicating its presence in the extracellular space. ***Aii***, Dendrites (de) and axons are sheathed by polySia labeling. ***B***, polySia-ir (white arrows) was found adjacent to some synapses (sy) likely in astrocytic processes, as a tripartite synapse. ***C–E***, polySia-ir is found within some dendrites (de) and axon terminals (te) of neurons. Black arrows indicate postsynaptic densities.

required for enzyme incubation of brain slices to remove sialic acids, measured by Western blot. Brain slices obtained and treated identically to those used for electrophysiological recordings were incubated in either aCSF ($n = 3$), aCSF containing the exosialidase neuraminidase from *Clostridium perfringens* (Neu; 0.1 U/ml, $n = 3$), which cleaves terminal α2,3-, α2,6-, and α2,8-linked sialic acids (Taylor, 1996), or aCSF containing the endosialidase, endoNF (1 μg/μl, $n = 3$), which is specific for polySia, as it cleaves α2,8 linkages within polymers with >8 sialic acid residues (Stummeyer et al., 2005; Taylor, 1996).

polySia-ir was stable during incubation in aCSF alone (Fig. 3*A*), and appeared to increase slightly during slice recovery, possibly due to increased synaptogenesis that occurs (Kirov et al., 1999). Densitometric evaluation, however, indicated no significant difference in expression during incubation in the absence of sialidases ($t_{(4)} = 2.007$, $p = 0.1152$; Fig. 3*B*). In contrast, one-way ANOVA revealed significant treatment effects when slices were incubated in exosialidases or endosialidases ($F_{(2,6)} = 18.01$, $p = 0.0029$), with polySia-ir reducing significantly within 45 min (endoNF (green); 0.10 ± 0.02 a.u. vs 1.82 ± 0.41 a.u., $t_{(6)} = 5.157$, $p = 0.0042$, $n = 3$) or 60 min (Neu (blue); 0.02 ± 0.07 a.u. vs 1.82 ± 0.41 a.u., $t_{(6)} = 5.237$, $p = 0.0039$, $n = 3$).

We next investigated whether enzymatic digestion of polySia altered the current density profiles of NTS neurons. In whole-cell voltage clamp recordings of neurons from slices incubated in aCSF, Neu (0.1, 1, and 10 U/ml), or endoNF (0.1 and 1 μg/ml) for 60 min, steady-state outward currents were evoked by 1000 ms, 10 mV depolarizing voltage steps. Two-way ANOVA revealed significant enzymatic effect on responses when slices were incubated in 0.1 U/ml Neu ($F_{(1/47)} = 21.54$, $p < 0.0001$), with increases in current density observed at mV ≥ 0 mV (0.1 U/ml Neu; 38.05 ± 4.73 pA/pF vs aCSF, 19.93 ± 1.70 pA/pF, $t_{(517)} = 4.290$, $p = 0.0002$, $n = 16$; Fig. 3*C*,*Ci*). Incubation in 0.01 U/ml Neu ($n = 11$) had no effect ($F_{(1/42)} = 0.03$, $p = 0.858$). Although a 10-fold higher concentration (1 U/ml, $n = 16$) resulted in a significantly enhanced response compared with control ($F_{(1/47)} = 25.75$, $p < 0.0001$), it did not evoke a greater response than slices incubated in 0.1 U/ml ($F_{(1/30)} = 1.65$, $p = 0.208$) (Fig. 3*Ci*). Incubation in endoNF (1 μg/ml) also showed a treatment effect relative to control ($F_{(1/67)} = 35.86$, $p < 0.0001$, $n = 36$; Fig. 3*D*), and at 0 mV evoked a 73% increase in current density (35.84 ± 2.45 pA/pF vs 20.66 ± 1.10 pA/pF, $t_{(737)} = 4.504$, $p < 0.0001$, $n = 36$), a profile matching that of Neu incubation ($F_{(50/500)} = 287.24$, $p < 0.0001$). A 10-fold lower (0.1 μg/ml, $n = 14$) concentration of endoNF had no effect ($F_{(1/45)} = 2.82$, $p = 0.099$, $n = 14$; Fig. 3*D*).

The location of 21 recorded neurons (biocytin-filled; Fig. 3*E*, left) was plotted (recovery rate = 55%), and all were found within the NTS (Fig. 3*E*). Consistent with our ultrastructural observations, analysis of a subset of recovered cells (from control slices not subjected to enzymatic treatment) consistently revealed punctate expression of polySia-ir enveloping both soma and proximal dendrites (Fig. 3*E*, left).

Enzymatic digestion of polySia enhances K^+-mediated outward currents and increases intracellular Ca^{2+} release in NTS neurons

Delayed rectifier (IKDR) and large conductance calcium-activated (BK) potassium channels regulate the excitability of NTS neurons (Champagnat et al., 1986; Dekin and Getting, 1987; Dekin et al., 1987; Moak and Kunze, 1993; Andresen and Kunze, 1994). We therefore examined the effect of polySia removal on outward currents in the presence of TEA (10 mM), a blocker of IKDR. TEA application significantly reduced the amplitude of steady-state currents in both endoNF ($F_{(1/18)} = 121.72$, $p < 0.0001$) treated and control slices ($F_{(1/10)} = 24.69$, $p = 0.0006$), but no difference in amplitude was observed between groups (2.78 ± 1.53 pA/pF vs 4.67 ± 2.10, $F_{(1/14)} = 1.15$, $p = 0.30$, $n = 10$; Fig. 4*A*,*Ai*), suggesting that polySia significantly contributes to IKDR channel function.

As TEA-sensitive channels include voltage-gated as well as BK channels (Coetzee et al., 1999), we investigated the effect of endoNF on BK channel activation, using the specific antagonist iberiotoxin (Ibtx, 50 nM) (Pedarzani et al., 2000). In keeping with previous observations (Mayer et al., 2009), application of Ibtx in control slices significantly reduced steady-state outward currents ($F_{(1/12)} = 3.60$, $p = 0.08$, $n = 7$; Fig. 4*B*,*Bi*). In contrast, Ibtx had

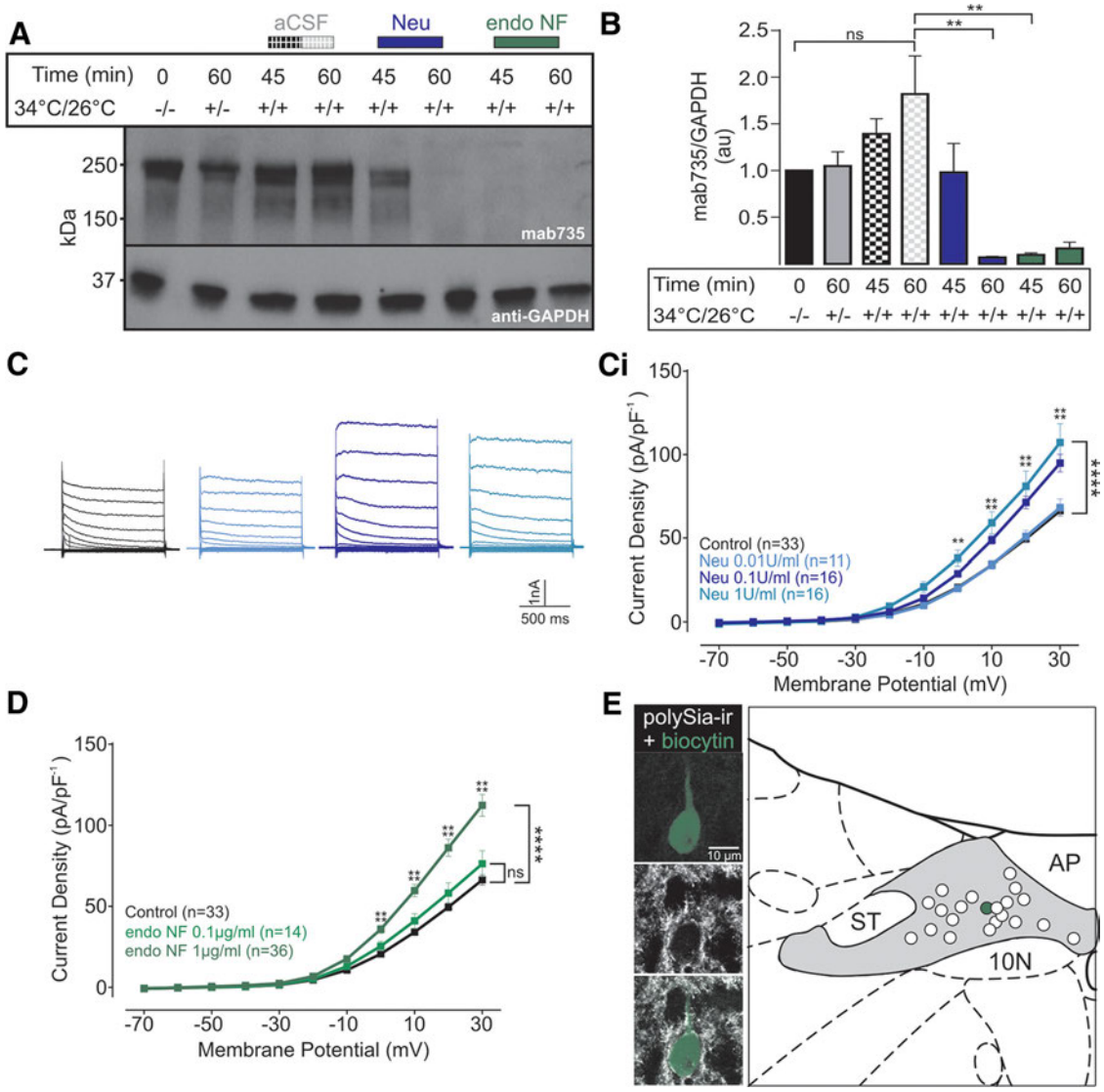

Figure 3. polySia removal enhances current voltage relationship within NTS neurons. ***A***, Representative Western blot using Mab735 to detect polySia during slice recovery, and following incubation in aCSF (gray/black box), Neu (0.1 U/ml, blue box), or endoNF (1 μg/ml, green box). GAPDH was used as a loading control. ***B***, Comparison of the amount of protein detected using Mab735 during slice recovery (black and gray), and incubation in aCSF, Neu, or endoNF. polySia-ir was significantly reduced after 60 min incubation in Neu (blue box, $p = 0.0039$, $n = 3$) or 45 min incubation in endoNF (green box, $p = 0.0042$, $n = 3$). Data are normalized to GAPDH with the zero time point value set to 1. Enzymatic removal of polySia in NTS brain slices increases steady-state outward currents. ***C***, Typical current traces (depolarizing voltage step: Δ10 mV) from NTS neurons incubated in aCSF (black), or Neu (0.01 U/ml, light blue, 0.1 U/ml, dark blue, and 1 U/ml, aqua, respectively). ***Ci***, Grouped data reveal that Neu (0.1 and 1 U/ml) significantly increased current density of neurons at depolarized potentials $\geq$ 0 mV ($p = 0.0002$, $n = 16$ and $n = 11$, respectively). ***D***, Grouped data show that incubation in endoNF at 1 μg/ml (dark green), but not 0.1 μg/ml (light green), significantly increased current density of neurons at depolarized potentials $\geq$ 0 mV ($p < 0.0001$, $n = 36$). Data are mean $\pm$ SEM. ***E***, Recovered cell (green) within the NTS surrounded by polySia-ir puncta (white) coating the soma and proximal dendrite. The recovered cell was recorded while superfused with aCSF (control). Schematic coronal section showing distribution of recorded neurons in the NTS recovered following incubation in aCSF or endoNF. **$p < 0.01$; ****$p < 0.0001$; ns, $p < 0.05$.

no effect in endoNF-treated slices ($F_{(1/6)} = 0.30$, $p = 0.60$, $n = 4$; Fig. 4*B*,*Bi*), suggesting that BK channel function was perturbed by polySia removal. Current injections did not alter the number of action potentials generated ($F_{(1/35)} = 0.21$, $p = 0.65$; Fig. 5*A*,*Ai*) or the amplitude of the AHP ($t_{(18)} = 0.133$, $p = 0.90$; Fig. 5*B*) in keeping with a reduced ability of Ibtx to close BK channels following polySia digestion (Yang et al., 2015). These data indicate that IKDR and BK channel function are both altered by the removal of polySia.

The effect of endoNF on steady-state currents was voltage-dependent and significantly enhanced at the equilibrium potential for Ca^{2+} (9 mV under the recording conditions), so we examined whether polySia altered Ca^{2+}currents. We first omitted Ca^{2+} from the external solution preventing Ca^{2+} influx during depolarization. Under these conditions, enzymatic digestion of polySia still enhanced steady-state currents ($F_{(1/28)} = 5.40$, $p = 0.027$, $n = 15$; Fig. 4*C*) that were indistinguishable from those evoked by endoNF under normal levels of external Ca^{2+} ($F_{(1,49)} = 0.002$, $p = 0.96$). Next, we substituted EGTA within the recording pipette for the fast Ca^{2+} chelator BAPTA (10 mM) to assess the contribution made by internal Ca^{2+} stores. We found that BAPTA eliminated the enhanced steady-state outward currents normally observed following polySia digestion ($F_{(1/28)} = 0.15$, $p = 0.70$, $n = 13$; Fig. 4*D*).

Together, these data indicate that removal of polySia from NTS neurons facilitated currents generated through K^+ channels, reduced inactivation of BK channels, and increased Ca^{2+} via release from intracellular stores.

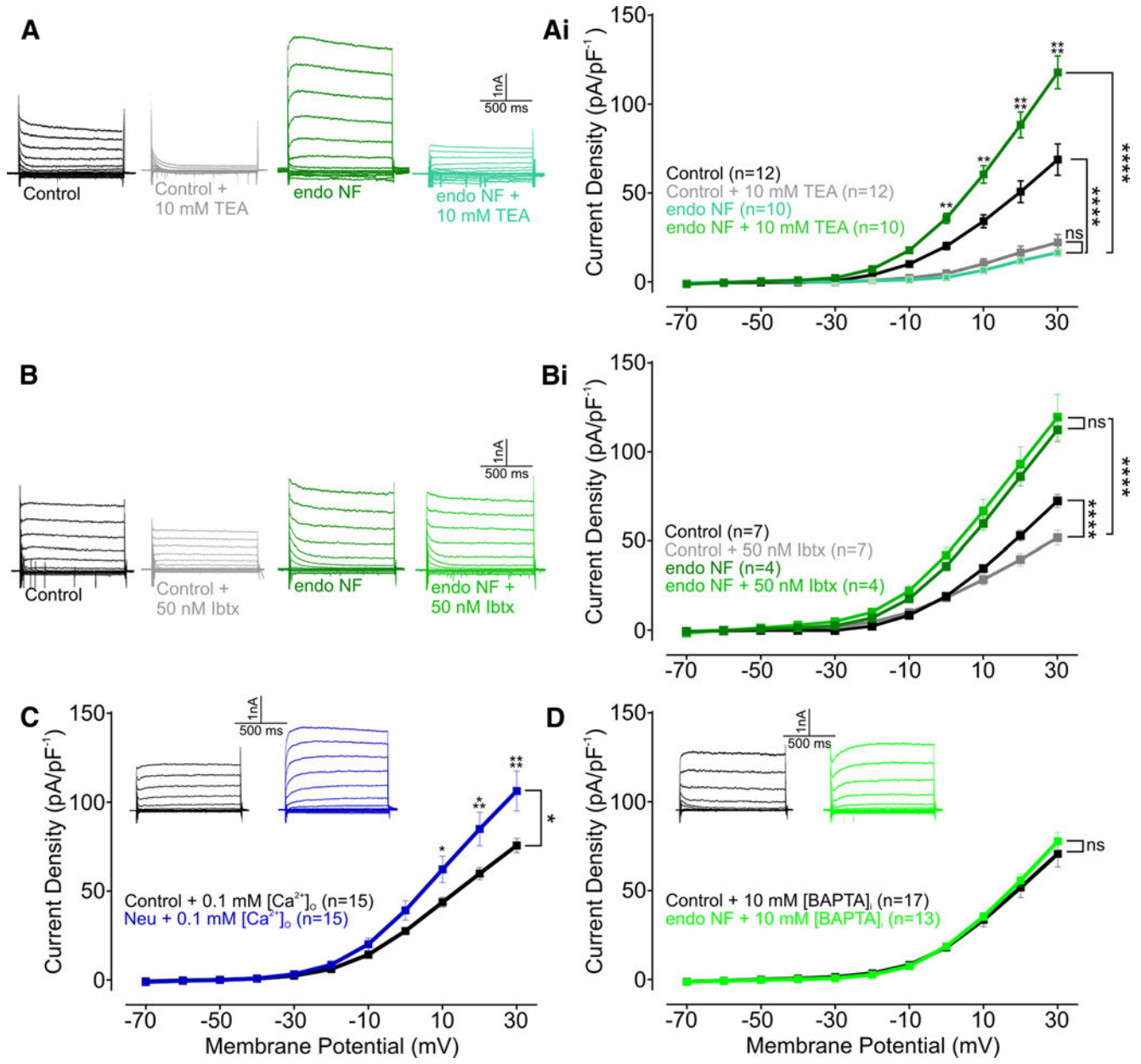

Figure 4. polySia removal enhances K^+ currents, and intracellular Ca^{2+} in NTS neurons. ***A***, Typical current traces (depolarizing voltage step: Δ10 mV) of NTS neurons recorded following slice incubation in either aCSF (black), aCSF containing TEA (10 mM, gray), endoNF (1 μg/ml, green), or endoNF containing TEA (10 mM, light green). ***Ai***, Grouped data reveal that TEA treatment reduced currents generated in aCSF ($p = 0.0006$, $n = 10$) and endoNF-treated slices ($p < 0.0001$, $n = 12$ and $n = 10$, respectively) with no difference between groups ($p = 0.30$, $n = 10$). ***B***, Typical current traces (depolarizing voltage step: Δ10 mV) of NTS neurons recorded following slice incubation in either aCSF (black), aCSF containing Ibtx (50 nm, light gray), endoNF (green), or endoNF containing Ibtx (50 nm, light green). ***Bi***, Grouped data reveal that Ibtx reduced currents generated in aCSF ($p = 0.08$, $n = 7$) but did not alter currents generated in endoNF-treated slices ($p = 0.60$, $n = 4$). Endo NF + Ibtx currents generated were significantly different to aCSF + Ibtx currents ($p = 0.0002$). ***C***, Typical current traces (depolarizing voltage step: Δ10 mV) of NTS neurons recorded following slice incubation in either aCSF or Neu with reduced extracellular Ca^{2+} concentration ($[Ca^{2+}]_0$, 0.1 mM, black and blue, respectively). Grouped data show that increased currents were generated by Neu when $[Ca^{2+}]_0$ was reduced ($p = 0.027$, $n = 15$). ***D***, Typical current traces (depolarizing voltage step: Δ10 mV) of NTS neurons recorded following slice incubation in either aCSF or endoNF with EGTA substituted for BAPTA in the recording pipette (10 mM, black and green, respectively). Grouped data reveal no change in currents generated between aCSF and endoNF ($p = 0.70$, $n = 13$). Hyperpolarizing spikes were truncated to aid visual representation. Data are mean ± SEM. *$p < 0.05$; **$p < 0.01$; ***$p < 0.001$; ****$p < 0.0001$; ns, $p > 0.05$.

polySia contributes to glutamatergic viscerosensory afferent transmission in NTS

We next investigated whether polySia removal affected viscerosensory afferent transmission. In second-order NTS neurons, identified as receiving monosynaptic input from viscerosensory afferents, enzymatic cleavage of polySia reduced the fidelity of action potentials generated by afferent activation (Fig. 6*A*). Consistent with previous observations (Bailey et al., 2007), consecutive, 1 Hz minimal amplitude electric stimulation generated action potentials with 86.0 ± 5.1% fidelity under control conditions previous shown to be mediated by AMPA receptors. In the same neurons, following polySia digestion with endoNF, fidelity decreased to 31.0 ± 3.3% ($t_{(4)} = 9.297$, $p = 0.0007$, $n = 5$; Fig. 6*Ai*). Furthermore, polySia digestion increased the latency of action potential propagation following stimulation of viscerosensory afferents (Fig. 6*B*) by 41.7% (8.79 ± 1.56 ms vs 5.12 ± 0.61 ms, $t_{(4)} = 3.96$, $p = 0.021$, $n = 5$; Fig. 6*Bi*). No significant differences were observed in basal action potential parameters, includ-

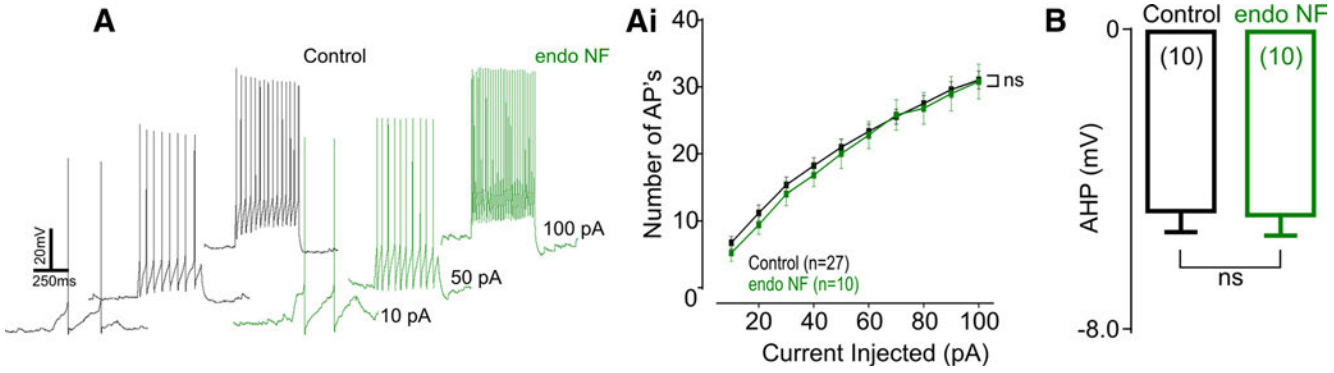

Figure 5. Action potential discharge and AHP following current injection are not altered after enzymatic digestion of polySia. ***A***, Typical current traces of action potentials generated by current injections (10, 50, and 100 pA) in cells incubated in aCSF (control, black) or endoNF (green). ***Ai***, Grouped data show that enzymatic digestion of polySia did not alter action potential discharge to current injections ($p = 0.65$, $n = 10$). ***B***, Grouped data revealed no change in AHP amplitude following enzymatic cleavage of polySia ($p = 0.90$, $n = 10$). Data are mean ± SEM.

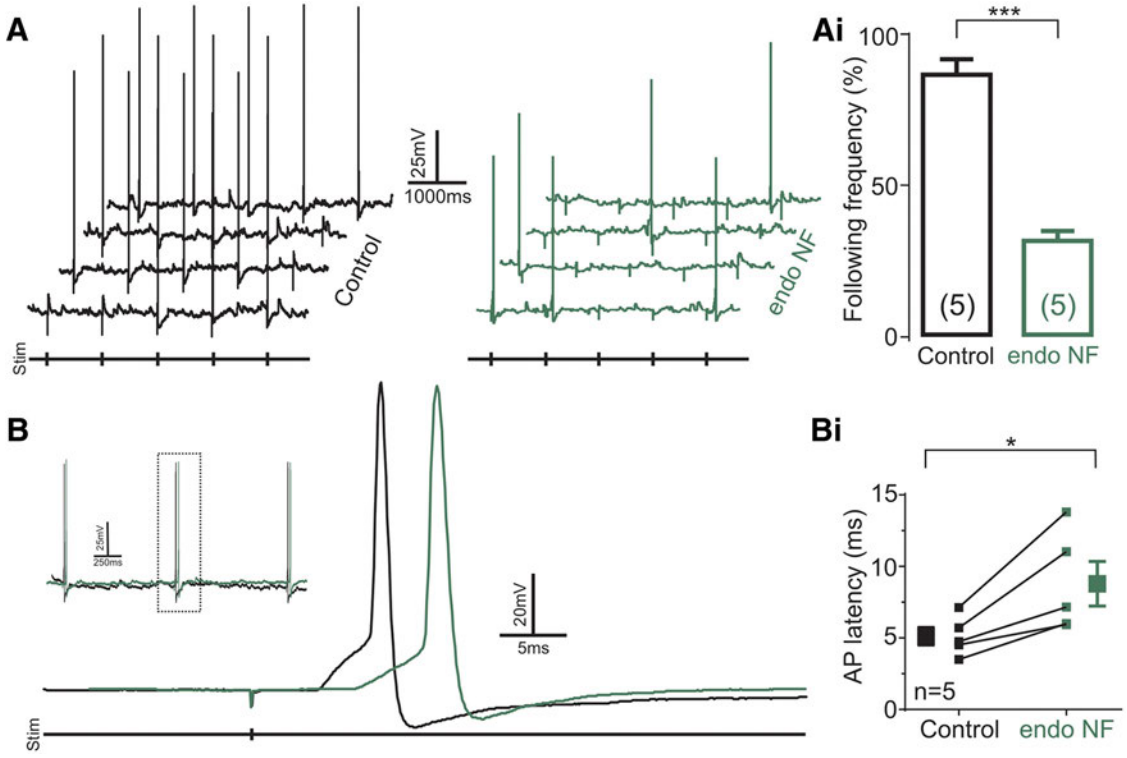

Figure 6. polySia removal reduces viscerosensory afferent signal transmission in the NTS. ***A***, Typical voltage trace of monosynaptically connected NTS neurons with action potentials generated following viscerosensory afferent stimulation (1 Hz) before (black) and 60 min after (green) endoNF incubation. ***Ai***, Grouped data show that endoNF decreased the following frequency in response to viscerosensory afferent stimulation from 86% to 31% ($p = 0.0007$, $n = 5$). ***B***, Typical voltage trace of monosynaptically connected NTS neuron showing action potential latency following viscerosensory afferent stimulation (1 Hz) before (black) and after (green) endoNF incubation. Inset, aCSF (black) and endoNF (green) traces overlaid and aligned to the stimulus artifact. ***Bi***, Grouped data reveal that endoNF treatment increased the latency in response to viscerosensory afferent stimulation (1 Hz) by 71.6% ($p = 0.021$, $n = 5$). Data are mean ± SEM. *$p < 0.05$; ***$p < 0.01$.

ing membrane potential (−51.60 ± 2.14 mV vs −49.20 ± 1.72 mV, $t_{(4)} = 2.59$, $p = 0.061$, $n = 5$), action potential amplitude (92.03 ± 7.27 mV vs 93.18 ± 3.50 mV, $t_{(4)} = 0.27$, $p = 0.80$, $n = 5$), half-width (1.54 ± 0.30 ms vs 1.10 ± 0.16 ms, $t_{(4)} = 2.40$, $p = 0.074$, $n = 5$), rise time (90%–10%; 1.72 ± 0.50 ms vs 1.68 ± 0.38 ms, $t_{(4)} = 0.13$, $p = 0.91$, $n = 5$), spike threshold (−39.80 ± 2.22 vs −33.31 ± 0.87, $t_{(4)} = 2.58$, $p = 0.061$, $n = 5$), or decay time ($T_{90\%–10\%}$; 1.96 ± 0.21 ms vs 1.64 ± 0.17 ms, $t_{(4)} = 1.40$, $p = 0.23$, $n = 5$). These data suggest that polySia expression enables monosynaptic transmission from viscerosensory afferents onto NTS neurons.

As the fidelity of action potential transmission is perturbed following polySia removal in the NTS, we investigated whether excitatory drive from viscerosensory afferents would similarly decline. As described previously (Doyle and Andresen, 2001), suprathreshold electrical stimuli applied to viscerosensory afferents evoke large monosynaptic EPSCs (eEPSCs), identified by low failure rates and jitters (<200 μs; 140.60 ± 13.63 μs, $n = 12$). Consistent with effects on action potential probability and latency, enzymatic digestion of polySia increased eEPSC latency by 31.1% (4.97 ± 0.44 ms vs 3.79 ± 0.38 ms, $t_{(9)} = 3.51$, $p = 0.0066$, $n = 10$; Fig. 7*A*,*Ai*), and decreased the amplitude of eEPSCs recorded in voltage-clamp mode by 54.4% (198.60 ± 31.14 pA vs 412.20 ± 59.93 pA, $t_{(9)} = 5.527$, $p = 0.0004$, $n = 10$; Fig. 7*A*,*Aii*). In contrast, jitter (159.90 ± 7.30 μs vs 134.60 ± 10.06 μs, $t_{(9)} = 2.242$, $p = 0.0517$, $n = 10$), paired-pulse ratio (EPSC2/EPSC1;

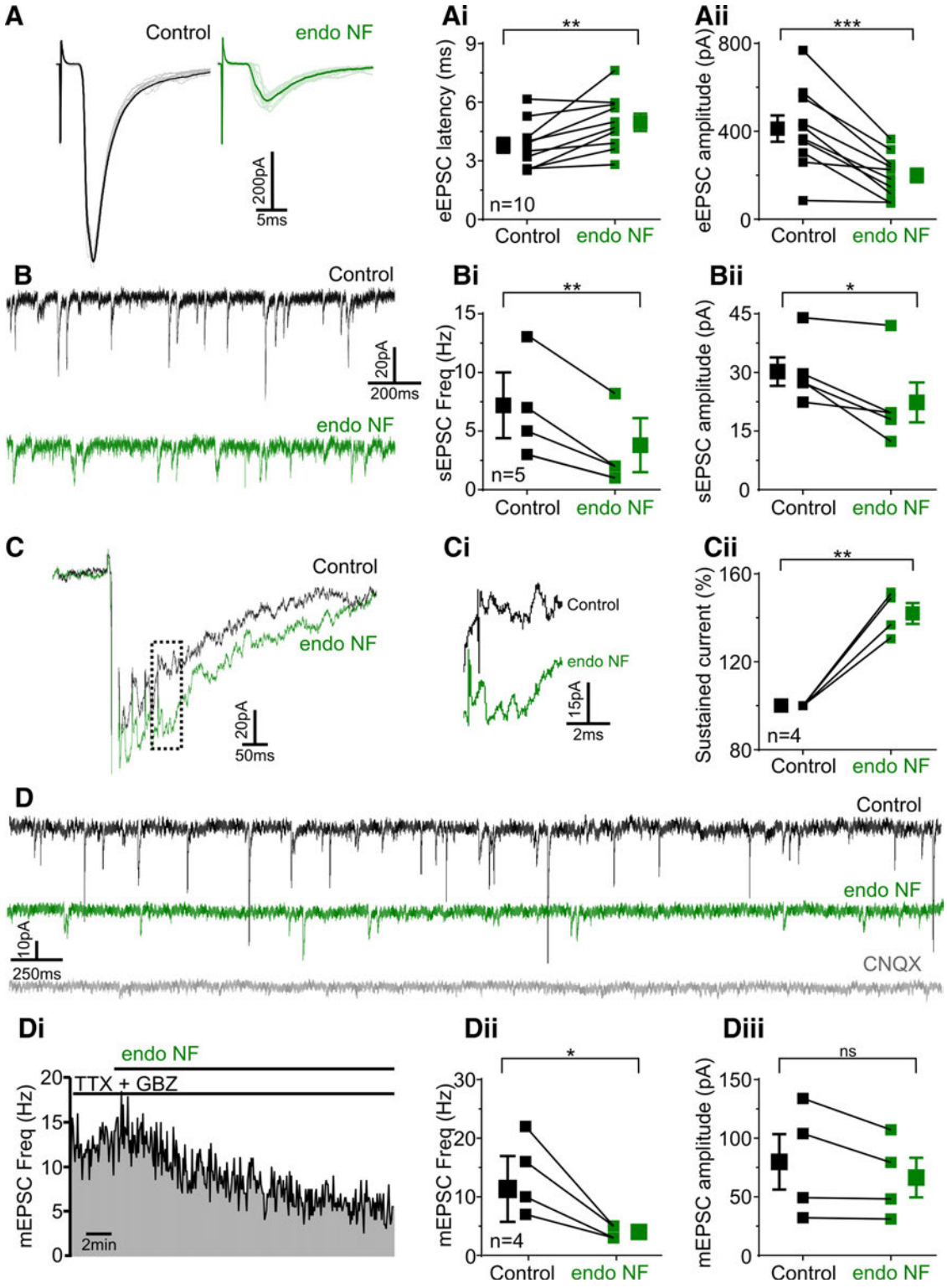

Figure 7. polySia removal in the NTS reduces glutamatergic synaptic input. ***A***, Typical current traces of monosynaptically connected NTS neurons with eEPSCs generated following viscerosensory afferent stimulation (5 Hz) before (black) and after (green) endoNF incubation. Individual trials are represented in gray and light green, respectively. ***Ai***, ***Aii***, Grouped data show that enzymatic digestion of polySia increased latency by 34.2% (***Ai***, $p = 0.0098$, $n = 9$) and decreased eEPSC amplitude by 54.4% (***Aii***, $p = 0.0002$, $n = 9$). ***B***, Typical current traces of sEPSCs in monosynaptically connected NTS neurons before (black) and after (green) endoNF incubation. ***Bi***, ***Bii***, Grouped data show that removal of polySia decreased frequency by 47.2% ($p = 0.0074$, $n = 5$) and amplitude by 26% ($p = 0.034$, $n = 5$). ***C***, Current trace of NMDA-mediated sustained currents in monosynaptically connected NTS neurons before (black) and after (green) endoNF incubation. ***Ci***, Sustained current 100 ms (hashed vertical line) after initial stimulus. ***Cii***, Grouped data show that enzymatic digestion of polySia increased sustained current by 42% ($p = 0.0031$, $n = 4$) in response to high-frequency stimulation of the solitary tract. Stimulus artifacts and current response to first shock were truncated to aid visual representation. ***D***, Current traces showing mEPSCs recorded before (black) and after endoNF treatment (green) with both TTX and GBZ present in the bath. CNQX (gray) was added to the superfusate at the end of experimentation. ***Di***, Frequency distribution over time shows a progressive decrease in mEPSC frequency (10 s bins) following addition of endoNF to the perfusate. ***Dii***, ***Diii***, Grouped data show that enzymatic digestion of polySia decreased frequency by 71% ($p = 0.04$, $n = 4$) but had no effect on mEPSC amplitude ($p = 0.156$, $n = 4$). Data are mean ± SEM. *$p < 0.05$; **$p < 0.01$; ***$p < 0.001$; ns, $p > 0.05$.

0.53 ± 0.08 vs 0.58 ± 0.05, $t_{(5)} = 1.54$, $p = 0.18$, $n = 6$), and eEPSC decay tau ($T_{90\%-10\%}$; 5.67 ± 1.70 ms vs 5.65 ± 0.60 ms, $t_{(5)} = 0.30$, $p = 0.78$, $n = 6$) remained unaffected following polySia digestion.

In the same neurons, we examined whether polySia was required for the maintenance of sEPSCs, arising from spontaneous glutamate release. Enzymatic digestion of polySia significantly decreased both the frequency of sEPSC by 58.80% (3.80 ± 2.30 Hz vs 7.70 ± 2.80 Hz, $t_{(4)} = 5.01$, $p = 0.0074$, $n = 5$), and amplitude by 27.80% (22.34 ± 5.10 pA vs 30.21 ± 3.65 pA, $t_{(4)} = 3.18$, $p = 0.034$, $n = 5$; Fig. 7*B*,*Bii*). Together, these data indicate the importance of polySia expression within the NTS in facilitating excitatory synaptic transmission from viscerosensory afferents mediated by AMPA receptor activation.

In a subset of monosynaptically connected neurons, we investigated the effect of polySia removal on NMDA-mediated sustained currents, recently identified in second-order NTS neurons (Zhao et al., 2015). Neurons were voltage clamped at −60 mV and recorded in Mg^{2+}-free aCSF to remove the Mg^{2+} block on NMDA receptors (Mayer et al., 1984). In 4 of 5 neurons tested, stimulating the solitary tract at 50 Hz consistently evoked large sustained currents (Fig. 7*C*,*Ci*), that were not observed at lower stimulating frequencies (1 Hz, data not shown). Enzymatic digestion of polySia increased the current generated to high-frequency stimulation of the solitary tract by 42 ± 4.80% ($t_{(3)} = 8.758$, $p = 0.0031$, $n = 4$; Fig. 7*Cii*).

Collectively, these data suggest that the fidelity of excitatory synaptic transmission during high- and low-frequency afferent input is maintained by polySia expression, and that its removal may alter the appropriate charge required to open and close AMPA and NMDA receptors as previously suggested (Vaithianathan et al., 2004; Hammond et al., 2006).

polySia contributes to presynaptic glutamate release in the NTS

To determine whether polySia removal impacts neurotransmission postsynaptically or presynaptically we recorded, in the presence of TTX (10 μM) and GBZ (25 μM), mEPSCs, and measured responses before and during polySia digestion (Fig. 7*D*,*Di*). Enzymatic digestion of polySia decreased mEPSC frequency by 68.75% (endoNF, 4.00 ± 0.57 Hz vs control, 13.75 ± 3.30, $t_{(3)} = 3.47$, $p = 0.040$, $n = 4$; Fig. 7*Dii*) without altering amplitude (62.00 ± 15.70 pA vs 74.50 ± 22.08 pA, $t_{(3)} = 1.88$, $p = 0.156$, $n = 4$; Fig. 7*Diii*). CNQX was added at the end of experimentation demonstrating that mEPSCs were dependent on non–NMDA-type glutamate receptors (Fig. 7*D*). These data indicate that removal of polySia reduces glutamatergic release from presynaptic terminals at NTS neurons, and this mechanism likely contributes to the reduction in viscerosensory afferent transmission (both evoked and spontaneous) seen following polySia digestion.

Enzymatic cleavage of polySia within the NTS increases sympathetic nerve discharge *in vivo*

Finally, as multiple pathways emerge from the NTS that influence presympathetic neurons regulating the sympathetic outflow (Guyenet, 2006), we determined whether the changes to intrinsic neuronal properties and/or viscerosensory afferent transmission resulting from polySia digestion within the NTS *in vitro*, would be sufficient to alter function *in vivo*. sSNA and arterial pressure recorded before and after microinjection of neuraminidases directly into the caudal and intermediate NTS, in urethane-anesthetized rats. Bilateral microinjections of endoNF (2 μg/μl, total volume 800 nl) elicited sympathoexcitation (Fig. 8*A*; $F_{(1,8)} = 34.06$, $p = 0.0004$) with peak increases in sSNA of 140.80 ± 7.63% compared with control (saline, 96.50 ± 4.48%, $t_{(104)} = 4.991$, $p < 0.0001$, $n = 6$; Fig. 8*Ai*). Brains were removed at the end of each experiment and the degree of polySia digestion determined using Western blot analysis. polySia was present following PBS microinjection but absent following endoNF microinjection (0.94 ± 0.05 a.u. vs 0.09 ± 0.02 a.u., $t_{(21)} = 5.71$, $p < 0.0001$, $n = 6$; Fig. 8*Bi*,*Biv*). Microinjection of the neuraminidase targeting only terminal α2–3 and α2–6 sialic acids (α2–3 + α2–6 Neu, 0.1 U/μl) had no effect on sSNA ($F_{(1,8)} = 2.580$, $p = 0.15$, $n = 5$; Fig. 8*A*,*Ai*) and similarly did not alter the expression of polySia relative to control ($t_{(21)} = 0.81$, $p > 0.99$, $n = 5$; Fig. 8*Bii*,*Biv*).

polySia also terminates α2–3 and α2–6 sialic acid-linked glycans (Schnaar et al., 2014), which would be untouched by α2–3 + α2–6 Neu; we therefore determined the combined effect of enzymatically removing polySia together with α2–3- and α2–6-linked sialic acid residues by combining both enzymes (α2–3 + α2–6 Neu + endoNF). Microinjection of the combined enzymes bilaterally caused rapid sympathoexcitation (Fig. 8*A*; $F_{(1,7)} = 20.43$, $p = 0.0027$) with a peak effect of 162.50 ± 13.73% ($t_{(91)} = 4.760$, $p < 0.0001$, $n = 5$; Fig. 8*Ai*) and in support of a specific role for polySia, no polySia was detected at the protein level (0.01 ± 0.002 a.u. vs 0.94 ± 0.05 a.u., $t_{(21)} = 5.90$, $p < 0.0001$, $n = 5$; Fig. 8*Biii*,*Biv*). Similarly, microinjection of Neu (0.1 U/μl) also produced rapid sympathoexcitation ($F_{(1,8)} = 68.18$, $p < 0.0001$) and peaked at a higher level (179.33 ± 14.56%, $t_{(104)} = 4.315$, $p = 0.0005$, $n = 6$; Fig. 9*A*,*Ai*) that was significantly greater than endoNF alone ($p = 0.041$, Mann–Whitney *U* test, $n = 6$; Fig. 9*B*) but did not differ from that evoked by α2–3 + α2–6 Neu + endoNF ($p = 0.628$, Mann–Whitney *U* test, $n = 5$).

The effects on arterial pressure were more variable following enzymatic digestion of polySia. Neu evoked the largest and most rapid sympathoexcitation (see above) which acutely elevated mean arterial pressure (MAP) compared with control (15 min: 152 ± 10.97 vs 87.75 ± 7.32 mmHg, $t_{(13)} = 4.425$, $p = 0.0014$, $n = 6$; Fig. 9*A*,*B*,*Ci*). This MAP increase however, returned to baseline within 60 min (108 ± 3.1 vs 92.5 ± 7.5 mmHg, $t_{(13)} = 1.91$, $p = 0.157$, $n = 6$; Fig. 9*Cii*). As endoNF evoked smaller and slower sympathoexcitation, little to no effect on MAP was seen acutely (15 min: 98.24 ± 9.11 vs 87.75 ± 7.32 mmHg, $t_{(13)} = 0.713$, $p = 0.97$, $n = 6$; Fig. 9*Ci*) or at 60 min (95.02 ± 6.38 vs 92.5 ± 7.5 mmHg, $t_{(13)} = 0.301$, $p > 0.99$, $n = 6$; Fig. 9*Cii*).

Together these results demonstrate that removal of polySia in the NTS increases sympathetic nerve activity, which is consistent with a net disfacilitation in the NTS or experimental visceral deafferentation (Iggo and Vogt, 1962; Fagius et al., 1985). Thus, our findings indicate that polySia expression within the NTS is required to maintain appropriate (i.e., "normal") levels of sympathetic outflow. Figure 10 depicts the cellular mechanisms and network effects modified by polySia in the NTS highlighting the consequences of polySia's removal.

Discussion

We demonstrate that polySia expression in the dorsal medulla is required for normal excitatory neurotransmission within the NTS, and that its disruption is sufficient to acutely increase sympathetic outflow. We draw these conclusions based on the following observations: First, neurons in the NTS were ensheathed by polySia, expressed predominantly in or on the fine processes of astrocytes and within the extracellular space. Second, enzymatic removal of polySia-enhanced currents in NTS neurons, mediated by changes at IKDR and BK channels, and altered release of Ca^{2+} from internal stores. Third, enzymatic removal of

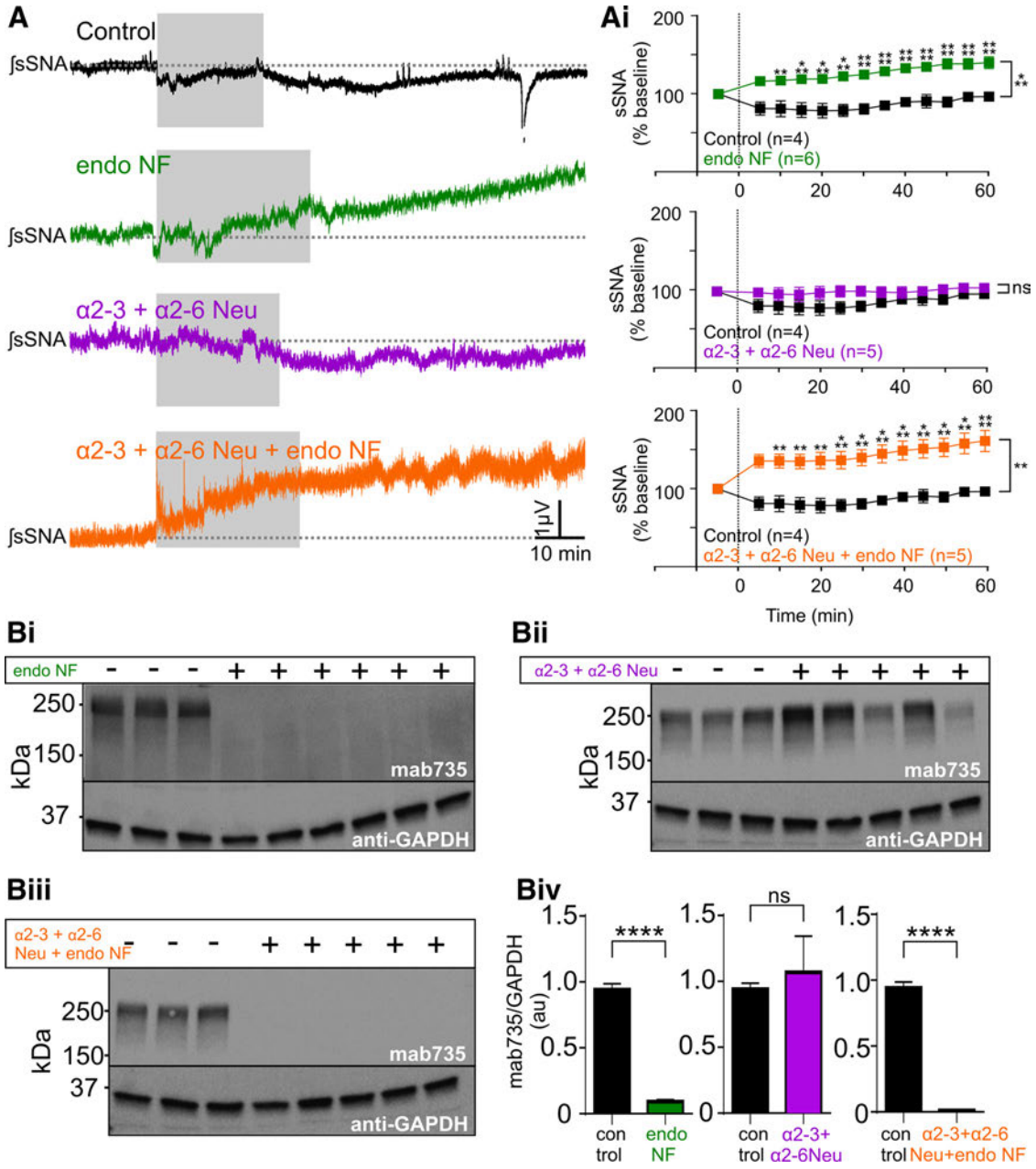

Figure 8. polySia removal in the NTS increases sympathetic nerve activity. ***A***, Integrated and smoothed representative traces of sSNA recorded in urethane-anesthetized, paralyzed, and ventilated rats following saline (black), endoNF (green 2 μg/μl), α2–3 + α2–6 Neu (magenta, 0.1 U/μl), or α2–3 + α2–6 Neu + endoNF (orange) microinjections bilaterally into the NTS. Gray represents the period of injection. ***Ai***, Grouped data show that endoNF ($n = 6$) and α2–3 + α2–6 Neu + endoNF ($n = 5$) significantly increased sSNA by 40.8% and 62.5%, respectively ($p <$ 0.0001). Microinjection of α2–3 + α2–6 Neu alone had no effect compared with control ($p = 0.15$, $n = 5$). ***B***, Western blots of NTS dissected from the animals in (***Ai***) following microinjection of control, endoNF (***Bi***, 2 μg/μl, green), α2–3 + α2–6 Neu (***Bii***, 0.1 U/μl, magenta), or α2–3 + α2–6 Neu + endoNF (***Biii***, orange). ***Biv***, Grouped data showing quantitative changes in polySia protein (detected using Mab735) from animals in ***B***. polySia-ir was virtually absent following microinjection of either endoNF (green box, $p < 0.0001$, $n = 6$) or α2–3 + α2–6 Neu + endoNF (orange box, $p < 0.0001$, $n = 5$), and was not altered following microinjection of α2–3 + α2–6 Neu alone (magenta box, $p > 0.99$, $n = 5$). Data are mean ± SEM. $^{**}p < 0.01$; $^{***}p < 0.001$; $^{****}p < 0.0001$; ns, $p > 0.05$.

polySia reduced AMPA-mediated excitatory transmission following viscerosensory afferent stimulation by decreasing evoked EPSCs, attenuating action potential generation and propagation and diminishing spontaneous and mEPSCs, whereas high-frequency stimulus-evoked NMDA-dependent sustained currents were increased. Finally, enzymatic removal of polySia from the NTS *in vivo* increased splanchnic sympathetic nerve activity, whereas microinjection of sialidases that do not target polySia had little effect. Collectively, our studies indicate that polySia plays a hitherto unrecognized role in the modulation of neural transmission within the NTS, and demonstrate that polySia expression is required for the appropriate processing of viscerosensory afferent activity and its transmission to downstream networks, including the sympathetic outflow.

We extend earlier studies that describe the location of polySia in the CNS (Bonfanti et al., 1992; Bouzioukh et al., 2001a, b) demonstrating abundant polySia expression throughout the rostrocaudal extent of the NTS. Our ultrastructural analysis revealed polySia expression at sites that influence neurotransmission: in the extracellular space and intricate processes of astrocytes that

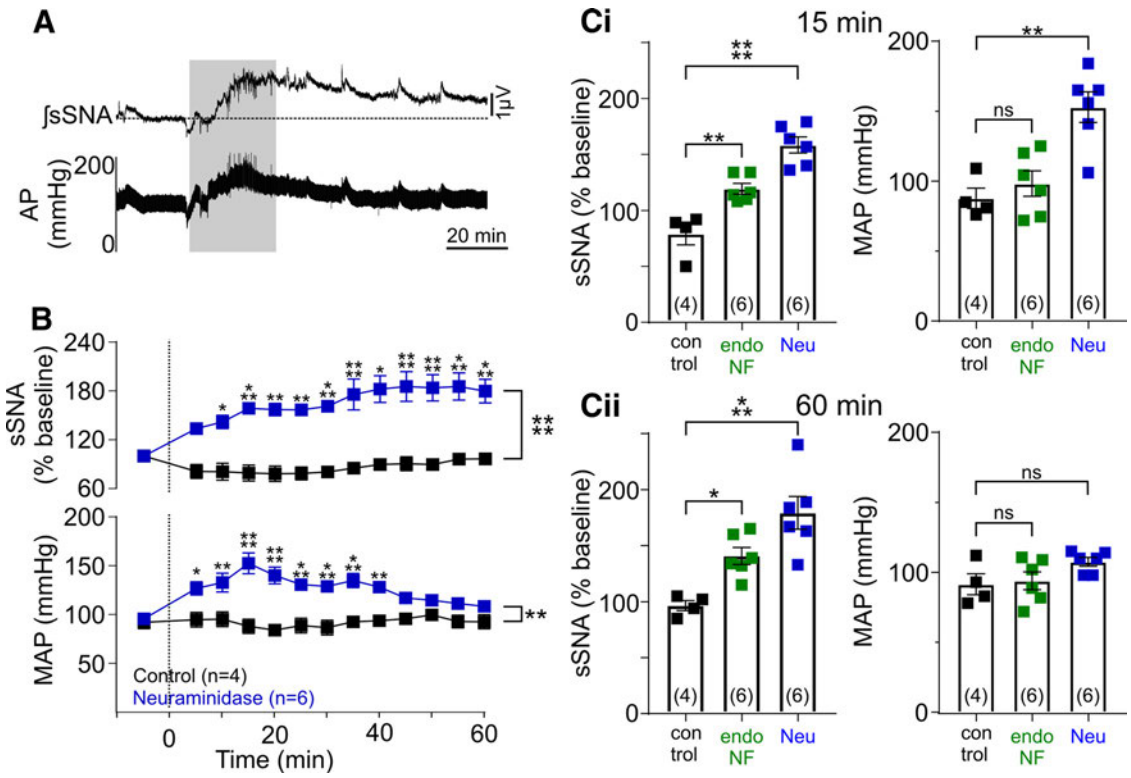

Figure 9. Removal of all sialic acids in the NTS causes rapid sympathoexcitation and acute hypertension. ***A***, Representative traces of integrated and smoothed neurogram of sSNA and arterial pressure following Neu (blue, 0.1 U/μl) or saline (control) microinjected into the NTS. Gray represents the period of injection. ***B***, Grouped data show the time course of response in sSNA and MAP following Neu microinjection ($n = 6$). sSNA increased by 79.3% ($p < 0.0001$) and arterial pressure increased acutely ($p = 0.0014$), returning to baseline after 60 min ($p = 0.157$). ***Ci***, Grouped data at 15 min after injection show that, compared with control, Neu significantly increased sSNA (158.5 $\pm$ 1.2 μV, $p < 0.0001$, $n = 6$) and MAP (152.8 $\pm$ 10.9 mmHg, $p = 0.0014$), whereas endoNF evoked a smaller increase in sSNA (119.3 $\pm$ 4.80%, $p = 0.0039$, $n = 6$) but did not change MAP (98.24 $\pm$ 9.12 mmHg, $p = 0.977$). ***Cii***, Grouped data at 60 min after injection show that, compared with control, both Neu and endoNF increased sSNA (179.3 $\pm$ 14.56 and 140.80 $\pm$ 7.63 μV, $p = 0.0004$ and $p = 0.0357$, respectively) but had no significant effect on MAP (108.5 $\pm$ 3.12 and 95.02 $\pm$ 6.40 mmHg, $p = 0.157$ and $p > 0.99$, respectively). Data are mean $\pm$ SEM. *$p < 0.05$; **$p < 0.01$; ***$p < 0.001$; ****$p < 0.0001$; ns, $p > 0.05$.

envelop neurons and synapses, as well as in some dendrites and axon terminals, consistent with our synaptophysin/polySia double labeling (Fig. 10*A*). Supporting our finding of polySia expression in astrocytic fine processes, blockade of microtubular function in the neurosecretory hypothalamus caused accumulation of polySia in astrocyte cell bodies (Theodosis et al., 1999, 2008). Expression around neurons found here is consistent with previous studies in the hippocampus, striatum, and cortex where polySia is linked with synaptic plasticity (Muller et al., 1996; Uryu et al., 1999; Eckhardt et al., 2000; Hildebrandt and Dityatev, 2015). Enzymatic digestion of polySia has no effect on presynaptic or postsynaptic neuronal structures examined by electron microscopy (Theodosis et al., 1999; Brusés et al., 2002), suggesting that functional effects result from disruption of signaling mechanisms, rather than major morphological changes.

In exploring the cellular mechanisms influenced by polySia in the NTS, we found that enzymatic removal of polySia increased TEA-sensitive currents, inhibited the closure of BK channels, and produced effects consistent with the increased release of Ca^{2+} from intracellular stores (Fig. 10*A*). The effects of TEA differed to those of Ibtx, indicating effects at multiple K^+ channels, including at delayed rectified K^+ channels, common in NTS neurons (Andresen and Kunze, 1994). Functional effects of NTS desialylation were not unexpected given that voltage-gated K^+ channels present on NTS neurons are heavily glycosylated, often with glycans likely capped by sialic acids (Cartwright and Schwalbe, 2009; Ednie and Bennett, 2012). A range of effects of desialylation have been described in other cell types, including both depolarizing and hyperpolarizing shifts in channel activation (Ednie and Bennett, 2012; Scott and Panin, 2014), which appear dependent upon the cell type examined and the channel isoform investigated. These complications arise as desialylation of the same ion channel in different cell types can produce varying effects (Ednie and Bennett, 2012; Scott and Panin, 2014) and channel isoforms can also vary in the glycan structures they carry (Schwalbe et al., 2008). Curiously astrocytes express abundant voltage-gated K^+ channels (Contet et al., 2016), so it is possible that polysialylation may also impact K^+ spatial buffering. Although both sialic acids and polySia are associated with voltage-gated Na^+ channels in rat brain (Zuber et al., 1992; Bennett et al., 1997; Ednie and Bennett, 2012) we saw no impact of polySia removal on action potential properties generated by current injection or following afferent stimulation.

We found that removal of polySia disrupted information transfer from viscerosensory afferents as evoked and spontaneous AMPA-dependent EPSCs were reduced, and NMDA sustained currents increased, indicating a role for polySia in regulating excitatory neurotransmission (Fig. 10*A*). As viscerosensory afferents innervate both somata and dendrites of NTS neurons (Anders et al., 1993), the astrocytic, neuronal, and extrasynaptic location of polySia seen here, together with the close association with synaptophysin shown by us and others (Bouzioukh et al., 2001a), are consistent with such a role. It is plausible that polySia on astrocytes may also influence synaptic or extrasynaptic glutamate availability as astrocytes express abundant glutamate transporters such as EAAT2 responsible for 90% of glutamate reuptake in brain.

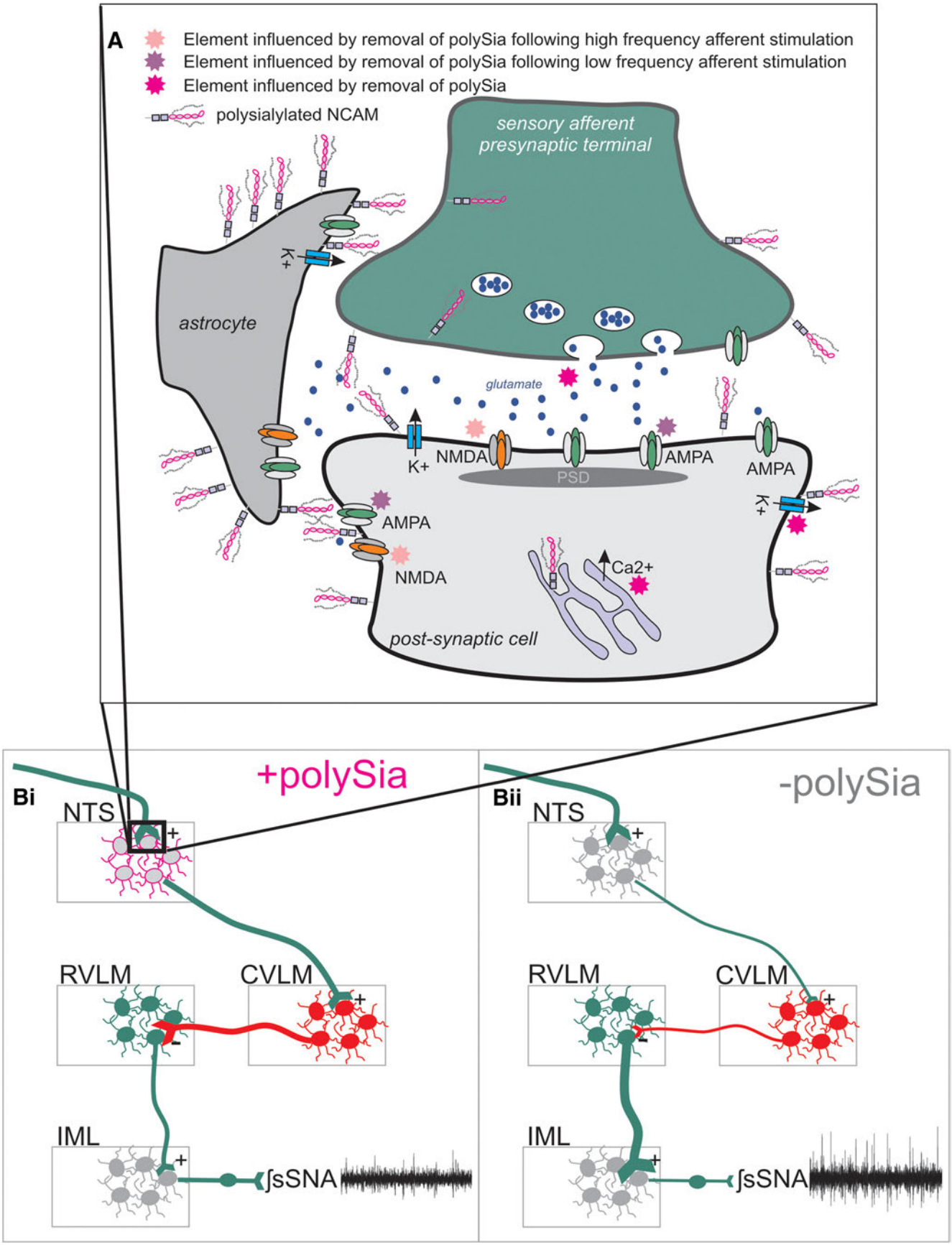

Figure 10. Overview depicting the structural location of polySia as well as the cellular mechanisms modified and functional consequences following removal of polySia from the NTS. ***A***, Astrocytic, terminal, and extrasynaptic expression of polySia influences Kv, intracellular calcium, and viscerosensory afferent glutamatergic transmission: during low-frequency input (magenta stars), and high input (pink stars), maintaining appropriate transmission through the NTS. ***B***, Schematically, the local and network impact of polySia in the NTS under *in vivo* (*Figure legend continues.*)

Within the NTS, variations in synaptic strength usually result from differences in the number of contact or release sites between afferent axons and postsynaptic membranes, rather than glutamate release probability or uptake capacity (Bailey et al., 2006b; Peters et al., 2008). Reduced action potential generation has been demonstrated in the NTS when K^+ channels are activated before viscerosensory afferent stimulation (Bailey et al., 2006a, 2007), or when glutamate release sites from single afferents are reduced (Bailey et al., 2006b). It appears paradoxical that polySia is not present within synapses in the NTS, given that its removal perturbs all forms of afferent excitation (e/s/mEPSC). However, polySia likely modulates transmission via effects directly at K^+ channels, and/or by altering availability of glutamate to the postsynaptic density, or via mechanisms at multiple release site recently described in NTS neurons (Fawley et al., 2016).

Also in keeping with effects seen here on evoked transient and sustained currents, polySia can modulate AMPA and NMDA receptor function (Vaithianathan et al., 2004; Hammond et al., 2006; Varbanov and Dityatev, 2017). Both receptor types are present within the NTS and are activated by differing afferent input (Aylwin et al., 1997; Zhang and Mifflin, 1998), with low-frequency stimulation evoking a large transient AMPA-mediated current (Andresen and Yang, 1990), and high-frequency stimulation (>5 Hz) a sustained NMDA-mediated current (Zhao et al., 2015). In support of our findings, activation of AMPA receptors in reconstituted lipid bilayers, in the presence of bacterially derived polySia, potentiated currents (~67%) and increased the opening probability of these receptors (~360%) (Vaithianathan et al., 2004), with opposing effects observed at NMDA receptors (decreased opening probability in the presence of polySia) (Hammond et al., 2006). Our findings therefore support previous suggestions that the anionic charge of polySia directly influences the positive amino acid residues of AMPA and NMDA receptors, as suggested for other polyanionic polysaccharides, such as heparin (Hall et al., 1996; Sinnarajah et al., 1999) and dextran (Suppiramaniam et al., 2006; Chicoine and Bahr, 2007). Whether GluN2B subunits containing NMDA receptors are targeted by removal of polySia as found previously (Kochlamazashvili et al., 2010) remains to be determined. Nevertheless, it is plausible that the anionic polySia provides optimal conditions for regulating glutamatergic transmission in the NTS.

The effects seen following polySia removal at the single neuron strongly support our findings in the whole animal, where enzymatic removal of polySia from the NTS region increased splanchnic sympathetic nerve activity (Fig. 10*B*). This finding is consistent with net disfacilitation of the NTS, effectively reducing information throughput resulting in sympathoexcitation via increased activity of premotor neurons (Pilowsky and Goodchild, 2002). Baroreceptor afferents provide tonic activation of the NTS altering activity on a heartbeat to heartbeat basis. Under basal conditions (as recorded here), baroreceptor firing frequency is low, favoring AMPA receptor activation with minimal input from NMDA receptors (Seagard et al., 1990; Gordon and Leone, 1991). When baroreceptor afferent traffic is reduced, sympathetic nerve activity increases (Sved et al., 1997) suggesting that polySia could influence such transmission. The inverse relationship between vagal afferent traffic and polySia expression in the NTS previously described (Bouzioukh et al., 2001a, b), and the sympathoexcitatory effect evoked by polySia removal seen here, appears to provide a mechanism to explain why stimulation of vagal afferents increases lumbar sympathetic nerve activity (Sun and Guyenet, 1987). The lack of a consistent blood pressure response following removal of polySia may be due to a threshold effect where blood pressure is not increased by the small, slow changes in sympathetic nerve activity induced by endo N alone, whereas Neu induced larger and more rapid changes in sympathetic nerve activity elevating blood pressure. Alternatively, polySia removal in the NTS may result in opposing changes in different vascular beds or influence splanchnic sympathetic fibers that innervate targets other than the vasculature. Nevertheless, the data indicate that sympathetic outflow is dependent on the expression of polySia within the NTS, which can be modified by changes to viscerosensory afferent traffic.

Targeting polySia consistently evoked sympathoexcitation. However, effects were enhanced by exo-neuraminidases that target α2–3, α2–6, in addition to α2–8 linked sialic acids, suggesting a role for other types of sialylation in regulating sympathetic outflow. However, endoNF only cleaves polySia polymers of five to eight α2–8 linked sialic acids (Stummeyer et al., 2005), potentially leaving some sialic acids (including single, di, or oligo sialic acids) that could be cleaved by the other enzymes used. Our Western blotting would not have detected these residual sialic acids because Mab735 recognizes octamers of α2–8 linked sialic acids (Evans et al., 1995; Nagae et al., 2013).

Collectively, our data show that removal of polySia alters neuronal properties and transmission of viscerosensory excitatory traffic through the NTS and that these effects alter transmission to downstream networks increasing sympathetic outflow (Fig. 10). This study expands the repertoire of signaling molecules, particularly those located on the cell surface or in astrocytes, which influence information transfer within sensory nuclei. The NTS governs autonomic, hormonal, and behavioral activity indicative of the wide spectra of functions that polySia may impact (Craig, 2003). Furthermore, the findings described here may define the neuronal mechanisms modified by polySia in higher brain regions (Rutishauser and Landmesser, 1996; Rutishauser, 2008) as well as at several sensory nuclei expressing abundant polySia (Bonfanti et al., 1992; El Maarouf et al., 2005). Finally, we demonstrate the importance of glycosylation modifications, such as sialylation, in altering neuronal function and show the importance of the level of polySia expression for appropriate information processing in the dorsal medulla, which ultimately regulates the activity of multiple downstream neural networks.

References

Aicher SA, Kurucz OS, Reis DJ, Milner TA (1995) Nucleus tractus solitarius efferent terminals synapse on neurons in the caudal ventrolateral medulla that project to the rostral ventrolateral medulla. Brain Res 693:51–63. CrossRef Medline

Anders K, Ohndorf W, Dermietzel R, Richter DW (1993) Synapses between slowly adapting lung stretch receptor afferents and inspiratory beta-neurons in the nucleus of the solitary tract of cats: a light and electron microscopic analysis. J Comp Neurol 335:163–172. CrossRef Medline

Andresen MC, Kunze DL (1994) Nucleus tractus solitaries: gateway to neural circulatory control. Annu Rev Physiol 56:93–116. CrossRef Medline

Andresen MC, Paton JF (2011) The nucleus of the solitary tract. In: Processing information from viscerosensory afferents. Oxford: Oxford UP.

Andresen MC, Yang MY (1990) Non-NMDA receptors mediate sensory afferent synaptic transmission in medial nucleus tractus solitarius. Am J Physiol 259:H1307–H1311. Medline

←

(*Figure legend continued.*) conditions. Control conditions (***Bi***) and highlight effects (***Bii***) following removal of polySia. Under both conditions, afferent input remains constant (equal line weight); however following removal of polySia, neurotransmission through the NTS is attenuated and intrinsic properties are modified, reducing the gating provided by the inhibitory CVLM on tonically active sympathoexcitatory premotor RVLM neurons resulting in elevated sympathetic nerve activity.

Appleyard SM, Marks D, Kobayashi K, Okano H, Low MJ, Andresen MC (2007) Visceral afferents directly activate catecholamine neurons in the solitary tract nucleus. J Neurosci 27:13292–13302. CrossRef Medline

Aylwin ML, Horowitz JM, Bonham AC (1997) NMDA receptors contribute to primary visceral afferent transmission in the nucleus of the solitary tract. J Neurophysiol 77:2539–2548. Medline

Bailey TW, Hermes SM, Andresen MC, Aicher SA (2006a) Cranial visceral afferent pathways through the nucleus of the solitary tract to caudal ventrolateral medulla or paraventricular hypothalamus: target-specific synaptic reliability and convergence patterns. J Neurosci 26:11893–11902. CrossRef Medline

Bailey TW, Jin YH, Doyle MW, Smith SM, Andresen MC (2006b) Vasopressin inhibits glutamate release via two distinct modes in the brainstem. J Neurosci 26:6131–6142. CrossRef Medline

Bailey TW, Hermes SM, Whittier KL, Aicher SA, Andresen MC (2007) A-type potassium channels differentially tune afferent pathways from rat solitary tract nucleus to caudal ventrolateral medulla or paraventricular hypothalamus. J Physiol 582:613–628. CrossRef Medline

Bennett E, Urcan MS, Tinkle SS, Koszowski AG, Levinson SR (1997) Contribution of sialic acid to the voltage dependence of sodium channel gating: a possible electrostatic mechanism. J Gen Physiol 109:327–343. CrossRef Medline

Bonfanti L (2006) PSA-NCAM in mammalian structural plasticity and neurogenesis. Prog Neurobiol 80:129–164. CrossRef Medline

Bonfanti L, Olive S, Poulain DA, Theodosis DT (1992) Mapping of the distribution of polysialylated neural cell adhesion molecule throughout the central nervous system of the adult rat: an immunohistochemical study. Neuroscience 49:419–436. CrossRef Medline

Bou Farah L, Bowman BR, Bokiniec P, Karim S, Le S, Goodchild AK, McMullan S (2016) Somatostatin in the rat rostral ventrolateral medulla: origins and mechanism of action. J Comp Neurol 524:323–342. CrossRef Medline

Bouzioukh F, Tell F, Jean A, Rougon G (2001a) NMDA receptor and nitric oxide synthase activation regulate polysialylated neural cell adhesion molecule expression in adult brainstem synapses. J Neurosci 21:4721–4730. Medline

Bouzioukh F, Tell F, Rougon G, Jean A (2001b) Dual effects of NMDA receptor activation on polysialylated neural cell adhesion molecule expression during brainstem postnatal development. Eur J Neurosci 14:1194–1202. CrossRef Medline

Browning KN, Travagli RA (2010) Plasticity of vagal brainstem circuits in the control of gastric function. Neurogastroenterol Motil 22:1154–1163. CrossRef Medline

Browning KN, Travagli RA (2014) Central nervous system control of gastrointestinal motility and secretion and modulation of gastrointestinal functions. Compr Physiol 4:1339–1368. CrossRef Medline

Brusés JL, Chauvet N, Rubio ME, Rutishauser U (2002) Polysialic acid and the formation of oculomotor synapses on chick ciliary neurons. J Comp Neurol 446:244–256. CrossRef Medline

Burke PG, Li Q, Costin ML, McMullan S, Pilowsky PM, Goodchild AK (2008) Somatostatin 2A receptor-expressing presympathetic neurons in the rostral ventrolateral medulla maintain blood pressure. Hypertension 52:1127–1133. CrossRef Medline

Cartwright TA, Schwalbe RA (2009) Atypical sialylated N-glycan structures are attached to neuronal voltage-gated potassium channels. Biosci Rep 29:301–313. CrossRef Medline

Champagnat J, Jacquin T, Richter DW (1986) Voltage-dependent currents in neurones of the nuclei of the solitary tract of rat brainstem slices. Pflugers Arch 406:372–379. CrossRef Medline

Chen X, Varki A (2010) Advances in the biology and chemistry of sialic acids. ACS Chem Biol 5:163–176. CrossRef Medline

Chicoine LM, Bahr BA (2007) Excitotoxic protection by polyanionic polysaccharide: evidence of a cell survival pathway involving AMPA receptor-MAPK Interactions. J Neurosci Res 85:294–302. CrossRef Medline

Coetzee WA, Amarillo Y, Chiu J, Chow A, Lau D, McCormack T, Moreno H, Nadal MS, Ozaita A, Pountney D, Saganich M, Vega-Saenz De Miera E, Rudy B (1999) Molecular diversity of K^+ channels. Ann N Y Acad Sci 868:233–285. CrossRef Medline

Contet C, Goulding SP, Kuljis DA, Barth AL (2016) BK channels in the central nervous system. Int Rev Neurobiol 128:281–342. CrossRef Medline

Craig AD (2003) Interoception: the sense of the physiological condition of the body. Curr Opin Neurobiol 13:500–505. CrossRef Medline

Damanhuri HA, Burke PG, Ong LK, Bobrovskaya L, Dickson PW, Dunkley PR, Goodchild AK (2012) Tyrosine hydroxylase phosphorylation in catecholaminergic brain regions: a marker of activation following acute hypotension and glucoprivation. PLoS One 7:e50535. CrossRef Medline

Dekin MS, Getting PA (1987) In vitro characterization of neurons in the ventral part of the nucleus tractus solitaries: II. Ionic basis for repetitive firing patterns. J Neurophysiol 58:215–229. Medline

Dekin MS, Getting PA, Johnson SM (1987) In vitro characterization of neurons in the ventral part of the nucleus tractus solitaries: I. Identification of neuronal types and repetitive firing properties. J Neurophysiol 58:195–214. Medline

Doyle MW, Andresen MC (2001) Reliability of monosynaptic sensory transmission in brain stem neurons in vitro. J Neurophysiol 85:2213–2223. Medline

Eckhardt M, Bukalo O, Chazal G, Wang L, Goridis C, Schachner M, Gerardy-Schahn R, Cremer H, Dityatev A (2000) Mice deficient in the polysialyltransferase ST8SiaIV/PST-1 allow discrimination of the roles of neural cell adhesion molecule protein and polysialic acid in neural development and synaptic plasticity. J Neurosci 20:5234–5244. Medline

Ednie AR, Bennett ES (2012) Modulation of voltage-gated ion channels by sialylation. Compr Physiol 2:1269–1301. CrossRef Medline

El Maarouf A, Kolesnikov Y, Pasternak G, Rutishauser U (2005) Polysialic acid-induced plasticity reduces neuropathic insult to the central nervous system. Proc Natl Acad Sci U S A 102:11516–11520. CrossRef Medline

Evans SV, Sigurskjold BW, Jennings HJ, Brisson JR, To R, Tse WC, Altman E, Frosch M, Weisgerber C, Kratzin HD (1995) Evidence for the extended helical nature of polysaccharide epitopes: the 2.8 A resolution structure and thermodynamics of ligand binding of an antigen binding fragment specific for alpha-(2->8)-polysialic acid. Biochemistry 34:6737–6744. CrossRef Medline

Fagius J, Wallin BG, Sundlöf G, Nerhed C, Englesson S (1985) Sympathetic outflow in man after anaesthesia of the glossopharyngeal and vagus nerves. Brain 108:423–438. CrossRef Medline

Fawley JA Hofmann ME, Andresen MC (2016) Distinct calcium sources support multiple modes of synaptic release from cranial sensory afferents. J Neurosci 36:8957–8966. CrossRef Medline

Frosch M, Görgen I, Boulnois GJ, Timmis KN, Bitter-Suermann D (1985) NZB mouse system for production of monoclonal antibodies to weak bacterial antigens: isolation of an IgG antibody to the polysaccharide capsules of *Escherichia coli* K1 and group B meningococci. Proc Natl Acad Sci U S A 82:1194–1198. CrossRef Medline

Glaum SR, Brooks PA (1996) Tetanus-induced sustained potentiation of monosynaptic inhibitory transmission in the rat medulla: evidence for a presynaptic locus. J Neurophysiol 76:30–38. Medline

Gogolla N, Galimberti I, DePaola V, Caroni P (2006) Staining protocol for organotypic hippocampal slice cultures. Nat Protoc 1:2452–2456. CrossRef Medline

Gordon FJ, Leone C (1991) Non-NMDA receptors in the nucleus of the tractus solitarius play the predominant role in mediating aortic baroreceptor reflexes. Brain Res 568:319–322. CrossRef Medline

Guyenet PG (2006) The sympathetic control of blood pressure. Nat Rev Neurosci 7:335–346. CrossRef Medline

Hall RA, Vodyanoy V, Quan A, Sinnarajah S, Suppiramaniam V, Kessler M, Bahr BA (1996) Effects of heparin on the properties of solubilized and reconstituted rat brain AMPA receptors. Neurosci Lett 217:179–183. CrossRef Medline

Hammond MS, Sims C, Parameshwaran K, Suppiramaniam V, Schachner M, Dityatev A (2006) Neural cell adhesion molecule-associated polysialic acid inhibits NR2B-containing N-methyl-D-aspartate receptors and prevents glutamate-induced cell death. J Biol Chem 281:34859–34869. CrossRef Medline

Hermes SM, Mitchell JL, Aicher SA (2006) Most neurons in the nucleus tractus solitarii do not send collateral projections to multiple autonomic targets in the rat brain. Exp Neurol 198:539–551. CrossRef Medline

Hildebrandt H, Dityatev A (2015) Polysialic acid in brain development and synaptic plasticity. Top Curr Chem 366:55–96. CrossRef Medline

Iggo A, Vogt M (1962) The mechanism of adrenaline-induced inhibition of sympathetic preganglionic activity. J Physiol 161:62–72. CrossRef Medline

Jin YH, Cahill EA, Fernandes LG, Wang X, Chen W, Smith SM, Andresen MC (2010) Optical tracking of phenotypically diverse individual synapses on solitary tract nucleus neurons. Brain Res 1312:54–66. CrossRef Medline

Kirov SA, Sorra KE, Harris KM (1999) Slices have more synapses than perfusion-fixed hippocampus from both young and mature rats. J Neurosci 19:2876–2886. Medline

Kline DD (2008) Plasticity in glutamatergic NTS neurotransmission. Respir Physiol Neurobiol 164:105–111. CrossRef Medline

Kochlamazashvili G, Senkov O, Grebenyuk S, Robinson C, Xiao MF, Stummeyer K, Gerardy-Schahn R, Engel AK, Feig L, Semyanov A, Suppiramaniam V, Schachner M, Dityatev A (2010) Neural cell adhesion molecule-associated polysialic acid regulates synaptic plasticity and learning by restraining the signaling through GluN2B-containing NMDA receptors. J Neurosci 30: 4171–4183. CrossRef Medline

Llewellyn-Smith IJ, Dicarlo SE, Collins HL, Keast JR (2005) Enkephalin-immunoreactive interneurons extensively innervate sympathetic preganglionic neurons regulating the pelvic viscera. J Comp Neurol 488:278–289. CrossRef Medline

Mayer CA, Macklin WB, Avishai N, Balan K, Wilson CG, Miller MJ (2009) Mutation in the myelin proteolipid protein gene alters BK and SK channel function in the caudal medulla. Respir Physiol Neurobiol 169:303–314. CrossRef Medline

Mayer ML, Westbrook GL, Guthrie PB (1984) Voltage-dependent block by Mg^{2+} of NMDA responses in spinal cord neurones. Nature 309:261–263. CrossRef Medline

McDougall SJ, Peters JH, Andresen MC (2009) Convergence of cranial visceral afferents within the solitary tract nucleus. J Neurosci 29:12886–12895. CrossRef Medline

Miles R (1986) Frequency dependence of synaptic transmission in nucleus of the solitary tract in vitro. J Neurophysiol 55:1076–1090. Medline

Moak JP, Kunze DL (1993) Potassium currents of neurons isolated from medical nucleus tractus solitarius. Am J Physiol 265:H1596–H1602. Medline

Muller D, Wang C, Skibo G, Toni N, Cremer H, Calaora V, Rougon G, Kiss JZ (1996) PSA-NCAM is required for activity-induced synaptic plasticity. Neuron 17:413–422. CrossRef Medline

Nagae M, Ikeda A, Hane M, Hanashima S, Kitajima K, Sato C, Yamaguchi Y (2013) Crystal structure of anti-polysialic acid antibody single chain Fv fragment complexed with octasialic acid: insight into the binding preference for polysialic acid. J Biol Chem 288:33784–33796. CrossRef Medline

Oltmann-Norden I, Galuska SP, Hildebrandt H, Geyer R, Gerardy-Schahn R, Geyer H, Mühlenhoff M (2008) Impact of the polysialyltransferases ST8SiaII and ST8SiaIV on polysialic acid synthesis during postnatal mouse brain development. J Biol Chem 283:1463–1471. CrossRef Medline

Parker LM, Kumar NN, Lonergan T, Goodchild AK (2013) Neurochemical codes of sympathetic preganglionic neurons activated by glucoprivation. J Comp Neurol 521:2703–2718. CrossRef Medline

Paxinos G, Watson CR (2006) The rat brain in stereotaxic coordinates. San Diego: Academic.

Pedarzani P, Kulik A, Muller M, Ballanyi K, Stocker M (2000) Molecular determinants of Ca^{2+}-dependent K^{+} channel function in rat dorsal vagal neurones. J Physiol 527:283–290. CrossRef Medline

Peters JH, McDougall SJ, Kellett DO, Jordan D, Llewellyn-Smith IJ, Andresen MC (2008) Oxytocin enhances cranial visceral afferent synaptic transmission to the solitary tract nucleus. J Neurosci 28:11731–11740. CrossRef Medline

Pilowsky PM, Goodchild AK (2002) Baroreceptor reflex pathways and neurotransmitters: 10 years on. J Hypertens 20:1675–1688. CrossRef Medline

Rutishauser U (2008) Polysialic acid in the plasticity of the developing and adult vertebrate nervous system. Nat Rev Neurosci 9:26–35. CrossRef Medline

Rutishauser U, Landmesser L (1996) Polysialic acid in the vertebrate nervous system: a promoter of plasticity in cell–cell interactions. Trends Neurosci 19:422–427. CrossRef Medline

Schauer R (2009) Sialic acids as regulators of molecular and cellular interactions. Curr Opin Struct Biol 19:507–514. CrossRef Medline

Schindelin J, Arganda-Carreras I, Frise E, Kaynig V, Longair M, Pietzsch T, Preibisch S, Rueden C, Saalfeld S, Schmid B, Tinevez JY, White DJ, Hartenstein V, Eliceiri K, Tomancak P, Cardona A (2012) Fiji: an open-source platform for biological-image analysis. Nat Methods 9:676–682. CrossRef Medline

Schnaar RL, Gerardy-Schahn R, Hildebrandt H (2014) Sialic acids in the brain: gangliosides and polysialic acid in nervous system development, stability, disease, and regeneration. Physiol Rev 94:461–518. CrossRef Medline

Schwalbe RA, Corey MJ, Cartwright TA (2008) Novel Kv3 glycoforms differentially expressed in adult mammalian brain contain sialylated N-glycans. Biochem Cell Biol 86:21–30. CrossRef Medline

Scott H, Panin VM (2014) The role of protein N-glycosylation in neural transmission. Glycobiology 24:407–417. CrossRef Medline

Seagard JL, van Brederode JF, Dean C, Hopp FA, Gallenberg LA, Kampine JP (1990) Firing characteristics of single-fiber carotid sinus baroreceptors. Circ Res 66:1499–1509. CrossRef Medline

Sinnarajah S, Suppiramaniam V, Kumar KP, Hall RA, Bahr BA, Vodyanoy V (1999) Heparin modulates the single channel kinetics of reconstituted AMPA receptors from rat brain. Synapse 31:203–209. CrossRef Medline

Stummeyer K, Dickmanns A, Mühlenhoff M, Gerardy-Schahn R, Ficner R (2005) Crystal structure of the polysialic acid-degrading endosialidase of bacteriophage K1F. Nat Struct Mol Biol 12:90–96. CrossRef Medline

Sun MK, Guyenet PG (1987) Arterial baroreceptor and vagal inputs to sympathoexcitatory neurons in rat medulla. Am J Physiol 252:R699–R709. Medline

Suppiramaniam V, Vaithianathan T, Manivannan K, Dhanasekaran M, Parameshwaran K, Bahr BA (2006) Modulatory effects of dextran sulfate and fucoidan on binding and channel properties of AMPA receptors isolated from rat brain. Synapse 60:456–464. CrossRef Medline

Sved AF, Schreihofer AM, Kost CK Jr (1997) Blood pressure regulation in baroreceptor-denervated rats. Clin Exp Pharmacol Physiol 24:77–82. CrossRef Medline

Szele FG, Dowling JJ, Gonzales C, Theveniau M, Rougon G, Chesselet MF (1994) Pattern of expression of highly polysialylated neural cell adhesion molecule in the developing and adult rat striatum. Neuroscience 60:133–144. CrossRef Medline

Talman WT, Perrone MH, Reis DJ (1980) Evidence for L-glutamate as the neurotransmitter of baroreceptor afferent nerve fibers. Science 209:813–815. CrossRef Medline

Taylor G (1996) Sialidases: structures, biological significance and therapeutic potential. Curr Opin Struct Biol 6:830–837. CrossRef Medline

Theodosis DT, Bonhomme R, Vitiello S, Rougon G, Poulain DA (1999) Cell surface expression of polysialic acid on NCAM is a prerequisite for activity-dependent morphological neuronal and glial plasticity. J Neurosci 19:10228–10236. Medline

Theodosis DT, Poulain DA, Oliet SH (2008) Activity-dependent structural and functional plasticity of astrocyte-neuron interactions. Physiol Rev 88:983–1008. CrossRef Medline

Titz S, Keller BU (1997) Rapidly deactivating AMPA receptors determine excitatory synaptic transmission to interneurons in the nucleus tractus solitarius from rat. J Neurophysiol 78:82–91. Medline

Uryu K, Butler AK, Chesselet MF (1999) Synaptogenesis and ultrastructural localization of the polysialylated neural cell adhesion molecule in the developing striatum. J Comp Neurol 405:216–232. CrossRef Medline

Vaithianathan T, Matthias K, Bahr B, Schachner M, Suppiramaniam V, Dityatev A, Steinhaüser C (2004) Neural cell adhesion molecule-associated polysialic acid potentiates alpha-amino-3-hydroxy-5-methylisoxazole-4-propionic acid receptor currents. J Biol Chem 279:47975–47984. CrossRef Medline

Varbanov H, Dityatev A (2017) Regulation of extrasynaptic signaling by polysialylated NCAM: impact for synaptic plasticity and cognitive functions. Mol Cell Neurosci 81:12–21. CrossRef Medline

Venstrom KA, Reichardt LF (1993) Extracellular matrix: 2. Role of extracellular matrix molecules and their receptors in the nervous system. FASEB J 7:996–1003. Medline

Yang H, Zhang G, Cui J (2015) BK channels: multiple sensors, one activation gate. Front Physiol 6:29. CrossRef Medline

Zhang J, Mifflin SW (1998) Differential roles for NMDA and non-NMDA receptor subtypes in baroreceptor afferent integration in the nucleus of the solitary tract of the rat. J Physiol 511:733–745. CrossRef Medline

Zhao H, Peters JH, Zhu M, Page SJ, Ritter RC, Appleyard SM (2015) Frequency-dependent facilitation of synaptic throughput via postsynaptic NMDA receptors in the nucleus of the solitary tract. J Physiol 593:111–125. CrossRef Medline

Zhou Z, Champagnat J, Poon CS (1997) Phasic and long-term depression in brainstem nucleus tractus solitarius neurons: differing roles of AMPA receptor desensitization. J Neurosci 17:5349–5356. Medline

Zoccal DB, Furuya WI, Bassi M, Colombari DS, Colombari E (2014) The nucleus of the solitary tract and the coordination of respiratory and sympathetic activities. Front Physiol 5:238. CrossRef Medline

Zuber C, Lackie PM, Catterall WA, Roth J (1992) Polysialic acid is associated with sodium channels and the neural cell adhesion molecule N-CAM in adult rat brain. J Biol Chem 267:9965–9971. Medline